IMMUNOLOGICAL AND TOXICOLOGICAL STUDIES ON THE BENZOPYRONES

A thesis submitted for the degree of Ph.D.

by

Aoife Lacy B.Sc. (Hons)

April, 2004.

Based on research carried out

at

The School of Biotechnology,

Dublin City University,

Dublin 9,

Ireland.

Under the supervision of Professor Richard O'Kennedy

Declaration:

I hereby certify that this material, which I now submit for assessment on the programme of study leading to the award of Doctor of Philosophy, is entirely my own work, and has not been taken from the work of others, save and to the extent that such work is cited and acknowledged within the text of my work.

Signed _____

Date: _____

This thesis is dedicated to my Mum and Dad, without their love and guidance I would not be where I am today.

Acknowledgements:

In the course of my studies and research, I have met extraordinary people and received generous help in so many ways that I will be forever grateful for all the encouragement and support. First and foremost, I owe a tremendous debt to my supervisor, Professor Richard O'Kennedy. I appreciate with much gratitude all the time and energy he invested in guiding me along the sometimes rocky path that was my PhD studentship. A million thanks, Richard, for all the support and advice and for your patience and understanding.

My time as part of the Applied Biochemistry Group has had its ups and downs and I feel incredibly fortunate that I was surrounded by a wonderful group of people. Someone would always listen to my woes and the atmosphere was always pleasant even on the most stressful days. No matter how busy anyone was, there was always time to listen and help out. Thanks in order of appearance to John, Bernie, Brian, Paul D, Stephen D, Jane, Lorna, Joanne, Lynsey, Fred, Sharon, Liz and Mary. Now a few special thanks. I'd like to thank Brian for all his help with the warfarin antibody. Who knows where I'd have ended up if I didn't have clone 4-2-25 and all his support. Thanks to John who helped me with the dreaded Solution phase assays (and so much more) and for his good humour when it was really needed. Paul D & Stephen D, thanks with much appreciation, for your help and encouragement. The immunology section of my thesis wouldn't be what it is without all you guys and I'm all the saner for it! Paul L, thanks for all the support over the years and especially towards the end where your advice and help really made a difference. Finally, to Stephen H, I really appreciate that you listened to all my woes and gave such sound advice. You've been a good friend, thanks for everything.

I should also mention all the staff and fellow students in the School of Biotechnology I've met along the way. My DCU experience was all the more pleasant for all their input, both intellectual and social. A special mention to the "Karaoke Girls" you know who you are...and why I am so grateful. To Bella, Grace and Paul, I owe so much... I don't think I'd have survived the undergrad years without you guys.

Now, to my other life...the one outside DCU. Firstly, thanks to those who inspired me and helped my confidence over the years - John & Daphne and Liam. To all my friends along the way, Marie, Karen, Jude and Julie, thanks for the wonderful memories. My best friend Susan, you really have been through it all with me. Your friendship has enriched my life in so many ways. You are like a sister to me (& you know what that means to me) and your family, my family. I am eternally

grateful. Noreen (my 2nd mother across the road), thanks for EVERYTHING. I could write a list as long as this thesis and it still wouldn't cover all you've done for me over the years. Now, to my actual family. Mum, a heartfelt thanks for listening and being there whenever I needed you throughout my life, which was quite often! I found out about Biotechnology in DCU thanks to you and will always be grateful for your inquisitive and selfless nature. To my Dad, thanks for being there. Your generous nature, great advice and walks out in Howth helped to ease the stress and make my life so much better. To Conor, thanks for caring and always showing an interest in what I've been up to. I couldn't ask for a better big brother! You've all helped me become the person I am today - much love and respect. To the rest of my family, I want to say a big THANK YOU – especially Beryl, Pauline, Karen, Silvana and Ger. It is very important that I thank some special people who have come into my life since I started my PhD. To Mary, we were reunited nearly four years ago now, but you've always had a place in my heart. Thank you for being part of my life and enriching it, which means so much to me. I couldn't imagine life without you now. Thanks Alan for the warmth and humour, which has made getting to know you such a joy (I appreciate the new nickname of Dr. Doolittle!). Thanks to the rest of my newfound family – it's a great feeling to know you're there.

Last, but definitely not least, Fai. It's difficult to put into words how much you mean to me. I've made it to the end in one piece because of you. I am sure you're sick of hearing it but, what would I do without you? Your humorous replies to that often asked question and caring nature, lifts my spirits. Thanks for helping me keep it together, and even if you don't believe it, you've been my rock.

My acknowledgements would be complete without a quick mention to my furry friends Homer, Marge and Benji who never get stressed about anything – I am working towards that philosophy.

"To see a thing uncoloured by one's own personal preferences and desires is to see it in its own pristine simplicity."

Bruce Lee

■

"Research shows that you begin learning in the womb and go right on learning until the moment you pass on. Your brain has a capacity for learning that is virtually limitless, which makes every human a potential genius."

Michael J. Gelb

v

TABLE OF CONTENTS

xi

List of Figures

List of Tables

Abbreviations

| 4'-AW | 4'-aminowarfarin |
| Ab | Antibody |

ADME/T	Absorption, distribution, metabolism, excretion and toxicity profiles
ADP	Adenosine diphosphate
AFM_1	Aflatoxin M_1
AIDS	Acquired immune deficiency syndrome
ALT	Alanine aminotransferase
AMI	Acute myocardial infarction
AP	Acid phosphatase
AR	Acquired resistance
ATP	Adenosine triphosphate
ATP-TCA	ATP-based tumour chemosensitivity assay
BIA	Biomolecular interaction analysis
BSA	Bovine serum albumin
BsDb	Bispecific diabody
CD-DST	Collagen gel droplet embedded culture-drug sensitivity test
CDK	Cyclin-dependent kinases
CDKIs	CDK inhibitors
CDR	Complementarity determining regions of antibody
cNOS	Constitutive nitric oxide synthase
CM	carboxymethylated
CYP	Cytochrome P450
CTLA-4	Cytotoxic T lymphocyte-associated antigen 4
DMEM	Dulbecco's Minimum Essential Medium
DMSO	Dimethyl sulfoxide
DNA	Deoxyribonucleic acid
DTT	Dithiothreitol
DVT	Deep vein thrombosis
E_2	Estradiol
ECAR	Extracellular acidification rate
EDC	N-ethyl-N'-(dimethylaminopropyl) carbodiimide
EDTA	Ethylene diamine tetraacetic acid
EGF	Epidermal growth factor
EGF-R	Epidermal growth factor receptor
ELISA	Enzyme-linked immunosorbent assay
ER	Estrogen receptor
ERK	Extracellular regulated kinase

Fab	Binding region of antibody above the hinge region
Fc	Constant region of antibody molecule
FCS	Foetal calf serum
FDA	Food and Drug Administration (U.S.)
FDH	Familial dysalbuminemic hyperthyroxinemia
FGF-R	Fibroblastic growth factor receptor
FPT	Farnesyl protein transferase
FR	Framework region
FTIs	Farnesyl transferase inhibitors
FTS	Farnesylthiosalycyclic acid
5-FU	5-Fluorouracil
Fv	variable binding region of antibody
FX	Factor X
GAP	GTPase activating protein
GC-MS	Gas chromatography-mass spectrometry
GCR	G-protein coupled receptor
GDP	Guanosine diphosphate
GTP	Guanosine triphosphate
Gla	γ-carboxyglutamate
Glu	Glutamate
GN	Glomerulonephritis
Grb	Growth factor receptor binding protein
GRF	Guanine nucleotide releasing factor
GTP	Guanosine triphosphate
HAT	Hypoxanthine aminopterin thymidine
HAMA	Human anti-mouse antibody
HBS	Hepes buffered saline
HCC	Hepatocellular carcinoma
HCV	Hepatitis C virus
HGPRT	Hypoxanthine guanine phosphoribosyltransferase
HIV	Human immunodeficiency virus
HLE	Human leukocyte elastase
HPLC	High performance liquid chromatography
HPO	High protein oedema
HR	Hereditary resistance

HRP	Horseradish peroxidase
HSA	Human serum albumin
HT	Hypoxanthine thymidine
HV	Hypervariable
i.v.	Intravenous
IC_{50}	50% Inhibitory Concentration *i.e.* Drug concentration causing 50% growth inhibition
IFC	Integrated μ-fluidic cartridge
IFN	Interferon
Ig	Immunoglobulin
IgA	Immunoglobulin class A
IgD	Immunoglobulin class D
IgE	Immunoglobulin class E
IgG	Immunoglobulin class G
IgM	Immunoglobulin class M
IL	Interleukin
iNOS	Inducible nitric oxide synthase
INR	International Normalized Ratio
ISI	International Sensitivity Index
Ka	Association affinity constant
ka	Association rate constant
Kd	Dissociation affinity constant
kd	Dissociation rate constant
kDa	Kilodalton
LAPS	Light-addressable potentiometric sensor
LDH	Lactate dehydrogenase
LED	Light-emitting diode
Log	Logarithmic
LPS	Lipopolysaccaride
mAb	Monoclonal antibody
MAP	Mitogen-activated protein
MDR	Multi-drug resistance
MEK	MAP/ERK kinase
MHC-II	Major histocompatibility complex class II molecules
8-MOP	8-methoxypsoralen
mRNA	Messenger RNA

MTT	3-[4,5-dimethylthiazol-2-yl]-2,5-diphenyltetrazolium bromide
MW	Molecular weight
n	Refractive index
NEAA	Non-essential amino acids
NF-κB	Nuclear factor-κB
NGF	Nerve growth factor
NHS	N-hydroxysuccinimide
NIOSH	National Institute for Occupational Safety and Health
NO	Nitric oxide
NSAIDs	Non-steroidal anti-inflammatory drugs
OAT	Oral Anticoagulant Therapy
2-OHC	2-hydroxycoumarin
4-OHC	4-hydroxycoumarin
7-OHC	7-hydroxycoumarin
o-HPAA	o-hydroxyphenylacetic acid
o-HPLA	o-hydroxyphenyllactic acid
pI	Isoelectric point
p.o.	peroral
PAGE	Polyacrylamide gel electrophoresis
PBS	Phosphate-buffered saline
PDA	Photodiode array
PDGF	Platelet-derived growth factor
PEG	Polyethylene glycol
PG	Prostaglandin
pH	Log of the hydrogen ion concentration
pNPP	para-Nitrophenyl phosphate
PI3K	Phosphatidylinositol 3-kinase
PIVKAs	Proteins Induced by Vitamin K Antagonism or Absence
PKC	Protein kinase C
PRB	Retinoblastoma protein
PSA	Prostate specific antigen
PT	Protrombin time
PTB	Phosphotyrosine binding domain
P-Tyr	Phosphorylated tyrosine
PUVA	Psoralen & UVA

R	Regression coefficient
RBD	Ras binding domain
RCC	Renal cell carcinoma
Req	Equilibrium binding response
RI	Refractive index
RIA	Radioimmunoassay
Rmax	Maximum binding response
RNA	Ribonucleic acid
ROS	Reactive oxygen species
RTK	Receptor tyrosine kinase
S.D.	Standard deviation
scFv	Single chain Fv antibody derivative
SDS	Sodium dodecyl sulphate
SE	Standard error
SPR	Surface plasmon resonance
TBS	Tris-buffered saline
TBZ	Benzimidazolecarboxylic acid
TGF	Transforming growth factor
TIR	Total internal reflection
TLC	Thin layer chromatography
TM	Transverse magnetic
TMB	Tetramethyl-benzidine
TNF	Tumour necrosis factor
Tris	Tris(hydroxymethyl)aminomethane
TYR	Tyrphostin
UV	Ultraviolet
UVA	Artificial long wavelength ultraviolet
V_H	Variable region of heavy chain
V_L	Variable region of light chain
VSMC	Vascular smooth-muscle cells
WISN	Warfarin-induced skin necrosis
WF-BSA	Warfarin-BSA
χ^2	Chi squared (i.e. averaged squared residual per data point)

Units

μg	microgram
(k)Da	(kilo) Daltons
μl	microlitre
μM	micromoles
°C	degrees Celcius
AU	arbitrary units
cm	centimetres
g	grams
h	hours
K	degrees Kelvin
kg	kilogram
l	litre
m	metre
M	molar
mg	milligram
min	minute
ml	millilitre
mm	millimetres
nm	nanometre
nM	nanomolar
mol	molar
pg	picograms
rpm	revolutions per minute
RU	response units
sec, s	seconds
v/v	volume per unit volume
w/v	weight per unit volume

Publications and Presentations

Lacy, A. & O' Kennedy, R. (2001) The application of rapid analytical systems and sensors to the detection of cancers and other diseases, *West Indian Med. J.,* **50:** 100-104.

Lacy, A. & O' Kennedy, R. (2004) Radioimmunoassays, In: *Encyclopaedia of Analytical Science,* Second Edition, In Press.

Lacy, A. & O' Kennedy, R. (2004) Studies on the coumarins and coumarin-related compounds to determine their therapeutic role in the treatment of cancer, *Curr. Pharm. Design,* In Press.

Lacy, A., Cooke, D., O'Kennedy, R. (2004) The effects of benzopyrones on the growth, metabolism and signalling pathways of human tumour cells, (In Preparation).

Lacy, A. & O' Kennedy, R. (Dec., 2002) Immunological and toxicological studies on the benzopyrones, PhD Transfer meeting, DCU.

Abstract

The Benzopyrones are a group of compounds whose members include coumarins (e.g. esculetin, warfarin) and flavonoids (e.g. genistein).

An anti-warfarin monoclonal antibody (mAb) was successfully used to develop assays for the detection of warfarin in biological matrices. Warfarin was reproducibly detected in PBS and urine utilising both the enzyme-linked immunosorbent assay (ELISA) technique and BIAcore, a biosensing instrument. Cross reactivity studies illustrated that acenocoumarin exhibited the highest degree of cross reactivity with the anti-warfarin mAb, as expected, due to its high degree of structural similarity to warfarin. Coumarin displayed negligible cross reactivity due to its low degree of structural similarity to warfarin. Kinetic studies of mAb preparations yielded both dissociation constant (K_D) and association constant (K_A) values for warfarin and three structurally similar analogues. The mAb was successfully characterised.

Toxicological effects of four benzopyrone compounds were investigated on two carcinoma cell-lines (A549 and MCF-7). Three different types of 96-well microtitre assays determined that genistein and esculetin respectively, were the most potent inhibitors of cell proliferation and metabolism. These results were compared to the results from the Cytosensor microphysiometer, a biosensor that detects cellular metabolism. Genistein was the most potent inhibitor on cellular metabolism followed by esculetin. In all assays both warfarin and 7-hydroxycoumarin showed weak inhibition of proliferation and metabolism. Other studies performed, illustrated the ability of genistein and esculetin to inhibit cell proliferation by DNA synthesis suppression. Studies on tyrosine kinase activity in MCF-7 cells suggest that esculetin and warfarin may suppress tyrosine kinase activity, which in turn has an inhibitory effect on cell proliferation. Overall, the potency of growth and metabolic inhibition by genistein was greater than esculetin, which was far greater than warfarin.

Chapter 1

Introduction to the Benzopyrones

1.1. Introduction

Coumarins owe their class name to 'Coumarou', the vernacular name of the tonka bean (*Dipteryx odorata* Willd., Fabaceae), from which coumarin itself was isolated in 1820 (Bruneton, 1999). Coumarin is classified as a member of the benzopyrone family of compounds, all of which consist of a benzene ring joined to a pyrone ring (Ojala, 2001). The benzopyrones can be subdivided into the benzo-α-pyrones to which the coumarins belong and the benzo-γ-pyrones, of which the flavonoids are principal members (Figure 1.1.).
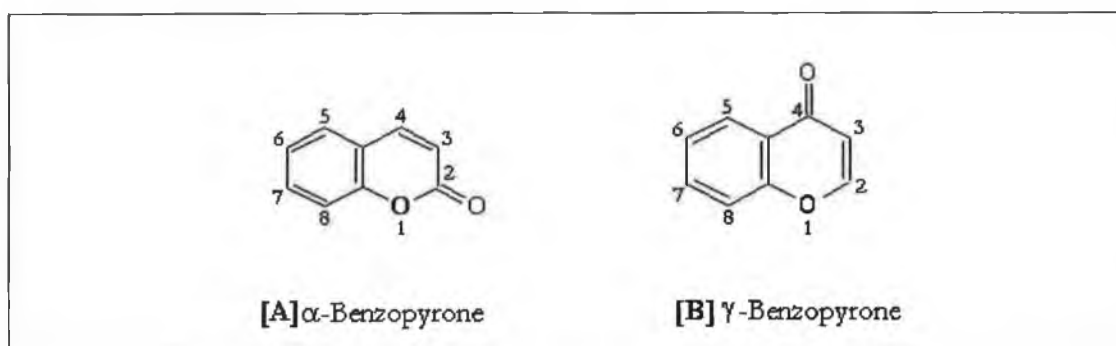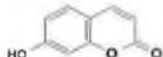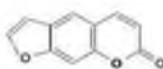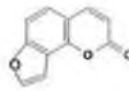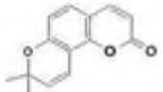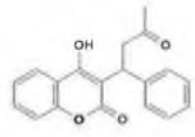
Figure 1.1: *The chemical structures of benzopyrone subclasses, with the basic coumarin structure (benzo-α-pyrone) [A], and flavonoid (benzo-γ-pyrones) structure [B].*

1.2. Occurrence

There are four main coumarin sub-types: the simple coumarins, furanocoumarins, pyranocoumarins and the pyrone-substituted coumarins (Table 1.1). The simple coumarins (e.g. coumarin, 7-hydroxycoumarin and 6,7-dihydroxycoumarin), are the hydroxylated, alkoxylated and alkylated derivatives of the parent compound, coumarin, along with their glycosides. Furanocoumarins consist of a five-membered furan ring attached to the coumarin nucleus, divided into linear or angular types with substituents at one or both of the remaining benzoid positions. Pyranocoumarin members are analogous to the furanocoumarins, but contain a six-membered ring. Coumarins substituted in the pyrone ring include 4-hydroxycoumarin (Keating & O'Kennedy, 1997). The synthetic compound warfarin belongs to this coumarin subtype. By virtue of its structural simplicity coumarin has been assigned as head of the benzo-α-pyrones, although it is generally accepted that 7-hydroxycoumarin be regarded as the parent compound of the more complex coumarins (Table 1.1) (Murray *et al.*, 1982). Genistein is an isoflavone and belongs to the benzo-γ-pyrones. It is a natural component of soy and

2

has been intensively investigated as a chemopreventitive agent, mainly against hormonally regulated breast and prostate cancers in animal models (Constantinou *et al.*, 1998).

Table 1.1: *The four main coumarin subtypes. The main structural features and examples of each coumarin subtype are illustrated in this table.*

Classification	Features	Examples
SIMPLE COUMARINS	Hydroxylated, alkoxylated or alkylated on benzene ring	7-hydroxycoumarin
FURANOCOUMARINS	5-membered furan ring attached to benzene ring. Linear or Angular	Psoralen Angelicin
PYRANOCOUMARINS	6-membered pyran ring attached to benzene ring. Linear or Angular	Seselin Xanthyletin
PYRONE-SUBSTITUTED COUMARINS	Substitution on pyrone ring, often at 3-C or 4-C position	Warfarin

Coumarins comprise a very large class of compounds found throughout the plant kingdom (Finn *et al.*, 2002). They are found at high levels in some essential oils, particularly cinnamon bark oil (7000 ppm), cassia leaf oil (up to 87,300 ppm) and lavender oil. Coumarin is also found in fruits (e.g. bilberry, cloudberry), green tea and other foods such as chicory (Lake, 1999). Most coumarins occur in higher plants, with the richest sources being the Rutaceae and Umbelliferae. Although distributed throughout all parts of the plant, the coumarins occur at the highest levels in the fruits, followed by the

3

roots, stems and leaves. Environmental conditions and seasonal changes can influence the occurrence in diverse parts of the plant (Keating & O'Kennedy, 1997). Recently six new minor coumarins have been isolated from the fruits and the stem bark of *Calophyllum dispar* (Clusiaceae). The genus *Calophyllum* which comprises 200 species is widely distributed in the tropical rain forest where several species are used in folk medicine (Guilet, 2001).

Although most of the natural coumarins in existence have been isolated from the higher plants, some members have been discovered in microorganisms. Some important coumarin members have been isolated from microbial sources e.g. novobiocin and coumermycin from *Streptomyces*, and aflatoxins from *Aspergillus* species (Cooke *et al.,* 1997; Cooke, 1999). The aflatoxins are a group of highly toxic fungal metabolites and the most commonly occurring member of the group is aflatoxin B_1 (Keating & O'Kennedy, 1997). Coumarin group antibiotics, such as novobiocin, coumermycin A_1 and clorobiocin, are potent inhibitors of DNA gyrase. These antibiotics were isolated from various *Streptomyces* species and all possess a 3-amino-4-hydroxy-coumarin moiety and a substituted deoxysugar; noviose, as their structural core that is essential for their biological activity. Chlorobiocin differs from novobiocin in that the methyl group at the C-8 of the coumarin ring is replaced by a chlorine atom, and the carbamoyl at the 3' of the noviose is substituted by a 5-methyl-2-pyrrolcarboxyl group. Coumermycin A_1 contains two of the coumarin-noviose core joined by a 3-methyl-2,4-dicarboxyl pyrole linker and has the same substituted noviose as in chlorobiocin (Chen & Walsh, 2001).

1.3. Biosynthesis

In the higher plants, coumarins are generally produced via the shikimate-chorismate biosynthetic pathway as a derivative of cinnamic acid, which is also a precursor of many other natural products such as methyl salicylate, cinnamic aldehyde and amygdalin. The shikimate-chorismate pathway is responsible for the formation of the aromatic amino acids (Keating & O' Kennedy, 1997). This pathway is a central biosynthetic route in plants and micro-organisms. Shikimate and chorismate are key intermediates in the biosynthesis of the aromatic acids L-phenylanine, L-tyrosine and L-tryptophan (Murray *et al.,* 1982). Shikimate is converted to chorismate through sequential phosphorylation, condensation and elimination reactions. Chorismate is converted to prephenate, which is achieved enzymatically. Aromatisation of prephenate yields phenylpyruvate that is transaminated to become phenylalanine. Enzymatic elimination of ammonia from phenylalanine produces *trans*-cinnamic acid, which is a precursor for the production of all coumarin species (Murray *et al.,* 1982; Weinmann, 1997).

4

At this stage the biosynthetic pathway diverges (pathways 1 and 2 in Figure 1.2), giving rise to two distinct coumarin types - those which are oxygenated at carbon-7 and those that are not. In the latter case (pathway 1, Figure 1.2) trans-cinnamic acid is converted to coumarinyl glucoside via the three steps illustrated in Figure 1.2. This is the primary form in which coumarin exists. The simple 7-oxygenated coumarins follow a similar scheme (pathway 2, Figure 1.2). The difference being the initial step where trans-cinnamic acid is converted to *p*-coumaric acid by a *para*-hydroxylation. *P*-coumaric acid undergoes three steps to convert to umbelliferyl glucoside (Keating & O' Kennedy, 1997).

Details of Pathway 1 and 2 in Figure 1.2 are as follows:

Pathway 1

1. Ortho hydroxylation of *trans*-cinnamic acid to *trans*-2'-hydroxycinnamic acid.

2. Glucosylation of *trans*-2'-hydroxycinnamic acid to *trans*-2'-glucosyloxycinnamic.

3. *Cis*-isomerisation to form coumarinyl glucoside.

Pathway 2

A. *Para*-hydroxylation of *trans*-cinnamic acid to *p*-coumaric.

B. *Ortho*-hydroxylation of *p*-coumaric to *trans*-2',4'-dihydroxycinnamic.

C. Glucosylation to yield *trans*-2'-glucosyloxy-4'-hydroxycinnamic.

D. *Trans-cis*-isomerisation to form umbelliferyl glucoside.
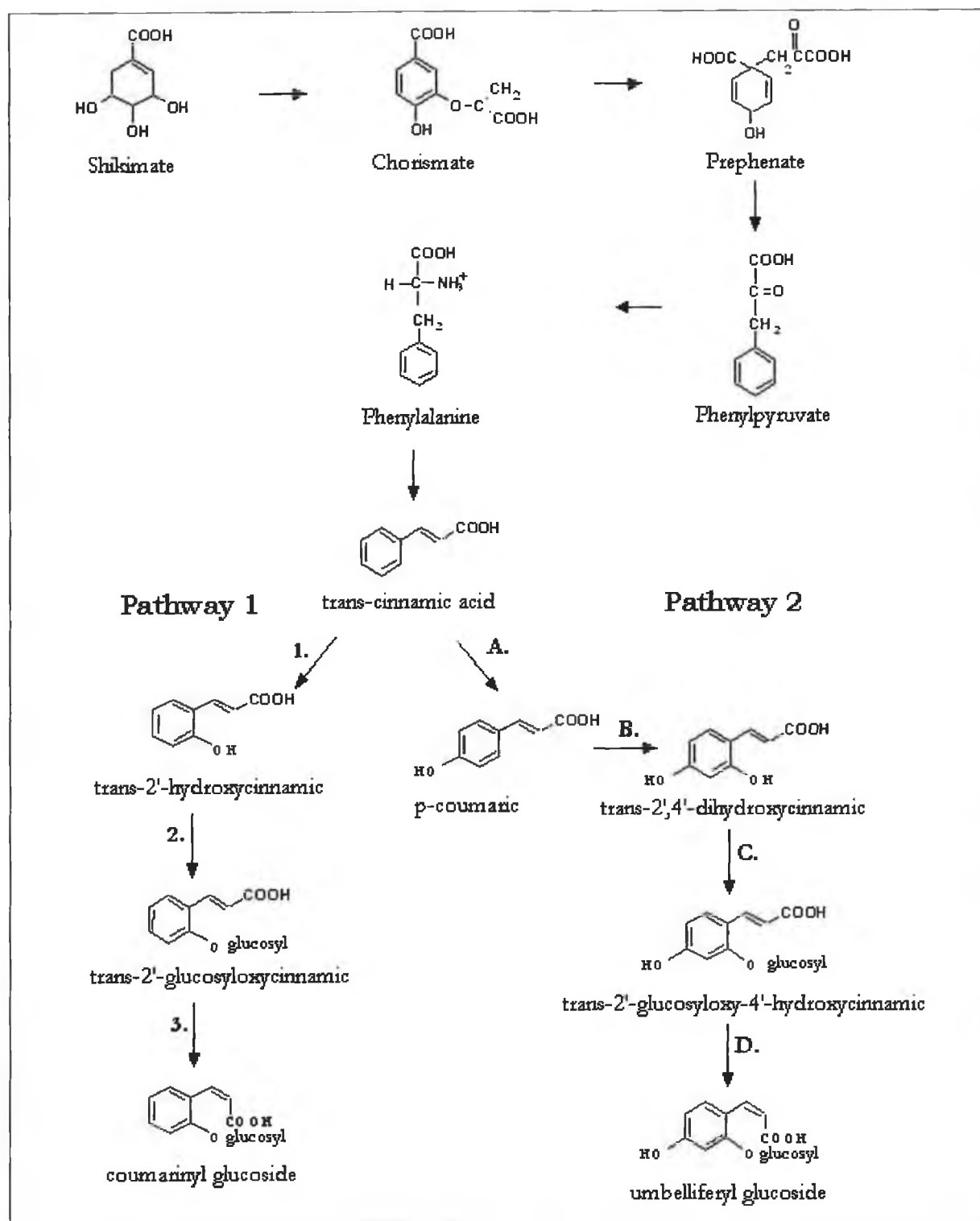
Figure 1.2: *Biosynthetic routes for the natural production of coumarin and 7- hydroxycoumarin. Details of the pathways are included in the text.*

1.4. Pharmacokinetics

The area of study, which elucidates the time course of drug concentration in the blood and tissues, is termed pharmacokinetics. It is the study of the kinetics of absorption, distribution, metabolism and excretion of drugs and their corresponding pharmacologic, therapeutic, or toxic response in animals and man (Rang & Dale, 1987). The pharmacokinetics of coumarin, including the excretion of various metabolites, was elucidated over many years. Coumarin is rapidly and almost completely metabolised with little unchanged compound excreted (Pelkonen *et al.,* 1997).

The biological response to a drug is the result of an interaction between the drug substance and functionally important cell receptors or enzyme systems. The magnitude of the response is related to the concentration of the drug achieved at the site of its activation. This drug concentration depends on the dosage of the drug administered, the extent of its absorption and distribution to the site, and the rate and extent of its elimination from the body.

For a drug to exert its biologic effect, it must be transported by the body fluids, traverse the required membrane barriers, escape widespread distribution to unwanted areas, endure metabolic attack, penetrate in adequate concentration to the site of action, and interact in a specific fashion, causing an alteration of cellular function. The absorption, distribution, biotransformation (metabolism), and elimination of the drug from the body are dynamic processes that continue from the time the drug is taken until the drug has been removed from the body (Ansel *et al.,* 1999).

A simplified diagram of this complex series of events between drug administration and its elimination is presented in Figure 1.3.
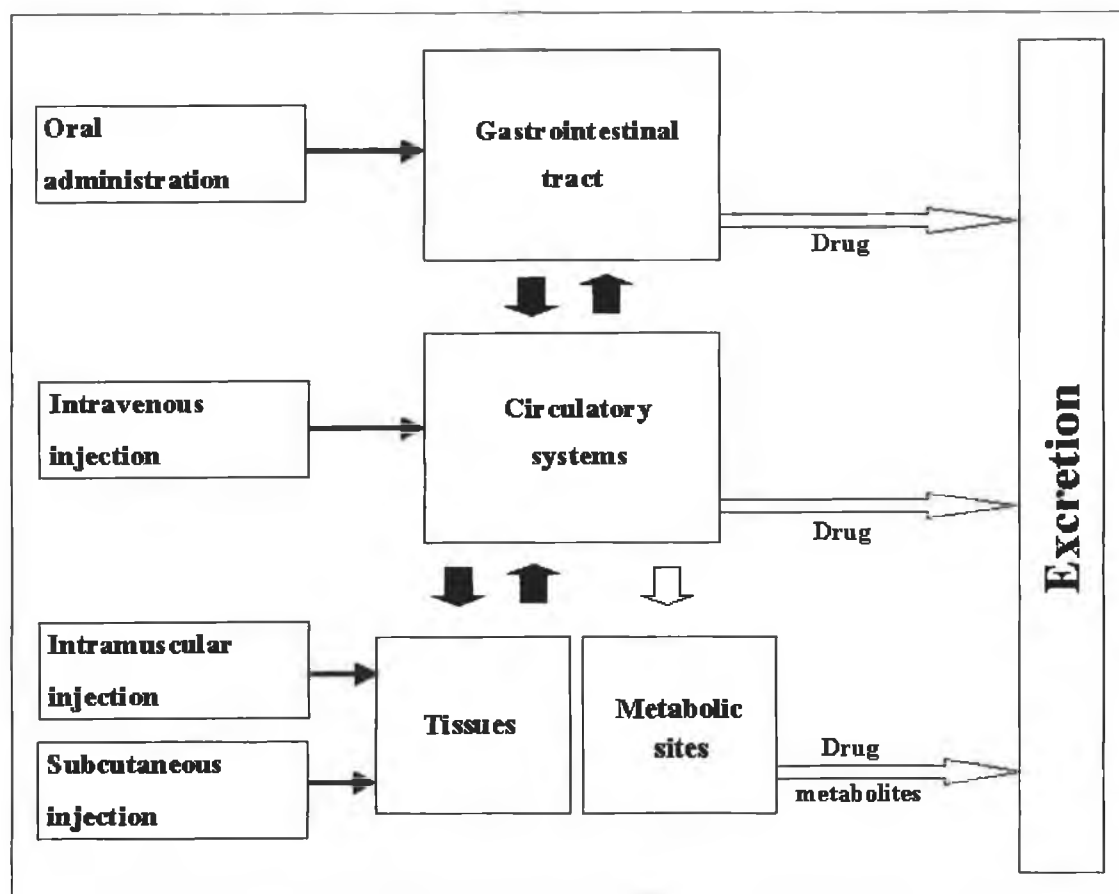
Figure 1.3: Schematic representation of events of absorption, metabolism, and excretion of drugs after their administration by various routes.

1.4.1. Absorption and Distribution

Absorption refers to the passage of a drug from its site of administration into the plasma. Following oral administration, coumarin is rapidly absorbed from the gastrointestinal tract and is distributed throughout the body (Lake, 1999). The ability of a compound to be absorbed well in the gastrointestinal tract following oral administration relies heavily on its physico-chemical characteristics.

Coumarin and 7-hydroxycoumarin are both poorly soluble in water (0.22 and 0.031 %, respectively). This characteristic is cause for concern with respect to their bioavailability *in vivo*, as 0.3% solubility in water is considered the critical value at which the distribution of a compound limits its rate of absorption. However, both compounds have high partition coefficients (21.5% for coumarin and 10.4% for 7-hydroxycoumarin), which is considered favourable for the rapid absorption of

8

compounds once they are in aqueous solution. This coupled with the fact that coumarin is non-polar, suggests that in theory coumarin should cross lipid bilayers easily by passive diffusion (Ritschel *et al.*, 1981; Pelkonen *et al.*, 1997).

In reality absorption from the gastro-intestinal tract (GIT) has been shown to be quite high, with most of the dose absorbed within an hour of administration. Pharmacokinetic studies in humans have demonstrated that coumarin is completely absorbed from the GIT after oral administration and extensively metabolised by the liver in the 1st pass with only between 2 and 6% reaching the systemic circulation intact (Lake, 1999). The low bioavailability of coumarin, in addition to its short half-life has brought into question its importance *in vivo* and it is now accepted that coumarin is a pro-drug, with 7-hydroxycoumarin being the compound of main therapeutic relevance. Once absorbed any active compound must be distributed via plasma to its target site (Rang & Dale, 1987).

At normal therapeutic plasma concentrations many drugs exist in the plasma mainly in the bound form. The fraction of drug that is free in aqueous solution can be as low as 1%, the remainder being associated with plasma protein. Ritschel *et al.* (1981) have shown that 35% of coumarin and 47% of 7-hydroxycoumarin bind plasma proteins. Availability of the compounds at their target tissues should not be problematic since the proportions that bound were well below the accepted critical value of 80% binding. Once a drug is administered and drug absorption begins, the drug does not remain in a single body location, but rather is distributed throughout the body until its ultimate elimination (Ansel *et al.*, 1999).

Coumarin has a short half-life *in vivo*, which is independent of the route of administration (1.02 hrs peroral v_s 0.8 hrs intravenous) as shown by Ritschel *et al.*, (1977). As mentioned previously, coumarin is rapidly metabolised to form 7-hydroxycoumarin, which quickly becomes conjugated as the glucuronide, such that concentrations of 7-hydroxycoumarin are always low and rarely exceed 2.2% of the levels of 7-hydroxycoumarin-glucuronide (Ritschel *et al.*, 1977).

The pharmacokinetics of coumarin were studied in a number of species including the rat, dog, gerbil, rhesus monkey and in man. Specific antibody recognition for its antigen is the basis for very selective and sensitive analytical methods, and has been exploited in numerous formats for the pharmacokinetic determination of coumarin and its derivatives. Immunoanalytical approaches have included ELISA-based methods for the detection of coumarin and 7-hydroxycoumarin in urine (Egan & O'Kennedy, 1993b). Antibody biosensors have also been employed, with either electrochemistry, or surface plasmon resonance (BIAcore) facilitating label-free detection of coumarin compounds in

various matrices (Dempsey *et al.*, 1993; Keating, 1998). Tests in animals, using radio-labelled coumarin, have demonstrated its distribution throughout the body to nearly all organs and tissues, and highlighted its accumulation in the liver and kidney. This information has proven useful in illustrating which species are appropriate animal models for studies on the toxicity and therapeutic relevance of coumarins (Lake, 1999).

1.4.2. Metabolism

Although some drugs are excreted from the body in their original form, many drugs undergo biotransformation prior to excretion. Biotransformation is the term used to indicate the chemical changes that occur with drugs within the body as they are metabolised and altered by various biochemical mechanisms (Ansel *et al.*, 1999). Traditionally coumarin was viewed by pharmacologists as the ideal model for studying the complex metabolism of a structurally simple organic molecule, and as such, its metabolic fate has been extensively researched (Shilling *et al.*, 1969; Moran *et al.*, 1987; Lake, 1999). Determining the metabolic fate of coumarin is important in order to utilise the fact it is metabolised at several sites and to access the possible dependence of coumarin-induced toxicity on metabolism (Pelkonen *et al.*, 1997).

The superfamily of cytochromes P450 (CYPs) consists of microsomal hemoproteins that catalyse the oxidative, peroxidative and reductive metabolism of a wide variety of endogenous and exogenous compounds. The CYP superfamily is divided into families and subfamilies according to their nucleotide sequence homology. Most biotransformations of xenobiotics (such as drugs) are performed by enzymes from the families CYP1, CYP2 and CYP3. The CYP2 family were examined using the rat, mouse and rabbit model systems. This family includes seven subfamilies in mammals. In humans, the most important CYPs regarding drug metabolism are CYP2A6, CYP2C9, CYP2C19, CYP2D6 and CYP2E1 (Taavitsainen, 2001).

Coumarin is metabolised initially by specific cytochrome P-450-linked mono-oxygenase enzyme (CYP2A6) system in liver microsomes, resulting in hydroxylation to form 7-hydroxycoumarin. After 7-hydroxylation, coumarin undergoes a phase II conjugation reaction resulting in a glucuronide conjugation associated with 7-hydroxycoumarin. The 7-hydroxylase activity is exceptionally high in human liver microsomes compared with its activity in the livers of other animal species. The activity of coumarin 3-hydroxylase is very high in rodent microsomes but is absent in human microsomes.

Although coumarin may be metabolised by hydroxylation at all six possible positions (i.e. carbon atoms 3, 4, 5, 6, 7, and 8.), the most common routes of hydroxylation are at positions 7 and 3 to yield 7-hydroxycoumarin and 3-hydroxycoumarin, respectively. Hydroxylation at carbon 3 results in further metabolism via ring opening, yielding two further products, *o*-hydroxyphenyllactic acid (*o*-HPLA) and *o*-hydroxyphenylacetic acid (*o*-HPAA) (Pelkonen *et al.,*1997; Lake, 1999). The expression of CYP enzymes (e.g. CYP2A6) varies between individuals due to genetic and environmental factors. These factors produce inter-individual variation in the metabolism of drugs such as coumarin. The frequency of poor metabolisers varies between species, races and ethnic groups. It has been shown that there exists large inter-species and inter-individual variability in the activity of these enzymes (Taavitsainen, 2001).

1.4.2.1. Metabolism in Man

The metabolism of coumarin has been investigated *in vivo* and *in vitro* in a wide range of species including humans. Human metabolic studies usually involve oral dosage followed by urine collection with or without timed fractionation (Egan & O'Kennedy, 1992; Bogan *et al.,* 1995). Analysis is by one of a number of techniques including spectrofluorimetry, HPLC and capillary electrophoresis (Rautio *et al.,*1992; Egan and O'Kennedy, 1993a; Bogan *et al.,* 1996). Human metabolic studies usually involve oral dosage followed by urine collection with or without timed fractionation. Recent *in vitro* systems employed include tissue slices, hepatocytes, subcellular fractions, and purified and cDNA-expressed enzymes (Lake, 1999). In the majority of human subjects studied coumarin is extensively metabolised to 7-hydroxycoumarin. Some data for various coumarin dose levels and collection periods are shown in Table 1.2. The measurement of urinary 7-hydroxycoumarin following an oral dose of coumarin has been employed as a biomarker of human hepatic CYP2A6, the cytochrome P-450 (CYP) isoform which is responsible for coumarin 7 hydroxylation in human liver (Pelkonen *et al.,* 1997). Some individuals can metabolise a considerable proportion of coumarin through pathways other that 7-hydroxylation. Humans can metabolise coumarin by the 3,4-epoxidation and other pathways to *o*-HPAA (Figure 1.4.).

Table 1.2: Extent of coumarin metabolism to 7-HC in various species. [a]Coumarin administered orally unless otherwise stated [b]Shilling et al. (1963). [c]Egan et al. (1990).

Species	Dose (mg/kg)[a]	Collection time (hr)	Urinary 7-HC (% of Dose)
Rat	100	890 or 120	0.4
Mouse	21. i.p.	22	25
Syrian Hamster	200	24	5
Squirrel Monkey	200	24	1
Baboon	200	24	60
Human	200mg/subject	24	[b]79 (range 68-92)
	200mg/subject	24	[c]63 (range 40-97)

In humans, there are three genes in the CYP2A subfamily, however, CYP2A6 is mainly of greater importance, as the other two gene products (CYP2A7 and CYP2A13) are either inactive or are not expressed in the liver. CYP2A6 codes the enzyme catalysing coumarin 7-hydroxylation (about 10% of total P450) (Pelkonen *et al.,* 2000). Recently, CYP2A6 was reported to be polymorphically expressed in the human liver. It was shown that CYP2A6 participates in metabolism of nicotine and its metabolite cotinine. Some drugs and chemicals, including coumarin which is widely used as a probe substance for CYP2A6 both *in vitro* and *in vivo*, are also metabolised by this enzyme (Pelkonen *et al.,* 1998). Substrates and inhibitors currently known to be metabolised by or interfere with CYP2A6 *in vitro* and *in vivo* have been summarised by Pelkonen *et al.,* (2000). Although 7-hydroxycoumarin is the main human metabolite, other hydroxylation pathways are important in humans and as such the therapeutic relevance of non-7-hydroxymetabolites should be examined rather than disregarded.

1.4.2.2. Metabolism in Other Species

Studies have examined the metabolism of coumarin and marked species differences have been reported. The extent of coumarin 7-hydroxylation appears to be species rather than dose dependent. Several species including the rat, most mouse strains, Syrian hamster, guinea pig, ferret, dog, marmoset and squirrel monkey appear to be poor 7-hydroxylators of coumarin excreting 5% or less of the administered dose of urinary 7-hydroxycoumarin. Fentem *et al.,* (1992) have indicated that coumarin 3,4-epoxide is the metabolic intermediate responsible for hepatotoxicity in the rat. Certain mouse strains, such as DBA/2 and 129/Rr strains, which have relatively high hepatic coumarin 7-hydroxylase activity, excrete up to 26% of an administered dose of coumarin as 7-hydroxycoumarin.

In a study by Gangolli *et al.*, (1974) the baboon has been reported to be an extensive 7-hydroxylator of coumarin with 60-66% of the dose being rapidly excreted in the urine as 7-hydroxycoumarin.
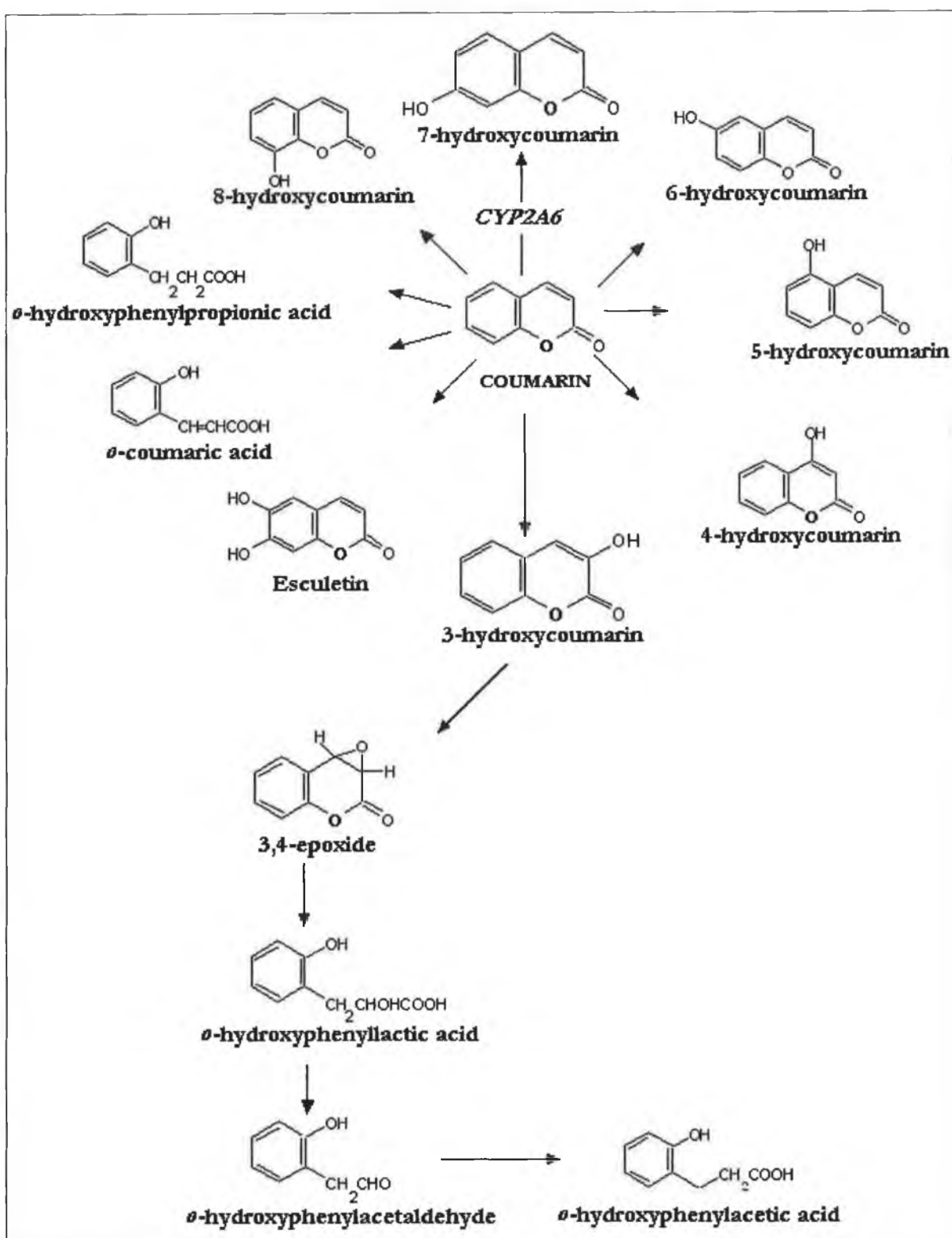
Figure 1.4: *Metabolism of coumarin. All biotransformations are possible, although the metabolism is species-specific.*

1.5. Toxicology

Since 1954, coumarin has been classified as a toxic substance by the FDA, following reports of its possible liver tumour-producing properties in rats (Byrden, 1996). The FDA banned its use, labelling as adulterated, all foods containing coumarin. Due to tests performed on rodents coumarin was referred to as a chemical carcinogen by NIOSH [National Institute for Occupational Safety and Health]. However, caution needs to be taken in extrapolating this information to human situations. Various tests (Ames, micronucleus) have shown that coumarin and its metabolites are non-mutagenic (Egan *et al.*, 1990). Preliminary results from early studies indicated that coumarin was a toxin, but it was shown since, that the rat is a poor model to compare with the human for this particular metabolic process (Deasy, 1996). A number of studies have examined the acute, chronic and carcinogenic effects of coumarin in the rat and mouse. In studies involving the rat, hepatic biochemical and morphological changes have been examined for various periods of coumarin administration (1 week to 2 years). Depending on dose administered, coumarin treatment results in an increase in relative weight and changes in various hepatic biochemical parameters. Single oral doses of coumarin were shown to produce liver necrosis and increase plasma transaminase activities in DBA/2 strain mice (Lake, 1999).

In contrast, studies involving baboons, syrian hamsters and certain mice strains seem to be resistant to acute coumarin-induced hepatotoxicity. Species differences in coumarin-induced toxicity *in vitro* were investigated in cultured hepatocytes. These studies provide evidence for species differences in coumarin-induced toxicity *in vitro*. The relative resistance of human and cynomolgus monkey liver slices and/or hepatocytes to coumarin toxicity correlates with coumarin 7-hydroxylation, the major pathway of coumarin metabolism in these species, being a detoxification pathway of coumarin metabolism. However, while coumarin-7-hydroxylation pathway is a detoxification pathway this does not appear to be the only explanation for resistance of a species to coumarin-induced toxicity. In the rat coumarin-induced hepatotoxicity appears to be partially attributable to the excretion of coumarin metabolites in the bile. This may result in enterohepatic circulation enhancing the exposure of liver cells to toxic coumarin metabolites. Species such as syrian hamster, baboon, and humans excrete coumarin metabolites primarily in urine. Low-level exposure to coumarin from diet and from fragrances used in cosmetic products would not be expected to produce any hepatotoxicity even in individuals with deficient 7-hydroxylase activity (Pelkonen *et al.*, 1997, Lake, 1999).

1.6. Applications of Coumarin and Coumarin Derivatives

The coumarins are of great interest due to their biological properties. In particular, their physiological, bacteriostatic and anti-tumour activity makes these compounds attractive for further backbone derivatisation and screening as novel therapeutic agents. Weber *et al.*, (1998) have shown that coumarin and its metabolite 7-hydroxycoumarin have antitumour activity against several human tumour cell lines. Both coumarin and coumarin derivatives have shown promise as potential inhibitors of cellular proliferation in various carcinoma cell lines (Egan *et al.*, 1997; Cooke, 1999; Cooke & O'Kennedy, 1999). In addition it has been shown that 4-hydroxycoumarin and 7-hydroxycoumarin inhibited cell proliferation in a gastric carcinoma cell line (Budzisz *et al.*, 2003).

1.6.1. Simple Coumarins

Coumarins and the benzopyrones are representative of a very diverse and potentially useful groups of drugs.

1.6.1.1. Industrial Uses

Coumarin has many uses in industry, mainly due to its strong fragrant odour (Egan *et al.*, 1993). It is applied in a variety of industrial settings, the most important being the perfumery industry. Coumarin is used as a fixative and enhancing agent in perfumes and is added to toilet soap and detergents, toothpaste, tobacco products and some alcoholic beverages. Large quantities are used in rubber and plastic materials and in paints and sprays to neutralise unpleasant odours. It is evident that coumarins are of analytical importance and are utilised as dyes, labels and derivatising agents. Coumarin heterocycles that are substituted in the 7-position with an amine function (azole coumarins) constitute an important class of fluorescent materials (Jones, 1999). Coumarin of the azole type may find use as fluoroprobes of the microenvironment of proteins and other biological macromolecules and as agents for pH sensing (Jones, 2001). The coumarin family of compounds have found widespread use in many analytical applications, resulting from their natural fluorescence. These compounds have found application as laser dyes, labelling agents and in enzyme assays where fluorescence is required (Cooke *et al.*, 1997).

Work by Luo *et al.*, (2001) involved synthesis of coumarins containing N-alkylsulfonamide groups built into benzoxazolyl, benzothiazolyl, or benzimidazolyl systems. These were then reacted

16

with NaCN to give fluorescent red compounds. Results from a determination of the spectral properties and dyeing characteristics of these new dyes suggest that they are potential commercial solvent dyes. Ishibashi *et al.,* (2000) have applied fluorescence techniques to the detection of ˙OH formed on a photo-illuminated surface using coumarin, which readily reacts with ˙OH to produce highly fluorescent products. This method has been used in radiation chemistry, sonochemistry and biochemistry for the detection of ˙OH generation in water.

1.6.1.2. Clinical Uses

Due to its biochemical properties coumarin has been proposed for use in clinical medicine. It was evaluated for the treatment of various clinical conditions, resulting in the employment of a variety of dosing regimens. Recommended doses range from 8mg for the treatment of venous constriction to 7000mg/day in anti-neoplastic therapies.

1.6.1.2.1. High Protein Oedema (HPO)

The lymph system is responsible for drainage of interstitial fluid within human tissues. If excess fluid is present, as a result of injury or lymph vessel blockage, the transport capacity of the lymph system is compromised, and oedema (swelling of tissue) develops. There are numerous detrimental effects of oedemas to the patient as often there is extensive injury to blood vessels, with fibrin deposition and fibrosis common effects. The oedema interferes with the metabolism of the tissue cells and reduces oxygen transport, resulting in problematic wound healing (Casley-Smith & Casley-Smith, 1986). In the case of high protein oedemas (HPO), there is an accumulation of protein in the tissue following trauma or inflammation, with resulting permeability of the capillaries causing water leakage in the tissue spaces. Many disease states are associated with high protein oedemas, ranging from extremely severe and chronic (*e.g.* lymphoedema and elephantiasis) through more common and acute forms (*e.g.* burns, accidental and surgical traumas). All forms have been shown to benefit from benzopyrone treatment (Casley-Smith & Casley-Smith, 1997).

Coumarin and numerous other benzopyrones have been tested in high protein oedema, and all have been shown to successfully reduce the swelling. The objective of a recent study was to evaluate the oedema-protective effect of a combination vasoactive drug, coumarin/troxerutin (SB-LOT) plus compression stockings in patients suffering from chronic venous insufficiency after decongestion of the legs as recommended by the new guidelines. The study confirms the oedema-protective effect of SB-LOT in chronic venous insufficiency and provides a treatment option for patients who discontinue

17

compression after a short time (Vanscheidt *et al.*, 2002). In addition to laboratory-based work, Casley-Smiths team has been very closely involved with many clinical investigations. All trials have shown that coumarin either alone, or in combination with other benzopyrones, leads to both objective (circumference and volume), and subjective (tension, heaviness, fullness, pain) improvement, and has lead to the introduction of coumarin as a lymphoedema treatment in a number of western and developing countries.

1.6.1.2.2. Chronic Infections

In addition to its stimulatory effect on macrophages, coumarin has been shown to activate other cells of the immune system. Hence, coumarin has been used clinically to treat chronic infections such as brucellosis (Thornes, 1983). In chronic brucellosis *Brucella abortis* infects macrophages, thus eluding the immune response. When immunostimulatory drugs such as coumarin are administered, the symptoms of chronic brucellosis disappear. Coumarin was found by Thornes (1983) to be the most effective and least toxic immunostimulant. It was also effective at augmenting and maintaining IgA levels (normally suppressed in chronic brucellosis) and restoring delayed hypersensitivity reactions. These results have encouraged the use of coumarin in other chronic infections such as mononucleosis, mycoplasmosis, toxoplasmosis and Q fever.

A new antiplasmodial coumarin has been isolated from the roots of *Toddalia asiatica*. This finding supports the traditional use of this plant for the treatment of malaria (Oketch-Rabah, 2000).

1.6.1.3. Coumarins in Cancer

The modern era of cancer chemotherapy began in the late 1940s with the demonstration that the nitrogen mustards showed anti-cancer activity in malignant lymphoma. At about the same time the coumarins were chemically described as a group of natural compounds, present in a wide variety of vegetables and fruits. Over time research has indicated that the coumarins may be clinically important in the treatment and maintenance of cancer patients.

Anti-cancer drugs have traditionally been targeted to damage the aberrantly dividing cell by interrupting the cell division process (Carter *et al.*, 1989). Reagents used include DNA intercalating agents (*e.g.* adriamycin), DNA cross-linking agents (*e.g.* cis-platin), topoisomerase inhibitors (*e.g.* campothecins), cytoskeleton-disrupting agents (*e.g.* vinblastin) and anti-metabolites (*e.g.* mercaptopurine). These drugs though effective, are cytotoxic, and thus exhibit severe side effects,

particularly on normal proliferating tissues such as the haematopoietic system. Often combination therapies, whereby several cytotoxic agents are combined in the treatment regime, offer better results with fewer toxic side-effects, as they are carefully regulated to allow recovery of normal, but not malignant cells, from drug exposure (Carter *et al.*, 1989).

Currently, chemotherapy, radiotherapy and surgery combined offer the best outcomes for cancer patients, and treatment combinations were successfully applied to particular cancer types, for example, Hodgkin's lymphoma, testicular cancer and various leukaemias. Coumarins can be used not only to treat cancer but to treat the side effects caused by radiotherapy. A recent study investigated the efficacy of coumarin/troxerutine combination therapy for the protection of salivary glands and mucosa in patients undergoing head and neck radiotherapy. The results suggest that coumarin/troxerutine have a favourable effect in the treatment of radiogenic sialadentis and mucositis (Grotz *et al.*, 2001).

The interest in coumarin and 7-hydroxycoumarin as anti-cancer agents, arose from reports (Section 1.6.1.3.1 – 1.6.1.3.3.) that these agents had achieved objective responses in some patients with advanced malignancies. To date, the particular mode of action of these agents in cancer cells is obscure, although various possibilities have been hypothesised, and these are outlined in the following sections. While a significant amount of research regarding the clinical applications of the benzopyrones has been reported it is important to emphasise that only the 'warfarin-type' anticoagulants belong to mainstream pharmacotherapy. Other types of coumarin compounds are either at the experimental or early clinical trial phase. Hence, additional studies on the elucidation of their mechanism of action are necessary to facilitate a greater understanding of these compounds if they are to have future clinical applications.

1.6.1.3.1. Coumarin in Malignant Melanoma

Early diagnosis of malignant melanoma facilitates surgical removal of the primary lesion and achieves a good prognosis. However, if the lesion progresses, the risk of recurrence becomes serious and represents a major challenge to the oncologist, as no satisfactory treatment for recurrent malignant melanoma currently exists. Studies have shown that five years after removal of the primary lesion, the recurrence of malignant melanoma is observed in 55-80% of high risk patients (Wcislo & Szczylik, 2003).

Original work with coumarin derivatives in the treatment of melanoma focused on the use of warfarin as a maintenance therapy. This compound was known to inhibit tumour spread, and to

stimulate granulocytes, lymphocytes and macrophages (Thornes *et al.,* 1968). In 1980, Maat illustrated that the decrease in tumour metastases due to warfarin was macrophage-dependent. This data prompted Thornes to assess the potential application of coumarin, the parent compound of warfarin, as an adjuvant therapy in melanoma. Like warfarin, the *in vivo* actions of coumarin were known to be macrophage-derived. Coumarin was non-toxic and conveniently administered, it had no anti-coagulant activity, and a previous administration resulted in subjective improvement in cancer patients (Thornes, 1997).

Coumarin was first compared to warfarin in a small-scale trial on patients with stage I and stage II melanomas after primary resection. Five patients were anti-coagulated with warfarin and six were given 25mg coumarin daily. During the first year, coumarin matched warfarin in its therapeutic effectiveness, with one patient in each group recurring (Thornes, 1993). In 1984, a placebo-controlled, randomised, double-blind trial (50mg coumarin alone, daily for 2 years) was established, with twenty-seven patients admitted. All patients were treated with standard surgical excision of the melanoma lesions prior to coumarin treatment. In 1987 the trial results were published, and showed 10 recurrences in the control (N=14), but only 2 in the treated group (N=13). Since the trial termination, two more patients in the treated group have recurred, at two and four years (Thornes, 1997).

Only one further trial in melanoma patients has yielded results: an open trial in Australia found a dosage of 300mg of coumarin daily to be of no benefit to treated patients (Thornes, 1997). Thornes has continuously stated the importance of optimal dosing in the establishment of trials, believing that high doses of coumarin may inhibit rather than stimulate the immune system. Such a hypothesis may explain these conflicting results, but it is evident that further dosing trials are required to determine the real benefit of coumarin in malignant melanoma therapy. A more recent study by Velasco-Velazquez *et al.,* (2003) determined the *in vitro* effects of 4-hydroxycoumarin (4-HC) employing the murine melanoma cell line B16-F10 and the non-malignant fibroblastic cell line B82. 4-HC disorganized the actin cytoskeleton in B16-F10 cells, but not in B82 fibroblasts. Adhesion of tumour cells to extracellular matrix is required during the metastatic process, therefore, 4-HC might be useful as an adjuvant therapy for melanoma.

1.6.1.3.2. Coumarin in Renal Cell Carcinoma

The clinical course of renal cell carcinoma (RCC) has been well documented, with long-lasting stable periods and rapid tumour growth its principal features. Surgery remains the standard care for patients whose tumour is confined to the kidney. However, many of these patients develop recurrent or metastatic disease within months, where the lungs, liver and bones are the common sites of secondary occurrence (Ebbinghaus *et al.,* 1997). RCC is characterized by a lack of early warning signs, resulting in a high proportion of patients with metastases at the time of diagnosis or relapse following nephrectomy. Despite extensive investigations with many different treatment modalities, metastatic RCC remains a disease highly resistant to systemic therapy. The outlook for patients with metastatic RCC is poor, with a 5-year survival rate of less than 10% (Vuky *et al.,* 2000).

Interest in the coumarin family of compounds stemmed from reports by Thornes, of the immunomodulatory activity of coumarin and its utility in malignant melanoma (Thornes, 1982). The clinical activity of coumarin in renal cell carcinoma patients was investigated by applying a treatment regime courtesy of Thornes [coumarin at 100mg/day oral dosage, with the addition of cimetidine 4 X 300mgs/day from day 15]. This preliminary study yielded some interesting results, with 14 objective results among 45 patients with metastatic RCC, and almost no toxic side effects. Validation of this anti-tumour activity was further demonstrated by other investigators (Dexeus *et al.,* 1990; Kokron *et al.,* 1991).

Following this success, it became clear that additional information regarding doses and toxicity's was required, and Marshall and colleagues implemented a phase I trial to define the maximally tolerated dose, and dose-limiting toxicity's of coumarin and cimetidine. 54 patients with a variety of advanced malignancies were admitted to this trial, with 3 patients each, given one coumarin dose in the range 400mg-7000mg. Coumarin was administered as a single, oral dose continuously during the trial, with cimetidine [4 doses of 300mg daily] added to the dosage regime on day 15. All coumarin doses were well tolerated, with the most common side effect of nausea attributable to the intense aroma of coumarin. Objective responses were observed in 7 patients, all with renal cell carcinoma, these responses being observed across a range of coumarin doses [600-5000mgs] (Marshall *et al.,* 1991).

In vitro cytotoxic potential and mechanism of action of selected coumarins (coumarin, 7-hydroxycoumarin, esculetin and nitro-coumarins) using renal cell lines were investigated recently (Finn *et al.,* 2002). The results obtained suggest that the nitro-coumarin (6-Nitro-7-hydroxycoumarin)

21

and daphnetin (7,8-dihydroxycoumarin) examined may merit further investigation in relation to renal cell carcinoma.

1.6.1.3.3. Coumarin in Prostate Cancer

Prostate cancer is the most common invasive malignancy in males and is characterised by a very slow growth rate and a wide biological variability, especially with regard to hormonal sensitivity (Bosland, 1991; Agarwal, 2000). These two traits have curbed attempts at curative treatments for patients, as most effective chemotherapeutic drugs rely on fast growth kinetics in the tumour mass. At present, early detection, and removal of clinically significant tumours by surgery or radiation, has been the focus of therapeutic strategies. However, patient survival is dependent on metastases where principal metastatic sites are regional lymph nodes and bone. Eventually, almost every prostate carcinoma that initially regressed on androgen deprivation will relapse into a hormonal-insensitive state and grow in the absence of androgen. Evidently, better therapeutic approaches to control both metastases and hormone-insensitive prostate carcinomas are required.

Coumarin had previously appeared to exert immunomodulating effects in other cancers, hence, a small-scale study to test the efficacy of coumarin in prostate cancer was set up (Marshall *et al.*, 1990). 14 patients received a single oral dose of 100mg coumarin daily continuously during the trial, with 300mg of cimetidine 4 times daily added to the regime from day 15 onwards. Both drugs were continued until disease progression was observed. No objective responses were observed, but a significant subjective improvement in bone pain was noted in patients, which prompted further studies. A phase I trial involving 40 patients with metastatic, hormone-naïve or hormone-refractory prostatic cancer was conducted (Mohler *et al.*, 1992). Participants were administered 3g of coumarin daily, and evaluated for toxicity and anti-tumour responses. 3 partial responses occurred, all in-patients with low tumour loads. One responder remained with 3 responsive bone metastases and stable prostate specific antigen (PSA) levels for 7 years following the trial. Myers *et al.*, (1994) examined the effects of various concentrations (0-500 µg/ml) of coumarin on the proliferation of two renal cell carcinoma cell lines (786-O and A-498) and two malignant prostatic cell lines (DU145 and LNCaP). After 5 days of treatment, coumarin inhibited the growth of the four cell lines. The LNCaP prostatic cell line was most sensitive to the inhibitory effects of coumarin.

1.6.1.4. Other Simple Coumarins

1.6.1.4.1. Cloricromene

Cloricromene is a coumarin derivative (8-monochloro-3-β-diethylaminoethyl-4-methyl-7-ethoxy-carbonylmethoxy coumarin) with beneficial effects on splanchnic, hemorrhagic and endotoxic shock. The drug is semi-synthetic with anti-platelet and anti-leukocyte properties, it inhibits tumour necrosis factor-α (TNF-α) and prevents the expression of inducible nitric oxide synthase [iNOS protein] (Zingarelli *et al.,* 1993; Maltese & Bucolo, 2002). Previous work has shown that cloricromene modifies several granulocyte as well as monocyte/macrophage functions, which explains at least in part its protective action in ischemia (Zatta & Bevilacqua., 1999). It decreases superoxide anion production, inhibits chemotaxis of polymorphonuclear cells, reduces levels of platelet-activating factor, and leukotriene B_4 and decreases the release of arachidonic acid by interfering with phospholipase A_2 activation. Cloricromene decreases myocardial infarct size after ischemic-reperfusion injury *in vivo*, and it has been suggested that this is due to inhibition of TNF-α. It was established that cloricromene inhibts lipopolysaccharide-induced cellular oxidative activity, which is important for nuclear factor-κB (NF-κB) activation. Cloricromene interferes with early signal transduction pathway triggered by lipopolysaccharide (Corsini *et al.,* 2001). A rapid and simple method was developed for the simultaneous separation and quantification of cloricromene and its active metabolite cloricromene acid, in rabbit aqueous humor. The assay provided good reproducibility and accuracy for both analytes and proved suitable for pharmacokinetic studies of cloricromene (Maltese & Bucolo, 2002).

1.6.1.4.2 Daphnetin

Aerial parts of *Daphne oleoides* are used to treat rheumatoid arthritis and lumbago in Turkish folk medicine. 17 compounds were isolated and their structures were elucidated. Daphnetin showed potent *in vitro* inhibitory activity on inflammatory cytokines such as interlukin-1 and TNF-α (Ullah *et al.,* 1999; Yeilada *et al.,* 2001). Protein kinases play key roles in the control of cell proliferation, differentiation and metabolism. The effect of coumarin and its derivatives, including daphnetin, esculin, 2-hydroxycoumarin (2-OH-coumarin), 4-hydroxycoumarin (4-OH-coumarin) and 7-hydroxycoumarin, on the activity of protein kinases was investigated by Yang and co-workers (1999). Only daphnetin was reported to be a protein kinase inhibitor. This compound inhibited tyrosine specific protein kinase, EGF-R and serine/threonine-specific protein kinases, including cAMP-dependent protein kinase (PKA) and protein kinase C *in vitro*. The structural comparison of daphnetin

with coumarin and other coumarin derivatives suggests that the hydroxylation at C8 may be required for daphnetin to act as a protein tyrosine kinase inhibitor. Recently two new coumarin glycosides along with two known coumarin glycosides, daphnetin glucoside and daphnin were isolated from the aerial parts of *Cruciata taurica*. It is possible that these new compounds will have important clinical applications (De Rosa *et al.,* 2002).

1.6.1.4.3. Scoparone

Scoparone (6,7-dimethoxycoumarin), is a known anti-asthmatic coumarin derivative extracted from the traditional Chinese herb *Artemisia capillaries herba*. Broncial asthma is a chronic inflammatory disease of the airways with obscure etiologies. It has been documented that elevations in intracellular calcium ion concentration is the main reason for contraction of the bronchi and increased sensitivity to bronchi sensitizers. Scoparone has been reported to directly reduce intracellular calcium ion concentrations in isolated guinea-pig tracheal smooth muscle. These *in vivo* and *in vitro* pharmacological experiments indicate that scoparone exerts strong anti-asthma action, along with both prophylactic and therapeutic properties for the treatment of asthma (Liu *et al.,* 2002). In order to elucidate the clinical effects of scoparone, it is necessary to clarify its pharmacokinetics, especially species-specific differences in pharmacokinetics among various animal models, and then to compare this data to those from human studies. Therefore, the pharmacokinetics of scoparone was determined in rabbit plasma by HPLC. Distribution and elimination of this compound in rabbit plasma were both relatively rapid. These results indicate that scoparone could be easily administered by spray inhalers with few associated side effects expected (Fang *et al.,* 2003).

In organ transplantation, the ischemic injury during cold preservation is a most challenging problem, especially in liver transplantation. Scoparone antioxidant effects can be utilised in cold-preserved hepatocytes where it is used as an additive to preservation solutions or as an agent given to the recipient to reduce ischemic injury (Cho *et al.,* 2000). Scoparone has other important therapeutic properties which include its ability to act as a vasodilator on rat aortic rings precontracted with phenylephrine (Huang *et al.,* 1992). It was reported to exhibit immunosuppressive effects on human peripheral blood mononuclear cells (IL-1, IL-2 production and IL-2 receptor expression were reduced in presence of scoparone). Immunosuppressive effect may be due to inhibition of protein tyrosine kinase and release of arachidonic acid metabolites. Differential oxidation of scoparone can be used as a sensitive indicator for distinguishing between different cytochrome P450 isoforms. Regioselective 7-demethylation of scoparone is regularly employed as an indicator of Phenobarbital-like induction of

24

rat liver cytochrome P450 isoform CYP2B1, e.g. by the antiepileptic drug phenytoin (Meyer *et al.*, 2001).

1.6.1.4.4. Osthole

Osthole (7-methoxy-8-[3-methylpent-2-enyl] coumarin), is a coumarin compound isolated from medicinal plants, such as *Cnidium monnieri* and *Angelica pubescens*. It possess a variety of pharmacological and biochemical properties, and is considered to have potential therapeutic applications (Okamoto *et al.*, 2003). It has both anti-inflammatory and analgesic activities and has been reported to inhibit platelet aggregation and suppresses thromboxane formation and breakdown of phosphoinositides (Wu *et al.*, 2002). Osthole also exhibits vasorelaxant action by elevation of cGMP levels of vascular smooth muscle and inhibition of calcium influx (Ko *et al.*, 1992; Tsai *et al.*, 1996). It has also been reported to have an antiproliferative effect on vascular smooth muscle cells. The antiproliferative effect occurs at the early G_1 phase of the cell cycle and is due to the increase in cyclic AMP and cyclic GMP contents. Abnormal VSMC proliferation is a major component of vascular disease, including atherosclerosis, vein graft occlusion and re-stenosis following angioplasty. An important therapeutic aim is to inhibit VSMC proliferation without interfering with endothelial repairs (Guh *et al.*, 1996).

Fas ligand is a major inducer of apoptosis, and Fas-mediated apoptosis is involved in the development of various diseases such as hepatitis. Fas and Fas ligand are expressed in the livers of hepatitis C virus (HCV)-induced chronic hepatitis. This Fas system plays a major role in the development of apoptosis in virus-induced chronic hepatitis. Recently, it has been indicated that normalisation of alanine aminotransferase (ALT) prevents the development of hepatocellular carcinoma (HCC) in HCV-induced chronic hepatitis. Thus, inhibition of Fas-mediated liver injury leads to preventing the development of HCC in virus-induced hepatitis. The effect of osthole on hepatitis induced by anti-Fas antibody in mice was studied. Pretreatment of mice with osthole prevented the elevation of plasma ALT caused by anti-Fas antibody. The results indicated that osthole prevented anti-Fas antibody-induced hepatitis by inhibiting the Fas-mediated apoptotic pathway (Okamoto *et al.*, 2003).

1.6.2. Applications of the Furanocoumarins

As stated in Section 1.2. there are four main coumarin subtypes the simple coumarins, furanocoumarins, pyranocoumarins and pyrone-substituted coumarins. The furanocoumarins are a

therapeutically important subtype as they have various significant clinical applications. The furanocoumarins consist of a 5-membered furan ring attached to a benzene ring. Two of the most important and well known furanocoumarins are Psoralen (Linear) and Angelicin (Angular). The terms linear and angular refer to the orientation of the furan ring with respect to the coumarin nucleus (Keating & O'Kennedy, 1997).

The linear furanocoumarins (or psoralens) are naturally occurring plant biosynthetic metabolites that have been used since ancient times in skin photochemotherapy to treat a number of skin disorders including mycosis fungoides, psoriasis and vitiligo (Diawara *et al.*, 1997). Most psoralens have strong absorption bands in the range 200-350 nm, with lower absorbances towards the visible region of the spectrum. Their planar aromatic structure and hydrophobic nature facilitate their intercalation with DNA bases. Purified 8-methoxypsoralen (8-MOP) has been used for over 50 years for treatment of vitiligo. It was determined that artificial long wavelength ultraviolet (UVA) radiation was the most efficient for activating 8-MOP. This photochemotherapy became known as PUVA (psoralen & UVA). The therapy met with unprecedented success from the outset, leaving little perceived need to understand the underlying science. However, in recent years there has been a new found interest in the basic aspects of psoralen photobiology and molecular mechanistic events contributing to therapeutic responses as well as to the development of skin cancers in PUVA patients (Bethea *et al.*, 1999).

Psoralens have recently found application in the regulation of human cervical carcinoma cell proliferation in conjunction with anti-sense technology (Murakami *et al.*, 2001). Oligonucleotides and their analogs have been used to inhibit protein biosynthesis by suppressing the gene expression in a sequence specific manner. The method is called antisense strategy and has been applied to gene therapy for incurable diseases such as cancers and viral infections. Among various reports regarding antisense technology, many have presented clear evidence that the antisense mechanism participated in the regulation of cell growth. Some of the antiproliferative effects of oligo(nucleoside phosphorothioate)s (S-oligo) may be attributed to the interaction of S-oligo with certain proteins such as growth factors. Upon UVA irradiation psoralen derivatives have the ability to crosslink covalently with pyrimidine bases (e.g. thymine and uracil). As psoralen derivatives can inactivate gene expression via cross-linking, they were conjugated with oligonucleotides to reinforce antisense effects. During *in vitro* experiments psoralen-conjugated S-oligos have shown resistance to nucleases and, therefore, have exhibited significant inhibitory effects upon UVA irradiation. Psoralen-conjugated S-oligos (Ps-S-oligo) were prepared and used to inhibit the proliferation of human cervical carcinoma cells. Upon UVA irradiation of Ps-S-oligo treated cells, Ps-S-oligo complementary to the initiation

codon region (Ps-P-As) of human papillomavirus (HPV)18-E6*-mRNA of human cervical carcinoma cells significantly inhibited proliferation. The E6* protein is tightly correlated with the transformation of human cervical cells and, therefore, its suppression may regulate cellular proliferation. The psoralen-conjugated antisense DNA has significant potential to regulate gene expression, which may provide useful information to explore novel gene regulating agents (Murakami *et al.*, 2001).

Angelicin is a naturally occurring furanocoumarin that shows anti-fungal activity. A broad range of opportunistic pathogenic fungi are making their appearance in the medical scene. *Candida* is now ranked at the third most common causative agent of blood stream infections in most hospitals. There are many anti-fungal compounds of plant origin. These compounds can be constitutive and are present in plant tissues most of the time or they can be induced so that they are produced only in special circumstances such as infection. Coumarins can be classified in the latter group. Anti-fungal activities of the synthesised coumarins and angelicin derivatives have been reported against *Candida albicans, Cryptococcus neoformans, Saccharomyces cerevisiae* and *Aspergillus niger.* The development of azoles has transformed the treatment of many fungal infections, however, treatment can often necessitate application of highly toxic drugs such as amphotericin B. Therefore, it is desirable to develop natural antifungals with low toxic side effects. Toxicity of several coumarins was evaluated against KB cells derived from human carcinoma of the nasopharynx. Angelicin and several potent antifungals were found to be non-toxic in this assay (Sardari *et al.*, 1999).

Nitric oxide (NO) is synthesised from l-arginine by constitutive and inducible nitric oxide synthase (cNOS and iNOS) in numerous mammalian cells and tissues. Inducible NOS is an important pharmaceutical target in inflammatory and mutagenesis research. Therefore, inhibition of NO production by iNOS may have potential therapeutic value when related to inflammation and septic shock. NO is known to cause mutagenesis and deamination of DNA bases, and to play an important role in the formation of carcinogenic N-nitroso compounds *in vivo*. Chronic inflammation of the colon increases the risk of colorectal cancer in rats. On the basis of this evidence, iNOS inhibition has become a new approach for cancer chemoprevention. Various naturally occurring furanocoumarins such as angelicin, pimpinellin and sphondin have shown iNOS inhibition in lipopolysaccharide-activated macrophage cells (Wang *et al.*, 2000).

27

1.6.3. Applications of the Pyranocoumarins

Plant materials have a long history of being successfully used in the treatment of cancer, both as chemotherapeutic agents and as complementary treatments. The pyrano-coumarin compound ($\pm$)-3-angeloyl-4-acetoxy-cis-khel-lactone was isolated from *Radix peucedani*, a herb well-known for the treatment of respiratory diseases and pulmonary hypertension. Resistance of cancer cells to chemotherapeutic agents remains one of the major obstacles in achieving an effective treatment for cancer. The molecular mechanism of multi-drug resistance (MDR) in cancer cells may involve over-expression of membrane drug efflux pumps, p53 mutations, and up-regulation of bcl-2, DNA repair or cellular detoxification enzymes. P-glycoprotein is over-expressed in various MDR cell lines and functions as an ATP-dependent drug efflux pump that rapidly extrudes anti-tumour drugs from target cancer cells, which prevents the drugs from exerting their cytotoxic effects. ($\pm$)-3-angeloyl-4-acetoxy-cis-khel-lactone is a P-glycoprotein inhibitor and studies were recently performed to determine its effect on MDR cell lines. Work by Wu and co-workers (2003) demonstrated that this pyranocoumarin causes apoptotic cell death for drug sensitive KB-3-1 and multidrug resistant KB-V1 cancer cell lines. Strong synergistic interactions were demonstrated when the pyranocoumarin was combined with common anti-tumour drugs such as vincristine, doxorubicin and paclitaxel. The results suggest that pyranocoumarins could be a potential MDR reversing agent (Wu *et al.*, 2003). Some pyranocoumarins isolated from *Calaphyllum* species have been shown to inhibit HIV-1 replication and cytopathicity through their interaction with HIV-1 reverse transcriptase. Pyranocoumarins may provide a new class of anti-HIV compounds (Dharmaratne *et al.*, 1998).

1.6.4. Applications of Other Coumarin Derivatives

Synthesis of many 4-(aryloxymethyl) coumarins and 3-heteroaryl-coumarins as anti-microbial and anti-inflammatory agents were recently reported by Ghate and colleagues (2003). Vanillins have been found to exhibit anti-microbial properties. It was therefore, of interest to react 4-(bromomethyl)-coumarins with vanillins to obtain the corresponding ethers. The ethers were then converted to the corresponding 4-(2-benzo[b]-furanyl) coumarins by intramolecular aldol condensation. Eight compounds were screened for their anti-inflammatory activity. 5,6-benzo-4,2-benzo[b]-furanyl coumarin was the most active anti-inflammatory compound among those tested (Ghate *et al.*, 2003).

Serine proteases play an important role in numerous physiological processes and are also involved in pathological states. Among these proteases, human leukocyte elastase (HLE) has the ability to degrade various structural proteins and has been implicated as a causative factor in

emphysema, chronic bronchitis, acute respiratory distress syndrome, cystic fibrosis and arthritis. Thrombosis is one of the leading single cause of morbidity and mortality in developed countries. The most widely studied target for antithrombotic intervention has been the serine protease thrombin. A new series of coumarins have been developed which target serine proteases such as HLE and thrombin. 6-Chloromethylcoumarin derivatives are known serine protease inhibitors. Mass spectrometry was used to confirm a previously postulated inhibition mechanism for these coumarin derivatives. The results demonstrated that the serine protease inhibition resulted from a nucleophilic attack on the intracyclic carbonyl group (Pochet *et al.*, 2003).

The 4-(1-piperazinyl)coumarins were evaluated *in vitro* to determine their inhibitory properties towards human platelet aggregation induced in platelet-rich plasma by ADP, collagen or the calcium ionophore A23187. The results indicated that these coumarin derivatives showed high activity as *in vitro* anti-platelet agents (Roma *et al.*, 2003).

Atherosclerotic cardiovascular disease is the leading cause of death in developed countries. Current therapies mostly focus on lowering LDL-cholesterol (a risk factor) and statins used for this purpose are quite effective and safe. However, most patients still experience adverse coronary events despite statin therapy. Coumarins are known to have anti-oxidant potential and it was demonstrated that a 2-ethoxy-3-propanoic acid coumarin derivative can lower blood glucose levels in animal models. Coumarin derivatives of different heterocycles were designed based on cyclisation of 2-ethoxy-3-phenylpropanoic acid and 2-benzylmalonic acid as novel lipid-lowering agents and their preliminary *in vivo* screening indicates one of the novel coumarin derivatives has moderate triglyceride-lowering activity (Madhavan *et al.*, 2003).

1.7. Pyrone-Substituted Coumarins: Warfarin

The previous sections in this introduction deal with the simple coumarins, pyranocoumarins and furanocoumarins. However, a significant amount of work was carried out on warfarin, a pyrone-substituted coumarin (Chapter 3 & 5). It has anti-coagulant properties, which will be described separately from the other coumarins.

1.7.1. Introduction to Warfarin

The emergence of warfarin as a drug of therapeutic potential can be attributed to the work of Karl Paul Link and his team at the University of Wisconsin during the late 1930's and early 1940's.

Previous to their work observations by Schofield in Canada and Roderick in North Dakota indicated that a haemorrhagic disorder affecting cattle was caused by the consumption of spoiled sweet clover hay from the *Melitotus alba* or the *M. officinalis* family.

When sweet clover hay spoils in the curing process it is easy for it to become contaminated with moulds because of its succulent stems. *Penicillium nigricans, P. jensi* and *Aspergillus* metabolise coumarin present into dicoumarol. In 1933 work began in the laboratory of K.P. Link to isolate the unknown agent causing the disease in cattle. After extensive research, an elaborate extraction scheme was developed whereby the anti-coagulant was crystallised by Campbell in 1939 and identified by Heubner as 3,3'-methylbis-4-hydroxycoumarin or dicoumarol (Figure 1.5.). More than 100 related structural compounds of dicoumarol were synthesised in order to find the portion that contains the highest anti-coagulant potency.
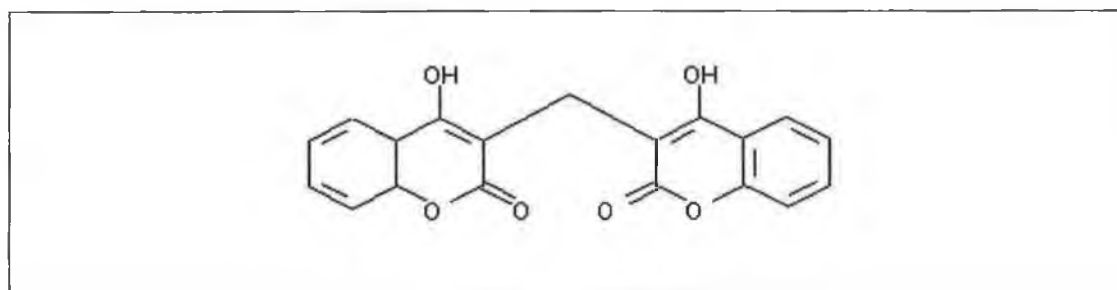
Figure 1.5: *Structure of Dicoumarol (3,3'-methylenebis-4-hydroxycoumarin)*

Work of Stahmann concluded that the minimal structural requirements for anti-coagulant activity were an intact 4-hydroxycoumarin residue with the 3-position substituted by a carbon residue or H-atom, whilst maximum anti-coagulant activity requires 4-hydroxycoumarin with the 3-position containing a keto group in a 1,5-spatial relationship with respect to the 4-hydroxycoumarin group. Warfarin (3-[acetonylbenzyl]-4-hydroxycoumarin) was subsequently synthesised by Ikawa in 1944, with the name warfarin arising out as a combination of the letters from Wisconsin Alumni Research Foundation and coumarin (Figure 1.6.).
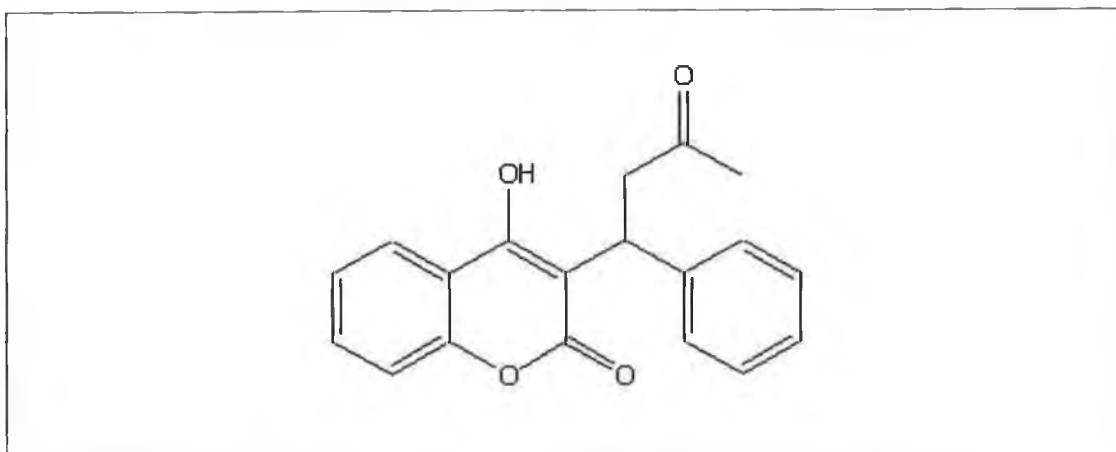
Figure 1.6: Structure of Warfarin (3-(α-acetonylbenzyl)-4-hydroxycoumarin)

1.7.2. Pharmacology of Warfarin

1.7.2.1. Mechanism of Action of Coumarin Anticoagulant Drugs

Warfarin, a coumarin derivative, produces an anticoagulant effect by interfering with the cyclic interconversion of vitamin K and its 2,3 epoxide (vitamin K epoxide). Vitamin K is a cofactor for the carboxylation of glutamate residues (Glu) to γ-carboxyglutamate (Gla) on the N-terminal regions of vitamin K-dependent proteins in the presence of vitamin K and molecular oxygen. These proteins, which include the coagulation factors II, VII, IX, and X, require γ-carboxylation by the vitamin K conversion cycle. Warfarin induces hepatic production of partially decarboxylated proteins with reduced coagulant activity (Hirsh *et al.*, 2003). The epoxidation reaction occurs in conjuction with the carboxylase reaction, where the active form of vitamin K is converted to vitamin K 2,3-epoxide, which is in turn converted back to the quinone form by vitamin K_1 epoxide reductase to complete the vitamin K cycle (Suttie, 1993). Due to the fact warfarin does not affect the activity of previously synthesised and circulating coagulation factors, depletion of these mature factors through normal catabolism must occur before the anticoagulant effects of warfarin are observed. Each factor varies in its degradation half-life (Table 1.3.), and this results in the requirement of 3-4 days therapy before a complete response to warfarin is observed. Warfarin is completely absorbed after oral administration and then is highly bound to albumin in the plasma. An inverse relation between the albumin and free warfarin levels is one reason why postoperative or acutely ill patients require lower doses of warfarin (Gage *et al.*, 2000). Warfarin also interferes with the carboxylation of Gla proteins synthesised in bone. Although these effects contribute to foetal bone abnormalities when mothers are

31

treated with warfarin during pregnancy, there is no evidence that warfarin directly affects bone metabolism when administered to children or adults (Hirsh *et al.*, 2003).

Table 1.3: Degradation half-lives of both coagulation and anti-coagulation factors.

Coagulation/Anticoagulation Factors	Degradation Half-Life (Hrs)
Coagulation Factor II	60
Coagulation Factor VII	4-6
Coagulation Factor IX	24
Coagulation Factor X	48-72
Anticoagulant Protein C	8
Anticoagulant Protein S	30

1.7.2.2. Vitamin K Cycle

A combination of dietary intake and microbiological synthesis in the gut provides the vitamin K requirement of mammals and phylloquinone is the most active source to meet the vitamin K requirements in humans. O'Reilly (1976) outlined the major factors necessary to prevent vitamin K deficiency as: (a) normal dietary intake of the vitamin (b) the presence of bile in the intestine (c) a normal absorptive surface in the liver and (d) a normal liver.

The direct link between vitamin K and blood coagulation was first established by Heinrik Dam whilst studying the dietary effects of chickens fed a 'lipid-free' diet. Dam (1929) discovered that the blood of chickens maintained on such a diet was devoid of clotting activity. However, when cereals were replaced back into the diet, the coagulation status of the chickens returned to normal. Vitamin K (phylloquinone, 2-methyl-3-phythyl-1,4-naphtoquinone) was identified as the agent necessary to cure the clotting defect in the chickens. The haemorrhagic condition was initially believed to be solely due to the depletion of the concentration of prothrombin (factor II). However, it was later discovered that the levels of factors VII, IX and X were also depleted and these proteins subsequently became known as the Vitamin K-dependent clotting factors (Suttie, 1993). A unique feature of the vitamin K-dependent proteins is the γ-carboxyglutamate residues (Gla) formed during post-translational modification of these proteins (Section 1.7.2.1. and Figure 1.4).

1.7.2.3. Vitamin K-dependent Carboxylase

The enzyme responsible for the post-translational modification of the glutamic residues on precursor clotting factors to γ-carboxyglutamate residues, necessary for the clotting ability of clotting factors is the vitamin K-dependent carboxylase (Berkner, 2000). The carboxylation reaction requires molecular oxygen, carbon dioxide and vitamin K as a cofactor. The hydroquinone form of vitamin K (vitamin KH_2) is reduced to the epoxide form of the vitamin (vitamin K 2,3-epoxide) in conjunction with the carboxylation reaction. Vitamin K 2,3-epoxide is then recycled to the quinone form of the vitamin by a vitamin K-epoxide reductase. Elevated levels of the epoxide form of the vitamin can be found in the plasma of orally anticoagulated patients (Nakamura *et al.*, 1994). The quinone form of the vitamin is subsequently reduced back to the hydroquinone form of the vitamin by a vitamin K reductase (Figure 1.7.) to complete the vitamin K cycle.

Oral anticoagulants exert their anticoagulant effect by inhibiting the cyclic inter-conversion of vitamin K, by inhibition of the epoxide- and vitamin K-reductases leading to a depletion of the hydroquinone (i.e. active) form of the vitamin. By inhibiting this regeneration of the epoxide form of the vitamin back to the hydroquinone form, partially carboxylated forms of the vitamin K-dependent clotting factors of varying Gla content are secreted; and pools of these partially carboxylated forms of prothrombin have been isolated and studied (Malhotra *et al.*, 1981; 1985; Takamiya & Yoshioka, 1996). A decrease in the number of Gla residues on the prothrombin molecule from 10 to 9 was found to result in a 30% decrease in coagulant activity, whilst a decrease to below 6 Gla residues reduces the coagulant activity by almost 95%.
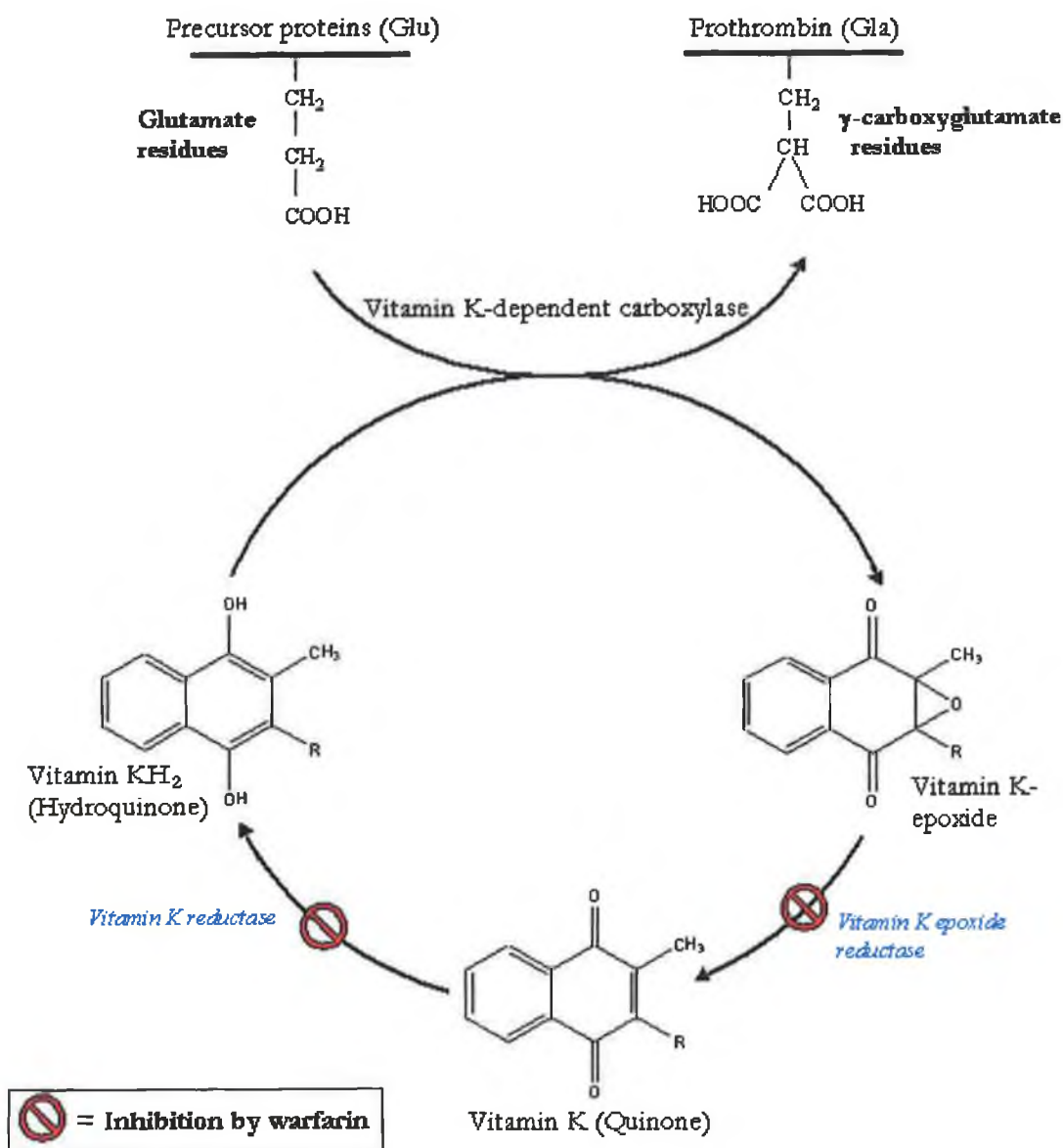
Figure 1.7: *The vitamin K cycle and its link to carboxylation of glutamate residues on vitamin K-dependent coagulation proteins. Vitamin K obtained from food sources is reduced to vitamin KH_2 by a warfarin-resistant vitamin K reductase. Vitamin KH_2 is then oxidised to vitamin K epoxide (vitamin KO) in a reaction that is coupled to carboxylation of glutamic acid residues on coagulation factors. This carboxylation step renders the coagulation factors II, VII, IX and X and the anticoagulant factors protein C and S functionally active. Vitamin KO is then reduced to vitamin K in a reaction catalysed by vitamin KO reductase. By inhibiting vitamin KO reductase, warfarin blocks the formation of vitamin K and vitamin KH_2, thereby removing the substrate (vitamin KH_2) for the carboxylation of glutamic acids.*

1.7.3. Pharmacokinetics and Pharmacodynamics of Warfarin

Warfarin is a widely prescribed oral anticoagulant which is available in the form of a racemic mixture consisting of equal amounts of R-and S-warfarin (Figure 1.8.) and displays both stereoselective metabolism and pharmacologic potency. The asymmetric carbon at position 9 of warfarin gives rise to these two entantiomers which are differentially metabolised, a process termed stereoselective metabolism. Different forms of P450 enzymes (Section 1.7.3.3.) catalyse metabolism of warfarin at different sites, and this process is referred to as regioselective metabolism (Kaminsky & Zhang, 1997). The S-enantiomer of warfarin is approximately three to five times as potent as the R-enantiomer and has a shorter half-life of elimination. Enantiomers have the same chemical composition, but are mirror images of each other. Both enantiomers are extensively metabolised in the body, and their metabolism involves highly stereospecific pathways catalysed by the cytochrome P450 system (Gage *et al.*, 2000; Linder, 2001; Zhou & Chan, 2002).

(R)-Warfarin   *(S)*-Warfarin
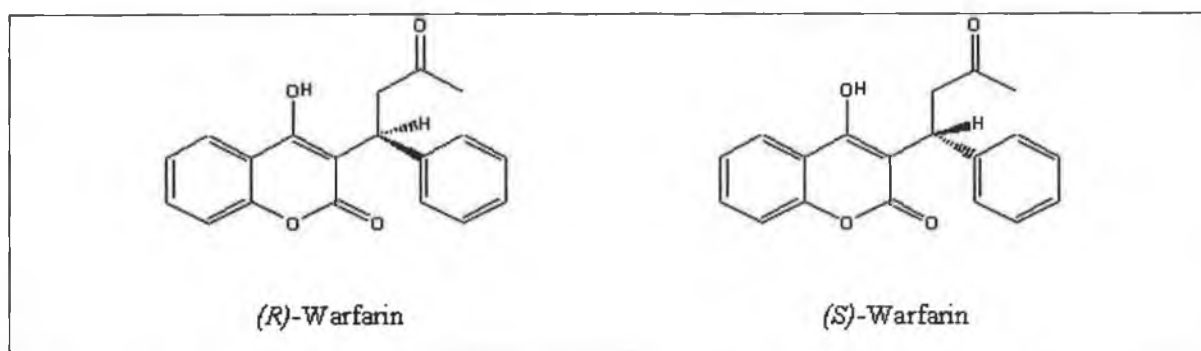
Figure 1.8: *Optical enantiomers of warfarin.*

The relationship between the dose of warfarin and the response is influenced by genetic and environmental factors, including common mutations in the gene coding for cytochrome P450 the hepatic enzyme responsible for oxidative metabolism of the warfarin S-isomer. Several genetic polymorphisms in this enzyme have been described that are associated with lower dose requirements and higher bleeding complication rates compared with the wild-type enzyme CYP2C9* (Hirsh *et al.*, 2003). The pharmacodynamic effect of warfarin is measured using the prothrombin time or the INR. The INR is calculated by dividing the patient's prothrombin time by the mean of the normal prothrombin time and then raising this ratio to an exponent, the international sensitivity index. That index reflects the sensitivity of the thromboplastin reagent to warfarin-induced changes in the levels of the clotting factors (Gage *et al.*, 2000).

1.7.3.1. Absorption

Warfarin is rapidly absorbed from the gastrointestinal tract, has high bioavailablilty, and reaches maximal blood concentrations in healthy volunteers 90 minutes after oral administration. Racemic warfarin has a half-life of 36-42 hours, circulates bound to plasma proteins (mainly albumin), and accumulates in the liver, where the 2 enantiomers are metabolically transformed by different pathways.

1.7.3.2. Distribution & Protein Binding

Following absorption the drug is highly protein bound (>99%), leaving only a small portion of free active drug circulating in the plasma (Table 1.4.). The binding of warfarin and its analogues to human serum albumin have been extensively studied (Ferrer *et al.* 1998; Bertucci *et al.*, 1999; Dockal *et al.*, 1999). Human serum albumin is composed of three structurally similar globular domains, HSA I, HSA II and HSA III (Dockal *et al.*, 1999). The primary warfarin-binding site was found to be located on domain II with a secondary binding site was found on domain I. Bertucci *et al.* (1999) demonstrated that the (S)-enantiomer has a higher affinity for HSA using competitive displacement studies. This high degree of protein binding predisposes warfarin to a range of possible drug interactions, which can have a dramatic effect on the degree of anticoagulation achieved (Section 1.7.5.). A recent study investigated the effect of familial dysalbuminemic hyperthyroxinemia (FDH) on warfarin pharmacokinetics. Warfarin was selected as a model compound to study FDH human serum albumin (HSA)/drug interactions since it binds to the HSA subdomain IIA and its pharmacokinetics are significantly influenced by HSA binding. The findings of this study indicated that FDH patients had elevated serum free warfarin concentrations which resulted in about a 5-fold reduction in the serum half-life of the drug (Petersen *et al.,* 2000).

Table 1.4: Extent of Plasma protein Binding and Plasma Half-Life

Oral Anticoagulant	Plasma Half-life ($t_{1/2}$) (hrs)	Protein Binding (%)
R-Warfarin	35-58	99
S-Warfarin	24-33	99
R-Acenocoumarol	8-10	99
S-Acenocoumarol	0.5-1.0	99
Phenprocoumon	72-120	99
Dicoumarol	24-96	99
Ethylbiscoumate	2-5	90

1.7.3.3. Warfarin Metabolism

Inter-patient variability in warfarin sensitivity appears to be linked to inherited differences in metabolic capacity (Loebstein *et al.*, 2001; Tabrizi *et al.*, 2002). Warfarin is essentially catalysed by a series of Cytochrome P450 enzymes to a series of hydroxylated metabolites (Kaminsky & Zhang, 1997). A series of carbonyl reductases in the endoplasmic reticulum and cytosol reduce the carbonyl side chain to yield diastereomeric alcohols (Herman & Thijssen, 1989) (Figure 1.9). The S enantiomer (possessing the predominant anticoagulant effect) is oxidised by a cytochrome P450 enzyme in the liver (CYP2C9) and then excreted in the bile, while the R enantiomer is metabolised by a different enzyme to an inactive alcohol that is excreted in the urine. Both enantiomers block the regeneration of the reduced form of vitamin K. By interfering with the vitamin K-dependent carboxylation of glutamate residues on the procoagulant forms of the clotting factors, warfarin inhibits the formation of several functional clotting factors (II, VII, Ix, and X) (Gage *et al.*, 2000).

The principal metabolism of warfarin in humans is catalysed by a variety of cytochromes P450 (P450 or CYP specific forms) to a series of monohydroxylated metabolites. The P450 enzymes belonging to the CYP2C subfamily have been shown to constitute the major forms of P450 in mammalian livers and play important roles in the oxidation of clinically used drugs. CYP2C9 is one of the major CYP2C gene products that catalyses oxidation of a variety of clinically used drugs such as torsemide, diazepam and warfarin in human liver microsomes. *In vitro* experiments have shown that the formation of the two main metabolites of S-warfarin, S-7-hydroxywarfarin and S-6-hydroxywarfarin, is catalysed primarily by CYP2C9 (Ragueneau-Majlessi *et al.*, 2001), whereas R-warfarin 7-hydroxylation appears to be catalysed by several P450 enzymes such as CYP1A2 and CYP3A4. (Kaminsky & Zhang, 1997; Yamazaki & Shimada, 1997).

Early studies involving warfarin metabolism identified the hydroxywarfarins, namely 6- and 7-hydroxywarfarin, and the warfarin diastereomeric alcohols, as the primary metabolites of warfarin (Lewis & Trager, 1970). Studies using human microsomes and recombinant P450's have extensively probed the regio- and stereoselectivity of warfarin (Takahashi *et al.*, 1997). Zhang *et al.* (1995) probed the (R)- warfarin metabolism using two isozymes (CYP4501A1 and CYP4501A2), and found that (R)- warfarin 6-hydroxylation rates could be used as markers of hepatic P4501A2, whilst 6-hydroxylation/8-hydroxylation rates could be used as markers for P4501A1. These particular isozymes were shown to be of particular importance because of their ability to bioactivate chemical carcinogens. The predominant human P450 catalysing S-warfarin metabolism is CYP2C9. Since this P450 also catalyses the metabolism for numerous drugs, the potential for warfarin-drug interactions is substantial (Section 1.7.5.). Both CYP1A2 and CYP3A4 are the major contributors to R-warfarin metabolism. Like CYP2C9, both of these enzymes catalyse the metabolism of various drugs. Therefore, there is a potential for R-warfarin and drug interactions (Kaminsky & Zhang, 1997).
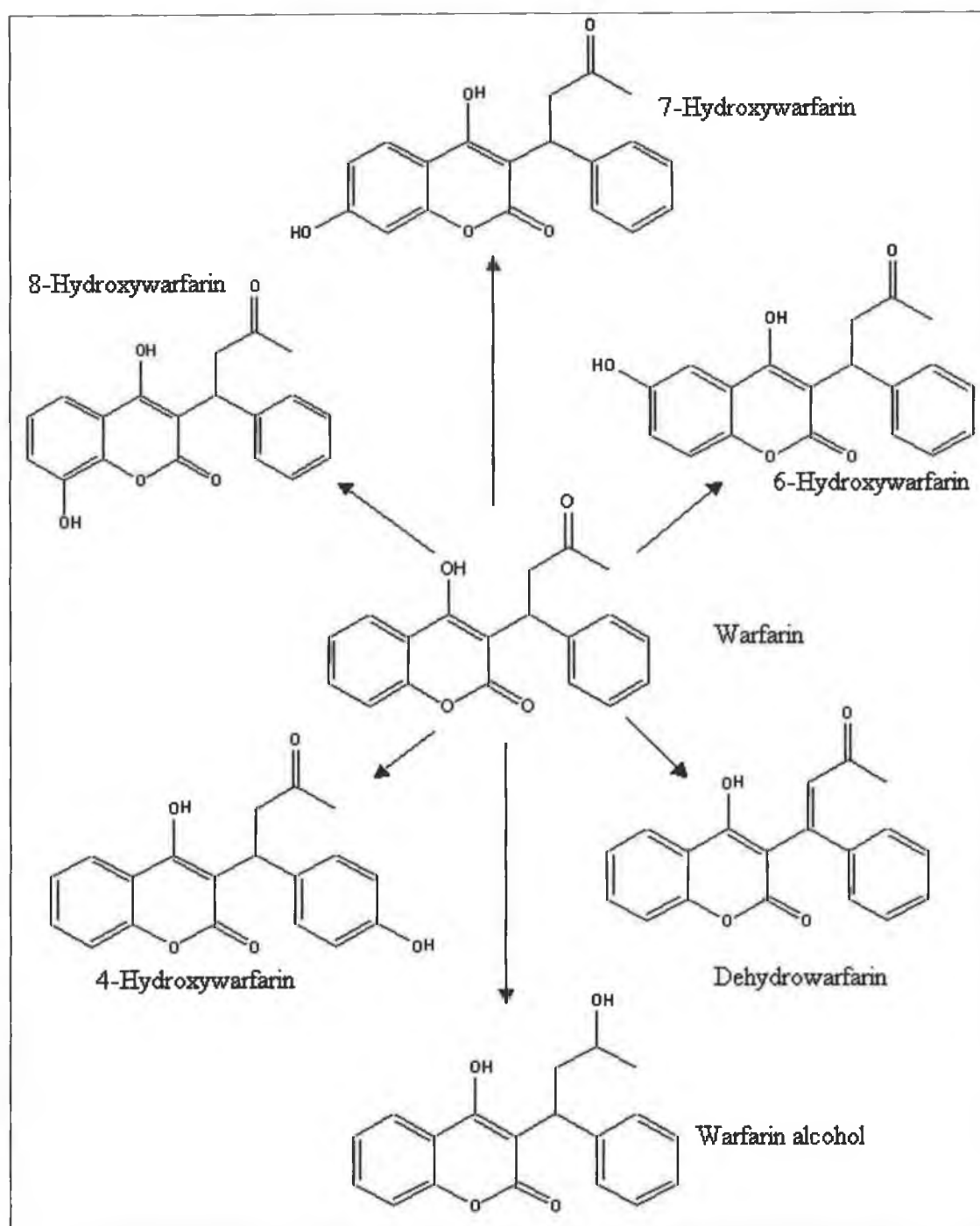
Figure 1.9: Main metabolic pathways of warfarin in humans

1.7.3.3.1. Genetic Variability

A high affinity hepatic S-warfarin 7-hydroxylase ascribed to cytochrome P4502C9 is responsible for both regioselective and stereoselective metabolism of S-warfarin. The cytochrome P4502C9 is encoded by the CYP2C9 gene. This gene exhibits structural polymorphism leading to two gene variants (alleles) which encode qualitatively different proteins with differing catalytic activities with respect to the 7-hydroxylation of S-warfarin. Studies performed to date strongly support a role for CYP2C9 polymorphism in the etiology of warfarin hypersensitivity. More in depth studies which include identification of all relevant CYP2C9 alleles and ratios are needed to strengthen the relationship between CYP2C9 genetics and warfarin maintenance dose requirements (Linder, 2001).

A recent study investigated population differences in the metabolic activity of cytochrome P450 (CYP) 2C9 between genotypically matched Caucasian and Japanese patients by using the unbound oral clearance of S-warfarin as an *in vivo* phenotypic trait measure. The findings of this study indicate that population differences in the frequencies of known variant CYP2C9 alleles account only in part for the variability observed in *in vivo* CYP2C9 activity in different populations. CYP2C9 genetic polymorphisms (e.g. allelic variants 2C9*2 and 2C9*3) markedly influence warfarin dose requirements and metabolic clearance of the S-warfarin enantiomer, although nongenetic factors may also contribute to their large interindividual variability (Scordo *et al.,* 2002). Further studies are required to identify currently unknown factors (e.g. transcriptional regulation) responsible for the large intrapopulation and interpopulation variability in CYP2C9 activity (Loebstein *et al.,* 2001; Takahashi *et al.,* 2003). CYP2C9 appears to be the predominant route of warfarin elimination, but alternative metabolic pathways and other genetic variants may potentially influence the response to warfarin therapy. Polymorphisms of the CYP2C9 subfamily are common, are associated with significant reductions in warfarin dose and may partially account for inter-patient variability in warfarin sensitivity. When interactions between genetic factors and other variables that influence warfarin effect are more completely understood, CYP analysis may prove useful for guiding warfarin prescription, particularly at the onset of therapy (Tabrizi *et al.,* 2002).

1.7.3.4. Excretion

Elimination of warfarin is primarily related to alterations in the degree of drug-protein binding, which affects the plasma concentration of circulating free drug available for metabolism. The major metabolites of warfarin (6- and 7-hydroxywarfarin) and the two diasteromeric warfarin alcohols are eliminated in the urine with less than 2 % of the administered dose excreted as warfarin. The rate

of elimination shows high interindividual variability with plasma half-lives ranging from 20-60 hours (Palaretti & Legnani, 1996).

1.7.4. Warfarin Resistance

Resistance to warfarin has been defined as: "the inability of Oral Anticoagulant Therapy (OAT) to bring the Prothrombin Time (PT) down to adequate levels of anticoagulation when administered at a dose near or equivalent to the normally recommended doses" (LeFrere *et al.*, 1987). In order to simplify understanding of warfarin resistance in this section, it shall be described as either hereditary resistance (HR), or acquired resistance (AR).

1.7.4.1. Hereditary Resistance

Hereditary resistance is believed to be caused by an abnormal receptor with an increased affinity for vitamin K and a reduced affinity for the coumarins. This form of resistance was first described over 30 years ago with the inability of patient to attain the desired degree of anticoagulation even with greater than 20 times the normal therapeutic concentration (O' Reilly, 1964). Other family members were tested and their response was similar to that of the patient. It was postulated then (O' Reilly, 1964), that HR is an autosomal dominant characteristic. Warrier and coworkers (1986) reported that the resistance was not absolute and could be overcome with large doses of the drug, suggesting an altered affinity of the enzyme or hepatic receptor for warfarin.

Two potential forms of hereditary warfarin resistance were reported in man. One mechanism appears to be a pharmacokinetic mechanism where the clearance of (S)-warfarin was increased 4-fold compared to control subjects. A second mechanism for hereditary warfarin resistance appears to be dependent upon pharmacodynamic mechanism of the drug action. This form of resistance is characterised by the relatively high doses of warfarin required to achieve therapeutic effect, normal warfarin pharmacokinetics, extremely high warfarin concentrations in blood, normal concentrations and half-lives of blood clotting proteins and the pattern of inheritance that of a monogenetic dominant trait. Although a considerable amount of progress was made in identifying genetic mechanisms contributing to variability in the response to warfarin, several questions remain to be answered in order to raise the level of knowledge to the point where this information can be routinely applied to patient care (Linder, 2001).

1.7.4.2. Acquired Resistance

Several cases of warfarin resistance associated with *intra-venous* lipid administration have also been documented (Lutomski *et al.*, 1987; MacLaren *et al.*, 1997). The use of heparin therapy was recommended for patients receiving lipid emulsions in order to overcome this complication. The precise mechanism of this particular interaction is not fully understood and was suggested to be due to enhanced binding of warfarin to albumin, or a result of enhanced clotting factor production.

The literature contains one report of warfarin resistance in a patient due to malabsorption (Talstad *et al.*, 1994). The case study involves a patient who after two years of satisfactory anticoagulation therapy with warfarin experienced selective malabsorption of warfarin. At this stage of warfarin therapy the dosage required was now 5 times the initial prescribed dosage. The reported malabsorption was not due to drug interactions or gastrointestinal disease. Enhanced clearance of warfarin has been reported and found to be due to an intrinsically high oral clearance of the more active S enantiomer (Hallak *et al.*, 1993).

Chu *et al.* (1996) described the first reported naturally occurring mutation in the propeptide sequence of Factor IX that directly affects the carboxylation by γ-glutamyl carboxylase. A patient whose PT was in the desired therapeutic range was admitted to hospital with bleeding complications. It was subsequently found that the patients Factor IX activity was <1% on warfarin therapy, but returned to normal levels when warfarin therapy was terminated. A mutation predicting a substitution of an Ala- residue to a Thr-residue at position 10 in the pro-peptide region of Factor IX was found. Ala-residues at position 10 in vitamin K-dependent proteins are highly conserved and, therefore, likely to be important in the binding of the carboxylase for γ-carboxylation. This in turn results in a reduced affinity of the carboxylase for the Factor IX precursor and demonstrates a previously unreported mechanism of warfarin 'sensitivity'. Bentley *et al.* (1986) produced a dosage-algorithm from a study of well-controlled patients, in order to aid the physician in the diagnosis of patients with an abnormal response to warfarin. The study provides two algorithms that can help the physician identify the causes of the abnormal warfarin response and dose accordingly.

1.7.5. Drug Interactions

Many potentially fatal diseases can be completely cured by modern treatments. However, the number of patients suffering from particular chronic diseases has been increasing (Makino *et al.*, 2001). The potential for pharmacokinetic drug interactions is of concern with any new drug,

particularly if given for chronic diseases such as epilepsy and cardiovascular conditions, as patients are likely to receive concomitant therapy for other underlying disorders. Since modern drugs do not cure chronic diseases but prevent further deterioration associated with them, patients must take drugs for extended periods of time. This increases the chances of interaction with other drugs as shown in Table 1.5.

Table 1.5: Drug Interactions. List of drugs that either inhibit the metabolism of warfarin
(i.e. increase the warfarin effect) or induce the metabolism of warfarin (i.e. decrease the
warfarin effect).

Increase in Warfarin Effect		*Decrease in Warfarin Effect*	
CNS DRUGS	• Tricyclic antidepressants (TCAs) • Selective serotonin reuptake inhibitors (SSRIs)	**CNS DRUGS**	• barbiturates • carbamazepine • phenytoin
ANTIBACTERIALS	• cotrimoxazole • isoniazid • metronidazole	**ANTIBACTERIALS**	• rifampicin
ANTI-RETROVIRALS	• indinavir • ritonavir • saquinavir	**ALCOHOLS**	• ethanol
CARDIOVASCULAR	• amiodarone • quinidine • verapamil		
ANTIFUNGALS	• miconazole • fluconazole • itraconazole		
ANTILIPIDAEMICS	• clofibrate • gemfibrozil • statins		
GASTRO-INTESTINAL	• cimetidine • omeprazole		

The anticoagulant response to warfarin is influenced both by pharmacokinetic factors, including drug interactions that affect its absorption or metabolic clearance, and by pharmacodynamic factors, which alter the haemostatic response to given concentrations of the drugs. Other drugs may influence the pharmacokinetics of warfarin by reducing the gastrointestinal absorption or disrupting metabolic clearance. For example, the anticoagulant effect of warfarin is reduced by cholestyramine, which impairs its absorption, and is potentiated by drugs that inhibit warfarin clearance. Inhibition of S-warfarin metabolism is more important clinically because this enantiomer is 3-5 times more potent than the R-isomer as a vitamin K antagonist. Phenylbutazone, sulfinpyrazone, metronidazole, and trimethoprim-sulfamethoxazole inhibit clearance of S-warfarin, and each potentiates the effect the effect of warfarin on the prothrombin time. In contrast, drugs such as cimetidine and omperazole, which inhibit clearance of the R-isomer, potentiate the PT only modestly in patients treated with warfarin. Amiodarone inhibits the metabolic clearance of both S- and R-enantiomers and potentiates warfarin anticoagulation. Drugs such as aspirin, NSAIDs, penicillins (in high doses), and moxolactam increase the risk of warfarin-associated bleeding by inhibiting platelet function. Of these aspirin is the most important because of its widespread use and prolonged effect. Aspirin and NSAIDs can produce gastric erosions that increase the risk of upper gastrointestinal bleeding.

The anticoagulant effect is inhibited by drugs like barbiturates, carbamazepine and rifampicin, which increase hepatic clearance. Chronic alcohol consumption has a similar potential to increase the clearance of warfarin, but ingestion of even relatively large amounts of wine has little influence on PT in subjects treated with warfarin.

With the increasing use of orally active fluropyrimidine prodrugs such as capecitabine and 5-Fluorouracil (5-FU) in the treatment of colorectal, breast and other cancers, the potential for drug interactions will increase. 5-FU is a pyramidine analog that is widely used in the treatment of a variety of solid tumours. The cytotoxicity of 5-FU is mainly attributed to the formation of fluoro-deoxyuridine-monophosphate that inhibits thymidylate synthetase, as well as to the incorporation of the drug into ribonucleic acid. It was postulated that 5-FU interferes with the synthesis of hepatic cytochrome CYP2C9, leading to impaired metabolism of warfarin (Zhou & Chan, 2002). Capecitabine is an oral prodrug of 5-FU and hence it is likely that the interaction with warfarin occurs by the same mechanism. Interacting drugs affecting the metabolism of warfarin in a stereoselective manner could result in marked differences in modifying the anticoagulant response to warfarin (Buyck *et al.*, 2003).

1.7.6. Monitoring Anticoagulant Therapy

1.7.6.1. Protrombin Time and INR

The start of anti-coagulant treatment is a critical period, as the hemorrhagic risk lies mainly in the induction phase. Warfarin has a narrow therapeutic index, so even a modest change in dose-response can lead to either thrombosis or haemorrhage. There is a great inter- and intraindividual pharmacokinetic and pharmacodynamic variability. It is therefore, difficult to predict the correct induction dose and obtain a more rapid and accurate individualisation of the dose of warfarin (Bertola *et al.*, 2003). The risk of bleeding with warfarin can be markedly reduced without affecting efficacy by using a low intensity therapeutic range. The prothrombin time (PT) assay is the most common test used to monitor oral anticoagulant therapy. The PT responds to reduction of 3 of the 4 vitamin K-dependent procoagulant clotting factors (II, VII, and X) that are reduced by warfarin at a rate proportionate to their respective half-lives (Table 1.3.).

The PT assay is performed by adding a mixture of calcium and thromboplastin to citrated plasma. The term "thromboplastin" refers to a tissue factor/phospholipid-containing extract, usually from brain, lung, or placenta, which promotes the activation of factor X by factor VII. Warfarin-induced responsiveness of a given thromboplastin to reduction in clotting factors reflects its potential for factor X activation. A responsive or sensitive thromboplastin produces a greater prolongation of the PT for a given reduction in the plasma concentrations of these factors (Hirsh, 1995). Thus, during the first few days of warfarin therapy, the PT reflects mainly the reduction of factor VII, the half-life of which is ~6 hours. Subsequently, reduction of factors X and II contributes to prolongation of the PT. PT monitoring of warfarin treatment is very imprecise when expressed as a PT ratio (calculated as a simple ratio of the patient's plasma value over that of normal control plasma) because thromboplastins can vary markedly in their responsiveness to warfarin (Hirsh *et al.*, 2003).

It was noticed that the PT would vary from laboratory to laboratory and even with the same analyser from time to time. The problem was traced to varying sensitivities of the materials used to perform the test. A mathematical formula was devised to take this variance into account (Table 1.6.). This is called the International Normalized Ratio or INR. If the patient INR is in the desired range there is a greater chance of avoiding a clot with the least chance of developing major bleeding. Major bleeding is usually defined as needing two units of blood or more. However, it is not a very good predictor of who will have minor bleeding. It measures clotting time, so it is not a good indicator of some other factors in the blood. The INR calibration model, adopted in 1982, is now used to

46

standardise reporting by converting the PT ratio measured with the local thromboplastin into an INR calculated as follows:

$$INR = (\text{patient PT/mean normal PT})^{ISI}$$

Or

$$\text{Log INR} = ISI(\text{log observed PT ratio}),$$

Where ISI denotes the International Sensitivity Index of the thromboplastin used at the local laboratory to perform the PT measurement. The ISI reflects the responsiveness of a given thromboplastin to reduction of the vitamin K-dependent coagulation factors. The more responsive the reagent, the lower the ISI value (Hirsh *et al.*, 2003). In a patient who is starting warfarin for the first time, no demographic or clinical information reliably predicts the steady-state dose that will achieve a given INR. The mean steady-state dose is 4 to 5 mg per day, but warfarin doses range from 0.5 to more than 50 mg per day (Gage *et al.*, 2000).

Table 1.6: Recommended International Normalised Ratios (INRs) for various thromboembolic conditions.

INDICATION	PT RATIO	RECOMMENDED INR
Acute Myocardial Infarction	1.3-1.5	2.0-3.0
Atrial Fibrillation	1.3-1.5	2.0-3.0
PE Treatment	1.3-1.5	2.0-3.0
Mechanical Prosthetic Valves	1.5-2.0	3.0-4.5
Venous Thrombosis	1.3-1.5	2.0-3.0
Tissue Heart Valves	1.3-1.5	2.0-3.0
Valvular Heart Disease	1.3-1.5	2.0-3.0
Systemic embolism prevention	1.3-1.5	2.0-3.0

It takes an average of almost 2 weeks to achieve a steady-state INR response. This long delay arises from warfarin's long half-life of accumulation, the time required for functional clotting factors to fall to low levels, and the time required to establish the correct daily dose empirically (Gage *et al.*, 2000). Information concerning patient sensitivity during the first 24 h of treatment could allow the practitioner to adapt the dose according to the patient's individual requirement as early as the second intake of warfarin. This early adaptation will improve the monitoring of oral anticoagulation in elderly

patients by reducing the risk of over or under anticoagulation and by shortening the time required to reach the correct maintenance dosage.

1.7.6.2. Warfarin -The 'Rebound Phenomena'

The expression 'rebound-phenomena' is used to describe a hypercoagulable state that exists following withdrawal of warfarin treatment. The first reported effects of 'rebound phenomenon' in patients following cessation of warfarin treatment was reported by Cosgriff & Stuart (1953). Withdrawal of warfarin therapy commonly results in the low-grade activation of the coagulation system, although the degree of activation is transient in most cases. However, higher levels of activation were observed for certain individuals predisposing them to an increased incidence of thrombotic complications (Palaretti & Legnani, 1996).

Two theories may explain the nature of the increased levels of blood coagulation and thrombin generation following warfarin withdrawal. The first explanation is that the reduced prothrombin levels during warfarin therapy balance the levels of increased coagulation, and when anticoagulant therapy is withdrawn the activation of coagulation is no longer 'counterbalanced' by the oral anticoagulant effect. This 'catching up' effect of the procoagulant factors was first described by Wright (1960) and later by Hirsh (1982). The second explanation describes how an actual 'rebound phenomena' may actually occur following cessation of warfarin therapy. The levels of Factor VII (has a role in thrombotic events) and Factor IX showed recovery times of 2 days (Schofield *et al.*, 1987). The return to normal levels of the anticoagulant proteins C and S was slower creating an imbalance between pro- and anticoagulant factors which may lead to activation of blood coagulation (Palaretti and Legnani, 1996). It was shown that the degree of hypercoagulability is more marked when discontinuation of warfarin is immediate rather than gradual. When anticoagulants are phased out gradually, the differences between the procoagulant and anticoagulant proteins are less marked reducing the likelihood of blood activation and the possibility of the 'rebound phenomenon'.

Recent studies on the risk of warfarin withdrawal due to impending surgical procedures indicate that the risk of bleeding is outweighed by the risk of serious thromboembolic events. Aside from anecdotal reports, there is little data available on the risk of thrombotic complications in patients in whom use of warfarin and aspirin is discontinued before cutaneous operation. It was reported that thrombotic events included strokes, cerebral and pulmonary embolism, myocardial infarction, transient ischemic attack and deep vein thrombosis (DVT). Since there are no reports of severe hemorrhagic complications during continued use of warfarin before surgery it is recommended not to

discontinue warfarin therapy due to surgery (Kovich & Otley, 2003). Chronic anticoagulation therapy with warfarin is not uncommon in the elderly population of patients requiring cataract surgery. Preoperative cessation of anticoagulant therapy carries a significant risk of thromboembolic events and is particularly hazardous for certain patients, such as those with artificial heart valves. Several studies document the safety of cataract surgery in patients treated with warfarin. In summary, cataract surgery can be safely performed without discontinuing anticoagulation medication and without exposing patients at risk for systemic and life-threatening complications (Rotenstreich *et al.*, 2001).

For dental extractions, patients who have been taking warfarin are at an increased risk of perioperative thromboembolism if the drug is stopped but may be at an increased risk of bleeding if continued. In addition, several antibiotics that are prescribed as prophylaxis during dental extraction against bacterial endocarditis may increase the effects of warfarin and the risk of bleeding. However, a study has shown that continuation of warfarin after dental extractions showed no evidence of increased clinically important bleeding. Since there are serious risks associated with stopping warfarin, the practice of routinely discontinuing it before dental extractions should be reconsidered (Evans *et al.*, 2002).

1.7.7. Clinical Uses

Warfarin is the therapeutic of choice for treatment of a variety of thromboembolic disorders, including atrial fibrillation, deep vein thrombosis and threatened stroke. The dosage required to achieve the desired therapeutic effect varies up to 120-fold (5 - 80mg/ml) between individuals (Linder, 2001). The clinical effectiveness of oral anticoagulants was established by well-designed clinical trials in a variety of disease conditions. Oral anticoagulants are effective for primary and secondary prevention of venous thromboembolism, for prevention of systemic embolism in patients with prosthetic heart valves or atrial fibrillation, for prevention of acute myocardial infarction (AMI) in patients with peripheral arterial disease and in men otherwise at high risk, and for prevention of stroke, recurrent infarction, or death in patients with AMI (Hirsh *et al.*, 2003). Brief descriptions of several alternative applications of warfarin are described below.

1.7.7.1. Anti-Coagulant Therapy

In vivo, the coumarin anti-coagulants act by blocking the synthesis of four blood factor proteins essential to the blood clotting process. The factors (Factor II, VII, IX and X) are necessary components of the prothrombin complex, and vitamin K is essential for their correct post-translational

modification. It is known that warfarin and other coumarin anti-coagulants interfere with this vitamin K-dependent process, by inhibiting the formation of vitamin K from its precursor (Vitamin K epoxide). This interference causes abnormal processing of blood factors, leading to accumulation of abnormal prothrombin proteins called PIVKAs (Proteins Induced by Vitamin K Antagonism or Absence), with a resultant depression of clotting activity.

The coumarin anti-coagulants are thus employed therapeutically to depress blood clotting. They have been applied in the treatment of venous thromboembolism, acute myocardial infarction and threatened stroke. Warfarin (also known as coumadin) is particularly extensively used in the clinical treatment of all thromboembolic disorders. Indeed it is the ninth most widely prescribed drug in the US.

1.7.7.2. HIV-1 Inhibitor

The urgent requirement for suitable therapeutic agents to arrest the development of the AIDS epidemic has led to considerable progress in recent years in the field of drug development against HIV. The anti-HIV activity of drugs and immunomodulating substances such as warfarin, cimetidine, levamisole and gramicidin may be used in a cocktail drug combination for HIV therapy (Bourinbaiar & Jirathitikal, 2003). Warfarin has shown promising results as a potent HIV inhibitor *in vitro*. A single dose of warfarin exhibited a specific inhibition of HIV replication in lymphocytes (Bourinbaiar *et al.*, 1993). Tummino *et al.* (1994) showed that warfarin inhibits the HIV retroviral protease in a competitive manner in the micromolar concentration range.

Retroviruses are known to share structural epitope domains with host-cell proteins (i.e., molecular mimicry). Molecular mimicry has been suggested as a fundamental mechanism underlying the pathogenicity of autoimmune disease. Tishkoff and co-workers have identified regions of sequence similarity shared between plasma-derived blood-clotting factor X (FX), major histocompatibility complex class II molecules (MHC-II), and human immunodeficiency virus-1 envelope glycoprotein 120 (HIV-1 env gp 120) that may possibly act as shared epitopes. FX zymogen could be the initial requirement for activation of viral envelope glycoprotein-fusegenic activity and may play a key role in host protease-dependent viral tropism. It is a vitamin K-dependent trypsin-like serine protease that may interrupt host viral tropism by down-modulation of vitamin K action using specific vitamin K antagonists, such as warfarin. Kinetic analysis *in vitro* supports warfarin as a competitive inhibitor of HIV-1 protease (Tishkoff *et al.*, 2000).

50

1.7.7.3. Anti-metastatic Properties

Metastasis involves several distinct steps, including one in which the tumour cell, after entry into the bloodstream, comes to rest in a capillary located at the distant site where a metastatic tumour will ultimately form. Components of the blood-clotting pathway may contribute to metastasis by trapping cells in capillaries or by facilitating adherence of cells to capillary walls. Conceivably, anticoagulants could interfere with this step in the metastatic process (Hejna *et al.*, 1999). Warfarin has shown particularly promising results in the treatment of SCCL (Small Cell Carcinoma Lung) a tumour cell type that is characterised by a coagulation associated pathway (Aisner *et al.*, 1992; Maurer *et al.*, 1997; Fitzpatrick, 2001). Studies by Mousa (2002) have shown that anticoagulation with commonly used agents such as unfractionated heparin and warfarin (Coumadin) prevent tumour formation by limiting the ability of tumour cells to be retained in the pulmonary microvasculature. Other anti-coagulants have shown promise in cancer treatment. Among drugs available for testing, aprotinin and low molecular weight heparin have particular appeal. The former blocks a pathway of tumour cell growth, invasion and metastasis while the latter blocks growth factor activity, angiogenesis, and other tumour growth mechanisms as well as coagulation activation (Zacharski, 2002).

Recent studies suggest that anticoagulant drugs and cimetidine therapy in malignancy may improve cancer survival and inhibit the metastatic process. A study investigated and compared the effects of anticoagulant drugs (e.g. warfarin and heparin), cimetidine and a combination of cimetidine with anticoagulants on adhesion of highly invasive breast cancer cell lines BT-549 and MDA-MB-231 *in vitro*. A high anti-adhesion effect was observed with cimetidine and warfarin. Anticoagulants such as warfarin can decrease adhesion and tumour angiogenesis. Application of cimetidine and anticoagulant drugs intensifies the anti-adhesion effect together with other anti-metastatic effects (Bobek *et al.*, 2003). There is now considerable evidence that the blood coagulation system plays an important role in the biology of malignant tumours. This evidence was derived from a combination of clinical, biochemical, histological, and pharmacological observations that point to the possibility of favourably affecting the course of malignant disease with agents that interfere with blood coagulation pathways (Mousa, 2002).

1.7.7.4. Ig A Nephritis

Human glomerulonephritis (GN) remain one of the most important causes of end-stage kidney disease worldwide. Although there is no cure for this type of kidney disease, the current therapeutic

measures serve to retard the progression to end stage renal failure. Dipyridamole (well-known vasodilator) and low dose warfarin was found to be successful in retarding progression to end-stage renal failure in patients with Ig A nephritis (Leim, 2001).

1.7.8. Warfarin Contraindications

Although the most common side effect associated with the use of warfarin is bleeding, other nonhemorrhagic side effects including skin necrosis have been reported. Deleterious effects on bone are also suggested by warfarin's ability to induce embryopathy when administered to women during their first trimester of pregnancy (Simon *et al.*, 2002).

The first reports of a possible connection between the drug and skin damage were by Flood *et al* who described a migratory thrombophlebitis in 1943 and Verhagen who was the first to describe skin necrosis in 1954. Warfarin-induced skin necrosis occurs in 0.01-0.1% of warfarin-treated patients (Ad-El *et al.*, 2000). To date approximately 300 cases have been reported worldwide. This rare but dramatic complication of warfarin therapy is characterised by rapidly developing skin and subcutaneous tissue death that usually occurs 3-10 days after the initiation of warfarin therapy. Skin necrosis may mimic the clinical findings of fulminant purpura, breast cancer, necrotising fascitis, microembolisation and decubitis ulcers (Babu & McIntyre, 2001; Kurtoglu *et al.*, 2001). There are also several adverse skin manifestations associated with the use of anticoagulants, ranging from purpura, haemorrhagic necrosis to maculopapular vesicular urticarial eruptions (Zimbelman *et al.*, 2000; Roche-Nagle *et al.*, 2003). A few cases of warfarin-induced skin necrosis are found in the orthopaedic literature where warfarin can induce skin necrosis after total hip arthroplasty (Clark & Bremner, 2002). Warfarin-induced skin necrosis (WISN) is often associated with large initial loading dose of warfarin. It is thought to be due to a rapid elimination of protein C (a natural anticoagulant) compared with other vitamin K-dependent clotting factors. WISN is mainly seen in middle aged, peri-menopausal, and obese women (Roche-Nagle *et al.*, 2003). Therefore, it is recommended to introduce warfarin gradually, especially in middle-aged, obese women treated for venous thromboembolism in order to avoid this serious and at times life-threatening complication (Lennox *et al.*, 2001).

Warfarin provides effective protection against thromboembolism, but its use in pregnancy is associated with an augmented rate of abortion and the risk of warfarin-induced embryopathy. The risk of maternal thromboembolic events is heightened during pregnancy because of the patient's hypercoagulable state, which is characterised by increased levels of clotting factors and of fibrinogen and platelet adhesiveness (Vitale *et al.*, 1999; Brooks *et al.*, 2002; Vitale *et al.*, 2002). Following

numerous reports on adverse pregnancy outcomes related to oral anticoagulants, the manufacturers have contraindicated their use during pregnancy since the late 1970s. Warfarin therapy during pregnancy has been implicated in two major adverse effects. Warfarin embryopathy was attributed to the inhibiting effect of warfarin on vitamin K reductase activity. Vitamin K is involved in the carboxylation of two essential components of bone and cartilage development. The effect of warfarin on embryonic calcium desposition and subsequent bone formation and growth in a critical period of embryological ossification (6-9 weeks' gestation) results in stippled calcification, extremity shortening, vertebral abnormalities, and nasal hypoplasia. The other adverse effect results from warfarin over-anticoagulation of the foetus. Since warfarin readily crosses the placenta, anticoagulation may occur any time during pregnancy and may cause haemorrhage in every foetal organ. In patients with mechanical prosthetic heart valves, long-term anticoagulation is mandatory to prevent thromboembolic phenomena. In a recent retrospective Multicenter survey, the Working Group on Valve Disease of the European Society of Cardiology concluded that heparin is neither effective nor safe for long-term use during pregnancy in patients with mechanical heart valve, bringing an increased risk of both thromboembolism and bleeding to mother and foetus. There is a close dependency between warfarin dosage and foetal complications. Patients whose warfarin dose was greater than 5mg per day had a significantly higher number of foetal complications in comparison to patients on less than 5mg per day. Recently protocols of low intensity anticoagulation with coumarin derivatives and studies suggesting that foetal adverse effects of anticoagulation might be dose-dependent led to the American Heart Association to recommend low dose warfarin administration from the first trimester to the 35th week of pregnancy (Cotrufo *et al.*, 2002).

Other uncommon adverse reactions that occur with warfarin administration include agranulocytosis, alopecia, anaphylactoid reactions, anorexia, cold intolerance, diarrhoea, dizziness, elevated hepatic enzymes, exfoliative dermatitis, headache, hepatitis, jaundice, leukopenia, nausea and/or vomiting.

1.8. Isoflavones

For many years now, isoflavones have been investigated by clinicians, pharmacologists and plant physiologists. Isoflavones have exceptionally interesting, multidirectional therapeutic properties and the biological activity of these substances is conditioned by the location of the phenyl ring near the third carbon of the benzo-γ-pyrone. Hence, these compounds, in addition to antiflammatory, antimycotic and radical scavenging properties, also exhibit both estrogenic and anti-estrogenic effects (Luczkiewicz & Glod, 2003). Genistein (4,5,7-trihydroxyisoflavone) is a natural isoflavone

phytoestrogen present in soybean (Figure 1.10). In the gastrointestinal tract, the β-glucoside conjugates of soy are converted by the natural gut microflora into free genistein and other related isoflavones, which are present in circulating blood, accumulate in tissue and are excreted in urine of people who consume high amounts of soy in their diet. Studies have revealed that individuals who consume a traditional diet high in soy products have a low incidence of certain types of cancer, such as breast, prostatic and colon cancer (Fioravanti *et al.*, 1998). Genistein has been shown to inhibit cancer cell proliferation *in vitro* and this effect may be attributed to the fact that it is a known tyrosine kinase inhibitor (Section 4.9). Therefore, this compound was chosen to determine its effect on two cell lines *in vitro* (Chapter 5.). The following section gives background details on this therapeutically important compound.
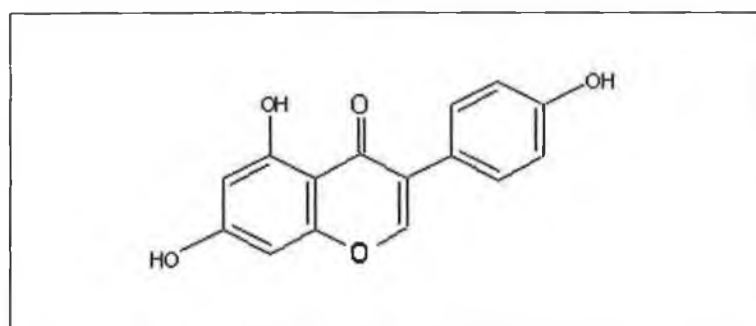
Figure 1.10: *The basic chemical structure of genistein. It belongs to the benzo-γ-pyrone subclass.*

1.8.1. Genistein

Although genistein belongs to the benzopyrones is not classed as a coumarin (benzo-α-pyrone). It is a flavonoid and belongs to the benzo-γ-pyrones. Genistein is a phytoestrogen, which belongs to the 'isoflavone' class of compounds. These diphenolic compounds structurally resemble estradiol (E_2) and were shown to have weak estrogenic activity (Tanos, 2002).

Reports about environmental estrogens, or xenoestrogens, have been widespread in the last few years. There are important distinctions between estrogenic compounds of industrial origin and those that come from plants. Compounds such as insecticide DDT and industrial PCBs were implicated by some researchers in causing estrogen-dependent cancers in exposed populations. Unlike some industrial xenoestrogens, which tend to bioaccumulate in adipose tissue and persist in the body for years, phytoestrogens are readily metabolised and spend relatively little time in the body. The timing of exposure, repeated exposures and levels of exposure to phytoestrogens are important.

The two major classes of phytoestrogens that have captured the most scientific attention are isoflavones and lignans. Diet rich in natural anti-estrogenic substances such as isoflavones has been considered as one of the main reasons for significantly lower incidence of breast cancer in China, Japan, and South East Asia. Soybeans are a particularly abundant source of isoflavones such as genistein and daidzein (Barrett, 1996).

1.8.1.2. Genistein and Cancer Research

Genistein has been shown to inhibit cancer cell proliferation *in vitro*. This effect was attributed to inhibition of several key enzymes, especially tyrosine kinase, which plays a critical role in cell proliferation and transformation. Tyrosine kinase is also associated with oncogene expression in breast cancer. Breast cancer is one of the most frequently diagnosed malignancies in women, and its incidence is increasing in industrialised nations. Tanos *et al.*, (2002) have investigated the effect of genistein on human dysplastic and malignant epithelial breast cell lines, expressing low and high metastatic potentials. They discovered that genistein has a significant *in vitro* inhibitory effect on the growth rate of dysplastic (fibrocystic cells) and cancerous breast cells. The results obtained, illustrate that genistein has not only anti-proliferative effect on cancer cells but also on pathological (non-malignant) cells. *In vitro* studies show that genistein also exhibited a synergistic additive effect when cancer cells were exposed to a genistein and tamoxifen treatment. These results indicate the potential of genistein administration alone or in combination with tamoxifen for the treatment of breast cancer (Tanos, 2002).

A separate study has shown that genistein treatment has a role in triggering cell death and promotes cell cycle arrest on γ-irradiated K562 myeloid leukaemia cells (Papazisis *et al.*, 2000). Genistein structurally resembles estradiol (E_2) and demonstrates weak estrogenic activity in several studies (Fioravanti *et al.*, 1998; Ratna, 2002; Tanos *et al.*, 2002). In humans, this compound appears to have both estrogenic and anti-estrogenic effects, depending on the concentrations of circulating endogenous estrogens and estrogen receptor (ER). Genistein binds to the estrogen receptor with an affinity approximately 100-fold lower than that of estradiol, resulting in enhanced proliferation activity. The estrogen agonistic activity in the absence of estrogen may account for the beneficial effects of genistein against atherosclerosis, coronary artery disease, osteoporosis and post-menopausal manifestations of hot flushes. The protective effect of genistein against other forms of hormone-dependent cancers, such as prostate cancer, may be due to similar mechanisms (Ratna, 2002).

1.9. Chapter Summary

In this chapter the coumarin family of compounds were reviewed, as a prelude to the work described in this thesis. The occurrence, biosynthesis and pharmacokinetics of coumarins were described. Particular focus was given to the metabolism and toxicology of the parent compound, coumarin, with the importance of coumarin metabolites addressed. Many of these metabolites, and other coumarin derivatives are very important, both clinically and industrially, and the uses of coumarins in these settings were summarised. A review of the use of benzopyrones in cancer therapy, the focus of chapter 5 was given. Since warfarin is the main focus of chapters 3 and 4, and is also of importance in chapter 5, its origins and uses were described in detail. Finally, the isoflavones are described with emphasis on genistein, as it is relevant to the work described in chapter 5 and facilitates understanding of the clinical importance of this compound and its potential benefits for use in cancer patients.

Chapter 2
Materials & Methods

2.1. Equipment

Table 2.1: Equipment model used and suppliers.

Class	Model	Source
Cytosensor® Microphysiometer	Cytosensor single unit (4) Serial No: C04706	Molecular Devices
BIAcore™	BIAcore™ 3000	BIACORE AB
Centrifuges	Heraeus Christ Labofuge 6000	Heraeus Instruments Inc.
	Biofuge A Microcentrifuge	Heraeus Instruments Inc.
	Sorvall refrigerated centrifuge	Du Pont Instruments
CO_2 Tissue culture incubator	EG 115 IR	Heraeus Instruments Inc./Jouan
Microscope	Nikon Diaphot inverted microscope	Micron Optical Co. Ltd.
pH meter	3015 pH meter	Jenway Ltd.
Rocker Platform	Stuart Platform Shaker STR6	Lennox
Protein Electrophoresis Apparatus	Atto dual minislab system AE-6450	Atto Corp.
Spectrophotometers	U.V.-160A Spectrophotometer	Shimadzu Corp.
	Titertek Multiscan plate reader	Medical Supply Company
Sonicator & Waterbath	RM6 Lauda waterbath	A.G.B. Scientific Ltd.
Laminar Flow Unit	Holten 2448K laminar air flow unit	Holten Laminar A/S
Millipore Filtration Apparatus	Millipore Filtration Device	A.G.B. Scientific Ltd.
Ultrafiltration Cell	Stirred Cell 8400	Amicon Inc.

Full Addresses:

AGB: Dublin Industrial Estate, Dublin 11, Ireland.

Amicon Inc.: Beverly, Massachusetts 01915, U.S.A.

Atto Corp.: 2-3 Hongo 7-Chrome, Bunkyo-Kui, Tokyo 113, Japan.

BIACORE AB: St. Albans, Hertfordshire AL13AW, England.

Molecular Devices: Unit 6, Raleigh Court, Rutherford Way, Crawley, West Sussex, England.

Du Pont Instruments: Instrument Products Division, Newtown, Connecticut 06470, U.S.A.

Heraeus Instruments Inc.: 111-a Corporate Boulevard, Sth Plainfield, New Jersey 07080,U.S.A.

Holten Laminar A/S: Gydevang 17, DK 3450 Allerod, Denmark.

Jenway Ltd.: Gransmore Green, Felsted Dunmow, Essex, CM6 3LB, England.

Lennox: P.O Box 212A, John F. Kennedy Dr., Naas Rd., Dublin 12, Ireland.

Medical Supply Company: Damastown, Mulhuddart, Dublin 15, Ireland.

Nikon Corporation: 2-3 Marunouchi 3-chome, Chiyoda-ku, Tokyo, Japan.

Pharmacia Biosensor: St. Albans, Hertfordshire AL1 3AW, England.

Shimadzu Corp.: 1 Nishinokyo-Kuwabaracho, Nakagyo-ku, Kyoto 604, Japan.

2.2. Consumable Items

2.2.1. Plastic Consumables

Table 2.2: Consumables used and suppliers

Class	Item	Source
Plastics	Eppendorf tubes, sterile universal containers and gilson tips	Sarstedt Ltd.
	Cytosensor capsules/ Reference Electrode kit	Biosciences
	Nunc Maxisorp plates	Nunc
	Tissue Culture plastic-ware	Corning Costar
Miscellaneous	CM5 Chips	Pharmacia Biosensor
	Nanosep™ Ultrafiltration membranes	Amicon Inc.
	Milipore 0.2 µm filters	A.G.B. Scientific Ltd.

Full Addresses:

AGB: Dublin Industrial Estate, Dublin 11, Ireland.

Corning Costar: High Wycombe, Buckinghamshire HP13 6EQ, England.

Biosciences: 3, Charlemont Terrace, Dunlaoire, Co. Dublin, Ireland.

Nunc: P.O. Box 280-Kamstrup DK, Roskilde, Denmark.

Sarstedt Ltd.: Sinnottstown Lane, Drinagh, Co. Wexford.

2.3. Reagents and Chemicals

All chemicals were reagent grade and were purchased through Sigma Aldrich Company Ltd, (Airton Road, Tallaght, Dublin 24.) except as noted below.

Table 2.3: Reagents & Chemicals used and suppliers:

Class	Chemical	Supplier
Chemicals	Acencoumarin (Sintrom®)	Ciba-Geigy
Biochemical & Immunological Reagents	Anti-phosphotyrosine monoclonal antibody	Promega
	Alkaline phosphatase-labelled antibodies	Southern Biotechnology Ltd.
	Phosphate buffered Saline tablets	Oxoid Ltd.
	BCA Kit	Pierce
	MTT, LDH and BrdU Kits	Roche
Tissue culture	MCF-7 cells	N.C.T.C.C.
	Dulbecco's modification of Eagles medium	Gibco BRL
	Foetal calf serum	Gibco BRL
	HEPES	Gibco BRL
	Trypsin	Gibco BRL
	L-glutamine	Gibco BRL
	Non-essential amino acids	Gibco BRL
	Phosphate-buffered saline tablets	Oxoid
	Sodium pyruvate	Gibco BRL

Full Addresses:

Ciba-Geigy: CH-4002 Basle, Switzerland.

Gibco BRL: Trident House, Renfrew Rd., Paisley PA4 9RF, Scotland.

N.C.T.C.C.: National Cell and Tissue Culture Centre, DCU, Dublin 9, Ireland.

Oxoid: Basingstoke, Hampshire, England.

Pierce: 3747 North Meridian Road, PO box 117, Rockford, IL 61105, U.S.A.

Promega Corporation: 2800 Woods Hollow Road, Madison, WI 53711, U.S.A

Roche Diagnostics Ltd: Bell Lane, Lewes, East Sussex BN7 1LG, United Kingdom

Southern Biotechnology: 160A Oxmoor Boulevard, Birmingham, Alabama 35209, U.S.A.

2.4. Standard Solutions

Phosphate Buffered Saline (PBS-1):

One tablet was dissolved per 100 mls of distilled water according to the manufacturer's instructions. When dissolved, the tablets prepare Dulbecco's A PBS which contains 10 mM phosphate buffer and 0.14 M NaCl, pH 7.2-7.4 (referred to in text as PBS-1).

Phosphate Buffered Saline 2 (PBS-2):

PBS-1 was prepared as described above, with 0.3 M NaCl added (referred to in text as PBS-2).

Wash Buffer:

PBS-1 containing 0.05% (v/v) Tween-20.

Diluent Buffer:

PBS-1 containing 0.05% (v/v) Tween-20 and 5% (v/v) FCS.

HBS Buffer:

Hepes Buffered Saline (HBS):

Hepes buffered saline (BIACORE running buffer) containing 50 mM NaCl, 10 mM HEPES, 3.4 mM EDTA and 0.05% (v/v) Tween-20 was prepared by dissolving 8.76 g of NaCl, 2.56 g of HEPES, 1.27 g of E.D.T.A. and 500 µl of Tween 20 in 800ml of distilled water. The pH of the solution was then adjusted to pH 7.4 by the addition of 2M NaOH. The final volume was then made up to 1,000 ml in a volumetric flask. The solution was filtered through a Milipore 0.2 µm filter and degassed prior to use.

SDS-PAGE (Sodium Dodecyl Sulphate-PolyAcrylamide Gel Electrophoresis) solutions:

Stock Solutions:

(A) 30% (w/v) acrylamide containing 0.8% (w/v) bis-acrylamide.

(B) 1.5 M Tris-HCl, pH 8.8, containing 0.4% (w/v) SDS.

(C) 0.5 M Tris-HCl, pH 6.8, containing 0.4% (w/v) SDS.

(D) 10% (w/v) ammonium persulphate.

Table 2.4: *The quantities of stock solutions required for the preparation of resolving and stacking gel used for polyacrylamide gel electrophoresis.*

Solution	Resolving Gel	Stacking Gel
Acrylamide (A)	3.3. ml	0.83 ml
Distilled Water	4.17 ml	2.9 ml
Resolving Gel Buffer (B)	2.5 ml	--------
Stacking Gel Buffer (C)	--------	1.25 ml
Ammonium Persulphate (D)	100 μl	25 μl
TEMED	10 μl	5 μl

Coomassie Blue Stain Solution

Coomassie Blue R-250	1.25 g
Methanol	227 ml
dH$_2$O	227 ml
Glacial acetic acid	46 ml

The components were dissolved, mixed thoroughly, filtered through Whatman paper grade number 1, and stored at room temperature (R.T.) in a dark bottle.

Destain Solution

Methanol	150 ml
Glacial acetic acid	50 ml
dH$_2$O	300 ml

The above components were mixed, thoroughly, and stored at R.T.

Electrophoresis Buffer

Tris. HCl	3.00 g
Glycine	14.40 g
SDS	1.00 g

The components were dissolved in 1L of dH$_2$O, and stored at R.T.

Sample Buffer

1M Tris.HCl (pH 6.8)	0.60 ml
50% (v/v) Glycerol	5.00 ml
10% (w/v) SDS	2.00 ml
2-ME (2-Mercaptoethanol)	0.50 ml
1% (w/v) Bromophenol blue	0.90 ml

The components were thoroughly mixed together, and stored at -20°C.

Acrylamide Stock Solution (A)

Acrylamide	29.20 g
Bisacrylamide	0.80 g

The components were dissolved in 100ml dH$_2$0, and stored in the dark at 4°C.

4X Resolving Gel Buffer (B)

2M Tris-HCl (pH 8.8)	75.0 ml
10% (w/v) SDS	4.0 ml
dH_2O	21.0 ml

The components were thoroughly mixed together, and stored at 4°C.

4X Stacking gel Buffer (C)

1M Tris.Cl (pH 6.8)	50.0 ml
10% (w/v) SDS	4.0 ml
dH_2O	46.0 ml

The components were thoroughly mixed together, and stored at 4°C.

Ammonium Persulphate Solution (D)

Ammonium persulphate	0.10 g
dH_2O	1.00 ml

The components were mixed thoroughly and stored at R.T.

Electrophoresis buffer

Tris	3.10 g
Glycine	14.40 g
Methanol	200.0 ml

The components were dissolved in 1,000 ml of dH_2O, and stored at R.T.

2.5. Methods

2.5.1. Mammalian Cell Culture

All mammalian cell cultures were grown in a humidified 5% CO_2 atmosphere, at 37^0C. All cell counts were made using a Neubauer Counting Chamber. Viable cell counts were obtained by mixing cells, with a 1/5 volume of a commercial 0.4% (w/v) isotonic Trypan blue solution. Dead cells were stained blue. The viable cell count was carried out within 5 mins of the addition of Trypan blue. Cells were visualised with a phase contrast microscope. All cells were pelleted by centrifugation and all centrifugations were at 2000 rpm for 10 min. unless otherwise stated.

2.5.1.1. Cell Lines and Media Preparation

The cell lines used in the experimental work and their appropriate culture media are outlined in Table 2.5. In all cases, the culture medium was supplemented with FCS (at either 5 or 10% (v/v) as outlined in Table 2.5.), L-glutamine (2mM), HEPES (1mM) and gentamycin (5µg/ml). Sodium pyruvate (1mM) and non-essential amino acids (1% (v/v)) were also used to supplement the MCF-7 media.

Table 2.5: *List of cell lines and their culture media used throughout this work.*

Cell Line	ATTC No.	Description	Culture Medium
MCF-7	HTB 22	Human Caucasian Breast Carcinoma	$DMEM.S_{10}$
A549	CCL 185	Human Caucasian Lung Carcinoma	$DMEM.S_5$
Clone 4.2.25	NA	Murine Hybridoma(Balb/C-Sp2)	$DMEM.S_5$

2.5.1.2. Recovery of Frozen Cells

Cells were recovered from liquid nitrogen by thawing rapidly at 37°C and transferring to a sterile universal tube containing 10mls of $DMEM.S_{10}$ [DMEM containing 10% (v/v) Foetal Calf Serum (FCS)]. The cells were centrifuged at 2000 rpm for 10 mins, resuspended in fresh medium, transferred to culture flasks, and incubated at 37°C in a humid 5% CO_2 incubator.

2.5.1.3. Culture of Cells in Suspension

4.2.25. hybridoma cells (derived from fusion of mouse spleenocytes to Sp2/0 cells ATTC No. CRL 1581) were maintained in DMEM.S$_{10}$. The cells were subcultured, using a split ratio of 1:4, at approximately 70% confluency. For subculturing, the cells were flushed off the surface of the flask using a Pasteur pipette, collected and centrifuged at 2,000 rpm. The pellet was then resuspended in 4 ml of fresh culture medium. 1 ml of the resuspended pellet was then transferred to T-75 flasks containing 14 ml of fresh DMEM

2.5.1.4. Culture of Adherent Cells

The two other cell lines used (A549 and MCF-7) in the experiments were adherent cell lines. All cells were strongly adherent and required trypsinisation for harvesting prior to subculturing or experimental usage.

For trypsinisation the medium was decanted and 1 ml of trypsinising solution (Gibco 0.025% (w/v) trypsin with 0.02% (w/v) EDTA in 0.1M PBS, pH 7.4) was used to rinse the flask, thus removing residual FCS which contains a trypsin-inhibitory activity. After this volume was decanted a further 4mls of the trypsinising solution was added to the flask and the flask was incubated at 37°C until all the cells had detached from the flask surface. 6mls of DMEM.S$_{10}$ was added to this cell suspension, which was then transferred to a sterile universal tube and centrifuged at 2000 rpm for 10 mins. The cells were resuspended in culture medium and seeded at 1×10^6 cells/ml, using 15mls of DMEM per 75cm^2 culture flask.

2.5.1.5. Cell Counts and Viability Testing

Trypan Blue was used routinely to determine cell numbers and viabilities. 20µl of Trypan Blue stain (Sigma, 0.25% (w/v)) was mixed with 100µl of cell suspension and allowed to incubate for 3 mins. A sample of this mixture was loaded onto the counting chamber of an improved Neubauer Haemocytometer slide, and cell numbers and viabilities were determined. Viable cells excluded the dye and remained white, while dead cells stained blue. In all cases the minimum number of cells counted was 200.

2.5.1.6. Long-Term Storage of Cells

Cells required for long-term storage were frozen in liquid nitrogen. Harvested cells were pelleted and resuspended in freezing medium (90% FCS, 10% DMSO, (v/v)) to a concentration of 1 X 10^6 cells/ml. 1ml aliquots were then transferred to sterile cryotubes, and lowered slowly (over a 3 hour period) into the gas phase, before being eventually immersed in liquid nitrogen.

2.5.2. Solid Phase Immunoassays

2.5.2.1. ELISAs for Titration of Antibody Levels in Hybridoma Supernatants

100 µl of a solution of 50 µg/ml warfarin-BSA conjugate prepared in PBS-1, was added to all of the wells of a Nunc maxisorp plate, and incubated at room temperature overnight. Wells were washed with 5 x 200 µl of wash buffer, and 100 µl of a 5% (v/v) solution of FCS in PBS-1 was added to each well, and incubated for 90 minutes at 37^0C. This was to 'block' any remaining adsorption sites on the plastic surface. Wells were then washed out with 5 x 200 µl of wash buffer. 100 µl of test sample (i.e. the appropriate dilution of hybridoma supernatant) was added to the wells of the plate. Samples were diluted (serial doubling dilutions including neat sample) in PBS-1 containing 0.05% (v/v) Tween-20 and 5% (v/v) FCS. Samples were incubated for 90 minutes at 37°C.

Wells were washed with 5 x 200 µl of wash buffer, 100 µl of secondary antibody (alkaline phosphatase conjugated to a goat anti-mouse antibody), diluted as required in diluent buffer, was added to each well and incubated for 90 minutes at 37°C. Wells were washed with 5 x 200 µl of wash buffer, and 100 µl of substrate was added per well. The substrate used was para-nitrophenyl phosphate (pNPP) provided in tablet form (final concentration 25mM), and dissolved in the required volume of dH$_2$O immediately before use, according to the manufacturer's instructions. Substrate was left to develop in the dark at room temperature, or overnight at 4°C. Absorbance readings were read at 405 nm using a Titertek plate reader.

2.5.2.2. Isotyping of Monoclonal Antibodies

ELISA plates were coated and blocked as described in section 2.5.2.1. 100 µl of hybridoma supernatant was then added to each well of the coated plate. Alkaline-phosphatase-labelled goat anti-

mouse immunoglobulin subtypes were then added to the wells and the ELISA developed as described in section 2.5.2.1. Wells giving positive results defined the monoclonal antibody isotype.

2.5.2.3. Determination of Antibody Working Dilution

ELISA plates were coated and blocked as described in section 2.5.2.1. Serial dilutions of purified monoclonal antibody were then prepared in diluent buffer, starting dilutions at 1/10. Sixteen serial dilutions were then prepared by doubling dilution in diluent buffer. 100 µl of test sample was then added to the wells of the plate in triplicate, and incubated at 37°C for 90 minutes.

Wells were then washed with 5 x 200 µl of wash buffer, and 100µl of the appropriate secondary antibody (i.e. alkaline phosphatase conjugated to a goat anti-mouse antibody) prepared in diluent buffer was added to each well, and the plate incubated at 37°C for 90 minutes. Wells were then washed with 5 x 200 µl of wash buffer and 100 µl of substrate (pNPP) was added per well. The plate was developed at room temperature in the dark or overnight at 4°C. Absorbance was measured at 405 nm using a Titertek plate reader. The antibody dilution that gave half the maximum absorbance was chosen. For the 4.2.25 monoclonal antibody producing clone supernatant, a 1/800 dilution of antibody was used in ELISA.

2.5.2.4. Determination of Optimal Conjugate Loading Density

Warfarin-BSA conjugate was prepared in PBS-1 at various concentrations, namely, 100, 50, 25, 12.5, 6.25, 3.125 and 0 µg/ml. A 50µg/ml solution of BSA control was also prepared in PBS-1 as a control. 100µl of the respective conjugate concentration was used to coat two rows of a Nunc Maxisorp immunoplates overnight at room temperature. The ELISA was developed as per section 2.5.2.3. The optimal conjugate loading density was defined as that coating density that gave the widest linear working range over the greatest range of antibody dilutions used.

2.5.2.5. Competitive ELISA

Nunc Maxisorp plates were coated and blocked as described in section 2.5.2.1. Serial dilutions of warfarin ranging in concentration from 7.81 -1000 ng/ml were prepared in diluent buffer. 50 µl of each drug concentration was then added to the wells of a coated microtitre plate, and 50 µl of purified antibody at 2 x working dilution was added to the wells of the plate. The plate was then developed as

described in section 2.5.2.1. Absorbance values were then measured at 405 nm using a Titertek plate reader. Absorbance values at each antigen concentration were then divided by the absorbance measured in the presence of zero antigen concentration to give normalised absorbance readings. A plot of the normalised absorbance reading versus antigen concentration (ng/ml) was used to construct the calibration curve.

2.5.2.6. Affinity Analysis Using ELISA

The method of Friguet *et al.* (1985) was employed. Briefly, the day before the ELISA analysis, a series of antibody-antigen mixtures were prepared in eppendorf tubes and placed on a rocking platform at room temperature overnight, and allowed to reach equilibrium. These solutions each contained a constant but unknown concentration of antibody. This concentration was nominally referred to as "1". The antibody:antigen solutions each contained a constant concentration of antibody, and varying but known concentrations of antigen ([A]). Additionally, serial doubling dilutions of antibody were prepared from that antibody dilution given the nominal antibody concentration of "1". These dilutions were used to construct a standard curve of nominal antibody concentration versus absorbance at 405 nm. The following morning, the nominal concentration of free antibody in each solution was determined by ELISA, as per section 2.5.2.1. Absorbance readings at 405nm values were related to nominal concentration values, by reference to the constructed standard curve of nominal antibody concentration versus absorbance at 405 nm. The fraction of total antibody, bound by antigen (v), was calculated for each antigen concentration. The slope of a plot of $1/v$ versus $1/[A]$ (Klotz plot) defined the dissociation constant for the interaction.

2.5.2.7. Determination of Mouse Immunoglobulin Concentrations by Affinity-Capture ELISA

Goat anti-mouse immunoglobulin which was previously affinity-purified (according to section 2.5.3.2.), was diluted to a final concentration of 1 μg/ml in PBS-1, and 100 μl added to the wells of an ELISA plate and allowed to coat overnight at room temperature. The plate was then blocked as described in section 2.5.2.1. Dilutions of mouse IgG of known concentration ranging from 3.90-1000 ng/ml were prepared in diluent buffer. Dilutions of purified antibody ranged from 1/10 to 1/10,000 and were also prepared in diluent buffer. 100 μl of the solutions containing mouse IgG of known concentration and the dilutions of purified antibody were added to the wells of the ELISA plate in triplicate. The ELISA was developed as described in section 2.5.2.1. using a goat anti-mouse alkaline phosphatase-labelled secondary antibody. A calibration curve of absorbance at 405 nm versus log of

mouse IgG concentration allowed for the determination of the mouse IgG concentration in the affinity-purified and hybridoma supernatants.

2.5.3. Monoclonal Antibody Purification

2.5.3.1. Concentration of Tissue Culture Supernatant

200 ml of conditioned supernatant from the 4.2.25 hybridoma cell line was collected over a period of time as described in section 2.5.1.3. Sodium azide was added to a final concentration of 0.02% (w/v) to the supernatants to prevent microbial growth, and stored at 4°C until required. The supernatant was concentrated 10-fold to a final volume of 20 ml, using a stirred ultrafiltration cell with a 76 mm diaflo ultrafilter membrane, with a molecular weight cut-off of 100,000 daltons, and the concentrate stored at 4°C until required.

2.5.3.2. Protein G/A Affinity Purification of Murine and Goat Anti-Mouse Immunoglobulin

1ml of a suspension of immobilised protein G (immobilised on Sepharose 4B) (stored in PBS-1 containing 20% (v/v) ethanol) was equilibrated in a column with 20ml of PBS-1. 10 ml of concentrated hybridoma supernatant, or, 2 ml of goat serum containing anti-mouse immunoglobulin was passed through the column, the eluate collected and passed through the column a second time. 25 ml of wash buffer was passed through the column and, subsequently, the retained protein was eluted with 0.1 M glycine-HCl buffer (pH 2.5). 850 μl fractions of eluate were collected in eppendorf tubes containing 150 μl of Tris-HCl (pH 8.5). Tris-HCl was used to neutralise the pH of the fractions collected so that the mAb present would not denature. The absorbance of each fraction was measured, at 280 nm. Those fractions containing significant protein were pooled, dialysed against PBS-2 and stored at −20°C until required for further use.

2.5.4. Toxicity Testing

2.5.4.1. Drug Preparations

Drug solutions (benzopyrones) were prepared fresh for each experiment. Stock solutions of all drugs were made in DMSO, from which all required drug dilutions were made into culture medium, in such a way that the final concentration of solvent exposed to cells was always less than 0.1% (v/v). In all experiments, control cells were exposed to 0.1% (v/v) DMSO in culture medium.

2.5.4.2. In Vitro Proliferation Assays

Cells were seeded into $25cm^2$ flasks at the appropriate density (see Table 2.6.) and allowed to adhere for 6 hours, prior to addition of the drug of interest (warfarin, genistein and esculetin) at the desired concentration. Incubation of cells with drugs was continued for 96 hours, after which the cell number and viability was determined using Trypan Blue as outlined in section 2.5.1.5. All experiments were carried out in duplicate on at least three separate occasions. The increase in cell number for drug-treated cells was expressed as a percentage of the increase for untreated control cells, and growth curves were constructed from this data.

Table 2.6:   *Seeding Densities for In Vitro Proliferation Assays.*

Cell Lines	Seeding Density
A549	1×10^5 cells/flask
MCF-7	2.5×10^5 cells/flask

2.5.4.3. Cytotoxicity Detection: Lactate Dehydrogenase (LDH) Assay

This assay is based on the cleavage of a tetrazolium salt when LDH is present in the culture supernatant. The principle of the LDH assay is illustrated in Figure 2.1. Cells were seeded at 5×10^4 cells/well in sterile 96 well plates, allowed to adhere (over 24hrs.) and exposed to drug concentrations (range 0-250µg/ml) for 24 hours at 37^0C. Each drug concentration was tested in 5 separate wells (in duplicate), with each experiment repeated on at least three separate occasions.

Immediately prior to testing supernatants, LDH reaction mix was prepared from the kit components as follows: 250µl of catalyst solution (Diaphorase/NAD+ mixture) was mixed with 11.25mls of dye solution (iodotetrazolium chloride (INT) and sodium lactate). Test supernatants were prepared by centrifugation of the cells in their 96 well plates at 250g for 10 mins. From each well, 100µl of supernatant was transferred to a second 96 well plate, 100µl of LDH reaction mix was added, and the plates were incubated for 30 minutes at room temperature. Absorbances at 492nm were determined on a Titertek plate reader, with a reference wavelength of 620nm. The absorbances obtained were compared to that of cells exposed to a 1% (v/v) Triton X-100 solution (maximal LDH release).
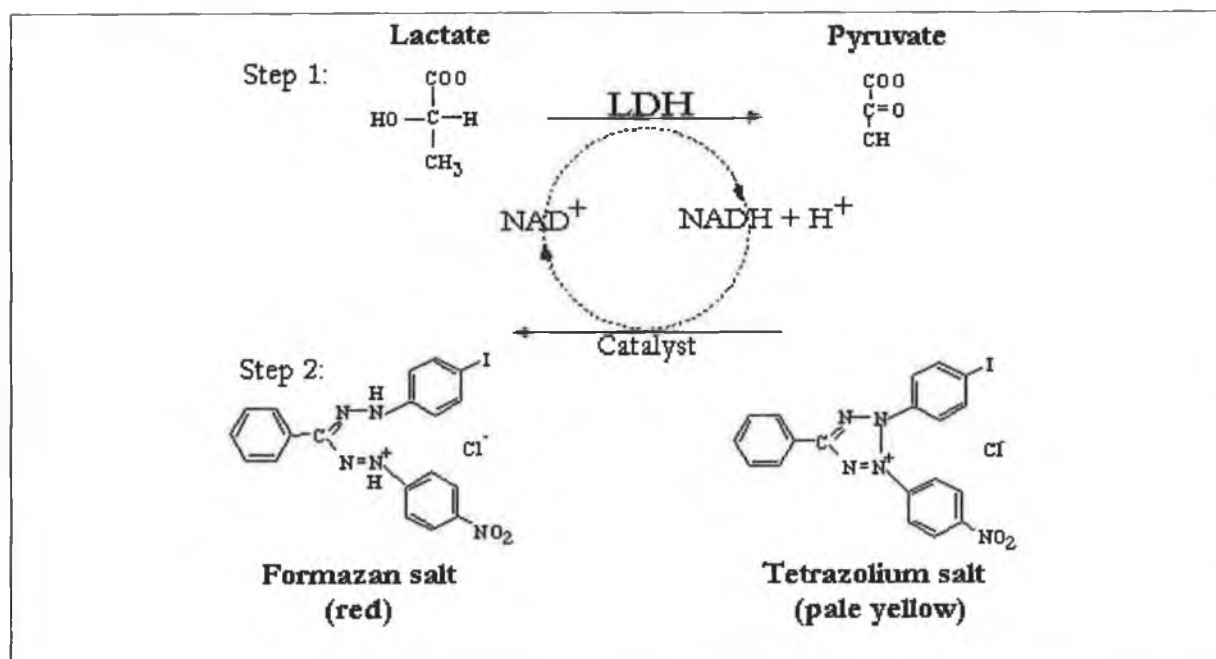
Figure 2.1: *Principle of the LDH Assay. In the 1st step, released lactate dehydrogenase (LDH) reduces NAD$^+$ to NADH + H$^+$ by oxidation of lactate to pyruvate. In the 2nd enzymatic reaction 2 H are transferred from NADH + H$^+$ to the yellow tetrazolium salt INT (2-[4-idophenyl]-3-[4-nitrophenyl]-5-phenyltetrazolium chloride) by a catalyst (diaphorase).*

2.5.4.4. MTT Assay

This non-radioactive colourimetric assay system is a modification of that first described by Mosmann *et al.* (1983), and involves the use of a tetrazolium salt, MTT (3-[4,5-dimethylthiazol-2-yl]-2,5-diphenyltetrazolium bromide). In metabolically active cells, this yellow MTT salt is cleaved to form purple formazan crystals, and as such can be used to assess the cellular metabolism and viability as shown in Figure 2.2.
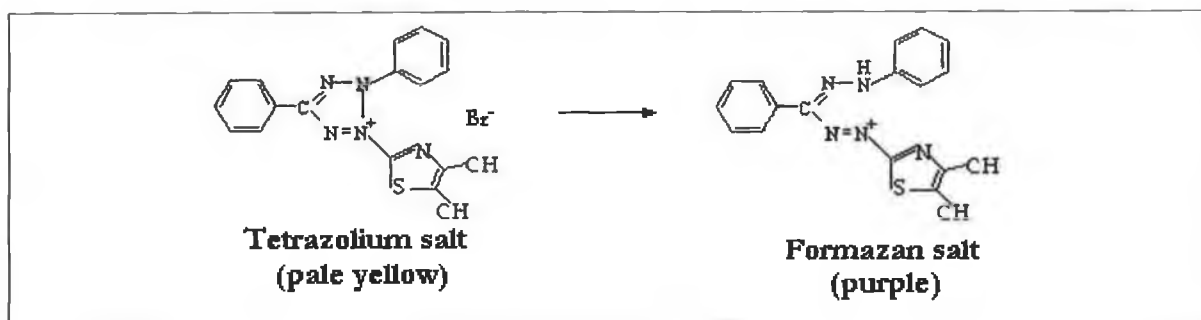
Figure 2.2: *Metabolisation of MTT to a formazan salt by viable cells.*

Cells were seeded at 5×10^5 cells/well into sterile 96 well plates, and allowed to adhere prior to the addition of 100μl of the appropriate drug solution (concentration range: 0-500μg/ml). Incubation with drug was continued for 24 hours. Following this time period, 10μl of MTT [3-[4,5-dimethylthiazol-2-yl]-2,5-diphenyl tetrazolium bromide] labelling reagent (5mg/ml in 0.1M PBS) was added to each well, and the plates were incubated at 37°C for 4 hours to allow for formazan crystal formation. 100μl of solubilisation buffer (10% (w/v) SDS in 0.01M HCl) was added to dissolve the crystals overnight. The following morning the absorbance at 560nm was read on a Titertek Twinplus plate-reader. Drug-treated cells were compared to untreated control cells. Each drug concentration was tested in 7 separate wells in a randomised manner and each experiment was repeated on at least three separate occasions.

2.5.4.5. Acid Phosphatase Assay

Acid phosphatase activity is correlated with membrane integrity and cell viability. The principle of the assay is based on the conversion of p-nitrophenyl phosphate (p-NPP) to a yellow compound called p-nitrophenol that can be quantified simply by measuring absorbance of light at 405nm as shown in Figure 2.3. Acid phosphatase activity is an accurate indicator of cell number because the amount of enzyme remains relatively constant in most cell types.
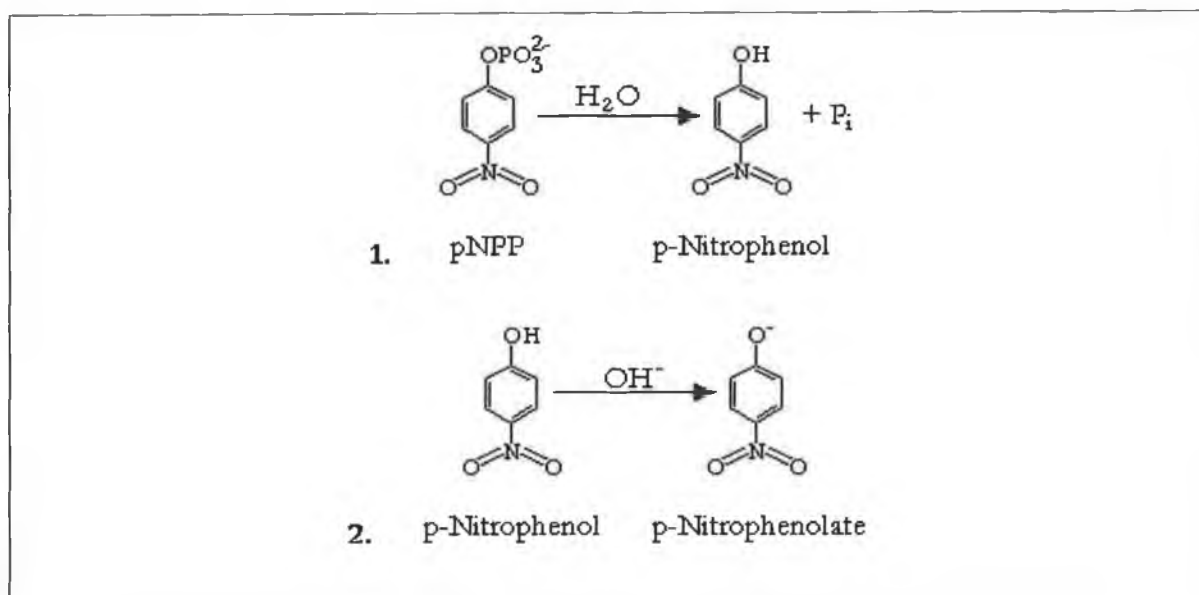
Figure 2.3: *This assay utilises the fact that viable cells have acid phosphatase activity and non-viable cells do not. Therefore, when detergent (in buffer) lyses viable cells the acid phosphatase acts on substrate pNPP also in buffer. This phosphatase-catalysed reaction changes pNPP to p-nitrophenol and inorganic phosphate. In the second part of the reaction NaOH is added to end the phosphatase assay after the two-hour incubation step. The hydroxide reacts with the p-nitrophenol to remove the phenolic proton and p-nitrophenolate is formed, which is a yellow coloured compound absorbing at 405 nm.*

Cells were seeded at 1×10^3 cells/well into sterile 96 well plates, and allowed to adhere over-night prior to the addition of 100µl of the appropriate drug solution (concentration range: 0-500µg/ml). Incubation with drug was continued for 96 hours. Following this time period, cell-culture media was poured off, and wells were washed with PBS. A substrate containing buffer (10mM p-NPP, 0.1% (v/v) Triton X in 0.1M sodium acetate, pH 5.5) was prepared and 100µl was added to each well. The plates were then incubated at 37 °C for 2 hours. After incubation the reaction was stopped by adding 50µl of 1.0M NaOH solution to each well. The absorbance at 405nm was read on a Titertek Twinplus plate-reader. Drug-treated cells were compared to untreated control cells. Each drug concentration was tested in 6 separate wells and each experiment was repeated on at least three separate occasions.

2.5.5. Cytosensor Microphysiometer Studies on Toxicity

2.5.5.1. Pre-Experimental Preparations

On the day prior to the experiment MCF-7 cells were seeded into transwell cell capsules at a density of 2.5 X 10^5 cells/capsule in DMEM.S_{10} and allowed to adhere overnight.

On the day of the experiment, running media was prepared from stock liquid 10X DMEM, as a 1X DMEM solution with a low buffering capacity i.e. without HEPES or sodium bicarbonate. Sodium chloride was added at 0.044M to compensate for the osmolarity as a result of the absence of sodium bicarbonate. Other supplements included L-glutamine (2mM), gentamycin (5μg/ml) and FCS (0.5% (v/v)). After all these additions, the pH was adjusted to 7.35 with 1M NaOH, and the media was filter-sterilised (0.22μm) using a Millipore apparatus. This media was heated to 37 °C prior to use.

2.5.5.2. Toxicity Studies

On the day of the experiment the cells were assembled onto the Cytosensor Microphysiometer, and running medium (37°C) was passed over them at a 50% flow-rate (~ 100μl/min). The cells were allowed to stabilise on the instrument for 3-4 hours. A pump cycle of 4 minutes duration was used with the acidification rate being measured in the final 30 secs of this 4-minute cycle. Once a steady base-line acidification rate was obtained the cells were exposed to drugs (Warfarin and esculetin) in the concentration range 0-100μg/ml (final concentrations in running medium) for 24 hours. The acidification rate was measured and recorded every 4 mins during this exposure period.

2.5.6. Cell Signalling Studies

2.5.6.1. ELISA for Detecting Tyrosine Kinase Activity in Whole Cells

This ELISA was developed as a modification (optimise conditions for use with different cell line) of a method published by Cooke, (1999). Sterile 96 well plates were seeded with MCF-7 cells at a density of 5×10^4 cells/well and allowed to adhere for 6 hours in DMEM.S_{10}. The cells were then subjected to a 16hr period of serum-depletion. Following this serum-free period, each well (containing MCF-7 cells) was stimulated with 100ng/ml EGF for 15 minutes at 37°C. The medium was immediately removed and the wells were washed with ice-cold PBS containing 100µM sodium orthovanadate, after which the cells were fixed with methanol for 10 minutes at -20°C. Figure 2.4 illustrates the basic steps involved in this assay.
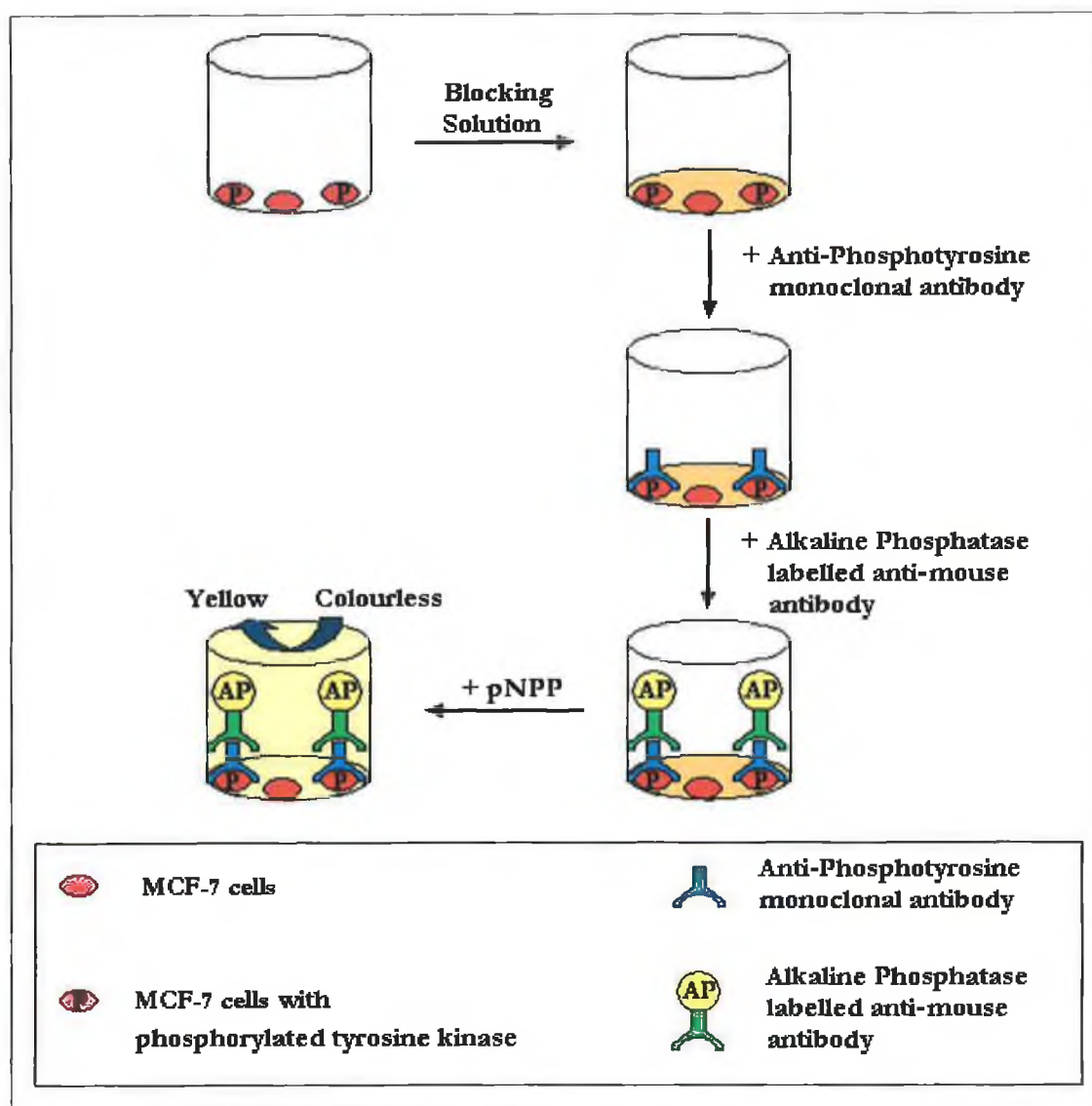
Figure 2.4: *Diagram outlining the basic protocol involved in the ELISA for the dectection of tyrosine kinase activity in MCF-7 cells.*

200μl of blocking solution (10% (v/v) FCS, 0.2% (v/v) Tween-20, 100μM sodium orthovanadate in Tris Buffered Saline, TBS, [10mM Tris-HCl, pH 8.0, 150mM NaCl]) was added per well and the plates were incubated at 37°C for 1.5 hours. After incubation, the blocking solution was removed and the plate was washed once with TBS containing 0.1% (v/v) Tween-20. 100μl of primary antibody (anti-phosphotyrosine, dilution of 1/750 in TBS containing 10% (v/v) FCS, 0.1% (v/v) Tween-20) was added per well. The plates were incubated for 1 hour at 37°C.

Following incubation the plates were washed five times with TBS containing 0.1% (v/v) Tween-20, and twice with TBS. Anti-mouse IgG-alkaline phosphatase conjugate was diluted 1/2000 in TBS containing 10% (v/v) FCS, 0.1% (v/v) Tween-20. 100μl of this solution was added per well and incubation was carried out at 37°C for 1 hour. Following incubation the plates were washed five times with TBS containing 0.1% (v/v) Tween-20 and twice with TBS. 100μl of pNPP was added per well with colour development for 45 minutes before the absorbance at 405nm was measured.

To determine the effect of the benzopyrones on tyrosine phosphorylation, the ELISA was performed as outlined above, with cells being pre-exposed to drug solutions (in the concentration range 0-100μg/ml), for 1 or 6 hours (as appropriate) prior to EGF stimulation. Controls were used which were positive tyrosine kinase inhibitors (Genistein, 1 hour and 6 hour exposure). In all experiments, increases in absorbances (405nm) in stimulated cells compared to unstimulated cells were determined. Absorbance increases for drug-treated cells were normalised versus untreated control cells. Inhibition of tyrosine kinase activity was demonstrated if the absorbance increase for the drug-treated cells was diminished compared to the absorbance increase for control cells.

2.5.6.2. Cytosensor Studies for Detecting Tyrosine Kinase Activity

2.5.6.2.1. Pre-experimental Preparations

On the day prior to the experiment, MCF-7 cells were seeded into transwell cell capsules at a density of 2.5×10^5 cells/capsule in DMEM.S_{10} and allowed to adhere for 6 hrs. Serum-free medium was then used to replace the culture medium and the cells were serum-starved for 16 hours. Running media was prepared from stock liquid 10X DMEM, as a 1X DMEM solution with a low buffering capacity i.e. without HEPES or sodium bicarbonate. Sodium chloride was added at 0.044M to compensate for the osmolarity as a result of the absence of sodium bicarbonate. Other supplements included L-glutamine (2mM), gentamycin (5μg/ml) and BSA (1mg/ml). After all these additions the pH was adjusted to 7.35 with 1M NaOH, and the media was filter-sterilised (0.22μm) using a Millipore apparatus. The media was heated to 37°C prior to use.

2.5.6.2.2 Optimisation of EGF Stimulation

On the day of the experiment the cells were assembled into the Cytosensor Microphysiometer and running medium (37°C) was passed over them at a 60% flow-rate (~120μl/min). The cells were allowed to stabilise on the instrument for 3-4 hours. A pump cycle of 2 minute duration was used, with

the acidification rate being measured in the final 30 secs of this 2 minute cycle. Once a steady base-line acidification rate was obtained, the cells were exposed to various concentrations of EGF in the range (0-100ng/ml). By carrying out these experiments in triplicate, it was determined that the maximal response was obtained at 200ng/ml of EGF and this was used in all subsequent experiments (Section 2.5.6.2.3.)

2.5.6.2.3. EGF-Receptor Tyrosine Kinase Inhibition Studies

The passing of EGF (200ng/ml) over MCF-7 cells on the Cytosensor Microphysiometer was shown from experiments in Chapter 4 to cause a substantial (~ 20%) increase in the acidification rate of the cells. This increase was mainly due to the activation of the receptor-associated tyrosine kinase (on EGF binding to the receptor), and could be blocked by pre-exposure of the cells to the tyrosine kinase inhibitor, genistein.

In order to determine if the benzopyrones could inhibit the activation of the EGF-RTK the cells were pre-exposed to warfarin (0-20µg/ml) or esculetin (0-20µg/ml) for either 1 or 6 hours prior to the EGF stimulation (200ng/ml). In all the cytosensor (tyrosine kinase inhibition) experiments genistein was used as the positive control.

2.5.6.3. BrdU ELISA for DNA Synthesis Determination

The BrdU ELISA is designed as a precise, simple and fast colorimetric alternative to determine DNA synthesis in viable cells by measurement of pyramidine analogue, 5-bromo-2'-deoxyuridine (BrdU) incorporation during DNA synthesis in actively proliferating cells. After its incorporation into newly synthesised DNA, BrdU is detected by ELISA. This is achieved with the help of a murine monoclonal antibody conjugated with peroxidase. This monoclonal antibody recognises and binds to BrdU incorporated into the DNA of proliferating cells and is known as Anti-BrdU-POD. When the substrate solution, tetramethyl-benzidine (TMB) is added it reacts with the anti-BrdU-POD to give a colour change which can be detected using a plate reader set at the appropriate wavelength (Figure 2.5.).
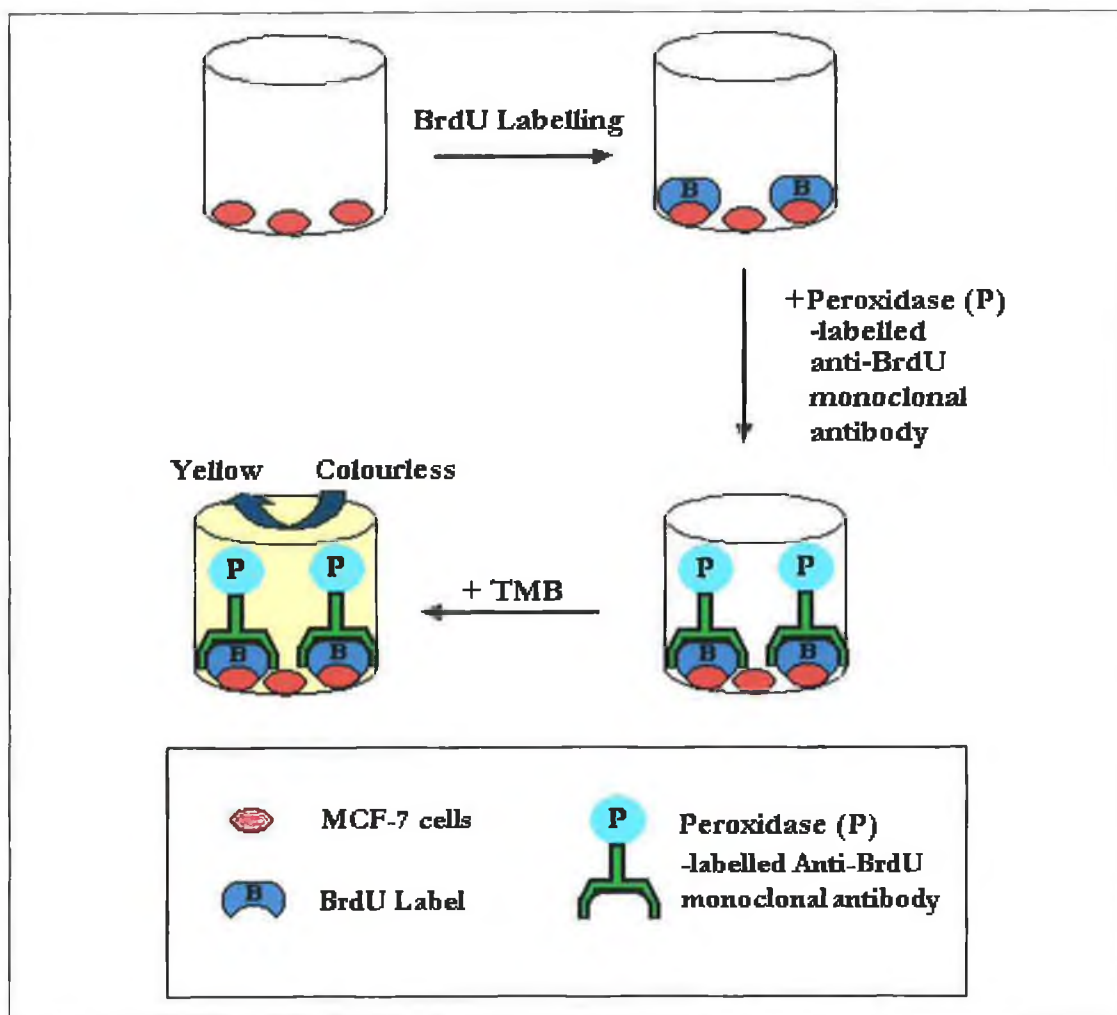
Figure 2.5: *Diagram outlining the basic protocol involved in the BrdU ELISA.*

MCF-7 cells were seeded at 5×10^5 cells/well (100μl/well) into sterile 96 well plates, and allowed to adhere over night (37°C, CO_2 incubator) prior to the addition of 100μl of the appropriate drug solution (concentration range: 0-100μg/ml) and final volume was 200μl/well. Incubation with drug was continued for 24 hours. Following this time period 20μl/well of BrdU labelling solution was added to each well (final concentration: 10μM BrdU). The cells were then reincubated for an additional 2 hours at 37°C. After this time the labelling medium was removed by tapping off. 200μl/well of FixDenat solution (cell fixing solution) was added to each well and the microtitre plate was incubated for 30 mins at room temperature. The FixDenat solution was then removed from each well by flicking off and tapping plates. 100μl of anti-BrdU-POD working solution was added to each well except the wells reserved as background controls. The microtitre plates were then incubated for 90 mins at room temperature. The antibody conjugate was removed by flicking off and rinsing the

wells three times with 200µl/well wash solution (PBS). This wash solution was removed by tapping and 100µl of substrate solution (TMB) was added to each well. Finally, microtitre plates were incubated at room temperature until colour development was sufficient for photometric detection (5-30 mins) at 370nm.

2.5.7. Protein Techniques

2.5.7.1. BCA Protein Assay

The BCA assay was used to detect protein quantitatively and was obtained commercially as a kit from Pierce, Rockford IL. In this assay, Cu^{2+} reacts with protein under alkaline conditions to give Cu^+, which reacts with BCA to give a coloured product. Two separate reagents are supplied as part of the kit: Reagent A, an alkaline bicarbonate buffer, and Reagent B, a 4% (w/v) copper sulphate solution. The working solution was prepared fresh each time by combining 50 parts of Reagent A to 1 part Reagent B. Protein standards in the range 0-1mg/ml were prepared in 0.1M PBS, pH 7.4.

For the assay 10µl of sample or standard was placed in the well of a 96-well plate. 200µl of the BCA working solution was added and the plate was gently swirled to ensure mixing of the solutions. The plate was then incubated at 37°C for 30 mins, before the absorbance of each well at 560nm was determined on a Titertek Twinplus plate-reader. All standards and samples were determined in triplicate. The absorbances of the standard solutions were used to construct a standard curve from which the protein concentration of the samples could be determined.

2.5.7.2. Polyacrylamide Gel Electrophoresis (PAGE)

Polyacrylamide gel electrophoresis (PAGE) was carried out using the discontinuous system, in the presence of sodium dodecyl sulphate (SDS), as described by Laemmli (1970). 8% (w/v) resolving and 4% (w/v) stacking gels were normally used and prepared from the following stock solutions as outlined in Table 2.4.

2.5.7.3. Staining of Gels with Coomassie Brilliant Blue

Gels were stained with Coomassie staining solution for visualisation of protein bands. Gels were stained for 1 hour in 0.2% (w/v) Coomassie Brilliant Blue in methanol:acetic acid:distilled water (3:1:6). Gels were destained overnight in methanol:acetic acid:distilled water (3:1:6).

2.5.8. BIAcore Studies

2.5.8.1. Preconcentration Studies

The BIAcore™ with CM5 chips, was used for all 'real-time' analyses. For a detailed description of the theory and practice of this instrument, the reader is referred to Jönnson *et al.* (1991) and Chapter 5 of this thesis. For preconcentration studies, warfarin-BSA was dissolved at a concentration of 50 µg/ml in 10 mM sodium acetate buffer, at a range of pH values between 3.8-5.5. These were passed, sequentially, over an underivatised chip surface, and that pH giving the greatest mass (measured in terms of response units (RU)) pre-concentrated at the surface of the chip, was used for subsequent warfarin-BSA immobilisation procedures.

2.5.8.2. Immobilisation of Drug-Protein Conjugates

The chip surface was activated, by passing 35 µl of a solution containing 0.05 M NHS and 0.2 M EDC in ultra-pure (UP) H_2O, over the chip surface at a flow rate of 5 µl/min. 35 µl of a solution of warfarin-BSA in 10 mM acetate buffer, pH 4.8, was passed over the surface at a flow rate of 5 µl/min. Unreacted NHS groups were 'capped' by passing 35 µl of a 1 M ethanolamine (pH 8.5) solution over the surface at a flow rate of 5 µl/min.

2.5.8.3. Direct Immobilisation of Drug on to the Chip Surface

Direct immobilisation of drug directly onto the chip surface, was performed manually outside the BIAcore instrument. The chip was first allowed to equilibrate to room temperature. 40 µl of HBS buffer (Section 2.4.) was added to the sensor chip well and left for 5 minutes (in order to prime the chip surface). This solution was then removed using lint-free adsorbent paper, without the paper touching the dextran matrix. Equal volumes of 0.4 M EDC and 0.1 M NHS were then mixed, and 40 µl of the resulting solution, containing 0.05 M NHS and 0.2 M EDC in UPH_2O, was added to the chip well and left for 15 minutes. The EDC/NHS was then removed using adsorbent paper. 4'-aminowarfarin, at a concentration of 50 µg/ml in 10m M sodium acetate buffer, pH 5.5, was then added to the chip well and allowed to react for 20 minutes. The chip was then blocked by adding 40 µl of a 1.0 M ethanolamine (pH 8.5) solution to the chip well and left for 20 minutes. The chip was then extensively washed with distilled water and dried under nitrogen. The chip could then be stored in HBS or in a desiccator for use with subsequent assays (1-2 months).

2.5.8.4. Regeneration Studies

To assess the stability of the immobilised drug-protein conjugates or directly immobilised drug surfaces, a known concentration of antibody was passed over the chip surface and the surface regenerated with mild acid/base solution (10-25 mM HCl was usually sufficient to dissociate the complex). This cycle of binding and regeneration was usually completed for greater than 50 cycles, and the binding signal measured to assess the stability and suitability of the immobilised surface for assay purposes.

2.5.8.5. Non-Specific Binding Studies

Bovine serum albumin (BSA) (~8000 RU) was immobilised on one of the flow cell surfaces of a sensor chip. A separate flow cell surface was left blank (no compound immobilised) and allocated as the dextran surface for non-specific binding studies. Purified monoclonal antibody solutions, and hybridoma supernatants at the requisite dilution (i.e. 1/100 dilution) were passed over the blank CM-dextran and BSA-immobilised sensor chip surfaces. The degree of non-specific binding of the monoclonal antibody to both the dextran layer and the immobilised BSA portion of the drug-protein conjugate was determined from the sensogram data which evaluated the amount of antibody bound (in RU) to either surface.

2.5.8.6. Competitive/Inhibition Assays

Warfarin was prepared at a series of concentrations ranging from 0.03-5,000 ng/ml by serial dilution, using Hepes Buffered Saline (HBS), pH 7.4 as diluent (Section 2.4). Antibody was then mixed with the various antigen concentrations using the BIAcore autosampler. The antibody:antigen mixture was allowed to equilibrate for a specified time interval (normally 5-10 minutes). The equilibrium mixtures were then passed sequentially, in random order, over the chip surface at 10 μl/min for 4 minutes, and the chip surface regenerated between cycles by pulses of the appropriate regeneration solution for each antibody type. The amount of bound antibody following injection of the antibody:antigen mix was measured in terms of response units (R). The respective responses (R), were then divided by the response measured for the antibody:antigen mixture containing zero antigen (R_0), to give normalised binding responses (R/R_0). A plot of antigen concentration ng/ml versus normalised binding responses (R/R_0) could then be used to construct the calibration plot using BIAevaluation 3.1 software.

2.5.8.7. Solution Affinity Analysis Using Biacore

Warfarin-BSA (13,000 RU) was immobilised using the conventional EDC/NHS coupling chemistry. Serial dilutions of Protein G-purified anti-warfarin monoclonal antibodies of known concentration were passed over the immobilised surface, and a calibration curve was constructed of mass bound measured in terms of response units, versus antibody concentration (nM). A known concentration of antibody was then incubated with varying concentrations of warfarin (nM), and allowed to reach equilibrium overnight. The equilibrium samples were then sequentially passed over the immobilised surface and the binding response calculated. The response values measured were used to calculate the amount of 'free antibody' in the equilibrium mixtures, from the constructed calibration curve. A graph was then constructed of drug concentration (nM) versus 'free antibody concentration' (nM), and using the solution phase interaction models in BIAevaluation 3.1 software, the overall affinity constant could be determined.

2.5.8.8. Steady State Affinity Analysis Using Biacore

Warfarin-BSA (~1200 RU) and BSA (~1500 RU) were immobilised on separate flow cell surfaces of a sensor chip. Serial dilutions of purified monoclonal antibodies to warfarin of known concentration, were then sequentially passed over the chip surfaces using 'on-line' reference curve subtraction. A graph was then constructed of the equilibrium binding response (Req) measured versus antibody concentration (nM). Using the steady-state interaction model in BIAevaluation 3.1 software, the affinity constant could then be calculated for the interaction.

Chapter 3

Characterisation and Applications of Monoclonal Antibodies to Warfarin

3.1. Introduction

Antibodies are serum-proteins called immunoglobulins that are produced by B-lymphocytes in response to a foreign substance (i.e. antigen). Antibodies may be raised to almost all classes of substances including, proteins, polysaccharides, nucleic acids and complex particles (e.g. pollens, infectious agents and cells). They typically exhibit high binding affinities for the target antigen and mediate many biological effector functions as part of the humoral immune system. Those most commonly produced and used for analytical applications have been either entire or partial antibodies of the subclass immunoglobulin G (IgG) (Jefferis & Deverill, 1992).

3.1.1. Antibody Structure

An illustration of a typical antibody, an immunoglobulin G (IgG) molecule, is shown in Figure 3.1. An antibody is a Y-shaped molecule that possesses two identical antigen-binding sites. Each binding site is formed from two polypeptide chains, one heavy (H) chain (50 kDa) and one light (L) chain (25 kDa) that are coupled together by a disulphide bridge. The heavy chain consists of four domains named from the binding site as V_H, C_H1, C_H2, and C_H3. C stands for constant domain (Crowther, 1995). The variable region is composed of the variable heavy (V_H) and variable light (V_L) domains, which demonstrate amino acid variability between antibodies. The variable region is further subdivided into hypervariable (HV) and framework (FR) regions (Steward, 1984). Hypervariable regions have a high ratio of different amino acids in a given position, relative to the most common amino acid in that position. Within light and heavy chains, three hypervariable regions exist – HV 1, 2 and 3. Four FR regions, which have more stable amino acids sequences, separate the HV regions. The HV regions directly contact a portion of the antigen's surface. For this reason, HV regions are also sometimes referred to as complementarity determining regions (CDRs). The FR regions form a beta-sheet structure, which serves as a scaffold to hold the HV regions in position to contact the antigen. The CDRs differ in length and sequence between different antibodies and are mainly responsible for the specificity (recognition) and affinity (binding) of the antibodies to their target markers. Proteolytic digestion of antibodies releases different fragments termed Fv (Fragment variable), Fab (Fragment antigen binding) and Fc (Fragment crystallisation). Antibody engineering can join the separate segments of the heavy and light chains in the Fv with a flexible peptide linker to form a single-chain Fv (scFv).

X-ray crystallographic studies have established that six CDRs form the strongest contacts with the antigen and define the antibody binding properties. The CDRs from both V_H and V_L domains

associate in three-dimensional space to form the antigen-binding site (idiotype). The CDR region can be further sub-divided into three different regions (i.e. CDR1, CDR2 and CDR3) of about 10 amino acid residues in length between which lies more conserved sequences known as the framework residues. When the heavy and light chains are created, the variable (V) region is formed and the CDR sequences are exposed, forming a cleft that serves as the antigen-binding pocket. It is the precise amino acid sequence, shape and positioning of this cleft or pocket resulting from the combination of the six CDR sequences which form hypervariable loops that confers the particular antibody specificity. Furthermore, studies indicate that the V_H region plays a greater role in antigen-binding than the V_L region (Davies, 1994a).

There are five main classes of antibody (isotypes) that have been resolved, which differ in the structure of their heavy chains (Table 3.1). The basic four-chain model holds for all antibody isotypes with specific heavy chains for each class, γ for IgG, μ for IgM, δ for IgD, α for IgA and ε for IgE (Cahill *et al.*, 1995; Bengten *et al.*, 2000). The light chains are serologically divided into κ and λ chains, although these are similar in each isotype class. In addition, each antibody isotype is segregated into sub-classes such as IgG_1 and IgG_{2a} (Jefferis & Deverill, 1992). Antibody function is largely determined by the specificity and affinity of the antigen-binding site and by the heavy chain isotype.

Table 3.1: *Functions and Structural Features of Antibody Isotypes*

Characteristic	IgG	IgM	IgD	IgA	IgE
Molecular Weight	150 kDa	950 kDa	175 kDa	165 kDa (monomeric) 390 kDa (secretory)	190 kDa
Subunits	1	5	1	1,2 or more	1
Heavy chain domains	4	5	4	4	5
Heavy chain	γ	μ	δ	α	ε
Light chain	κ or λ	κ or λ	κ or λ	κ or λ	κ or λ
Molecular Formula	$\gamma_2\kappa_2,$ $\gamma_2\lambda_2$	$\mu_2\kappa_2,$ $\mu_2\lambda_2$	$\delta_2\kappa_2,$ $\delta_2\lambda_2$	$(\alpha_2\kappa_2)1,2,3$ or 4 $(\alpha_2\lambda_2)1,2,3$ or 4	$\varepsilon_2\kappa_2,$ $\varepsilon_2\lambda_2$
Subclasses	IgG_1, IgG_2, IgG_3 & IgG_4	none	none	IgA_1 & IgA_2	none
Valency	2	5/10	2	4	2
Concentration in serum	8-16 mg/ml	0.5-2 mg/ml	40 µg/ml	1-4 mg/ml	0.4 µg/ml
Half-life	$IgG_{1,2}$ & $_4$: 23 days IgG_3: 8 days	5 days	3 days	6 days	2.5 days
Polymer unit	Monomer	Monomer (membrane) Pentamer (secreted)	Monomer	Monomer, dimer, trimer & tetramer	Monomer
Function	• Main serum antibody in secondary response • ability to bind many cell types and to fix complement (varies with subclass)	• First to be produced in a primary response • low affinity but high avidity to multivalent antigens • complement fixation	• Primarily a cell surface receptor • expression varies during B cell differentiation	• Chief Ig component of external secretions (e.g. saliva, sweat, tears)	• Triggers inflammatory reactions via specific receptors on mast cells and basophils • elicits effector responses to some gut parasites
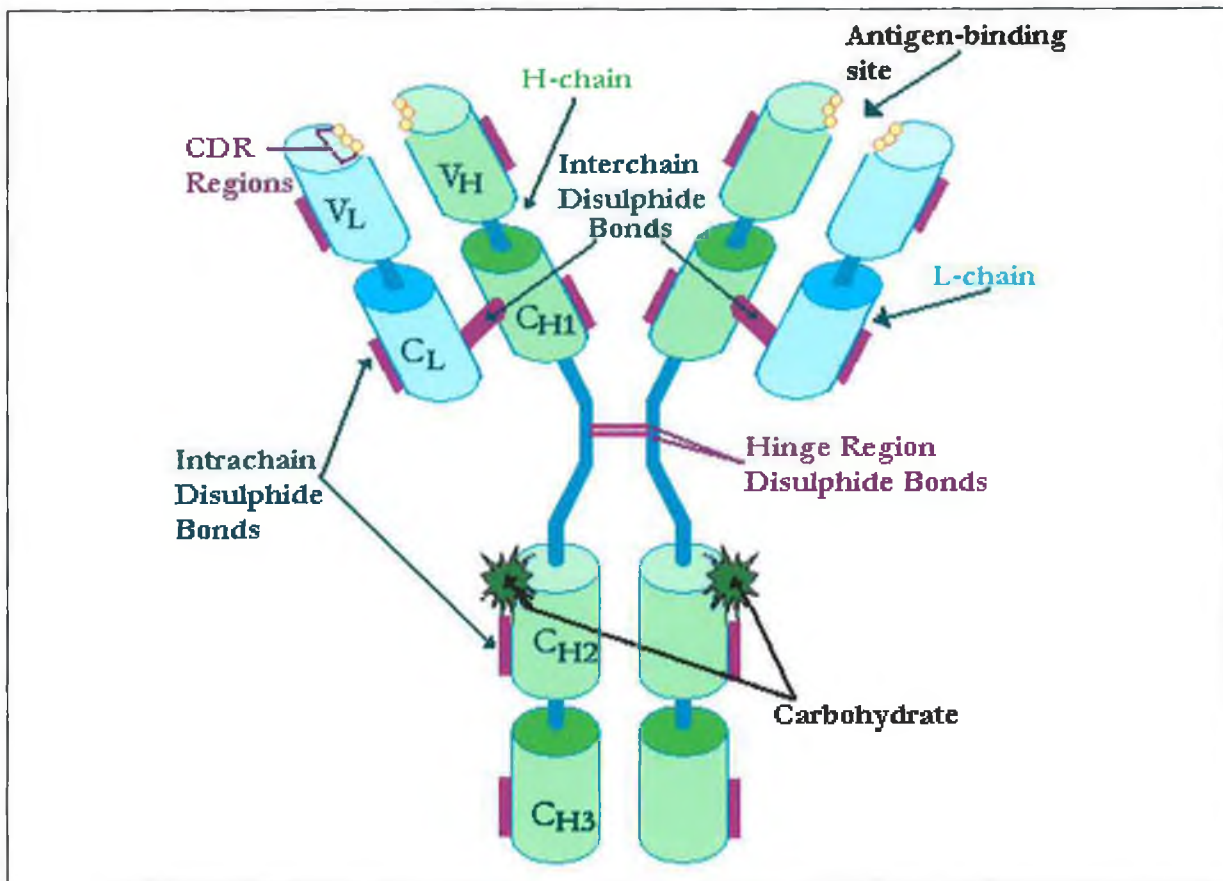
Figure 3.1: *Illustration of an immunoglobulin G molecule. The molecule is composed of four peptide chains that fold into domains, which are stabilised by disulphide bonds. Interchain disulphide bridges connect the heavy and light chains; there are also intrachain disulphide bonds that form loops within the chain. Both antigen-binding sites are formed by association of the variable region of the heavy chain (V$_H$) with the variable region of the light chain (V$_L$) and the amino acid residues that form the binding contacts with the antigen are located in the CDR regions. The CDR regions confer specificity to the particular antibody-binding site, and exhibit high amino acid sequence variability. Carbohydrate residues are commonly located along the constant domains but the biological role of these residues is uncertain.*

3.1.2. Monoclonal Antibodies

Traditionally, all antibody sera were purified from whole blood extracted from an animal that had undergone an immunisation procedure against the target antigen. These polyclonal antibody preparations are composed of many antibody isotopes with specificities for a range of epitopes located

on the antigen surface. This heterogeneity limited the application of polyclonal antibodies in many areas.

In 1975, César Milstein and Georges Köhler at the Medical Research Council's (MRC) Laboratory of Molecular Biology (LMB) in Cambridge (UK) worked out a way to produce "custom-built" antibodies *in vitro* with relative ease (Köhler & Milstein, 1975). Monoclonal antibodies (mAbs), derived from the progeny of a single immune cell, were pure and available in potentially unlimited quantities. Since then mAbs have become essential reagents for both highly specific protein detection and the characterisation of protein structure and function. The combined properties of hybridoma immortality and the exquisite specificity of the monoclonal antibody (mAb) produced have been readily exploited for the creation of standardised reagents for diagnostic assays and, more recently, novel therapeutic agents (Bruce *et al,* 2002).

3.1.2.1. Production of Monoclonal Antibodies Following Immunisation

In order to produce monoclonal antibodies, an animal such as a mouse or rat is initially immunised with the antigen of interest. The serum response of the animal is directly monitored for antibody production to the antigen. When an adequately high serum titre is attained the animal is sacrificed and the spleencocytes are harvested for cell fusion procedures (Sikora & Smedley, 1984). A variety of myeloma cell lines are commercially available as suitable fusion partners and the most frequently employed include X63-Ag8.653 and Sp2/0-Ag14 cell lines, which were produced from a myeloma cell line developed following the injection of mineral oil into the peritoneal cavity of mice (Delves, 1995). Kohler and Milstein (1975) developed a method, by which spleen lymphocytes were activated *in vivo* and then fused to myeloma cells using polyethylene glycol (PEG), yielding hybridoma cells. Even though the initial report by Köhler & Milstein used Sendai virus as the fusogen, almost all researchers subsequently used PEG to induce cell fusion and procedures are well established for fusing cells with PEG (Gefter *et al.,* 1977; Herzenberg *et al.,* 1978). Once spleenocytes are fused with myeloma cells it is necessary to eliminate unfused cells as not all myeloma cells will have fused with spleenocytes to form hybridomas and remain growing healthily in an unfused state. This is accomplished by utilising a myeloma cell line deficient in the enzyme responsible for incorporation of hypoxanthine into DNA. Cells can synthesize DNA in two ways, either by *de novo* synthesis or via the 'salvage' pathway using exogenous sources of preformed bases as summarised in Figure 3.2a. If myeloma cells are grown in the presence of a purine analogue, for example 8-azaguanine or 6-thioguanine, the hypoxanthine guanine phosphoribosyltransferase (HGPRT) enzyme catalyses the incorporation of the purine analogue into DNA where it interferes with normal protein

synthesis and so the cells die. Gene coding for the HGPRT enzyme is on the X chromosome, so only a single copy per cell is expressed. Cells will arise that are deficient in the HGPRT gene and therefore do not incorporate the purine analogue, i.e. HGPRT-deficient cells which are unable to utilise hypoxanthine and therefore, can only synthesise ribonucleotides by *de novo* synthesis (Figure 3.2b). A selective medium containing Hypoxanthine, Aminopterin, and Thymidine (HAT medium) is used. Aminopterin (analogue of folic acid) binds folic acid reductase and blocks the coenzymes required for *de novo* synthesis DNA. To grow in this medium a cell must make DNA via the 'salvage' pathway. If HGPRT-deficient myeloma cells are fused with normal spleenocyte cells and then placed in HAT medium, only the hybrids between myelomas and normal cells will grow (myeloma cell provides immortality; spleenocyte provides the HGPRT enzyme – Figure 3.2c) The hybridoma cells are a permanent cell line and have the ability to grow in culture and to secrete a defined antibody. The secreted antibodies can then be screened for binding to antigen by enzyme-linked immunosorbent assay (ELISA). Those hybridoma cells secreting antibody that binds to antigen are cloned by limiting dilution to yield one cell per well. Therefore, all resulting cells are derived from a single parent cell (Sikora & Smedley, 1984).
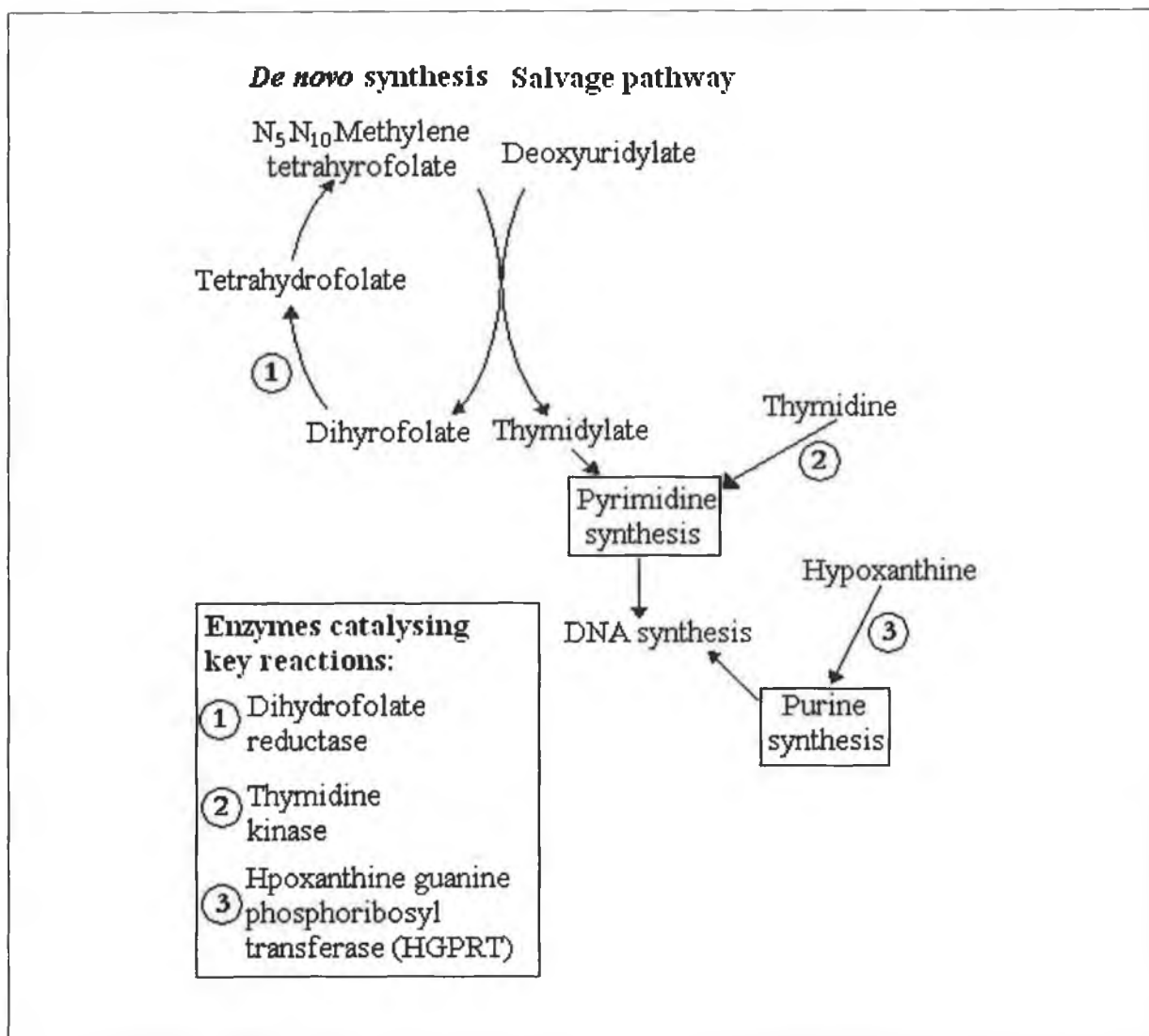
Figure 3.2a: Pathways of DNA synthesis in cells. Most cells can make DNA either by de novo synthesis or via the 'salvage' pathway, using an endogenous or exogenous source of preformed bases (Hay & Westwood, 2002).

Block *de novo* pyrmidine synthesis

Aminopterin (A) blocks the enzyme dihyrofolate reductase

Block salvage pathway of preformed bases (pyrimidines and purines) by selecting for myeloma fusion partners that lack key enzymes HGPRT and TK

DNA

Supply of key enzymes HGPRT and TK from normal spleenocyte fusing with mutant myeloma allows synthesis of pyrimidines and purines from hypoxanthine (H) and thymidine (T) present in HAT medium

Figure 3.2b: In order to select cells which are solely the result of fusion with a normal antibody-forming cell with a myeloma cell, de novo DNA synthesis is partially stopped with aminopterin A. This reagent blocks the enzyme dihydrofolate reductase, while the 'salvage' pathway is blocked by preselecting for the myeloma cells that can survive in the presence of the lethal purine analogues, 8-aza or 6-thioguanine. These cells lack the key salvage pathway enzymes: hypoxanthine guanine phosphoribosyltransferase (HPGRT) and thymidine kinase (TK). These enzymes are then supplied by the normal antibody-forming partner cell (Hay & Westwood, 2002).
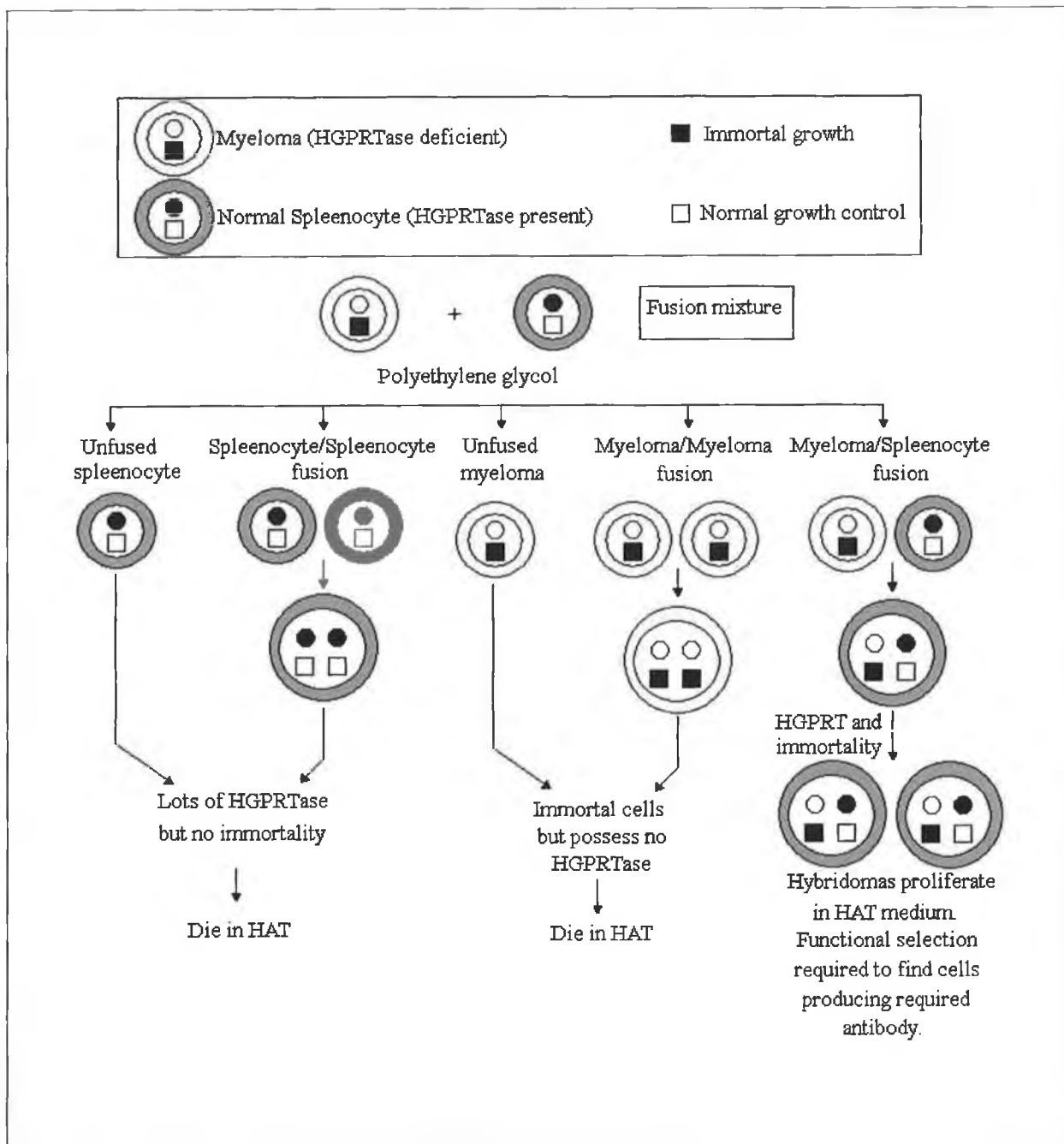
Figure 3.2c: *The myeloma 'parent' is HGPRT-deficient and so is unable to grow in HAT medium. HAT contains either the folic acid analogue aminopterin or the amination inhibitor, azaserine, which block de novo synthesis. Since these cells cannot use hypoxanthine they die. Hybrid cells grow out from HAT medium because DNA from the normal partner provides the information to synthesize HGPRT and the myeloma cell DNA provides the 'message' for unrestricted proliferation (Hay & Westwood, 2002).*
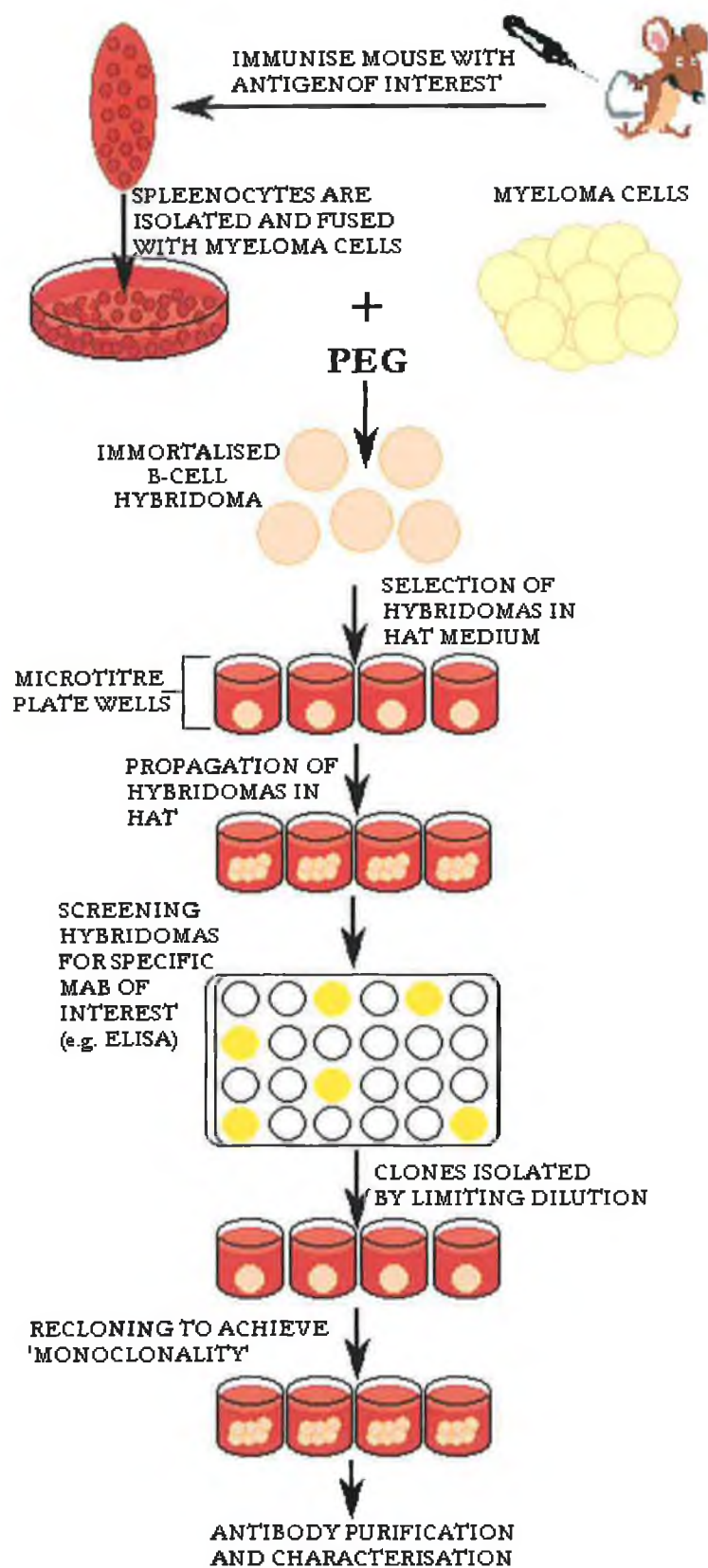
Figure 3.3: *Principle of Monoclonal Antibody Production*

3.1.2.1.1. Production of Monoclonal Antibodies to Small Haptens

The ability of a particular molecule to provoke an immune response is known as immunogenicity and is dependent upon a variety of factors such as molecular weight, chemical composition and 'foreignness'. Substances with a molecular weight of approximately 100,000 Da are the best immunogens, while molecules with a molecular mass of less than 1,000 Da (haptens) do not usually cause antibody production (Kuby, 1997). The prospect of raising mAbs with high affinity for the target antigen is greatly reduced for haptens with a molecular weight of <1000 Da and mAbs to such small haptens can only be generated using the hapten conjugated to a carrier molecule. One of the potential problems is that a hapten alone is too small to cross-link lymphocyte cell-surface receptors and so will not stimulate B-cell differentiation to plasma cells and antibody production. The B-cell response to antigen, in the majority of cases, requires co-operation by T-cells. Again because of its small size, the hapten cannot stimulate two lymphocytes simultaneously. This may be overcome by hapten conjugated to an immunogenic protein. The T-cells will recognise this protein, or carrier molecule, and so co-operate with B cells to produce anti-hapten antibody (anti-carrier antibody is also produced) (Hay & Westwood, 2002). The most frequently used carriers are highly immunogenic proteins (e.g. Bovine Serum Albumin [BSA]; 67kDa, Ovalbumin; 45kDa), but lipid bilayers, polymers (e.g. dextran), and synthetic organic molecules have also been used (Hermanson, 1996). Carriers must be inherently immunogenic, possess suitable functional groups for covalent linkage and be non-toxic *in vivo*.

Fasciglione *et al.,* (1996) recognised three crucial aspects for the production of conjugates (e.g. warfarin-BSA). These consist of the hapten conjugation method employed, the choice of carrier molecule and the amount of neodeterminants introduced. The conjugation method should enhance the specific antibody response to the hapten. It was determined that the choice of carrier protein specifically modulates the serum titre and affinity of clones generated. Hydrophobic haptens are capable of modifying the tertiary structure of carrier proteins and become hidden in the core of protein, thereby limiting the interaction with the immune response and serum response generated. Hence, it was suggested that specific hydrophilic carriers such as poly-L-lysine and sepharose be used for small hydrophobic haptens (Fasciglione *et al.,* 1996). Hapten-protein conjugates can be utilised at the screening stage of antibody production. When screening for the presence of specific antibody it is necessary to use a conjugate containing a different protein moiety than the immunogen to minimise false positive results. This finding is supported by reports of difficulties associated with the selection of antibodies to small molecular weight haptens during screening procedures, resulting in the selection of antibodies sharing a combined drug-protein epitope (Danilova, 1994; Keating, 1998; Killard, 1998).

97

The use of conjugates employing different coupling chemistries and carrier protein homology than those used for immunisation procedures is thus strongly recommended. Danilova (1994) suggested that, when dealing with very small haptens, the conjugate used for screening should possess a different carrier molecule and coupling chemistry than that used for immunisation.

There are a variety of coupling chemistries available for coupling proteins to small molecules such as warfarin. The choice of coupling chemistry employed is generally selected as a result of the chemical residues available for coupling and whether or not spacer molecules need be employed to distance the molecule from the carrier protein. Many aromatic ring systems contain active hydrogens, which can easily be displaced by attacking electrophilic groups. Diazonium groups are particularly reactive with these active hydrogens, and are a useful means of attachment for molecules with few available functional groups (Hermanson, 1996). Amino groups on phenolic compounds can be converted to diazonium groups by reaction with sodium nitrite in acidic conditions. The diazonium group reacts rapidly with the aromatic ring of tyrosine and histidine residues on protein molecules. Fitzpatrick (2001) used this conjugation procedure for the coupling of (4'-AW) 4'-aminowarfarin to various proteins (i.e. thyroglobulin, keyhole limpet haemocyanin (KLH), bovine serum albumin (BSA) and ovalbumin). Drug-protein conjugates containing diazonium bonds yield highly coloured complexes that are also extremely stable. Examples of haptens to which mAb were raised against include 5-benzimidazolecarboxylic acid (TBZ) a broad-spectrum anthelmintic and O,O-diethyl O-(5-carboxy-2-flurophenyl) phosphorothioate a conserved structure of organophosphorus pesticides (Jang *et al.*, 2002; Moran *et al.*, 2002). A recent application of using mAbs to detect haptens concerns the development of an immunochemical rapid test for multiresidue analysis of antimicrobial drugs in milk using a hapten-glucose oxidase conjugate (Strasser *et al.*, 2003).

3.1.2.1.2. Clinical Applications of Monoclonal Antibodies

Monoclonal antibodies have become the cornerstone of most diagnostic kits, immunoaffinity procedures and are extensively used for the detection of a wide variety of target antigens ranging from pesticides, illicit drugs and toxins to blood markers (Markowska, 2003). Their use in the monitoring of environmental (e.g. pesticides, pollutants) and food (e.g. growth promoters) residues were recently reviewed (Fitzpatrick *et al.*, 2000). Monoclonal antibodies have become an extraordinarily important resource for medical research, diagnosis and therapy. However, the design of a therapeutic strategy requires consideration of certain factors including short- and long-term side-effects as well as benefits of monoclonal antibody use. Particular attention needs to be paid to deciding which therapeutic effect is most desirable and how it is expected that the antibody may produce that effect (Waldmann, 1989).

Over a century ago, Paul Ehrlich proposed that antibodies could be used as "magic bullets" to target and destroy human diseases. This vision is still being pursued today for many kinds of therapy, such as in the treatment of malignancies, where a "toxic payload" (such as a radioactive element or a plant toxin) attached to the antibody can be accurately delivered to the target. This confers potential suitability for homing in on and killing cancer cells, infectious diseases (bacteria, viruses and their toxins) as well as modulating the immune system by binding and inhibiting or enhancing its regulatory molecules and thus curing autoimmune and inflammatory diseases.

The impact of mAbs in the treatment of human tumours has greatly increased in recent years (Bestagno *et al.*, 2003). Lin and co-workers (2003) investigated the effects of an anti-basic fibroblast growth factor mAb (bFGF-mAb) on the proliferation, invasion and angiogenesis of ovarian cancer. They determined that the bFGF-mAb was capable of inhibiting the *in vitro* proliferation of SKOV3 human ovarian cancer cells in a concentration dependent manner. Thus, this mAb shows promise in the biological treatment of ovarian cancer. Other forms of cancer such as small cell lung cancer (SCLC), B-cell non-Hodgkin's lymphoma and renal cancer have shown promising results following monoclonal antibody treatment, in clinical trials (Coleman *et al.*, 2003; Heidenreich *et al.*, 2003; Shepherd, 2003).

Some applications of monoclonal antibody therapy have already met with success. Abciximab, a Fab monoclonal antibody fragment that blocks the platelet glycoprotein IIb/IIIa receptor, is increasingly used as an adjunct to coronary intervention. A clinical study has confirmed that abciximab remains clinically efficacious when readministered as an adjunct to percutaneous coronary intervention. However, concomitant heparin administration must be carefully monitored and warfarin therapy should be avoided. Reduced dosing may be necessary when abciximab is readministered within days of the initial administration (Madan & Tcheng, 2000).

3.1.2.1.3. Antibody Humanisation for Therapeutic Applications

The development of mAbs has had a considerable impact on the area of clinical diagnostics, but the expected success in the area of human therapy to date has not been fully realised (Clark, 2000). Although the first mAb to be approved as a human therapeutic was a murine antibody (OKT3) it was generally not well tolerated and certain problems were initially encountered with the use of these monoclonal antibodies. They did not always trigger the requisite effector function, and had a short life-span *in vivo*, due to the fact the antibodies often elicited a HAMA (Human anti-Mouse Antibody) response. The HAMA response resulted in the increased clearance of the antibody from the circulation

thereby negating the therapeutic potential. Murine antibodies also possess the potential to be highly immunogenic in humans (Jaffers *et al.*, 1986; Kellermann & Green, 2002). In order to circumvent this response it was necessary to minimise the non-human sequence of the mAbs (Figure 3.4.). This was achieved by constructing chimaeric antibodies where the mouse variable regions were joined to human constant regions (Boulianne *et al.*, 1984). This technology was advanced by humanisation, which led to the successes of infliximab (anti-tumour necrosis factor α) and trastuzumab (anti-human epidermal growth factor 2). Chimaerisation solved some of the initial problems associated with murine mAbs: as it allowed for increased half-life in the circulatory system through interaction with the Brambell receptor (FcRn), which protects the IgG from catabolism thereby recycling it back to the serum pool (Ghetie & Ward, 2000); and the ability to recruit effector cells such as complement and cytotoxic cells (Glennie & Johnson, 2000; Rader *et al.*, 2003). Infliximab is a promising agent for the treatment of Hidradenitis suppurativa (HS) a chronic disease characterized by significant morbidity. The initial findings suggest that infliximab is associated with objective and subjective improvement in HS. Further controlled studies of the efficacy of infliximab and its effect on the course of the disease are warranted (Sullivan *et al.*, 2003)

Research into the use of chimaeric Fab fragments for radioimmunoscintigraphy has shown promise due to the fact that the chimaeric fragments half-life is longer than intact mAb and can accumulate rapidly in tumours thus helping in the early diagnosis of pancreatic carcinoma (Otsuji *et al.*, 2003). A chimaeric and complementary-determining region (CDR) grafted monoclonal antibody (mAb) was generated by Forero and co-workers (2003) to help reduce the immunogenicity problem in radioimmunotherapy with monoclonal antibodies. However, humanization has prolonged the circulation of radiolabeled antibodies, resulting in an increased normal tissue exposure to radioactivity and greater dose-limiting bone marrow suppression. To overcome this problem, a tumour-associated glycoprotein (TAG)-72-specific CDR grafted mAb with C(H)2 domain deletion (DeltaC(H)2) was developed from the mAb CC49. Preliminary studies were preformed with metastatic colorectal carcinoma patients. These studies support the further clinical investigation of this agent in phase I trials by intravenous and intraperitoneal routes. Although there are many promising applications of chimaeric and humanised antibodies, there are some drawbacks. Chimaeric antibodies may still be considered immunogenic, and humanisation requires sophisticated molecular biological techniques and may sacrifice the affinity and potency of the original antibody.
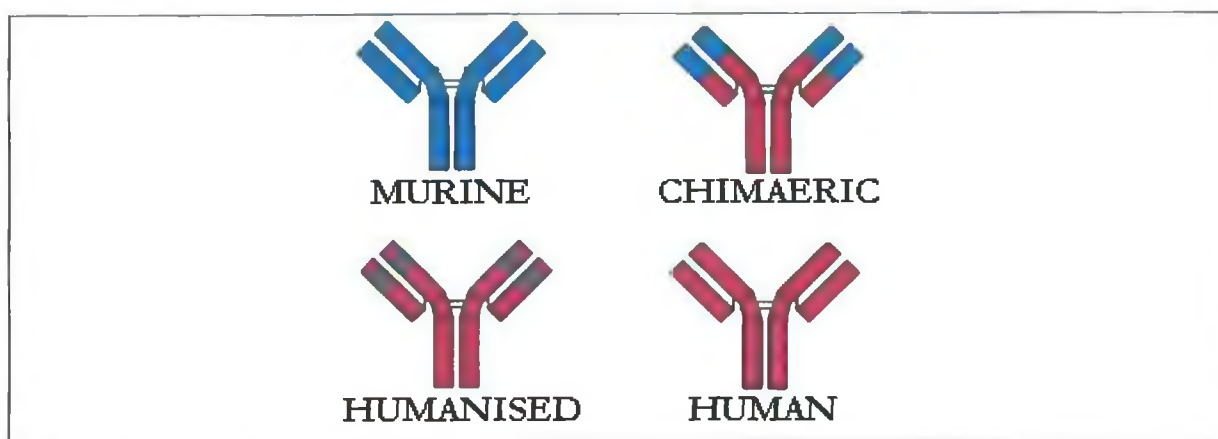
Figure 3.4: This diagram illustrates the concept of mouse, chimaeric, humanised and human antibodies (Blue = murine, Red =human).

Although display technologies using systems such as phage, ribosomes or yeast can be powerful tools to generate human antibodies (Table 3.2.), optimising such antibodies for high affinity and potency can be labour intensive. Two strategies have evolved, which utilise recombinant antibody technology through the expression of naïve variable regions expressed on the surface of bacteriophage and the use of transgenic mice (Vaughan *et al.,* 1998). The rationale behind mice transgenic for human immunoglobulin loci is to harness the natural recombination and affinity maturation machinery to generate human antibodies of wide diversity and high affinity.

The evolution of transgenic mouse technologies was first marked by the report of a transgenic mouse containing a predominantly human IgH minilocus, permitting the expression of IgM antibodies with human μ chains, but containing mouse light chains (Bruggermann *et al.,* 1989). The XenoMouse^{TM} strains of transgenic mice were the first engineered mice to include a majority of both the human VH and Vκ repertoire. The mice immunoglobulin genes were replaced with human Ig genes on YAC (Yeast Artificial Chromosomes) transgenes, which carry the majority of the human variable repertoire as well as the possibility of undergoing class-switching from IgM to IgG and efficient affinity maturation. Xenomouse™ strains of mice recognise human antigens as foreign, and are capable of producing antibodies with sub-nanomolar affinities (Mendez *et al.,* 1997). Due to the fact that the YAC transgenes are integrated into a mouse chromosome, they offer superior genetic stability. Currently, five fully human antibodies from the XenoMouse^{TM} strains have been used in clinical trials (Green, 1999; Galka *et al.,* 2000). The first transgenic-mouse-derived fully humanised antibody entered clinical trials in 1998 (Yang *et al.,* 1999a). Since then other mAbs have followed including antibodies against epidermal growth factor, CD4, CTLA-4 (cytotoxic T lymphocyte-

101

associated antigen 4) CD69, and several cancer-specific target antigens (Tistravik *et al.,* 1999; Yang *et al.,* 1999b; Molina *et al.,* 2003). XenoMouse™ antibodies are also adaptable to production directly from hybridomas, transgenic plants or recombinant cell lines with many in preclinical and early clinical testing stages at the present time. Laboratory and initial clinical studies suggest that epratuzumab, a humanized anti-CD22 monoclonal antibody, may have anti-lymphoma activity in both unlabeled and radiolabeled forms. Efforts are underway to establish the utility of epratuzumab as a treatment for B-cell malignancies, through single agent and combination regimens, to define the optimal settings for its clinical application (Coleman *et al.,* 2003).

Table 3.2: *Classification of existing therapeutic antibodies and the strategies currently available for their production.*

Antibody Type	*Description*
MURINE MONOCLONAL ANTIBODIES:	These have been used therapeutically and the first mAb to be FDA approved was OKT3 a mouse IgG2a (1986). These mAbs tend to provoke strong (HAMA) immune responses, which restricts their usefulness for repeated application in the same patient.
CHIMAERIC ANTIBODIES:	The whole of the variable regions of a mouse or rat antibody are expressed along with human constant regions. This provides the antibody with human effector functions and also reduces immunogenicity (HAMA) caused by the murine Fc region.
HUMANISED ANTIBODIES:	An alternative to chimaeric antibodies where only the complimentarity determining regions from the rodent antibody V-regions are combined with framework regions from human V-regions. These antibodies should be more 'human-like' than chimaeric and, thus, less immunogenic than chimaeric antibodies.
HUMAN ANTIBODIES FROM IMMUNE DONORS:	Some antibodies have been rescued from immune human donors using either EBV transformation of B-cells or by PCR cloning and phage display. By definition these antibodies are completely human in origin.
FULLY HUMAN ANTIBODIES FROM PHAGE LIBRARIES:	Synthetic phage libraries created which utilising randomized combinations of synthetic human antibody V-regions. By selection on antigen fully humanised abs can be made where it is assumed the V-regions are very 'human-like' in nature.
FULLY HUMAN ANTIBODIES FROM TRANSGENIC MICE:	Transgenic mice have been created which have a repertoire of human immunoglobulin germline gene, segments. These mice when immunised thus make human-like antibodies.

3.1.2.1.4. Antibody Engineering

In the late eighties initial steps in antibody engineering revolutionized the technology of antibody production, particularly in the area of immunotherapy and diagnostics and is reviewed by Kramer & Hock, (2003). Recombinant DNA technology and antibody engineering have supplemented, and in some instances, replaced hybriboma technology in the production of 'tailor-made' antibodies of high affinity to any particular antigen (Hoogenboom & Chames, 2000; Hudson & Souriau, 2001). With the advent of this technology, antibody genes can be amplified and selected using phage display and in addition, cell surface and cell free display systems. An advantageous feature of these display systems is the linking of the phenotype (binding specificity) and genotype (antibody V regions) of the antibodies during selection, thus allowing simple co-selection of the desired antibodies and their encoding genes based on the binding characteristics of the displayed antibodies (Yau *et al.*, 2003). Phage display involves cloning DNA into bacteriophage genome as a fusion to one of phage coat proteins. Following expression the antibody fragments are presented on the surface of the phage with the encoding DNA residing within the phage. The phage display library can then be panned by selection of phage with specific binding affinity towards a particular immobilised target ligand. The affinity of the antibodies created was reported to be proportional to the size of the antibody library (Sblattero & Bradbury, 2000).

Recombinant antibody libraries can be constructed from naïve or immunised donors, and also from synthetic libraries. Immunised donors are previously enriched for specific immunoglobulin, with some undergoing affinity maturation. The affinity of the selected antibodies is frequently not adequately elevated and may necessitate *in vitro* affinity maturation to produce antibodies of suitable affinity (Hemminki *et al.*, 1998). This can be achieved in a variety of ways from the use of mutator strains, the use of error prone PCR (Harayama, 1998), chain or oligonucleotide-directed mutagenesis shuffling (Jirholt *et al.*, 1998). The introduction of diversity into the V genes allows for the creation of a 'mature' secondary library from which higher affinity variants may be selected. BIAcore-based selection procedures allows for the selection of particular variants with respect to specific affinity and kinetic rate constants (Dueñas *et al.*, 1996). High affinity antibodies may be selected from naïve libraries that are particularly useful for selection of human antibodies (Hoogenboom *et al.*, 1998).

ScFvs with femtomolar association constants, the highest yet reported for monovalent ligands have been produced using a similar approach of 'molecular breeding' involving repeated cycles of affinity mutagenesis (Boder *et al.*, 2000). The potential applications of such higher affinity variants with association constants 1000 fold greater than possible by *in vivo* maturation, is particularly

104

interesting for developing areas such as immunotherapy and tumour targeting. scFv antibodies have recently been directed towards several pathogenic targets such as the highly infectious *Brucella melitensis* (Hayhurst *et al.,* 2003). A recombinant scFv antibody to the exotoxin from *Burkholderia pseudomallei* was constructed by phage display and exhibited good specificity towards the exotoxin (Su *et al.,* 2003). Antibodies from phage and ribosome display libraries have found application in microarray technology (He & Taussig, 2001; Tomlinson & Holt, 2001) and may prove useful for studying protein-protein interactions and proteomics (Haab *et al.,* 2001; Kodadek, 2001).

3.1.2.1.5. *Alternative Expression Systems and Novel Antibody Constructs*

A variety of expression systems are available for the production of antibodies and antibody fragments, including the use of bacteria, yeast, plants, insect cells and mammalian cells. Each one has advantages and limitations with respect to ease of production and the glycosylation pattern of antibodies recorded. Two potentially relatively low cost antibody expressions systems are described. The concept of using plants as heterlogous expression hosts for recombinant antibodies is more than a decade old (Hiatt *et al.,* 1989). It was reported that genetically engineered tobacco plants were capable of synthesising correctly folded immunoglobulin heavy and light chains. Plants represent an inexpensive, efficient and safe alternative to traditional systems used for the commercial-scale synthesis of recombinant antibodies (Nolke *et al.,* 2003). Therefore, it is not surprising that a variety of 'plantibodies' have since been constructed, three of which are currently in use as immunotherapeutic products for the treatment of caries and cancer (Larrick *et al.,* 1998). Plantibodies offer several advantages as potential protein sources and they represent a viable alternative to prokaryotic and mammalian expression systems. Advantages include the production of antibodies on an agricultural low-cost scale, and potential increased safety as plants do not serve as human pathogen hosts (e.g. HIV, prions). Contemporary applications in agronomic research include immunomodulation of physiological processes and engineering of antibody-mediated resistance to pathogen infection (Stoger *et al.,* 2003). The most advanced application, however, is the utilisation of plants as bioreactors to produce antibodies required for medical use or industrial processes (Fischer & Emans, 2000; Daniell *et al.,* 2001; Larrick & Thomas, 2001).

One of the challenges created by the biotechnology revolution is the development of methods for the cost-effective large-scale production of highly purified proteins. Recent developments indicate that expression of recombinant proteins in the milk of transgenic animals may be suited for the production of complex polypeptides (Pollock *et al.,* 1999). Expression vectors containing the gene encoding the specific protein fused to milk specific regulatory genes can be introduced by

microinjection into embryo cells. Following a period of *in vitro* culture the embryos can be transferred to pseudopregnant animals and development to full term (Little *et al.,* 2000). Following integration into the germline, the mammary gland specific transgene is transmitted in Mendelian fashion and, if expressed, will become a dominant genetic characteristic inherited by offspring of the mammalian originator. The identified animals can then be bred or induced to lactate. Dairy goats were shown to be excellent animals for the production of transgenic milk, capable of producing between 1 and 5 g/l of recombinant antibody (Pollock *et al.,* 1999). The efficiency of microinjection has limited the development of this technology as the integration into the genome of specific transgenes is typically low, 0.1% in cattle to 5% in mice. The antibodies can be separated from the majority of milk proteins by standard dairy procedures to relatively pure antibody (~60%), which can be further, purified by traditional chromatography procedures (e.g. Ion exchange, Protein A/G chromatography). A variety of antibodies have been produced in the milk of transgenic animals, and in particular cases been shown to be produced at levels 160,000 fold times those recorded in cell culture systems whilst retaining all biological activity (Newton *et al.,* 1999).

A scFv (single chain variable fragment) antibody contains a synthetic amino acid linker peptide (usually a glycine-serine repeat linker), which acts to stabilise the antibody fragment without interfering with the domain association. Diabodies are recombinant, dimeric, antibody-based molecules (55-60kDa) composed of two non-covalently associated single-chain antibody fragments (scFv) that bind to an antigen in a divalent manner (Aubrey *et al.,* 2003). The construction of scFv fragment, with a short linker (5-10 amino acid residues) between the variable heavy and light domains, permits interchain, but not intrachain, pairing of the variable domains (Lu *et al.,* 2003). Careful selection of the linker length dictates the size (kDa), and thus the valency of the scFv multimer formed (Hudson & Kortt, 1999). Reducing the linker length below 3 residues forces the scFv to form triabodies (90 kDa) or tetramers (120 kDa). As a result of the increase in valency, scFv multimers exhibit very high avidity and reduced off rates as a result of multiple binding and re-binding when one Fv dissociates (Pluckthhun & Pack, 1997). In BIAcore studies conducted, Iliades *et al.,*(1997) found that the trimers produced from a scFv exhibited an approximate 4-fold apparent slower off-rate compared to the monomeric unit.

The association of two diverse scFv molecules from different parent IgG will result in the formation of bispecific diabodies (Hollinger *et al.,* 1993), which have been successfully used for ELISA, immunohistochemistry and immunoblotting procedures (Kontermann *et al.,* 1997).
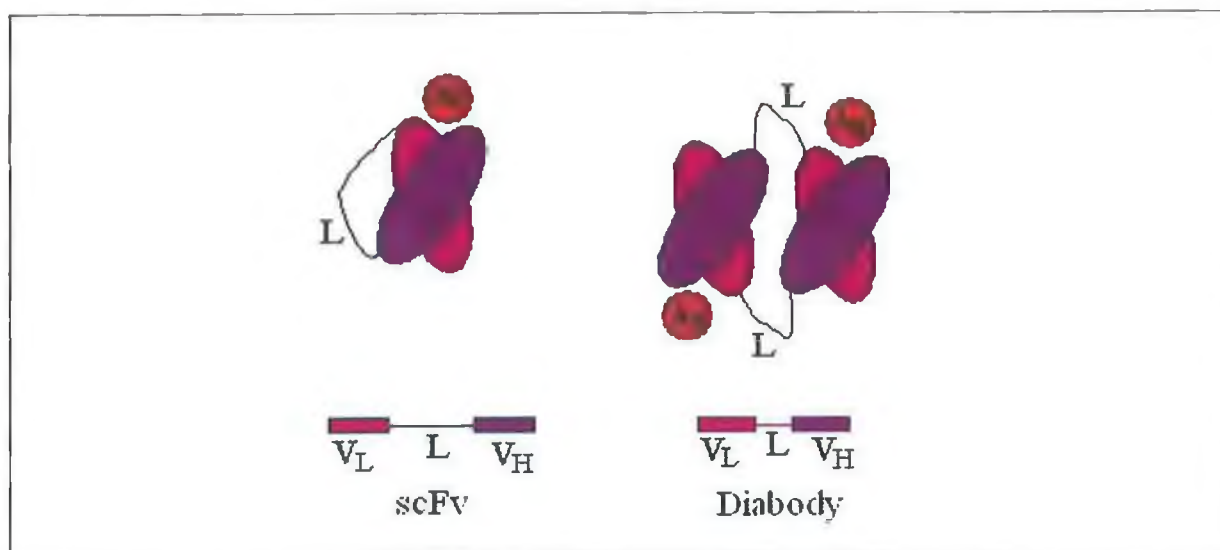
Figure 3.5: *Schematic diagram of scFv and diabodies showing antigen binding sites. When joined by a peptide linker (L) at least 12 residues long scFv's are predominantly monomeric, diabodies (~60Kda) are formed by selecting linkers between 3 and 12 residues. Reducing the linker length below 3 residues can force scFv into triabodies (~90 kDa) and tetramers (~120 kDa).*

The use of diabodies has gained increasing interest particularly in the areas of immunotherapy and tumour imaging (Arndt & Krauss 2003; Kipriyanov, 2003). The reduced size of diabodies compared to whole Ig for tumour targeting has the advantage of increased tumour penetration and faster clearance rates *in vivo*. To target NK cells against non-Hodgkin's lymphoma, Kipriyanov *et al.,* (2002) constructed a bispecific diabody (BsDb) with reactivity against both human CD19 and FcγRIII (CD16). It was able to induce specific lysis of tumour cells in the presence of isolated human NK cells and the results obtained demonstrated the synergistic effect of small recombinant bispecific molecules recruiting different populations of human effector cells to the same tumour target. Bispecific diabodies have also been shown to induce cytotoxic and 'vaccine effects' *in vivo* (van Spriel *et al.,* 2000), and a number are currently under trial for the treatment of various cancer cell types. Two bispecific diabodies (BS1.5 and BS1.5H) were produced and tested as potential agents for pretargeted delivery of radiolabelled bivalent haptens to tumours expressing carcinoembryonic antigen. These results indicate that both diabodies are promising candidates for use in a variety of pretargeting applications, including tumour therapy with radionucleotides and drugs (Rossi *et al.,* 2003).

The combination of genetic engineering and advanced selection techniques has led to the development of a novel range of protein ligands, 'affibodies' (affinity ligands). Despite their small size and simple structure, these proteins have been shown to possess binding features similar to

antibody variable domains in that selective binding with high affinity can be achieved towards various target molecules (Hansson *et al.,* 1999; Ronnmark *et al.,* 2002). Knottins, are a small group of small disulphide-bonded proteins capable of binding to target molecules. Smith and colleagues (1998) created knottin scaffolds with binding capacities in the micromolar range for target antigens such as alkaline phosphatase. Nord *et al.,*(1997) have also created 'affibodies', in which 13 surface-located positions of the 58 amino acid three-helix bundle protein Z, and a one-domain analogue of staphylococcal protein A, have been targeted for random mutagenesis during library constructions (Andersson *et al.,* 2003). This affibody was revealed to be exceptionally stable to pH extremes and harsh regeneration conditions and thus potentially useful in areas such as affinity purification (Nord *et al.,* 2000). The potential for improving binding affinity has also been exploited through the use of *in vitro* affinity maturation strategies, such as α-helix shuffling strategy employed by Gunneriusson *et al.,*(1999) which resulted in a 20-30-fold increase in functional affinity.

3.1.3. Antibody Purification

Immunoglobulins are relatively robust molecules capable of maintaining biological activity following exposure to extremes of pH for short periods of time, and storage for relatively long periods at –20°C. It is widely accepted that purified antibodies are superior to crude animal antisera, cell culture supernatant and cell lysates in ELISA, Western blot analyses, and immunohistochemical staining (Sun *et al.,* 2003). Affinity purification is a crucial step in obtaining antibodies from the antiserum of animals immunised with a peptide antigen conjugated to a carrier protein. Protein A and G may be used for the isolation of IgG. Protein G is a 30 kDa bacterial cell wall protein isolated from the group G streptococci, and binds to immunoglobulin molecules primarily through their Fc regions. Protein G binds with a higher affinity to particular immunoglobulin molecules such as mouse IgG_1 that do not bind particularly well to Protein A. Protein A is a 42 kDa cell wall component of several strains of *Staphylococcal aureus* and binds specifically to the Fc region of immunoglobulin molecules. Protein A and G can be easily coupled to sepharose to produce solid supports with high immunoglobulin capacity, exhibiting low degrees of non-specific binding. Following application of the crude antibody preparation to such column supports and subsequent washing to remove non-specifically bound protein, the bound antibody can be eluted by exposure to high/low pH solutions. Recent developments include the generation of an affinity column for antibody purification by semi-synthetic intein-mediated protein ligation and an chromatographic procedure utilising a thermally responsive poly(N-isopropylacrylamide)-dextran derivative conjugate (Anastase-Ravion *et al.,* 2001; Sun *et al.,* 2003).

3.1.4. Immunoassay

Immunoassays with high accuracy and specificity that are inexpensive, fast and convenient to perform are always advantageous (Yau *et al.*, 2003). One of the most commonly employed techniques for measuring antibody-hapten interactions, is the use of ELISA, which is now far more commonly employed than radioimmunoassay techniques, primarily as a result of the hazardous nature and disposal of radioimmunoassay reagents. Immunoassays are classified into one of two types, heterogeneous or homogenous. In heterogeneous assays the antigen-antibody complex is separated from free antigen and antibody, while in homogenous assays, no such physical separation occurs. ELISA is a good example of a heterogeneous assay (Watanabe *et al.*, 2000; Webb & Hall, 2001).

Enzyme immunoassays can be further classified as competitive and non-competitive. A wide variety of ELISA formats are possible. However, a competitive ELISA format is described in the context of the assay format utilised for the detection and development of a competitive immunoassay for warfarin (Figure 3.6). The hapten of interest that is covalently coupled to a protein (e.g. warfarin-BSA), is added to the wells of a 96-well immunoplate, and binds to the immunoplate predominantly through hydrophobic interactions. Loosely bound protein is then removed by washing with a solution containing detergent. A blocking agent (e.g. 5% FCS in PBS-1) is then added to the wells to 'block' any remaining available adsorption sites on the surface of the plate. The use of such blocking agents is necessary to ensure that no non-specific binding of either primary or secondary-labelled antibody to the wells of the plate occurs. A solution containing a limiting constant amount of monoclonal antibody and varying known concentrations of antigen (warfarin) are then applied to the wells of the immunoplate, and incubated for a specified time interval. Competition then occurs between free warfarin in solution and warfarin-BSA immobilised to the immunoplate for binding to the anti-warfarin monoclonal antibody. The contents of the well are then removed and the plate washed to remove any non-specific antibody. The presence of antigen-specific antibody (i.e. monoclonal anti-warfarin antibodies) in the wells of the immunoplate can then be determined using a species-specific secondary enzyme-labelled antibody for the primary antibody (e.g. alkaline phosphatase-labelled goat anti-mouse immunoglobulin). The substrate for the enzyme is added and a coloured product is formed, which can be measured spectrophotometrically at the appropriate wavelength.

In such assay formats as the concentration of free antigen (i.e. warfarin) in solution increases, less antibody is available to bind to the solid-phase immobilised antigen (i.e. warfarin BSA). Consequently, an inverse relationship exists between the intensity of the coloured solution formed and the concentration of free antigen in solution. In this way, the concentration of warfarin in unknown

solutions can be determined by reference to a suitable standard curve. The sensitivity of such competitive ELISA formats can be optimised using the appropriate dilution of antibody preparation and immobilised conjugate. However, the ultimate sensitivity of all immunoassay procedures is primarily a factor of the intrinsic affinity of the antibody preparation for the particular antigen (Yau *et al.*, 2003).
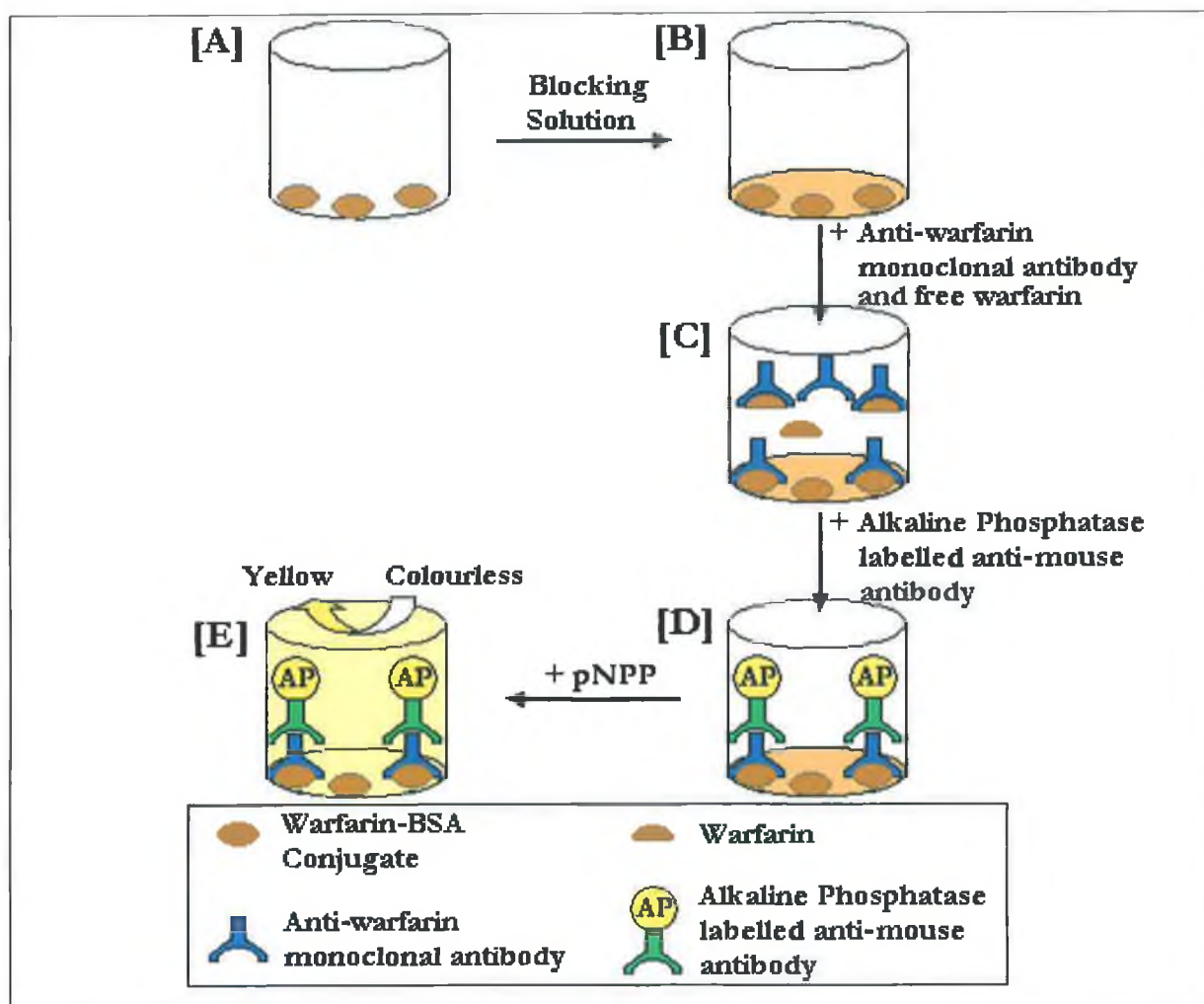
Figure 3.6: Schematic of the principle of direct ELISA. Warfarin-BSA is used to 'coat' the wells of a 96-well immunoplate and sticks to the γ-irradiated plate primarily by hydrophobic interactions [A]. The wells of the immunoplate are then blocked with a suitable blocking solution (e.g. 5% (v/v) F.C.S. solution in PBS-1) to block any remaining absorption sites on the plate [B]. The antibody-containing samples are then added to the wells of the immunoplate, and, following a suitable incubation step, washed (i.e. wash buffer section 2.3.) to remove non-specific protein [C]. A species-specific secondary enzyme-labelled antibody is then added to the wells of the immunoplate and incubated for a suitable period of time [D]. The wells are washed extensively again, and substrate added to the wells of the plate. In the presence of enzyme (i.e. the enzyme-labelled secondary antibody) a coloured product is formed and its absorbance can then be measured spectrophotometrically at the appropriate wavelength for the substrate [E].

3.1.4.1. ELISA Applications

ELISA is very versatile and as a result was applied to a variety of sectors including the food industry and drug screening for the pharmaceutical industry.

Regarding the food industry ELISA is very useful for the detection and quantification of many contaminants (e.g. toxins) and pathogenic organisms such as *Salmonella* and *E. coli*. A study was undertaken by Sarimehmetoglu and co-workers in the University of Ankara, Turkey (2004) in order to determine the presence and levels of aflatoxin M_1 (AFM_1) in cheeses. AFM_1 is a hepatic carcinogenic metabolite found in the milk of lactating animals that consume aflatoxin B_1. A total of 400 cheese samples were used as the study material. The competitive ELISA determined 110 out of 400 samples contained levels of AFM_1 that exceeded the legal limit established. In an attempt to develop a standard for ELISA-PCR detection of Shiga toxin producing *E. coli* O157, six published PCR tests were evaluated in a comparative study on a panel of 277 bacterial strains isolated from foods, animals and humans. Since its recognition in 1982, enterohaemorrhagic *E. coli* O157 is recognised as an important human pathogen predominantly associated with haemorrhagic colitis and the more serious severe complications of haemolytic uraemic syndrome. It causes high morbidity and mortality especially among the young and elderly (Fach *et al.*, 2003).

Another significant area of ELISA application is drug screening with several recent developments highlighting the importance of ELISA in this sector. ELISA in microtitre plate format is widely used for high throughput screening of chemicals and drugs for their effects on various biological activities (Svojanosky *et al.*, 1999; Itoh *et al.*, 1999; Elian, 2003). These assays make it possible to rapidly evaluate a large number of compounds and can be readily adapted for automatic manipulations. Cell-based ELISAs are especially valuable as they reflect the ability of drugs to permeate cell membrane and to affect cellular targets and functions. Apoptosis plays an important role in human disease and drugs, which stimulate or inhibit apoptotic cell death, may have valuable clinical applications. Thus, specific and sensitive screening procedures are required to select drugs affecting apoptosis. Based on this requirement a solid-phase ELISA was developed for the specific and sensitive detection of apoptotic cells. The assay involved the binding of cells to microtitre plates. The attached cells were then treated with formamide to denature DNA in apoptotic cells, which is followed by staining of the denatured DNA with a mixture of anti-ssDNA mAb and peroxidase-conjugated anti-mouse IgM. Two human carcinoma cell lines (leukaemic cells and breast carcinoma cells) treated with drugs (e.g. etoposide, cisplatin and staurosporine), were examined using this assay format. It was determined from these assays that the absence of an apoptotic signal in the breast cancer cells treated

112

with cytotoxic concentrations of cisplatin that this drug kills cells by non-apoptotic mechanisms, whereas apoptosis was the dominant mechanism of cell-death caused by staurosporine. This illustrates the potential of this assay format to provide a foundation for high-throughput screening of drugs based on their ability to induce or suppress apoptosis (Frankfurt & Krishan, 2001).
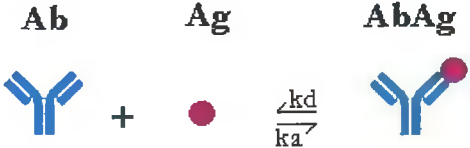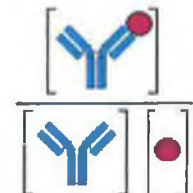
In order to successfully screen drugs in a variety of applications it is important to develop ELISAs capable of detecting the target drug in a various biological matrices (e.g. blood, urine, saliva), especially if the drug has clinical or therapeutic significance in both animals and humans. An important example involves recent developments utilising a competitive ELISA format for the quantification of plasma and intracellular levels of the HIV protease inhibitor, ritonavir. Successful HIV treatment is critically dependent on drug potency, viral susceptibility and plasma drug levels. However, serum pharmacokinetics of this inhibitor revealed large inter-individual variations caused by low or variable oral bioavailablity of current formulations and by extensive cytochrome P450 metabolism. Therefore, a simple and sensitive analytical method for the routine determination of serum and intracellular levels of ritonavir is likely to represent a useful clinical tool. A convenient one-step competitive ELISA was developed by Akeb and colleagues (2002) for measuring plasma and intracellular ritonavir levels in HIV patients. Anti-ritonavir polyclonal antibodies were raised in rabbits using a ritonavir-KLH conjugate as immunogen. This assay format accurately and specifically detected 3-4ng/ml of ritonavir in plasma and intracellular drug levels in the peripheral blood mononuclear cells of patients undergoing ritonavir therapy.

ELISAs are becoming very popular within the forensic toxicology community because of their relative ease to perform, potential for automation, the small sample size requirement, lack of radioisotopes, and their ability for use with blood and urine specimens. Clonazepam is a benzodiazepine derivative approved for use as an anticonvulsant in 1975. However, in recent years it is used in drug-facilitated assaults and for this reason it is important to be able to detect clonazepam and 7-aminoclonazepam in whole blood and urine for use as evidence in such cases (Elian, 2003).

3.1.5. Antibody Affinity

The net interaction between an antibody's antigen binding site and the corresponding antigen epitope dictates the affinity of the interaction between the two molecules. Merging of the antigen binding site with antigen can be investigated thermodynamically. To measure the affinity of a single antigen binding site, it is necessary to use a monovalent antigen, or even a single isolated antigenic determinant (a hapten). Due to the fact that the non-covalent bonds between antibody and epitope are

113

dissociable, the overall binding of antibody and antigen must be reversible. Therefore the Law of Mass Action can be applied to the reaction and the equilibrium constant K_A can be determined. This is the affinity constant.

Antigen-Antibody reactions are reversible	Applying the Law of Mass Action
Ab **Ag** **AbAg** $\quad + \quad \frac{\angle kd}{ka}$	Equilibrium constant of affinity, K_A, is given by: $K_A = \frac{[AbAg]}{[Ab][Ag]} \; ; \; K_A = \dfrac{\left[\; \right]}{\left[\; \right]\left[\; \right]}$

(1)

All antigen-antibody reactions are reversible. The Law of Mass Action can therefore be applied, and the antibody affinity (given by the equilibrium constant K_A) can be calculated. (Square brackets refer to the concentrations of the reactants).

Antibody avidity indicates the overall strength of interaction between antibody and antigen and is dependent upon the number of antigen binding sites with which it makes contact. If an antibody has more than one antigen binding site (in the case of IgG two and in the case of IgM five) then these multivalent molecules will be more likely to lock tightly onto their target antigen (Sikora & Smedley, 1984). In addition, antigen can also be monovalent (e.g. hapten) or multivalent (e.g. microorganism). The strength with which a multivalent antibody binds a multivalent antigen is termed avidity, to differentiate it from the affinity of a single antigenic determinant for an individual combining site. The avidity of an antibody for its antigen is dependent on the affinities of the individual combining sites for the determinants on the antigen. It is greater than the sum of these affinities if both antigen-binding sites can combine with the target antigen. This is because all of the antigen-antibody bonds must be broken simultaneously before the antigen and antibody dissociate. In normal physiological situations avidity is likely to be more relevant than affinity, as naturally occurring antigens are multivalent. However, the precise measurement of hapten-antibody affinity is more likely to give an insight into the immunochemical nature of the antigen-antibody reaction.

Measurements of antibody affinity relate to equilibrium conditions. Affinity indicates the tendency of the antibodies to form stable complexes with the antigen. However, for many biological

114

activities of antibodies, it is possible that the kinetics of the reaction may also be significant. Kinetics measures the forward rate (on-rate) constant or association constant ka and the reverse rate (off-rate) or dissociation constant kd. At equilibrium, the ratio of the two constants gives the equilibrium constant, or affinity of the antibody.

The affinity of the interaction between an antibody and antigen is the net result of the intermolecular forces between the two molecules, and four types of such intermolecular forces have been identified. They include hydrogen bonding, ionic interactions, 'van der Waals' forces and hydrophobic interactions. Hydrogen bonding involves the interaction of a H-atom covalently linked to an electronegative atom with the unshared electron pair of another electronegative atom. Ionic interactions are the result of the attraction between oppositely charged groups and consequently can be disrupted by changes in salt concentration or pH. Hydrophobic interactions involve the association of non-polar (hydrophobic) residues in aqueous environments. 'Van der Waals' forces are the result of interactions between electron clouds of neighbouring molecules as two polar groups come in close contact. This results in the induction of oscillating dipoles between the two molecules resulting in a net attractive force. The strength of these particular forces is only effective over short distances, which can usually be disrupted by high ionic strength or extremes of pH (Fitzpatrick, 2001).

3.1.6. Chapter Outline

This chapter outlines the characterisation and application of anti-warfarin monoclonal antibody (mAb) produced and purified from clone 4.2.25. Optimisation of ELISA using this mAb was performed in phosphate buffered saline (PBS) and in urine. Cross reactivity studies investigated the specificity of the mAb to compounds that were structurally similar to warfarin (e.g. acenocoumarin). Finally, kinetic studies involving a method developed by Friguet *et al.,* (1985) were utilised to determine the dissociation constant (K_D) of the mAb to warfarin and its analogues.

3.2. Results and Discussion

3.2.1. Monoclonal Antibody Purification

200mls of 'spent' hybridoma supernatant from clone 4.2.25 was concentrated using an Amicon™ filtration device as described in section 2.5.3.1. The concentrate was then passed through a Protein G column as described in section 2.5.3.2. The fractions were then assayed at 280nm, using a

spectrophotometer, and the fractions containing protein were pooled and dialysed against 3-4 changes of PBS-2.
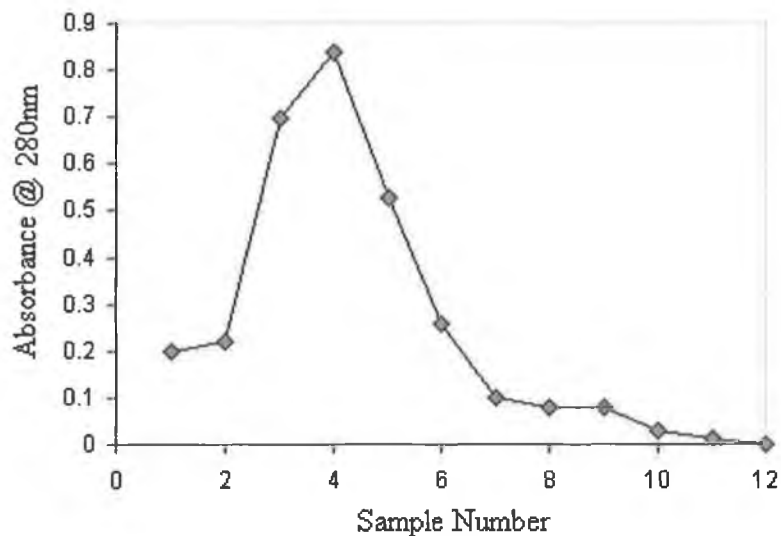
Figure 3.7: *Elution profile of monoclonal 4.2.25 following purification on a Protein G column. 20 ml of concentrated 'spent' hybridoma supernatant was applied to the 1ml Protein G column, which was then washed with two column volumes of wash buffer. 0.1 M Glycine-HCl (pH 2.5) was then applied to the column and 850 μl extracts were collected in eppendorf tubes containing 150 μl of 1 M Tris-HCl (pH 8.0). The samples were then measured for protein content by recording absorbance 280 nm, and those fractions (i.e. fractions 1-6) containing immunoglobulin were pooled and dialysed against several changes of PBS-2 at 4°C.*

3.2.2. Characterisation of Purified Antibody by SDS-PAGE

The purity of the protein G-purified anti-warfarin monoclonal antibody was assessed by sodium dodecyl sulphate polyacrylamide gel electrophoresis (SDS-PAGE) as described in Section 2.5.7.2. and Table 2.4. SDS-PAGE allows the separation of proteins according to their size. Figure 3.8. depicts the SDS-PAGE gel of the purified anti-warfarin monoclonal antibody with molecular weight bands at 50 kDa and 25kDa. These bands represent the heavy (50kDa) and light (25kDa) chains of the antibody.

116
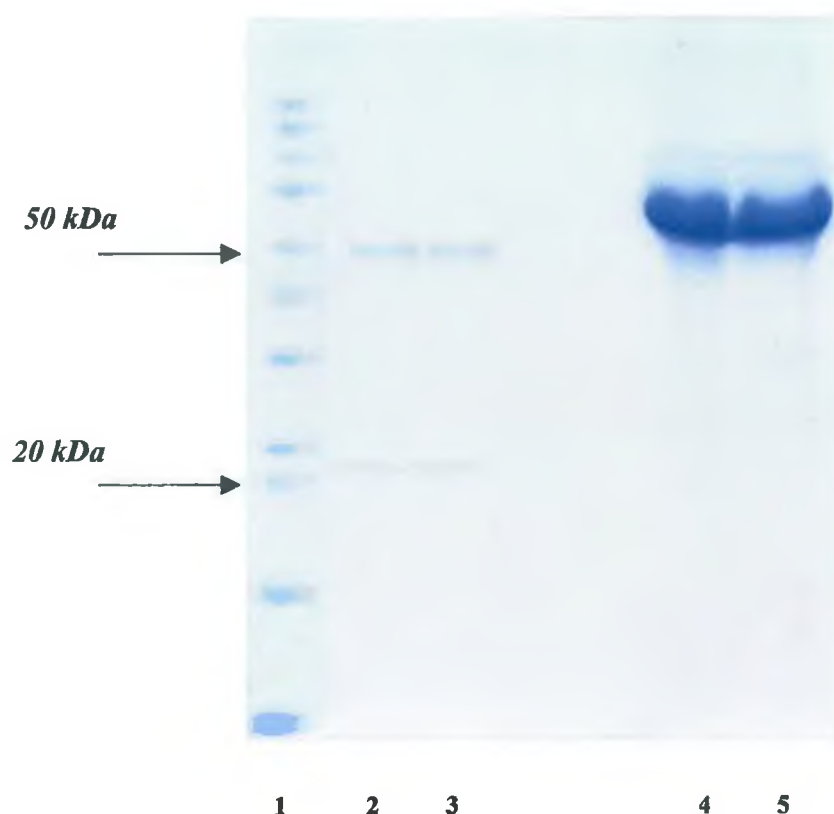
Figure 3.8: *SDS-PAGE gel of the protein-G purified anti-warfarin monoclonal antibody.*
Lane [1] contains Sigma Marker wide range M.W. 6,5kDa-205kDa
Lane [2] shows purified heavy (50KDa) and light (25kDa) chains of
anti-WF mAb. Lane [3] shows purified heavy (50kDa) and light (25kDa) chains of
anti-WF mAb. Lane [5] shows anti-WF mAb in supernatant before purification. Lane
[6] shows anti-WF mAb in supernatant before purification.

Once the purity of the monoclonal antibody was established the purified antibody fractions were then assayed for antibody activity as described in section 2.5.2.3. Titres of the hybridoma supernatant following concentration, and after affinity purification are shown in Figure 3.9. Both SDS-PAGE and antibody titre results confirm the mAb is well purified and binds warfarin.
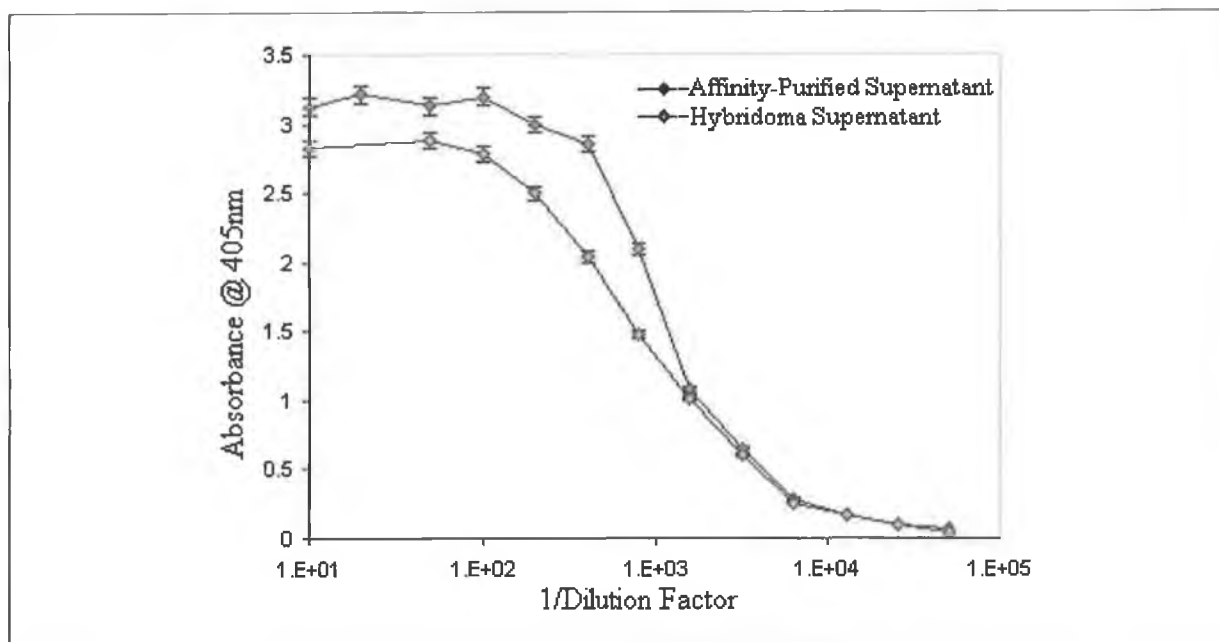
Figure 3.9: *Typical antibody titre for clone 4.2.25 from 'spent' hybridoma supernatant and affinity-purified antibody sample were greater than 1/50,000 and 1/100,000, respectively. Results shown are the mean of triplicate measurements ±S.D.*

3.2.3. Development of a Competitive ELISA for Warfarin

A competitive ELISA was developed for the detection of warfarin in solution using a warfarin-BSA conjugate and the protein G-purified mAb.

3.2.3.1 Determination of Optimal Conjugate Loading Density and Antibody Working Dilution

Utilising too high a conjugate loading density (i.e. solid-phase form of immobilised antigen) will shift the binding equilibrium in favour of binding to the ELISA plate and cause reduced sensitivity to free antigen in solution (i.e. the desired detectable analyte). Similarly, utilising too high an antibody concentration, will require high concentrations of free antigen in solution to inhibit antibody binding to the ELISA plate, and therefore result in decreased assay sensitivity. It is essential, therefore, to optimise both the concentration of the solid-phase antigen and the concentration of antibody (i.e. the working dilution of antibody) to be used for competitive ELISA techniques.

118

A checkerboard ELISA was carried out as described in section 2.5.2.4. in order to determine optimal conjugate loading density. A concentration range of warfarin-BSA from 0 - 100 μg/ml was prepared in PBS-1 and applied to a 96-well microtitre plate. Dilutions of purified mAb from 1/100 to 1/100,000 were prepared and added to the plate. The optimal conjugate loading density was defined as that conjugate coating density (μg/ml) that gave the widest linear detection range over the range of antibody dilutions used. The optimal warfarin-BSA coating concentration was found to be 50 μg/ml, as shown in Figure 3.10.

The optimal dilution of antibody to be used in competitive ELISA experiments was determined by setting up a standard curve of serial doubling dilutions of purified mAb as described in section 2.5.2.3. using the optimal warfarin-BSA conjugate loading density. The optimal working dilution of mAb for competitive ELISA was taken from the linear portion of the dilution curve, where there is greatest change in absorbance for similar change in antibody dilution. The optimal working dilution of purified mAb was determined to be a 1/800 dilution (Figure 3.11.).
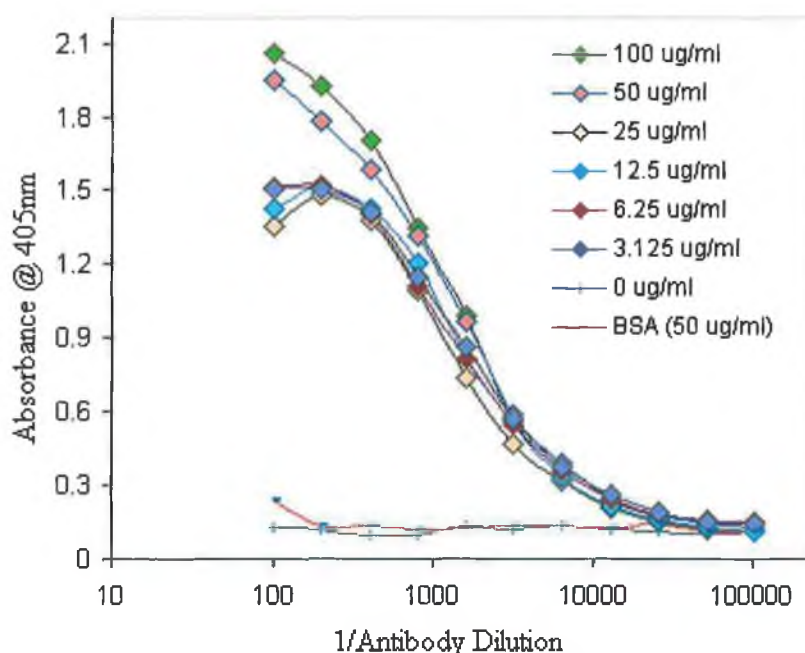
Figure 3.10: Determination of optimal conjugate loading density. Wells of an immunoplate were coated with varying concentrations of conjugate ranging from 0 -100 μg/ml. Serial doubling dilutions of mAb were then added to the wells of the plate as described in section 2.5.2.4. The conjugate loading density that gave the widest linear detection range over the antibody dilution series was used, and 50 μg/ml was chosen as the optimal conjugate loading density. The results shown are the average of duplicate results.

119
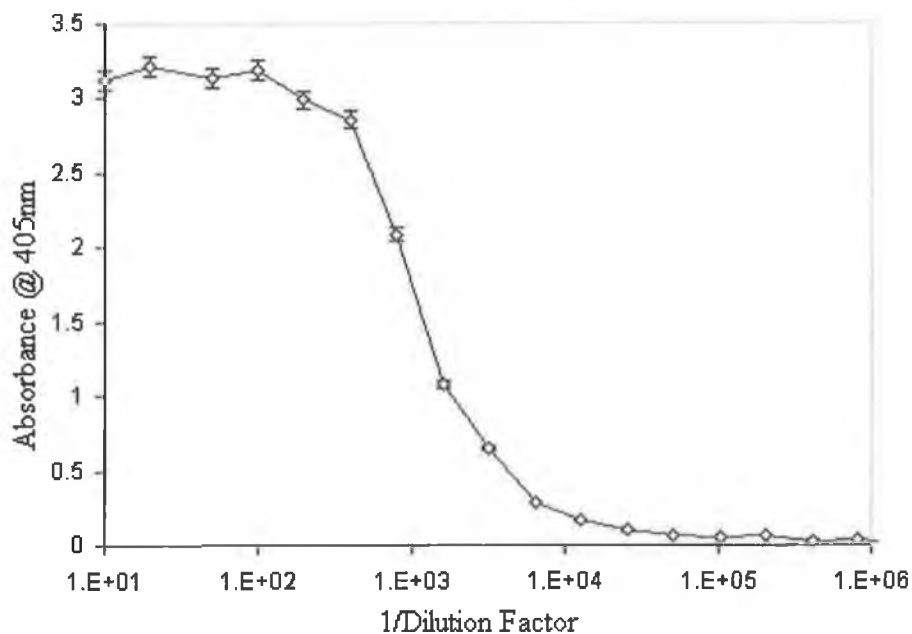
Figure 3.11: Determination of mAb optimal working dilution. The working dilution of mAb for competitive ELISA was taken from the linear portion of the sigmoidal mAb dilution curve, where the greatest change in absorbance for a similar change in antibody dilution occurs. A 1/800 working dilution was determined from the above curve.

3.2.3.2. Antibody Concentration Determinations

Affinity-based techniques such as ELISA and other biosensor-based techniques provide a unique means of determining the biologically active concentration of antibody, unlike spectroscopic techniques that provide total protein concentrations, and consequently inaccurate thermodynamic constants. Concentration of purified mAb was determined using a well-based ELISA capture system employing purified polyclonal anti-mouse immunoglobulin (M6149) as the capture antibody as described in section 2.5.2.7.

3.2.3.2.1. Mouse IgG Determination by Antibody Capture ELISA

Goat anti-mouse immunoglobulin (M6149) was initially purified on a Protein-G sepharose column as described in section 2.5.3.2. The concentration of protein in the purified fraction was estimated by means of UV absorbance at 280 nm (1 mg/ml IgG $O.D._{280\ nm} \approx 1.35$) (Hudson & Hay, 1988). The wells of an ELISA microtitre plate were coated with a solution containing approximately

120

1µg/ml goat anti-mouse immunoglobulin (M6149) in PBS-1, and blocked as described in section 2.5.2.1. Serial dilutions of murine IgG of known concentration ranging from 3.90-1000 ng/ml were prepared in blocking buffer. Dilutions of protein G purified mAb ranging from 1/10 to 1/10,000, were prepared. The known concentrations of murine IgG and the dilutions of purified mAb were then added to the wells of the microtitre plate and the ELISA was then developed as described in section 2.5.2.1. The concentration of antibody in the purified antibody fraction was calculated by constructing a standard curve of the log of mouse immunoglobulin concentration versus absorbance at 405 nm. A spline calibration plot was constructed using BIAevaluation 3.1 software™. From the results from the spline calibration plot (Figure 3.12.) concentration of antibody in the affinity-purified fraction for clone 4.2.25. was calculated to be approximately 32.97 µg/ml.
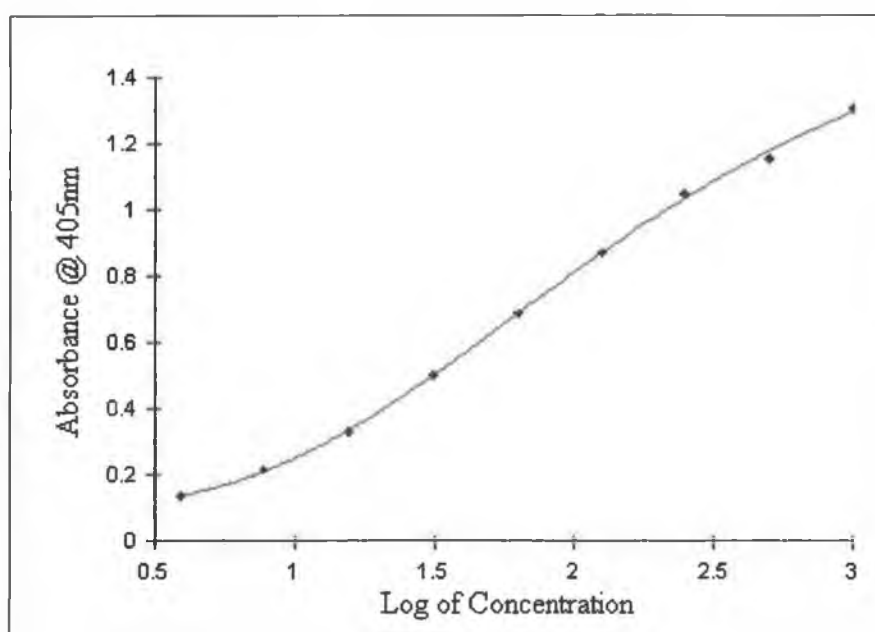
Figure 3.12. Mouse IgG calibration plot constructed using BIAevaluation^{TM} software. A spline is fitted to the data set for non-linear plots, allowing for calculation of the mouse IgG in protein G purified fraction. Each point on the curve is the mean of three replicates.

3.2.3.3. Competitive ELISA for the Detection of Warfarin in PBS

Protein G affinity-purified monoclonal antibody from clone 4.2.25. was used in a competitive ELISA format for the detection of warfarin in solution as described in section 2.5.2.5. Immunoassays are generally best modelled using a four-parameter fit equation, of the form:

$$R = R_{HI} - \frac{R_{HI} - R_{LO}}{1 + \left(\dfrac{Conc}{A_1}\right)^{A_2}} \qquad\qquad (2)$$

Where R_{HI} =   Response at infinite concentration

             R_{LO} =   Response at zero concentration

             $Conc$ =   Analyte Concentration (M)

             A_1 =   Fitting constant

             A_2 =   Fitting constant

Four-parameter equations of the form above were fitted to the data sets obtained for immunoassays curves using BIAevaluation 3.1 software. Such calibration curves also allowed for the determination of unknown values from the constructed plot. In this way it was possible to calculate the degree of precision of analytical measurements at different concentrations points relative to the fitted four-parameter equation.

Fitting a four-parameter curve to the data set as opposed to utilising the straight-line portion of the sigmoidal plot conventionally obtained with ELISAs, greatly extends the working range of the plot at the asymptotes of the curve for both ends of the concentration range employed. 4-parameter curves were fitted to the data obtained using BIAevaluation software™. A comparison of the extended working range obtained can be observed in Table 3.4 and 3.5 and Figures 3.13 and 3.14, which illustrates that the working range of the ELISA was extended with no significant effect on the degree of assay precision.

In order to measure the accuracy of the immunoassay, intra-day variability studies were performed. Five sets of warfarin standards ranging from 1.95 - 500 ng/ml were prepared, and assayed on the same day and their means plotted. These absorbance values (A) were then divided by the absorbance measurement in the presence of zero antigen concentration (A_0) to give normalised absorbance values (A/A_0). A calibration plot of the mean normalised absorbance value versus warfarin concentration in ng/ml was then constructed using BIAevaluation software™ (Figure 3.13). From the calibration curve it was possible to calculate the mean, standard deviation, coefficient of variation and precision for intra-assay measurements. The coefficient of variation (CV's) were determined to assess the precision of the analytical method, expressing standard deviation as a percentage function of the mean. These values ranged from 1.05 - 7.29 % indicating the assay had a high degree of precision and the results are shown in Table 3.3.

To measure the intermediate precision (precision of repeated measurements, taking into account sources of variation such as runs, days and reagents), inter-day assay variability studies were performed with the anti-warfarin monoclonal antibody. Five sets of warfarin standard ranging from 3.91 - 500 ng/ml were prepared, and assayed five times over five days. A separate calibration curve plotting normalised values (A/A_0) versus concentration values (ng/ml) was then constructed for each assay curve. The normalised values from each curve for each concentration determination were then back-calculated using the calibration curve and BIAevaluation software. The mean back-calculated concentration from each of the calibration curves was then used to calculate the mean, standard deviation and coefficient of variation for the inter-assay curve. The CVs were determined and ranged from 3.16 - 8.62 %. The percentage accuracies of the curve (Figure 3.15) were good (Table 3.5) especially in the linear range of the assay (96-102 %), which indicates that the curve provides an accurate representation of the sigmoidal relationship between the measured response and the logarithm of concentration observed for the immunoassay. Residual plots for the calibration curves are included for each calibration curve, which illustrate the 'goodness of the fit' of the applied 4-parameter equations (Figure 3.13 & 3.15). The residual plots also illustrate the precision profile of the calibration curves over the assayed concentration range and illustrate that the 4-parameter equation demonstrates no bias over the assayed concentration range, unlike linear plots (Figure 3.14) which have a tendency to demonstrate increased bias at the extremities of the linear plot (Findlay *et al.,* 2000).

Table 3.3: Intra-day Assay coefficients of variation (CVs) and percentage accuracies data for the anti-warfarin monoclonal antibody in PBS. Coefficients of variance (a quantitative measure of precision) were calculated utilising the equation % CV = (S.D./Mean) x 100, where the standard deviation (S.D.) is computed from replicate (5 replicates) analyses within a single validation run. Percentage accuracy is the difference between the actual warfarin concentration (AWC) of the prepared warfarin standards and the mean back calculated warfarin concentration (MBCW) value obtained from the 4-parameter calibration curve: (AWC/MBCW) x 100

Actual Warfarin Concentration (ng/ml)	Mean Back Calculated Warfarin Concentration from calibration curve (ng/ml)	% CV	% Accuracies
500.00	646.90	6.19	77.29
250.00	245.65	6.17	101.77
125.00	105.21	6.37	118.81
62.50	65.24	7.29	95.80
31.20	32.50	4.06	96.00
15.60	15.59	1.05	100.06
7.81	7.52	2.19	103.86
3.91	4.00	3.63	97.75
1.95	1.91	3.05	102.09
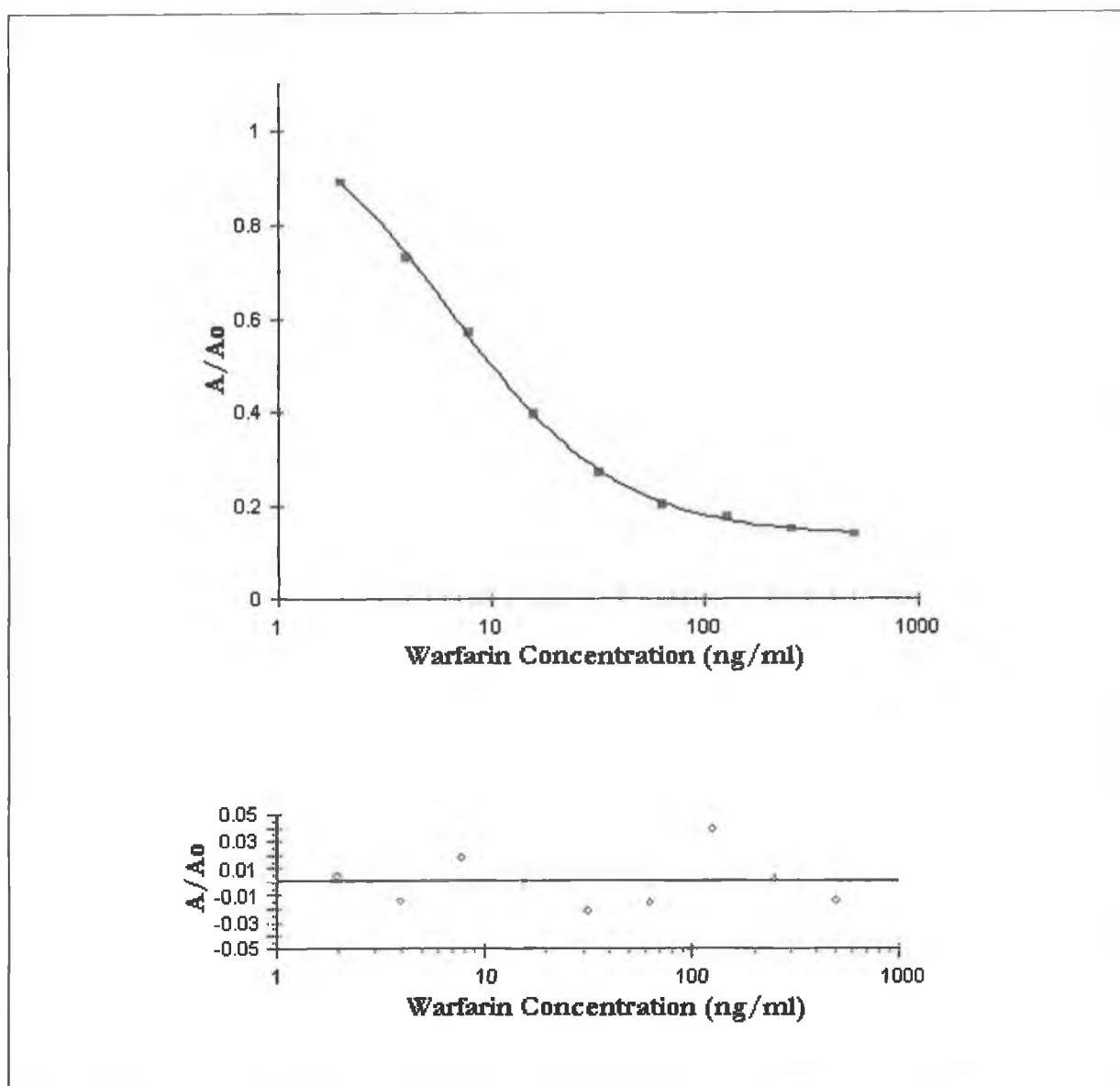
Figure 3.13: *Intra-day Assay calibration curve for the detection of warfarin in PBS utilising an anti-warfarin mAb. A 4-parameter equation was fitted to the data set using BIAevaluation 3.1. software. The intraday means and coefficients of variation are tabulated in Table 3.3. Each point on the curve is the mean of five replicate measurements analysed within a single validation run. Residual plots for the calibration curves are included for each calibration curve, which illustrate the 'goodness of the fit' of the applied 4-parameter equations and supports the % accuracy findings.*

Table 3.4: *Intra-day Assay coefficients of variation (CVs) and percentage accuracies data for the anti-warfarin monoclonal antibody in PBS (using linear regression). Coefficients of variance (a quantitative measure of precision) were calculated utilising the equation % CV = (S.D./Mean) x 100, where the standard deviation (S.D.) is computed from replicate (5 replicates) analyses within a single validation run. Percentage accuracy is the difference between the actual warfarin concentration (AWC) of the prepared warfarin standards and the mean back calculated warfarin concentration (MBCW) value obtained from the 4-parameter calibration curve: (AWC/MBCW) x 100*

Actual Warfarin Concentration (ng/ml)	Mean Back Calculated Warfarin Concentration (ng/ml)	% CV	% Accuracies
31.20	29.37	4.06	106.23
15.60	16.96	1.05	91.98
7.81	7.83	2.19	99.74
3.91	3.90	3.63	100.26
1.95	1.91	3.05	102.09
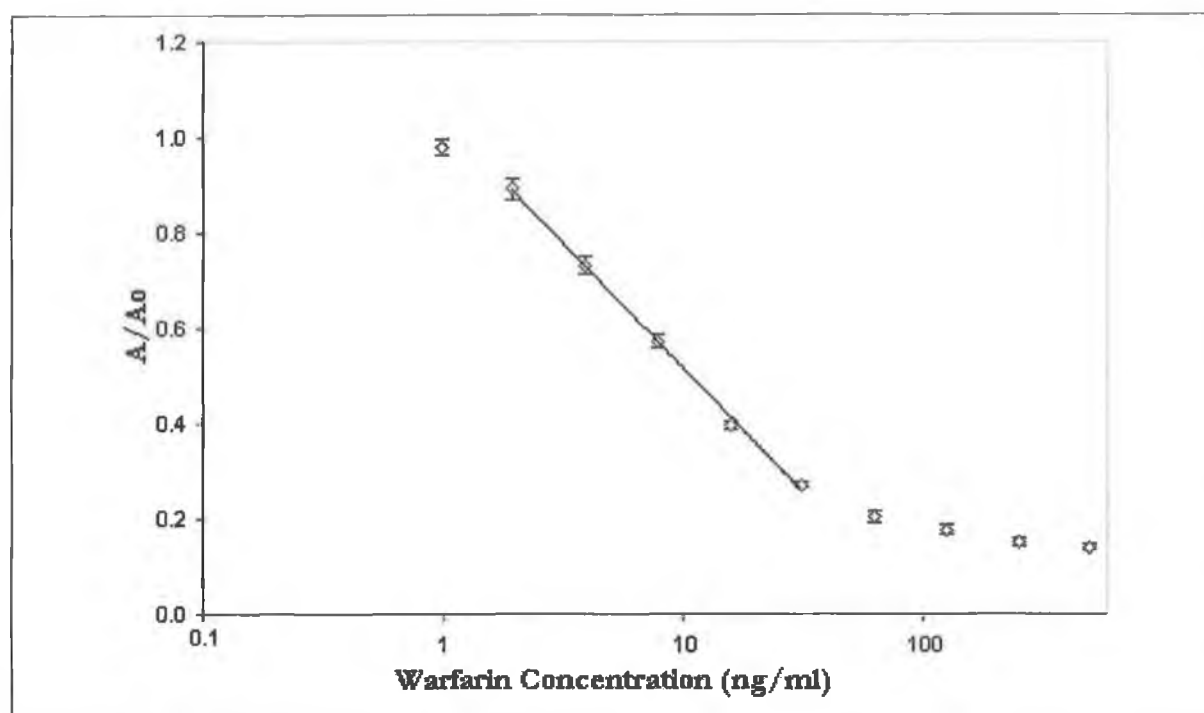
Figure 3.14: *Intra-day Assay curve:*

Linear regression analysis was applied to the data set giving the line of best fit, from which the intra-assay mean, coefficient of variation and precision were calculated and shown in the above table. Each point on the curve is the mean of (n=5) replicate measurements carried out on a single day ± standard deviation.

Table 3.5: *Inter-day Assay coefficients of variation (CVs) and percentage accuracies data for the anti-warfarin monoclonal antibody in PBS. Coefficients of variance (a quantitative measure of precision) were calculated utilising the equation % CV = (S.D./Mean) x 100, where the standard deviation (S.D.) is computed from replicate (5 replicates) analyses over 5 validation runs on 5 separate days. Percentage accuracy is the difference between the actual warfarin concentration (AWC) of the prepared warfarin standards and the mean back calculated warfarin concentration (MBCW) value obtained from the 4-parameter calibration curve: (AWC/MBCW) x 100.*

Actual Warfarin Concentration (ng/ml)	Mean Back Calculated Warfarin Concentration from calibration curve (ng/ml)	% CV	% Accuracies
500.00	499.95	3.78	100.01
250.00	243	3.86	102.88
125.00	129.97	5.17	96.18
62.50	61.10	4.42	102.30
31.25	31.26	3.16	99.97
15.63	15.53	7.92	100.64
7.81	8.42	7.11	92.76
3.91	4.07	8.62	96.07
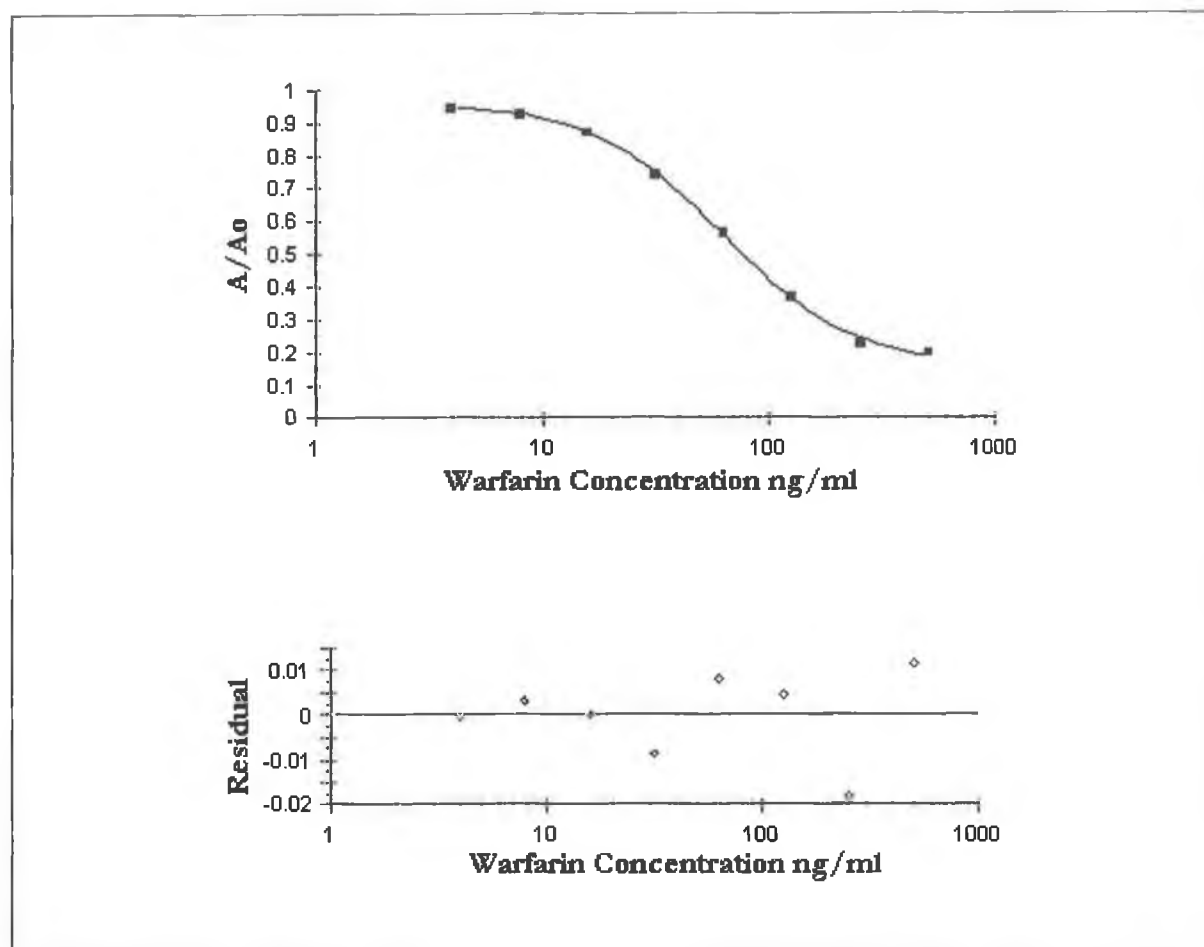
Figure 3.15: *Inter-day Assay calibration curve for the detection of warfarin in PBS utilising an anti-warfarin mAb. A 4-parameter equation was fitted to the data set using BIAevaluation 3.1 software. The interday means and coefficients of variation are tabulated in Table 3.5. Each point on the curve is the mean of five replicate measurements analysed over five days. Residual plots for the calibration curves are included for each calibration curve, which illustrate the 'goodness of the fit' of the applied 4-parameter equations and supports the % accuracy findings.*

3.2.3.4. Competitive ELISA for the Detection of Warfarin in Urine

Quantitative determination of mAb in urine samples was also investigated. The ionic composition of urine can vary considerably from sample to sample. To compensate for the potential of great inter-individual variability in the salt composition of urine, the mAb sample was prepared in PBS of twice the normal ionic strength. Warfarin samples ranged approximately from 3 - 500ng/ml. These samples were spiked into control urine and assayed for the presence of free drug with mAb.

To carry out intra-day assay variability studies in urine, five sets of warfarin standards ranging from 3.91 - 500 ng/ml were prepared, and assayed on the same day and their means plotted. These absorbance values (A) were then divided by the absorbance measurement in the presence of zero antigen concentration (A_0) to give normalised absorbance values (A/A_0). A calibration plot of the mean normalised absorbance value versus warfarin concentration in ng/ml was then constructed using BIAevaluation software™. From the calibration curve it was possible to calculate the mean, standard deviation, coefficient of variation and precision for intra-assay measurements. The CVs were determined to assess the precision of the analytical method, expressing standard deviation as a percentage function of the mean. These values ranged from 3.47 - 15.41 % as shown in Table 3.6, where it can be seen that there was a much greater degree of variance in comparison to PBS assays (Table 3.3). This is due to the undefined nature of urine, however this assay is still reproducible as the results show in Figure 3.16 and Table 3.6.

To carry out inter-day assay variability studies, 5 sets of warfarin standard ranging from 3.91 - 500 ng/ml were prepared, and assayed five times over five days. A separate calibration curve plotting normalised values (A/A_0) versus concentration values (ng/ml) was then constructed for each assay curve. The normalised values from each curve for each concentration determination were then back-calculated using the calibration curve and BIAevaluation software. The mean back-calculated concentration from each of the calibration curves was then used to calculate the mean, standard deviation and coefficient of variation for the inter-assay curve. The CVs were determined and ranged from 3.63 - 17.16 %. Again there was a greater degree of variance than the PBS assays however, this assay is still reproducible and the results are shown in Figure 3.16 and Table 3.7. The percentage accuracies of the curve (Figure 3.17) were good (Table 3.7) especially in the linear range of the assay (99-102 %), which indicates that the curve provides an accurate representation of the sigmoidal relationship between the measured response and the logarithm of concentration observed for the immunoassay. Residual plots for the calibration curves are included for each calibration curve, which illustrate the 'goodness of the fit' of the applied 4-parameter equations.

130

Table 3.6: Intra-day Assay coefficients of variation (CVs) and percentage accuracies data for the anti-warfarin monoclonal antibody in urine. Coefficients of variance (a quantitative measure of precision) were calculated utilising the equation % CV = (S.D./Mean) x 100, where the standard deviation (S.D.) is computed from replicate (5 replicates) analyses within a single validation run. Percentage accuracy is the difference between the actual warfarin concentration (AWC) of the prepared warfarin standards and the mean back calculated warfarin concentration (MBCW) value obtained from the 4-parameter calibration curve: (AWC/MBCW) x 100.

Actual Warfarin Concentration (ng/ml)	Mean Back Calculated Warfarin Concentration from calibration curve (ng/ml)	% CV	% Accuracies
500.00	496.98	15.41	100.61
250.00	255.70	15.19	97.77
125.00	120.91	13.63	103.38
62.50	63.46	11.28	98.49
31.25	32.37	11.04	96.54
15.63	14.74	4.83	106.04
7.81	7.58	4.94	103.03
3.91	4.25	3.47	92.00
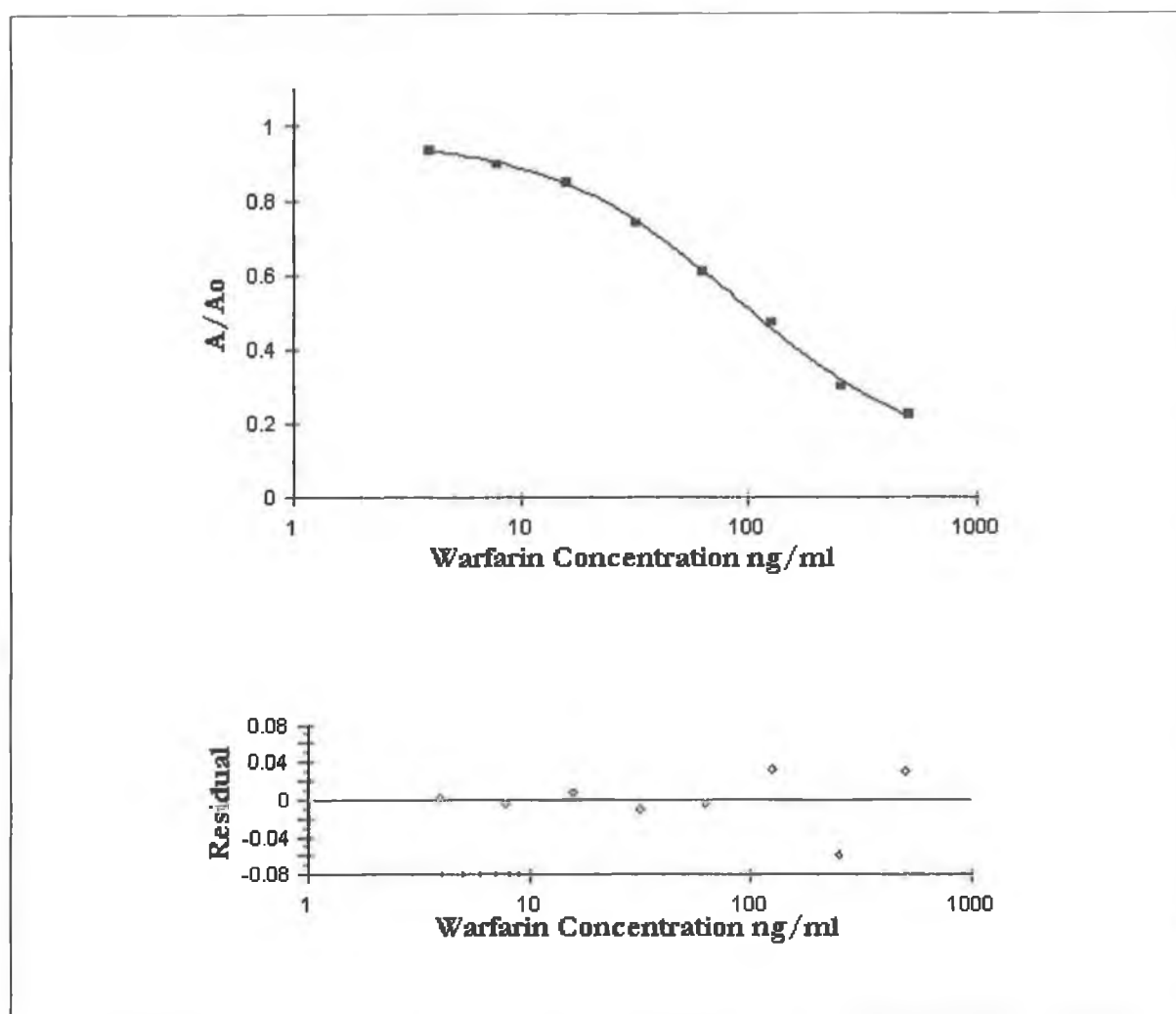
Figure 3.16: *Intra-day Assay calibration curve for the detection of warfarin in urine utilising an anti-warfarin mAb. A 4-parameter equation was fitted to the data set using BIAevaluation 3.1. software. The intraday means and coefficients of variation are tabulated in Table 3.6. Each point on the curve is the mean of five replicate measurements analysed within a single validation run. Residual plots for the calibration curves are included for each calibration curve, which illustrate the 'goodness of the fit' of the applied 4-parameter equations and supports the % accuracy findings.*

Table 3.7: Inter-day Assay coefficients of variation (CVs) and percentage accuracies data for the anti-warfarin monoclonal antibody in urine. Coefficients of variance (a quantitative measure of precision) were calculated utilising the equation % CV = (S.D./Mean) x 100, where the standard deviation (S.D.) is computed from replicate (5 replicates) analyses over 5 validation runs on 5 separate days. Percentage accuracy is the difference between the actual warfarin concentration (AWC) of the prepared warfarin standards and the mean back calculated warfarin concentration (MBCW) value obtained from the 4-parameter calibration curve: (AWC/MBCW) x 100.

Actual Warfarin Concentration (ng/ml)	Mean Back Calculated Warfarin Concentration from calibration curve (ng/ml)	% CV	% Accuracies
500.00	499.29	17.16	100.14
250.00	251.44	13.69	99.43
125.00	123.04	9.12	101.59
62.50	64.54	9.01	96.84
31.25	29.99	5.63	104.20
15.63	16.01	4.46	97.63
7.82	7.67	8.28	101.96
3.91	3.99	3.63	97.99
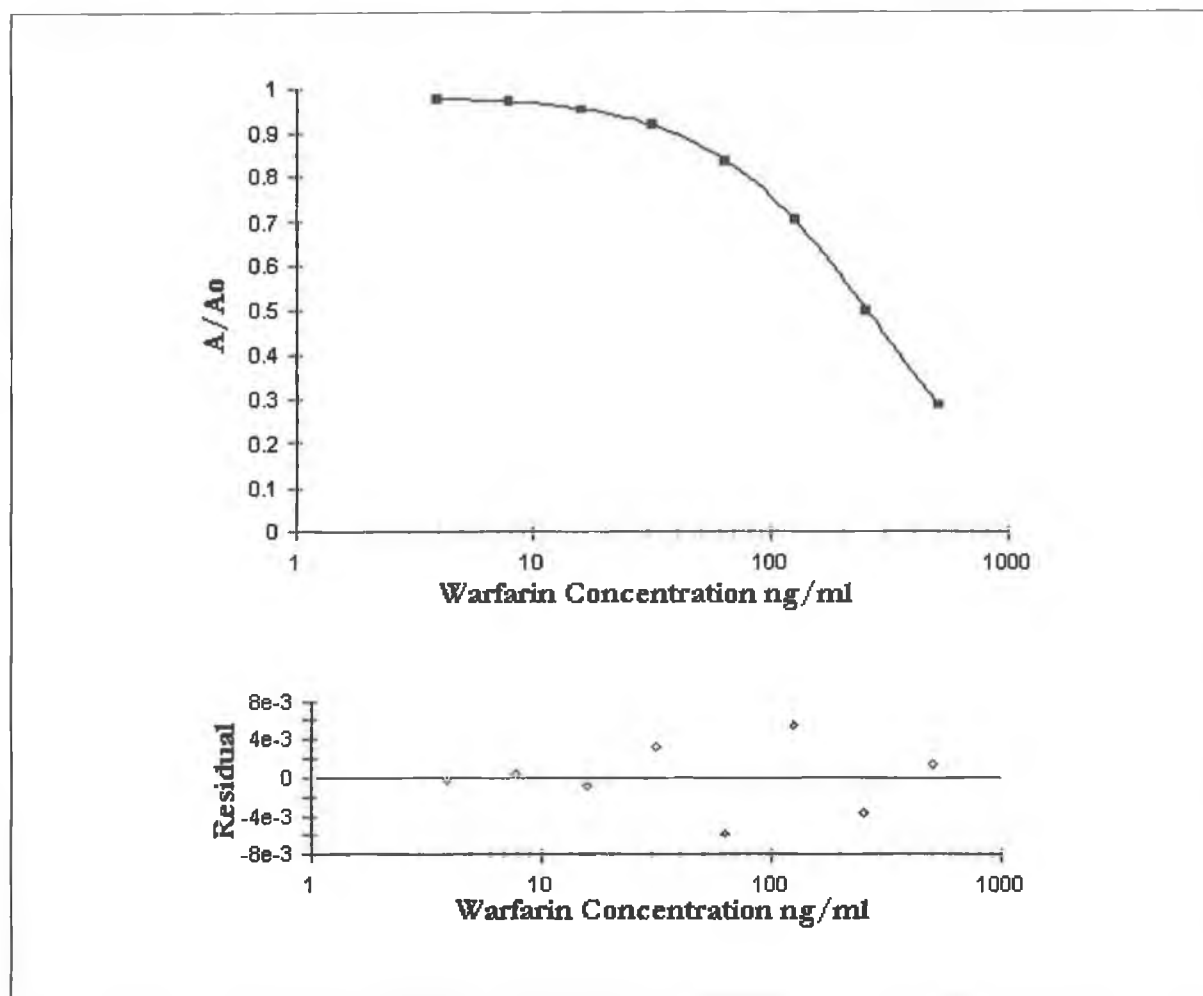
Figure 3.17: *Inter-day Assay calibration curve for the detection of warfarin in urine utilising an anti-warfarin mAb. A 4-parameter equation was fitted to the data set using BIAevaluation 3.1 software. The interday means and coefficients of variation are tabulated in Table 3.7. Each point on the curve is the mean of five replicate measurements analysed over five days. Residual plots for the calibration curves are included for each calibration curve, which illustrate the 'goodness of the fit' of the applied 4-parameter equations and supports the % accuracy findings.*

3.2.4. Cross-Reactivity Studies

Cross-reactivity may be defined as a measure of the antibody response to structurally related molecules, as a result of shared epitopes (Findlay *et al.*, 2000). Given the unique specifity of antibodies, one of the first steps in immunoassay design is the assessment of reactivity towards structurally related molecules that share such common epitopes (Davies, 1994b). Cross-reactivity can be assessed by setting up serial dilutions of the competing antigen in parallel with similar dilutions of the specific antigen as described in section 2.5.2.5. Cross-reactivity can be defined as the point where the reduction in signal recorded in the presence of a particular analyte concentration (A_x) gives a 50% reduction in the signal in the presence of zero analyte (A_0) (i.e. A_x/A_0=50%). This concentration value at 50% inhibition (EC_{50}) can then be expressed as a percentage of the analyte giving the same decrease in signal (Figure 3.18).

Therefore,

$$\% \text{ Cross-reactivity} = \frac{\text{Concentration of analyte giving 50\% decrease in signal}}{\text{Concentration of the cross-reactant giving 50\% decrease in signal}} = \frac{Z_1}{Z_2} \times 100\% \quad \text{(X)}$$
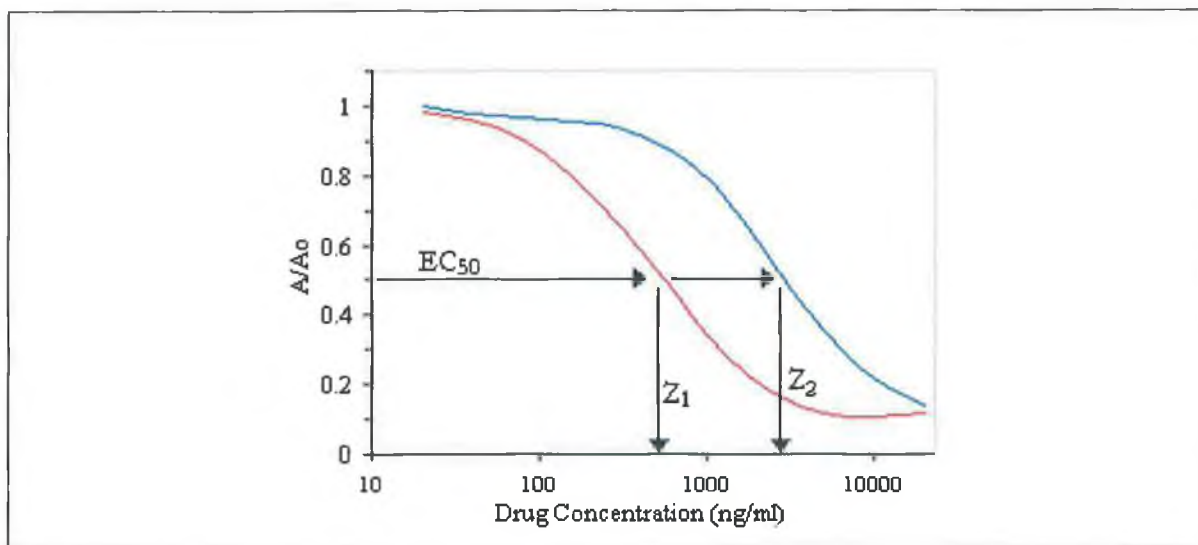
Figure 3.18: *Typical plot illustrating the potential cross reactivity of a particular antibody preparation towards a structurally related compound using the ratio of concentrations of each compound that gives 50% inhibition. (The % cross reactivity is calculated by expressing the antigen concentration, Z_1, as a percentage of the cross reactant concentration, Z_2.).*

The nitro-group on the parent molecule (4-hydroxycoumarin) was chosen as the point of attachment for two particular reasons. Firstly, it provided a convenient means of conjugation.

135

Secondly, as the major human metabolites of warfarin involve hydroxylations of the 4-hydroxycoumarin ring structure and carbon side chain of the molecule, it was believed that conjugation via the phenyl substituent would confer a greater degree of specificity to the antibodies produced against warfarin.
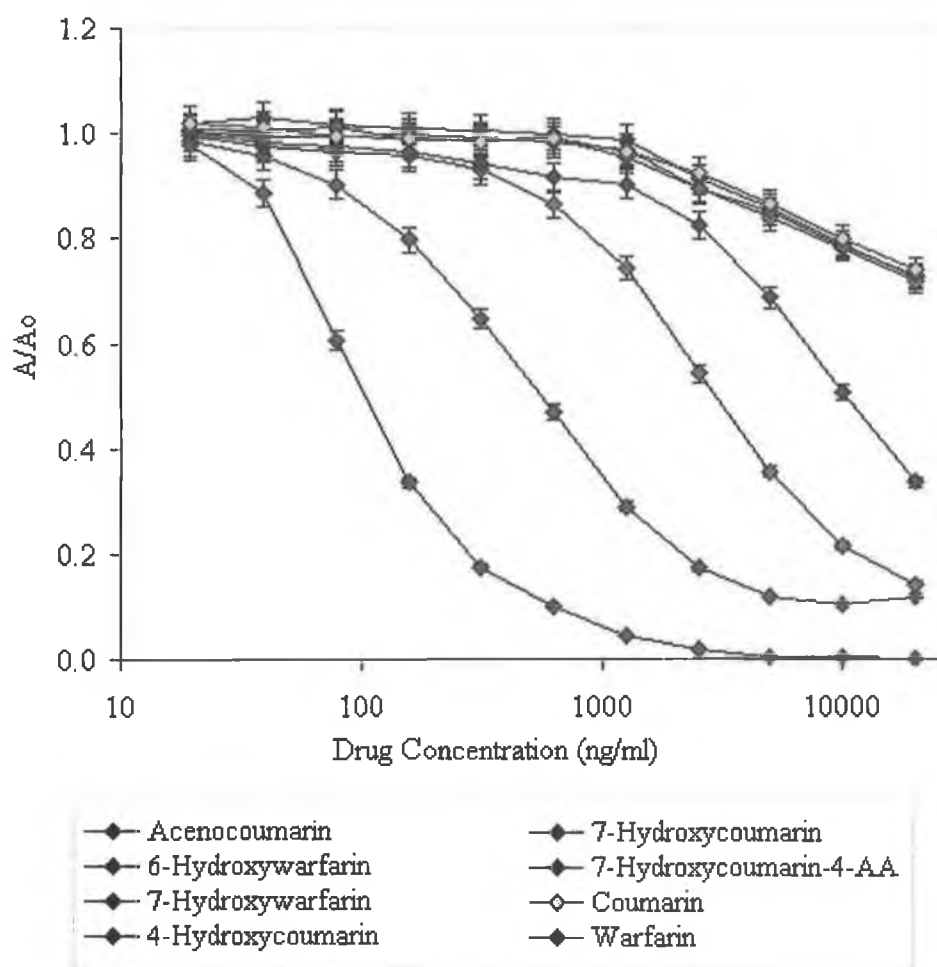
Figure 3.19: Cross-reactivity studies of monoclonal antibodies. Cross-reactivity studies were carried out on the Protein-G- purified anti-warfarin monoclonal antibodies, as described in section 2.5.2.5., to structurally related warfarin derivatives. The antibody demonstrated little or no reactivity towards coumarin-based molecules (e.g. 7-HC, 4-HC, Coumarin) suggesting that the presence of the carbonyl group and possibly the phenyl ring are also required for antibody recognition.

The results from the cross-reactivity study are shown in Figure 3.19 and Table 3.8. The cross-reactivity of the purified monoclonal antibody demonstrated the highest degree of cross-reactivity (18.18%) towards acenocoumarin, as expected given that the two compounds are essentially identical

except for the presence of the nitro group. Since this particular region does not confer any antibody specificity being the point of conjugation, this would explain the similar affinity of the monoclonal antibody preparation to acenocoumarin. The monoclonal antibody showed cross-reactivity of approximately 8 and 1% towards 6- and 7-hydroxywarfarin, respectively. Cross reactivity studies were also carried out using 4-hydroxycoumarin (which comprises half of the molecule), coumarin, 7-hydroxycoumarin, and 7-hydroxycoumarin-4-acetic acid. Cross-reactivities towards these particular compounds in each case was negligible and typically of the order of < 0.001%.

Table 3.8: Cross-Reactivity of protein G-purified anti-warfarin monoclonal antibody

Compound	*% Cross Reactivity*
Warfarin	100.00
Acenocoumarin	18.18
6-Hydroxywarfarin	8.33
7-Hydroxywarfarin	1.00
7-Hydroxycoumarin	0.09
4-Hydroxycoumarin	0.09
Coumarin	0.09
7-Hydroxycoumarin-4-acetic acid	0.09

3.2.5. Affinity Constant Determinations

An ELISA-based approach originally published by Friguet *et al.*, (1985) was used to measure the affinity of the anti-warfarin mAb to warfarin and structurally related analogues by calculation of the dissociation constant (K_D) of antibody:antigen mixtures at equilibrium in solution. An unknown but constant concentration of mAb is incubated with known varying concentrations of the antigen of interest. The antibody:antigen mixtures are allowed to attain equilibrium and the 'bound' concentration of antibody (V) can be can then be calculated by indirect ELISA as described in section 2.5.2.6. by the expression:

$$V = \frac{A_0 - A_1}{A_0}$$
(3)

Where A_0 = Absorbance in the absence of antigen

A_1 = Absorbance in the presence of antigen

The concentration of bound antibody can be related to the antigen concentration by the following equation:

$$\frac{1}{V} = \frac{KD}{Ag} + 1$$
(4)

A plot of 1/(V) versus 1/[Ag] will thus yield a straight line graph with a y-intercept of 1, with the slope of the regression line (K_D), describing the overall equilibrium constant for the antibody: antigen interaction at equilibrium.
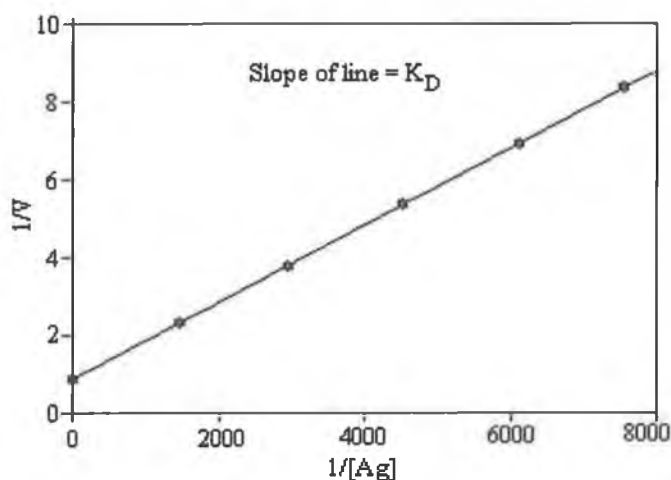
Figure 3.20: *Typical plot obtained using the method of Friguet et al., (1985). A plot of the reciprocal of bound antibody (1/V) versus the reciprocal of antigen concentration (1/[Ag]) should yield a straight line plot with a y-intercept of 1 and whose slope defined the dissociation constant for the particular antibody: antigen interaction at equilibrium.*

Two points must be addressed if this technique is to be used correctly to obtain reliable dissociation constants. The first prerequisite is to demonstrate the correlation between 'free' (i.e. unbound) antibody concentration in solution and enzymatic activity, and adding various dilutions of

138

antibody to antigen-coated wells of an ELISA plate as described in section 2.5.2.6. and constructing a calibration plot of nominal antibody concentration versus absorbance. A straight line plot similar to that in Figure 3.22. of 'nominal' antibody concentration (i.e. 1/dilution factor) versus enzymatic activity at 405 nm is attained, demonstrating the linear correlation between antibody concentration and enzymatic activity. This calibration plot can then be used to calculate the concentration of antigen bound antibody at equilibrium in the antibody: antigen mixtures.

The 'free' antibody concentration, i, following incubation with the antigen can be related to absorbance by the following equation:

$$\frac{i}{i_0} = \frac{A}{A_0}$$

(5)

Where A_0 = absorbance in the absence of antigen.

   A   = absorbance in the presence of antigen.

   i_0 = total antibody concentration.

The second prerequisite is that no readjustment of the antibody:antigen equilibrium mixture should occur during the incubation in the antigen-coated wells. This can be demonstrated experimentally by placing serial dilutions of antibody into the wells of an antigen-coated ELISA plate for a specified time interval. The contents of these wells can then be transferred into adjacent antigen-coated wells on the ELISA plate for a similar incubation period. An overlay of the plots for the developed ELISA of wells 1 and 2, as shown in Figure 3.21, should demonstrate no significant decrease in the antibody bound in the second set of wells. This implies that the amount of antibody bound by the solid phase antigen is negligible compared to the amount of antibody in solution, and is therefore unlikely to cause any significant displacement of the antibody:antigen mixture at equilibrium. The fraction of antibody retained by the first set of wells, f, can be calculated by the following equation:

$$f = \frac{A_1(c) - A_2(c)}{A_1(c)}$$

(6)

139

Where

f	=	fraction of antibody retained
$A_1(c) / A_2(c)$	=	enzymatic activities in the first and second set of wells, respectively. (i.e. absorbance measurements)
c	=	initial concentration of antibody

The antigen concentration was shown to have the greatest effect on the solid phase disruption of fluid phase equilibrium in affinity assays (Friguet *et al.,* 1985; Seligman, 1994). Reducing the incubation period in the antigen-coated wells also minimises the disruption of the fluid phase equilibrium. The optimal incubation period for clone 4.2.25 on the 96-well microtitre plate was typically of the order of 15-20 minutes. The value of f calculated for clone 4.2.25, was approximately = 0.03, demonstrating that the amount of bound antibody is negligible compared to overall antibody concentration. By calculating the amount of unbound antibody at equilibrium by reference to the antibody concentration calibration plot, the amount of ligand-bound antibody (V), can thus be estimated and used to calculate the overall affinity constant.

Table 3.9: *Calculation of free antibody concentrations.*

The nominal concentrations of antibody were calculated by reference to the constructed antibody standard curve and substituting the value obtained into equation 4. The value for the bound antibody was calculated to yield the values of 1/V. from which a plot of 1/[Ag] versus 1/V was constructed, whose slope (K_D) defined the dissociation constant K_D of the overall reaction.

[Warfarin] mol/l	1/[Warfarin] l/mol 1/[Ag]	Abs at 405nm	Nominal Antibody concentration NC	1/V
$1.62\,e^{-6}$	616000	0.072	0.126	1.085
$8.12\,e^{-7}$	1232000	0.101	0.165	1.115
$4.06\,e^{-7}$	2464000	0.304	0.435	1.469
$2.03\,e^{-7}$	4920000	0.432	0.606	1.373
$5.07\,e^{-8}$	19680000	0.647	0.892	1.610
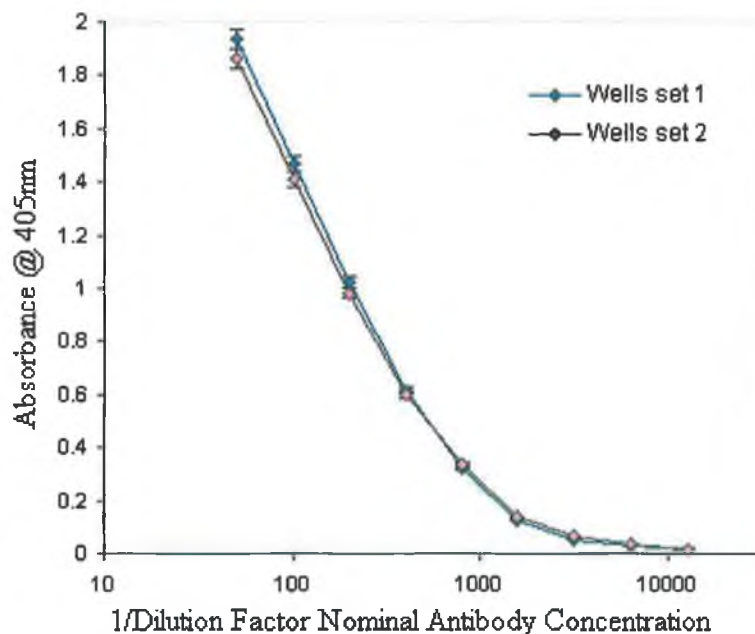
Figure 3.21: *The value for f (equation 6), represents the small amount of antibody that is captured in the ELISA and should represent a small fraction of the total free antibody. The above figure shows that for the anti-warfarin antibody, negligible readjustment occurred for the determination of the affinity constant by the Friguet method.*

141
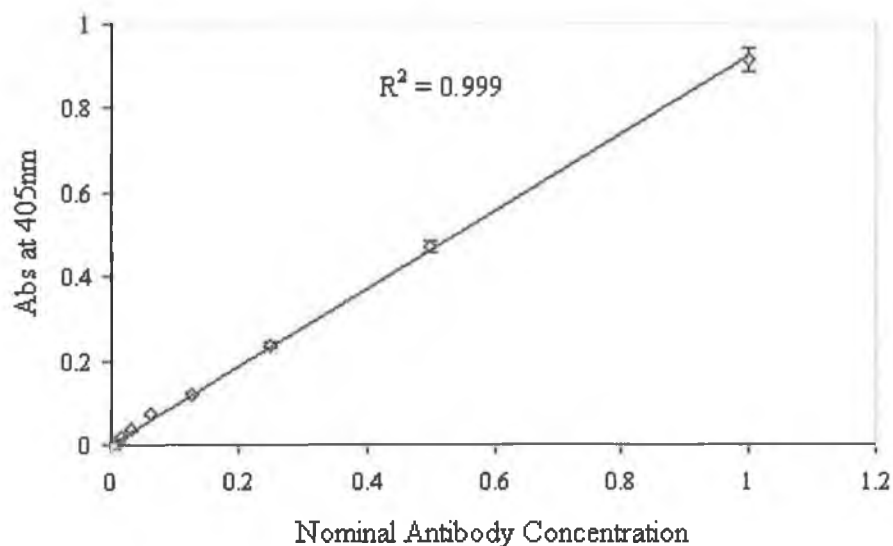
Figure 3.22: *A standard curve of nominal antibody concentration versus Absorbance at 405 nm was constructed as described in section 2.5.2.6. The highest antibody concentration used was given the nominal antibody concentration of '1' and serial doubling dilutions up to 1/256 dilution were prepared from this, of nominal concentration of 0.5, 0.25, 0.125, 0.0625, 0.03125, 0.0156, 0.0078 and 0.0039, respectively. The antibody dilutions were then applied to the microtitre plated for a predetermined incubation period to ensure that there would be minimal disturbance of the fluid phase equilibrium of the antibody:antigen mixture as described in equation 6. A linear plot of nominal antibody concentration versus absorbance at 405 nm was used to construct the antibody standard curve to determine the bound fraction of antibody present at equilibrium in the equilibrium mixtures. The results shown are the mean of triplicate measurements $\pm$ standard deviation.*

The chart shows a plot with 1/(V) on the y-axis and 1/[Ag] on the x-axis, with the equation:

$$1/V = (6.0 \times 10^{-8}) \times 1/[Ag] + 1.045 \quad R^2 = 0.997$$
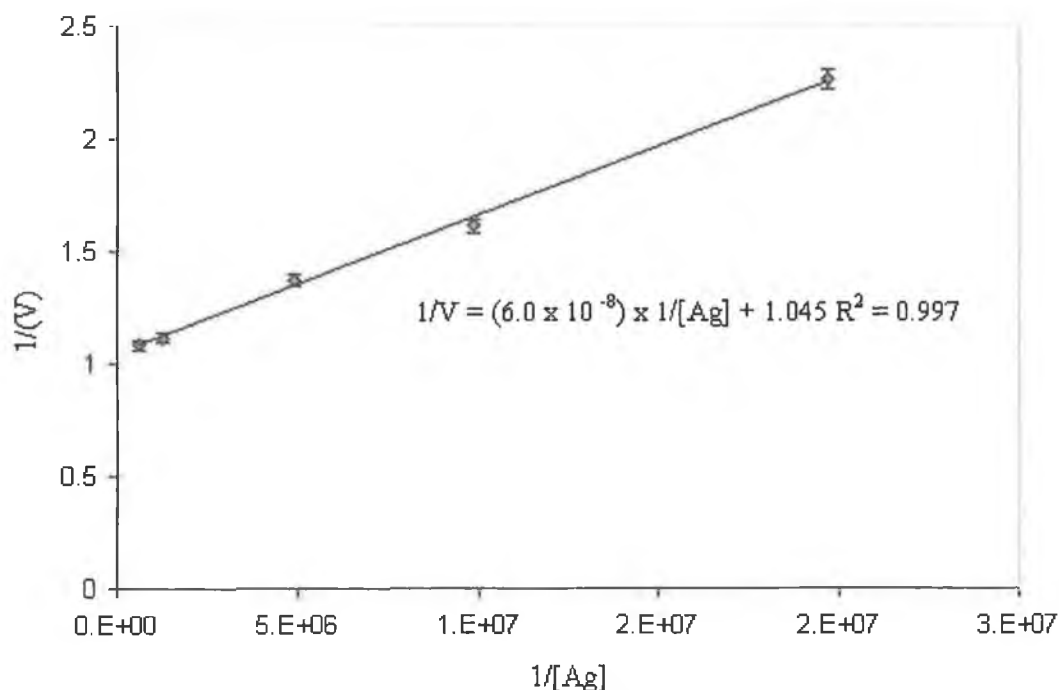
Figure 3.23: *Determination of the equilibrium dissociation constant for the interaction between warfarin and clone 4.2.25 by the method of Friguet et al., (1985). The nominal unbound antibody concentrations were calculated using the standard curve constructed in Figure 3.22, and equation (3.3) from which the values of 1/V were subsequently determined at the respective antigen concentrations as shown in Table 3.9. The calculated equilibrium dissociation constant for the interaction between warfarin and monoclonal antibody 4.2.25 was calculated to be 6.0 x 10^{-8} M.*

However, an antibody (e.g. anti-warfarin antibody), whether monovalently bound or completely non-bound to its specific antigen in solution, will still be able to bind to the coated wells of an ELISA plate. The concentration of antibody complex measured at equilibrium (Friguet method) does not take into account the fact that monovalently bound antibodies may also bind to the plate (Bobrovnik, 2003). The apparent binding constant measured will therefore not equal that of the corresponding antibody Fab fragments. Stevens (1987) developed a 'correction factor' based on the binomial distribution theory to provide the 'correct' concentration of liganded antibody binding sites to allow for the calculation of the 'correct' thermodynamic constant. Stevens (1987) postulated that if the probability that a Fab binding site is bound is taken as, z, then the probability that the binding site is free can then be interpreted as 1-z. For the case of an intact IgG molecule, the following relationships can be used to describe the three populations of antibody fractions existing within the equilibrium complex:

143

Completely Unbound:	$(1-z^2)$	
Monovalently bound:	$2z\,(1-z)$	
Bivalently bound:	z^2	(7)

On the basis of binomial distribution, assuming that the binding of one Fab does not preclude the binding of a second Fab (which is the case for small haptens, not necessarily true for larger molecular weight haptens due to steric hindrance factors (Quinn & O'Kennedy, 2001)), of the three antibody populations present at equilibrium, only the bivalently bound antibody, (z^2), is incapable of binding to the ELISA plate. The fraction of free antibody assayed by ELISA (m) is therefore equal to $1-z^2$.

$$m = 1 - z^2 \qquad (8)$$

and

$$z = \sqrt{1-m} \qquad (9)$$

represents the corrected fraction of liganded binding sites in terms of the apparent free IgG. The method of Friguet et al.,(1985) measures the 'bound' fraction of unbound IgG (V), using the relationship:

$$V = \frac{A_0 - A_1}{A_0} \qquad (10)$$

It can be seen, therefore, that as the concentration in equation (7) represents the bivalently bound antibody fraction, the corrected fraction of occupied antibody binding sites at any antigen concentration is given by:

$$z = \sqrt{V} \qquad (11)$$

Stevens (1987) found that overall association constants were overestimated by a factor of at least 2, with the level of error inversely proportional to the level of binding site occupancy. By substituting the corrected value of liganded binding sites a more 'realistic' value of association constants is determined which takes into account the bivalent nature of the antibody giving association constants for whole IgG that closely mirror those for Fab fragments (Bobrovnik, 2003).

Table 3.10: *'Corrected' Free Antibody Concentrations according to Stevens (1987).*

[Warfarin] mol/l	1/[Warfarin] l/mol 1/[Ag]	Nominal Antibody concentration NC	1/V	Corrected Free Antibody concentration $1/z=(1/V)^{1/2}$
$1.623\ e^{-6}$	616000	0.126	1.085	1.042
$8.12\ e^{-7}$	1232000	0.165	1.115	1.056
$4.06\ e^{-7}$	2464000	0.435	1.469	1.172
$2.03\ e^{-7}$	4920000	0.606	1.373	1.269
$5.07\ e^{-8}$	19680000	0.892	1.610	1.503
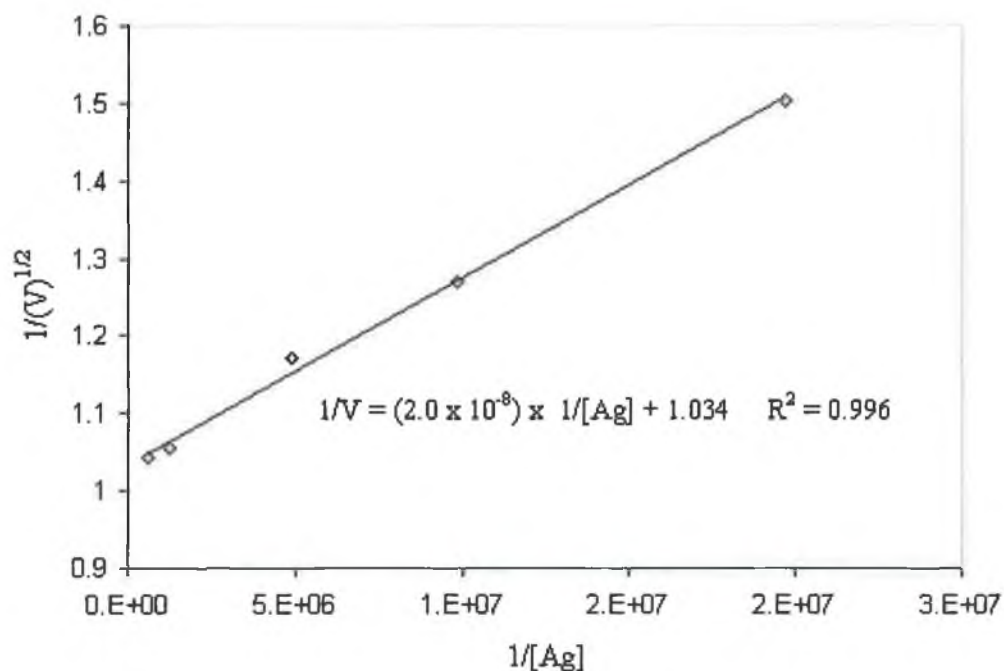
Figure 3.24: *Friguet assay for warfarin clone 4.2.25 using 'corrected' IgG concentrations described by Stevens (1987) to account for bivalency of IgG. The corrected overall dissociation constant ($K_D = 2.0 \times 10^{-8}M$) indicates that there is a 3 fold increase in estimation of overall affinity constant compared to the 'uncorrected' IgG concentration shown in Figure 3.22 ($K_D = 6.0 \times 10^{-8}M$).*

It could be argued that the method of Friguet *et al.*, (1985) only works particularly well for high affinity antibodies, as the incubation step in ELISA must be sufficiently short not to perturb the antibody:antigen equilibrium complex. For low affinity antibodies (high off rates) such a condition

145

can be difficult to achieve in practice. Friguet assays for the anti-warfarin antibody with particular antigens are shown in Figures 3.25 and 3.26 and overall affinities shown in Table 3.11.

The top graph shows a linear plot of $1/V$ versus $1/[Ag]$ with equation $1/V = (4.0 \times 10^{-7})\,x + 1.269$ and $R^2 = 0.997$.

The bottom graph shows a linear plot of $1/V$ versus $1/[Ag]$ with equation $1/V = (6 \times 10^{-6})\,x + 1.902$ and $R^2 = 0.984$.
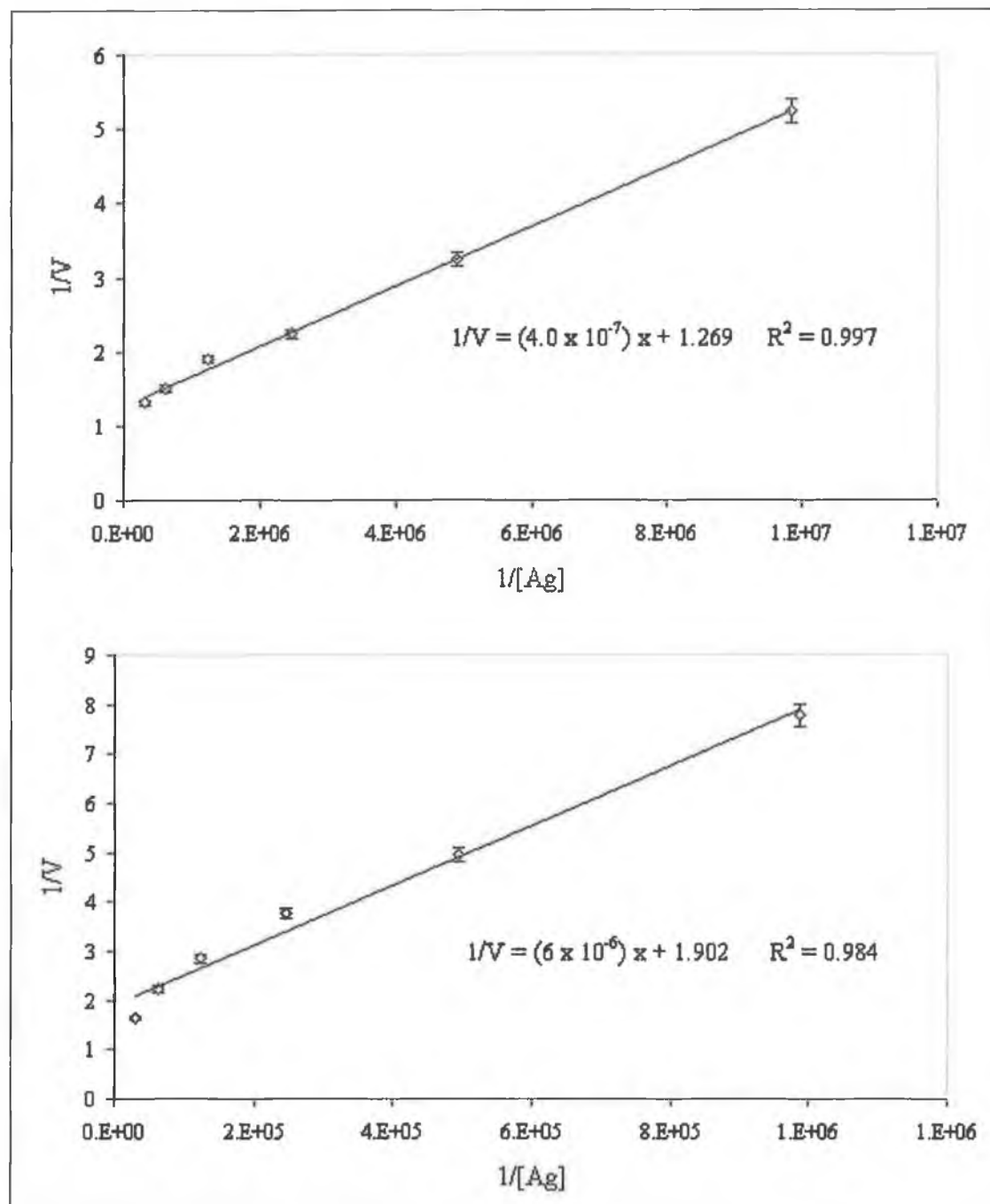
Figure 3.25: *Friguet affinity determinations of equilibrium dissociation constants for the interaction between clone 4.2.25 and antigens acenocoumarin (Top) and 6-hydroxywarfarin (Bottom).*

146

The equation shown in the figure:

$$1/V = (2 \times 10^{-6}) x + 3.181 \quad R^2 = 0.991$$

Axes: y-axis labelled $1/V$, x-axis labelled $1/[Ag]$
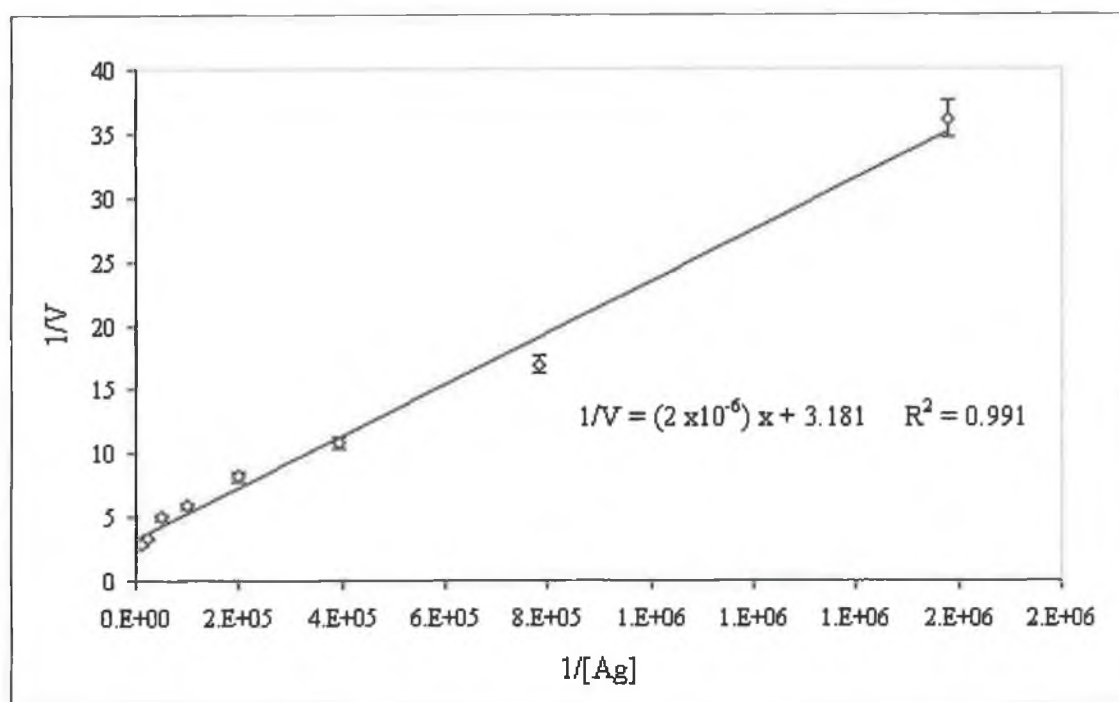
Figure 3.26: *Friguet affinity determination of equilibrium dissociation constant for the interaction between clone 4.2.25 and antigen 7-hydroxywarfarin.*

Table 3.11: *Equilibrium dissociation constants (K_D) determined using the method of Friguet et al., (1985) for the interaction between warfarin and mAb from clone 4.2.25. The affinity of the mAb to structurally related molecules of warfarin was also measured, and the equilibrium dissociation constants determined are tabulated below.*

Antigen	Clone 4.2.25 (M)
Warfarin	2.0×10^{-8}
Acenocoumarin	4.0×10^{-7}
6-hydroxywarfarin	6.0×10^{-6}
7-hydroxywarfarin	2.0×10^{-6}

147

3.3. Conclusions

The results presented in this chapter describe the development and validation of an competitive immunoassay for the detection of warfarin in biological samples. This was accomplished by utilising an anti-warfarin mAb, which was purified (Section 3.2.1) and characterised (Section 3.2.2) prior to assay development. The purity of the mAb was assayed by SDS-PAGE analysis (Figure 3.8). Purified mAb was initially utilised in the development of a model competitive assay for the detection of warfarin in PBS. In order to determine the optimal warfarin coating concentration (Figure 3.10) and optimal working dilution (Figure 3.11), a checkerboard ELISA was performed as described in Section 3.2.3. Varying dilutions (0-100 µg/ml) were coated on a microtitre plate and the optimal conjugate loading density was determined to be 50 µg/ml, which correlates well with previous findings, by Fitzpatrick (2001). The optimal working dilution of antibody was determined from the standard curve (Figure 3.11) to be a 1/800 dilution. For all immunoassay calibration plots the use of a 4-parameter function in BIAevaluation™ software was adopted which fitted an advanced smoothed curved cubic polynomial to the data set. Immunoassay curves are inherently non-linear in origin and adopt a familiar sigmoidal bell shaped curve on log-linear plots. The fitting of a linear plot (Figure 3.14) to the data set ignores the inherent shape of the plot, with the resulting 'linear' plot showing a greatly reduced dynamic range with reduced precision at both the upper and lower ends of the calibration set. Fitting 4-parameter equations to immunoassay curves offers a much more realistic fitting of the data set, and can increase the detection range by 4-fold at both ends of the linear range increasing the dynamic range considerably with no significant effect on the degree of assay precision or performance.

A competitive ELISA was developed as described in Section 2.5.2.5. and 3.2.3.3. and a four-parameter equation fitted to the data using BIAevaluation 3.1 software. Intra- and Inter-day studies were performed in order to determine the accuracy and precision of repeated measurements of both assays. The coefficient of variance values of each assay provide a quantitative measure of precision of the analytical method. The inter- and intra-assay variation for the competitive ELISA in PBS were typically of the order of 3-8%, and demonstrated the accuracy and reproducibility of the technique. This compares well to intra- and inter-day CV's for a radio-immunoassay (RIA) developed for the detection of small hapten coumestrol, which ranged from 2-9% (Lapcik *et al.*, 2003). These values are well within the current recommended guidelines for immunoassay calibrations, that suggest that tolerance limits of 20% be applied to immunoassay curves with respect to assay precision (Findlay *et al.*, 2000). The percentage accuracies values obtained in the linear part of the inter-day plot (Figure 3.15) indicate the fitted four-parameter curves provide an accurate representation of the sigmoidal

relationship between the measured response and the logarithm of concentration observed for the immunoassay. The assay results compare well to previous studies by Fitzpatrick (2001) involving the detection of warfarin in PBS using an anti-warfarin monoclonal antibody. The working range of the assay was similar to the present assay (Section 3.2.3.3.) working range (3.91-500 ng/ml). The CV's determined by Fitzpatrick for the intra- and inter-day variability studies ranged from 1.0-9.10% and 4.07-14.37%, respectively. The percentage accuracies for intra- and inter-day curves ranged from 91.05-109.79% and 95.64-102.09%, respectively. In the work presented in this chapter the CV's for the intra- and inter-day studies ranged from 1.05-7.29% and 3.16-8.62%, respectively. The intra- and inter-day % accuracies ranged from 96-102%.

In order to assess the feasibility of detecting warfarin in a biological matrix, samples of urine were acquired and spiked with known concentrations of warfarin. It was evident from the intra- and inter-day variation studies in Section 3.2.3.3 that the anti-warfarin mAb was suitable for use in the development of a competitive ELISA for the detection of warfarin in complex biological matrices. Standards of warfarin ranging from 3.9 – 500μg/ml were prepared in urine and mixed with purified mAb (1/800 dilution). The inter- and intra-assay variation for the competitive ELISA in urine were typically of the order of 3 – 17%. Although there is a higher degree of variation due to the undefined nature and sample variation of urine, these values are still within the recommended limit of 20%. This immunoassay format is a suitable complement to the instrumental methods (i.e. High performance liquid chromatography [HPLC], Gas chromatography-mass spectrometry [GC-MS] and BIAcore) especially for screening purposes, for samples with low concentrations of analyte and for small volume samples such as body fluids, cell and tissue culture supernatants (Maurer & Arlt, 1998; Lombardi *et al.*, 2003; Anfossi *et al.*, 2004).

One of the initial steps in designing an immunoassay is the assessment of reactivity towards structurally similar molecules. The cross-reactivity studies carried out demonstrated that the anti-warfarin mAb shared a common epitope between the 4-hydroxycoumarin ring structure and the carbonyl substituent. As Table 3.8 illustrates, acenocoumarin shows the highest degree of cross-reactivity (18%) due to its structural similarities to warfarin. Both 6-hydroxywarfarin and 7-hydroxywarfarin show varying degrees of cross-reactivity (8% & 1%) with the anti-warfarin mAb. Previous cross reactivity studies by Fitzpatrick (2001) involving polyclonal antibodies showed that these type of antibodies have much higher cross reactivities with regard to acenocoumarin (98%), 6-hydroxywarfarin (28%) and 7-hydroxywarfarin (3%). However like the anti-warfarin monoclonal antibody the polyclonal antibody showed negligible cross reactivity with the other compounds tested (7-hydroxycoumarin, 4-hydroxycoumarin, coumarin and 7-hydroxycoumarin-4-acetic acid).

Fitzpatrick utilised a Hyperchem® molecular modelling software package in order to analyse the 3 dimensional structure models of warfarin and its metabolites (e.g. 6-and 7-hydroxywarfarin). The models indicated that the 4-hydroxycoumarin residue and the carbonyl side chain appear to lie along the same plane, orthogonal to the phenyl substituent (i.e. the point of conjugation). It can be postulated therefore that the majority of the antibody-binding site is directed against the 4-hydroxycoumarin ring structure and carbonyl side-chain. Consequently, substitutions (e.g. hydroxylations to the coumarin ring) could lead to differing specificities of antibody binding pocket for the antigen, as the 'complementarity' of the binding domain is disturbed. In this context, the hydroxylation at position-7 of the 4-hydroxycoumarin ring could be expected in the context of a polyclonal antibody population, to have a more marked effect on the antibody affinity given the suggested epitope region, than a hydroxylation at position 6 of the 4-hydroxycoumarin residue, which would concur with the experimental observations noted. The fact that the degree of cross-reactivity towards the coumarin and its hydroxylated metabolites is negligible implies that the antibodies require both the coumarin ring structure and the presence of the carbonyl side chain for antibody recognition.

The final section of this chapter deals with the measurement of the affinity of anti-warfarin mAb to warfarin and structurally related analogues by calculation of the dissociation constant (K_D) of antibody:antigen mixtures at equilibrium in solution. The method of Friguet *et al.* (1985) was used to assess the overall dissociation constants for the anti-warfarin mAb to warfarin and structurally related analogues. The affinity profile of the monoclonals produced measured by the equilibrium dissociation constants, was generally of the order: warfarin > acenocoumarin > 7-Hydroxywarfarin ≥ 6-hydroxywarfarin. These results suggest that the majority of the antibodies were directed against an epitope on the coumarin portion of the molecule. This implies that the monoclonal antibody produced from clone 4-2-25 was directed against a combined epitope near the 4-hydroxycoumarin residue and the branched keto substituent at position 3 part of the coumarin molecule. This also explains why there was a reasonably high degree of affinity of the mAb for the hydroxylated metabolites. The dissociation constants determined by the method of Friguet *et al.* (1985) demonstrate the method to be an accurate means of determining equilibrium affinity constants.

Chapter 4

Development of a BIAcore-based Inhibition Assay for the Detection of Warfarin in Biological Matrices

4.1. Introduction

Biosensors are analytical devices composed of a recognition element of biological origin, a physico-chemical transducer and the processing unit. The biological element is capable of sensing the presence, activity or concentration of a chemical analyte in solution. The sensing takes place either as a binding event or a biocatalytical event. These interactions produce a measurable change in a solution property, which the transducer converts into a quantifiable electrical signal (D'Orazio, 2003). The biological component of the biosensor is composed of two distinct groups: catalytic (e.g. enzymes, micro-organisms, and tissues) and non-catalytic (e.g. antibodies, receptors and nucleic acids) (Griffiths & Hall, 1993). A promising area of development in biospecific interaction analysis (BIA) is the use of biosensors to detect and measure interactions in 'real-time' (Jonsson *et al.,* 1991; Liedberg & Lundstrom, 1993). Biosensors can be segregated into four fundamental groups, depending on the process of signal transduction (e.g. optical, electrochemical and thermal sensing) (Goepel, 1991; Seyhi, 1994; Goepel & Heiduschka, 1995). Biosensors based on the optical phenomenon of surface plasmon resonance (SPR) are among the most versatile of those processes (Williams & Addona, 2000). Biosensor technology is moving towards miniaturised, chip-based, microarrays capable of multi-analyte detection in order to achieve inexpensive, portable, robust and easy to use analytical systems (Ekins, 1998; de Wildt *et al.,* 2000).

4.1.1. SPR Biosensors

Surface plasmon resonance biosensors allow the label free detection of biomolecular interactions in 'real-time' and have become well established as laboratory tools in the biopharmaceutical industry. (Myszka & Rich, 2000). In receptor-driven drug discovery, crude tissue extracts and cell homogenates are screened for potential ligands of orphan receptors, an approach termed 'ligand-fishing' that can identify possible interacting pairs of molecules and target agents (Cooper, 2003). SPR instruments offer a unique means of monitoring reaction kinetics and determining equilibrium constants and also allow for the determination of active analyte concentrations (Zhu *et al.,* 2000; Schindler *et al.,* 2002; Ahmad *et al.,* 2003). SPR systems can also be used to detect pathogens such as *Escherichia coli* O157:H7 in biological matrices (Kai *et al.,* 2000), and were successfully used as analytical tools in the food and drink industries (Gaudin *et al.,* 2001; Mello & Kubota, 2002; Leonard *et al.,* 2003, McCarney *et al.,* 2003).

There are a number of SPR-based devices currently commercially available including the BIAcore range of instruments (BIAcore AB). Affinity Sensors manufactures the IAsys line of

instruments, which is a cuvette-based system utilising evanescent-wave technology (Bertucci & Cimitan, 2003). Windsor Scientific Limited markets the IBIS system, which can be configured as a flow- or cuvette-based system. Nippon Laser & Electronics Lab developed the SPR-CELLIA system and Texas Instruments latest SPR device (Spreeta 2000) can be configured for a variety of applications (Myszka & Rich, 2000). However, since the research described in this thesis involves the use of the BIAcore 3000, the mode of operation and the principle of SPR are described in the context of the BIAcore range of instruments. The mode of operation of the miniaturised SPR device is briefly explained (Section 4.1.3.).

4.1.2. BIAcore System

Pharmacia Biosensor was created in 1984 as a separate company within Pharmacia, to develop biosensing technology. In 1990 they introduced their first commercial biosensor (BIAcore) system to the market (Robinson, 1995). BIAcore is a fully automated instrument that monitors biomolecular interactions and includes sample handling equipment that performs the biomolecular interactions, SPR analysis, and the regeneration of the sensor surface. Three features of BIAcore are essential for a complete system for real-time BIA:

1.   *Sensor chip* and *optical system*, responsible for generation and detection of the SPR signal
2.   *Integrated micro-fluidic cartridge*, for optimal transport of samples to the sensor surface
3.   *Autosampler* for unattended handling of long series of analyses.

153
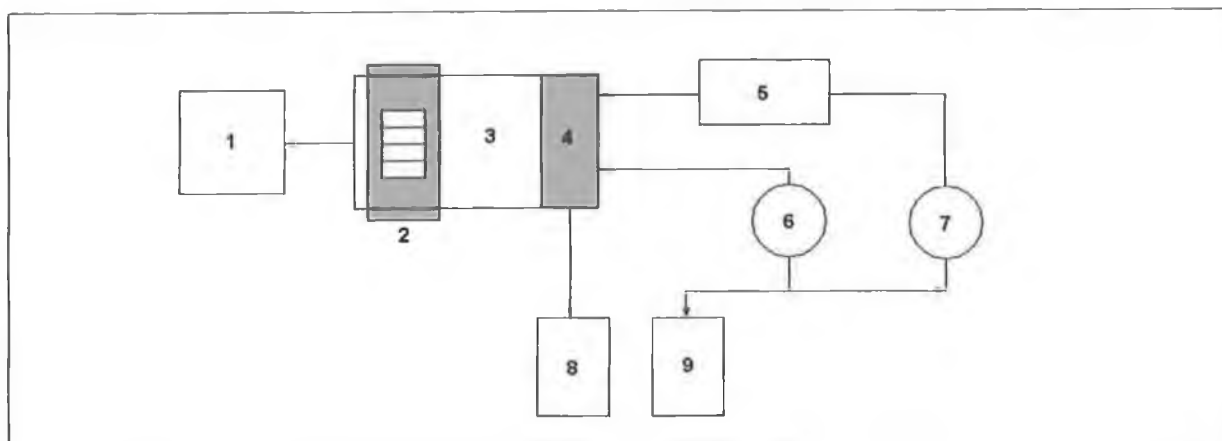
Figure 4.1: *Basic components of BIAcore(TM) instrument: (1) optical detection system; (2) sensor chip; (3) integrated microfluidic cartridge (IFC); (4) connector block; (5) autosampler; (6) eluent pump; (7) autosampler pump; (8) waste bottle; (9) buffer bottle.*

The entire system is controlled by a microprocessor, enabling development of programs to run multiple samples simultaneously without intervention. Since the introduction of the first BIAcore system, BIAcore AB have introduced more instruments to target specific areas of the biosensor market. These instruments include BIAlite[TM] (1994), BIAcore X[TM] (1996), BIAquadrant[TM], BIAcore S51 and BIAcore J (2001) and these systems offer varying degrees of automation and parameter specifications (Leonard *et al.*, 2003). Several generations of the original BIAcore were developed, (BIAcore 1000, 2000 and 3000) which are enhanced versions of the original.

4.1.2.1. CM5 Sensor Chip

One of the most essential features of an SPR biosensor is the interface between the sensor surface and the immobilised ligand (Myszka & Rich, 2000). BIAcore technology utilises a sensor chip that consists of a glass slide coated on one side with a thin gold film, to which a matrix of carboxymethylated dextran is covalently attached. The gold film is essential for the generation of an SPR signal at a convenient combination of reflectance angle and light wavelength, and is in addition chemically inert to solvents and solutes used in biochemical interactions. The dextran layer comprises the outermost layer of the chip surface and is a linear polymer of glucose units modified by carboxymethylation (Lofas & Johnsson, 1990). Dextran exhibits very low non-specific adsorption of biomolecules and therefore provides a very favourable matrix for biomolecular interactions (O'Shannessy *et al.*, 1992). There are several reasons why dextran facilitates biomolecular interactions and they are as follows:

1.   Covalent immobilisation of biomolecules.

2.   Surface binding capacity is increased.

3.   Hydrophillic surface environment is provided, which is favourable for most interactions of biological interest.

4.   Surface is provided with a low degree of non-specific binding.

The sensor chip forms one wall of the micro-fluidic cell. The dextran surface of the chip makes contact with the solution being examined. There are four independent flow cells on the sensor chip surface. Therefore each chip can be utilised for up to four separate series of measurements (Sjolander & Urbanicky, 1991).
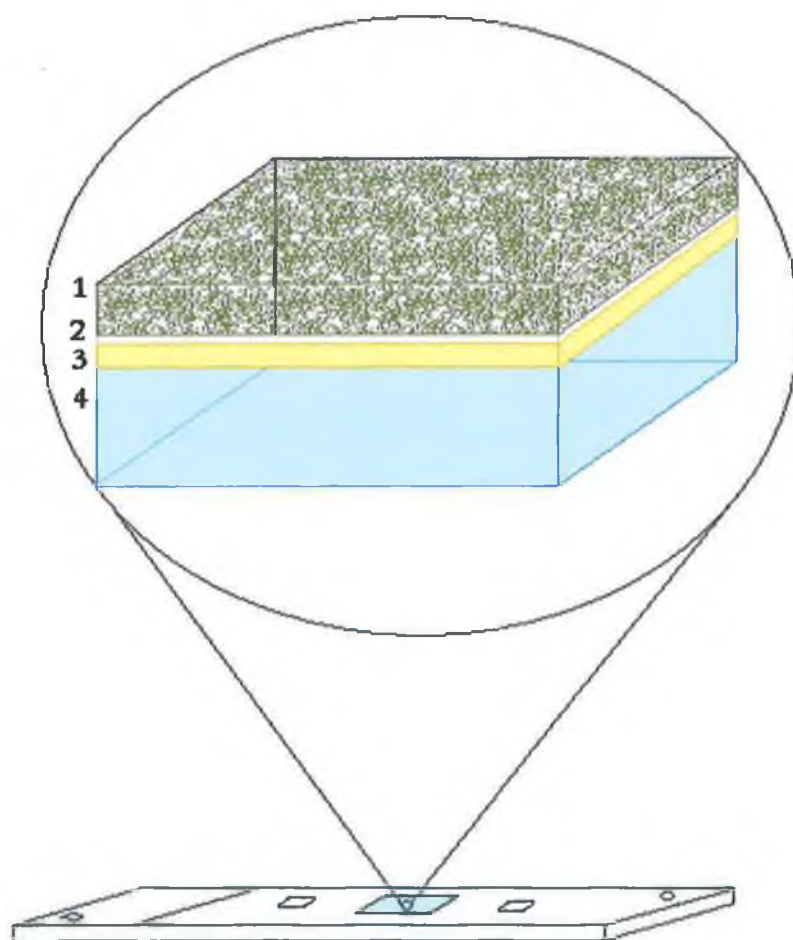
Figure 4.2: Sensor chip components. The sensor chip surface consists of three layers ([4] glass, [3] thin gold film and [1] dextran surface). The dextran layer is bonded to the gold film through an inert [2] linker layer.

155

4.1.2.1.1. Dextran Activation

For carboxymethylated dextran to be useful for immobilisation reactions, the carboxyl group must first be activated so that it can participate in covalent binding. Generally this involves activation of the surface by derivatisation with N-hydroysuccinimide (NHS), mediated by N-ethyl-N'-(dimethylaminopropyl) carbodiimide (EDC) according to the reaction scheme illustrated in Figure 4.3. (Nuzzo & Allara, 1983; Bain *et al.*, 1989). Typically, 30-40% of the carboxyl groups on the dextran are converted to reactive NHS esters (which are receptive toward primary amino functions) and reducing the activation contact period is the simplest method for regulating the yield of immobilised ligand. Many biomolecules have uncharged amino groups available for interaction with NHS esters to yield a covalent immobilisation to the dextran layer. For those biomolecules that do not possess amino groups it is possible to add this functionality or to react the biomolecules using different coupling strategies (e.g. thiol coupling) (Lofas *et al.*, 1991). The reaction works best between pH 6 and 9, whilst the efficiency of the reaction decreases rapidly below pH 4.5.
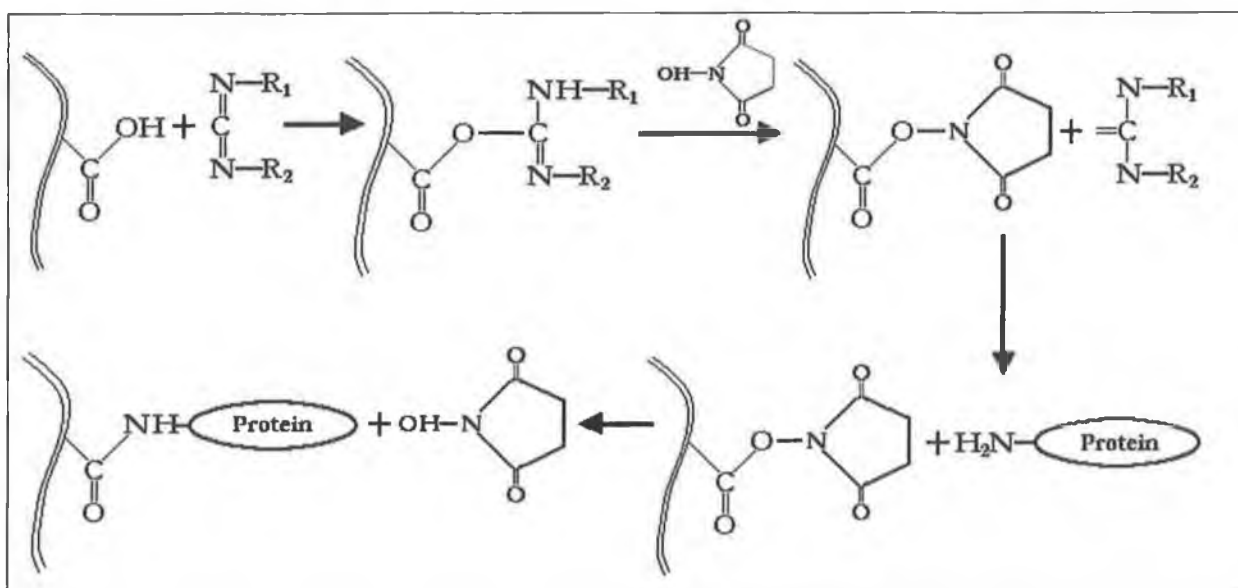
Figure 4.3: *Activation chemistry of the carboxymethylated dextran surface with N-hydroysuccinimide / N-ethyl-N'-(dimethylaminopropyl) carbodiimide (NHS/EDC). Protein at a pH lower than its isoelectric point is injected over the surface following EDC-mediated NHS derivatisation. Unreacted sites are capped with ethanolamine.*

4.1.2.2. Optical System

In BIAcore, the optical phenomenon used for detection is SPR and the light source is a high-efficiency near-infrared light-emitting diode (LED). The polarised light from the LED (760nm) is focused onto the gold film giving a fixed range of incident angles. The SPR response is monitored by a fixed array of light-sensitive diodes covering the whole beam of reflected light.

4.1.2.2.1. Surface Plasmon Resonance (SPR)

SPR is a unique optical surface sensing technique involving an electron charge density wave phenomenon that arises at the surface of a metallic film when light is reflected at the film under specific conditions. In order to describe SPR it is useful to begin with the phenomenon of total internal reflection (TIR), which occurs at an interface between non-absorbing media. When light is incident on two media of different refractive index (e.g. glass and water), a portion of the light coming from the medium of higher refractive index is refracted and the remainder of the light is reflected (Figure 4.5.). When the angle of incident light is greater than the critical angle of incidence, the light is totally internally reflected and no light is refracted across the interface between the two surfaces of different refractive index. Under conditions of total internal reflection (TIR), the incident light leaks an electrical field intensity (a distance of approximately one wavelength) called an evanescent field wave into the low refractive index medium. The amplitude of this evanescent wave decays exponentially with the distance travelled from the interface into the lower dense medium (Figure 4.4). The penetration depth of the evanescent field wave is usually defined as the distance over which the wave decays to 1/e, or about 37%, of its maximum intensity.
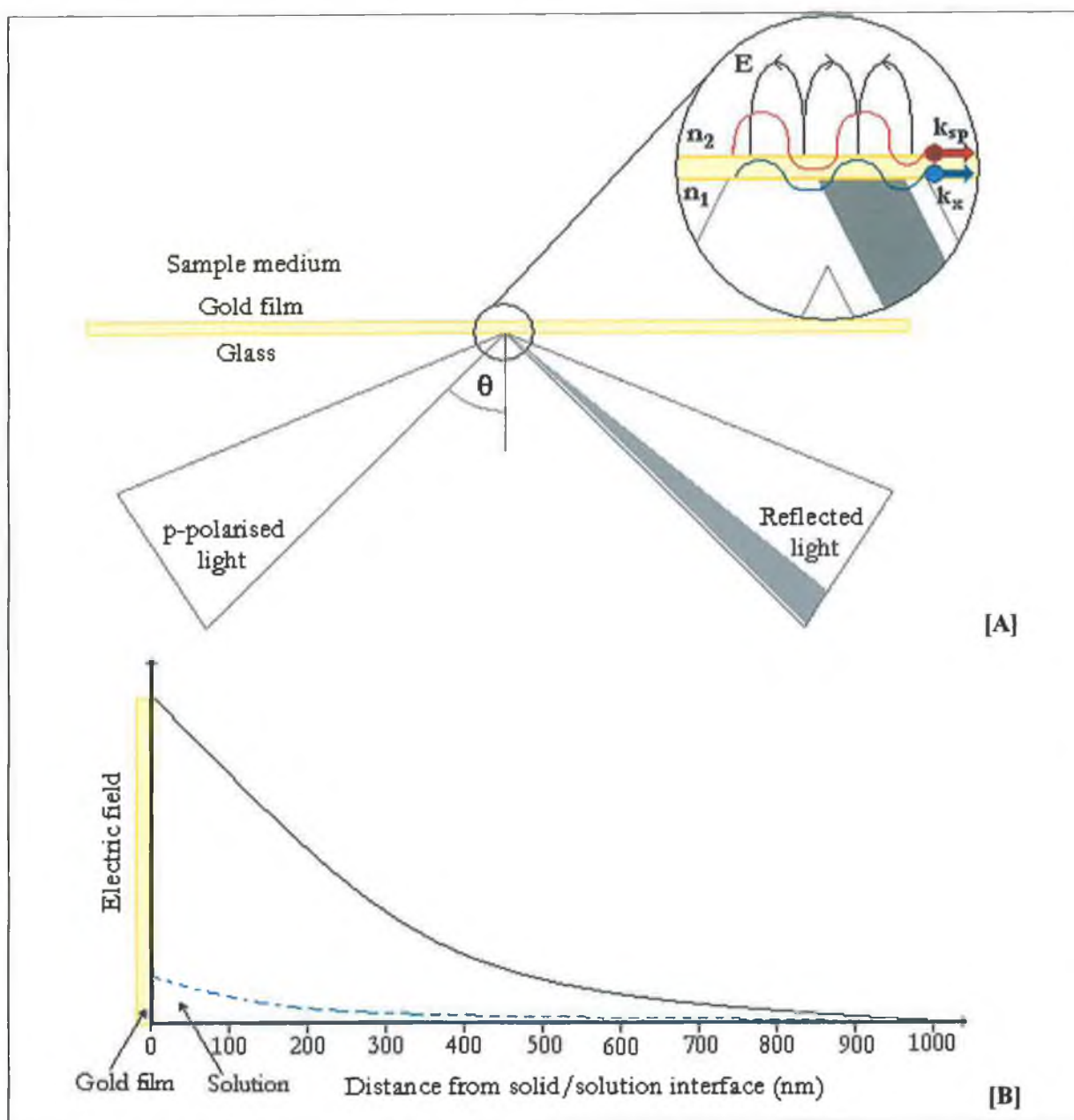
Figure 4.4: *[A] SPR is excited by p-polarised totally internally reflected (TIR) light at a glass/metal film interface. The evanescent field, E, is a non-transverse wave that has components in all spatial orientations. The incident p-polarised light is focused into a wedge-shaped beam providing a continuous interval of light wave vectors* **k$_x$**. *The wavevector of the plasmon wave,* **k$_{sp}$** *depends on the refractive indices of the conductor* **n$_1$** *and the sample medium* **n$_2$**. θ *refers to the angle of incidence. [B] Relative evanescent electric field amplitude versus distance to solid/solution interface (nm). The continuous line represents the SPR-evanescent wave (gold film), whereas the dashed blue line represents non-absorbing TIR (no gold film). Adapted from BIAcore manual.*

158

In BIAcore the TIR-interface between the glass and water layer is coated with a thin layer of a suitable conducting material (e.g. gold, silver). The p-polarised component of the evanescent wave can be transferred to the metal layer, causing the electrons to resonate, which results in the generation of a surface plasmon wave. This resonance effect occurs when there is a match between the energy of the surface electrons and the energy of the incident light photons. By measuring the amount of light reflected by the metal surface the coupling of energy between the evanescent wave and surface electrons can be observed. All the light is reflected at most wavelengths, except for the SPR angle where most of the light is absorbed, which can be observed by a decrease in the intensity of the reflected light measured. As the wavelength of light and the properties of the metal film are constant, SPR can be used to probe the refractive index of the aqueous layer adjacent to the gold layer. Biomolecular interactions occurring at the sensor surface change the solute concentration and thus the refractive index within the evanescent wave penetration range (Figure 4.6.). The displacement of the SPR angle as result of biological interactions occurring at the chip surface is measured in 'real-time' and interpolated as a sensogram (Figure 4.7.).
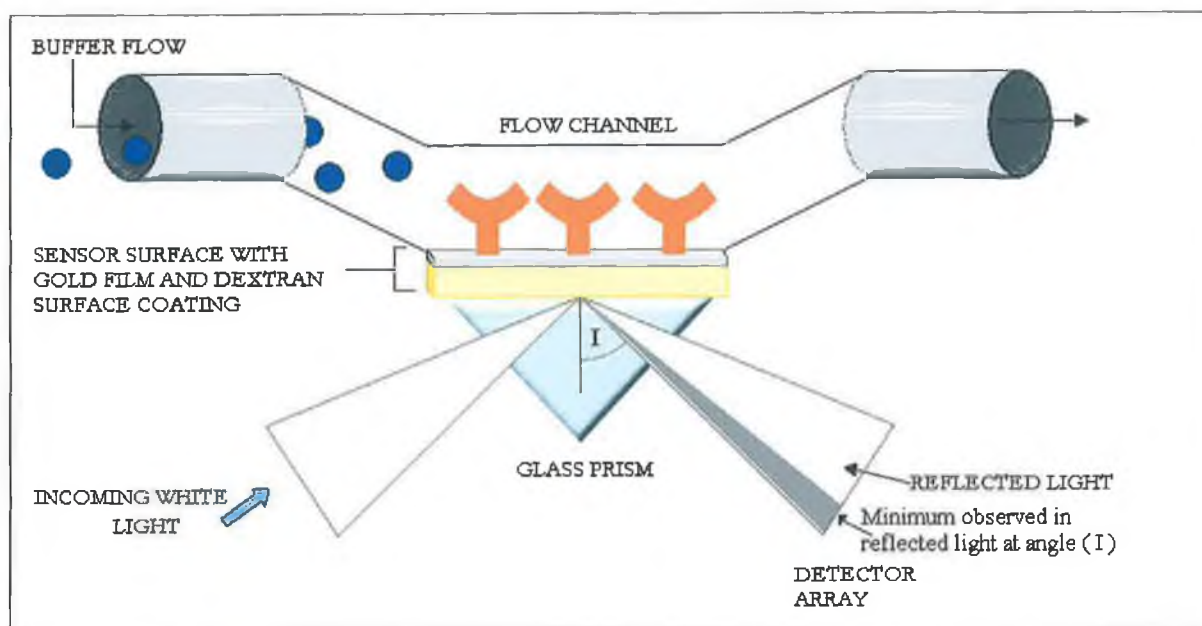
Figure 4.5: *Schematic depicting typical BIAcore SPR measurements. In the example illustrated, antibody (Y) is immobilised at the gold sensor chip surface using conventional coupling chemistries (e.g. EDC/NHS). Plane polarised light is emitted from a high efficiency light emitting diode and is focused onto the gold chip surface in the shape of a wedge shaped beam by means of a glass prism under conditions of total internal reflection. The reflected light is then measured by a two-dimensional photo-diode array. Under conditions of total internal reflection at a metal-coated interface an electromagnetic portion of the light known as the evanescent wave penetrates into the medium of lower refractive index. Buffer is passed over the surface and the dip in reflected light intensity (grey line) recorded at angle (I). The angle at which SPR occurs is dependent on a number of factors including the refractive index of the layer adjacent to the metal film. SPR can thus be used to probe and monitor the interactions occurring at the chip-surface in 'real-time'.*
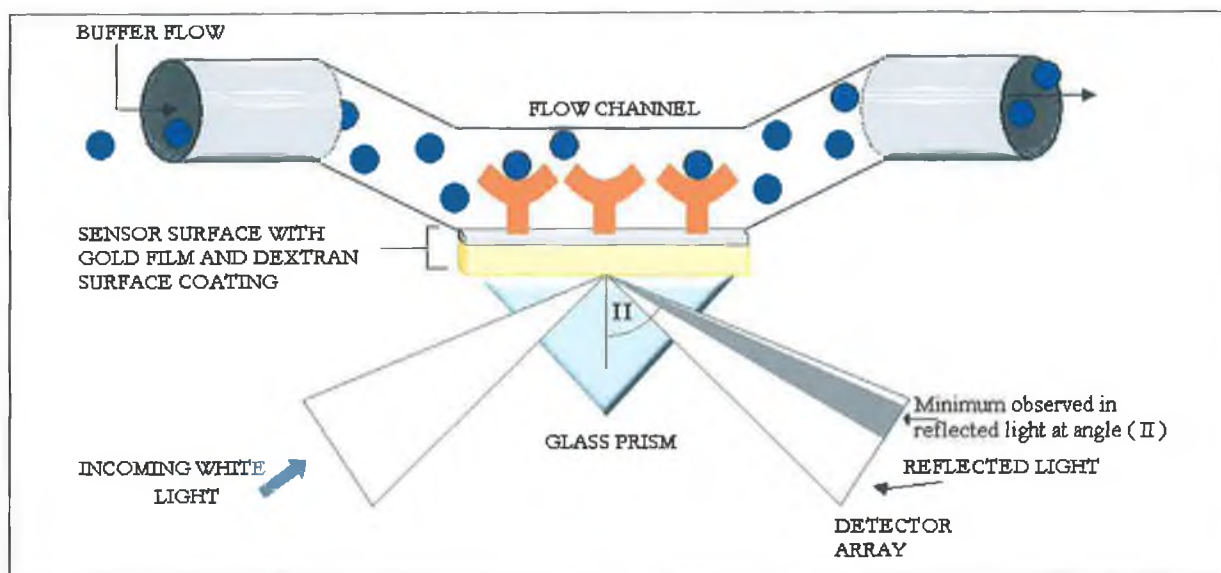
Figure 4.6: *Antigen (●) is then injected over the antibody-immobilised chip surface. Binding of antigen to immobilised antibody causes an increase in the mass bound at the sensor chip surface and a subsequent change in the refractive index at the sensor chip surface, causing a shift (θ) in the resonant angle of the reflected light (i.e. from angle I to angle II). The shift in the resonant angle is proportional to the change in the mass of analyte bound at the sensor chip surface.*
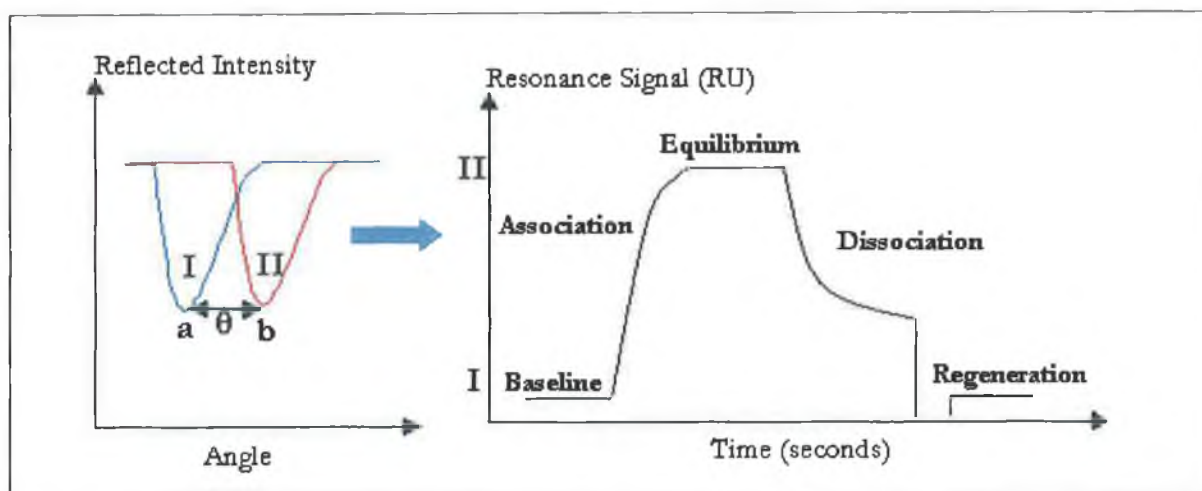
Figure 4.7: *A plot of the change in the resonant angle (θ) measured in 'real-time' following antibody: antigen binding versus time, is interpolated by the instrument software to generate the characteristic SPR response curve (Sensogram). The change in the SPR angle is converted to arbitrary response units by the instrument software. The response signal measured is proportional to the concentration of bound analyte. A change of approximately 1 kRU corresponds to a mass change in surface protein concentration of approximately 1 ng/mm^2. Before injecting antigen, the baseline response should be stable. Response increase during association phase represents complex formation in real-time. Equilibrium is achieved when an equal number of antigen molecules associate with and dissociate from the surface simultaneously. To monitor dissociation, the instrument automatically switches back to running buffer and information regarding the stability of the complex is collected. The surface is washed and any remaining complexes can be dissociated from the surface. Following regeneration, the binding response should return to the starting baseline position. (I & II = SPR angle; Figure 4.5 &4.6)*

4.1.2.3. Liquid Handling

Samples, reagents and buffers are supplied to the sensor chip surface through a precision liquid handling system. There are three main components that comprise this system. Firstly, stepper motor-driven syringe pumps are utilised and designed to deliver smooth pulse-free flow. One pump maintains continuous flow over the chip surface, while the other pump is utilised for injection of samples and reagents via the autosampler. The autosampler is responsible for sample handling and is designed to take defined volumes of liquid from specified sample positions and deliver them to other positions for mixing or into the micro-fluidic cartridge. Finally, the integrated μ-fluidic cartridge (IFC) controls the delivery of liquid to the sensor chip surface. It consists of a series of precision-cast

channels in a hard polymer plate, forming sample loops and flow channels for buffer and sample delivery. Operation of the whole IFC, including choice of sample loop and valve actuation, is automatically controlled through the instrument software.

4.1.2.4. BIAcore Software

Operation of BIAcore is controlled from a separate personal computer running BIAlogue software under Microsoft Windows. This program provides the user interface for the entire system, from pump control and sample injection to data collection and evaluation. The SPR signal (Section 4.1.2.2.1.) is expressed in resonance units (RU) and plotted against time in a sensorgram (Figure 4.7). The sensorgram is displayed directly on the computer screen in real-time as the analysis progresses. This data can be saved and evaluated (e.g. kinetics studies) with the help of BIAevaluation software.

4.1.2.5. Advantages and Limitations of BIAcore

In comparison to many other interaction technologies, SPR-based biosensors such as BIAcore exhibit several distinct advantages for characterising real-time BIA. Following the interactions as they happen, can yield valuable diagnostic information and provide rapid, quantitative kinetic data useful for pilot experiments to establish conditions for automated analyses. There are no labelling requirements, which results in minimal interference with the interaction being studied. Regeneration of the surface is normally included in the automatic analysis method, and the system can be programmed for unattended analysis of 1000 samples or more. The flexibility of BIAcore allows for the immobilisation of a wide range of biomolecules and the amount of materials required for immobilisation of ligands and regeneration solutions are minimal. In relation to assay performance, it is vital that the amount of complex (e.g. antibody:antigen) at equilibrium can be measured in the presence of unbound reactant, without disturbing the reaction equilibrium (Homola *et al.*, 1999; Myszka & Rich, 2000). The feature of multi-channel analysis, means that the interactions can be monitored over different immobilised ligand sensor surfaces, and provide direct comparison. It is advantageous to the user that BIAcore comes as a complete integrated system, which includes the processing unit, sensor chip, controlling computer and software for data collection and analysis.

Although the advantages of using BIAcore are numerous there are some limitations to its application, which should be noted. The initial cost of setting up BIAcore technology can be quite high and routine servicing is required to keep it running at optimal performance. Other drawbacks, which limit its applications, include the limited life-time of the biological components and

practicability in handling (Mello & Kubota, 2002). Biosensors, in general, offer an exciting alternative to conventional methods of analysis in various research areas. However, the sensitivity of each sensor system depends on improvements in several aspects including the biological elements, flow-cell design, transducer sensitivity, miniaturisation and antibody design and production. Future biosensor developments will evolve into highly sensitive, inexpensive devices, routinely used both in the field and the laboratory in a wide variety of applications ranging from rapid detection systems for the food industry to therapeutical analysis of biological matrices.

4.1.3. Miniature TI-SPR Device

The first mass-produced Spreeta device was introduced in 1999 by Texas Instruments. Their goal was to move SPR applications from high-cost systems to low-cost, portable electronic systems designed for field-work. This fully integrated miniature SPR sensor contains a light emitting diode (LED), polariser, thermistor (to allow for correction due to temperature fluctuations) and two 128 silicon photo diode arrays housed in an epoxy resin moulding which was designed in the form of the Kretschmann geometry prism (Figure 4.8a.).It measures approximately 3 cm x 1.5 cm x 4 cm and provides electrical connections using a 16-pin DIP connector device. Mirrored surfaces are thermally evaporated onto the internal surfaces of the device except for the SPR sensing portion of the device. The wedge shaped beam reflects off the SPR sensing layer and is reflected onto the PDA array by means of a mirror. The SPR minimum can then be measured in 'real-time' following dedicated signal processing (Kukanskis *et al.*, 1999). In 2001, Texas Instruments began production of the newest Spreeta device, the Spreeta 2000. This device is smaller than the original Spreeta (1.5 cm x 0.7 cm x 3 cm) and interfaces using a miniature 10-pin card-edge connector (Figure 4.8.b).

The Spreeta 2000 sensor consists of a plastic prism moulded to a microelectronic circuit contained on a printed circuit board (PCB) (Figure 4.8.a). The circuit contains an infrared LED (830 nm peak wavelength), a 128-pixel linear diode array detector, and a non-volatile memory chip for recording identification and calibration information. The LED emits a diverging beam that passes through a polariser and strikes an elliptical region of the sensor surface at a range of angles above the critical angle. The sensor surface is formed by a glass chip coated with a thin layer of gold (produces the SPR effect) and epoxied to the plastic prism. The thin layer of gold produces the SPR effect. For certain angles of incidence, part of the energy of the traverse-magnetic (TM) polarised incident light joins into a surface plasma wave travelling along the interface between the gold layer and the analyte. The loss of this energy is observed as a sharp attenuation of reflectivity. The angles at which this occurs vary with the surface refractive index (RI) of the analyte. Hence, it is possible to measure the

surface RI by measuring the reflection spectrum. The light reflected from the Spreeta 2000 sensor surface then reflects from the sensor's top mirror and back down onto the PCB. A fraction of this light strikes the diode array detector and each detector pixel collects this light that strikes the sensor surface at different angles. From this a reflectivity versus angle spectrum may be obtained by reading the detector array (Chinowsky *et al.*, 2003).
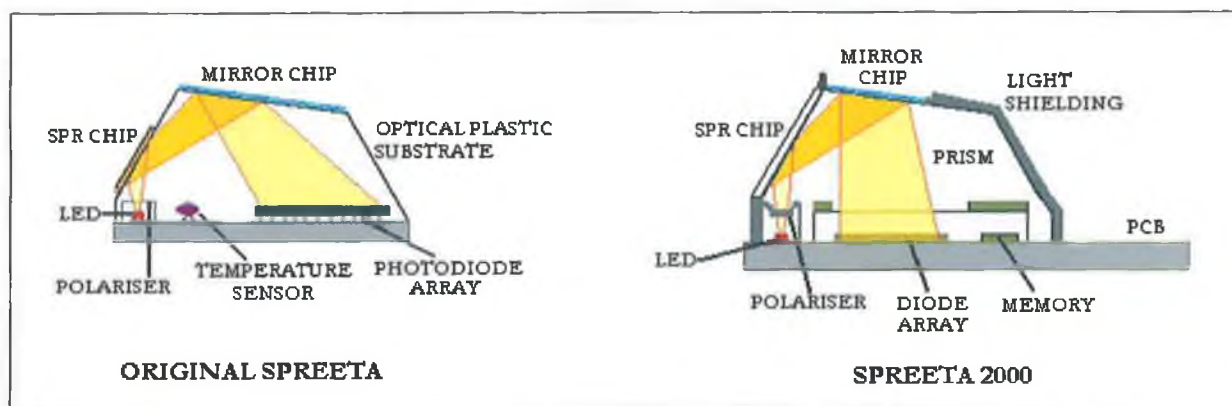
Figure 4.8(a): Cross-section of miniature Spreeta and Spreeta 2000 instruments, illustrating the components of the sensor. Mass changes are related to changes in the resonant angle and position of the reflectance minima, which can be detected using a dedicated software package in 'real-time'.

Figure 4.8 (b):Photograph of original Spreeta and enhanced Spreeta 2000 device (Chinowsky et al., 2003).

Spreeta technology appeals to a broad market base including medical diagnostics (in hospitals/physician's office), environmental monitoring and the food and drinks industries (Elkind *et al.*, 1999; Homola *et al.*, 1999; Leonard *et al.*, 2003).

4.1.4. Application of SPR Technology

Biosensors are increasingly becoming practical and they can be tailored to match individual analytical demands for almost any target molecule or compound that interacts specifically with a biological system (Scouten *et al.*, 1995). Surface plasmon resonance biosensors are amenable to characterising unmodified biopharmaceuticals, studying the interaction of drug candidates with macromolecular targets and identifying binding partners during ligand fishing experiments (Høyer-Hansen *et al.*, 2000; Myszka & Rich, 2000). There is an increasing number of potential applications of SPR technology driving forward the development of novel sensor devices such as miniaturised portable formats, thus making SPR instruments progressively more important in modern biophysical analytical laboratories.

4.1.4.1. SPR Biosensors in Drug Discovery

Pharmaceutical companies are always searching for technologies that will lower development costs and decrease the lead-time to market. The average costs of developing a small molecular weight drug was estimated to be approximately $800 million dollars with a lead-time to market of approximately 12-15 years. Biopharmaceuticals costs are less expensive ($200 million) with a development time of between 5-7 years (Hensley & Myszka, 2000). SPR biosensors can be implemented in many stages of the drug discovery process to increase throughput and lower costs, while generating a wealth of new information about drug candidates.

4.1.4.1.1. Target Characterisation and Small-molecule Detection

The use of SPR-based instruments is gaining increasing momentum in the area of biopharmaceutical discovery and characterisation of biomolecules. These instruments can monitor directly a particular molecule's binding activity and determine kinetic and thermodynamic parameters of receptor-ligand interactions (e.g. immobilisation conditions and sample concentrations). SPR biosensors provide a rapid and reliable method to assess the quality of molecules that are destined for further applications. Utilising these biosensors can enhance drug-screening methodologies where only functional targets will enter the screening phase of drug discovery. Recent improvements in SPR-based biosensor design, have made it possible to routinely detect the binding of low-molecular-mass analytes (<500 Da).

Recent research has demonstrated the applicability of SPR in characterising both high- and low-affinity small-molecule interactions. Kampranis *et al.* (1999) measured the kinetics of wild-type and mutant DNA gyrases binding to a number of anti-bacterial agents, including coumarin and cyclothialidine drugs (Molecular Weight < 700 Da). The study of these high-affinity drug-protein interactions (K_D = 1-150nM) allowed the identification of the particular gyrase residues that were responsible for drug binding. An excellent example of using SPR biosensors in small molecule screening was reported by Markgren *et al.* (1998, 2000). This group developed a rapid and informative assay to screen and rank a panel of HIV-1 inhibitors binding to HIV proteinase. Identification of the proteinase-binding compounds and their relative binding capabilities enabled ranking of the inhibitors based on their association and dissociation rates.

4.1.4.1.2. *Pharmacological Applications*

SPR biosensors can play an equally significant role in the general pharmacological assessment of drug candidates in addition to the benefits of characterising specific drug-target interactions. Novel biosensor applications are being developed for the predictive profiling of important pharmacokinetic parameters of target molecules in terms of their individual absorption, distribution, metabolism, excretion and toxicity (ADME/T) profiles (Cooper, 2003). Routine ADME applications are being developed for SPR biosensors to determine the binding tendency of compounds to carrier plasma proteins (e.g. serum albumin), their ability to pass through membranes and their role in signal transduction (e.g. cytochrome P450). Myszka and co-workers (2000) demonstrated the potential of SPR technology to collect high-resolution binding data on small molecules interacting with human serum albumin (HSA). They injected a series of warfarin samples over a sensor chip coated with a HSA surface. By utilising the kinetics software available with the system they were able to determine that HSA binds warfarin with an affinity of 17 µM and this value correlates well with values measured by traditional equilibrium assays. A more recent study detected differences in binding of enantiomeric drug compounds to immobilised albumins where warfarin was a control drug. The results indicated slight differences in binding patterns of the enantiomers to human and rat albumin (Ahmad *et al.*, 2003). In a similar assay, Frostell-Karlsson *et al.* (2000) investigated the interactions of a panel of 19 drug compounds with immobilised HSA. They demonstrated the possibility of ranking the panel of drugs as high, intermediate or low HSA binders using single drug concentrations.

Two new chips constructs (referred to as HPA and L1) released by BIACORE have made it possible to construct stable membrane surfaces within the flow cell. A comprehension of the intestinal absorption profile of new drug candidates is of importance for screening, especially in order to

differentiate between drugs that demonstrate low, medium or high absorption. As the majority of drugs are administered orally, the fraction of drug absorbed from the intestine is of substantial significance. *In vivo* studies of drug absorption are complicated to perform and the necessity for suitable *in vitro* models is increasing. Danelian *et al.* (2000) investigated the direct interaction of a panel of 27 drugs by mimicking drug adsorption to the human intestine through immobilisation of liposomes on a L1 chip surface and monitoring the binding response of the drugs as they flowed over the surface. The results correlated well with previously reported oral absorption data, and allowed for the classification of the compounds absorbed by the transcellular route into low, medium and high membrane permeability based on the measured responses. Applications are also being developed to characterise the activation of metabolic pathways such as cytochrome P450.

4.1.4.1.3. Proteomics

Proteomics can be defined as the qualitative and quantitative comparison of proteomes (PROTEin complement to a genOME) under different conditions to further unravel biological processes (Williams & Addona, 2000). SPR biosensors serve two main purposes in proteome analysis: [1] as a sensitive instrument to confirm detection and quantify direct binding of ligand from cell lysates and conditioned media and [2] to act as micropurification devices capable of recovery of sufficient quantities of analyte for subsequent analysis and characterisation. Attention has thus been focused on identifying new ligand-receptor pairs and the characterisation of protein-protein interactions. The SPR biosensor has the ability to detect and quantify analytes from complex fluids, cell lysates and conditioned media, which makes this technology a logical method for orphan ligand screening. This form of screening termed 'ligand-fishing' involves the process by which 'orphan receptors' are screened against multitudes of compounds, cells and tissue extracts to identify alleged targets. Furthermore, performing biosensor experiments in tandem with mass spectroscopy provides immediate molecular weight identification of the analytes that bind to the immobilised receptor.

A relatively new analytical platform combining BIA and mass spectrometry (MS) is referred to as BIA-MS. It is an integration of a surface plasmon resonance biosensor for real-time interaction analysis and mass spectrometry for the subsequent identification of interacting molecules (Natsume *et al.*, 2001). Traditional methods involving BIA require purification steps that are both time- and labour-intensive and case by case strategy is often needed. BIA-MS was developed to address these unfavourable conditions as biomolecules detected and captured on the sensor chip can now be analysed and identified by MS. To gain more flexibility and sensitivity in terms of choice of analytical procedure Sonksen and colleagues (1998) reported an novel microrecovery procedure for combined

BIAcore-Maldi-MS analysis that allows for elution of bound analytes in as little as 4µl of eluant. Mass spectrometry offers several advantages such as specificity, sensitivity and rapidity over the majority of protein identification techniques, which rely on proteolytic digestion of separated proteins and subsequent analysis of proteins by PAGE. Nelson *et al.* (1997a) performed MS analysis of analytes bound directly to the sensor chip surface, and also coupled MS with the use of the SPR probe instrument whose relatively large surface area allows for greater quantities of analytes to be recovered, and also given the exposed nature of the sensor surface collection and elution of analytes is also simplified (Nelson *et al.*, 1997b). Although biological applications of BIA-MS are still limited, the research described in this section indicates that it may be used to characterise both stable and transient interactions with relatively fast dissociation rates. It may also be utilised in crude protein mixtures to identify novel molecules and simultaneously monitor the interactions taking place (Natsume *et al.*, 2003).

4.1.4.2. Biosensors in Food and Drinks Analysis

Application of biosensor technology in the food and drinks industry looks promising as this industry needs suitable analytical methods for process and quality control. Biosensors offer advantages as alternatives to conventional methods due to their inherent specificity, simplicity and quick response and can provide important information about the physical and chemical characteristics of food (Mello & Kubota, 2002). In the food industry, the quality of a product is evaluated through periodic chemical (chromatography, spectrophotometry, titration, and electrophoresis) and microbial analysis. Conventional techniques for the detection and identification of micro-organisms mainly rely on specific microbiological and biochemical identification (e.g. enrichment methods, nucleic acid-based assays, immunological detection assays). Although these methods can be inexpensive, sensitive and yield reliable quantitative and qualitative information on the number and nature of the micro-organisms tested, they are greatly restricted by the time it takes to complete the assay (standard enrichment assays vary between 3-7 days). Commercial biosensors are available in several forms, such as autoanalysers, manual laboratory instruments and portable (hand-held) devices. A list of commercially available biosensors is specified in Table 4.1. The food industry is vast, but its profit margins are low and competition is intense. Although the rapid detection of pathogens, pesticides, micro-organisms and toxins is an attractive area for biosensor application within this industry, investment in modern, expensive analytical methods is not always feasible. Drawbacks that need to be addressed include the limited lifetime of the biological components, mass production as well as ease of use. (Mello & Kubota, 2002).

__Table 4.1:__ Summary of several available commercial biosensors in the food industry. In spite of much biosensor research in food analysis, only a few systems are commercially available. Very few biosensors are presently used in the food industry for on-line analysis, although in principle they could be combined with flow-injection analysis for on-line monitoring of raw-materials, product quality and, possibly, the manufacturing process. Biosensors have found application in the analysis of glucose and other carbohydrates or alcohols. BIAcore and several other devices are applied commercially for bacterial detection.

Company (Location)	Biosensor Device	Compounds Analysed
DANVERS (USA)	Apec glucose analyser	Glucose
EPPENDORF (GERMANY)	ESAT 6660 Glucose Analyser	Glucose
SOLEA-TACUSSEL (FRANCE)	Glucoprocesseur	Glucose
YELLOW SPRINGS INSTRUMENTS (USA)	ISI Analysers	Glucose, lactose, L-lactate, ethanol, methanol, glutamate and choline.
TOYO JOZO BIOSENSORS (JAPAN)	Models: PM-1000 & PM 1000DC (online), M100 and AS200	Glucose, lactate, L-amino acids, cholesterol, tryglicerides, glycerine, ascorbic acid and alcohol.
BIACORE AB (SWEDEN)	BIAcore	Bacteria, pantotheinic acid, folic acid, biotin, vitamin B_2 and B_{12}.
BIOTRACE (UK)	Unilite	Bacteria
BIOSENSORI SPA (ITALY)	Midas Pro	Bacteria

Detection of contaminants is a very active area of research since spoilage of foods by toxins (e.g. domoic acid in mussels, terodotoxin in fish), viruses (e.g. hepatitis A) or micro-organisms (e.g. *Escherichia coli, Salmonella, Listeria*) is a serious concern (Luong *et al.,* 1997). Detection utilising antibodies is perhaps the only technology that has been successfully employed for the detection of cells, spores, viruses and toxins. During the past decade, with the emergence of hybridoma techniques (Section 3.1.2.1.) and the development of recombinant antibody phage display technology, immunological detection of microbial contamination has become more specific, reproducible, sensitive and reliable. Biosensors offer the potential of detecting pathogens in 'real-time' but, unfortunately still require the time-consuming pre-enrichment step in order to detect low numbers of pathogens in food and water. Methods are available to reduce assay time and include microwave digestion, evaporation, acidic or alkaline hydrolysis and filtration.

Successful detection of micro-organisms requires optimisation of several parameters including antibody availability, immobilisation strategies, sample preparation and assay design (Kaclikova *et al.,* 2001; Quinn & O'Kennedy, 2001; Leonard *et al.,* 2003). BIAcore is utilised in the development of competitive and inhibitive immunoassays. With this system, either hapten (inhibitive) or antibody (competitive) is immobilised onto the sensor chip surface. In some cases immobilisation of hapten can prove difficult depending on the available functional groups. Hence, in some assays (referred to as an inhibition assay), hapten-protein conjugates (e.g. warfarin-BSA) are immobilised onto the surface. Free hapten standards are prepared and premixed with antibody. After an appropriate incubation time, the mixture is passed over the hapten-protein conjugate immobilised surface. The hapten in solution inhibits the binding of antibody to the immobilised hapten on the surface and the amount of antibody binding to the surface is inversely proportional to the amount of free hapten in solution. A competitive assay involves the immobilisation of antibody on the chip surface. A mixture of standard samples and high molecular mass hapten-conjugates is then passed over the surface allowing both to compete for the binding site on the antibody. These immunoassay results are then used in the construction of a standard curve and unknown concentrations determined from such a curve (Dillon *et al.,* 2003). The following section describes recent biosensor applications within the food industry and other areas for drug and pathogen detection.

4.1.4.2.1. Antibiotic Detection in Milk

Several biosensor-based immunoassays were developed for the detection of antibiotics in milk. Penicillins and other beta-lactam antibiotics constitute the antimicrobial drugs most frequently tested for in quality assurance programs for milk worldwide. They are used in veterinary medicine in

the treatment of septicaemia, urinary and pulmonary infections. The presence of penicillin residues in food of animal origin (milk, meat) can have several drawbacks including the reduction of hypersensitivity reactions and antibiotic resistance in the consumer. Gaudin and colleagues (2001) successfully developed a BIAcore-based immunoassay for screening penicillin residues in milk. This assay format involved the use of a commercial antibody directed against ampicillin, which had a much higher affinity for the open beta-lactam ring structure. A different approach was developed by Gustavsson and co-workers (2002) that involved a BIAcore inhibition assay for penicillin detection. A microbial receptor protein with carboxypeptidase activity was used as the detection molecule. One advantage of using this receptor protein over antibodies that are more commonly used is that only the active, intact beta-lactam structure is recognised, whereas most antibodies detect both active and inactive forms.

Other antibiotics of concern to the food industry are the aminoglycosides. These are broad spectrum antibiotics most commonly used in veterinary drug medicine in the treatment of infections caused by aerobic Gram-negative bacteria such as mastitis. The BIAcore 3000 biosensor was used in combination with a mixture of four specific antibodies to form a competitive inhibition assay for simultaneous detection of five relevant aminoglycosides in reconstituted skimmed milk (Haasnoot *et al.*, 2003a). Other molecules such as antibacterials (e.g. sulfonamides, nicarbazin) and hormones can be detected in milk and a range of other biological matrices including serum and liver samples (Gillis *et al.*, 2002; Crooks *et al.*, 2003; Haasnoot *et al.*, 2003b; McCarney *et al.*, 2003).

4.1.4.2.2. Pathogen Detection

Salmonella is of major significance as a pathogenic micro-organism in food-bourne infections in humans, causing mild to severe clinical effects (e.g. temperature, gastroenteritis). Therefore, detecting the presence of this bacterial species is quite apparent in prevention and treatment of infection (e.g. in *Salmonella* eradication programs for food-producing animals). The BIAcore 3000 was used to detect serum antibodies in chickens having current or recent *Salmonella* infections. The assay format involved the immobilisation of three well-defined flagellar recombinant DNA antigens (expressed in *E. coli)* onto the surface of the sensor chip. Sera from different batches of chicken with or without infection was passed over the surface in order to detect anti-*salmonella* antibodies. The sensitivity, specificity, precision and reproducibility obtained suggested that this approach could be used for detecting past or present infection with a range of pathogens in animals (Jongerius-Gortemaker *et al.*, 2002). A different approach to Salmonella detection was taken by Bokken *et al.*, (2003). In this study BIAcore was used to detect *Salmonella* through antibodies reacting with

Salmonella group A, B, D and E. Anti-*Salmonella* antibodies were immobilised to the chip surface and bacteria was injected over the surface and allowed to bind. Although further work is required to cover the detection of all relevant *Salmonella* serovars in food-producing animals and food products, this work demonstrates the merits of this alternative biosensor approach in terms of automation, sensitivity (serovars detected at 1 x 10^7 CFU/ml), simple handling and limited hands-on time.

A method was developed by Kai and co-workers (2000) for the rapid detection of pathogenic *E. coli* in human stool samples. Another area of significant interest that involves the testing of human samples is the detection of illicit drug residues. Different assay formats were utilised for the detection of morphine-3-glucuronide (M3G, the main metabolite of heroin and morphine). Polyclonal antibodies and recombinant antibodies were produced for the development of BIAcore inhibition assay for the detection of M3G in biological matrices (Brennan *et al.*, 2003; Dillon *et al.*, 2003).

4.1.4.3. Kinetic Studies

BIAcore is generally used for two main types of biomolecular studies, which involve concentration analysis (Zhu *et al.*, 2000) and kinetic determinations (Deprez *et al.*, 2002). Affinity and rate constants are frequently measured using the BIAcore instrument with a high degree of accuracy. The basis of kinetic interaction is described in greater detail in Section 4.2.3.6. The concentration and kinetic determinations possible with BIAcore are impressive considering that no labelling of the biomolecules is performed. Some recent applications include enzyme kinetic assays, the examination of the kinetic mechanism of MAP kinase and the kinetic analysis of estrogen receptor homo-and heterodimerisation *in vitro* (Stocklein *et al.*, 2000; Schindler *et al.*, 2002; Usami *et al.*, 2002; Jisa & Jungbauer, 2003).

4.1.5. Analysis of Warfarin

Currently there is an extensive assortment of sensitive analytical methods available for the quantitative determination of warfarin and it's metabolites in animal and human biological samples, which avail of various means of detection ranging from chromatography to phosphorescence-based measurements (Table 4.2.). The majority of techniques available require extensive sample pre-treatment (i.e. protein precipitation, liquid-liquid/ solid phase extraction, evaporation and reconstitution) to determine the plasma concentration levels of warfarin. Analysis of warfarin is not a new phenomenon and several of the earliest techniques for detection of warfarin in plasma were primarily based on thin-layer chromatography (TLC) of radiolabelled ligands followed by scintillation

173

counting (Lewis & Trager, 1970). Cook *et al.* (1979) developed a stereoselective radioimmunoassay (RIA) for the enantiomers of warfarin in rat-dosed subjects. The analytical procedure was based on a displacement radioimmunoassay (RIA) incorporating the use of tritium- labelled warfarin.

High-performance liquid chromatography (HPLC) development significantly advanced drug molecules research, allowing for precise determination of their pharmacokinetic profiles without the use of radiolabelled ligands. HPLC analysis of warfarin is predominantly carried out by reverse-phase HPLC, which employs the use of a suitable polar mobile phase and a non-polar stationary phase, typically employing hydrophobic C18 or C8 carbon chains. A number of investigators have employed the use of derivatisation schemes to enhance the detectability of warfarin by ultraviolet and fluorescence detection methods and to allow for resolution of warfarin enantiomers (Banfield & Rowland, 1984). Recent advances in column chromatography have allowed for the development of various columns incorporating β–cyclodextrin molecules capable of enantiomeric resolution of the warfarin enantiomers (Ring & Bostick, 2000). In the 2003 spring meeting of the South-Western Association of Toxicologists (USA) the determination of warfarin in post-mortem specimens by liquid chromatography (LC) and mass spectroscopy (MS) was discussed. A recent medical examiner case involving a suspected overdose of an anticoagulant prompted the development of an assay for warfarin in biological specimens. Warfarin and p-chloro-warfarin, as the internal standard, were isolated from acidified post-mortem fluid and tissue homogenate by extraction with n-butyl chloride. The n-butyl chloride fraction was extracted into base, acidified, extracted back into n-butyl chloride and evaporated to dryness. The residue was reconstituted in mobile phase for analysis by LC/MS. Warfarin concentrations were determined from heart blood (1.3 mg/L), vitreous humor (0.02 mg/L), and liver (1.1 mg/kg).

The pharmacokinetic profile of warfarin in man was extensively reviewed (King *et al.*, 1995). Cai *et al.* (1994) studied the pharmacokinetic profile of 12 stroke patients on warfarin therapy by developing a simplified method for direct determination of warfarin enantiomers by high-pressure liquid chromatography with fluorescence detection. This method involved solid phase extraction of warfarin in plasma, precolumn derivatization to form diastereoisomeric esters, and post-column reaction to discriminate each enantiomer separately. Ultrafiltration was employed in the separation of unbound warfarin enantiomers. The limits of detection routinely attainable by the many published chromatographic publications are often unable to accurately determine the levels of free plasma concentrations of warfarin in patient samples, which in the majority of cases are at least an order of magnitude outside the desired quantification limits. De Orsi and co-workers (1998) developed a method utilising HPLC for the determination of warfarin and acenocoumarin in raw materials and

174

pharmaceuticals. The current trend in anticoagulant therapy is towards lower intensity treatment (Lodwick, 1999). Consequently, there is a need to develop newer more sensitive analytical techniques capable of detecting lower concentrations of warfarin in biological fluids, for the accurate determination of the physiologically free fraction of warfarin in plasma (Fitzpatrick, 2001).

'Warfarin-like' anticoagulants were routinely used as rodenticides, where repeated ingestion of the rodenticide results in death by haemorrhage. The determination of such residues is often important in cases of accidental ingestion by non-target animals. A particular study of interest, involved the investigation of drug binding sites on chicken albumin using site selective fluorescent probes (warfarin and dansylsarcosine). Overall, the results suggest that chicken albumin, like mammalian albumins, has discrete binding sites for warfarin and dansylsarcosine (Rajaian *et al.,* 1997). Anticoagulant residues are not usually present in the stomachs of poisoned animals and the liver is usually the most useful material for diagnostic analysis, where residues are normally present in the affected animals at concentrations below 1 μg/g. Jones (1996) described a method for the detection of the same rodenticides in animal liver tissues using gel-permeation chromatography (GPC) as a clean-up procedure followed by post-column reaction with fluorescent detection. The reported limit of detection for warfarin was 0.010 μg/g and 0.002 μg/g for each of the other rodenticides.

Capitán-Vallvey *et al.* (1999) described a novel phosphorescence-based assay for the determination of warfarin in plasma and water samples using solid-phase room-temperature transmitted phosphorescence. Samples were spotted on Whatman No. 4 filter paper, together with iodide and NaOH solutions, after which they were dried and the transmitted phosphorescence intensity measured at 467 nm using two quartz plates to avoid the quenching effect produced by oxygen. A linear range of detection of warfarin between 300 and 4,000ng/ml was reported, with a lower limit of detection of 80 ng/ml. Some other recent warfarin analysis methodologies include site directed mutagenesis. A defined set of five recombinant proteins comprising combinations of domains and/or subdomains of the HSA N-terminal were prepared and utilised to determine the essential structural elements for the formation of the warfarin binding site on HSA. Affinity constants for binding to warfarin were estimated by fluorescence titration experiments and found to be highest for HSA- DOM I-II and HSA, followed by HSA-DOM IB-II, HSA-DOM II, and HSA-DOM I- IIA. In addition, ultraviolet difference spectroscopy and induced circular dichroism experiments indicated that the primary warfarin binding site is centered in subdomain IIA (Dockal *et al.,* 2000). Using a similar method Watanbe *et al.,* (2001) determined the conformational stability and warfarin-binding properties of HSA using recombinant mutants and fluorescence spectroscopy. Recently, Petersen and colleagues (2002) examined the binding of warfarin to human serum albumin (HSA) mutants

(K195M, K199M, F211V, W214L, R218M, R222M, H242V, and R257M). Warfarin bound to human serum albumin (HSA), exhibits an intrinsic fluorescence that is approximately 10-fold greater than the corresponding signal for warfarin in aqueous solution. This property of the warfarin/HSA complex has been widely used to determine the dissociation constant for the interaction. In the present study, such a technique was used to show that specific substitutions in subdomain IIA altered the affinity of HSA for warfarin.

Table 4.2: *Techniques and detection limits for warfarin analysis*

Detection Method	Limits of Detection/ Quantitation (ng/ml)	Reference
Thin Layer Chromatography (TLC)	(Primarily Qualitative detection limits not reported)	Breckenridge & Orme (1973)
RadioImmunoassay (RIA)	L.O.D pg range	Cook *et al.* (1979)
Phosphorescence	300-4,000 ng/ml	Capitán-Vallvey *et al.* (1999)
Capillary Electrophoresis	200-20,000 ng/ml	Gareil *et al.* (1993)
HPLC- Total:		
Fluorescence-	L.O. D. $\approx$ 0.2 ng/ml	Lee *et al.* (1981)
	1-100 ng/ml (free)	Steyn *et al.* (1986)
	500-10,000 ng/ml (total)	Steyn *et al.* (1986)
	6.0-450 ng/ml	King *et al.* (1995)
Ultraviolet-	40-800 ng/ml	Fasco *et al.* (1977)
	100-5,000 ng/ml	De Vries *et al.* (1982)
	100-1000 ng/ml	Chan & Woo (1988)
HPLC-Enantiomeric:		
Fluorescence-	25-2500 ng/ml	Boppana *et al.* (2002)
Ultraviolet-	L.O. D. $\approx$ 20 ng/ml	De Vries & Schmitz-Kummer (1993)
	L.O.D. $\approx$ 20 ng/ml	Takahasi *et al.* (1997)
	12.5-2500 ng/ml	Ring & Bostick (2000)
SPR based Immunoassay		
Monoclonal:	0.5-500 ng/ml	Fitzpatrick & O' Kennedy
Polyclonal:	10-2000 ng/ml	(2001)
Amperometric biosensor	1,500 ng/ml-150 µg/ml	Hutt *et al.* (1994)
Gas-chromatography Mass Spectrometry (GC-MS)	L.O. D. $\approx$2 ng/ml	Bush *et al.* (1983)
	L.O. D. $\approx$10 ng/ml	Kunze *et al.* (1996)
	L.O.D. $\approx$ 25 ng/ml	Maurer & Arlt (1998)

4.1.5.1. Measures of Analytical Performance

When developing a new analytical assay procedure, various parameters of analytical significance must be considered. Findlay *et al.* (2000) recently outlined particular issues regarding the bioanalytical validation of immunoassay procedures. Bruno (1998) addressed the growing need for validation of immunoassays performed on BIAcore instruments, and described the relevant validation parameters according to current ICH guidelines (International Congress of Harmonisation).

Immunoassays rely on the antibody-antigen interaction for the specific analyte measurement, and the constructed calibration plot is inherently sigmoidal in shape and best fitted with a four-parameter logistical fit. The working range of immunoassays is as a result slightly limited when compared to chromatographic procedures. Also, depending on the source of the antibody preparation (i.e. polyclonal or monoclonal), there can be significant variation in reagent variability, although the development of monoclonal and recombinant techniques has obviated the majority of these difficulties. The sample throughput of immunoassays is significantly better than chromatographic techniques, which can also involve extensive sample pre-treatment and derivatisation steps. Given the recent advances in genetic engineering, the possibility of producing antibodies and fragments thereof with enhanced affinities ($K_D \approx 10^{-15}M$) (Boder *et al.*, 2000), has advanced the possibility of determining even lower analyte concentrations in complex matrices without the need for extensive sample pre-treatment. Similarly, with the use of such antibody libraries and the unique specificity of the antibodies, common biosensor detection formats can be used for the analysis of a wide range of analytes, without the need for developing individual chromatographic assay separation techniques.

Findlay *et al.* (2000) suggested that the previously published minimum acceptable limits of accuracy at 15% (20% at the lower limit of quantitation (LLOQ)) should be increased to 20% (25% at the LLOQ). Wong *et al.* (1997) described the validation of an immunoassay for the detection of the concentrations of antibody in mouse serum. The main parameters addressed for the validation of the biosensor assay included: precision, accuracy, linearity, stability of the immobilised ligand, specificity and sensitivity. The stability of the immobilised ligand is an additional parameter that requires validation in the development of biosensor assays, unlike ELISAs. This must be determined prior to sample analysis through monitoring the binding capacity of the immobilised ligand by a series of consecutive binding-regeneration cycles. Depending on the nature of the immobilised ligand, the binding capacity may be drastically reduced by repeated regeneration exposure to mild acidic and basic pulses and/or the combined use of organic solvents (e.g. particularly for immobilised antibody molecules). Wong *et al.* (1997) suggested the use of independent positive controls to monitor the

178

ligand surface-binding capacity, and to continue with the use of the immobilised surface when the binding capacity for the positive controls remains within 20% of the original measured binding response value.

4.1.5.2. Measurement of Low Molecular Weight Analytes using BIAcore

Immunoassays are generally the method of choice for the detection of larger macromolecules and biomarkers. However, with recent developments in biosensor and antibody technology that has allowed for the standardisation of reagents, the use of immunoassays is continually growing for the measurement of smaller molecular weight molecules such as warfarin. For the detection of small molecular weight analytes, the most commonly employed assay format is the inhibition-based assay whereby an equilibrium drug-antibody mixture is passed over the derivatised chip surface (Section 4.2.3.3)
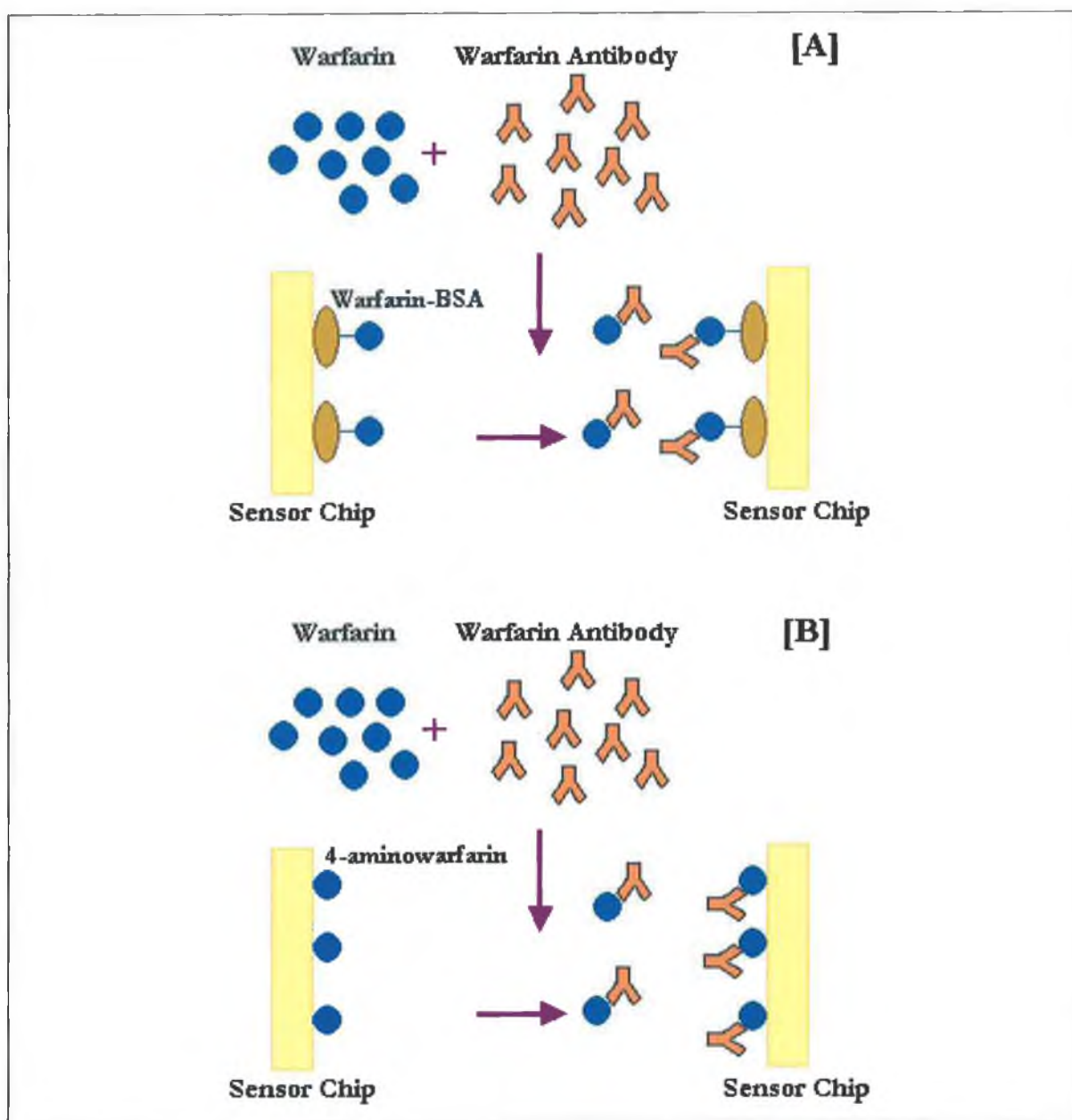
Figure 4.9: *Schematic of the antibody:antigen interaction occurring at the sensor chip surface. Equilibrated mixtures of antibody and antigen are injected over a functionalised sensor chip surface ([A] warfarin-BSA, [B] 4'-aminowarfarin). The amount of antibody available to bind to the chip surface will be 'inhibited' by the free warfarin concentration in solution (i.e. the greater the free analyte concentration in solution, the less free antibody available for binding to the chip surface).*

4.1.6. Chapter Outline

The development of a biosensor-based immunoassay for the detection of warfarin in biological matrices is described. An anti-warfarin mAb was used to develop the inhibition-based SPR immunoassay, and a schematic of the interaction occurring at the sensor surface is shown in Figure 4.9. The ability of the assay to measure free warfarin concentrations in urine were also assessed. Analytical issues regarding the accuracy, precision and robustness of the various immunoassays were investigated.

4.2. Results and Discussion

4.2.1. Preconcentration of Warfarin-protein Conjugates

For the successful immobilisation of drug-protein conjugates at the sensor chip surface it is essential to maximise the interaction between the carboxymethylated dextran (CM-dextran) surface and the target drug-protein molecule, in this instance warfarin-BSA. Electrostatic preconcentration of warfarin-BSA onto the sensor surface is a crucial step in the immobilisation process and relies on electrostatic interaction between unmodified carboxyl groups on the sensor surface and positive charges on the conjugate. This interaction is primarily influenced by the pH and ionic strength of the buffer. At pH values greater than 7, the CM-dextran surface has a net negative charge. Proteins at pH values below their isoelectric point (pI) will have a net positive charge and thus, have the ability to be electrostatically attracted to the chip surface. Therefore in order for electrostatic preconcentration to occur, it is necessary to use a buffer with pH below the pI of warfarin-BSA. Low ionic strength buffers (e.g. 10 mM acetate buffer) are employed for protein immobilisation procedures as they favour such electrostatic attractions between the dextran layer and the protein of interest. This 'preconcentration' step is an effective way of maximising the potential interaction between the warfarin-BSA conjugate and the CM-dextran layer for subsequent immobilisation, and increasing the potential yield of immobilised ligand.

A solution of 50 μg/ml warfarin-BSA was prepared in 10 mM acetate buffer and transferred into eppendorf tubes. The pH of each warfarin-BSA solution was adjusted to the desired pH value by the dropwise addition of a 10% (v/v) solution of acetic acid. Each solution was passed sequentially over an underivatised sensor chip surface at 10 μl/min for a period of 3 minutes as described in section 2.4.8.1. The differing degree of preconcentration can be measured by the response prior to the end of

the injection for each protein solution at the various pH values. Following injection, the flow of running buffer over the chip surface is usually sufficient to dissociate the electrostatic attraction between the protein and CM-dextran surface (Figure 4.10). The degree of preconcentration illustrates a significant increase at pH values below 5. From these preconcentration experiments, it was possible to determine that the optimal pH for warfarin-BSA immobilisation procedures, was pH 4.65 in 10 mM acetate buffer.

4.2.2. *Immobilisation of Warfarin-protein Conjugates*

Ligand immobilisation in BIAcore analysis involves the sequence of surface activation, ligand preconcentration/immobilisation and surface deactivation. In order for the CM-Dextran to be useful for immobilisation reactions, the carboxyl group must first be activated so that it can participate in covalent binding. There are different methods for accomplishing this but the most commonly employed strategy is the use of EDC (N-ethyl-N'-(dimethylaminopropyl)carbodiimide) and NHS (N-hydroxysuccinimide) chemistry. These reaction procedures and their underlying chemistries are described in section 4.1.2.1.1. and the accompanying Figure 4.3. Optimal pH reaction conditions are between pH 6 and 9, whilst the efficiency of the reaction decreases rapidly below pH 4.5. Hapten-protein conjugates are frequently characterised by low isoelectric points, which can make sufficient levels of surface immobilisation complicated when conventional EDC/NHS chemistry is applied. When this occurs, the pH chosen for immobilisation procedures is often a compromise between the effective preconcentration pH and a pH level at which EDC/NHS chemistry works well. Therefore, the pH selected for immobilisation procedures may not always be the pH at which the most effective preconcentration occurred. After immobilisation of warfarin-BSA, unreacted NHS-esters remaining on the sensor surface need to be deactivated. A high ethanolamine concentration ensures that the deactivation or 'capping' is effective. Deactivation was achieved by treatment with 1 M ethanolamine hydrochloride (pH 8.5), which also served to remove non-covalently bound protein by reducing the electrostatic attraction between the protein and CM-dextran surface.

For immobilisation of warfarin-BSA the procedure was carried out as described in Section 2.5.8.2. Immobilisation of the drug 4'-aminowarfarin directly onto the chip surface was carried out as described in section 2.5.8.3., direct immobilisation of drug was performed external to the BIAcore instrument due to the relatively high concentration of DMSO (5-10%) in the coupling buffer. Following surface deactivation, the chip surface was pulsed with two 30 second pulses of 30 mM HCl, which ensured complete removal of non-covalently bound protein. A typical immobilisation strategy for the coupling of warfarin-BSA to the sensor chip surface is demonstrated in Figure 4.11. Routinely,

182

it was possible to attain surface immobilisation of greater than 10,000 response units (RU) of warfarin-BSA. Immobilisation of 4'-aminowarfarin directly to the chip surface resulted in approximately ≈200 RU bound to the chip surface. The molecular weight ratio between 4'-aminowarfarin and warfarin-BSA (i.e. 318 Da to 84 kDa), represents a significantly large increase in epitope concentration at the sensor chip surface, and is reflected in the 20-fold dilution of antibody required with directly immobilised warfarin surfaces compared to warfarin-conjugate surfaces.

pH: 4.65
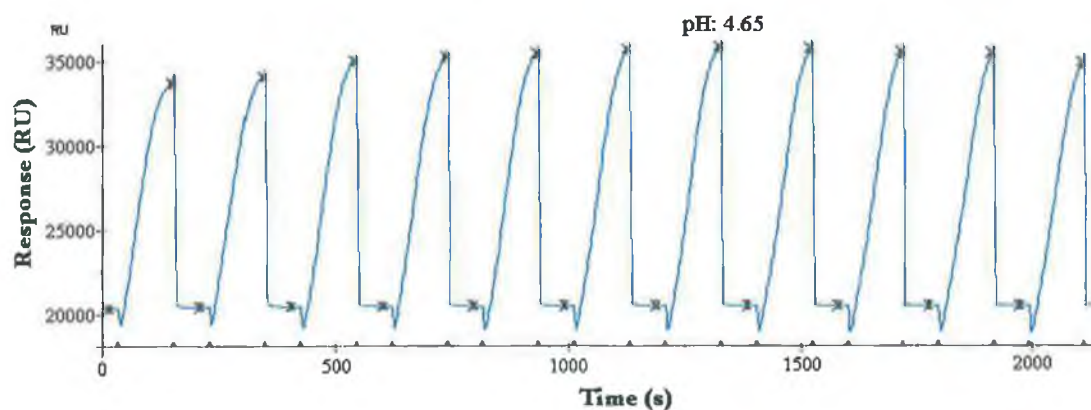
Figure 4.10: *Preconcentration of warfarin-BSA onto a CM-dextran chip surface. Solutions of 50 μg/ml of warfarin-BSA in 10 mM acetate buffer at various pH increments were passed over an unactivated CM-dextran surface at 10 μl/min for a period of 3 minutes. The low ionic strength of the buffer used favours the electrostatic attraction between the negatively charged dextran layer and the positively charged protein (i.e. below isoelectric point). The degree of 'preconcentration' was measured from the response prior to the end of each sample injection. The ionic strength of running buffer (150 mM NaCl) was sufficient to dissociate the electrostatically attracted conjugate from the chip surface. The optimal pH for immobilisation of warfarin-BSA onto a CM-dextran chip surface was calculated to be pH 4.65, and all subsequent immobilisation procedures of warfarin-BSA were thus prepared in 10 mM acetate buffer (pH 4.65).*
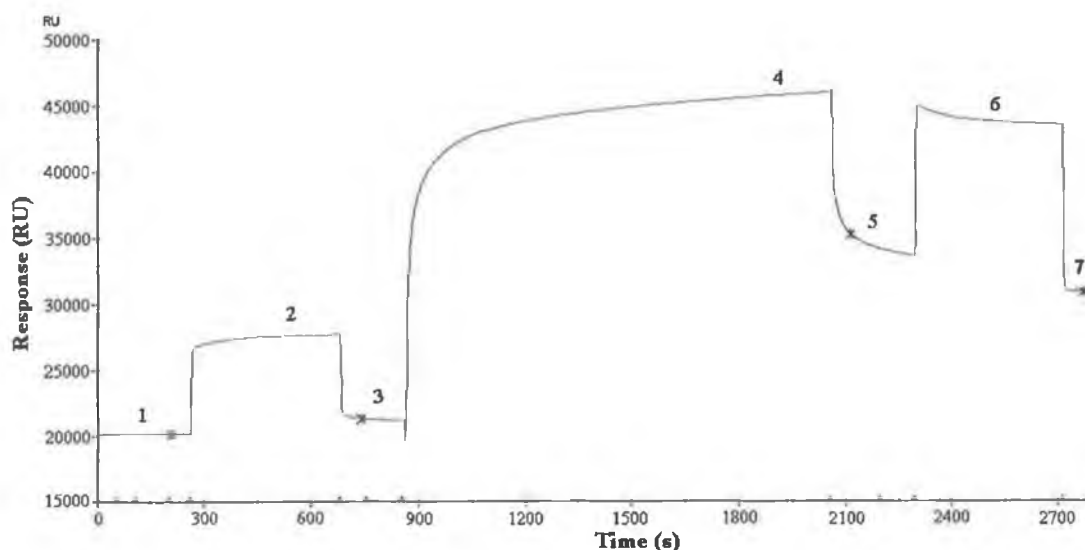
Figure 4.11: *Immobilisation of warfarin-BSA onto a CM-dextran chip surface:*

(1) HBS running buffer is initially passed over the chip surface and a baseline measurement recorded.

(2) Following mixing a solution containing 0.05 M NHS and 0.2 M EDC is passed over the chip surface to activate the chip, the large increase in SPR signal is due primarily to a bulk refractive index change.

(3) A small increase in baseline is recorded following activation of the chip surface (~200RU).

(4) A solution containing 50 µg/ml of warfarin-BSA in 10 mM acetate buffer (pH 4.65) is passed over the chip surface for a period of 10 minutes.

(5) The amount of bound ligand adsorbed is recorded whilst most of the non-covalently bound protein has been eluted.

(6) Deactivation of surface NHS-esters with 1M ethanolamine hydrochloride (pH 8.5), which also serves to elute non-covalently bound conjugate.

(7) One regeneration pulse with 25 mM HCl serves to remove any remaining non-covalently bound conjugate.

185

4.2.3. Development of an Inhibition Immunoassay for Warfarin

A model assay system was developed in Hepes Buffered Saline (HBS) running buffer, to establish effective working range concentration parameters for the detection of warfarin and suitable regeneration conditions for dissociation of the antibody-antigen complex following the binding of antibody to the derivatised chip surface. The analytical validation parameters as outlined by Wong *et al.* (1997) were initially used to assess the overall performance characteristics of the immunoassay. These parameters include accuracy, precision and the stability of the immobilised ligand. The use of directly immobilised 4'-aminowarfarin and warfarin-BSA conjugate were compared to ascertain which drug surface provided the optimal ligand binding characteristics and stability.

4.2.3.1. Regeneration Conditions

Regeneration of the surface of the sensor chip is an important feature of real-time BIAcore applications as regeneration conditions affect the performance and life-time of the chip surface. Therefore, it is necessary to optimise conditions for analysis of large numbers of samples, to evaluate the reproducibility of each measurement and to reduce the cost of the assay. Ideally, it is desirable to have the ability to perform multiple measurements (>50) on a single derivatised chip surface, allowing for routine sample analysis. Wong *et al.* (1997) suggested that the ligand binding capacity be maintained within 20% of positive control values, and be routinely checked throughout the course of the assay to monitor the ligand-binding capacity.

The binding-capacity of both directly immobilised drug surfaces and conjugate immobilised drug surfaces were determined by a series of binding and surface regeneration sequences, to assess at which point the binding capacity deviated outside the desired performance range (<20%). Monoclonal antibody detection of warfarin regeneration cycles were compared on both immobilised surface types (directly immobilised 4'-aminowarfarin/warfarin-BSA conjugate). Protein-G purified monoclonal antibody samples were serially diluted in HBS running buffer as described in section 2.5.8.4. Antibody solutions (nominally a 1/100 dilution of each antibody preparation) were then repeatedly injected and the surface regenerated. Monoclonal antibodies could be dissociated using mild acid (10-25 mM HCl) pulses. Surface regeneration studies conducted demonstrated that the sensor chip surfaces to which the drug 4'-aminowarfarin was directly coupled were essentially 'unlimited' with respect to antibody-binding capacity, and demonstrated no decrease in antibody-binding capacity over the course of greater than 80 cycles (Figure 4.13). Such surfaces were in fact used for in excess of 1,000 cycles (Fitzpatrick, 2001). The coefficient of variation of antibody binding over the course of 80

cycles was 0.89 %. The binding capacity of warfarin-BSA surfaces was also assessed (70 cycles) using the monoclonal antibodies to warfarin. The conjugate surfaces displayed an initially relatively high decrease in binding capacity that began to plateau out after approximately 10 cycles (Figure 4.12). Consequently, studies performed with such conjugate immobilised surfaces were exposed to at least 15 regeneration cycles prior to sample analysis. The monoclonal antibodies bound to the 4'-aminowarfarin immobilised chip surface demonstrated essentially no dissociation from the chip surfaces, which can be observed from the overlaid interaction curves at various antigen concentrations (Figure 4.15).

These results imply that directly immobilised drug molecules should be employed whenever target molecules with suitable reactive groups (e.g. the amine moiety on 4'-aminowarfarin) are available for direct coupling to the chip surface. In this instance such surfaces provided exceptional stability of the immobilised ligand (although, exposure to various pH extremes may affect the stability of the immobilised ligand molecule), and low coefficients of variation were observed over the course of binding studies (<4%). Clearly, the results generated demonstrate the use of drug-protein conjugates is applicable in many instances, provided the regeneration conditions maintain the binding capacity of the immobilised ligands. However, the use of drug-protein conjugates can be a limiting factor, particularly when trying to dissociate high affinity antibody and antigen interactions (Keating, 1998). The small molecular weight of warfarin (308 Da) is somewhat constrained in the type of immunoassay format available for the direct detection of analyte. Extremely high concentrations of IgG would need to be immobilised at the chip surface to attain any reasonable response for the direct detection of warfarin, which in turn would be reflected by a correspondingly large increase in the concentrations of analyte detectable. Direct chemical coupling of antibodies to the chip surface suffers from particular drawbacks; namely the regeneration conditions required too often result in significantly reduced surface binding capacity as a result of antibody denaturation. Secondly, direct immobilisation of antibodies does not afford any specific orientation of the antibody molecules for subsequent binding to antigen. The most reproducible assay condition for such assay formats has been to employ the use of suitable affinity-capture surfaces, typically those incorporating Protein A/G. Protein A-coated surfaces specifically bind ($K_D \sim 10^{-9}$ M) and orientates the antibody molecules through their Fc regions, and were shown to be capable of reproducibly being used for greater than 120 binding-regeneration cycles (Quinn et al., 1999). A notable feature of directly immobilised drug surfaces is the substantially reduced quantity (i.e. 10-fold) of antibody required for assay purposes, a direct result of the increased surface epitope concentration, which again can be an important parameter given the high cost of many commercial antibody preparations. The use of effective regeneration solutions such as guanidine hydrochloride and guanidine thiocyanate are routinely employed to dissociate bound antibody from

187
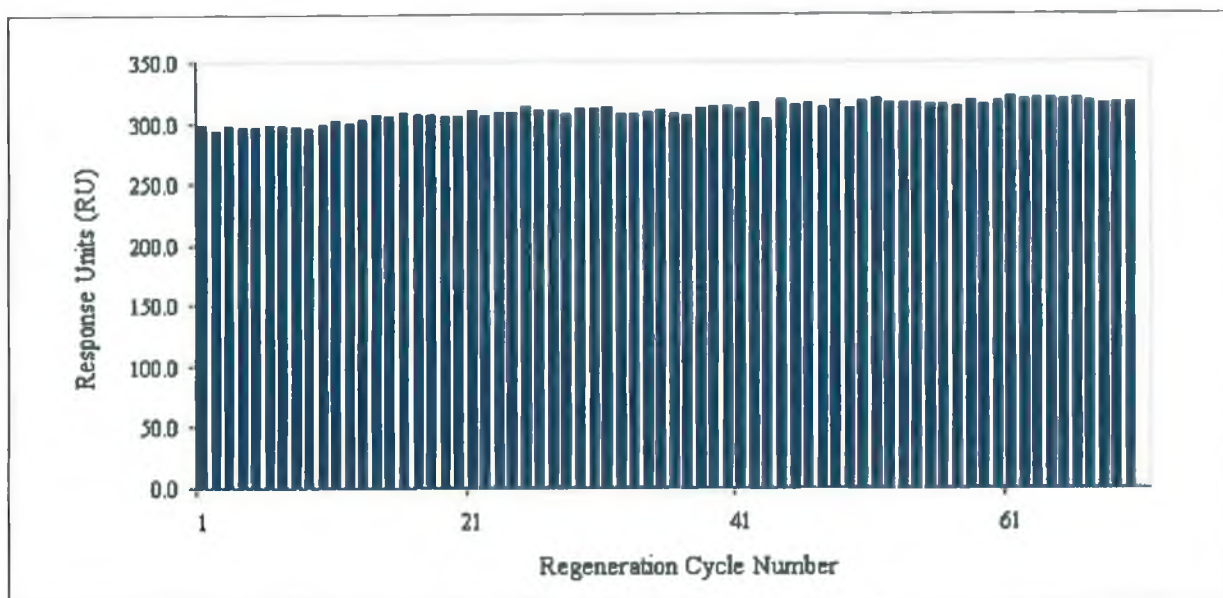
Figure 4.12: *70 consecutive regeneration cycles of a 4-minute binding of monoclonal antibody (4-2-25) to the warfarin-BSA drug surface. The surface was regenerated with one 30-second pulse of 25 mM HCl. The binding response demonstrated a coefficient of variation of 1.86% over the course of 70 cycles and no decrease in the measured binding response over the course of the regeneration study (i.e. cycle 1= 297.9, cycle 70 = 315.4).*
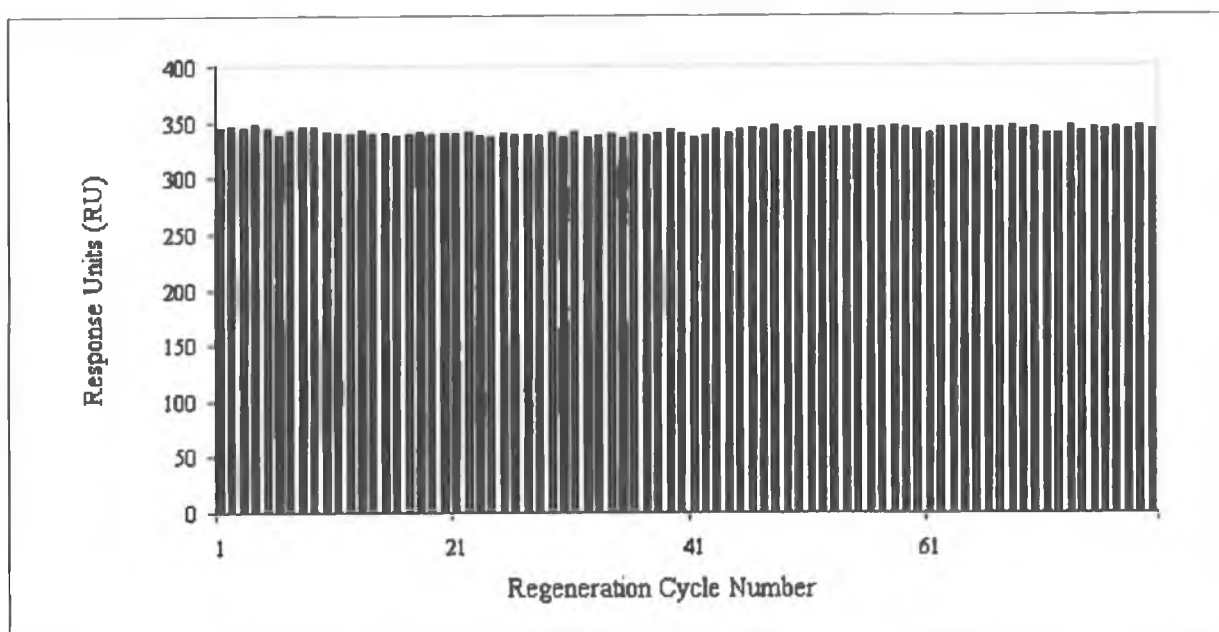
Figure 4.13: *80 consecutive regeneration cycles of a 4-minute binding of monoclonal antibody (4-2-25) to the directly immobilised 4'-aminowarfarin drug surface. The surface was regenerated with one 30-second pulse of 25 mM HCl. The binding response demonstrated a coefficient of variation of 0.89% over the course of 80 cycles and no decrease in the measured binding response over the course of the regeneration study (i.e. cycle 1= 345.1, cycle 80 = 343.0). Directly immobilised drug surfaces were essentially 'unlimited' with respect to antibody binding capacity and can be used for greater than 1,000 cycles (Fitzpatrick, 2001).*
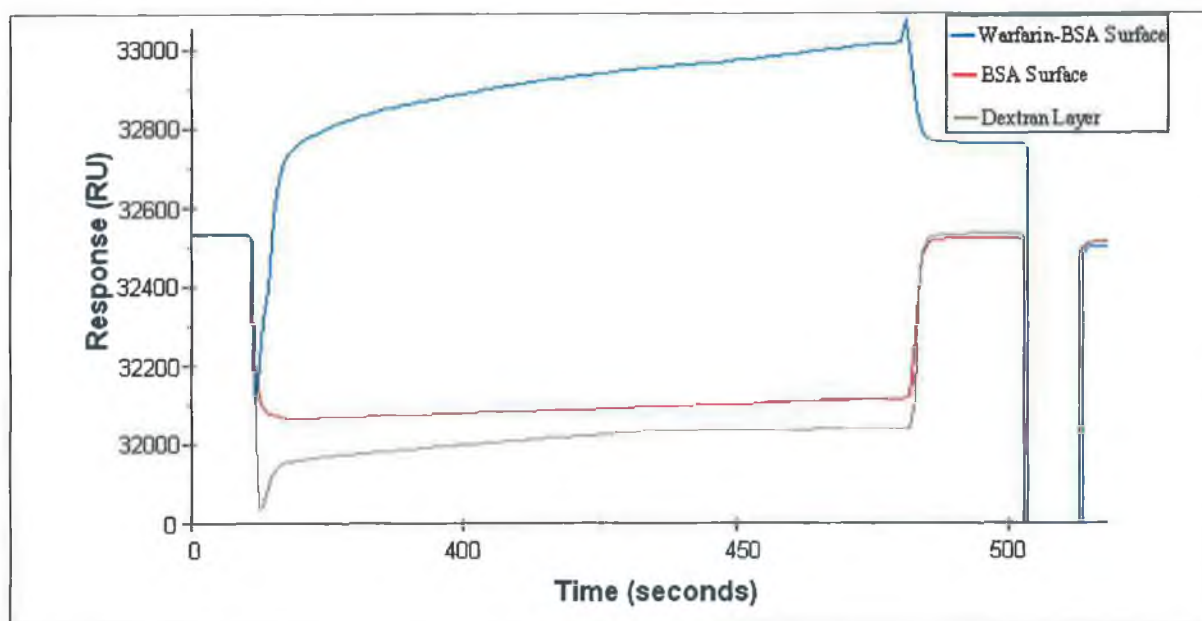
Figure 4.14: *Simultaneous injection of 1/5 dilution monoclonal antibody (4-2-25) sample over immobilised warfarin-BSA, dextran and BSA surfaces. The negligible degree of non-specific binding to BSA immobilised surface (1.1RU) compared to the response recorded on the immobilised warfarin-BSA (225RU), can be attributed primarily to the particular immunoaffinity purification procedures employed.*

4.2.3.3. Determination of Working Range of Model Inhibition Assay Range in PBS

Once the binding capacity and the degree of non-specific binding associated with the binding interactions was established, the working range of the biosensor assay for the monoclonal antibody 4-2-25 could then be evaluated. The validation criteria described by Wong *et al.* (1997) in the development of a biosensor-based immunoassay regarding sensitivity, ligand-binding capacity, accuracy, and precision were assessed for the detection of warfarin by mAb on two immobilised (i.e. drug/drug-protein) surfaces. A brief description of the main definitions and terminology used in reference to bioanalytical methods is included in Appendix 1A.

For the determination of the working range of the inhibition immunoassay, dilutions of warfarin were firstly prepared in HBS buffer as described in section 2.5.8.6. Dilutions of warfarin were prepared in HBS buffer ranging from 0.03 to 5000 ng/ml for the monoclonal antibody inhibition assays. The protein-G purified anti-warfarin monoclonal antibody preparations were mixed with the corresponding dilution of warfarin using the autosampler, and allowed to equilibrate for a period of 5-10 minutes. The samples were then passed in random order, over the derivatised chip surface and

regenerated using the appropriate predetermined regenerant. Typical antibody binding response curves are illustrated in Figure 4.15. The response measured following the binding of unliganded antibody from the equilibrium solution (warfarin:antibody) could be thus determined. In order to obtain normalised binding responses (allowing for direct inter-assay comparison), the binding response at each antigen concentration (R) was subsequently divided by the antibody binding response determined in the presence of zero antigen concentration (R_0).

These normalised (R/Ro) responses were then used to construct a calibration curve. It consisted of the normalised response plotted against the warfarin concentration (ng/ml) and a four-parameter logistic fit modelled to the data set using BIAevaluation™ 3.1 software (Section 2.5.8.6). The working range of the assay was calculated to be from 0.97-250 ng/ml. Examples of the calibration plots constructed for monoclonal antibody injected over either the 4'-aminowarfarin or warfarin-BSA chip surfaces are illustrated in Figures 4.16-4.19. In addition, the intra- (precision) and inter-assay (reproducibility) variability determined for the monoclonal antibody are displayed in Tables 4.3-4.6. The intra-assay variation (precision/repeatability) for the BIAcore-based inhibition assay was obtained by calculating the coefficient of variation between samples assayed during a single assay run. The inter-assay variation (reproducibility) for each antibody preparation was calculated by performing the assay on three separate days and calculating the precision, or coefficient of variation between batches.

In this context, based on the degrees of precision, reproducibility, sensitivity and accuracy recorded, a direct comparison could be made with respect to each immobilisation format and particular antibody preparation. The coefficients of variation for the assay were typically of the order of 4%, except as expected towards the asymptotes of the spline curves where the degree of precision decreased to ~9% at the higher limit of quantitation. The coefficients of variation for the complete curve including the lower limit of quantitation (LLOQ)(i.e. 0.97 ng/ml) are all well within the current recommended validation guidelines for immunoassay procedures (Findlay *et al.*, 2000). From the inter- and intra-assay data (Tables 4.3-4.6), a direct comparison could be made between both immobilisation formats, based on degrees of precision, reproducibility, sensitivity and accuracy recorded. The coefficients of variation (CV's) were determined to assess the precision of the analytical method, expressing standard deviation as a percentage function of the mean. For the immobilised warfarin-BSA conjugate chip the intra- and interday assay CV's ranged from 0.12 – 9.21% and 0.58 – 11.11% respectively. For the directly immobilised 4'-aminowarfarin chip the intra- and interday assay CV's ranged from 0.10 – 4.53% and 0.16 – 5.86%. These values indicate that the assay performed on both chip surfaces have a good degree of precision. The percentage accuracy values obtained in the linear part of the interday assay indicate that the fitted four parameter curve provides an accurate

192

representation of the measured response in the linear range of the assay. The % accuracy values for the warfarin-BSA conjugated chip and 4'-aminowarfarin chip ranged from 92 – 104% and 95 – 106%, respectively. It was concluded that the monoclonal antibody preparation 4-2-25 injected over a directly immobilised 4'-aminowarfarin drug surface performed with the highest degrees of accuracy, reproducibility and precision. Both surface types (warfarin-BSA and 4-aminowarfarin) were then selected for development of an inhibition biosensor assay for the detection of warfarin in urine.
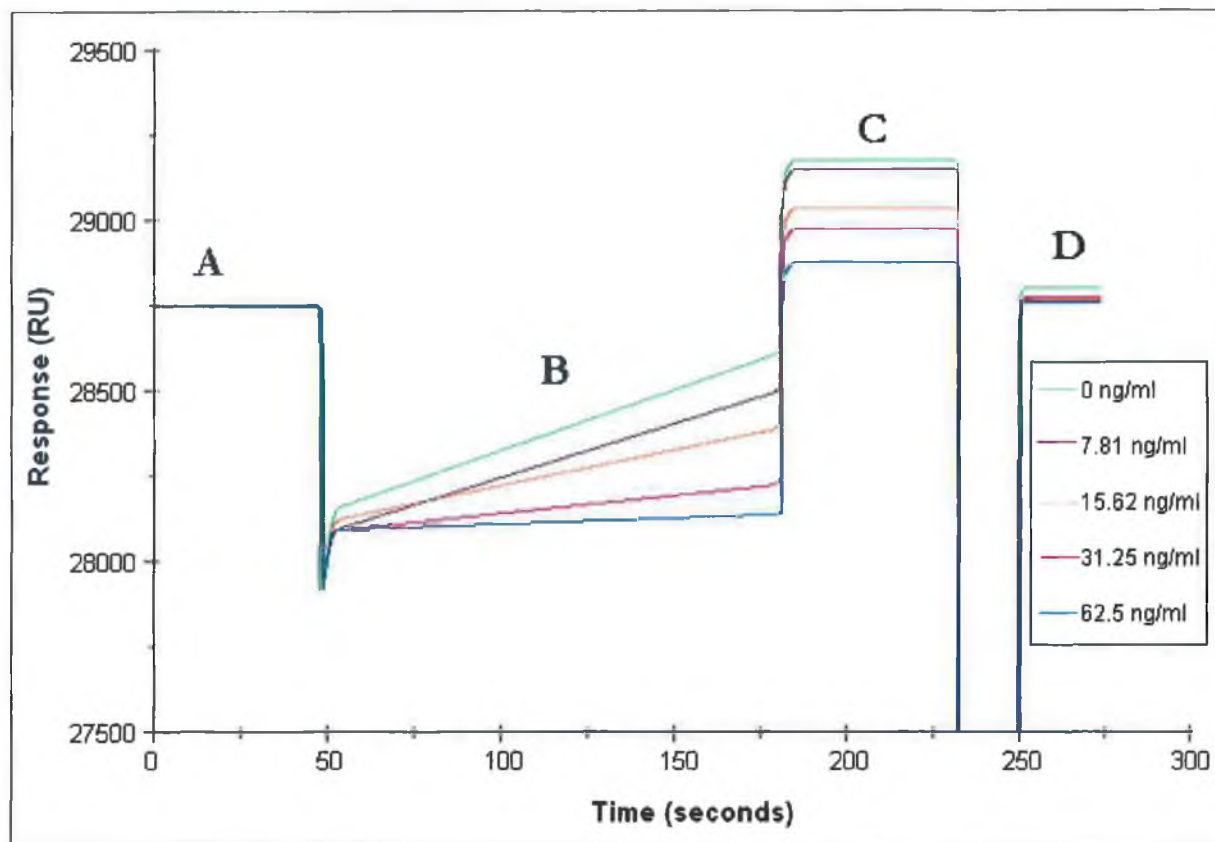
Figure 4.15: Overlay interaction curves demonstrating the decrease in binding of anti-warfarin mAb to the immobilised warfarin-BSA surface with increasing free warfarin concentrations in HBS. (A) shows the normalised baselines of each sensorgram when HBS is injected over the chip surface. (B) shows the increasing binding of free antibody with decreasing free warfarin concentrations. (C) shows the baseline shift when HBS buffer is passed over the surface after sample injection. The concentration of free warfarin used in each binding cycle is indicated beside each sensorgram. The measured binding response was used to calculate the normalised response values (R/Ro), which were subsequently used to construct the calibration curves. (D) The sensor chip could be easily regenerated using one 30 second pulse of 25 mM HCl.

Table 4.3: Intra-day Assay results (warfarin-BSA chip) for detecting warfarin in PBS. Coefficients of variance (a quantitative measure of precision) were calculated using the equation % CV= (S.D./Mean) x 100 where the standard deviation (S.D.) is computed from replicate (3 replicates) analyses within a single validation run. % Difference Accuracy is the difference between the actual warfarin concentration (AWC) of the prepared warfarin standards and the mean back calculated warfarin concentration (MBCW) value obtained from the 4-parameter calibration curve: (AWC/MBCW) x 100

Actual Warfarin Concentration (ng/ml)	Mean Back Calculated Warfarin Concentration from calibration curve (ng/ml)	% C.V.	% Accuracies
500.00	451.04	9.21	110.85
250.00	239.67	5.38	104.13
125.00	131.65	5.26	94.95
62.50	67.62	0.81	92.43
31.25	28.48	0.12	109.73
15.60	15.90	0.43	98.11
7.80	7.62	0.19	102.36
3.91	4.20	0.28	93.10
1.25	1.50	0.60	83.33
0.97	0.93	0.19	104.30
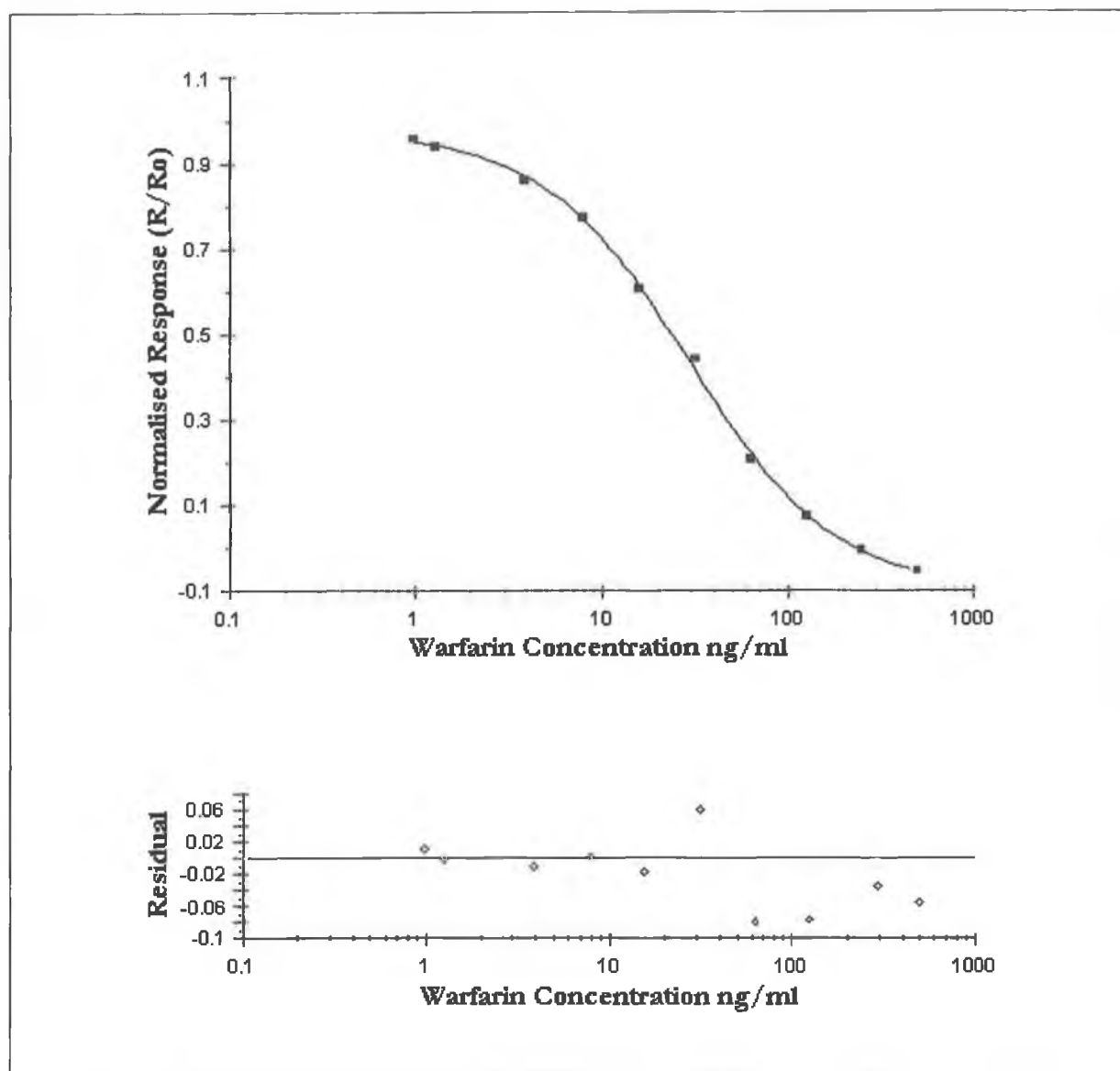
Figure 4.16: *Intra-day Assay calibration curve (warfarin-BSA chip) for the detection of warfarin in PBS utilising an anti-warfarin mAb. A 4-parameter equation was fitted to the data set using BIAevaluation 3.1. software. The intraday means and coefficients of variation are tabulated in Table 4.3. Each point on the curve is the mean of three replicate measurements analysed within a single validation run. Residual plots for the calibration curves are included (for each calibration curve), which illustrate the 'goodness of the fit' of the applied 4-parameter equations and supports the % accuracy findings.*

Table 4.4: Inter-day Assay results (warfarin-BSA chip) for detecting warfarin in PBS. Coefficients of variance (a quantitative measure of precision) was calculated using the equation % CV= (S.D./Mean) x 100 where for interday studies the S.D. is computed from replicate (3 replicates) analyses over 3 validation runs on 3 separate days. % Difference Accuracy is the difference between the actual warfarin concentration (AWC) of the prepared warfarin standards and the mean back calculated warfarin concentration (MBCW) value obtained from the 4-parameter calibration curve: (AWC/MBCW) x 100

Actual Warfarin Concentration (ng/ml)	Mean Back Calculated Warfarin Concentration from calibration curve (ng/ml)	% C.V.	% Accuracies
500.00	496.44	9.21	100.72
250.00	230.73	11.11	108.35
125.00	135.11	9.12	92.52
62.50	63.18	8.61	98.92
31.25	30.01	2.42	104.13
15.60	15.61	7.36	99.94
7.80	7.93	1.02	98.36
3.91	4.10	2.80	95.37
1.25	1.40	0.58	89.29
0.97	0.50	1.34	NA

Figure 4.17: *Inter-day Assay calibration curve (warfarin-BSA chip) for the detection of warfarin in PBS utilising an anti-warfarin mAb. A 4-parameter equation was fitted to the data set using BIAevaluation 3.1 software. The interday means and coefficients of variation are tabulated in Table 4.4. Each point on the curve is the mean of three replicate measurements analysed over three days. Residual plots for the calibration curves are included (for each calibration curve), which illustrate the 'goodness of the fit' of the applied 4-parameter equations and supports the % accuracy findings.*

Table 4.5: Intra-day Assay results (directly immobilised 4'-amino warfarin chip) for detecting warfarin in PBS. Coefficients of variance (a quantitative measure of precision) were calculated using the equation % CV= (S.D./Mean) x 100 where the standard deviation (S.D.) is computed from replicate (3 replicates) analyses within a single validation run. % Difference Accuracy is the difference between the actual warfarin concentration (AWC) of the prepared warfarin standards and the mean back calculated warfarin concentration (MBCW) value obtained from the 4-parameter calibration curve: (AWC/MBCW) x 100

Actual Warfarin Concentration (ng/ml)	Mean Back Calculated Warfarin Concentration from calibration curve (ng/ml)	% C.V.	% Accuracies
250.00	214.03	3.64	116.81
250.00	112.91	1.89	110.70
125.00	73.07	4.53	83.76
62.50	33.67	0.35	92.80
31.25	15.63	0.10	99.81
15.60	7.30	1.43	106.83
7.80	4.20	0.31	93.14
3.91	2.16	0.86	87.96
0.97	1.02	3.34	95.28

Figure 4.18: *Intra-day Assay calibration curve (4'-aminowarfarin chip) for the detection of warfarin in PBS utilising an anti-warfarin mAb. A 4-parameter equation was fitted to the data set using BIAevaluation 3.1. Software. The intraday means and coefficients of variation are tabulated in Table 4.5. Each point on the curve is the mean of three replicate measurements analysed within a single validation run. Residual plots for the calibration curves are included (for each calibration curve), which illustrate the 'goodness of the fit' of the applied 4-parameter equations and supports the % accuracy findings.*

Table 4.6: Inter-day Assay results (directly immobilised 4'-amino warfarin chip) for detecting warfarin in PBS. Coefficients of variance (a quantitative measure of precision) was calculated using the equation % CV= (S.D./Mean) x 100 where for interday studies the S.D. is computed from replicate (3 replicates) analyses over 3 validation runs on 3 separate days. % Difference Accuracy is the difference between the actual warfarin concentration (AWC) of the prepared warfarin standards and the mean back calculated warfarin concentration (MBCW) value obtained from the 4-parameter calibration curve: (AWC/MBCW) x 100

Actual Warfarin Concentration (ng/ml)	Mean Back Calculated Warfarin Concentration from calibration curve (ng/ml)	% C.V.	% Accuracies
250.00	209.00	3.45	119.62
125.00	105.22	5.86	118.80
61.20	72.75	4.49	84.12
31.25	33.79	2.48	92.48
15.60	15.66	0.65	99.62
7.80	7.30	0.60	106.85
3.91	4.10	0.37	95.37
1.90	2.10	0.16	90.48
0.97	0.96	1.05	101.04

Figure 4.19: *Inter-day Assay calibration curve (4'-aminowarfarin chip) for the detection of warfarin in PBS utilising an anti-warfarin mAb. A 4-parameter equation was fitted to the data set using BIAevaluation 3.1. software. The interday means and coefficients of variation are tabulated in Table 4.6. Each point on the curve is the mean of three replicate measurements analysed over three days. Residual plots for the calibration curves are included (for each calibration curve), which illustrate the 'goodness of the fit' of the applied 4-parameter equations and supports the % accuracy findings.*

4.2.3.4. Determination of Working Range of Assay in Urine

The inhibition immunoassay was also used for the detection of warfarin in urine as described in section 2.5.8.6. The ionic composition of urine can demonstrate considerable variation depending on an individual's liquid volume intake. The antibody sample was prepared in HBS of twice the normal ionic strength (i.e. 2 x [HBS]), in order to compensate for the potential of wide inter-individual variability in the salt composition of urine. A dilution step (i.e. 1 in 5 urine dilution) was also employed to reduce the potential effect on the measured binding response due to the altered salt composition. Warfarin dilutions were prepared for concentrations ranging between 0.97-500 ng/ml in the urine solution. Dilutions of antibody solution (i.e. nominally 1/100) were subsequently mixed with 20 µl of warfarin-spiked urine of known warfarin concentration, and allowed to attain equilibrium for five minutes on the BIAcore autosampler. The equilibrium mixtures were then serially passed over either the 4'-aminowarfarin or warfarin-BSA-coated surface in random sequence, to ensure there was no bias in the recorded measurements. The normalised responses were then used to construct a calibration curve of the normalised response versus warfarin concentration (ng/ml) as explained in section 4.2.3.3. The working range of this assay was calculated to be from 0.97-250 ng/ml. Examples of the calibration plots constructed for monoclonal antibody injected over either the 4'-aminowarfarin or warfarin-BSA chip surfaces are illustrated in Figures 4.20-4.23. In addition, both the intraday and interday assay variabilities were determined and are displayed in Tables 4.7-4.10. The coefficients of variation for the assay were typically of the order of 2%, except as expected towards the asymptotes of the spline curves where the degree of precision decreased to ~9% at the higher limit of quantitation. The coefficients of variation for the complete curve including the lower limit of quantitation (LLOQ)(i.e. 0.97 ng/ml) are all well within the current recommended validation guidelines for immunoassay procedures (Findlay *et al.*, 2000).

From the inter- and intra-assay data (Tables 4.7-4.10) a direct comparison could be made between both immobilisation formats based on degrees of precision, reproducibility, sensitivity and accuracy recorded. The coefficients of variation (CV's) were determined to assess the precision of the analytical method, expressing standard deviation as a percentage function of the mean. For the immobilised warfarin-BSA conjugate chip the intra- and interday assay CV's ranged from 0.8 – 8.33% and 4.53 – 15.16%, respectively. For the directly immobilised 4'-aminowarfarin chip the intra- and interday assay CV's ranged from 0.13 – 7.17% and 0.16 – 11.80%. These values indicate that the assays performed on both chip surfaces have a high degree of precision. The percentage accuracy values obtained in the linear part of the interday assay indicates that the fitted four parameter curve provides an accurate representation of the measured response in the linear range of the assay. The %

accuracy values for the warfarin-BSA conjugated chip and 4'-aminowarfarin chip ranged from 97.50 – 105.93% and 95.71 – 103.59%, respectively. It was concluded that the monoclonal antibody preparation 4-2-25, on a directly immobilised 4'-aminowarfarin drug surface performed with the highest degrees of precision and reproducibility. This immunoassay format compares well to previous research data obtained using HPLC (Takahashi *et al.*, 1997) and BIAcore analysis. Fitzpatrick & O'Kennedy (2001) utilised a panel of anti-warfarin monoclonal antibodies to establish a BIAcore detection method for warfarin in human plasma samples. The limit of detection was similar to the data presented in this thesis (L.O.D. = 0.97ng/ml). HPLC was utilised to detect warfarin in plasma samples, however, the L.O.D. = 5.0ng/ml which is not as sensitive as the BIAcore assays. Approximately 99% of warfarin present in plasma is protein-bound (Cai *et al.*, 1994; Fitzpatrick & O'Kennedy, 2001; Bertucci & Cimitan, 2003). Therefore, initially there should be relatively little (1%) warfarin free in plasma and in urine. Hence, the BIAcore assay utilising anti-warfarin mAb is sufficient for the detection of warfarin in the concentration range 0.97 – 250ng/ml. If a higher range of detection is required (e.g. monitoring an increase in warfarin dose), anti-warfarin polyclonal antibodies can be utilised as the working range of a BIAcore assay for the detection of warfarin in urine was demonstrated to be from 10-5,000 ng/ml.

Proper patient compliance is tremendously important in the management of warfarin anticoagulation, as dosage modifications are made based on the pharmacological end-point of warfarin therapy (i.e. Prothrombin time measurements). Accordingly, any dosage adjustments made on the basis of improper patient compliance can have extremely serious consequences upon return of the patient to the recommended dosage regime. Therefore, the current system could be utilised as an immunoassay screening technique to guarantee adequate patient compliance prior to dosage adjustment. A comparable strategy could also be used in cases of suspected warfarin ingestion. George *et al.* (2000) described a similar approach for monitoring methadone compliance in patient urinary samples by immunoassay. These screening procedures could potentially be applied for rapid determination of substance abuse to a wide range of residues, by employing broad-spectrum antibodies (either poly-or monoclonal) capable of detecting particular classes of drugs of abuse (e.g. amphetamines). The BIAcore 3000 used in this work shows great promise in this area as different residues of illicit drugs and their metabolites can be immobilised on the available flow cells (1-4). Once this is accomplished, a single injection over the prepared surface of patient sample (e.g. urine, plasma or saliva) could be rapidly used to identify the presence of such illicit residues in minutes. Such rapid screening techniques are essential to allow for rapid identification of drugs so that an appropriate antidote may be administered.

Table 4.7: Intra-day Assay coefficients of variance (CV's) and percentage accuracies for the anti-warfarin monoclonal antibody used for the detection of warfarin in urine. Warfarin-BSA was immobilised onto the sensor chip surface. The standard deviation (S.D.) is computed from replicate (3 replicates) analyses within a single validation run.

Actual Warfarin Concentration (ng/ml)	Mean Back Calculated Warfarin Concentration from calibration curve (ng/ml)	% C.V.	% Accuracies
250.00	228.83	4.78	109.25
125.00	143.98	8.33	86.82
62.50	55.40	0.80	112.82
31.25	35.42	3.64	88.23
15.60	13.12	1.31	118.90
7.80	8.77	2.04	88.94
3.91	4.71	1.31	83.01
1.90	1.17	2.36	NA
0.97	0.62	1.92	NA
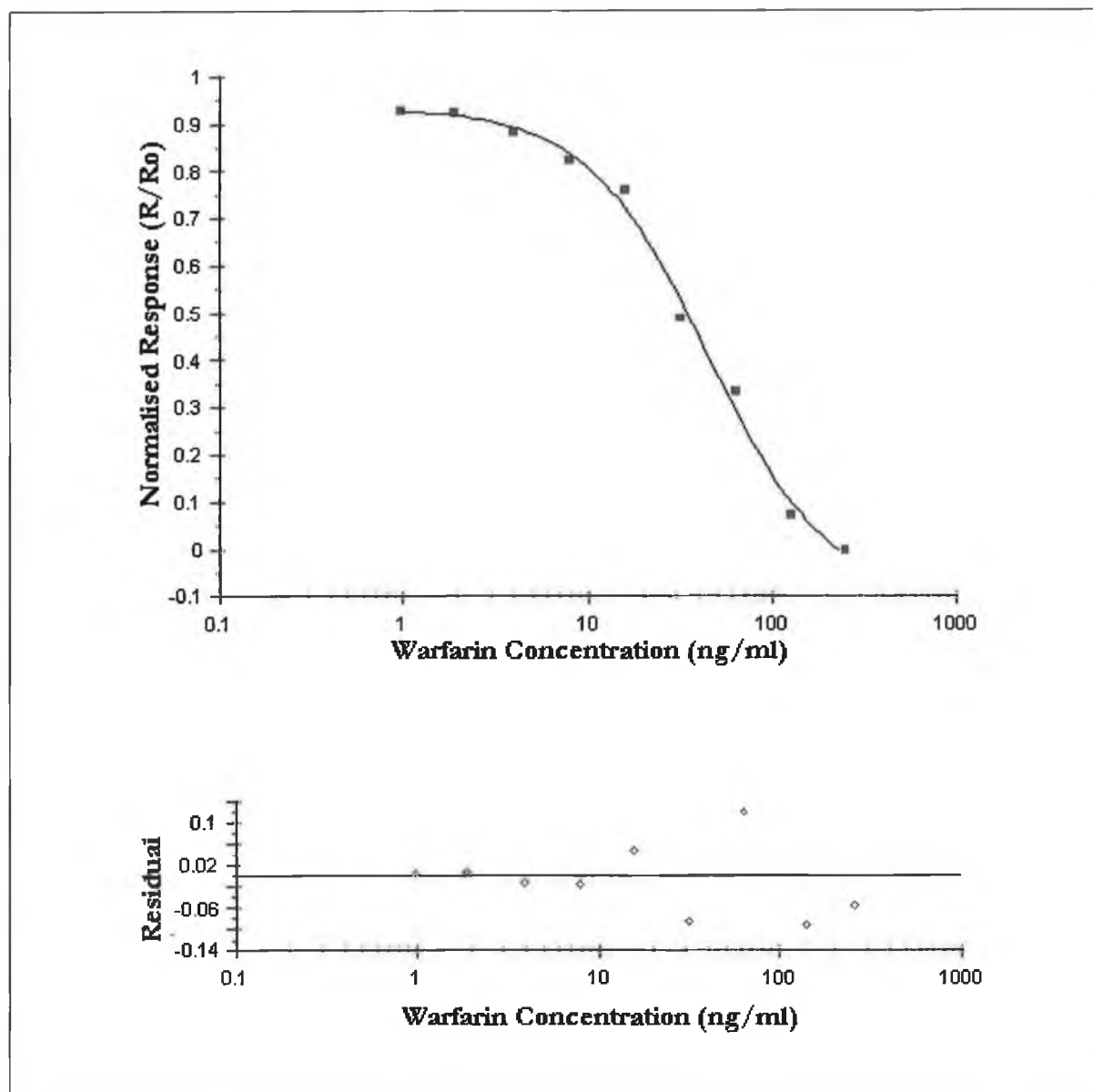
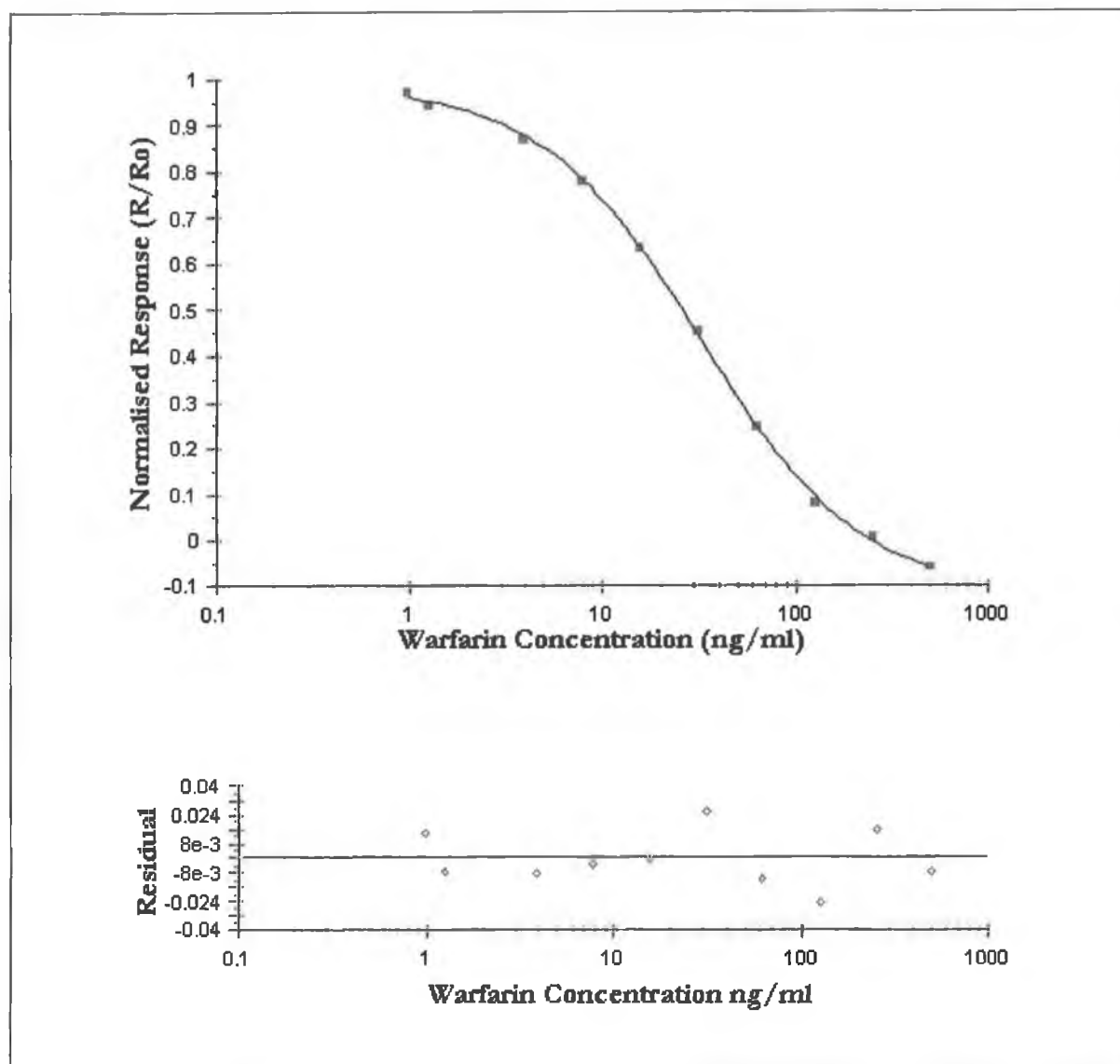***Figure 4.20:*** *Intra-day Assay calibration curve (warfarin-BSA chip) for the detection of warfarin in urine utilising an anti-warfarin mAb. A 4-parameter equation was fitted to the data set using BIAevaluation 3.1 software. The intraday means and coefficients of variation are tabulated in Table 4.7. Each point on the curve is the mean of three replicate measurements analysed within a single validation run. Residual plots for the calibration curves are included (for each calibration curve), which illustrate the 'goodness of the fit' of the applied 4-parameter equations and supports the % accuracy findings.*

Table 4.8: Inter-day Assay coefficients of variance (CV's) and percentage accuracies for the anti-warfarin monoclonal antibody used for the detection of warfarin in urine. Warfarin-BSA was immobilised onto the sensor chip surface. The standard deviation (S.D.) is computed from replicate (3 replicates) analyses over 3 validation runs on 3 separate days.

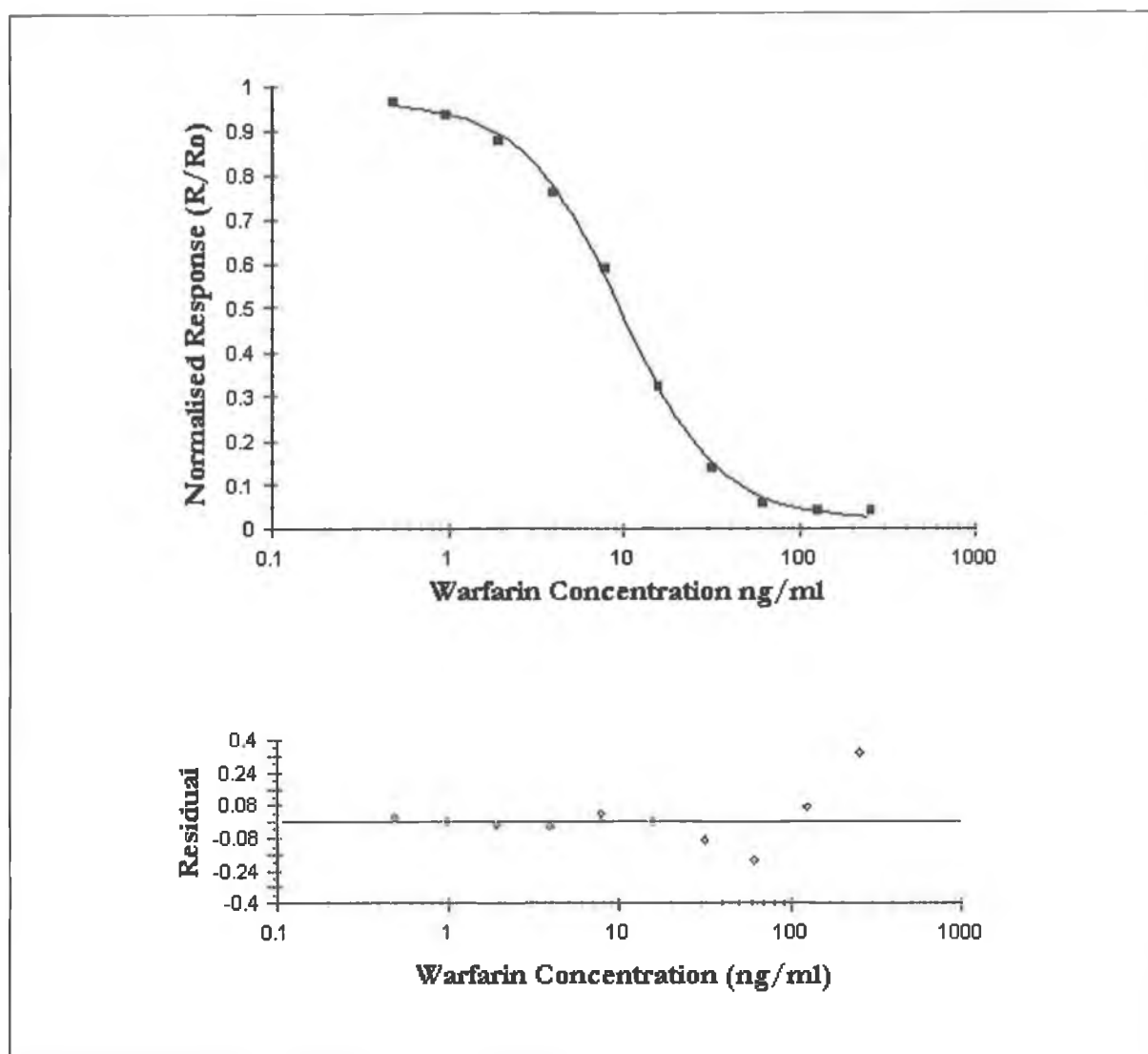| Actual Warfarin Concentration (ng/ml)	Mean Back Calculated Warfarin Concentration from calibration curve (ng/ml)	% C.V.	% Accuracies
250.00	256.40	5.40	97.50
125.00	118.00	6.77	105.93
62.50	63.40	11.05	98.58
31.25	32.10	13.87	97.35
15.60	15.65	15.16	99.68
7.80	7.51	11.69	103.86
3.91	3.65	4.53	107.12
1.90	1.74	7.27	109.20
0.97	1.20	10.32	80.83
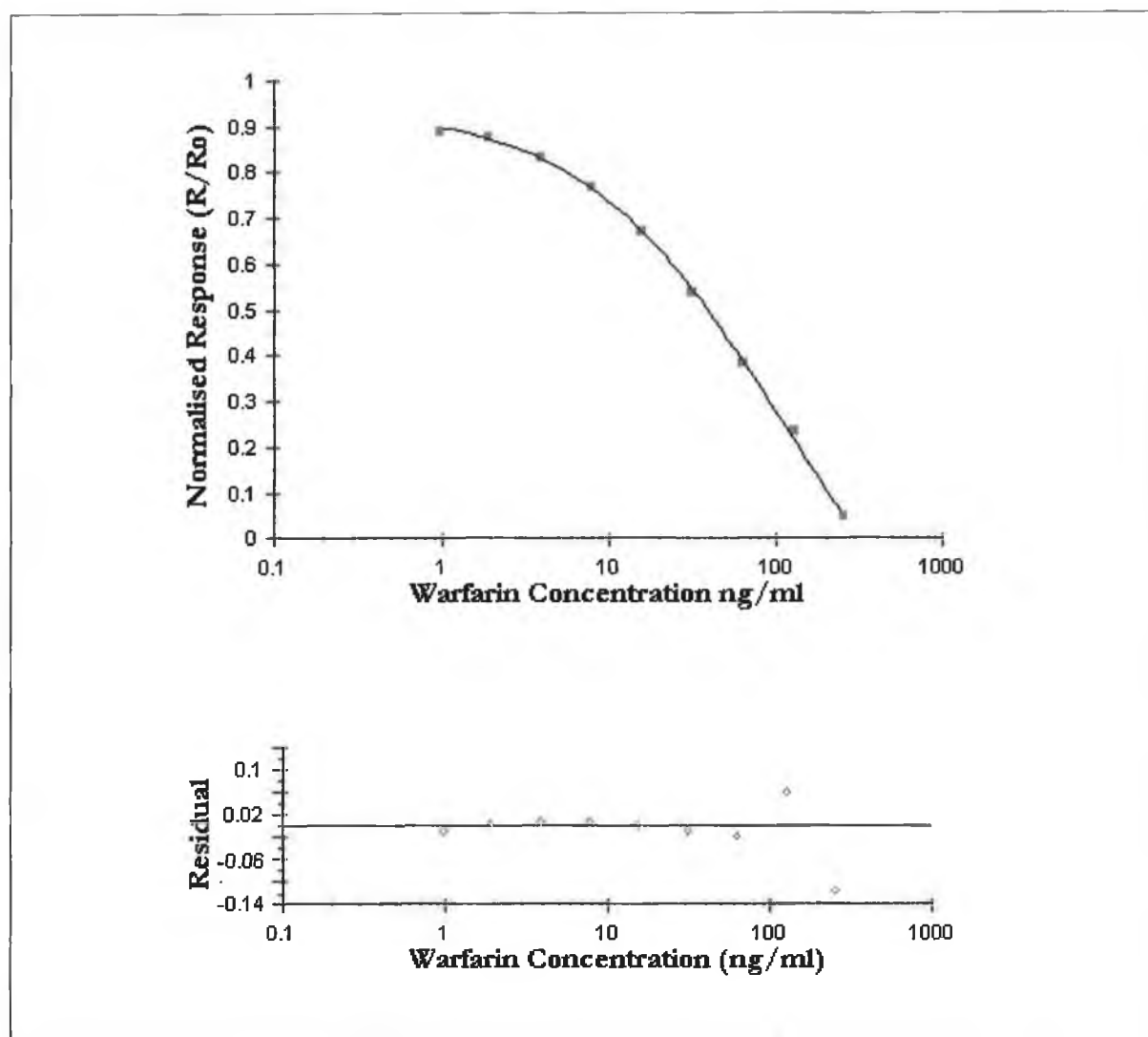
Figure 4.21: Inter-day Assay calibration curve (warfarin-BSA chip) for the detection of warfarin in urine utilising an anti-warfarin mAb. A 4-parameter equation was fitted to the data set using BIAevaluation 3.1 software. The interday means and coefficients of variation are tabulated in Table 4.8. Each point on the curve is the mean of three replicate measurements analysed over three days. Residual plots for the calibration curves are included (for each calibration curve), which illustrate the 'goodness of the fit' of the applied 4-parameter equations and supports the % accuracy findings.

Table 4.9: *Intra-day Assay coefficients of variance (CV's) and percentage accuracies for the anti-warfarin monoclonal antibody used for the detection of warfarin in urine. 4-aminowarfarin was immobilised onto the sensor chip surface. The standard deviation (S.D.) is computed from replicate (3 replicates) analyses within a single validation run.*

Actual Warfarin Concentration (ng/ml)	Mean Back Calculated Warfarin Concentration from calibration curve (ng/ml)	% C.V.	% Accuracies
250.00	214.00	7.17	116.82
125.00	111.00	4.88	112.61
61.20	70.00	0.95	87.43
31.25	33.00	0.41	94.70
15.60	15.63	0.54	99.81
7.80	7.30	0.17	106.85
3.91	4.01	0.35	97.51
1.90	2.10	0.13	90.48
0.97	1.00	0.33	97.00

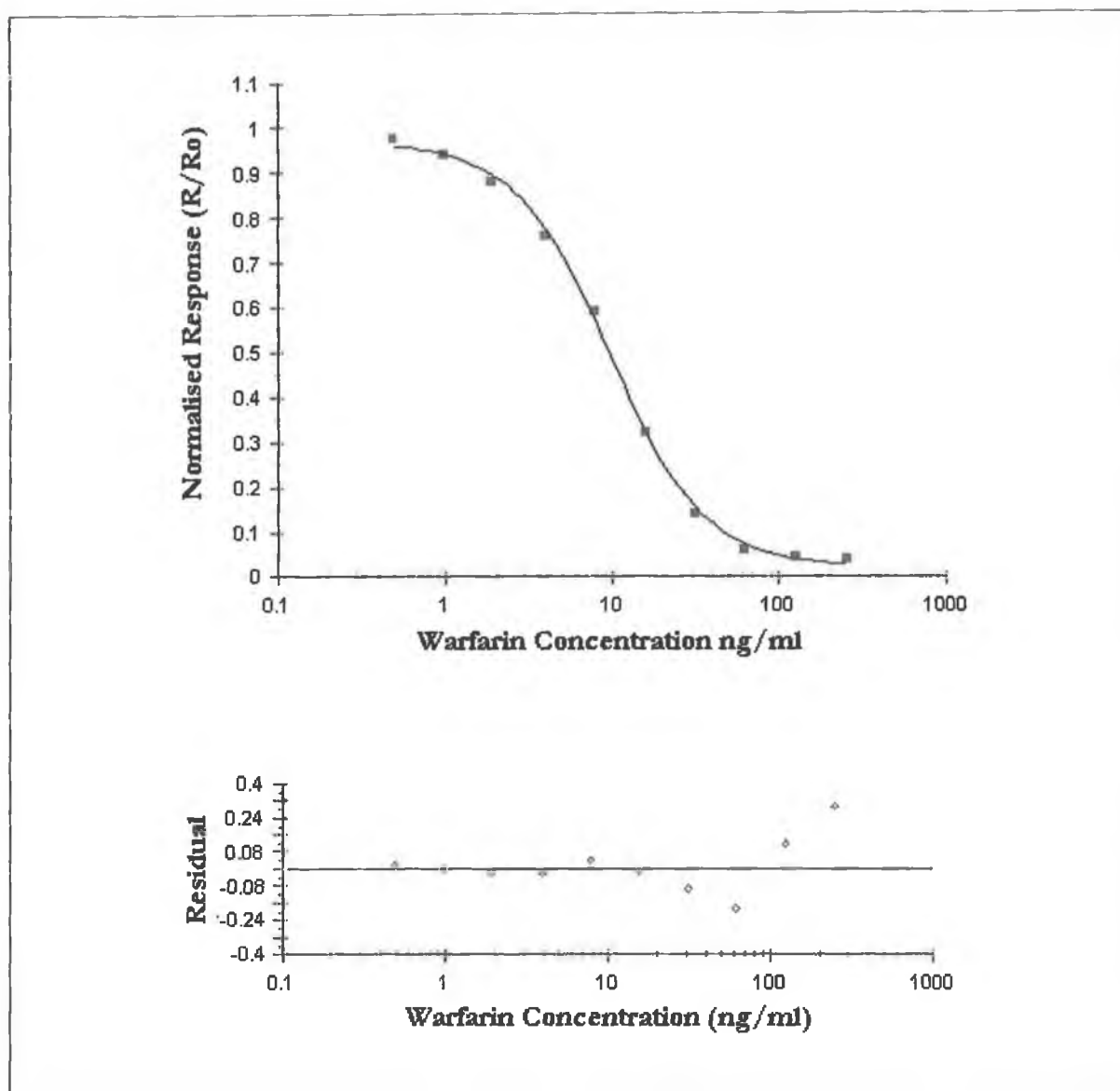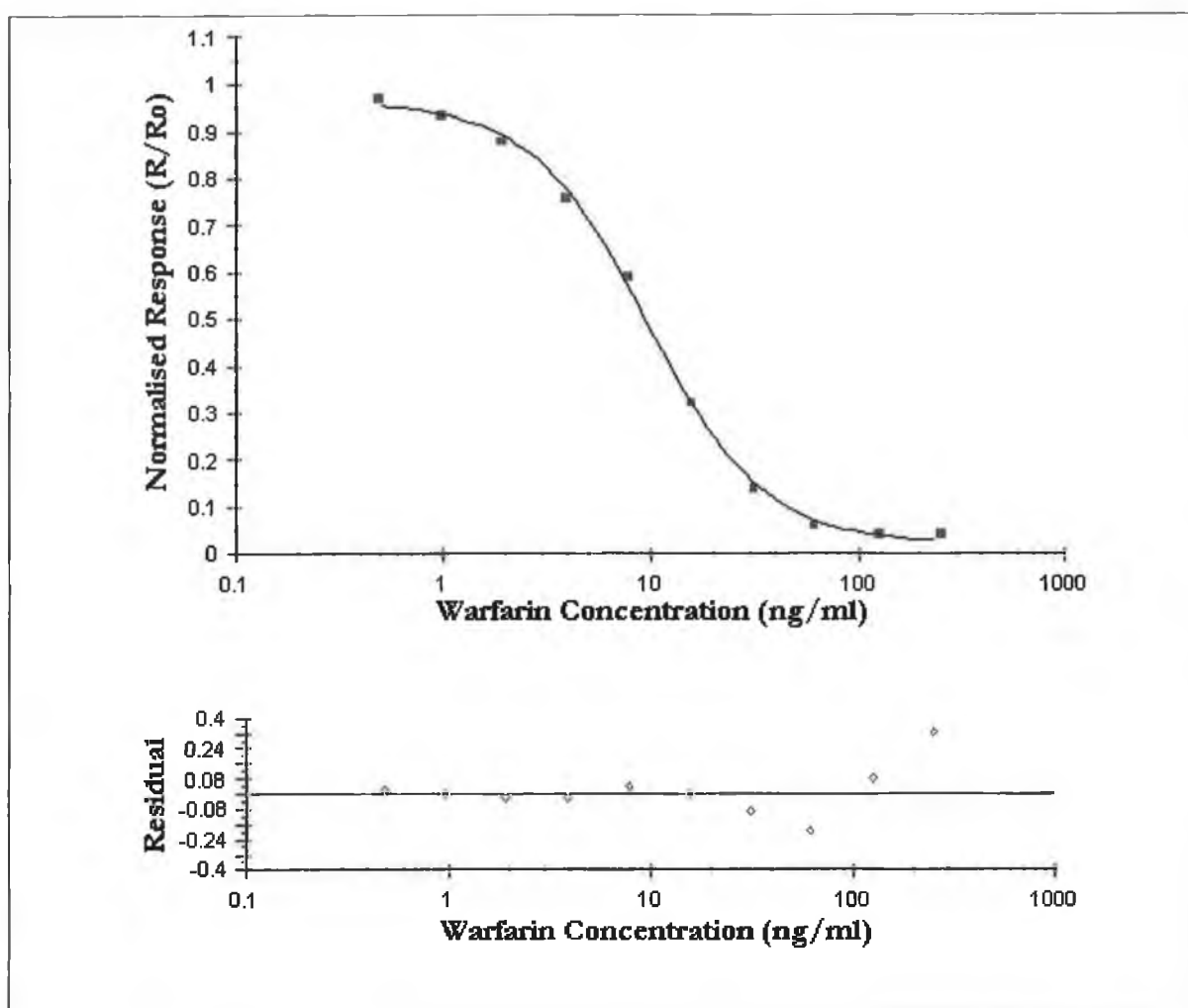***Figure 4.22:*** *Intra-day Assay calibration curve (4'-aminowarfarin chip) for the detection of warfarin in urine utilising an anti-warfarin mAb. A 4-parameter equation was fitted to the data set using BIAevaluation 3.1 software. The intraday means and coefficients of variation are tabulated in Table 4.9. Each point on the curve is the mean of three replicate measurements analysed within a single validation run. Residual plots for the calibration curves are included (for each calibration curve), which illustrate the 'goodness of the fit' of the applied 4-parameter equations and supports the % accuracy findings.*

Table 4.10: Inter-day Assay coefficients of variance (CV's) and percentage accuracies for the anti-warfarin monoclonal antibody used for the detection of warfarin in urine. 4-aminowarfarin was immobilised onto the sensor chip surface. The standard deviation (S.D.) is computed from replicate (3 replicates) analyses over 3 validation runs on 3 separate days.

Actual Warfarin Concentration (ng/ml)	Mean Back Calculated Warfarin Concentration from calibration curve (ng/ml)	% C.V.	% Accuracies
250.00	215.04	8.36	118.46
125.00	105.58	11.80	118.39
61.50	72.98	4.49	84.27
31.25	32.65	2.48	95.71
15.60	15.68	0.65	99.49
7.80	7.53	0.60	103.59
3.91	4.19	0.37	93.27
1.90	2.19	0.16	86.60
0.97	0.96	1.05	101.46
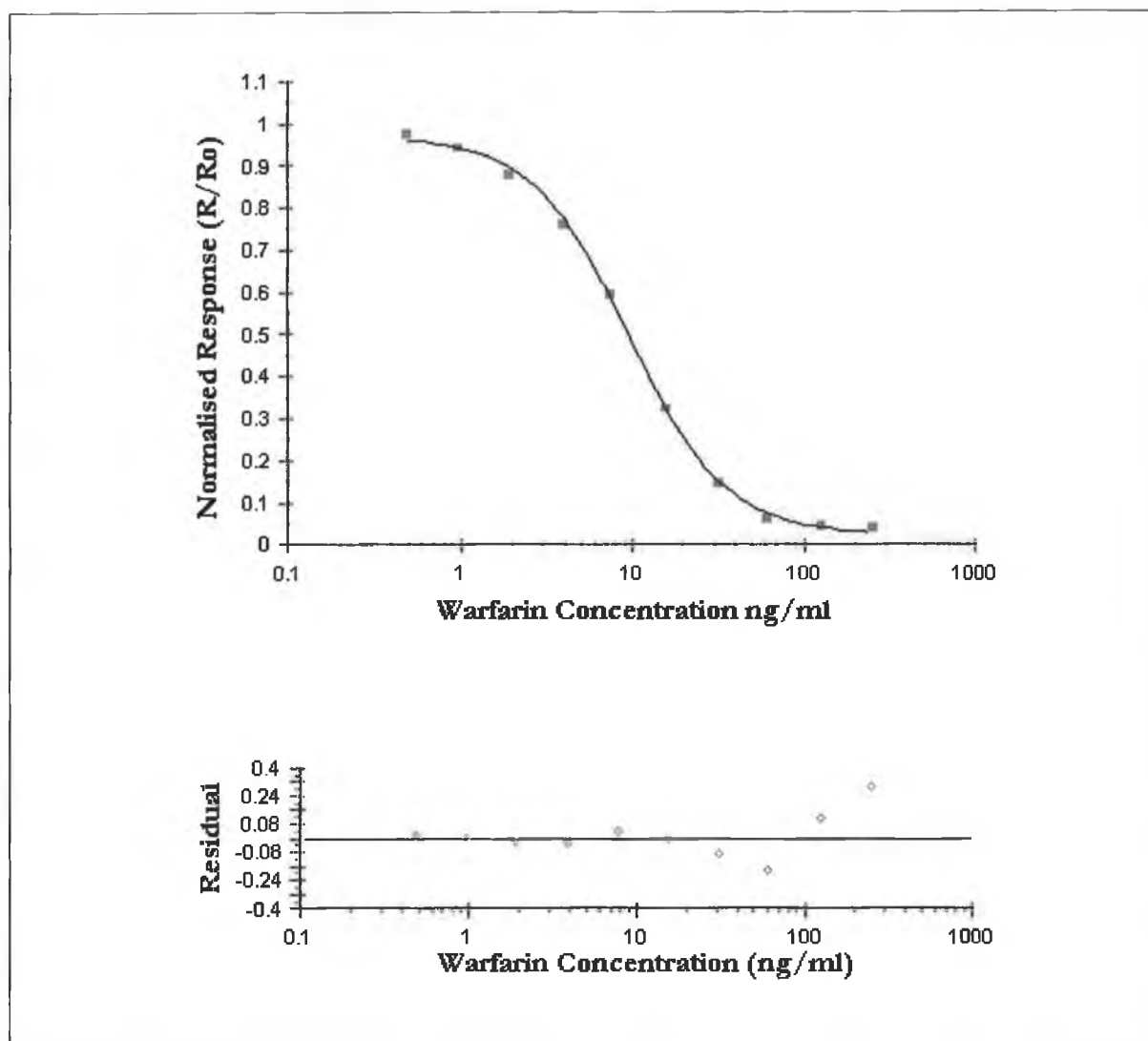
Figure 4.23: *Inter-day Assay calibration curve (4'-aminowarfarin chip) for the detection of warfarin in urine utilising an anti-warfarin mAb. A 4-parameter equation was fitted to the data set using BIAevaluation 3.1. software. The interday means and coefficients of variation are tabulated in Table 4.10. Each point on the curve is the mean of three replicate measurements analysed over three days. Residual plots for the calibration curves are included (for each calibration curve), which illustrate the 'goodness of the fit' of the applied 4-parameter equations and supports the % accuracy findings.*

4.2.3.5. Cross-Reactivity Studies

Cross reactivity studies with the monoclonal antibody 4-2-25 (defined in Section 3.2.4) were assessed utilising BIAcore. The procedure was similar to that performed for the ELISA cross-reactivity studies. Three compounds (acenocoumarin, 6-hydroxywarfarin and 7-hydroxywarfarin) where chosen in order to determine their cross-reactivity with the anti-warfarin monoclonal antibody. In Section 3.2.4 percentage cross-reactivity was assessed for warfarin and several structurally similar compounds utilising ELISA. It was found that 7-hydroxycoumarin, 4-hydroxycoumarin, coumarin and 7-hydroxycoumarin-4-acetic acid displayed negligible cross-reactivity (<0.1%) with the anti-warfarin mAb. Therefore, it was decided to focus the BIAcore cross-reactivity studies on the compounds (acenocoumarin, 6- & 7-hydroxwarfarin), which displayed significant percentage cross-reactivity with the anti-warfarin mAb. Cross-reactivity was assessed by preparing serial dilutions of warfarin or one of the other compounds (Section 2.5.8.6.), using HBS as diluent. Protein-G purified monoclonal antibody was then mixed with the various antigen concentrations using the BIAcore autosampler (incubation time 5-10 mins). The equilibrium mixtures were then injected over the chip surface. The results obtained as explained in Section 2.5.8.6. and Section 3.2.4 were plotted and displayed as a single graph as in Figure 4.24. Formula X in section 3.2.4 was then used to calculate percentage cross reactivity of each compound. From the calculations it was determined as expected that acenocoumarin displayed the highest cross-reactivity with the anti-warfarin monoclonal antibody (~30%). 6-hydroxywarfarin displayed the next highest degree of cross-reactivity at approximately 18% and this was followed by 7-hydroxywarfarin at approximately 10%.

In terms of detecting warfarin in biological samples such as urine it is important to know whether the anti-warfarin monoclonal antibody can detect other metabolites present in biological samples besides warfarin. Warfarin is excreted in urine along with two major metabolites 6- and 7-hydroxywarfarin. From the results it is evident that the anti-warfarin monoclonal antibody will detect warfarin. Although both warfarin metabolites can be detected by the monoclonal antibody they need to be present at higher concentrations than warfarin (which is likely in biological samples where less than 2% of warfarin is excreted as warfarin in urine). Acenocoumarin is also known as nitro-coumarin, which can be used as an anticoagulant to treat patients. Therapeutic plasma concentrations of acenocoumarin tend to be in the range of 30-100ng/ml. The binding of several warfarin derivatives (such as acenocoumarin) to HSA was previously characterized (Petitpas *et al.*, 2001). It is interesting to note that acenocoumarin binds more loosely to HSA than warfarin. Therefore, higher levels of free acenocoumarin are present in plasma and urine in comparison to warfarin. The weaker association of acenocoumarin probably occurs because the addition of an NO_2 group to the benzyl ring sterically

hinders its accommodation in the hydrophobic compartment formed primarily by Phe-211, Trp-214, Leu-219, and Leu-238. It is possible that acenocoumarin if administered to patients at similar doses to warfarin could be detected by the anti-warfarin monoclonal antibody at a higher detection range than warfarin.
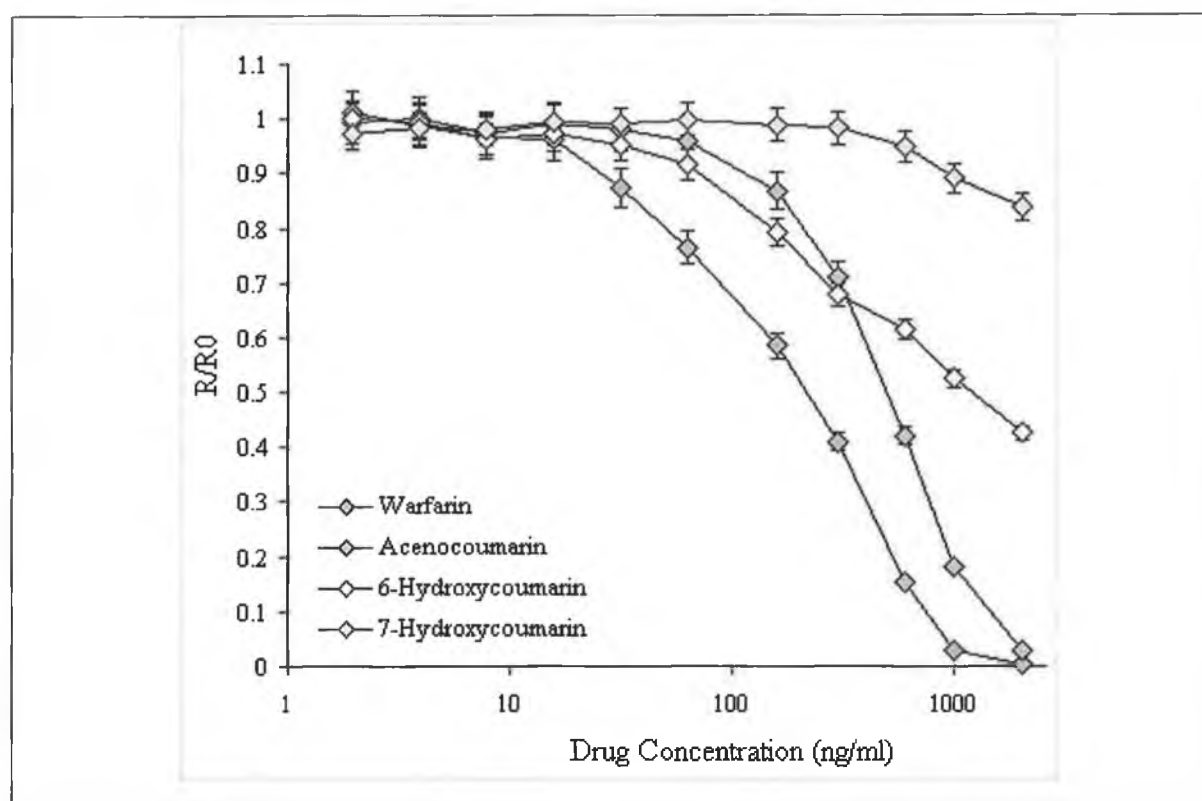
Figure 4.24: Overlay plot showing the cross reactivity of the anti-warfarin monoclonal antibody with several warfarin analogues using the BIAcore 3000 system (Section 2.5.8.6).

4.2.3.6. Solution Phase Steady State Affinity Determinations

BIAcore technology was employed to determine and evaluate the dissociation constants obtained using 'real-time' biomolecular interaction with those determined using a well-based ELISA analysis for the interaction between anti-warfarin monoclonal antibodies and specific target antigens. The protocol employed utilises the same principle as that employed in the ELISA method of Friguet *et al.* (1985), but has several advantages over the ELISA technique. The continual flow of fresh equilibrium mixture over the warfarin-coated sensor chip and the short contact time of the antibody:antigen equilibrium mixture in the flow cell (compared to incubation step in the ELISA) limits the possibility of a re-equilibration of the antibody:antigen mixture, and subsequent

underestimation of the affinity constant. The method requires no additional labelling of the reagents, or the addition of secondary reagents, which may affect the intrinsic thermodynamic binding constants.

A known concentration of anti-warfarin antibodies were serially doubly diluted in HBS buffer and used to construct a calibration curve of free antibody concentration versus response as described in section 2.5.8.7. A known concentration of antibody (M) was then mixed with serial doubling dilutions of warfarin of known concentration and allowed to attain equilibrium. Each equilibrium mixture was then assayed for 'free-unliganded' anti-warfarin antibodies by passing the equilibrated mixtures over a warfarin-coated sensor chip surface. The concentration of free antibody at equilibrium was determined by reference to the standard curve (Figure 4.25.).

The model described below is used to calculate the solution equilibrium dissociation constant:

$$B_{free} = \frac{B - A - K_d}{2} + \sqrt{\frac{(A+B+K_d)^2}{4} - A\,B} \qquad (12)$$

Where B_{free} is the free concentration of anti-warfarin IgG.

A is the total concentration of warfarin

B is the total anti-warfarin IgG concentration

K_d is the equilibrium dissociation constant.

The equilibrium dissociation constant can be calculated by constructing a plot of free anti-warfarin antibodies versus warfarin concentration as shown in Figure 4.25. Equation (12) describing the model for solution phase affinity assumes that the antibodies are monovalently bound. The assay format utilised is capable of detecting free and monovalently bound antibody, and a correction similar to that applied to the ELISA measurements may be applied, so that the concentration of free antibody in the equilibrated antibody:antigen mixture is not overestimated giving an underestimated affinity constant. Piehler *et al.* (1997) amended the solution phase model based on the binomial distribution principle described by Stevens (1987), and expressed the 'corrected' concentration of free antibody with at least one antibody binding site free by the expression:

$$B_{free} = \frac{B}{2} - \frac{\left[\frac{B + A + K_d}{2} - \sqrt{\frac{(A+B+K_d)^2}{4} - AB} \right]^2}{2B} \qquad (13)$$

The symbols have the same meaning as described for equation (12).

214

The model described in equation (13) assumes that the sensor responses for free and monovalently occupied antibody are similar. The assumption that the sensor responses measured would be similar for free and monovalently liganded antibodies particularly with larger target antigens is obviously incorrect, however with small molecules such as warfarin, the response measured for monovalently bound antibodies and free antibodies would be similar, given the small molecular weight of warfarin compared to an intact IgG molecule. The monovalent fit (Figure 4.26) appears to describe the interaction better between the antibody and the conjugate-immobilised drug surface (K_D=1.13 x 10^{-8} M). The data does not fit the bivalent model particularly well as seen in Figure 4.27, and the monovalent fit appears to describe the interaction better between the monoclonal antibody and the conjugate-immobilised drug surface.

Utilising BIAcore, affinity determinations were made by employing an immobilised monovalent ligand (warfarin-BSA) with a bivalent analyte (anti-warfarin monoclonal antibody) in solution, with the potential, of bivalent analyte binding. However, given the low epitope density and possible steric hindrance factors at the chip surface the probability of an antibody being bound to two immobilised conjugate-warfarin molecules simultaneously would be regarded as low. It is impossible to predict what conformation the protein (BSA)-bound warfarin molecules would assume when immobilised, given the inhomogenetity of the immobilised surface ligand (warfarin-BSA).
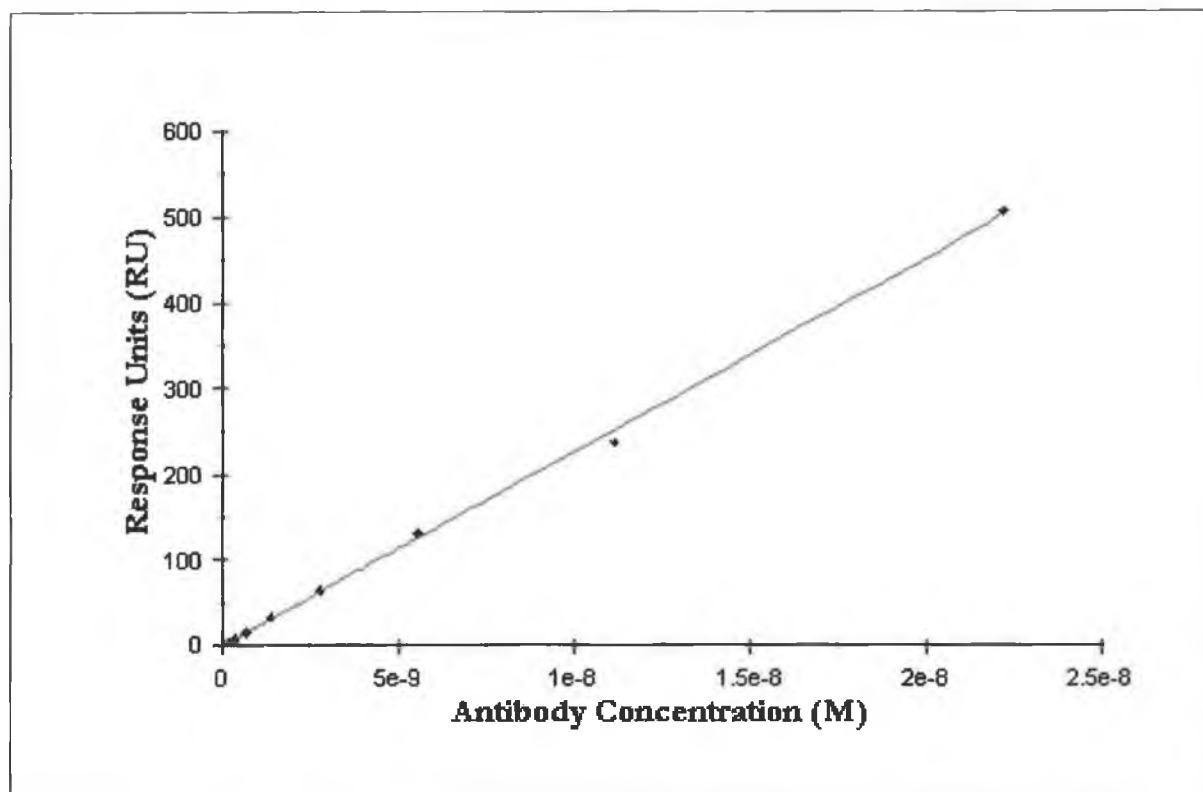
Figure 4.25: *Serial doubling dilutions of anti-warfarin antibodies of known concentration (M) were passed sequentially over a warfarin-coated (i.e. warfarin-BSA or 4'-aminowarfarin) sensor chip surface. A calibration plot was constructed of anti-warfarin antibodies (M) versus response measured (RU). The calibration plot was then used to calculate the concentration of free antibody at equilibrium. Results shown are the average of triplicate measurements.*
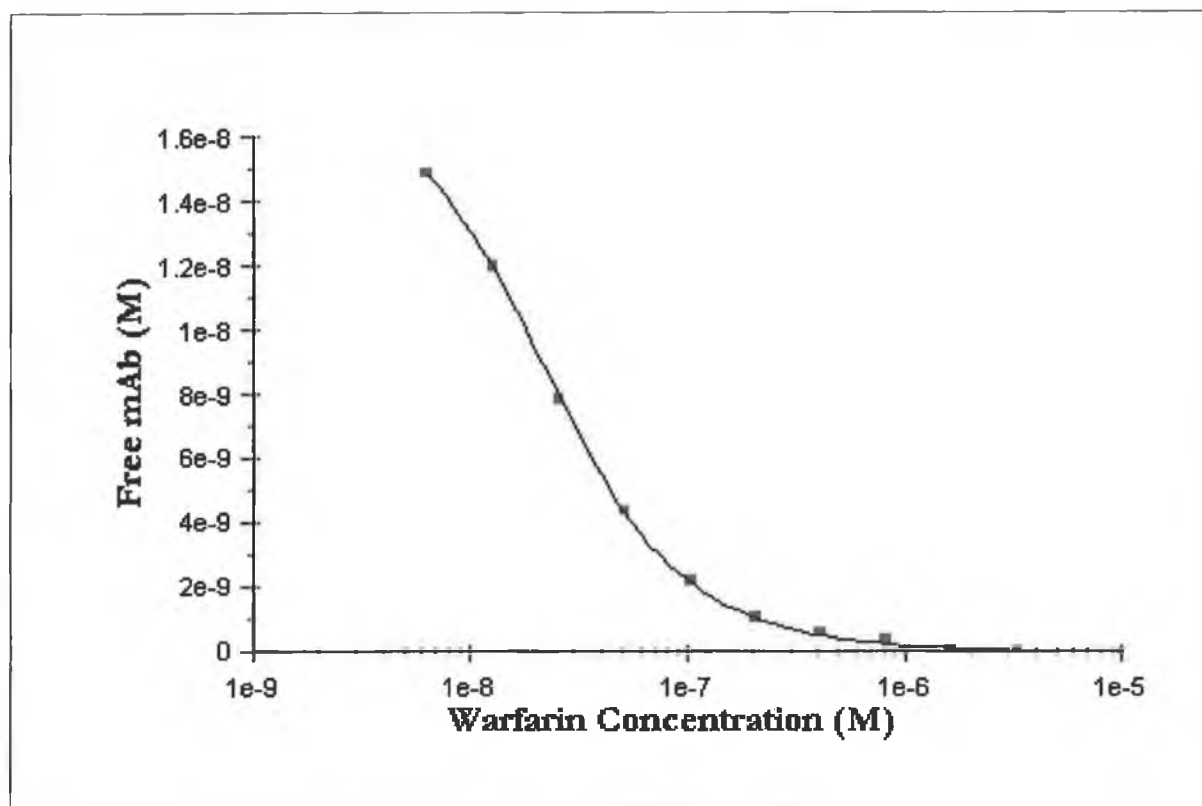
Figure 4.26: Determination of overall solution equilibrium affinity constant between mAb 4-2-25 and warfarin on a warfarin-BSA-coated chip surface. Warfarin concentrations were plotted against free anti-warfarin antibody concentration, determined by reference to a calibration plot of anti-warfarin antibodies. A 1:1 interaction model was used to describe the interaction (equation 12) and fitted to the data set using BIAevaluation software, deriving an equilibrium dissociation constant of K_D=1.13 x 10^{-8} M, for the interaction between clone 4-2-25 and warfarin.
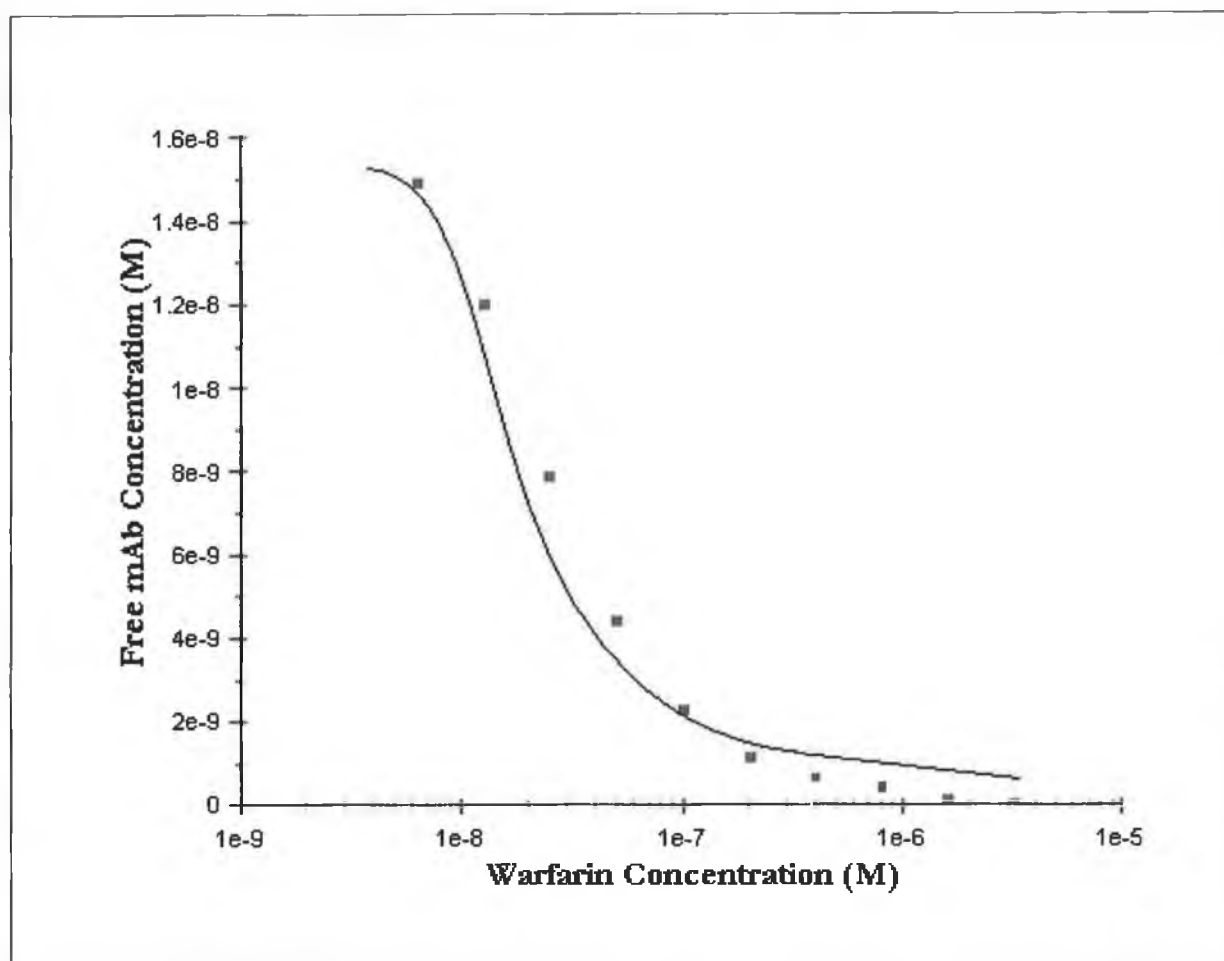
Figure 4.27: Solution phase affinity for warfarin and mAb 4-2-25 on warfarin-BSA -coated chip surface. The model describing bivalent binding was applied to the data set, giving an overall, equilibrium constant of $K_D = 4.51 \times 10^{-9}$ M. The bivalent model described in equation (13) fitted to the data using BIAevaluation software, does not describe the interaction particularly well as seen from the plot.

4.2.3.7. Steady-State Affinity Determinations

Warfarin-BSA was immobilised at an adequately low surface concentration in order to provide a maximum response of approximately 200 RU on the sensor chip surface using conventional coupling chemistry. Direct immobilisation of 4'-aminowarfarin at a sufficiently low ligand density on the chip surface was difficult to manage, and consequently the warfarin-BSA conjugate was immobilised. A second flow cell was used to immobilise BSA at a similar surface concentration as the conjugate. Fortunately BIAcore 3000 is capable of on-line reference curve subtraction, thereby removing matrix effects, and baseline jumps due to sample injection and refractive index changes.

Preferably, it would be ideal to immobilise the antibody to the chip surface by affinity capture using Protein A/G. However, direct immobilisation of the antibody would remove the complexity arising from a bivalent analyte binding to the drug surface, and possible avidity effects at the chip surface resulting in elevated affinity constant determinations. Previous work by Fitzpatrick (2001) demonstrated that the surface concentration of antibody required to achieve a quantifiable response signal following binding of warfarin to the affinity captured antibody proved to be a limiting factor and consequently the use of drug-protein conjugates was preferable. For example, affinity capture of 10,000RU of anti-warfarin antibody via protein G, (which is difficult to accomplish in practice) results in a maximal saturation response of 41RU even when taking antibody bivalency into account given the ratio of the molecular weights of the antibody (~150,000Da), and warfarin (308Da). Given the large concentration of antibody needed to generate such a quantifiable signal, it is very time consuming to attain equilibrium and saturation of the surface

The steady state affinity for a surface interaction can be described by the expression:

$$Req = \frac{Ka.(C_A)i.R\max}{Ka.n.(C_A)i + 1} \qquad (14)$$

Where n = Steric hindrance factor and represents the average number of ligand sites occupied per analyte molecule.

  Req = Response at equilibrium

  $(C_A)i$ = Injected concentration of analyte (M)

  Rmax = Maximal response

Ka = Equilibrium association constant

The value for steric hindrance factor, n, can be determined experimentally by calculating the fraction of the response measured versus the theoretical maximal response attainable given a specific immobilised ligand surface concentration. The value of n, could therefore not be calculated using drug protein conjugates and was set to 1, for the purposes of modelling experiments.

Serial dilutions of anti-warfarin antibody of known concentration were simultaneously injected over warfarin-BSA and BSA-coated surfaces at a flow rate of 2 μl/min for 40 minutes, using 'on-line' reference curve subtraction as illustrated in Figures 4.28 and 4.29. A plot of the equilibrium response (Req) measured versus the injected antibody concentration was constructed (Figure 4.30). The steady state affinity model detailed in equation (14) was fitted to the plot deriving an association

constant (K_A) value of $1.10 \times 10^7 \pm 0.21 \times 10^8$ M^{-1} for the steady-state interaction between clone 4-2-25 and warfarin.

    The steady-state affinity model derives an association constant higher than that obtained for the solution phase constant using immobilised drug conjugates, but less than that obtained with directly immobilised drug surface. The solution phase affinity constant is expected to defer a slightly higher value for the association constant, provided that both interacting molecules (i.e. antibody and antigen) are free in solution. The possibility of bivalent analyte binding to the chip surface also exists which is similar to the solution phase assay. However, since a low surface ligand concentration of warfarin-BSA is employed, the probability of a monovalently bound antibody bound to the conjugate surface, encountering a second free ligand site would be particularly small, given also the saturating concentrations of antibody employed. In this situation, the restrictions enforced by the small molecular weight of the analyte and the use of the warfarin-BSA surface allows for approximations of overall association constants, provided that values for the steric hindrance factor, n, were impossible to calculate given the inconsistency of the conjugate on the surface.
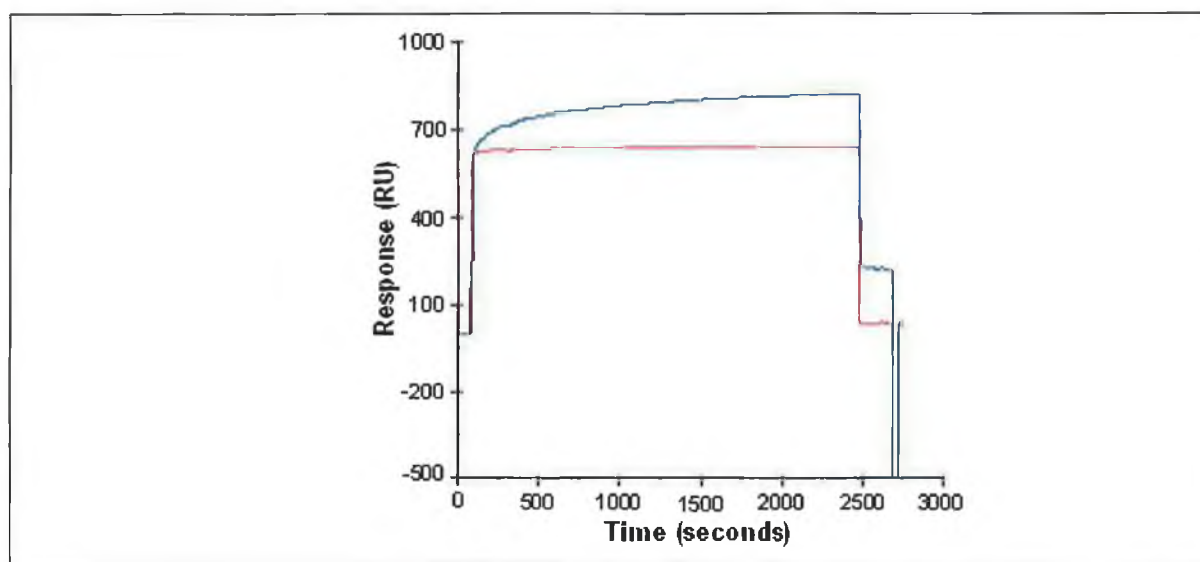
Figure 4.28: Warfarin-BSA (——) and BSA (——) were immobilised onto two flow (Fc) cells of a sensor chip surface, namely Fc2 and Fc1, respectively. 80nM of affinity-purified anti-warfarin antibodies were injected over the two sensor chip surfaces and monitored simultaneously using 'on-line' reference curve subtraction (i.e. Fc2-Fc1).
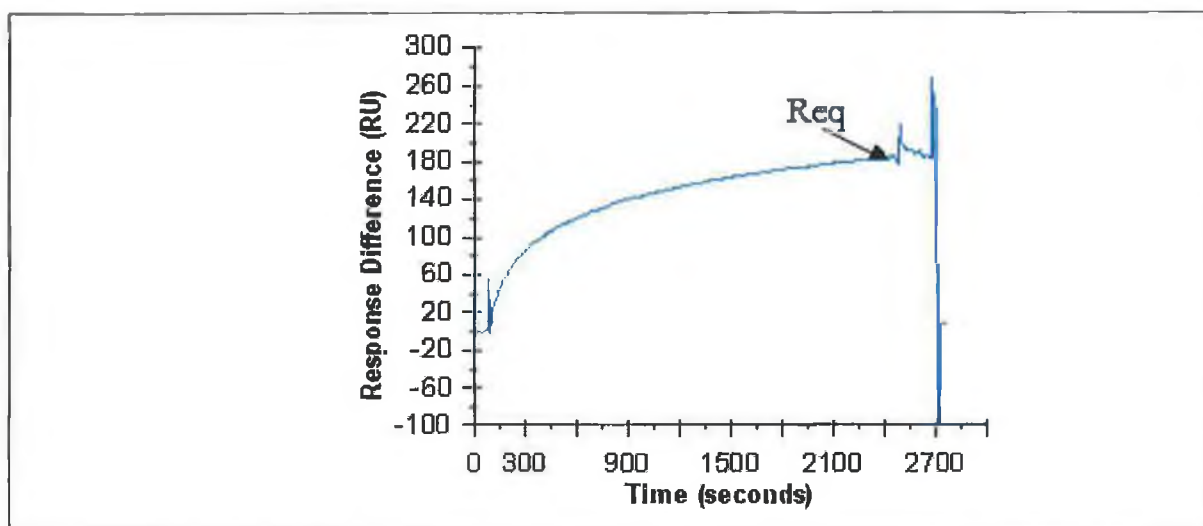
Figure 4.29: *Serial dilutions of anti-warfarin antibody of known concentration were simultaneously injected over warfarin-BSA and BSA coated surfaces at a flow rate of 2 μl/min for 40 minutes, using 'on-line' reference curve subtraction. The interaction curve from Figure 4.26, following 'on-line' reference curve subtraction, is shown. The equilibrium binding response was measured at a variety of injected antibody concentration and used to plot a curve of the binding response at equilibrium (Req) versus injected antibody concentration (Figure 4.28).*
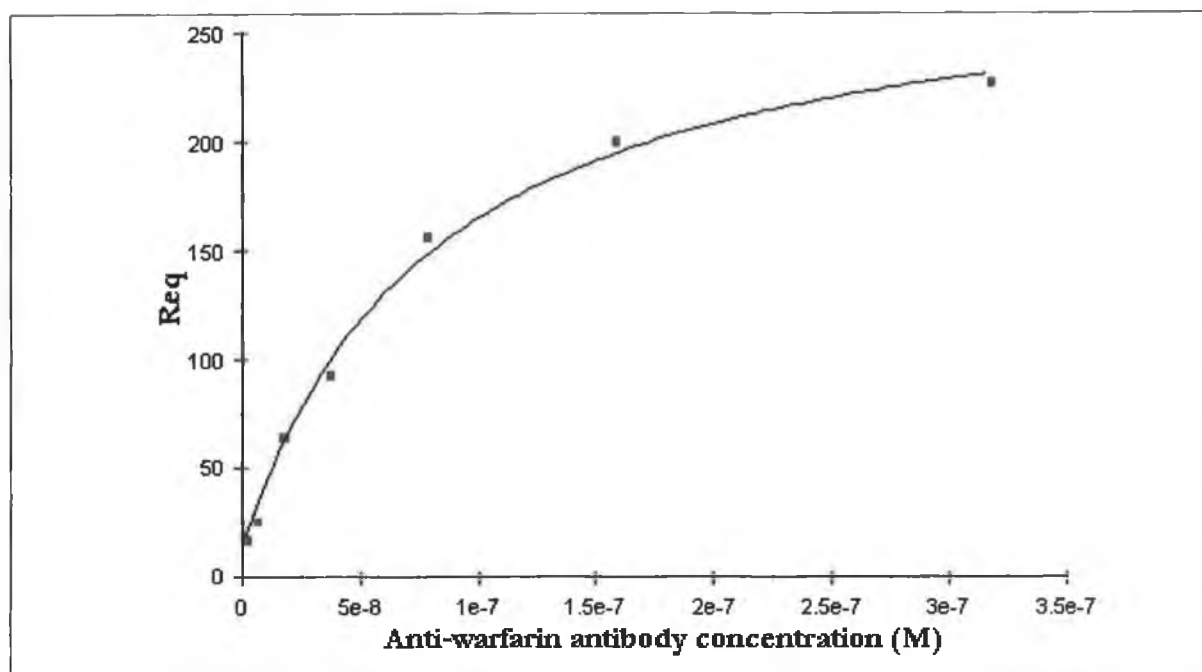
Figure 4.30: *The value obtained for Req was plotted against the molar concentration of antibody injected. The steady state model was fitted to the data, and assuming a value of n=1, the value for the association constant, K_A, for the interaction between warfarin and affinity-purified antibodies from clone 4-2-25 was determined using BIAevaluation software to be $1.10 \times 10^7 \pm 0.21 \times 10^8\ M^{-1}$.*

4.3. Conclusions

The results presented in this chapter describe the development and validation of an inhibition-based immunoassay for the detection of warfarin in biological samples. Both directly immobilised drug (4'-aminowarfarin) surfaces and the use of a drug-protein conjugate (warfarin-BSA) were utilised for ligand-binding capacity comparisons. In this instance it was demonstrated, that the directly immobilised drug surface offered considerably better binding reproducibility (% C.V. ~ 0.8%) over the binding-regeneration cycles studied (i.e. 80 cycles), which is primarily related to the exceptional stability of the immobilised drug molecule (4'-aminowarfarin) on the dextran surface. The use of hapten-protein conjugates offers an alternative when suitable reactive groups are not available for direct immobilisation of the drug. However, the use of hapten-protein conjugates can prove difficult particularly when trying to dissociate high affinity antibody:antigen interactions, where the use of adequately harsh regeneration solutions to regenerate the sensor surface, too often results in denaturation of the immobilised ligand. Similarly, immobilisation of sufficiently high yields of conjugate for routine sample analysis can sometimes prove difficult using EDC/NHS chemistry, as

222

many hapten-protein conjugates are characterised by very acidic isoelectric points. Inhibition assays (in PBS or urine) generated calibration plots for both chip surfaces in order to determine the assay precision and reproducibility. The coefficients of variation for all the assays developed were well within the current recommended validation guidelines for immunoassay procedures.

Using BIAcore analysis affinity determinations were made using the warfarin-BSA conjugate surface. The dissociation plot fitted to the data generated on drug-protein conjugate surfaces appeared to conform to the fit of monovalent binding. The reality is that the dissociation fit lies somewhere between the modelled mono- and bivalent fit. The likelihood of an antibody being bound to two immobilised protein-bound warfarin molecules simultaneously would be small as a result of the lower epitope concentration and possible steric hindrance factors at the chip surface, giving slightly lower association constants. The lower dissociation constant values generally obtained using solution phase assays compared to steady state analysis, agrees with what one might have predicted. For solution phase assays, both interacting molecules (i.e. antibody and antigen) are free in solution and hence have an increased collision frequency, thus affecting the kinetic rate constants and the measured affinity constants, unlike steady state analysis where one of the interactants is immobilised. Ultimately, the method (solution phase/steady state analysis) of measuring antibody affinity should resemble the environment for their intended use (i.e. steady state analysis should be used for measuring antibody affinity to surface bound molecules and solution phase assays for situations where the antibody might encounter the antigen in solution).

It is evident from Section 4.3.2.4. that anti-warfarin monoclonal antibodies can successfully detect warfarin in urine samples. In reality, most patients begin warfarin therapy by taking 5 mg per day. However, only less than 2% of the administered dose is excreted as warfarin (Kratochwil *et al.,* 2002). Therefore, in a regular setting anti-warfarin polyclonal antibodies are ideal as they have a broader range and cross-react with 6- and 7-hydroxywarfarin (warfarin metabolites). Warfarin dosing varies over time with some patients requiring lower or discontinued warfarin dosing. Monitoring warfarin levels at these times is very important to reduce the risk of thrombosis in patients. Both elderly patients and those with other medical complications (heart valves) require much lower doses than is regularly given (e.g. 0.5mg per day or lower) to patients. If surgery is required it may be recommended to discontinue warfarin therapy to prevent the risk of uncontrolled bleeding, however the patient is at risk from thrombosis prior to surgery. In this case, levels of warfarin in urine decrease to very low levels but can be monitored using anti-warfarin monoclonal antibodies, which have lower detection limits than anti-warfarin polyclonal antibodies (e.g. 0.9 ng/ml versus 10ng/ml). If a patient requires medication for other medical conditions this can affect the levels of warfarin in blood plasma

223

and in urine (Table 1.6.). When levels decrease below the detection range possible with polyclonal antibodies it is better to utilise anti-warfarin monoclonal antibodies with lower detection limits.

The use of biosensors for monitoring 'real-time' interactions is proving to be a viable and useful alternative to currently existing techniques for drug detection and drug-biomolecule interaction studies. The advantages of using biosensors such as BIAcore include speed, versatility and amenability to automation. The detection and separation of enantiomers is a problem routinely encountered in pharmaceutical drug discovery and chemical synthesis. A host of different analytical techniques either alone (HPLC) or in conjunction (LC-MS) are employed to address the issue of drug detection. HPLC in combination with UV spectroscopy, mass spectrometry (MS) or fluorescence spectroscopy were utilised for the detection of various drug compounds and metabolites in human urine and plasma (Takahashi *et al.*, 1997; Maurer & Arlt, 1998; Desta *et al.*, 2000; Naidong *et al.*, 2001). However, the development of the majority of chromatographic assays requires individual manipulation of mobile phases, extraction schemes and detection techniques for the detection of particular drug molecules. Hence, in comparison to BIAcore assays these techniques can be laborious and time consuming. Previous work by Fitzpatrick (2001) demonstrated excellent correlation between the BIAcore inhibition assay and a HPLC technique for the detection of warfarin in human plasma. The limits of detection (Table 4.2) attainable with the developed inhibition immunoassay were more than an order of magnitude below those attainable using HPLC with UV detection (i.e. L.O.D. inhibition immunoassay = < 0.3 ng/ml, HPLC with UV-detection ≈ 6ng/ml). The assay performance as measured by the conventional measures of analytical performance, namely precision, accuracy, reproducibility and robustness demonstrated that the assay performed comparably in every respect to the conventional chromatographic techniques. Several other studies involving HPLC analysis of warfarin also showed higher limits of detection, which ranged from 20-40 ng/ml down to 2.5-4.5 ng/ml (Takahashi *et al.*, 1997; Boppana *et al.*, 2002). Gas chromatography-mass spectrometry was utilised by Maurer and Arlt (1998) for the detection of warfarin in urine with a limit of detection at 25 ng/ml. The results presented in Section 4.2.3.4 demonstrate that the limit of detection (0.9 ng/ml) attainable with the inhibition immunoassay developed was lower than those obtained by conventional chromatographic methods (approx. 5 ng/ml).

The use of this inhibition BIAcore assay is amenable to the detection of a wide range of analytes in various matrices, as relatively facile manipulation of the experimental parameters (i.e. immobilised ligand, regeneration parameters and choice of antibody) can be achieved to tailor the assay for the detection of different analytes. Recent advances in genetic engineering with the development of phage-displayed libraries and various in-vitro affinity maturation techniques, has

realised the potential of generating antibodies of extremely high affinities (Brennan *et al.*, 2003) to almost any molecule. Allied with the sensitivity of current SPR devices, the ability to accurately quantitate sub-picogram quantities of analytes for detailed pharmacokinetic / environmental studies is now a reality.

Chapter 5

The Effects of Benzopyrones on the Growth, Metabolism and Signalling Pathways of Human Tumour Cells

5.1. Introduction to Chemosensitivity Testing

Cancer chemotherapy has witnessed a great deal of progress since the introduction of the nitrogen mustards in the 1940s. Unfortunately, chemotherapy today still faces the problem of determining which specific agent or agents are able to yield the desired clinical therapeutical effect for a particular tumour and patient. Attempts to individualise therapy have been the goal of oncologists since the 1950s. However, progress is delayed by the fact that cure rates are constrained not only by the limited range of agents currently available and their adverse side effects, but also by variations in individual responses (Clynes *et al.*, 2003). Since the 1950s a number of *in vitro* assays have been developed to predict therapeutic outcome (chemosensitivity and chemoresistance) prior to the start of therapy. These tests are also used for screening potential novel drugs. Three groups of tests can be defined:

a)   Cell viability tests e.g. the lactate dehydrogenase (LDH) assay.

b)   Cellular metabolism tests e.g. the tetrazolium salt (MTT) assay.

c)   Cellular proliferation tests e.g. *in vitro* proliferation assays.

Test time, tissue preparation, complexity of test performance, and correlation with the clinical progress of the disease are criteria used to judge how successful these tests are (Mestres-Ventura, 2003). As outlined in Section 1.6.3, current cancer therapies, even combination therapies, offer limited success for cancer patients. Therefore, the harsh reality for scientists and clinicians alike is that new drugs with novel mechanisms of action and better treatment strategies are still required for the progression in the successful treatment of cancer. Hence, a vast program of screening for compounds (both natural and synthetic) was instigated by government and private institutions worldwide (Cardenas *et al.*, 1998; Kong *et al.*, 2001; Zhu, 2003). Drug resistance can occur at the onset of the disease or can be acquired after previous chemotherapy. It was determined that chemosensitivity testing invariably shows a predictive accuracy of over 90% to identify drugs that will not work (chemoresistance).

5.1.1. Current Chemosensitivity Tests

To select the most appropriate anti-cancer drugs and their optimal doses, various chemosensitivity tests are now available. In examining the sensitivity of tumour cells (both biopsy and cultured cell samples) to compounds, one can examine the effect of the compound on one of a number of cellular mechanisms *e.g.* cellular proliferation, cellular metabolism and cell viability (Table 5.1). In

recent years colorimetric assays based on an enzymatic reaction such as the MTT assay, were used in an attempt to replace the conventional isotopic assay for cell-mediated cytotoxicity. In conventional chromium (^{51}Cr) release cytotoxicity assay there are problems with environmental pollution and poor labelling of some tumour cells. For these reasons, a variety of non-radioactive assays were developed as alternatives. These include flow cytometric analysis, time-resolved fluorometric assay, MTT colorimetric assay, the LDH assay and the AP assay. Among the colorimetric assays, the MTT assay is the most widely used (Niu, 2001). In order to better understand the most recent advances in chemosensitivity testing in cancer, a concise review of recent research follows.

The possibility of using the MTT assay as a substitute for the human tumour clonogenic assay (HTCA) was assessed in 5 human lung cancer cell lines. The results indicate that the MTT assay may be more convenient and less time-consuming in evaluating the effects of anticancer agents (Kawada *et al.*, 2002). This assay format has had further recent applications. Various malignant brain tumour cell lines were examined for their sensitivity to cisplatin, doxorubicin, etoposide and the antimitotic agents vincristine and paclitaxel by MTT-cytotoxicity assays. The tumour suppressor p33ING1 has growth-inhibitory and pro-apoptotic effects recruiting p53 and it plays a role in DNA repair. p33ING1 mRNA expression was determined by reverse transcriptase- polymerase chain reaction (RT-PCR) and these mRNA levels may be used to predict the chemosensitivity of brain tumour cells to vincristine (Tallen *et al.*, 2003). Another study was designed to determine whether this assay correlates with the clinical response. The effect of several compounds (cisplatin (CDDP), 5-fluorouracil (5-FU), mitomycin C, and adriamycin) on fresh human esophageal squamous cell carcinoma proliferation was investigated. The results suggest that the MTT assay may be useful in evaluating the optimum adjuvant chemotherapy for patients with regional lymph node positive (pN1) esophageal squamous cell carcinoma (Nakamori *et al.*, 2003).

Table 5.1: *Summary of the current chemosensitivity tests available. These tests can be utilised for screening novel chemotherapeutic agents, for determining mechanisms of action of current and new drugs and for testing drug combinations with other chemotherapy drugs or radiation therapy.*

Assay	Reference	Assay Description
CELLULAR PROLIFERATION		
In Vitro Proliferation	Lickiss *et al.* (1974) Brady *et al.* (2002)	Measures the total number of cells
BrdU Incorporation	Gratzner, (1982) Huong *et al.* (1991) Hawker Jr, (2003)	Amount of BrdU incorporated into viable cells is quantitated colorimeterical
Kenacid Blue	Clothier, (1985) Kowalska-Pylka *et al.* (2001)	Measures total cell protein
Clonogenic Assays	Hamburger & Salmon, (1977) Kawada *et al.* (2002)	Measures colony formation capability of cells
Xenografts	Tveit, (1983) Zembutsu *et al*, (2002)	Measures the change in size of human tumour cells transplanted into immuno-compromised mice
CELLULAR METABOLISM		
MTT Assay	Hansen *et al.* (1989) Chua *et al.* (2000)	Measures rate of reduction of tetrazolium salt (MTT) by mitochondrial dehydrogenases in metabolically active cells.
ATP Assay	Kangas *et al.* (1984) Kurbacher *et al.* (2003)	Measures intracellular ATP levels in cells (leaves decrease as cells die)
CELLULAR VIABILITY		
Dye Exclusion Assay	Weisenthal & Kern, (1991) Hartmann *et al.* (2003)	Measures ability of viable cells to exclude stains
Fluorescent Assay	Meitner, (1988) Ivasenko & Shlyakhto, (2001)	Measures ability of viable cells to retain fluorescein.
LDH Assay	Welder & Acosta, (1994) Putnam *et al.* (2002)	Measures release of intracellular enzyme (LDH) as a result of membrane damage

Currently, the ATP-based tumour chemosensitivity assay (ATP-TCA) can be regarded as the most sophisticated assay to investigate both solid samples and effusions derived from patients with various organ tumours. During the last 5 years, this assay has successfully revealed novel drug combinations for further clinical use in both ovarian and breast cancer such as mitoxantrone plus paclitaxel (NT) and treosulfan plus gemcitabine (TG), respectively (Sharma *et al.*, 2003). In a recent phase II clinical trial performed in 59 patients with relapsed ovarian carcinoma, ATP-TCA-directed therapy was able to triple the response rate and to double the survival time, compared with published empirical chemotherapy regimes. Preliminary results with ATP-TCA-directed therapy in breast cancer also provided promising response rates. A phase III trial that is now actively recruiting patients with platinum-refractory ovarian cancer to verify the promising phase II studies may prove the further value of the ATP-TCA as a predictor applicable in routine clinical oncology (Kurbacher *et al.*, 2003).

Collagen gel droplet embedded culture-drug sensitivity test (CD-DST) is a newly developed *in vitro* chemosensitivity test that has several advantages over the conventional tests. The clinical usefulness of this test in the prediction of response to chemotherapy in breast cancer patients was examined by Takamura and colleagues (2002). Their findings demonstrate that CD-DST can predict the response to CE (cyclophosphamide and epirubicin combination) and DOC (docetaxel) therapy with a high accuracy in breast cancer patients and seems to be superior to the conventional predictors. This chemosensitivity test has also been employed to determine the optimal chemotherapy regimens for patients with non-small cell lung cancer (NSCLC). An important advantage of this assay system is that it requires fewer cancer cells than conventional chemosensitivity tests and can be also used to assess cases of malignant effusion. The results suggest that the CD-DST is an effective method for chemosensitivity testing in unresectable NSCLC (Kawamura *et al.*, 2002).

5.2. Drug Discovery

Discovering and developing new treatments for cancer is a lengthy and expensive process. Hence, therapeutics utilising the latest knowledge and the best technology are absolutely essential for the development of new and improved treatments for cancer patients. The total length of time from initial discovery to FDA approval averages around 15 years and only one in 5,000 compounds or fewer make it to FDA approval. However, only through this meticulously thorough process (outlined in Table 5.2) of drug discovery and development do the many cancer drugs (e.g. trastuzumab) coming out every year reach the patients whose survival is improved by them.

Table 5.2: *Overview of the amount of research and time that must be undertaken over the period from initial drug discovery to FDA approval of the drug.*

Research Stage	Average Time Taken	Procedures
Identification and Preclinical Testing	4.4 Years	• 5000 compounds screened to identify 250 for preclinical testing • Laboratory/preclinical testing conducted to assess safety & biological activity in the laboratory and in animal models • Investigational New Drug (IND) application filed with Food & Drug Administration (FDA)
Clinical Trials	8.6 Years	• 5 of the 250 compounds advance to clinical testing • Phase I – Determines safe dosage and how treatment should be given • Phase II – Evaluates effectiveness and looks for side effects • Phase III – Determines whether the new treatment or new use of a treatment is a better alternative to the current standard
Post Clinical Trials	1.4 Years	• New drug application or Biologics Licence Application filed with FDA • FDA approval for one new drug

5.2.1. In Vitro Testing

Human risk assessment of new pharmaceuticals, pesticides, food additives, cosmetics and other chemicals requires the submission of a large battery of *in vivo* toxicity data derived from tests utilising laboratory animals. Although fairly well proven for evaluating toxicity, the use of laboratory animals may have limited predictive values for human risk assessment because of differences in factors such as bioavailability, pharmacokinetics, metabolism, receptor sensitivity, and repair mechanisms (Cao *et al.*, 1999). Ethical problems associated with the use of large numbers of laboratory animals for toxicity testing has also made the use of cell culture for measuring drug toxicity much more acceptable. Numerous organisations [e.g. the Fund for Replacement of Animals in Medical Experiments (FRAME), European Research Group for Alternate Testing (ERGAT), and the

international Multicenter Evaluation of *In Vitro* Cytotoxicity (MEIC)] are encouraging the development of alternative testing protocols (Cao *et al.*, 1999).

5.2.2. Benzopyrones in Cancer Therapy

The anti-cancer properties and mechanisms of action of the benzopyrones have been extensively researched and interest in these compounds arose as a result of the *in vivo* studies in patients with advanced malignancies (Section 1.6.1.3.).

5.2.2.1. In Vitro Testing of Coumarins

Chemosensitivity testing of coumarin and its chief human metabolite, 7-hydroxycoumarin, was accomplished by several investigators utilising *in vitro* cell proliferation-based methods. Total cell counts (Moran *et al.*, 1993; Marshall *et al.*, 1994) and MTT growth assays (Myers *et al.*, 1994; Cooke & O'Kennedy, 1999) were successfully utilised to determine the inhibitory effects of these compounds on cell proliferation. In these studies, a time- and dose-dependent inhibition of cell growth was observed on exposure to 7-hydroxycoumarin and, in some cases, to coumarin. 7-hydroxycoumarin is a pro-drug and exerts a more potent inhibitory activity than coumarin. A variety of cell-lines were tested. Renal, prostate, breast, glioblastoma and leukaemic cell lines appear to be the most susceptible to the cytostatic effects of coumarin (Ebbinghaus *et al.*, 1997). Several hydroxylated and/or methoxylated coumarin derivatives were tested for their relative cytotoxicity on four human tumour cell lines (oral squamous cell carcinoma HSC-2, HSC-3, melanoma A-375 and promyelocytic HL-60). Tumour cell-specific cytotoxicity was detected with all 6,7-dihydroxy-substituted coumarins only. The observations indicate that the tumour-specific cytotoxicity of the naturally occurring coumarin, esculetin, can be further enhanced by proper substitutions at 3- and/or 4-position(s) of the molecule. Agarose gel electrophoresis revealed that esculetin and its derivatives with tumour-specific cytotoxicity induce internucleosomal DNA fragmentation in HL-60 cells (Kawase *et al.*, 2003).

5.2.2.2. Other Coumarin Derivatives

A number of natural and synthetic coumarin derivatives have also been examined *in vitro* for their growth inhibitory activity. Egan *et al.* (1997) determined the *in vitro* activity of the synthesised derivative, 8-nitro-7-hydroxycoumarin. This compound displayed cytotoxic properties in two human cell lines (HL-60, promyelocystic leukaemia and K562, erythroleukaemia), inducing cell death by apoptosis. It also had a cytostatic effect on the three other cell lines (EJ, human bladder carcinoma;

CHOK1 & CHrC5 Chinese hamster ovary cells) tested, exerted through a perturbation in their cell cycle (Egan *et al.*, 1997). Kolodziej and co-workers (1997) evaluated the cytotoxicity of 22 simple coumarins on two human cell lines (colorectal and small cell lung carcinoma) using the MTT assay. While most compounds exhibited low toxicities on these cells lines over 96 hrs, they found the dihydroxy-compounds (6,7- and 6,8- dihydroxy-derivatives) acted as very potent anti-proliferative agents. A separate study involved four coumarin derivatives, theraphins A (1), B (2), C (3), and D (4), isolated from the bark of *Kayea assamica* (Clusiaceae). Theraphins A (1), B (2), and C (3) exhibited good cytotoxicity against Col2, KB, and LNCaP human cancer cell lines. Theraphin D (4) showed mild activity only against the KB cell line. The coumarins also exhibited mild antimalarial activities (Lee *et al.*, 2004).

5.3. *Introduction to the Cytosensor Microphysiometer*

The cytosensor microphysiometer system, introduced in 1992, is a powerful tool that allows researchers to evaluate directly the effect of a wide variety of chemical compounds on living cells. The cytosensor system incorporates a patented Light-addressable Potentiometric Sensor (LAPS) technology into a unique system that monitors the metabolic state of living cells in 'real-time' without destroying the cells. Cellular metabolism is central for maintaining the viability of cells. Hence, in the following section, a brief overview of cellular metabolism and methods for its measurement are described.

5.3.1. *Cellular Metabolism*

Metabolism is defined as the overall biochemical process through which living systems acquire free energy from their environment, and utilise this free energy to maintain their normal functioning (Figure 5.1.). Central to this overall process is the ubiquitous cellular energy transmitter, adenosine triphosphate (ATP), the measurement of which is often used to assess the physiological state of the cell (Stryer, 1995). Cells take in nutrients (e.g. glucose) as part of their metabolic cycle, and break them down to produce useful energy, which is harnessed (via ATP), for use in cellular processes such as growth, motion, biosynthesis of complex molecules and active transport. The primary carbon sources used are sugars, amino acids and fatty acids, with glucose and glutamine of major importance in *in vitro* cell culture.

The primary waste products that are excreted are lactic acid and carbonic acid (carbon dioxide). Glucose can be converted to lactic acid via glycolysis, or to CO_2 via respiration (glycolysis

233

followed by the citric acid cycle and oxidative phosphorylation). Respiration is more proficient energetically than glycolysis, and also produces much less acid per ATP generated (compare 1 H^+/ATP and 0.167 H^+/ATP, for glycolysis and respiration, respectively). However, although respiration is the predominant ATP source of cells *in vivo*, cells cultured *in vitro* utilise glycolysis as their major ATP-generating reaction. Glutamine metabolism has also been shown to contribute a proportion of ATP to mammalian cells in culture [estimated at 30-100% depending on cell type and culture medium composition] (Owicki & Parce, 1992).

The rate at which cells expel acids into their environment is strongly correlated to the rate at which they convert food to energy (e.g. metabolic rate). The cytosensor microphysiometer system measures the rate at which cells acidify their immediate environment. Cells respond to a particular stimulus, for example, a neurotransmitter binding to a cell-surface receptor, in complex ways that are reliably reflected in a change in the cells' metabolism. Responses to stimuli can be transient or sustained, but the response to a particular stimulus is reproducible under constant conditions. The cytosensor monitors these metabolic changes as alterations in the acidification rate of the medium surrounding the population of cells. In this way, the system provides a 'real-time', non-invasive means of measuring cellular responses to a wide variety of agents (such as chemotherapeutics and antibiotics).
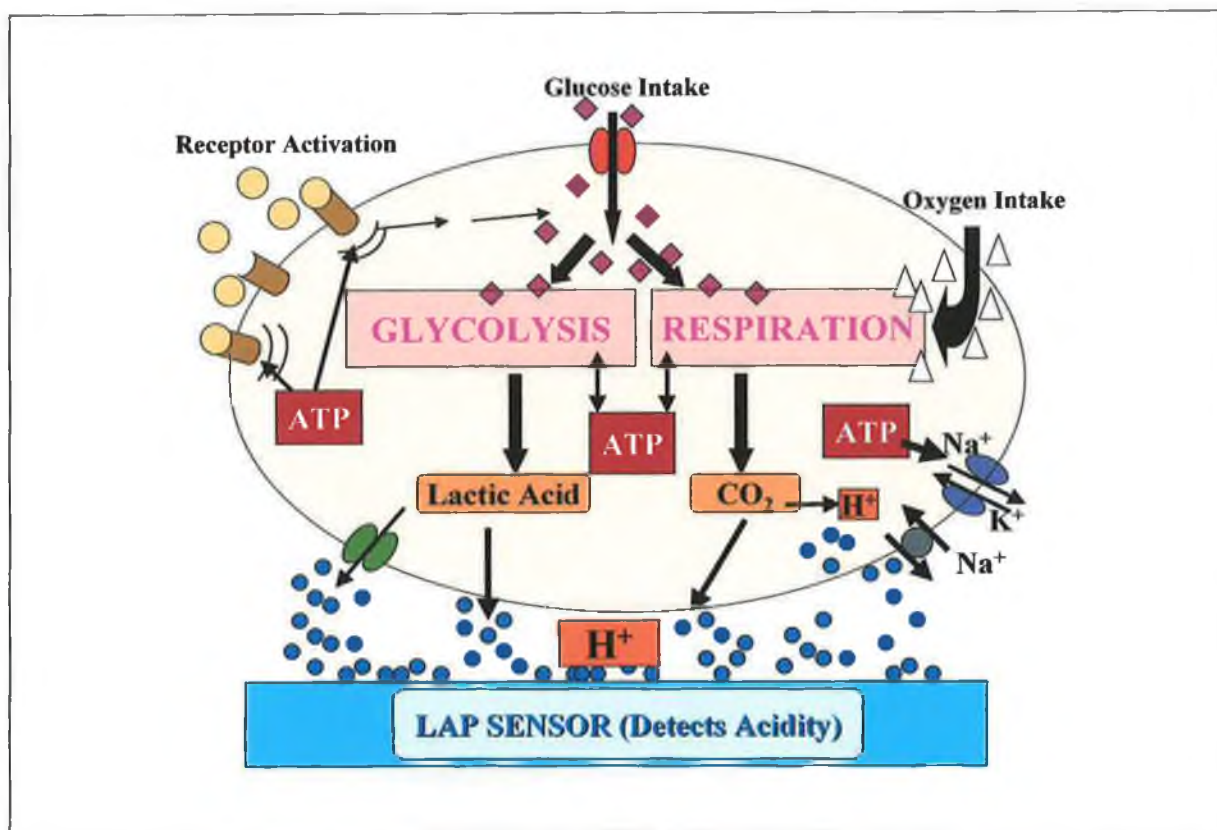
Figure 5.1: *Illustrative depiction of cellular metabolism and its affiliation to cellular processes such as receptor activation. Glucose and oxygen are utilised in the production of the cellular energy transmitter ATP, with the simultaneous manufacture of acidic waste products (lactic acid and carbon dioxide). ATP is consumed by a variety of cellular processes, e.g. growth, movement or receptor activation (as depicted in this diagram). In the Cytosensor Microphysiometer changes in metabolic rate, due to ATP, can be detected by measuring changes in the extracellular levels of acidic waste products, using the pH-sensitive LAPS sensor.*

5.3.2. The Cytosensor Microphysiometer Components

In the Cytosensor Microphysiometer, the cells are assembled into a disposable capsule, in such a way that they are sandwiched between two porous polycarbonate membranes. This assembly is then placed in a micro-flow chamber in aqueous diffusive contact with the silicon chip designed to function as an extremely sensitive pH detector. The chip is a light-addressable potentiometric sensor (LAPS), which serves as the bottom wall of the flow chamber (see Figure 5.2). The sensor chamber is the location at which all pH readings are taken. It is the heart of the instrument and with a volume of only 3μl it allows for the acquisition of very precise and sensitive readings.

235

Cytosensor Cell Capsule and Sensor Chamber

Fluid inlet

Fluid outlet

Plunger contact

Capsule insert

Spacer

Capsule cup

Sensor chamber body

Sensor chip

Living cells

LED
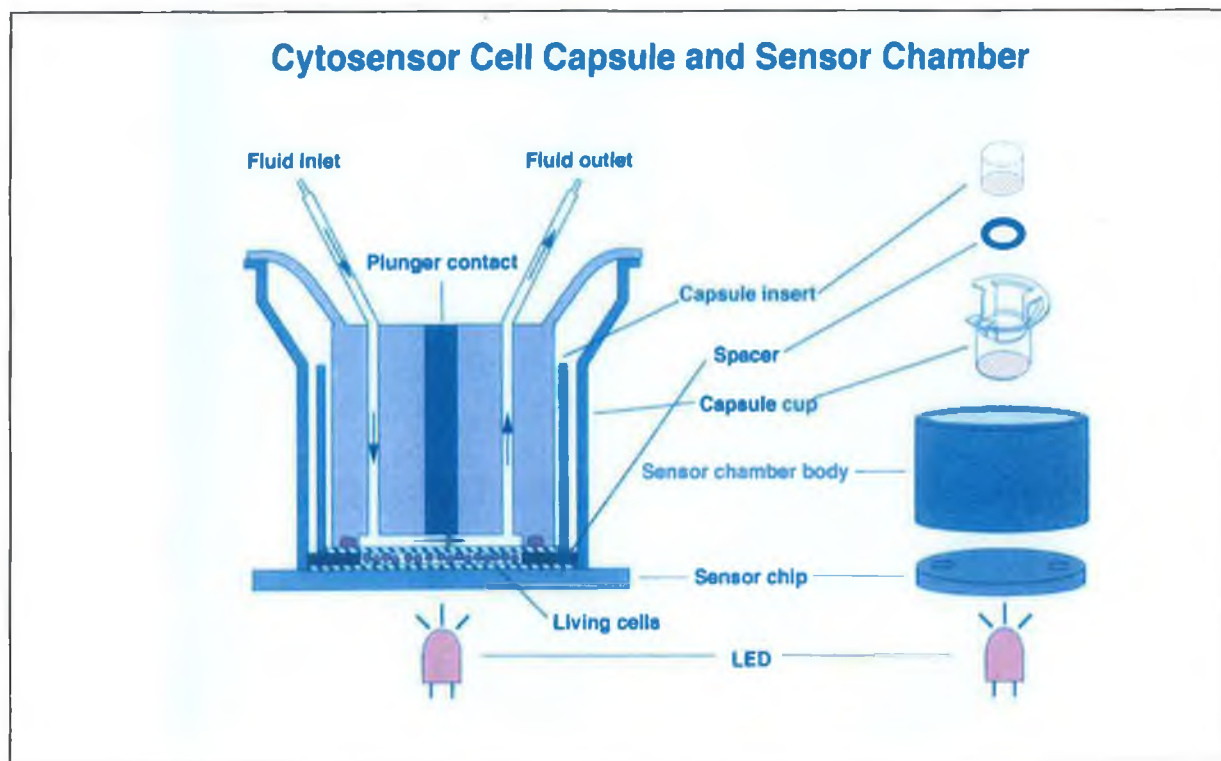
Figure 5.2: *Diagrammatic representation of the Cytosensor cell capsule and sensor chamber (Taken from Molecular Devices Users Manual).*

A light emitting diode (LED) positioned below the sensor chamber in the chamber pad enables pH readings in a 2mm diameter circular region in the centre of the cell capsule. Figure 5.3, a schematic diagram showing how the major components of the cytosensor system work together. A constant flow of fresh low-buffered running media is pumped through the system, and introduced into this sensor chamber, providing the encased cells with fresh nutrients and removing any waste products from their immediate environment.

Figure 5.3: *Schematic diagram of the major components of the Cytosensor Microphysiometer system (Taken from Molecular Devices Users Manual).*
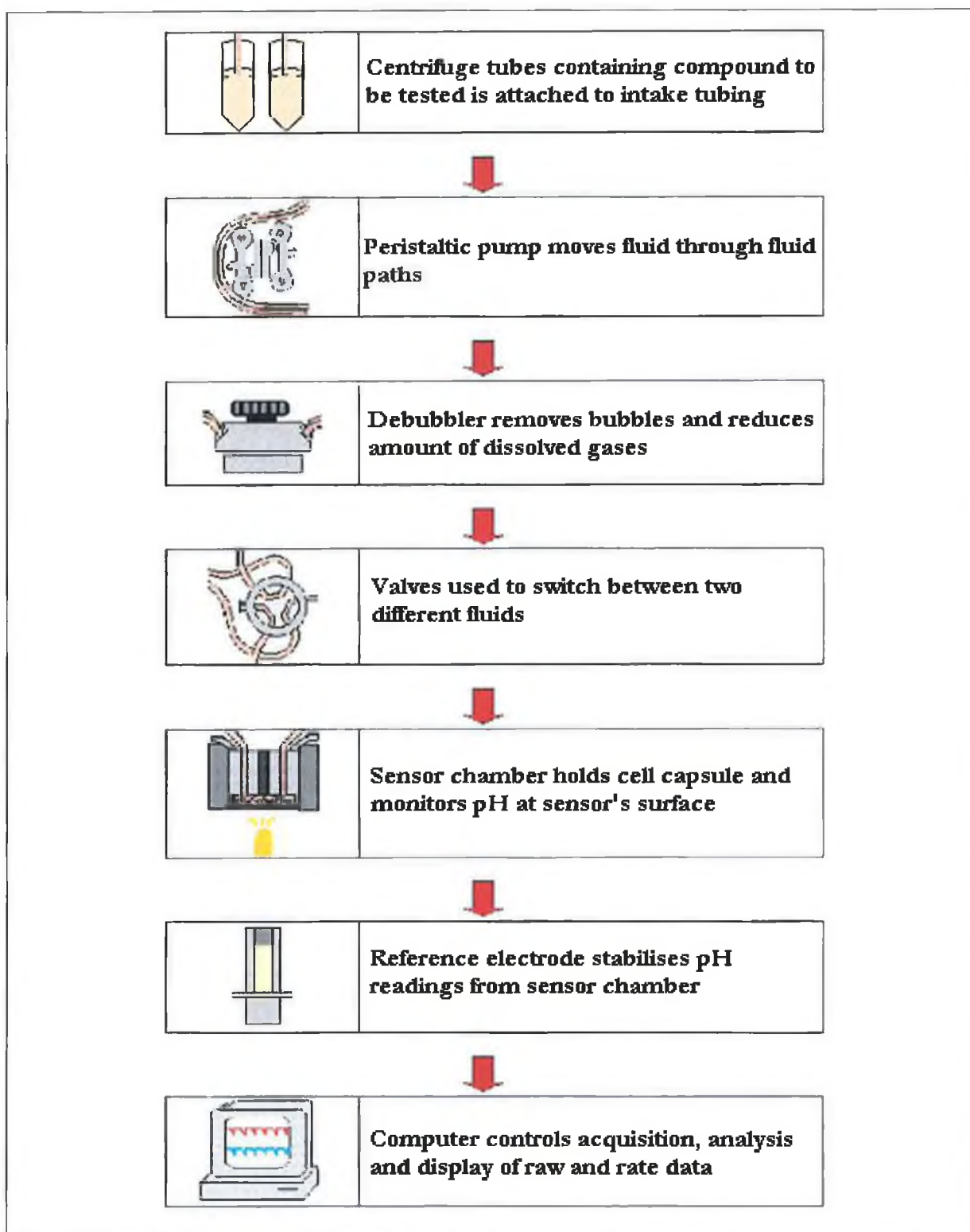
Figure 5.4: *Flow diagram describing what the major components contribute from start (fluid intake) to finish (display of raw & rate data) of a cytosensor run.*

5.3.3. Measuring Acidification Rates

The pH of the sensor chamber remains constant once media is allowed to flow through it, as no build-up of acidic waste products can occur. The pH remains steady at approximately the pH of the running medium (pH 7.3-7.4). When the pump is stopped (typically for 10-40 seconds), acid metabolites begin to build up in the sensor chamber and the pH begins to drop, which can be detected by the LAPS sensor chip. The extremely small volume of the flow chamber in which the cells are contained ensures that a minute increase in acidic metabolites causes a detectable change in the chamber's pH. When the pump is turned on again the flow sweeps out the acidic metabolites, returning the pH of the chamber to its original value, where it remains stabilised until the pump is stopped again. This pump on-off cycle generates data traces such as that shown in Figure 5.5.

The data obtained during the pump-off interval (also known as 'the get rate period') are fitted to a straight line, the slope [$-\mu$V/sec] of which is plotted as the acidification rate (Figure 5.5). If the metabolic rate of the cells changes in response to an effector agent (either stimulatory or inhibitory), the acidification rate data will reflect this change (Figure 5.5). The research in this thesis highlights the novel application of the microphysiometer for the analysis of the effects of benzopyrones on MCF-7 cells and the elucidation of their mode of action.
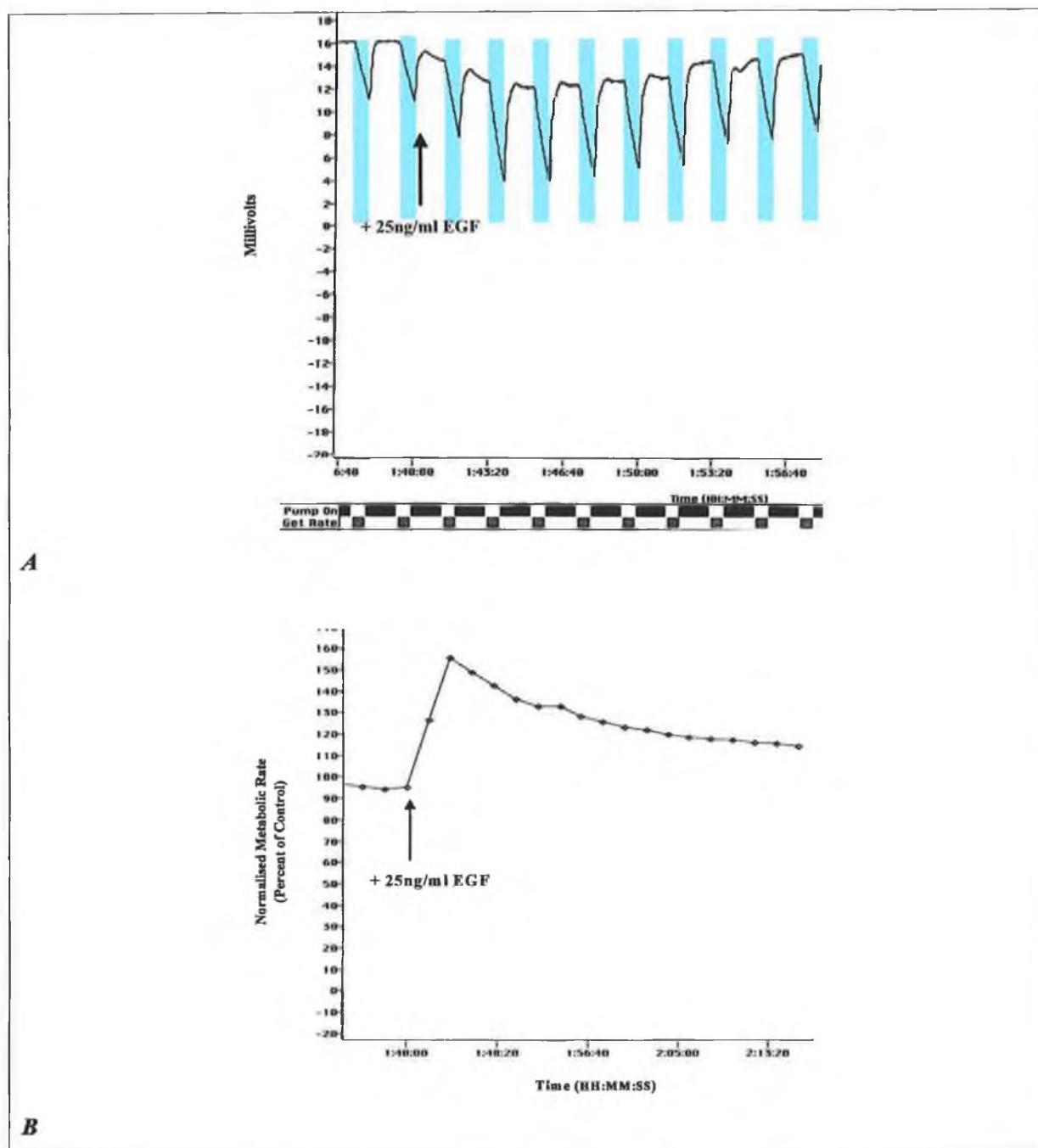
Figure 5.5: *Raw Data (A) and Rate (B) data derived from an experiment in which A431 cells were exposed to 25ng/ml EGF for 12 mins (Time of EGF exposure = 1:40:00). As can be seen from the raw data, a noticeable increase in the acidification rate during the pump-off cycle (highlighted in blue) denotes activation of the EGF-Receptor in these cells. This change in the cells metabolic rate is reflected in the Rate data (B). Molecular Devices Users Manual.*

5.3.4. Applications of the Cytosensor Microphysiometer

The cytosensor microphysiometer can be applied with mammalian cells (adherent and non-adherent cells, primary and established cell lines) yeast cells, prokaryotic cells and insect cells. The main application is the analysis of cell membrane bound receptors but the system can also be used to study non-receptor mediated events on cell metabolism, for example, the effect of viral infection and toxicological effects (Hafner, 2000). A major attribute of the Cytosensor Microphysiometer is its flexibility: it accurately measures a general cellular event (extracellular acidification), and as such is applicable to a variety of biological disciplines (Table 5.3.).

Since this is an assay system that reliably measures cell surface receptor activation, with subsequent intracellular signalling events, the cytosensor has been principally applied to pharmacological investigations, being particularly advantageous over traditional methods for determining agonist/antagonist profiles of receptors (Lang *et al.*, 2001; McCall *et al.*, 2002; Anderes *et al.*, 2003). Recently, the cytosensor has featured in toxicological evaluations of anti-cancer compounds and has been shown to be suitable as an *in vitro* alternative microtitre plate assays such as the MTT assay (Cooke & O'Kennedy, 1999; Cai *et al.*, 2002; Ekelund *et al.*, 2002). Other areas that have benefited from the application of cytosensor technology include studies in immunology, cell biology and microbiology (Hoelscher *et al.*, 2000; Sireci *et al.*, 2001; Landwojtowicz *et al.*, 2002).

Although general in its method of detection, the cytosensor can be used as a specific probe of signal transduction events in cells (Burvall *et al.*, 2002; Lui *et al.*, 2002). It has many advantages over traditional methods for examining signal transduction, as outlined in Table 5.4. In Section 5.4 signal transduction is introduced with the components of growth signalling pathways described.

Table 5.3: *Examples of the various research applications of the Cytosensor Microphysiometer in biological studies.*

Discipline	Application	References
Pharmacology	Receptor characterisation	Lang *et al.* (2001); Zambrano *et al.* (2002) McCall *et al.* (2002); Anderes *et al.* (2003)
	Signal transduction	Burvall *et al.* (2002); Lui *et al.* (2002)
Toxicology	Compound cytotoxicity	Cao *et al.* (1999)
	Tumour cytotoxicity	Liminga *et al.* (1999); Ekelund *et al.* (2000) Ekelund *et al.* (2001)
	Hepatotoxicity	Cao *et al.* (1998)
Cell Biology	Kinetics	Lanwojtowicz *et al.* (2002),
	Na^+/H^+ antiport studies	Wada *et al.* (1993); Fischer *et al.* (1999)
	Metabolic studies	Fan *et al.* (2002)
Immunology	T-cell activation	Wada *et al.* (1994); Sireci *et al.* (2001)
	Inflammatory Studies	Burvall *et al.* (2002)
	Macrophage/monocyte studies	Romano *et al.* (1996); DeVries *et al.* (1998)
Oncology	Chemotherapeutic efficacy	Wada *et al.* (1992); Ekelund *et al.* (2002)
	Apoptosis	Kuo *et al.* (1994); Cai *et al.* (2002)
Microbiology	Antibiotic susceptibility assays	Libby *et al.* (1998); Hoelscher *et al.* (2000)
	Anti-viral studies	Wada *et al.* (1992)
	Ion channel studies	Hahnenberger *et al.* (1996)

Table 5.4: Advantages of the Cytosensor Microphysiometer for research applications

Advantages of the Cytosensor Microphysiometer

Non-Invasive - Internal controls, Examine recovery.

Real-time Measurement – No need to do multiple assays for time course points

Rapid Results – Quicker than traditional assays (Ca^{2+} mobilisation, IP_3 assays)

High Reproducibility

Flexibility

No Radioactivity

Reduced Animal Usage

Reversibility studies – Efficient system

Increased Sensitivity – in comparison to MTT assay

5.4. Introduction to Signal Transduction and Cell Cycle Regulation

Signal transduction at the cellular level refers to the movement of signals from outside the cell to inside. Cell-surface receptors recognising and responding to extracellular stimuli are the key components required for the survival of any living organism (Bai, 2003). If cellular proliferation is desirable-for instance in wound healing, growth factors are generated which act as messengers for the cells wounded area stimulating them to proliferate. Growth factors are peptides or steroid hormones, which are recognised by specific cellular receptors. Binding of the growth factor to the receptor initiates a cascade of cell signalling events (Grunicke, 1995). The principal function of cell signalling is to co-ordinate the behaviour of different cells in order to achieve maximal benefits for the whole organism. The primary cellular mechanism for reception of a specific response commences with the binding of a ligand to its receptor, which in turn transmits a signal designed to express certain genes in a controlled manner (Helleday, 1998). These signalling pathways within cells are composed of chains

of interconnecting proteins. Each protein element in a pathway consolidates signals from activators upstream to itself, and passes these signals onto downstream effector proteins, this whole process being termed signal transduction (Hardie, 1991).

The significance of growth factors and the signalling pathways initiated by them to regulate cell cycle progression in eukaryotes has been identified as an important component of their function. Several studies have shown that cell signalling pathways determine cell growth as well as inhibition through cell cycle regulation (Agarwal, 2000). In the cell cycle of eukaryotes, DNA is replicated during S (synthesis) phase, and the replicated chromosomes are segregated into daughter nuclei during the M (mitosis) phase. A gap phase G_1 intervenes between mitosis and DNA synthesis, and another gap, G_2, occurs between DNA synthesis and mitosis. The two key decisions are when to enter S phase and subsequently, the M phase. Mitosis only begins after DNA synthesis has been completed and requires major changes in cell architecture (Stryer, 1995).

In order to stimulate a normal quiescent cell in G_0 to proliferate, the cell has to be exposed to growth factors, which can be recognised by corresponding cellular receptors. These growth factors have been classified as competence and progression factors. Combined activities of competence and progression factors lead to progression in G_1 until the restriction point is reached. The progression through G_1 phase of the cell cycle and the preparation for DNA replication requires the continuous signalling of progression factors, which are essential until the restriction point in G_1 is reached. EGF is an example of a competence factor needed for advancement of quiescent cells into G_1 phase. Beyond the restriction point, no further exogenous growth factors are required for the completion of the cell cycle (Grunicke, 1995).

Research in the area of signal transduction and cell cycle regulation has been stimulated by the belief that an understanding of signalling pathways interacting with cell cycle regulators responsible for cell growth in normal cells will provide an understanding into uncontrolled growth observed in cancer. In the remainder of the introduction to this chapter, the main elements of proliferative signalling pathways, as determined to date, will be reviewed. A detailed account of the cell cycle in normal cells is given so that comparisons can be made to cell cycle dysregulation leading to cancerous growth. The main focus of this work is with regard to breast cancer with particular emphasis on studies relating to the estrogen-positive MCF-7 cell line. Therefore, signal transduction and cell cycle regulation in breast cancer cells are discussed in detail.

5.5. *Components of Growth Signalling Pathways*

5.5.1. *Introduction to Phosphorylation in Signalling Pathways*

Receptor-ligand interactions launch downstream signalling cascades through intermediate cellular proteins, with the eventual effect of nuclear transcription. Stimulation of receptors by ligands can be of an autocrine, paracine or endocrine manner. It has been determined that phosphorylation reactions are the central mechanism for the progression of these growth signals from membrane to nucleus. Phosphorylation is one of the most common forms of protein modification. The most frequent targets for protein phosphorylation in eukaryotes are serine, threonine and tyrosine residues (Steen *et al.,* 2002). Receptor phosphorylation provides a pathway for cross-talk between responses initiated by steroid hormones, polypeptide growth factors, cyclic AMP, PKC or calmodulin (Strobl *et al.,* 1995).

Tyrosine phosphorylation plays an important role in the regulation of cell proliferation, differentiation, signal transduction and cell cycle progression. Induced tyrosine phosphorylation is mediated by activation of protein tyrosine kinases and/or inhibition of protein tyrosine phosphatases (Qian *et al.,* 2003). Phosphatases and protein kinases are enzymes that respectively remove or add phosphate residues, on either serine/threonine or tyrosine residues of proteins. ATP is utilised as a phosphate source. The signal transduction pathways in mammalian cells are being found to involve an increasing number of receptors and intracellular signals. However, many of these receptors and pathways can be grouped into superfamilies exhibiting high levels of identity at the protein level and similarities in the mechanism by which the signal is transmitted into the cell (Helleday, 1998).

5.5.2. *Receptor Classes*

The various growth factor receptor subtypes employ different mechanisms for post-receptor signalling. In order to understand the biological consequences of abnormal signal transducing elements in cancer, the various signal transmission pathways have to be briefly discussed (Grunicke, 1995). In this work, it is the importance of tyrosine phosphorylation in growth control and its deregulation in cancer that is addressed. Three distinct classes of receptors exist which use tyrosine phosphorylation to propagate proliferate signals. They are as follows:

1. Receptor Tyrosine Kinase (RTK) Family whose members have receptors with intrinsic intracellular tyrosine kinase domains, activated upon ligand binding. Downstream phosphorylation of proteins on tyrosine residues transduces the extracellular signal to the nucleus, e.g. EGF to EGF receptor.

2. Binary Receptor Tyrosine Kinase Family whose members do not possess an intracellular tyrosine kinase domain. They can only signal by association with a cytoplasmic tyrosine kinase molecule. This leads to a cascade of phosphorylation reactions, resulting in propagation of the external signal to the nucleus, e.g. IL-2.

3. G-protein-coupled Receptors cause activation of a number of signalling intermediates with eventual downstream activation of cytoplasmic kinases.

Tight regulation of RTK signalling is crucial for eliciting an appropriate type and level of response to external stimuli and they are the most important receptor subtype in proliferative signalling pathways (Chiarugi & Cirri, 2003). Therefore, the Receptor Tyrosine Kinase family shall now be discussed in more detail.

5.5.3. Receptor Tyrosine Kinases (RTKs) and Their Substrates

The Receptor Tyrosine Kinase (RTK) family of receptors consists of a group of cell-surface proteins, all members of which possess a large glycosylated extracellular ligand-binding domain, a single transmembrane domain, and an intracellular cytoplasm domain that contains a tyrosine kinase catalytic region. They are activated upon either ligand binding or receptor cross-linking (Qian *et al.*, 2003). Many subclasses of RTKs have been described based on sequence similarity and structural function, and the characteristics of the five principal subclasses are represented in Figure 5.6.
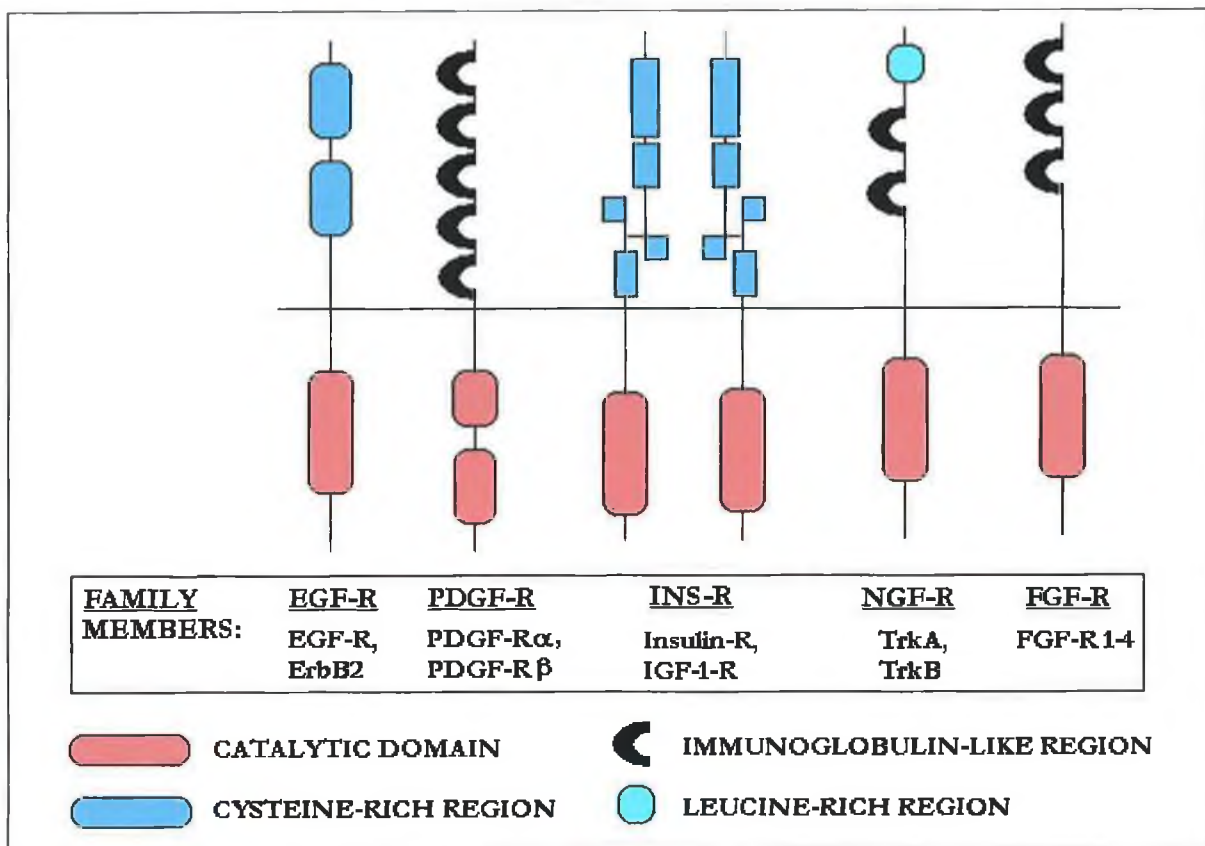
Figure 5.6: Schematic representation of the five principal Receptor Tyrosine Kinase subclasses. The family members include Epidermal growth factor-receptor (EGF-R), Platelet derived growth factor-receptor (PDGF-R), Insulin-receptor (INS-R), Nerve growth factor-receptor (NGF-F) and Fibroblast growth factor-receptor (FGF-R).

Many growth factors mediate their actions by binding to their cognate receptors e.g. the binding of epidermal growth factor (EGF) to the epidermal growth factor receptor (EGF-R). This causes activation of the intrinsic tyrosine kinase activity, which leads to the intracellular transmission and amplification of the extra cellular signal (Weiss & Schlessinger, 1998). Binding of the growth factor to the extracellular domain of the corresponding receptors activates the tyrosine kinase in the cytoplasmic domain and mediates a conformational change of the extra cellular domains, which induces receptor oligomerisation, usually dimerisation (Figure 5.7). Receptor dimerisation stabilises interactions between adjacent cytoplasmic domains, which in turn permits cross-phosphorylation of tyrosyl residues of the cytoplasmic domains. This process is termed autophosphorylation.
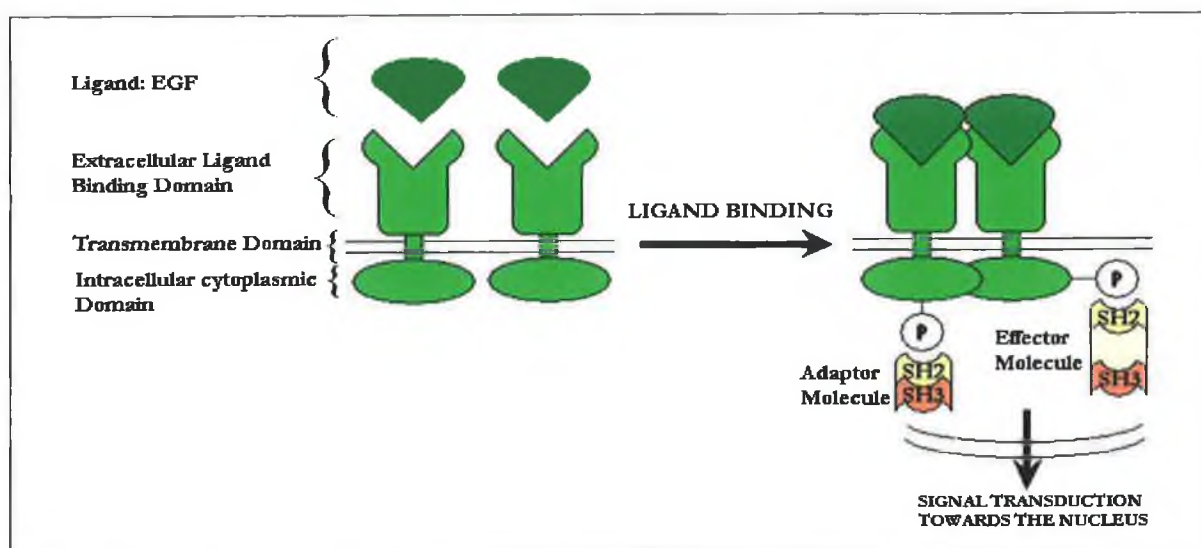
Figure 5.7: Diagram illustrating the events, which occur following ligand (e.g. EGF) – receptor interaction. The EGF-Receptor dimerises with a neighbouring receptor, allowing autophosphorylation of receptor tyrosine residues. Molecules containing SH2 domains (either adaptor e.g. GRB-2 or effector proteins e.g. PI3-K) can bind to tyrosine phosphorylated (P-Tyr) residues, leading to transduction of the binding signal towards the nucleus.

Receptor autophosphorylation enables the activated kinase to phosphorylate cytoplasmic molecules at tyrosine residues, thus initiating the cascade of signals downstream towards the nucleus. The phosphorylated tyrosyl moieties now serve as recognition signals for a variety of signalling molecules (substrates), which recognise specific autophosphorylated residues via their SH2 domains (domains homologous to a non-catalytic region of the src proto-oncogene) and bind only to these. The Src protein is a tyrosine kinase first identified as a transforming protein in Rous sarcoma virus. Subsequently, a cellular homologue was identified as c-Src. A number of RTK substrates have been identified to date. These include phosphatidylinositol-3-kinase (PI3-K), phospholipase Cγ (PLCγ), members of the nonreceptor Src family of tyrosine kinases, phosphatases and peptides. They consist almost entirely of SH2 and SH3 (responsible for accurate docking of appropriate downstream target) domains like growth factor receptor binding protein-2 (Grb-2). The latter links signalling molecules, including Ras, to tyrosine phosphorylated receptors (Grunicke, 1995). It was ascertained that certain molecules like Grb-2 contain only SH2 and SH3 domains, with no other functional domains. It is believed that these molecules function only as adaptor molecules to couple the activated receptor to other signalling intermediates. With regard to proliferative signal transduction, the SH3 domains couple with the Ras signalling pathway.

5.5.4. Ras Activation Pathway

Binding of ligand to its membrane receptor initiates a common sequence of events. The adaptor protein Shc binds to its peptide hormone receptor and becomes phosphorylated. Shc exists in three isoforms of 66, 52, and 46kDa and has three docking sites: an SH2, a phosphotyrosine binding domain (PTB) and a collagen homology (CH) site. Shc may be phosphorylated by the peptide receptor itself, by one of the SRC family kinases, or by other kinases (Santen *et al.*, 2002).

The receptor-Shc complex then further complexes with the adapter protein Grb-2. The guanine nucleotide release factor (GRF) SOS (mammalian homologue of "son of sevenless" genes in drosophila) is bound to activated receptor tyrosine kinases via the adapter protein Grb-2 (Santen *et al.*, 2002). Grb-2 is composed of one SH2 domain and two SH3 domains. The two SH3 domains bind to the carboxy-terminal proline-rich region of SOS, whereas the SH2 domain binds to the tyrosine phosphorylated sites in other proteins (Grunicke, 1995). When SOS enters the complex it is then able to catalyse the conversion of GDP to GTP-Ras.

The Ras protein has been assumed to act as a key regulator of cell growth and other functions. Ras is a 21kDa guanine nucleotide-binding protein whose biological activity is determined by the bound nucleotide. Activated protein contains bound GTP, while the inactive state binds GDP. Activation of Ras proteins is a key step in signal transduction process. Central to the activation of Ras is a family of GRFs, e.g. SOS. They are responsible for the release of bound GDP from the Ras protein, thereby enabling its activation. Deactivation of Ras occurs by hydrolysis of GTP to GDP, a reaction dramatically hastened by GTPase activating proteins (GAPs). Therefore, the relative activities of GRFs and GAPs acting on Ras at any instant determines its activation state (Figure 5.8.). Processed Ras proteins that have localised to the inner surface of the plasma membrane, function as a molecular switch that cycles between an inactive and active form (Caponigro, 2002). In transformed cells, however, the Ras protein usually has diminished GTPase activity, (as a result of mutations in the amino acids important for guanine nucleotide co-ordination), causing prolonged signalling periods since Ras can not switch from the active to inactive form to stop cell signalling when required.
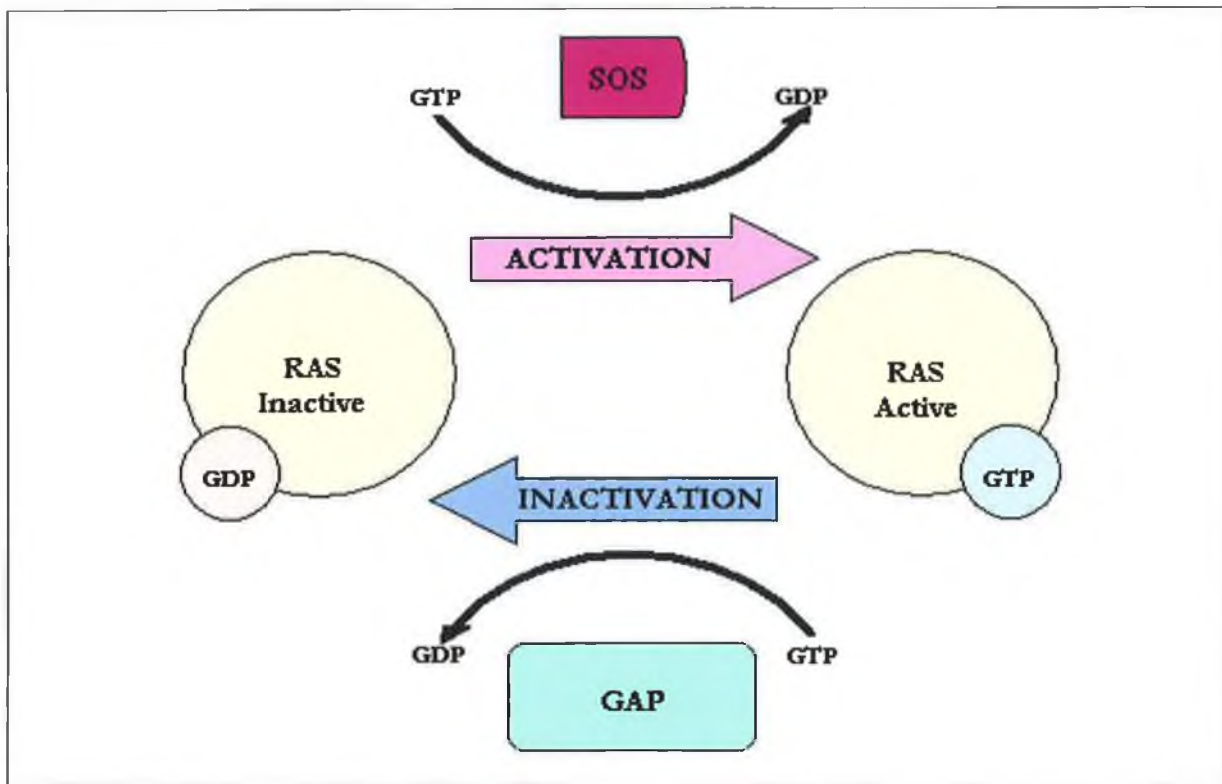
Figure 5.8: *Schematic representation of the activation/deactivation cycle of Ras. Inactive Ras binds GDP, while active Ras contains bound GTP. Two molecule types, the Guanine-nucleotide Releasing Factors (e.g. SOS) and the GTPase Activating Proteins (e.g. 120-GAP) control the activation state of Ras, with their relative activities at any instant, deciding its state of activation. The GRFs cause the release of bound GDP from Ras, enabling its activation. The deactivation of Ras occurs by hydrolysis of GTP to GDP, catalysed by GAPs.*

The GAP proteins do not account for all signals emanating from Ras. Activated GTP-Ras interacts with Raf-1 kinase. Raf-1 is a 70-75kDa protein, which is divided into three functional domains. The amino or N-terminal CR1 contains the domain responsible for interaction with Ras. CR2 contains the negative-regulatory domain. This domain regulates the kinase domain contained in CR3 that is located at the carboxyl-end of the protein. The fact that Ras has to be activated in order to associate with Raf-1 and that the binding of Raf-1 occurs through the Ras effector domain emphasizes the biological significance of this interaction. GTP-Ras binds to a site located at amino-acids 51-131 in the N-terminal region of Raf-1, which phosphorylates and activates the kinase properties of this peptide. Crystal structure analysis reveals that the Ras binding domain (RBD) of Raf involves direct contact of Ras with Gln 66, Arg 67, Lys 84, Arg 59, Gln 64, and Thr 68. GTP-Ras binds to this RBD with 100-fold higher affinity than GDP-Ras. Another Ras-binding domain for Raf was located in the cysteine-rich domain, which binds phosphatidylserine. There are two important steps involved in the

250

activation of Raf-1. Firstly, Ras interacts with Raf-1 and stimulates the translocation of Raf-1 to the plasma membrane. This facilitates further interaction with additional activators (Figure 5.9.). Secondly Raf-1 is phosphorylated on tyrosine and/or serine/threonine residues. When activated in this manner, Raf-1 in turn phosphorylates a second kinase, MEK kinase. This enzyme controls a third family of enzymes, the MAPK, again through phosphorylation on both the tyrosine and threonine residues (Santen *et al.*, 2002).
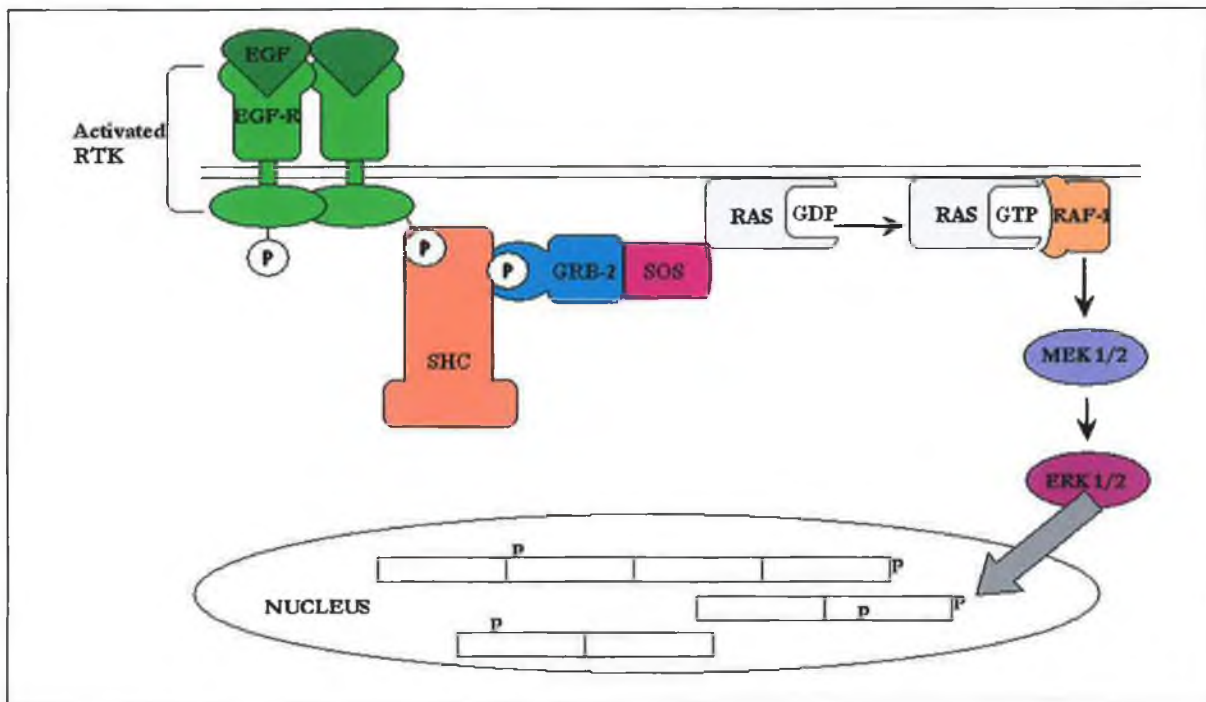
Figure 5.9: *Components of the RTK* ➡ *MAP Kinase pathway. Ligand binding to its cognate receptor at the membrane surface results in signal cascades towards the nucleus via the Ras/MAP Kinase pathway, with eventual nuclear phosphorylation of transcription factors (precise details in text).*

5.5.5. Role of Mitogen Activating Protein Kinase (MAPK) in Breast Cancer

Mitogen-activated protein kinase (MAP kinase) cascades transmit and amplify signals involved in cell proliferation as well as cell death. Three major MAP kinase pathways exist in human tissues:

a) Peptide growth factors acting through tyrosine kinase containing receptors are the major regulators of (extracellular-regulated kinase) ERK-1 and -2, e.g. EGF and EGF-R.

b) Estradiol, progesterone and other steroid hormones can act non-genomically via membrane-associated receptors to activate MAP kinase.

c) Various other ligands can activate MAP kinase by acting through heterotrimeric G protein receptors.

In this work the pathways of importance involve both the EGF and Estradiol stimulation of MAP kinase. Highly specific factors activate the MAP kinase pathway, usually through receptor-ligand interactions. Amplification of the signal then results from activation of a sequence of three or more linked kinase reactions. A small amount of active enzyme in the first kinase reaction acts upon a larger amount of substrate in the second and subsequent kinase reactions. The kinase sequence cascade usually involves three analogous proteins, a MAP kinase kinase kinase (MAPKKK), a MAP kinase kinase (MAPKK), and a MAP kinase (MAPK). One of the major mammalian MAP kinase cascades involves Raf-1 as the initial kinase in the sequence (i.e. MAPKKK); MAP/ERK kinase (MEK-1 and -2) as the second (i.e. MAPKK), and ERK-1 and -2 as the third sequential kinase (MAPK). It should be noted that MAP kinase is also called ERK and exists in the ERK-1 and -2 isoforms which are 85% homologous and have molecular weights of 42-44kDa, respectively (Santen *et al.*, 2002).

Since the work referred to in this section involves the estrogen receptor positive cell line MCF-7, emphasis shall be placed on the role of MAP kinase in breast cancer. Estrogen receptors (ER) belong to the steroid receptor gene superfamily, the members of which share some structural and functional similarities. The first estrogen receptor, now named ERα, was cloned in 1986, more than 20 years after it was identified by its affinity for 17β-estradiol. In 1996, the second ER, ERβ was reported (Weihua *et al.*, 2003). Clinical and experimental data have established that the leading cause of sporadic female breast cancer is exposure to estrogens, predominantly the steroid hormone 17β-estradiol (Foster *et al.*, 2001). Estradiol (E$_2$) was established as the pre-eminent breast epithelial cell mitogen in the development of human breast cancer and the polypeptide growth factors e.g. EGF also stimulate breast cancer growth in tissue culture. E$_2$ target tissues can be divided into two groups, the classical and non- classical E$_2$ target tissues, respectively. The classical targets are the uterus, mammary gland, placenta, liver, central nervous system (CNS), cardiovascular system and bone. These tissues have a high ERα content and respond to E$_2$ challenge with increases in transcription of certain E$_2$ responsive genes. The non-classical target tissues include prostate, testis, ovary, pineal gland and thyroid gland among others. In these tissues ERα expression is either very low or not

measurable. In the breast, E_2 stimulates growth and the estrogen receptor antagonist tamoxifen has been the most effective treatment for ERα-positive breast cancer (Weihua *et al.*, 2003).

Cell lines and breast tumour biopsies with high ER levels characteristically exhibit low or nonexistent EGF-R (170kDa). The inverse relationship between ER levels and receptors for epidermal growth factor is a clinically important observation. The ER+/EGF-R negative tumour types are better differentiated, whereas the ER-negative/EGF-R + types are associated with metastasis and shorter survival times. The down-regulation of ER levels by EGF observed in some tissue culture cell lines might provide a partial mechanism for the inverse relationship. Over expression or activation of receptor tyrosine kinase such as EGF-R is a poor prognostic indicator for breast cancer. The MCF-7 cell line contains high levels of ER with low levels of EGF-R (Strobl *et al.*, 1995).

Peptide growth factors utilising tyrosine kinase containing membrane receptors are the major regulators of ERK-1 and -2. However, numerous other receptor-ligand pathways can also stimulate ERK-1 and -2. For breast cancer estrogen can activate MAP kinase through interaction with ER, which co-opts the growth factor signalling pathway to activate MAP kinase (Santen *et al.*, 2002). ERα constantly shuttles between the cytoplasm and the cell nucleus, where it progressively stabilises, leading to an apparent permanent nuclear localisation (Seo *et al.*, 2003). Strong evidence now exists for the presence and importance of plasma membrane ERs in a variety of cells that are targets for steroid action. It is important to know the physical structure of the receptor and where it resides within the lipid bilayer, in order to better understand the function of the membrane ER. Signalling by growth factor receptor and non-growth factor tyrosine kinases as well as G protein receptors occurs at least in part after localisation to plasma membrane microstructures, known as caveolae (Levin, 2002).

Newly synthesised ER enters a phosphorylation/dephosphorylation process, continuously trafficking between cell compartments to achieve its physiological role before its final shipment into the proteosome (Seo *et al.*, 2003). The cell biologic roles of the two receptor pools may be quite complementary even though ER in the membrane and nuclear compartments appear to act by very different mechanisms (signalling versus transcriptional transactivation). It is possible that membrane kinase signalling can rapidly activate transcription, which can then be sustained by the nuclear receptor. The latter's action is probably facilitated by the phosphorylation of the co-activator proteins, and this could result from ER signalling from the membrane. Signalling from the membrane may also amplify the actions of the nuclear receptor. Furthermore, signalling appears to play an important role in the post-translational modification of proteins that can be upregulated in their synthesis via the nuclear receptor (Levin, 2002).

253

In MCF-7 breast cancer cells, estradiol binds to the membrane ER, which induces the phosphorylation of Shc and the binding of Shc to the ER. Shc proteins are substrates of activated tyrosine kinases and are involved in the cascade that leads to Ras activation and mitogenesis (Figure 5.10.) Both the SH2 and the phosphotyrosine binding (PTB) domains appear necessary for the interactions between Shc and the ER. Following Shc phosphorylation Shc binds to GRB-2 and SOS which in-turn activates the Ras pathway as described in Section 5.5.4. Once Raf-1 is activated in Ras signalling pathway it can phosphorylate MEK and activates its kinase activity by nearly 7000 fold. MEK exists in two molecular weight forms called MEK-1 and -2. Activated MEK then phosphorylates the tyrosine185 and threonine183 residues in the activation loop of ERK-1 and -2. This phosphorylation step increases the activity of MAP kinase by 1000-fold. ERK-1 and -2 then stimulate downstream events involved in gene regulation (Santen *et al.,* 2002). The MAP kinase pathway regulates the transcription of *c-fos* and *c-jun* two early response genes, which together dimerise to become the AP-1 nuclear transcription factor (Figure 5.10.).
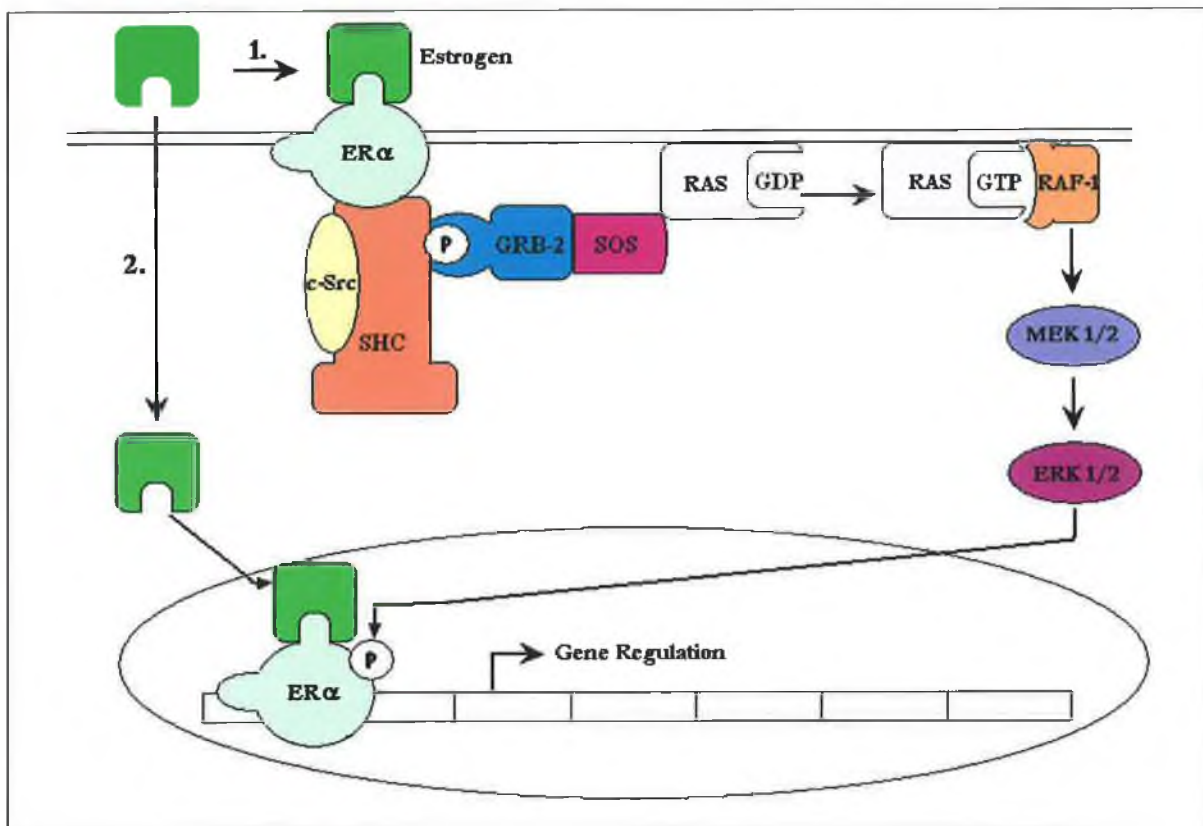
Figure 5.10: *Estrogen-activated MAP Kinase pathway. Estrogen may activate pathways, which utilise a membrane-associated ER or via nuclear ER. In breast cancer cells estradiol can bind to estrogen receptor-α (ER-α) molecules in the peri-membrane region which in turn initiates a cascade of protein reactions similar to Figure 5.8 involving Shc, GRB-2 and SOS to activate MAP kinase (Pathway 1). Estradiol can also initiate transcriptional events in the nucleus (Pathway 2).*

5.5.5.1. Events Downstream of MAP Kinase

The precise downstream events initiated by MAP kinase, which result in cell proliferation are still under investigation. Activation of other protein kinases such as the RSK proteins (RSK1, 2 and 3) is stimulated by MAP kinase. This occurs by MAP kinase mediated phosphorylation of serine 363 on the RSK protein. Once activated the RSK proteins can phosphorylate down stream targets involved in transcriptional activation such as cAMP response element binding protein (CREB), c-Fos and the estrogen receptor (Santen *et al.,* 2002). RSK proteins can enter the nucleus and phosphorylate the transcription factor c-fos, thus stimulating the transcription of genes under AP-1 control. Activated ERK-1 and -2 can elicit direct effects on transcription factors within the nucleus. It has been shown that phosphorylation of ERK-2 is necessary for its nuclear translocation. This nuclear translocation is important, as experiments have shown that when ERK2 was sequestered in the cytoplasm there was a

255

strong inhibition of cell cycle re-entry. Once ERK has been translocated to the nucleus it can directly phosphorylate c-Jun and c-Fos. It also has the ability to directly catalyse the phosphorylation of serine 118 of the ER and increase its transcriptional efficiency. RSK can also phosphorylate the ER at serine 167, which also increases its transcriptional efficiency (Figure 5.11.). Therefore it is true to say, MAP kinase is a key regulatory enzyme involved in mediating cell proliferation through phosphorylation of a number of important factors (Pan *et al.*, 2003).
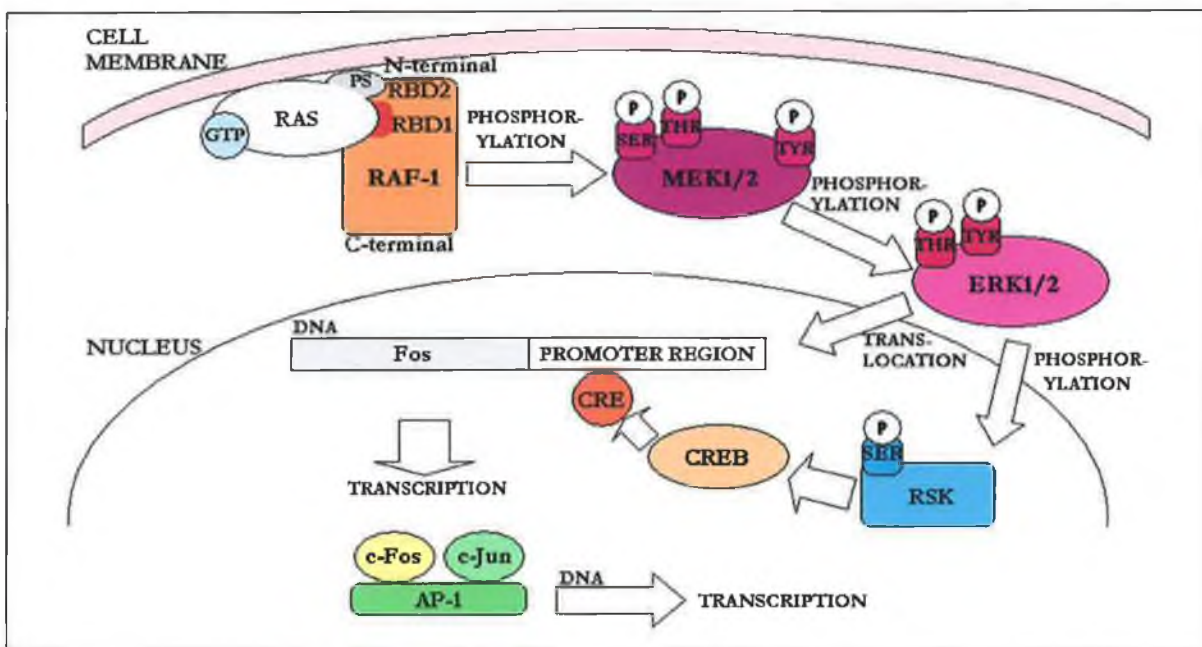
Figure 5.11: Schematic diagram illustrating in detail the events downstream of MAP Kinase. Once ERK has been translocated to the nucleus it can directly phosphorylate c-Jun and c-Fos. Activated ERK-1 and -2 can elicit direct effects on transcription factors within the nucleus. Activation of other protein kinases (by serine phosphorylation) such as the RSK proteins (RSK1, 2 and 3) is stimulated by MAP kinase. Once activated the RSK proteins can phosphorylate downstream targets involved in transcriptional activation and can enter the nucleus and phosphorylate the transcription factor c-fos, thus stimulating the transcription of genes under AP-1 control. [PS depicted on RAS molecule is phosphatidylserine, which binds to a RAS binding domain (RBD-2) on RAF-1 molecule. This interaction is explained in Section 5.5.4.]

5.5.6. PI3-K Signal Transduction Pathway

Since its discovery in 1988 the activity of PI3-K has been associated with the actions of mitogenic growth factors (Corvera, 2001). It is one of the intracellular signalling pathways that are

frequently activated in cancer cells (Van de Sande *et al.,* 2002). PI3-K heterodimer is an important mediator, of survival factors, protecting many cell types from multiple apoptosis-inducing stimuli (Barragan *et al,* 2002). Growth factor receptor activation causes receptor autophosphorylation of tyrosine residues, which recruits the SH2 domain containing p85 regulatory subunit coupled to the p110 catalytic subunit of PI3-K (Dangi *et al.,* 2003). PI3-K catalyses the formation of the 3-phosphoinositides, phosphatidylinositol 3,4-diphosphate and phosphatidylinositol 3,4,5-triphosphate. Increases in 3-phosphoinositides lead to transmembrane translocation of downstream effectors such as the serine/threonine protein kinase AKT (also known as protein kinase B). On translocation, AKT is phosphorylated and activated, ultimately resulting in stimulation of cell growth and survival (Van de Sande *et al.,* 2002). AKT is fully activated by phosphorylation at two sites, Thr308 and Ser473. In breast cancer cells activated AKT phosphorylates a serine residue on glycogen synthase kinase -3 (GSK-3) resulting in GSK-3 inactivation. Subsequently, inactive GSK-3 is unable to inhibit cyclin D1 expression (Figure 5.45). Cyclin D1 is an essential cell cycle regulator important in G_1 phase progression, which is discussed in more detail in Section 5.6. Activation of AKT is responsible for increasing and maintaining high levels of cyclin D1, resulting in the promotion of cell division and proliferation (West *et al.,* 2003).

Recently it has been reported that E_2 stimulates the phosphatidylinositol-3-kinase (PI3-K/AKT) pathway in MCF-7 cells. Interestingly, in these cells activation of Src and the PI3-K-dependent pathways is simultaneous and mediated by direct interactions of the two kinases with ERα. The sex steroid hormone signalling pathway activation in MCF-7 cells has been shown to lead to DNA synthesis and cell growth. E_2 treatment of MCF-7 cells activates the Src-Shc-Ras-Raf-MEK-1-Erk pathway as well as the PI3-K pathway. Activation of the two pathways is simultaneous and each item is required to trigger the S-phase entry of the cells. E_2 stimulates PI3-K/AKT pathway under the Src control and increases the transcriptional activity of the cyclin D1 promotor. This is of major importance as it is the first time that it has been found that E_2 controls expression of a cell cycle regulator through signalling pathway activation. As stated above, E_2 stimulation of S-phase entry of MCF-7 cells requires both MEK-1 and PI3-K activity. However, whereas MEK-1 activity is important at the beginning of hormone treatment, PI3-K is necessary for at least 3 hours. These findings indicate important differences between the action of the two pathways, although both converge on DNA synthesis (Migliaccio *et al.,* 2003).

5.6. Cell Cycle Regulation

Significant advances have been made towards understanding the eukaryotic cell cycle in the last twenty years. The cell cycle is divided into G_1 phase, S phase, G_2 phase and M phase. Eukaryotic cells have evolved signalling pathways to coordinate cell cycle transitions and ensure faithful replication of the genome before mitosis (Stewart *et al.*, 2003). Cell cycle progression requires the sequential activation of different cyclin-dependent kinases (CDKs), which are positively regulated by cyclins and negatively regulated by CDK inhibitors (CDKIs) (Barboule *et al.*, 1999). Cyclins are key components of the cell cycle progression machinery. They activate their partners, CDKs, which phosphorylate sequentially critical substrates that regulate the progression of the cell cycle. Normal, non-tumour cells express cyclin proteins in an orderly, scheduled fashion, at a given phase of the cell cycle. There are four types of cyclin important throughout the cell cycle. Cyclins D are expressed early in G_1 phase, and are degraded prior to entrance to S phase. Synthesis of cyclin E begins in mid-phase G_1 and its expression peaks at the G_1/S transition. It is degraded during the S phase. Synthesis of cyclin A starts in S phase, it peaks at S/G_2 transition and decreases stepwise during the latter part of the G_2 phase. Synthesis of cyclin B starts at the end of S phase, peaks as the cell enters M phase and breaks down at the transition to anaphase (Jimenez-Orozco *et al.*, 2001).

In the cell cycle there are 3 CDKs of importance, which are CDK4/6, CDK2 and CDK1. Activation of CDK4/6 by growth stimuli appears to govern exit from G_0 and entry into early G_1, activation of CDK2 occurs mid-to-late G_1 and regulates transition into, and passage through S phase, whereas late G_2 and completion of mitosis is regulated by CDK1. Normal cells do not progress from one phase to the next unless the events of the proceeding phase have been correctly completed (Foster *et al.*, 2001). The complexes cyclin-D-CDK4, cyclin-D-CDK6, cyclin-E-CDK2 and cyclin-A-CDK2 regulate the progression from G_1 phase to S phase (Stewart *et al.*, 2003). To prevent abnormal proliferation, cyclin-CDK complexes are precisely regulated by two families of CDKIs that block their catalytic activity. The first class of inhibitors includes the INK4a proteins (e.g. p16^{INK4A}) that bind only CDK4-CDK6 kinases and not to cyclins and are, therefore, specific for early G_1 phase. By forming dimers with CDK4 or CDK6 they can inhibit kinase activation by preventing the formation of complexes with members of the D-cyclin family. The second family of inhibitors is composed of CIP/KIP proteins (e.g. p21^{CIP1} and p27^{KIP1}), that inhibit all cyclin-CDK complexes and are not specific for a particular phase (Coqueret, 2003). These proteins form trimeric complexes with CDK2 bound to cyclin E or A and inactivate enzyme activity. Interaction of these proteins with CDK4/6 is, however, more complex, because at physiological concentrations, both p21^{CIP1} and p27^{KIP1} promote the formation of active D cyclin-CDK4/6 complexes (Foster *et al.*, 2001). Both p21^{CIP1} and p27^{KIP1} act as

a bridge between cyclin D and CDK4 to promote their association. Therefore, cyclin D-CDK4 complexes function to sequester $p21^{CIP1}/p27^{KIP1}$ away from cyclin E-CDK2 complexes, facilitating their activation and G_1/S transition (Figure 5.12.).

The retinoblastoma protein (pRB) is a crucial substrate of activated cyclin-CDK complexes in the G_1 phase. pRB is sequentially phosphorylated by cyclin D-CDK4 and cyclin E-CDK2 during G_1 phase progression, and either represses or activates transcription, depending on its phosphorylation state and associated proteins. Hypophosphorylated pRB binds to and inactivates members of the E2F family of transcription factors. Because E2F family members mediate transcription of genes required for DNA synthesis, binding of hypophosphorylated pRB to E2F arrests cells in the G_1 phase. During G_1-phase progression, CDK-mediated hyperphosphorylation of pRB results in the dissociation of pRB and E2F and entry into the S phase (Stewart *et al.,* 2003).
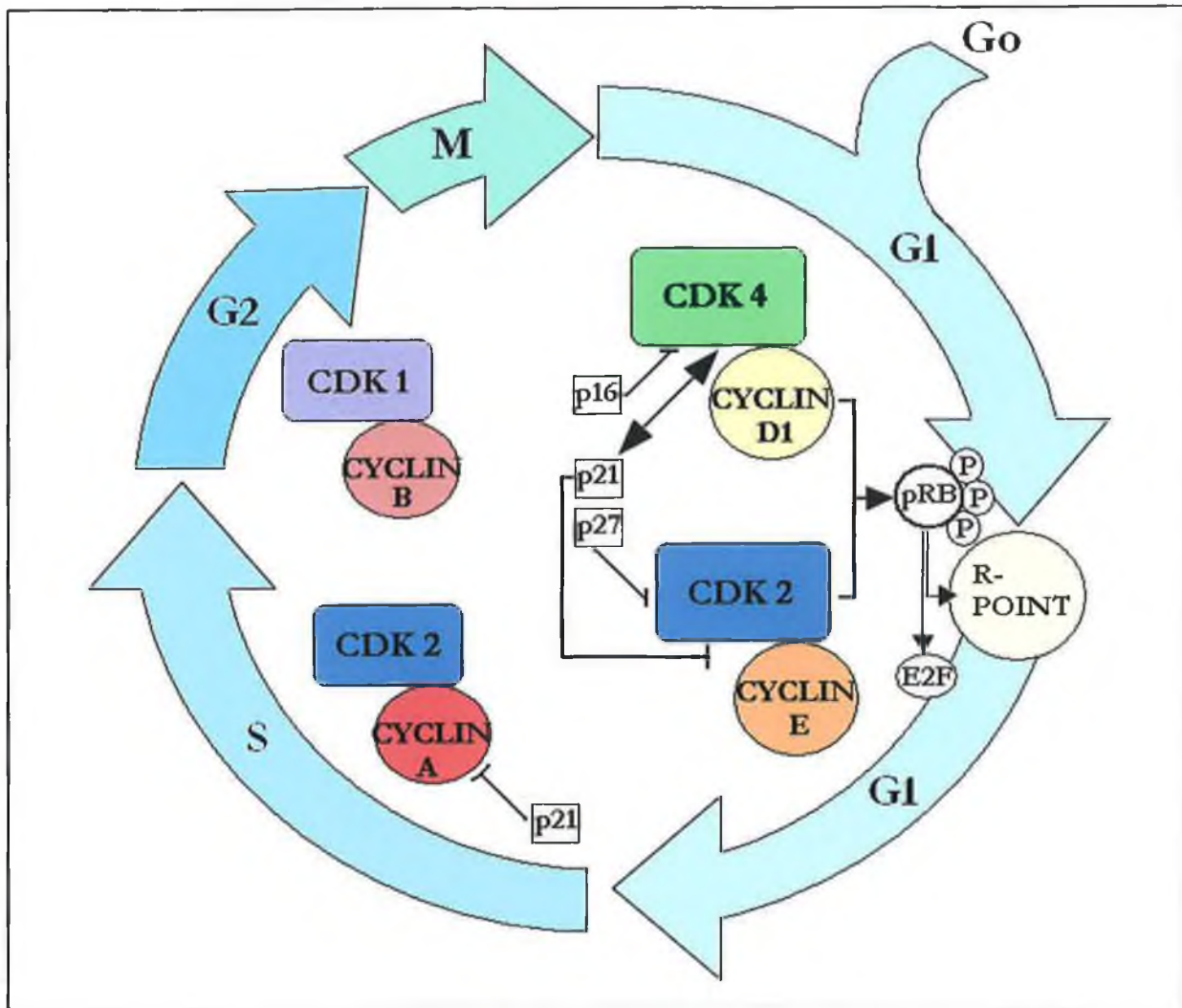
Figure 5.12: *Simplified scheme for cell cycle regulation in mammalian cells. The four phases G_1 , S, G_2 and M phase, reflect stages in cell cycle progression where DNA synthesis and replication (S phase) and mitosis (M) occur in a temporally regulated fashion, separated by two gap phases (G_1 and G_2). The restriction point (R-Point) is a point of control which determines when a cell becomes committed to cell cycle progression. The cyclin D1-CDK4 and cyclin E-CDK2 complexes phosphorylate pRB, which releases transcription factor E2F, resulting in progression through R-Point and entry into S-phase. Synthesis of cyclin A begins in S phase and complexes with CDK2 to regulate S phase progression. Cyclin B synthesis starts at the end of S phase and complexes with CDK1 in G_2 to help regulate late G_2 progression and completion of mitosis.*

5.6.1. Estrogens and Cell Cycle Regulation in Breast Cancer

Over the past thirty years, many groups have studied the effects of E_2 and estrogens on breast cancer cells in culture. Characterisation of the mammalian cell cycle has progressed rapidly in recent years. A considerable body of evidence indicates that, compared with normal ductal cells, cyclin D1 (mRNA and protein) is over expressed in nearly 50% of breast cancer cells. Overproduction of cyclin D1 protein and mRNA correlates strongly with ER synthesis in tumour tissues, and relates inversely to the level of cyclin E. In accordance with these results, cyclin D1 is a well-defined target of E_2 action in MCF-7 cells (Foster *et al.*, 2001). Through stimulation of cyclin D1, E_2 activates cyclinD1-CDK4 and this complex appears essential for E_2 action. Anti-estrogens are able to block the proliferative effect of E_2 on breast cancer cells. Treatment of MCF-7 cells with anti-estrogens elicits G_1 phase cell cycle arrest with a decrease in cyclin D1 expression and elevated expression of both $p21^{CIP1}$ and $p27^{KIP1}$ (Strobl *et al.*, 1995). Estrogens and, to the lesser extent, anti-estrogens, as well as protein kinase activators and growth factors increase phosphorylation of the ER and possibly other proteins in the ER-specific response pathway, suggesting that changes in cellular phosphorylation state will be important in determining the biological activity of the ER and the effectiveness of anti-estrogens as estrogen antagonists (Katzenellenbogen, 1996).

5.7. Breast Cancer Research and Treatment

Breast cancer is the second most common cancer among women in the world. In developed countries, it is the most common. What separates a malignant from a normal cell? This question has occupied scientists for decades. Although a simple answer remains elusive, several hallmarks of malignancy have been identified. These include evasion of apoptosis, lack of senescence and invasion and metastasis. Oncologists typically thought of systemic therapies for breast cancer as belonging to one of two categories: either cytotoxic chemotherapy or hormonal therapy. The growing complexity of cancer treatment, and more particularly of the biological basis underlying these therapies, suggest we re-consider our conceptual approach to the treatment of breast, and indeed all cancer (Sledge & Miller, 2003).

During normal growth and differentiation, cell proliferation is rigidly controlled. Cancer cells escape normal growth controls via mutations that result in over expression of differentially regulated growth factors or their receptors. Targeting self-sufficiency in growth signals in breast cancer has had profound effects. The biological underpinnings for hormonal therapy remained unexplained until the identification of the ER in the 1960s. The ER remains arguably the most important growth factor

261

receptor identified for breast cancer. The question remains, can other aspects of growth self-sufficiency be targeted in breast cancer? Leaving aside the introduction of new agents for old targets, an increased understanding of signalling pathways and the identification of other growth factors point to novel opportunities for therapy. Current efforts are underway to target downstream mediators of cell surface receptors (e.g. ras, MAP kinase and PI3-K pathways). Intact EGF-R is present in approximately 40% of breast cancers. Research has brought about the development of many inhibitors including the EGF-R kinase inhibitor Iressa/gefitinib (ZD 1839) (Liem *et al.*, 2002). Initial clinical trials of EGF-R blocking agents have proven disappointing with few responding patients. It is possible that inhibition of EGF-R alone is insufficient to limit self-sufficient growth as alternate pathways may come into play at this stage (Section 5.8.). In order to create more effective drugs, better understanding of this signalling pathway is essential (Sledge & Miller, 2003).

In human cancer, not only are the positive stimulators overactive: the negative controls fail to function properly. Altered expression of cyclins, CDKs and CDKIs are frequently found in malignancy. A considerable body of evidence indicates that in comparison with normal cells, cyclin D1 (mRNA and protein) is overexpressed in nearly 50% of breast cancer cells (Prall *et al.*, 1998; Foster *et al.*, 2001; Foster *et al.*, 2001a). Cyclin D1 is expressed relatively early in breast carcinogenesis. Overexpression of cyclins and related CDKs is associated with poor prognosis in breast cancer. Similarly, lack of expression of CDKIs (p21 and p27) also leads to a poor prognosis for breast cancer patients. Together these data suggest the importance of insensitivity to inhibitory signals in breast cancer.

Other important hallmarks of breast cancer beyond the scope of this work include, evasion of apoptosis, limitless replicative potential, invasion and metastasis, sustained angiogenesis and genomic instability. The ability to apply the hallmarks of cancer to clinical practice has been limited by the insufficiency of both available testing methods and knowledge of breast cancer biology. Today's research and treatment of cancer is fuelled by a host of technologies that analyse and manipulate genetic material at the molecular level. The first harvest of these technologies is now coming into focus. Genomic analysis of human breast cancers, using cDNA microarrarys 'gene-chips', reveals that breast cancer based on morphology in fact consists of several distinct subtypes. These subtypes have different 'tool-kits': for instance, different mechanisms of growth signal sufficiency. Due to the fact that the cancer 'tool-kit' is a finite package, and because cancer cells rely heavily on this limited repertoire for their survival, cancer should ultimately represent a calculable problem. In the future it is hoped that instead of stamping someone with the generic diagnosis "breast cancer," the patients illness will be treated according to which genes are mutated. Such a distinction could go a long way to

explaining why some cancers respond to certain drugs and others do not. It is also likely to change the way drugs will be designed and tested (Kahn, 2003).

5.8. Signal Transduction Therapy

Research in the area of signal transduction has always been stimulated by the belief that an understanding of signalling pathways responsible for cell growth in normal cells, will provide an understanding into the uncontrolled growth observed in cancer (Cooke, 1999). It is well known now that there is an important relationship between genes controlling normal cell growth, and those capable of inducing cell transformation. The genes that control normal cell growth, proliferation and differentiation, are known as proto-oncogenes and they are responsible for encoding proteins that are components of signalling pathways. Many oncogenes (cancer-causing genes) are altered versions of normal proto-oncogenes. The concept to employ elements of mitogenic signal transduction as targets for cancer chemotherapy originated as a result of increasing knowledge of the mechanism of transformation by oncogenes (Grunicke *et al.,* 1996). Signal transduction therapy involves utilising novel agents specifically designed to block signalling pathways or their components. Any component of the signalling pathway can be targeted. Inhibition of these pathways can be achieved by a variety of reagents. These include, small molecules such as peptides, antibodies, anti-estrogens, tyrosine kinase inhibitors, antisense oligodeoxynucleotides and target-specific RNA ribozymes (Levitzki, 1996). These inhibitors target different areas along the signalling cascade starting with the receptor and ending with transcription factors.

5.8.1. Signal Transduction Targets

5.8.1.1. Growth Factor Receptors

Proliferation, differentiation, and cell death are co-ordinated processes that help maintain homeostasis among diverse cell types in higher organisms. Growth factors play an important role in the control of these processes. They exert their function by triggering signal transduction cascades upon binding to their cognate membrane receptors. The varying efficacy and toxicity of traditional cancer therapies has driven the development of novel target-based agents. In particular, the EGF-R superfamily is an attractive therapeutic target because it is commonly overexpressed in malignant disease. Several selective inhibitors of this family of receptors are currently being evaluated in a number of cancers (Arteaga, 2003). EGF responsiveness has been reported in a variety of solid tumours, including breast, pancreatic, oesophageal, colon and prostate. There are at least 15 EGF-like

ligands, including transforming growth factor (TGF-α), heparin-binding, EGF-like growth factor, betacullin and epiregulin. For tumour cells, the final effects of signal transduction sequence are survival, proliferation, and blockage of differentiation, as opposed to apoptosis and senescence. Therefore, understanding the molecular interactions that occur from receptor occupation to induction of gene transcription will allow the rational design of chemotherapeutic drugs (Weinstein-Oppenheimer *et al.*, 2000). Several strategies have been developed to antagonise EGF-R family members and they will be discussed in the next paragraph.

Table 5.5: *Inhibitors of EGF-R-mediated MAP kinase pathway activation, which may prove useful as a single agent or combination treatment (radiation or chemotherapy) in cancer patients.*

INHIBITOR	*NAME*	*REFERENCE*
Anti-EGF-R mAb	Erbitux, Cetuximab, Trastuzumab	Huang *et al.*, 2003. Sridhar *et al.*, 2003
Tyrosine Kinase Inhibitor	Erlotinib, Gefitinib, OSI-774	Herbst, 2003 Grunwald & Hidalgo, 2003 Seymour, 2003
Fusion Protein	EGF-Genistein	Uckun *et al.*, 1998
Immunoconjugate	Mab806, Y10	Sridhar SS *et al.*, 2003
Anti-EGF Vaccine	YMB2000	Sridhar SS *et al.*, 2003

Recently Yang and co-workers (1999) generated a fully humanised monoclonal antibody (E7.6.3) to EGF-R. This mAb prevented engraftment of A431 xenografts in athymic mice. As a result eradication of pre-existing tumours was observed. This work was performed without the use of additional chemotherapy. These observations are encouraging to the development of humanised mAb, which should exhibit minimal immunogenicity and a longer half-life. Combination therapy is showing promise as illustrated by pancreatic cancer research performed by Huang and colleagues (2003). Pancreatic cancer remains a devastating disease, with 95% of all patients diagnosed with the disease

dying within 2 years. The combined therapy using an anti-EGF-R mAb (Erbitux), gemcitabine chemotherapy, and radiation caused complete tumour regression using a nude mouse model inoculated with pancreatic MiaPaCa-2 cells. Proliferation assays indicated that prolonged exposure to Erbitux increased the sensitivity of pancreatic cells to gemcitabine and radiation therapy. Research regarding drug resistance and the effect of Erbitux on signal transduction was also investigated. The results showed association of GRB-2 to EGF-R induced by EGF in the presence of Erbitux. This indicates an alternate pathway of Ras-MAPK activation, which may be related with tumour resistance to treatment.

The design of inhibitors to the tyrosine kinase activity of the EGF-R is an active area of research. Erlotinib (also known as OSI-774 or CP-358,774) is a small molecule selective inhibitor of the EGF-R tyrosine kinase that competes with ATP for binding with the intracellular catalytic domain of EGF-R tyrosine kinase, inhibiting phosphorylation. In preclinical studies, this compound inhibited the phosphorylation of the EGF-R in a dose-dependent and concentration dependent manner resulting in cell cycle arrest and induction of apoptosis in various human tumour xenografts alone and in combination with chemotherapeutic drugs. Both Phase I and II (monotherapy trial) data from patients with advanced NSCLC, ovarian cancer and head and neck squamous cell cancer showed erlotinib was well tolerated with favorable activity compared with single-agent chemotherapy in similar patient populations. Phase III trials with erlotinib in NSCLC and pancreatic cancer are in progress, as are a range of studies to optimise the use of erlotinib alone and in combination with chemotherapy, radiotherapy, and other targeted agents (Herbst, 2003). There is a definite need to opimise these trials as there has been some disappointing results from gefitinab phase III clinical trials (Seymour, 2003). While results from phase III trials with other agents such as erlotinib and cetuximab (monoclonal antibody studied as an anticancer drug) will be reported in the next 12 to 18 months, the early results indicate that present and future research efforts need to be directed towards the selection of patients with EGF-R-dependent tumours, identification of differences among the various classes of agents, and new clinical development strategies. Early data suggest a number of potential roles for these agents in the modulation of resistance and in combination with other inhibitors of signal transduction. The erlotinib clinical trials illustrate its potential as a novel inhibitor of EGF-R tyrosine kinase and is presently undergoing full development as an anti-cancer drug (Grunwald & Hidalgo, 2003). Uckun and co-workers (1998) have developed a fusion protein called EGF-Gen. Genistein is a tyrosine kinase inhibitor which is bound to the EGF to form a fusion protein. *In vitro* studies have shown the fusion protein caused apoptosis of EGF-R-expressing breast cancer cell lines.

5.8.1.2. Ras Protein

In 1993, a signal transduction cascade, starting from the membrane-anchored activated Ras protein and ending in nuclear gene transcription was first described. Ras proteins are present in every cell, with the highest levels in proliferating cells. Therefore, it is not surprising that Ras was implicated in the development of tumours that circumvent both the effects of therapy and the immune response. The MCF-7 cell line, transfected with an inducible Harvey- Ras (H-Ras) gene, showed increased resistance to cisplatin and mitomycin C (Fan *et al.*, 1997) Ras oncogenes (K-, H-, N-ras) are known to be involved in signal transduction pathways regulating cell growth and differentiation in many human cancers (Dempke, 2003). Ras was one of the first oncogenes targeted by pharmaceutical companies to develop anticancer drugs (Prendergast & Gibbs, 1994). Interruption of the Ras signalling pathway can be basically achieved in three ways, i.e. inhibition of Ras protein expression through antisense oligonucleotides, prevention of Ras membrane localisation and inhibition of Ras downstream effectors (Caponigro, 2002). The high incidence of mutated, transforming ras genes in human cancer and the restricted number of sites within the ras genes where transforming mutations occur spontaneously made these oncogenes attractive candidates for antisense technology.

Inhibition of Ras function is an alternative strategy for the interference with Ras controlled malignant growth. Ras activation requires its association with the plasma membrane. This process is initiated by the attachment of a farnesyl (15-C isoprenyl) group to the protein and is catalysed by the farnesyl transferase (Dempke, 2003). Farnesyl transferase inhibitors (FTIs) are a novel class of anti-cancer agents that competitively inhibit farnesyl protein transferase (FPT), and are currently being developed and tested across a wide range of human cancers (Lancet & Karp, 2003). These studies include both single-agent and combination (e.g. chemotherapy) clinical trials in pancreatic cancer, acute myeloid lymphoma, colon cancer, liver cancer and breast cancer (Caponigro, 2002; Gana-Weisz *et al.*, 2002; Dempke, 2003; Mazzocca *et al.*, 2003).

Both R-115777 and SCH-66336, are orally active heterocyclic FTIs undergoing research in phase III studies in patients with advanced pancreatic cancers. It is expected that these studies will determine the extent of clinical activity and whether these agents can be used as single agents or have to be used in combination with other cytostatic drugs. In addition, it remains to be clarified whether FTIs may sensitise drug-resistant cancers following conventional chemotherapy (Dempke, 2003). However other researchers have been able to shed light on this area. Recent studies by Gana-Weisz and co-workers (2002) demonstrated that treatment with S-trans, trans-farnesylthiosalycyclic acid (FTS) led to a marked increase in sensitivity to gemcitabine of the formerly resistant SW480 colon

cancer cells and a 100-fold increase in sensitivity to gemcitabine of Panc-1 pancreatic cancer cells. Their previous studies have shown that FTS disrupts Ras membrane anchorage, which contributes to inhibition of tumour growth and cell transformation. Most tumour cells develop resistance to anticancer agents. It was shown that Panc-1 pancreatic cancer cells and SW480 colon cancer cells exposed to FTS do not escape FTS-induced growth inhibition and do not develop drug resistance.

Phase I clinical trials using FTIs in acute myelogenous leukaemia (AML) and other myeloid malignancies have been performed, demonstrating enzyme target inhibition, low toxicity and promising response rates. These findings have prompted further development in phase II trials. It is anticipated that such information will ultimately define the optimal roles of FTIs in patients with AML and other myeloid disorders, facilitate the incorporation of FTIs into current therapeutic strategies for myeloid malignancies, and provide insight into effective methods of combining FTIs with other signal transduction inhibitors (Lancet & Karp, 2003). One aspect of FTI biology that is poorly understood is the ability of these drugs to induce cancer cell growth arrest at the G_2/M phase of cell cycle. The effects of FTI-277 on two human liver cancer cell lines (HepG2 & Huh7) were investigated by Mazzocca and colleagues (2003). It was shown that FTI-277 induced up-regulation of CDKI p27^{KIP1} without affecting the cellular levels of p53 and p21. This event correlated with reduced activity of CDK-2 and CDK-1. Increased expression of Bcl-2 protein was observed in both cell lines treated with FTI-277. Taken together, these results show that increased expression of p27 and Bcl-2 is concomitant with altered association between Ras, Raf-1 and Bcl-2 and suggests that this is responsible for the growth-inhibitory properties of FTI-277.

Nonsteroidal anti-inflammatory drugs (NSAIDs) have also been shown to inhibit Ras. The NSAID Sulindac is used in the therapy and treatment of tumours in patients with the inherited cancer predisposition familial adenomatous polyposis. Sulindac binds to Ras and inhibits activation of downstream Raf. It also inhibits the activation of the nucleotide exchange activating protein. However, the major limitation of these results was that they were performed at high doses of sulindac (Herrmann *et al.*, 1998). Vaccination with mutated Ras has been another approach to block Ras signalling. Peptides that correspond to mutated Ras were studied in a phase I vaccine trial. The response was modest, 3 out of 10 patients with advanced cancer showing cytotoxic T lymphocytes responses that were specific for the mutated Ras (Khleif *et al.*, 1999). Human reovirus therapy has become a novel approach to combat tumours expressing activated Ras (Coffey *et al.*, 1998).

5.8.1.3. Raf-1

Mutated forms of the Raf oncogenes have been observed in diverse neoplasias, including breast, cervical, renal, hepatocellular and small cell lung carcinomas. Raf-1 is the most extensively studied member of the Raf family. It was shown that for Raf-1 synergistic activation occurs with oncogenic Ras and activated tyrosine kinases. Certain residues are important in the regulation of Raf activity. Amino acids 340 and 341 of Raf-1 are both tyrosine phosphorylated which results in the activation of Raf-1 activity. The involvement of the different Raf oncogenes in various cancers is important to determine since they have different capacities to induce downstream signalling proteins. This may indicate that the development of inhibitors to the different Raf proteins will be complex. Inhibitors to each kinase may have to be developed, as they may have opposing roles in either stimulating or preventing cell cycle progression.

Until quite recently, the benzoquinone ansamycin antibiotic, geldanamycin (GA), was the only compound reported to inhibit Raf activity. It was demonstrated that this compound binds to the heat shock protein (hsp)90 and disrupts the Raf-1-hsp90 multimolecular complex, which prevents Raf-1 protein maturation. Other proteins are degraded in the presence of geldanamycin e.g. c-ErbB-2, EGF-R and ER components. c-ErbB-2 down-regulation is a desirable effect since this is a gene that is frequently mutated in tumours such as breast and non-small cell lung cancer. Kim and co-workers (2003) have shown that GA exhibits potent anti-tumour activity in certain cancer cell lines by destabilising important signal transduction proteins (e.g., Raf-1 and AKT). The purpose of the study was to determine whether GA alters the expression of Raf-1 and AKT, shown to be critical for neuronal cell survival, and induce apoptosis of neuroblastoma cells. It was determined that GA decreases cell viability and induces apoptosis in human neuroblastoma cells. These findings suggest that GA may be a novel therapeutic agent, which may be effective in treatment of neuroblastomas. A separate study utilised antisense oligonucleotides to antagonise Raf activity. A 20-base phosphorothioate oligonucleotide complementary to c-raf-1 mRNA (ISIS 5132) specifically suppresses Raf-1 expression both *in vitro* and *in vivo*. However, further development and optimisation is necessary before ISIS 5132 be properly evaluated as novel therapeutics (Barnard *et al.,* 1998; Rudin *et al.,* 2001).

5.8.1.4. Src Family of Tyrosine Kinases

The Src family of non-receptor protein tyrosine kinases plays critical roles in a variety of cellular signal transduction pathways, regulating such diverse processes as cell division, motility,

adhesion, angiogenesis and survival. Src family kinases are frequently overexpressed and/or aberrantly activated in a variety of epithelial and non-epithelial cancers. Activation is very common in colorectal and breast cancers. Exactly how Src family kinases contribute to individual tumours remains to be defined completely, however, they appear to be important for multiple aspects of tumour progression, including proliferation, disruption of cell/cell contacts, invasiveness, apoptosis resistance and angiogenesis. Given the ability of Src and its family members to participate in so many aspects of tumour progression and metastasis, Src family kinases are attractive targets for future anti-cancer therapeutics (Summy & Gallick, 2003). N-myristoylated peptides have been reported as src inhibitors. These modified peptides showed an improved potency compared with the original peptides (Ramdas *et al.,* 1999). 6-Aryl-pyrido-[2,3-*d*]pyramiding (PD089828) inhibits EGF-R and Src tyrosine kinase activity. This broad-spectrum tyrosine kinase inhibitor may be a valuable inhibitor of Raf activation, mediated by tyrosine phosphorylation (Oppenheimer-Weinstein *et al.,* 2000).

5.8.1.5. MAP/ERK Kinase (MEK)

The MEK pathway has been associated with a variety of neoplasias, including breast cancer renal cell carcinoma and hepatocellular carcinoma. MEK-2 is the most potent ERK-1 activator, followed by MEK-1, which is approximately 7 times less active in activating ERK-1 than MEK-2. In cells expressing normal MEK-1, the kinase appears as a 45kDa protein. The amino terminal end of the kinase has a negative regulatory domain, as deletion of these residues results in the constitutive activation of MEK-1. The catalytic activity is localised in the carboxyl terminus of the protein. Raf-1 activation of MEK-1 requires the phosphorylation of S residues 218 and 222. MEK activity can be blocked with the use of specific inhibitors. These kind of drugs, which inhibit MEK activity, show promise in turning off this pathway in rapidly proliferating malignant cells. One such inhibitor recently identified is 1,4-diamino-2,3-dicyano-1,4-bis[2-aminophenylthio] butadiene (U0126). This compound is selective for MEK-1 and MEK-2 (Favata *et al.,* 1998). The effects of U0126 on the growth of eight human breast cancer cell lines have been examined by Fukazawa and colleagues (2002). The results indicated that concurrent inhibition of MEK-ERK and S6K pathways induces apoptosis when cells are deprived of anchorage but not when anchored. These inhibitors may provide a therapeutic strategy to selectively target neoplasms proliferating at ectopic locations, with acceptable effects on normal cells in their proper tissue context. The effect of MEK inhibitor PD98059 on the growth of human pancreatic cancer was also investigated. Although tumour growth was not reduced by the MEK inhibitor, the findings suggest that the Ras signalling pathways are potential targets for manipulation of radiosensitivity, and that induction of an alternative pathway may enhance radiosensitivity of pancreatic cancer (Matsui *et al.,* 2003).

5.8.1.6. Extracellular Regulated Kinase (ERK)

ERK activity has been detected in increased levels in breast, colon, ovary and kidney cancer cell-lines. ERK mRNA expression was shown to be elevated in mammary adenocarcinoma cell lines with higher metastatic potential. In most solid tumours, a positive correlation has been found between Ras-activating mutations and ERK activation. In haematopoietic cells the situation seems different as it has been shown that 50% of patient with primary acute myeloid leukaemia exhibit constitutive ERK activation. However, leukaemia cells that exhibited the N-Ras mutations showed no signs of ERK activation. These observations are a reflection of the complexity of the signalling process and underscore the necessity to study different cell systems to avoid erroneous generalisations.

The role of nuclear translocation of ERK was demonstrated by sequestering both ERK-1 and-2 in the cytoplasm of the cell. Both Elk-1-dependent gene transcription and cell cycle re-entry were strongly inhibited (Brunet *et al.*, 1999). This research illustrates the potential for targets of ERK nuclear translocation.

5.9. Benzopyrones in Signalling Processes & Cell Cycle Regulation

Interest in the study of benzopyrones has originated in the clinical observation of its efficacy in cancer patients. Much presented work has shown that both coumarin and 7-hydroxycoumarin inhibit the *in vitro* growth of a range of cell lines in a dose-and time-dependent manner, with some cell lines more sensitive than others to these effects (Bogan *et al.*, 1996; Egan *et al.*, 1997; Cooke & O'Kennedy, 1999). In all cases 7-hydroxycoumarin was more potent than its parent compound. In order to exploit the effects of any drug optimally, it is essential to locate its precise cellular or molecular target. Recent advances made in both signal transduction and cell cycle research involving the use of benzopyrones will now be reviewed.

The central role of the Ras protein in growth signalling pathways was highlighted in Section 5.5.4. Recent research by Pan and colleagues (2003) has involved investigation into the inhibitory effects of esculetin on vascular smooth muscle cell (VSMC) proliferation and intimal hyperplasia by balloon angioplasty in the rat. Three predominant signalling pathways were found to be inhibited by esculetin:

a) Activation of MAP kinase and downstream effectors of c-fos and c-jun immediate early genes.

b) Activation of nuclear factor-κB and AP-1

c) Activation of PI-3K and cell cycle progression

Using western blot RT-PCR they found that esculetin inhibits serum-induced MAP kinase phosphorylation, expression of c-fos and c-jun mRNA and the DNA binding activity of AP-1. Furthermore, esculetin also inhibits Ras activation, a shared upstream event of these signalling cascades. It was recently suggested that PI-3K-mediated pathways play a key role in cyclin D1 expression and in turn effects progression of the cell cycle into S phase (Section 5.6.). Through these investigations it has been demonstrated that esculetin profoundly reduced cyclin D1 expression in the VSMC tested. Taken together it is clear from these results that esculetin inhibits the serum-induced events such as MAP kinase and PI-3K activation. It is likely that the cardinal target of esculetin is before these events. They concluded that esculetin inhibits VSMC proliferation via an upstream effector of Ras and downstream events such as MAPK and PI-3K activation.

The effect of esculetin, coumarin and 7-hydroxycoumarin on the cell cycle and its regulatory molecules have been investigated. Wang *et al.* (2002) have presented evidence that esculetin affected phosphorylation of pRB thus inducing G_1 arrest of human leukaemia HL-60 cells. The results demonstrated that the treatment with esculetin resulted in an accumulation of hypophosphorylated pRB in HL-60 cells along with reductions of both cyclin D1 and E. This induced the arrest of the cell cycle at the G_1 phase. Among the released proteins, the E2F family of transcription factor has central position. Not only does E2F induce gene expression necessary for DNA synthesis, it also contributes to the regulation of the cyclin D1 and E genes. Esculetin treatment also induced enhanced expression of the CDKI p27 and a reduced expression of CDK-4, thus inhibiting pRB phosphorylation (Wang *et al.*, 2002). A separate study set out to clarify mechanisms of action of 7-hydroxycoumarin and coumarin were studied with regard to their effects on cell cycle progression of human adenocarcinoma cell line A427. These cells are pRB positive and have homozygous deletions at the gene of p16^{INK4A}. The results showed that 7-hydroxycoumarin had greater cytostatic activity than coumarin. The inhibition of the cell-cycle at transition G_1/S is consistent with the cytostatic effect of 7-hydroxycoumarin. Furthermore, the decrease in the percentage of cells expressing cyclin D1 indicates that the action of 7-hydroxycoumarin involves early events in phase G_1. Absence of changes in the level of cyclin D1 mRNA suggests a post-transcriptional effect of 7-hydroxycoumarin. A pathway which regulates post-transcriptionally the levels of cyclin D1 is the PI-3K/AKT pathway (Section

271

5.6.). If this pathway is inhibited it cannot inhibit phosphorylation of GSK-3 which leads to cyclin degradation (Jimenez-Orozco *et al.*, 2001).

Flavonoid compounds in food items of plant origins (such as soybean), including isoflavone genistein, are known to have a wide spectrum of biological activities (Hua *et al.*, 2003). A very important biological activity of genistein regards its ability to inhibit cancer cell proliferation *in vitro* (Tanos *et al.*, 2002). It is also a well-known tyrosine kinase inhibitor and therefore many studies have been performed in order to better understand its mechanism of action in inhibiting cancer cell proliferation. The purpose of a study by Akimoto and colleagues (2001) was to test the potential effects of genistein on enhancement of radio-sensitivity as a therapeutic agent and to explore the molecular mechanism in human esophageal cancer cell lines. The investigations revealed that growth factor receptor-mediated signal transduction pathways play an important role in determining cellular response to radiation or other stresses. In this study, radiation activated both survival signals p42/p44 ERK and AKT/PKB. However, incubation with genistein for 9 hours greatly enhanced radio-sensitivity in the cell lines examined. In TE-2 esophageal cancer cells, there was a slight decrease in expression of (anti-apoptotic) Bcl-2 protein and an increase in (pro-apoptotic) Bax expression.

An earlier signal transduction study also demonstrated that genistein inactivates bcl-2 expression via phosphorylation. This compound can delay the G_2/M Phase of the cell cycle and induce apoptosis of MCF-7 breast cancer cells. Substantial changes in bcl-2 phosphorylation were detected following treatment with genistein. These changes involved increased bcl-2 phosphorylation, which was evident within 30 mins after genistein exposure. It was proposed that bcl-2 protects cells from apoptosis by forming heterodimer with bax and reducing the number of bax homodimers. Phosphorylated bcl-2 is incapable of forming heterodimer with bax, and it loses its anti-apoptotic potential. In genistein-treated MCF-7 cells, bcl-2 protein expression was down regulated and this was evident 48hrs after treatment. These results strongly suggest that an integral and independent early component of the apoptotic signalling is bcl-2 inactivation through phosphorylation. The combination of DNA targeting agents with protein tyrosine kinase inhibitors may prove especially beneficial in the treatment of breast cancer (Constantinou *et al.*, 1998).

It is evident from the above discussion, that the benzopyrones exert a number of effects on important components of cell signalling pathways. To further the investigation of the effects of the benzopyrones on signalling components and pathways it was decided to investigate the effect of esculetin and warfarin on tyrosine phosphorylation within cells as this type of phosphorylation is important to the accurate regulation of growth control.

5.10. Summary of Research Described in This Chapter

The effect of five benzopyrone compounds (warfarin, 4-hydroxycoumarin, 7-hydroxycoumarin, genistein, and esculetin) on proliferation in cultured human tumour cell-lines (MCF-7 and A549) was examined. Previous observations by Kolodziej and colleagues (1997) and Cooke & O'Kennedy (1999) indicated that a dihydroxy-function, in either an ortho- or meta-form of coumarin, was an extremely potent chemical structure for toxicity in human tumour cell lines. In the present study it was decided to concentrate on esculetin (6,7-dihydroxycoumarin), and 7-hydroxycoumarin in order to confirm the increased potency of esculetin in comparison to 7-hydroxycoumarin on the two tumour cell-lines examined. Previous clinical trials suggest warfarin may be more useful as an aid to the management and control of tumour growth rather than its eradication (Zacharski *et al.,* 1984; Zacharski, 1992). Therefore, as part of this research it was necessary to investigate the effect of warfarin on cell proliferation and draw comparisons with the antiproliferative effects of the other coumarins examined. Genistein has shown great promise in previous toxicity studies (Papazisis, 2000; Ratna, 2002; Tanos *et al.,* 2002). Determination of the effects of the benzopyrones on cell proliferation and metabolism was accomplished by performing *in vitro* proliferation assays, three microtitre format assays [Lactate Dehydrogenase assay, Tetrazolium Salt assay (MTT), Acid Phosphatase assay] and cytosensor studies. Signal transduction studies focused on the mechanism of action of esculetin, warfarin and genistein in MCF-7 cells. Investigation of the inhibitory effects of these compounds on tyrosine phosphorylation of the stimulated EGF-R was performed using ELISA. The cytosensor microphysiometer was utilised to determine the effect on tyrosine kinase activity of MCF-7 cells pre-exposed to benzopyrones. Finally, a BrdU ELISA was used to determine the effect of all the compounds on DNA synthesis of exposed MCF-7 cells.

5.11. Results and Discussion

5.11.1. In Vitro Proliferation Assays

Previous investigators have used cell proliferation-based assays in their chemosensitivity assessment of coumarin compounds (Myers *et al.,* 1994: Cooke, 1999). Recently a murine xenograft *in vitro* proliferation assay was utilised to determine the antitumour activities of SP500263, a novel next-generation selective estrogen receptor modulator (SERM), tamoxifen, and raloxifene in an *in vitro* and *in vivo* MCF-7 breast cancer model (Brady *et al.,* 2002). The insensitivity of many human tumour cell lines previously tested to growth inhibition by coumarin, seems to confirm the generally

held belief that coumarin is not responsible for the observed *in vivo* effects, but is a pro-drug for other active metabolites. Therefore, in our research we chose initially to examine three benzopyrone compounds, namely warfarin, esculetin, and genistein under similar assay procedures, for the MCF-7 cell line and the A549 cell line (Table 5.6.). The cell line was exposed to each of the three compounds for 96 hours as outlined in Section 2.5.4.2. In general, cells were exposed to drug concentrations in the range 0-25μg/ml for warfarin, 0-20μg/ml for esculetin, and 0-13.5μg/ml for genistein. Following exposure, cell counts were performed, and the decrease in cell number for drug-treated cells was expressed as a percentage of the increase for solvent-treated control cells, and growth curves were constructed from this data.

Figure 5.13. shows proliferation curves for cells exposed to the three benzopyrone compounds, for the cell line tested – MCF-7, a breast carcinoma cell line. Preliminary studies showed this cell line to be quite sensitive to all compounds and thus exposure to the three compounds is illustrated in the range 0-25μg/ml drug. As shown, all three compounds caused a significant cytostatic effect over the 96 hour exposure period, with genistein illustrating the most potent effect, followed by esculetin, and warfarin, in decreasing order of potency. Figure 5.14. illustrates the effect the three compounds tested have on A549 cells exposed to drug over 96 hours. As with the MCF-7 cell line, warfarin showed the least inhibitory effect over the drug range tested. At the highest concentration of warfarin tested (100μg/ml) there was only ~ 15% decrease in cell proliferation in comparison to control cells. Esculetin was far more potent at inhibiting cell proliferation in these cells, as at the highest concentration (20μg/ml) there was a decrease in cell proliferation by over 80%. For genistein there was a similar decrease of over 80% in cell proliferation at its highest concentration value of 13.5μg/ml. Although genistein at its highest concentration of 13.5μg/ml is just as effective as an inhibitor of cell proliferation as esculetin at the higher concentration of 20μg/ml, the IC_{50} is misleading, as esculetin appears to be a more effective inhibitor of proliferation than genistein. This illustrates the inadequacy of the *in vitro* proliferation assay to accurately determine the effects of drugs on cell proliferation. These results can only be guidelines for further assay development as can be seen in Sections 5.11.2.1 – 5.11.2.4.

274
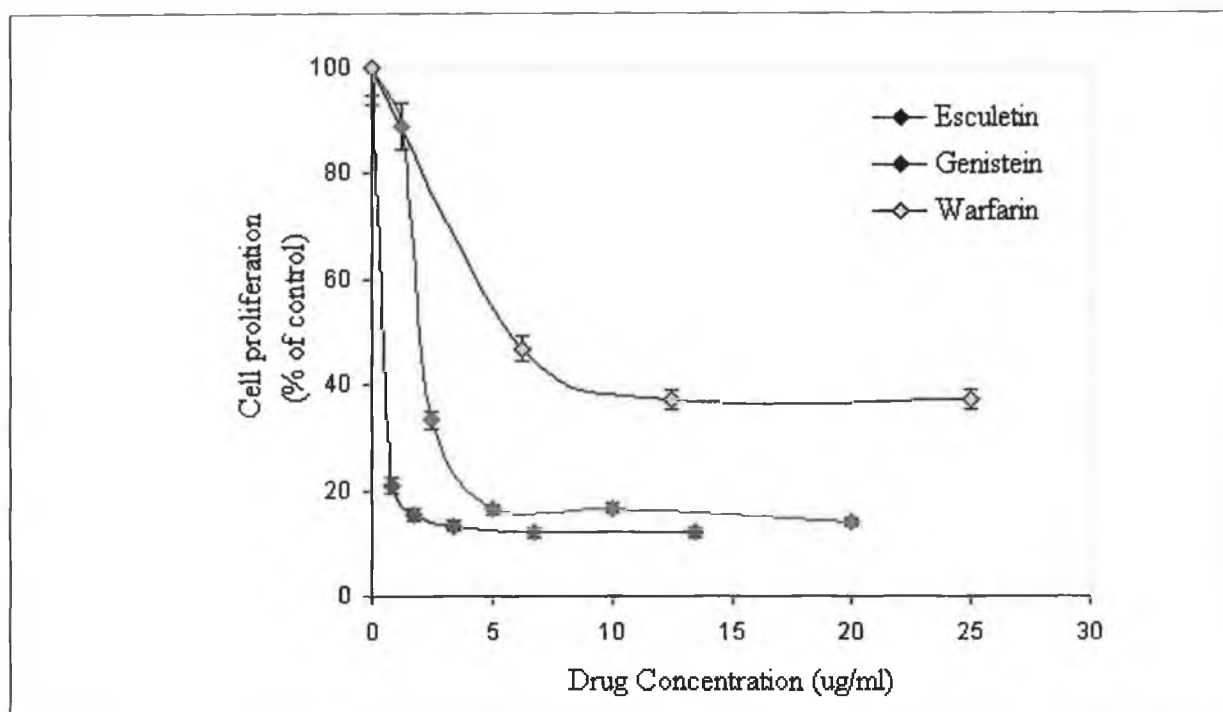
Figure 5.13: *In Vitro Cell Proliferation Assay following exposure of MCF-7 cells to 3 benzopyrone compounds for 96 hours. All experiments were conducted in duplicate on three separate occasions. The decrease in cell number for drug-treated cells was expressed as a percentage of the untreated control cells and plotted versus the appropriate drug concentration. Each experiment was carried out in duplicate on three separate occasions (n=3), and the mean IC_{50} value ($\pm$ standard deviation) for these experiments determined and tabulated (Table 5.6).*
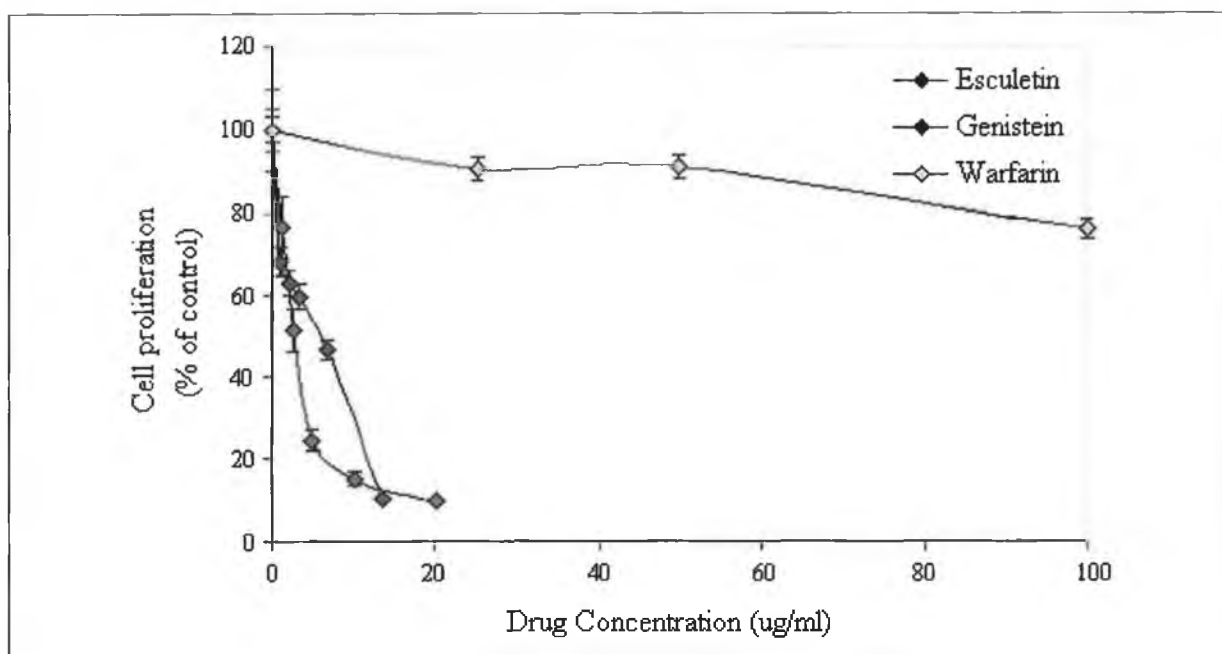
Figure 5.14: In Vitro Proliferation Assay following exposure of A549 cells to 3 benzopyrone compounds for 96 hours. All experiments were conducted in duplicate on three separate occasions. The decrease in cell number for drug-treated cells was expressed as a percentage of the untreated control cells and plotted versus the appropriate drug concentration. Each experiment was carried out in duplicate on three separate occasions (n=3), and the mean IC_{50} value ($\pm$ standard deviation) for these experiments determined and tabulated (Table 5.6).

The proliferation curves in the above Figure 5.14 were utilised to obtain IC_{50} values (IC_{50} value defined as the concentration of drug that causes a 50% inhibition of growth in drug-treated cells as compared to untreated control cells). The most evident trend from the proliferation curves and table of IC_{50} values (Table 5.6.) is the sensitivity of MCF-7 cells tested, to growth inhibition by esculetin (6,7-dihydroxycoumarin). Previous studies by Cooke (1999) have shown that this compound is 10-100 times more inhibitory to cell proliferation than the parent coumarin compound. This reflects well the previous observation by Kolodziej and colleagues (1997), that a dihydroxy-function in either an ortho- or meta-format, was an extremely potent chemical structure for toxicity in two human tumour cell lines, as ascertained by the MTT assay. Since this potency was not evident in either of the single-hydroxycoumarin compounds, the added potency must be due to the existence of a double hydroxy-function on the coumarin ring (Kawase *et al.,* 2003).

Previous studies by Tanos *et al.,* (2002) have shown that genistein inhibits cancer cell proliferation *in vitro*. This effect has been attributed to a competitive inhibition by occupying the

estrogen receptor (ER) of the cell or to inhibition of several key enzymes, especially tyrosine kinases, which are thought to be involved in the control of cell proliferation, carcinogenesis and are associated with oncogene expression in breast cancer (Tanos, 2002). From Figure 5.13 - 5.14 and Table 5.6. it can be seen that genistein is more potent inhibitor to cell proliferation than esculetin.

Cell Line	IC_{50} Warfarin ($\mu g/ml$)	IC_{50} Esculetin ($\mu g/ml$)	IC_{50} Genistein ($\mu g/ml$)
A549	> 150	3.0 ± 0.68	5.9 ± 0.10
MCF-7	5.8 ± 0.73	2.0 ± 0.28	0.5 ± 0.04

Table 5.6: IC_{50} *values determined for the exposure of 2 cell lines to benzopyrones. The* IC_{50} *value is defined as the concentration that causes a 50% inhibition of growth in drug-treated cells, as compared to untreated control cells. Each experiment was carried out in duplicate on three separate occasions (n=3), and the mean* IC_{50} *value (± S.D.) for these experiments determined and tabulated above.*

5.11.2. Further Chemosensitivity Testing

As outlined in Section 5.1, cell proliferation assays are only one of a number of chemosensitivity tests, which can be used to examine the response of cells to chemical agents. Therefore, as part of our study into the effects of benzopyrones on cultured cells, it was decided not to limit this investigation solely to the anti-proliferative effects of these agents, as many investigators in the past have done, but to also examine the effect of these compounds on other cellular mechanisms. In order to increase the number of assay formats performed and include signal transduction studies it was decided to limit this investigation to two human cell lines, the MCF-7 breast carcinoma and A549 a lung carcinoma cell line. The MCF-7 cell line was chosen for the presence of its estrogen receptor. Cellular proliferation is induced (Section 5.6.1) when this receptor is stimulated by estrogen or estradiol. Previous studies (Section 1.8.1.2.) have shown that genistein is a phytoestrogen. For cells possessing the estrogen receptor exposure to low doses (0.1-10μM) of genistein results in increased cellular proliferation due to the "estrogen-like" stimulation of the estrogen receptor. A549 cells do not possess the estrogen receptor. Hence, no estrogen receptor-induced cell proliferation should be observed when these cells are exposed to genistein. The microtitre assays described in the following sections were utilised to determine what effect genistein and the other benzopyrones had on the cellular proliferation of both cell lines.

5.11.2.1. Lactate Dehydrogenase (LDH) Assay

Cytotoxicity studies with culture systems provide useful information for understanding the effects of compounds on human tumour cell lines. Use of the LDH assay along with other types of assays (MTT, AP) can yield this information.

Although the LDH assay gives a rapid and simple quantification of cellular damage, one disadvantage of the assay is the possibility that the test compound may inhibit the LDH enzyme activity, causing underestimation of membrane damage. The test compound may also react with other assay components causing interference, which may lead to inaccurate results. Therefore, it is essential when assessing membrane damage with the LDH assay, that these two possible interferences are excluded. Inhibition of LDH activity is tested by incubating a standard LDH solution with various drug concentrations, and determining the activity of the enzyme in the presence of these drug concentrations. The second interference can be discounted by incubating the drug in culture media with the LDH Assay reagents and detecting whether presence of the drug gives rise to an increased absorbance at 492nm (assay absorbance wavelength) compared to drug-free culture medium. This interference testing was accomplished for all four coumarin compounds under investigation (esculetin, warfarin, 7-hydroxycoumarin, and 4-hydroxycoumarin as shown in Figure 5.15. This diagram illustrates that none of the four compounds are inhibitors of the enzyme activity (top), or react with the assay components yielding interfering species (bottom).

278
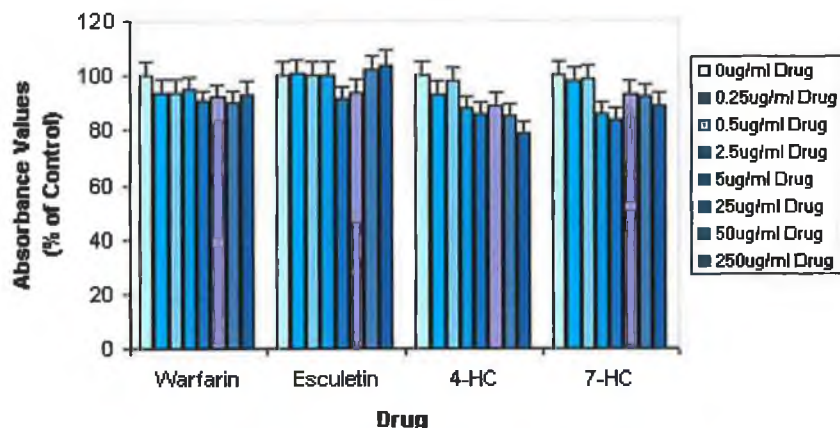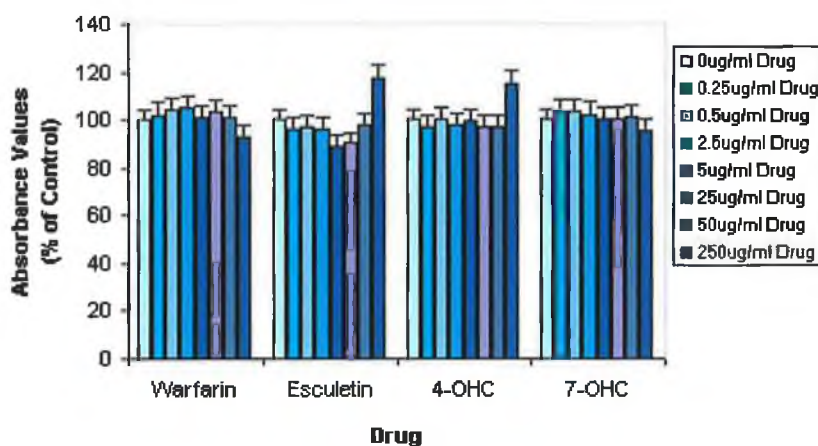
Figure 5.15: *Control tests confirming that coumarin compounds (0.25-250ug/ml) do not interfere with LDH Assay reagents. Results (A_{492nm}) for drug solutions are expressed as a percentage of control absorbance (A_0) at 492nm. The coumarins when incubated with an LDH standard (0.1U/ml) did not inhibit this LDH activity (top). A_0 for LDH standard (0.1U/ml) = 0.354 $\pm$ 0.024. The coumarins when incubated with culture medium alone did not interfere significantly with other LDH reagents (bottom). Ao for control medium = 1.376 $\pm$ 0.021*

Different cell types may contain different amounts of LDH. Therefore, it was necessary to determine the optimum cell concentration for both cell lines used in this experiment. This cell concentration (5 X 10^4 cells/well) was determined from graphs (Figure 5.16) in which the difference between the low (spontaneous LDH release) and high (maximal LDH release) control is at a maximum and this cell concentration was used in all subsequent assays.
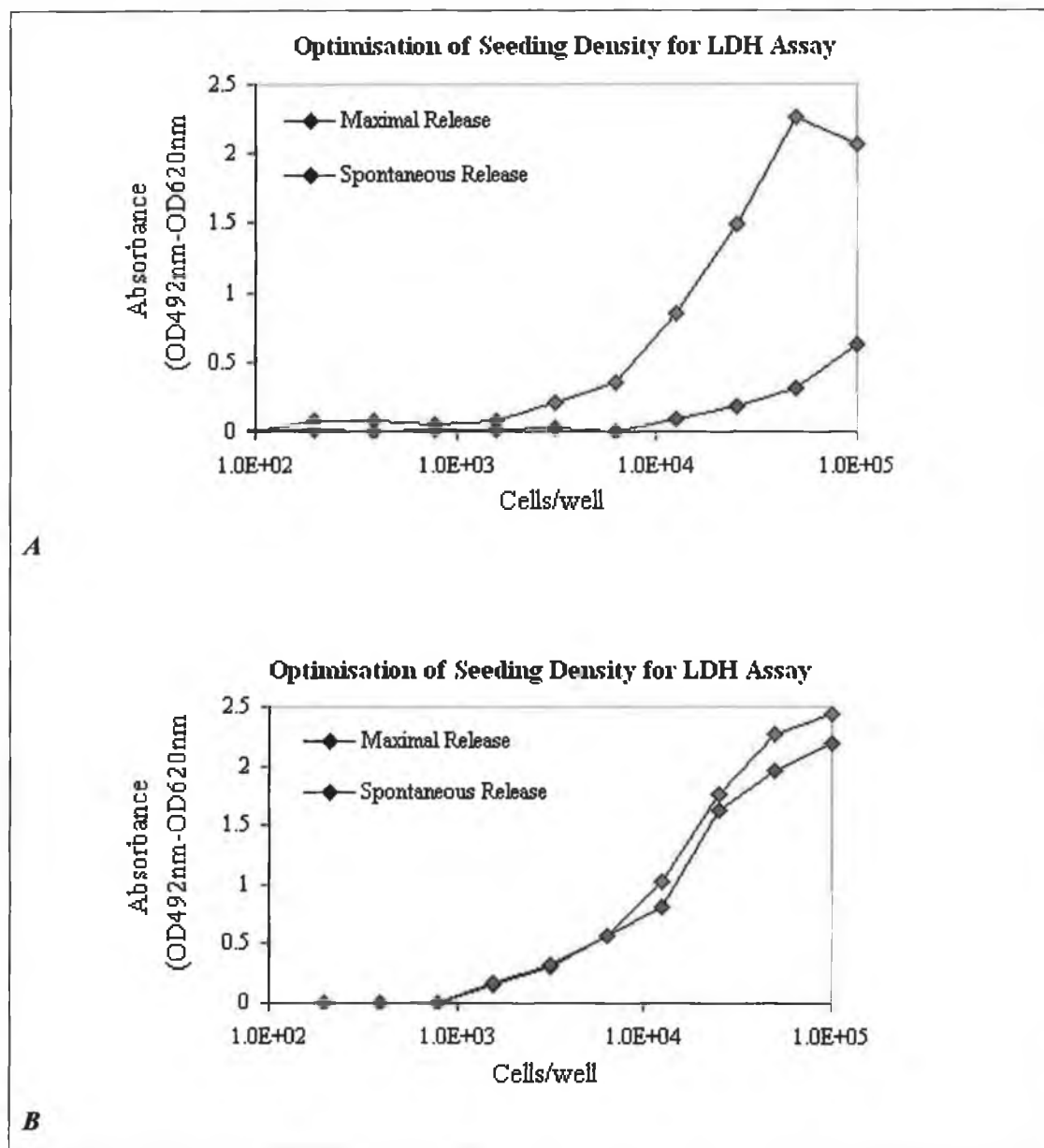
Figure 5.16: Determination of the optimal target cell concentration for both MCF-7 (A) and A549 (B) cell lines.

Having excluded interferences, both cell lines were incubated with the four coumarins (range 0.25-250μg/ml) for 24 hours and the culture supernatants assessed for enzyme release using the LDH assay as outlined in section 2.5.4.3. A 1% (v/v) Triton X-100 solution in culture medium was used as a positive control representing 100% membrane damage. The absorbances at 492nm for cells exposed to Triton X-100 were normalised at 100% and absorbances of cells exposed to the various drug concentrations expressed as a percentage of this positive control (Figure 5.17 and 5.18.). It is evident from the graphs that 24 hour exposure of both cell lines to 4-hydroxycoumarin warfarin and 7-hydroxycoumarin caused no significant membrane damage when compared to untreated cells. However, A549 cells (Figure 5.17) appeared to be sensitive to the effects of esculetin (25-250 μg/ml) as there was 30-40% LDH release indicating the occurrence of membrane damage to the cells. The MCF-7 cells did not appear to be as sensitive to the effects of esculetin (Figure 5.18). At the highest concentration (250 μg/ml) there was ~25% LDH release indicating slight membrane damage in comparison to control treated cells.
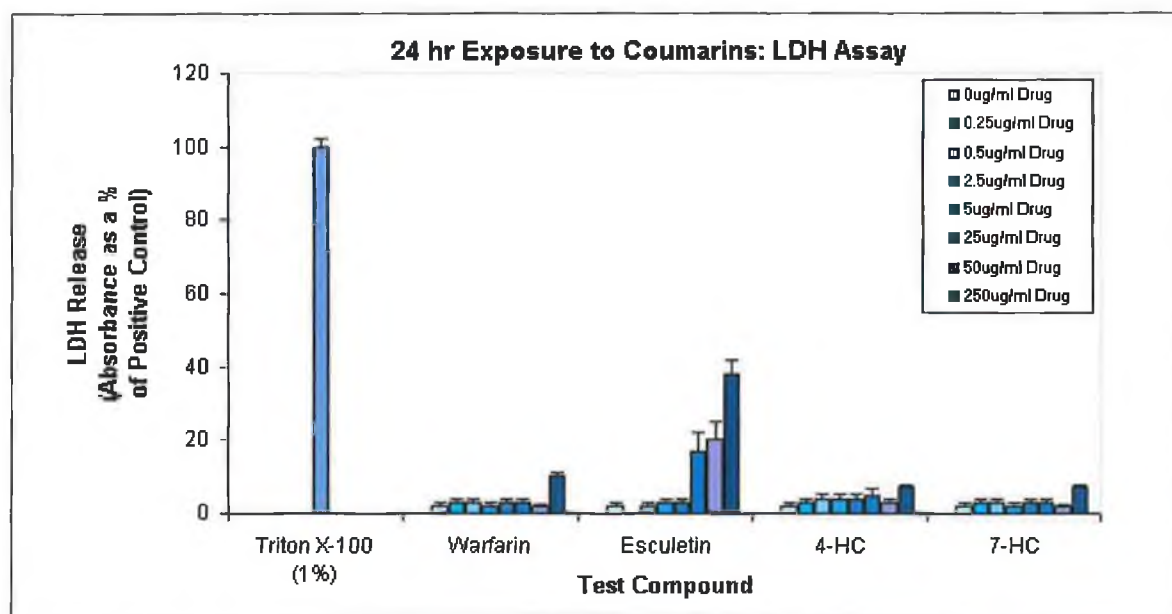
Figure 5.17: *LDH Assay of culture supernatants of A549 cells exposed to coumarins (0-250μg/ml) for 24 hours. Results (A492nm) for coumarin-treated cells are expressed as a percentage of A492nm of positive control (Triton X-100) cells (Abs=1.93± 0.019). Each drug was tested in five separate wells/plate, and the experiment was carried out on three separate occasions (n=3).*
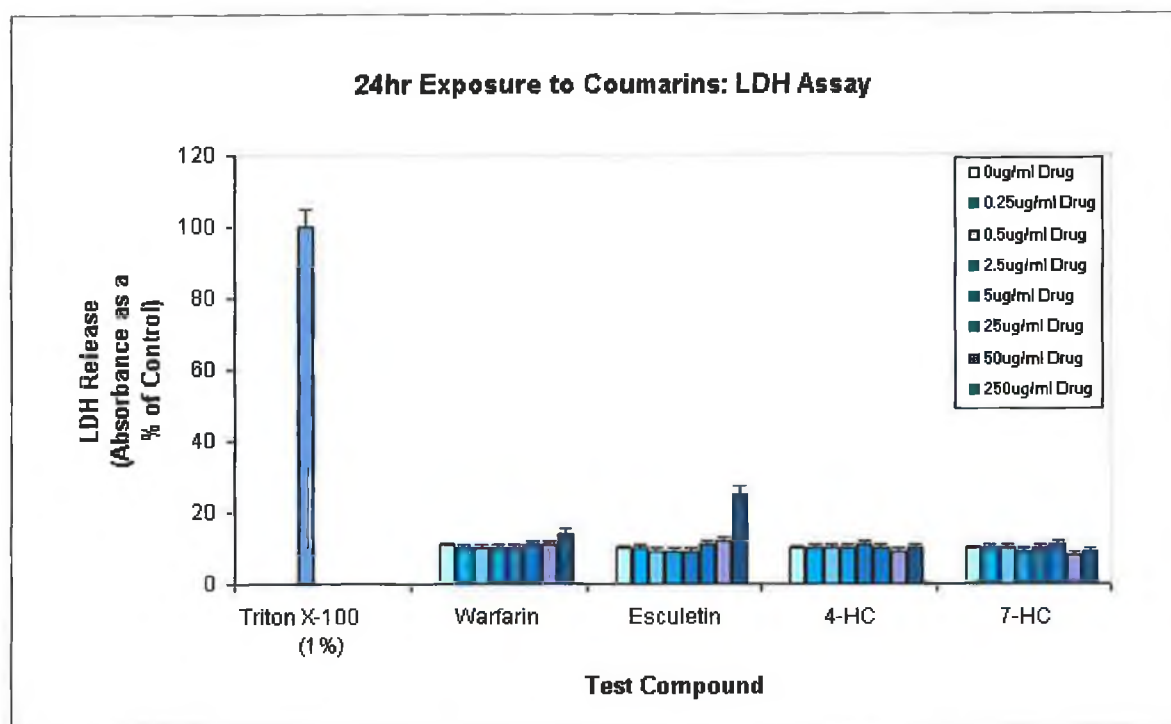
Figure 5.18: *LDH Assay of culture supernatants of MCF-7 cells exposed to coumarins (0-250µg/ml) for 24 hours. Results (A492nm) for coumarin-treated cells are expressed as a percentage of A492nm of positive control (Triton X-100) cells (Abs=1.823 ± 0.031). Each drug was tested in five separate wells/plate, and the experiment was carried out on three separate occasions (n=3).*

5.11.2.2. MTT Assay

The MTT Assay is a well-established colourimetric assay, which can be used to detect the effects of agents on cellular metabolism. The assay is based on the cleavage of the yellow tetrazolium salt, MTT (3-[4,5-dimethylthiazol-2-yl]-2,5-diphenyltetrazolium bromide), to purple formazan crystals by mitochondrial dehydrogenases. Therefore, cells must not only be alive, but also metabolically active for this reaction to occur (Cooke, 1999). The assay can be used in either a long- (96hr) or short-term (24hr) drug-exposure format, to assess the effects of a drug on cellular growth or metabolism, respectively. Previously, the MTT assay has been used to assess the anti-proliferative effects of coumarins (Kumi-Diaka, 2002; Krebs *et al.,* 2002).

The assay was carried out as outlined in Section 2.5.4.4. Prior to determining the effects of the benzopyrone compounds on cellular metabolism in MCF-7 cells and A549 cells, optimisation of cell seeding density (Figure 5.19) and interference testing (Figure 5.20) were necessary. Optimum seeding density of both cell lines was found to be 5 X 10^5 cells/ml, and this was used in all subsequent assays.

Incubating the MTT reagents with drug concentrations in the absence of cells (Figure 5.20) tested interference effects of the coumarins. Warfarin, 7-hydroxycoumarin and genistein did not interfere with the tetrazolium salt. However, esculetin reacts mildly with the tetrazolium salt in the concentration range 0-10µg/ml, but intensely at concentrations >10µg/ml. Therefore, all subsequent MTT assays were conducted with an esculetin concentration range of 0-25µg/ml and absorbance values were corrected for the interference effects. The significance of any reduction in cellular viability was determined using a paired Student's t-test with confidence limits set at 95%. A probability of 0.05 ($P<0.05$) or less was deemed statistically significant.

Figure 5.19: *Optimisation of seeding density of A549 (top) and MCF-7 (bottom) cells for MTT assay. 5 x 10⁵ cells/ml was chosen as the optimum density for both cell lines as it gave a high A560nm value at a pre-plateau point on the curve.*
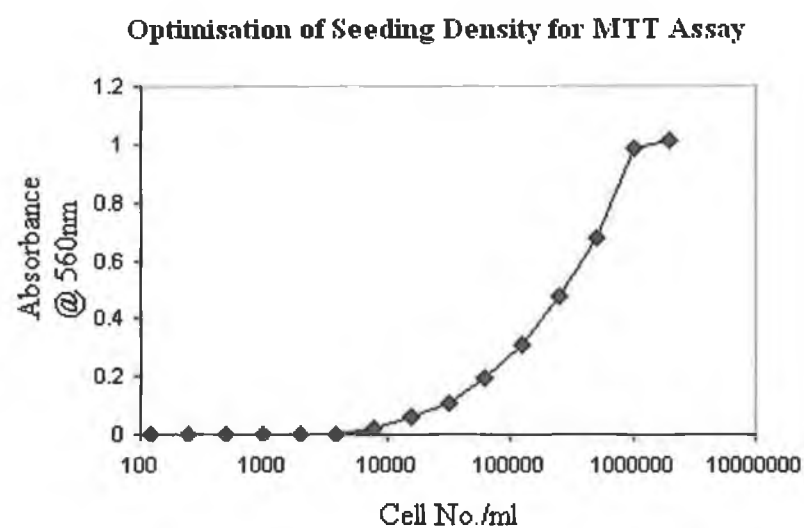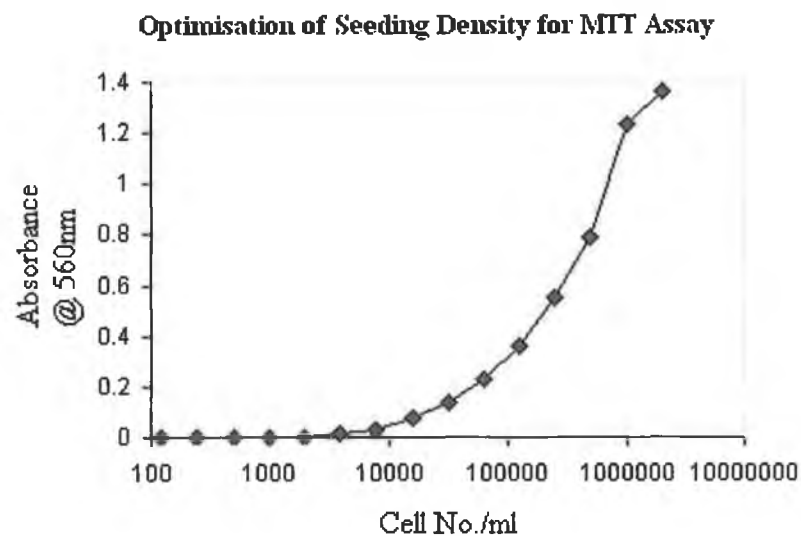
Figure 5.19: *Optimisation of seeding density of A549 (top) and MCF-7 (bottom) cells for MTT assay. 5 x 10^5 cells/ml was chosen as the optimum density for both cell lines as it gave a high A560nm value at a pre-plateau point on the curve.*
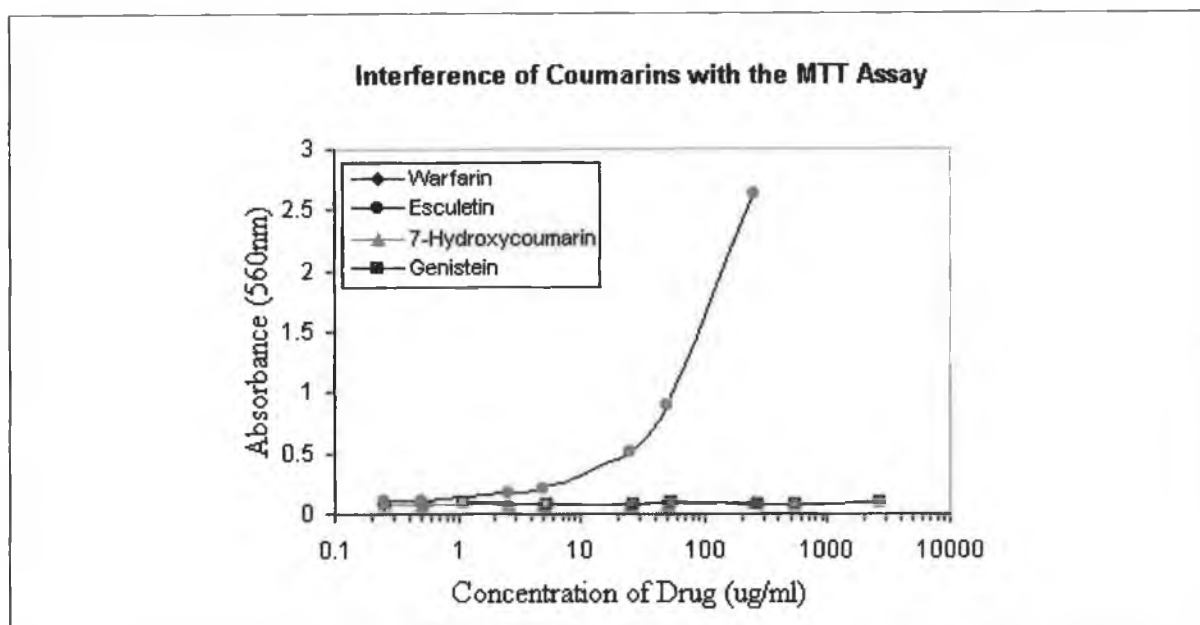
Figure 5.20: *Examination of the interference of benzopyrone compounds with MTT tetrazolium salt in the absence of cells. Neither warfarin, 7-hydroxycoumarin nor genistein interfere, but esculetin reacts intensely with the MTT salt especially at concentrations >10µg/ml.*

MTT assays were conducted on both cell lines for warfarin and 7-hydroxycoumarin in the concentration range 0-250µg/ml, esculetin concentration range 0-25µg/ml and genistein concentration range 0-100µM, with 24hr drug exposure. The results were plotted as A/Ao, where A represents the absorbance value at a given drug concentration (e.g. 100µg/ml esculetin) and Ao represents the absorbance value at 0µg/ml drug exposure. Therefore, the A/Ao value for cells exposed to 0µg/ml of drug should equal 1.0 or 100 when expressed as a percentage value. Figures 5.21 to 5.24 show the results for these experiments. From Figure 5.21 (A549 cells) and Figure 5.23 (MCF-7 cells) it can be seen that neither 7-hydroxycoumarin nor warfarin exerted any significant adverse effect on the metabolic activity of mitochondrial dehydrogenases in cells exposed to these drugs for 24hrs. Exposure of both cell lines to genistein (Figure 5.22 & Figure 5.24) indicates there is a slight decrease in mitochondrial dehydrogenase activity up to 10µM. From 25-100µM genistein there is an underestimation of the growth inhibitory effects of the drug, which is explained in Section 5.12. Esculetin was the only compound to show a significant decrease in mitochondrial dehydrogenase activity throughout the concentration range (0-25µg/ml) for both cell lines. Although interference effects were compensated for, these results require comparison with other assay formats (e.g. cytosensor and acid phosphatase assay) where interference effects are not a problem. Comparison to the Cytosensor microphysiometer shows that the MTT assay results are not as reliable as the Cytosensor results over 24 hours (Section 5.11.2.4.).

Figure 5.21: *MTT assay results determining the effect of 24hr exposure of benzopyrones on the metabolic activity of A549 cells. The above graphs represent 24hr exposure to 7-hydroxycoumarin (top) and warfarin (bottom) in the concentration range 0-250μg/ml. All drug concentrations were tested in five separate wells/plate on three separate occasions. All absorbances (550nm) of test wells were expressed as a percentage of control well absorbances (Ao).Ao for 7-hydroxycoumarin = 0.770 ± 0.024; Ao for warfarin = 0.790 ± 0.018. It is evident from Table 5.7 that both compounds have no significant effect on metabolic activity (formazan formation).*

24hr Exposure to Genestin: MTT Assay

24hr Exposure to Esculetin: MTT Assay

Figure 5.22: MTT assay results determining the effect of 24hr exposure of benzopyrones on the metabolic activity of A549 cells. The above graphs represent 24hr exposure to genistein (top) and esculetin (bottom) in the concentration range 0-100μM and 0-250μg/ml respectively. All drug concentrations were tested in five separate wells/plate on three separate occasions. All absorbances (550nm) of test wells were expressed as a percentage of control well absorbances (Ao). Ao for genistein = 0.750 ± 0.021; Ao for esculetin = 0.832 ± 0.023. An explanation for the increase in absorbance as genistein concentration (25-100μg/ml) increases, is explained in Section 5.12.

Figure 5.23: *MTT assay results determining the effect of 24hr exposure of benzopyrones on the metabolic activity of MCF-7 cells. The above graphs represent 24hr exposure to 7-hydroxycoumarin (top) and warfarin (bottom) in the concentration range 0-250μg/ml. All drug concentrations were tested in five separate wells/plate on three separate occasions. All absorbances (550nm) of test wells were expressed as a percentage of control well absorbances (Ao). Ao for 7-hydroxycoumarin = 0.826 ± 0.016; Ao for warfarin = 0.850 ± 0.017. There is slight decrease (5-10%) in formazan production and hence metabolic activity for both compounds (0-5μg/ml. At the higher concentrations (25-250μg/ml) there is an increase in absorbance values (overestimation), which may be due to cell cycle perturbations, or formazan production in lethally damaged cells.*

24hr Exposure to Genestein: MTT Assay

24hr Exposure to Esculetin: MTT Assay
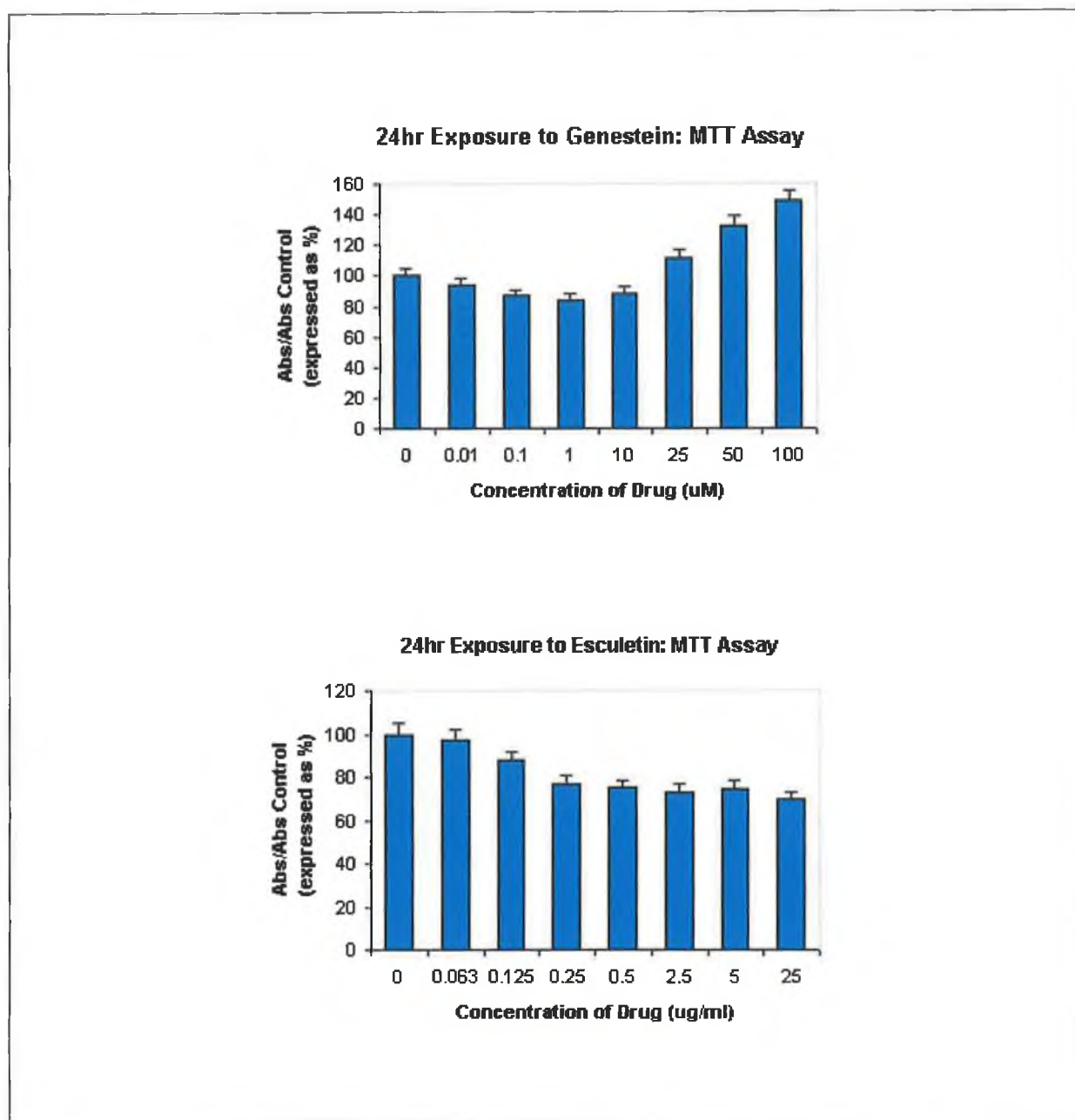
Figure 5.24: *MTT assay results determining the effect of 24hr exposure of benzopyrones on the metabolic activity of MCF-7 cells. The above graphs represent 24hr exposure to genistein (top) and esculetin (bottom) in the concentration range 0-100μM and 0-250μg/ml respectively. All drug concentrations were tested in five separate wells/plate on three separate occasions. All absorbances (550nm) of test wells were expressed as a percentage of control well absorbances (Ao). Ao for genistein = 0.848 ± 0.015; Ao for esculetin = 0.865 ± 0.028.*

Table 5.7: *Significance of the reduction in cellular viability. A probability of 0.05 (P<0.05) or less was deemed statistically significant.*

Compound	MCF-7 Significance P Value	A549 Significance P Value
Warfarin (μg/ml)		
0.25	>0.05	>0.05
0.5	<0.01	>0.05
2.5	<0.05	>0.05
5	<0.01	>0.05
25	>0.05	>0.05
50	<0.01	<0.01
250	<0.0001	<0.01
7-OHC (μg/ml)		
0.25	<0.01	>0.05
0.5	<0.0001	>0.05
2.5	<0.0001	<0.05
5	<0.0001	>0.05
25	<0.01	>0.05
50	<0.01	>0.05
250	<0.01	>0.05
Esculetin (μg/ml)		
0.063	<0.01	>0.05
0.125	<0.01	<0.01
0.25	<0.0001	<0.01
0.5	<0.0001	<0.0001
2.5	0.0001	<0.01
5	>0.05	0.01
25	<0.0001	<0.0001
Genistein (μM)		
0.01	0.01	>0.05
0.1	<0.0001	<0.05
1	<0.0001	>0.05
10	<0.01	<0.01
25	<0.01	>0.05
50	<0.0001	<0.0001
100	<0.0001	<0.0001

5.11.2.3. Acid Phosphatase Assay

The acid phosphatase assay can quantitate cells in culture by determination of intracellular enzyme activity (acid phosphatase). This assay was used as a different microtitre assay format (to yield benzopyrone cell proliferation inhibitory effects data) for comparison to the MTT microtitre assay results (Section 5.11.2.2). Following the removal of the growth medium from cells grown in 96-well culture plates, cells are lysed in buffer containing the detergent Triton X-100 and the phosphatase substrate *p*-nitrophenyl phosphate (pNPP). After two hours at 37°C, the reaction is stopped with sodium hydroxide, and colour development is determined using a rapid multiwell plate reader. In a paper by Connolly *et al.* (1986), linear activity of the enzyme was demonstrated for cell numbers over the range 100 to 10,000 endothelial cells per well. This miniaturised, semiautomated, colorimetric assay was used to determine growth curves for endothelial cells in the presence and absence of endothelial growth factor from bovine hypothalmus and to monitor fractions during purification of growth factors. In the work described in this thesis, the assay was applied to cytotoxicity testing (Martin, 1992).

Both 7-hydroxycoumarin and warfarin do not have a significant adverse effect on A549 cells over 96 hours in the range 0-50µg/ml. However, there is a decrease (approximately 50%) in proliferation at a concentration of 250µg/ml for both compounds (Figure 5.25.). There was a gradual decrease in proliferation in the A549 cell line when exposed to esculetin (range 0-25µg/ml). At the highest drug concentration there was approximately a 70% decrease in cell proliferation when compared to control cells with no drug present in the media. Genistein seems to be the most potent of all the compounds on A549 cells (Figure 5.26.). There was a significant decrease in cell proliferation (approx. 80%) at the highest concentration (100µM) of genistein.

Results were slightly different for MCF-7 cells due to the stimulation of the estrogen receptor (ER) present in this cell line by the compounds. Stimulation of the ER promotes cell proliferation and is evident with low dose levels of genistein exposed MCF-7 cells. 7-hydroxycoumarin has a detrimental effect on proliferation (~55%), which is most apparent in the concentration range 25-250µg/ml (Figure 5.27.). Warfarin has a slightly more effective inhibition (~60% decrease in proliferation) on MCF-7 cells than A549 cells. This compound may stimulate the estrogen receptor (ER) between 0.5 and 2.5µg/ml (Figure 5.27). However, it inhibits cell proliferation from 5-250µg/ml. Esculetin has a similar effect on MCF-7 cells as it did on A549 cells. It is evident from the graph in Figure 5.28. that there is approximately 70% decrease in proliferation of MCF-7 cells exposed to esculetin. Similar to previous studies (Hsieh *et al.*, 1998; Clarke *et al.*, 2001), it was expected that

291

genistein would act like estrogen at low concentrations (0.01 to 1µM). Figure 5.17 illustrates that in this concentration range there is a maximum increase of 30% in cell proliferation as compared to control cells. At higher concentrations (10-100µM) genistein inhibits cell proliferation by up to 75% in comparison to control cells (0 µg/ml genistein exposure). The significance of any reduction in cellular viability was determined using a paired Student's t-test with confidence limits set at 95%. A probability of 0.05 (P<0.05) or less was deemed statistically significant.

96hr Exposure to 7-Hydroxycoumarin: AP Assay

96hr Exposure to Warfarin: AP Assay
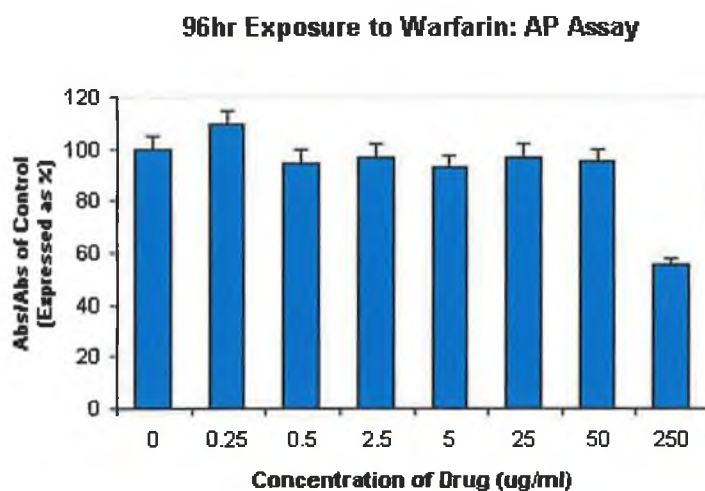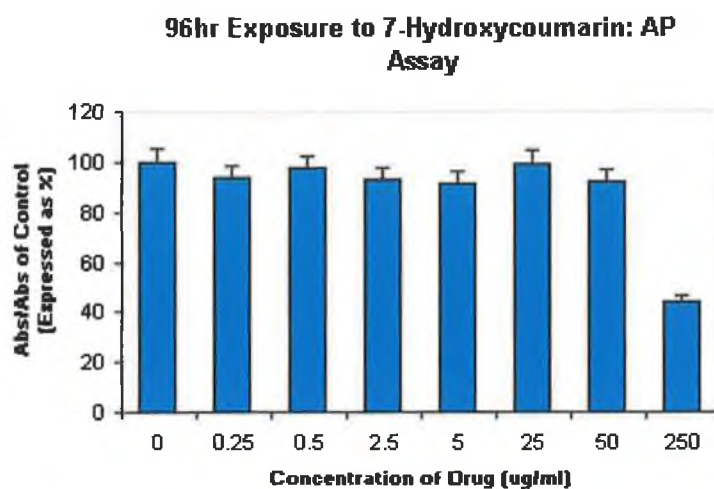
Figure 5.25: *Acid phosphatase assay results determining the effect of 96hr exposure of benzopyrones on the metabolic activity of A549 cells. The above graphs represent 96hr exposure to 7-hydroxycoumarin (top) and warfarin (bottom) in the concentration range 0-250μg/ml. All drug concentrations were tested in five separate wells/plate on three separate occasions. All absorbances (405nm) of test wells were expressed as a percentage of control well absorbances (Ao). Ao for 7-hydroxycoumarin = 0.929 ± 0.027; Ao for warfarin = 0.905 ± 0.023. Only at 250μg/ml exposure to both drugs is there a significant decrease in A/Ao values (~50%) indicating a decrease cell proliferation due to drug exposure.*
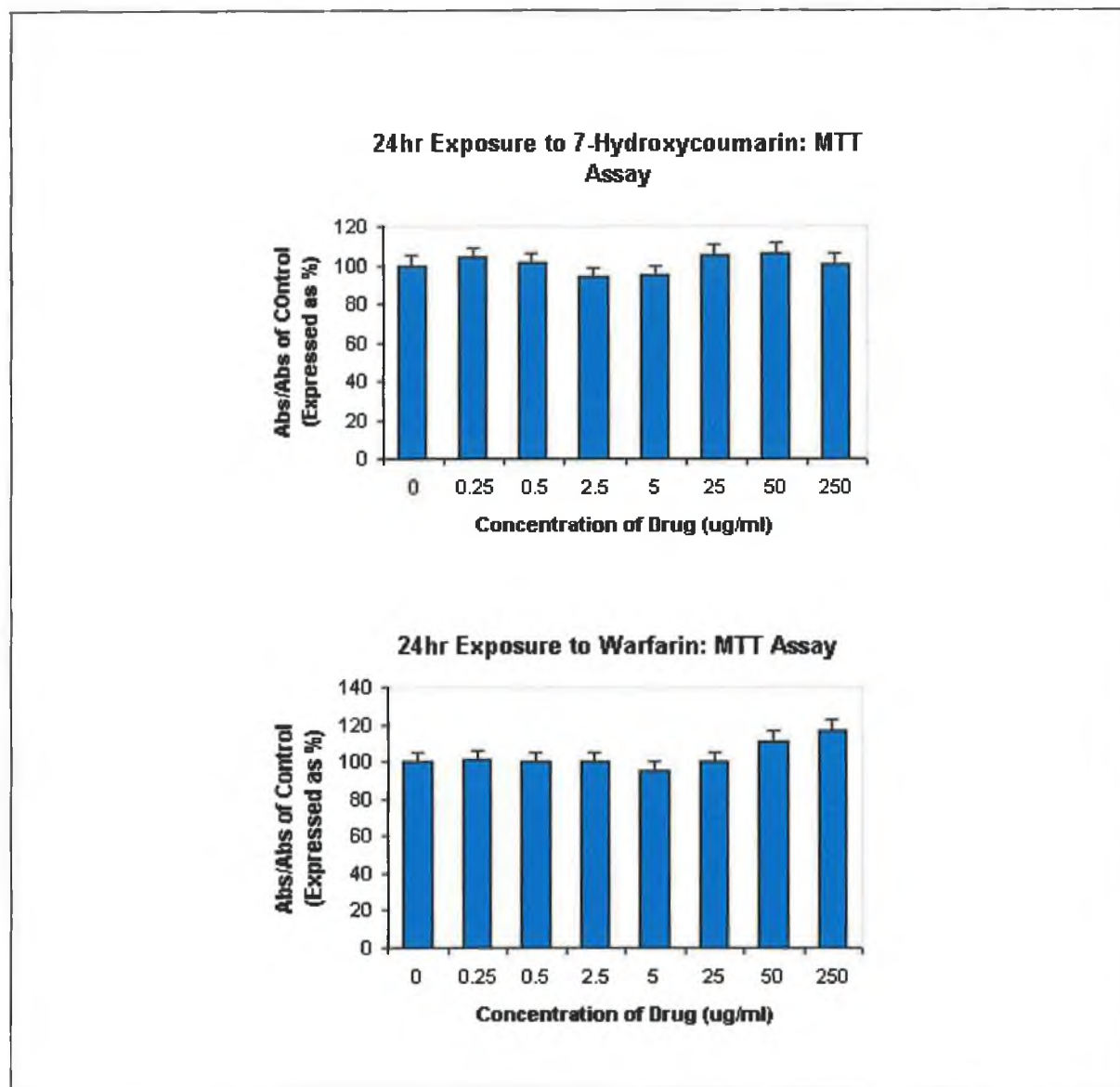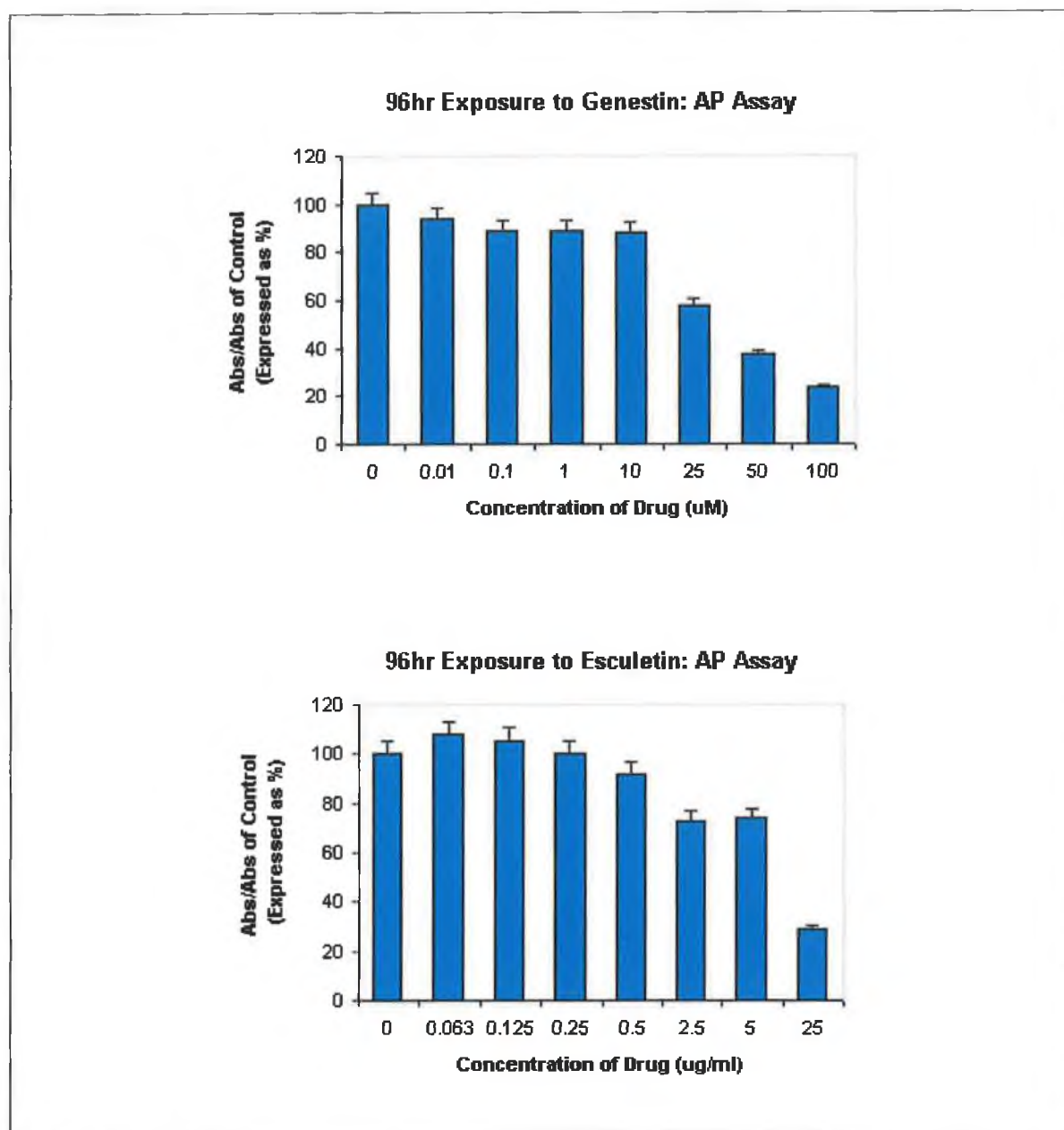
Figure 5.26: *Acid phosphatase assay results determining the effect of 96hr exposure of benzopyrones on the metabolic activity of A549 cells. The above graphs represent 96hr exposure to genistein (top) and esculetin (bottom) in the concentration range 0-100μM and 0-25μg/ml, respectively. All drug concentrations were tested in five separate wells/plate on three separate occasions. All absorbances (405nm) of test wells were expressed as a percentage of control well absorbances (Ao). Ao for genistein = 1.089 ± 0.029; Ao for esculetin = 1.012 ± 0.025.*

96hr Exposure to 7-Hydroxycoumarin: AP Assay

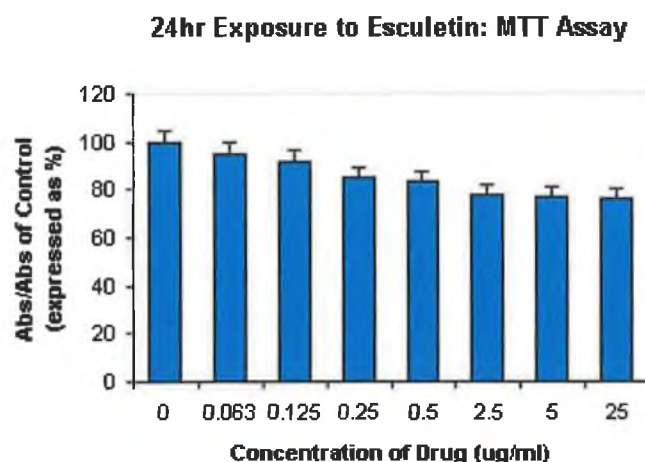**96hr Exposure to Warfarin: AP Assay**
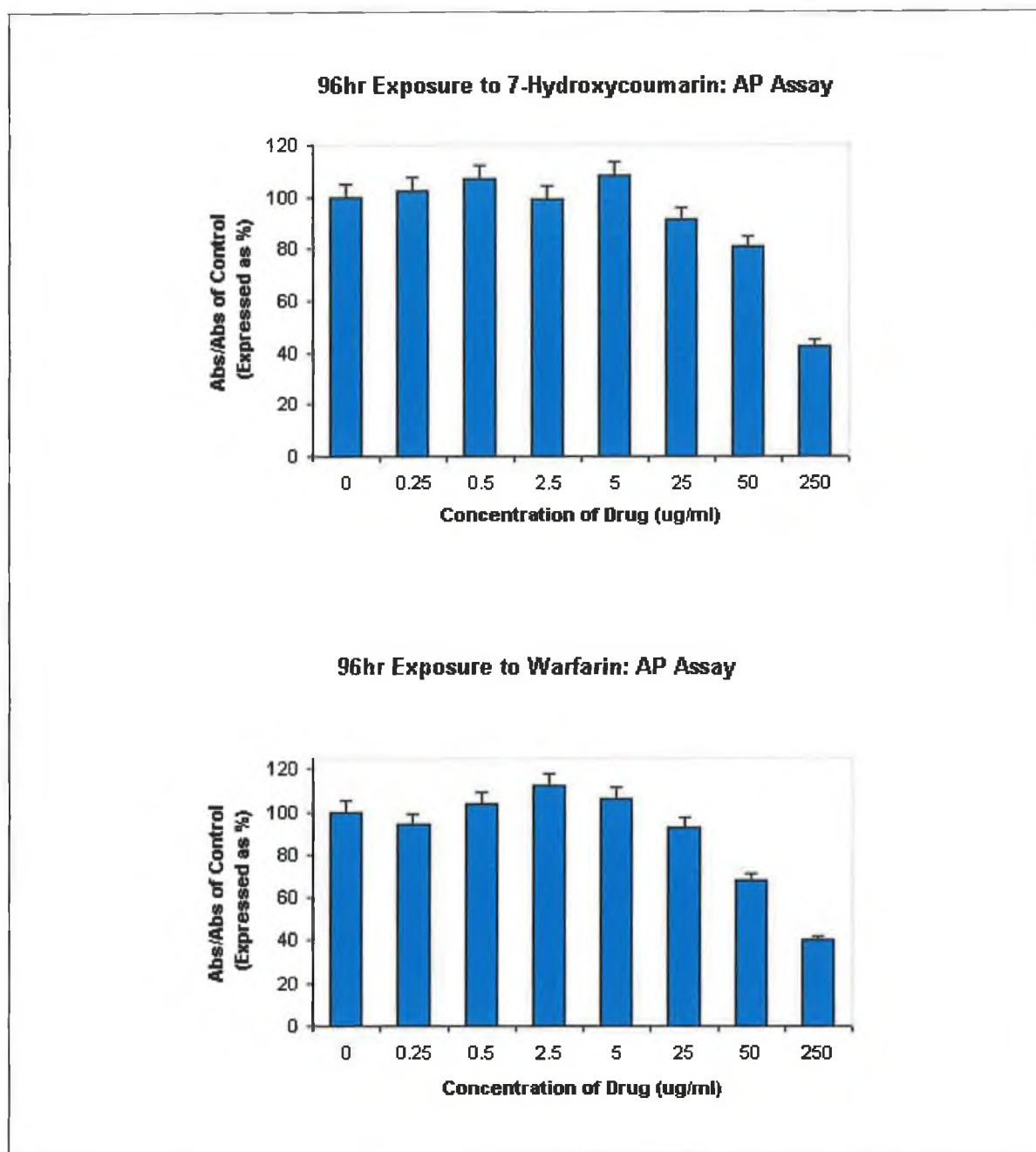
Figure 5.27: *Acid phosphatase assay results determining the effect of 96hr exposure of benzopyrones on the metabolic activity of MCF-7 cells. The above graphs represent 96hr exposure to 7-hydroxycoumarin (top) and warfarin (bottom) in the concentration range 0-250µg/ml. All drug concentrations were tested in five separate wells/plate on three separate occasions. All absorbances (405nm) of test wells were expressed as a percentage of control well absorbances (Ao). Ao for 7-hydroxycoumarin = 0.852 ± 0.031; Ao for warfarin = 0.869 ± 0.028.*

96hr Exposure to Genestin: AP Assay

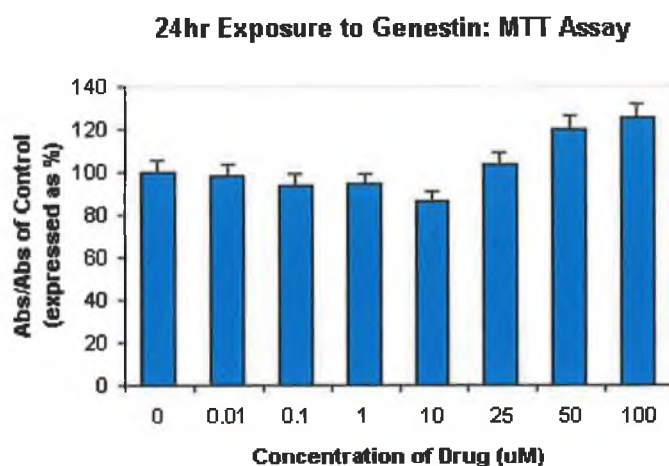**96hr Exposure to Esculetin: AP Assay**

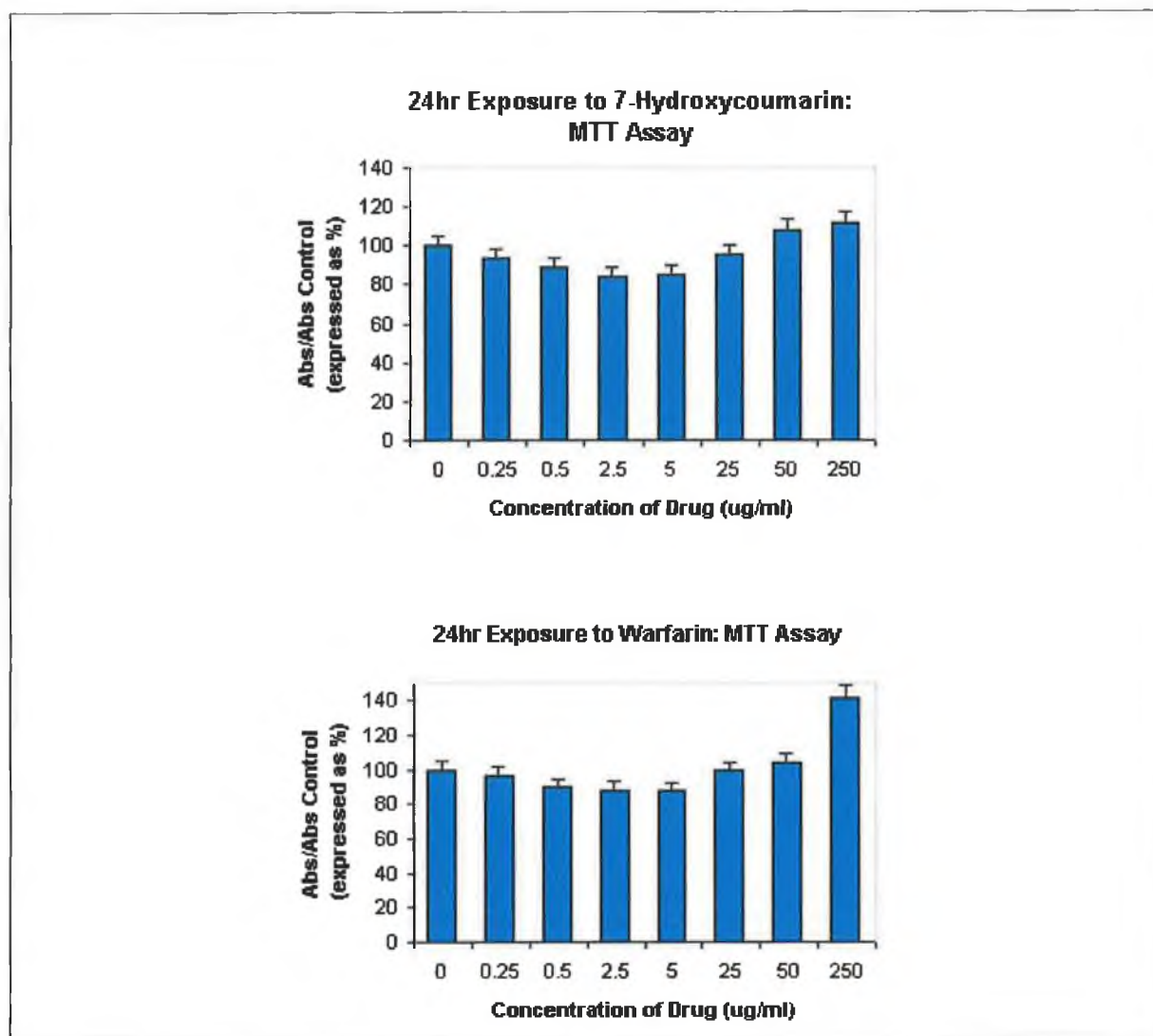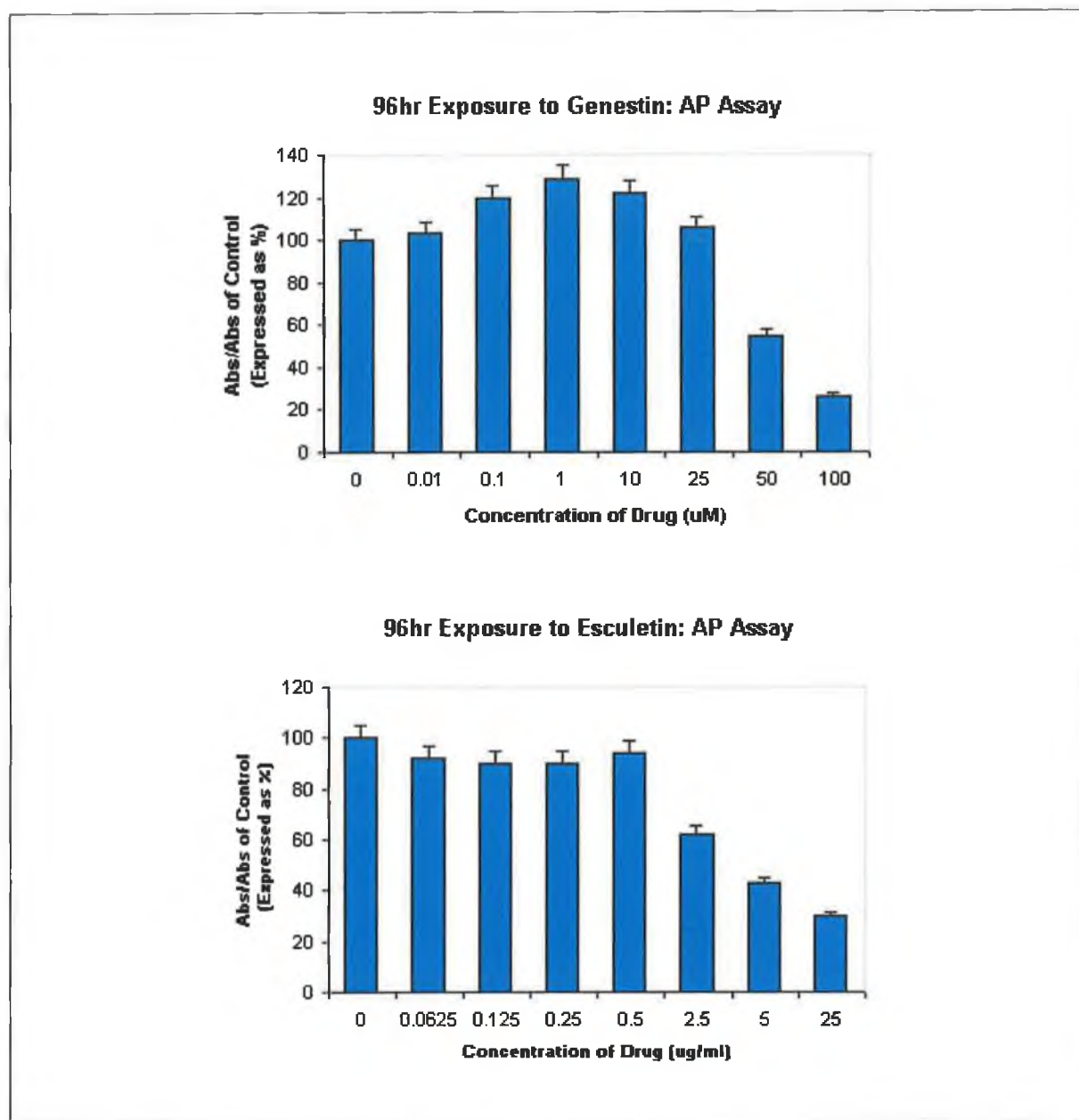*Figure 5.28:* *Acid phosphatase assay results determining the effect of 96hr exposure of benzopyrones on the metabolic activity of MCF-7 cells. The above graphs represent 96hr exposure to genistein (top) and esculetin (bottom) in the concentration range 0-100μM and 0-250μg/ml, respectively. All drug concentrations were tested in five separate wells/plate on three separate occasions. All absorbances (405nm) of test wells were expressed as a percentage of control well absorbances (Ao). Ao for genistein = 0.962 ± 0.018; Ao for esculetin = 0.951 ± 0.022. The Biphasic effect of genistein is explained in Section 5.12 and esculetin has a similar effect on MCF-7 cells as is evident on A549 cells (Figure 5.26).*

Table 5.8: *Significance of the reduction in cellular viability. A probability of 0.05 (P<0.05) or less was deemed statistically significant.*

Compound	MCF-7 Significance P Values	A549 Significance P Values
Warfarin (μg/ml)		
0.25	>0.05	>0.05
0.5	>0.05	>0.05
2.5	>0.05	<0.01
5	>0.05	<0.01
25	<0.01	<0.01
50	<0.01	<0.01
250	<0.01	<0.0001
7-OHC (μg/ml)		
0.25	>0.05	>0.05
0.5	<0.05	>0.05
2.5	>0.05	<0.01
5	>0.05	<0.0001
25	<0.01	<0.01
50	<0.01	<0.0001
250	<0.0001	<0.0001
Esculetin (μg/ml)		
0.063	>0.05	<0.01
0.125	>0.05	<0.01
0.25	<0.05	<0.01
0.5	>0.05	<0.05
2.5	<0.0001	>0.05
5	<0.0001	<0.05
25	<0.0001	<0.01
Genistein (μM)		
0.01	>0.05	>0.05
0.1	<0.01	>0.05
1	<0.0001	>0.05
10	<0.0001	>0.05
25	>0.05	<0.0001
50	<0.0001	<0.0001
100	<0.0001	<0.0001

5.11.2.4. Cytosensor Microphysiometer

An alternative method was used to evaluate the effect of coumarins on cellular metabolism. As described in detail in Section 5.3.2, this biosensing instrument determines the extracellular acidification rate of cells, which is closely coupled to their basal metabolic rate. Monitoring of cellular metabolism is achieved using a pH-sensitive sensor, in 'real-time', which offers distinct advantages over the end-point nature of the MTT assay, when examining the effect of chemical agents on cellular metabolism (Cooke, 1999). The effect of 24hr exposure of MCF-7 cells to two coumarin compounds (warfarin and esculetin) was examined using this technique (Figures 5.29.-5.31.). In these experiments the basal metabolic rate of the cells was determined prior to drug-exposure, and this value was normalised as 100%. This was achieved for each of the four separate sensor chambers in the Cytosensor. Following drug exposure all subsequent metabolic rates were expressed as a percentage of the basal rate of the particular sensor chamber, ensuring each chamber with its encased cells acted as its own internal control.

Figure 5.29 illustrates the dose-dependent depression of metabolism in MCF-7 cells, on exposure of the cells to warfarin over 24hrs. Concentrations required to achieve this were high when compared to levels of esculetin (Figure 5.30.). Initially, during the first 4 hours of exposure, concentrations of 25 and 50μg/ml caused a slight increase in the metabolic rate of the cells, (maximum 10% and 8%, respectively). This was followed by suppression of metabolism over the 24hrs monitored. The metabolic rate of the cells also declined steadily after 2hrs exposure to 100μg/ml warfarin, and attained a metabolic rate approximately 50% of the basal rate after 24hrs. Figure 5.30. illustrates the exposure of MCF-7 cells to a range of esculetin concentrations and the consequent depression of basal cellular metabolism as a result. It is obvious from this figure that esculetin concentrations greater than 20μg/ml severely damaged the metabolic functioning of cells over a 24hr exposure period – at these concentrations, the metabolism of cells 24hrs post-exposure was only in the region of 20% of the basal metabolic rate. At 50 and 100μg/ml the principal damage to the cells metabolism occurred within the first ten hours of exposure. At lower concentrations, damage was dose- and time-dependent.

In Figure 5.31. the effects of genistein on MCF-7 cells over 24hrs are illustrated. As expected from previous results (Section 5.11.2.3.), at the lower concentration range between 0.1-1μM, genistein acted as a phytoestrogen and increased the metabolic rate above the baseline values throughout the 24hr exposure. At 0.1μM genistein the metabolic rate peaked to 50% above normalised baseline values between 2-4hrs after exposure to the drug. After this time values leveled off to 20% above the

baseline values for the remainder of the 24 hr exposure time. At 1.0μM genistein the metabolic rate peaked to a higher point of 80% above baseline values over the same time period of between 2-4 hours. Again levels dropped to 60% above baseline values for the remainder of the 24 hr exposure. From the 10-100μM concentration range, genistein acted as a potent inhibitor of the metabolic rate in comparison to control cells. Cells exposed to 10μM genistein showed no significant decrease in metabolic rate for the first 10 hrs, after this time the metabolic rate decreased by 30%. For 25μM genistein there was a decrease in metabolic rate by 30% over the 24 hr drug exposure time. Both 50μM and 100μM genistein concentrations show similar inhibitory effects on metabolic rate with no significant effects observed in the first 12 hrs. From 12 to 24 hours genistein exposure for both concentrations there is a sharp decline to nearly 100% inhibition of metabolic rate of the MCF-7 cells exposed to genistein.

One of the findings of major importance from the data collected indicated that the cytosensor microphysiometer was more sensitive to the effects of the benzopyrones on cellular metabolism than the MTT assay. For example, the MTT assay detected a decrease in cellular metabolism of approximately 30% when MCF-7 cells were exposed to 20μg/ml esculetin for 24hrs (Figure 5.32.). The cytosensor results indicate that the cellular metabolism in cells exposed to 20μg/ml esculetin decreased by approximately 60% over this time period (Figure 5.32). Experimental data collected to determine the effect of genistein on MCF-7 cells over 24hrs confirms the superior sensitivity of the cytosensor over the MTT assay format. Genistein is a phytoestrogen and, therefore, one would expect to see a biphasic effect on the metabolic rate. The MTT results show very little variation of metabolic rate in comparison to control cells over the entire drug range (0-100μM). However, it is evident from Figure 5.32. that the cytosensor illustrates the biphasic result well, resulting in a metabolic rate increase in the range of 0.1-1.0μM genistein. At this concentration range the MTT assays indicate a mitochondrial dehydrogenase activity decrease, whereas, the cytosensor reveals up to a 60% increase in metabolic rate over this drug range. At the higher concentration range (10-100μM) there is a decline in metabolic rate to nearly 100% inhibition. This is not apparent from MTT values over the same drug range. MTT values show less than 20% decrease in mitochondrial dehydrogenase activity at the highest concentration whereas cytosensor values show almost complete inhibition of metabolic rate at the same concentration of genistein (Figure 5.32.). The MCF-7 cells exposed to warfarin also show differences in values obtained for both the MTT assay and the cytosensor (Figure 5.33). The MTT assay results indicate that there is no major suppression of metabolic mitochondrial activity in these exposed cells as there is only approximately 20% decrease in metabolism in comparison to control cells at 50μg/ml warfarin. The cytosensor results suggest there is a much higher (than MTT results) suppression of metabolic rate in comparison to the basal rate as at a concentration of between 50-

100µg/ml there is approximately 50% decrease in the metabolic rate of exposed cells. It would appear from these findings that the cytosensor microphysiometer is a much more sensitive predictor of metabolic inhibition (Table 5.9). These results concur with the findings of Cooke (1999) with regard to the cell line A431 and further backup the importance of utilising several different assay types when investigating the effects of a particular compound on any cell type.

24 hr Exposure to Warfarin: Cytosensor studies

Legend:
- 0ug/ml Warfarin
- 25ug/ml Warfarin
- 50ug/ml Warfarin
- 100ug/ml Warfarin

Y-axis: Metabolic Rate (% of Normalised Control)
X-axis: Time (hours)
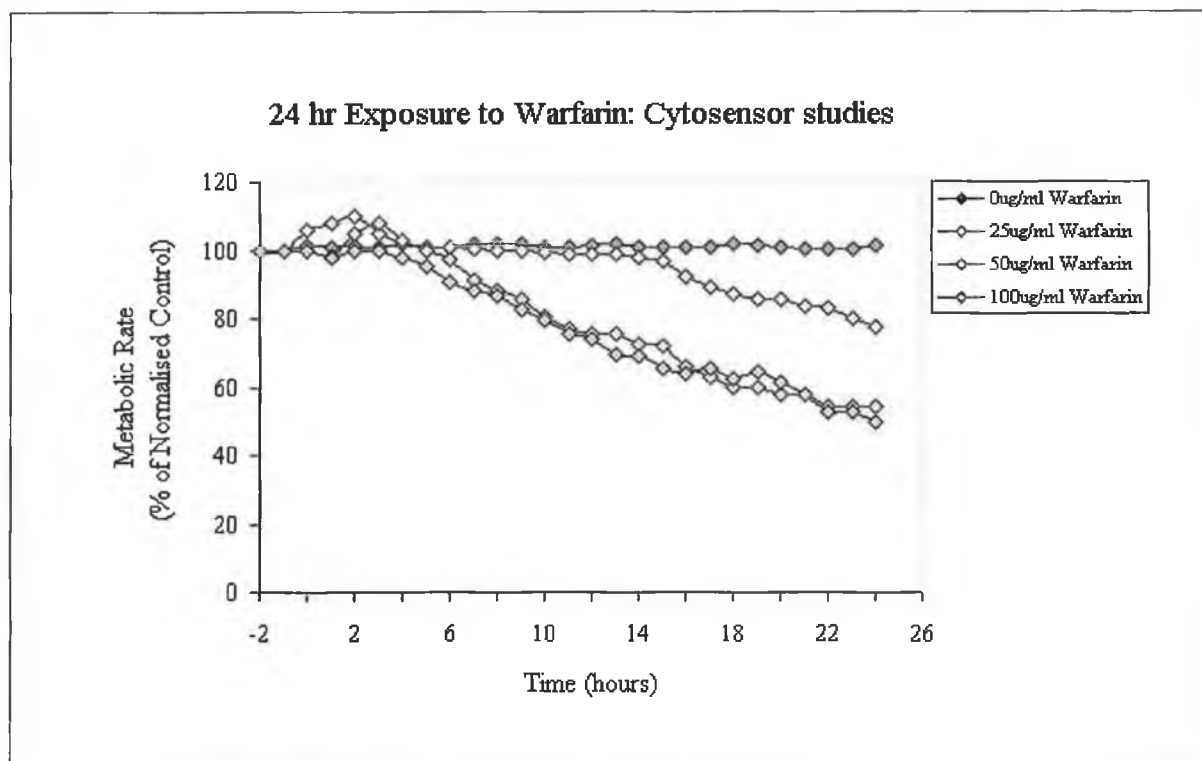
Figure 5.29: *Exposure of MCF-7 cells to various concentrations of warfarin for 24hrs. The above plot shows mean of three experiments conducted on the Cytosensor Microphysiometer, to determine the effects of the drug on cellular metabolism (Section 2.5.5). The cellular acidification rate for each sensor chamber was determined prior to drug exposure, using a 4 min pump cycle, with the acidification rate measured in the final 30secs. of this cycle. This rate was normalised at 100% and all subsequent acidification rates during drug-exposure expressed as a percentage of this normalised value. These values of metabolic rate (mean of three experiments) were plotted vs time in the above graph.*
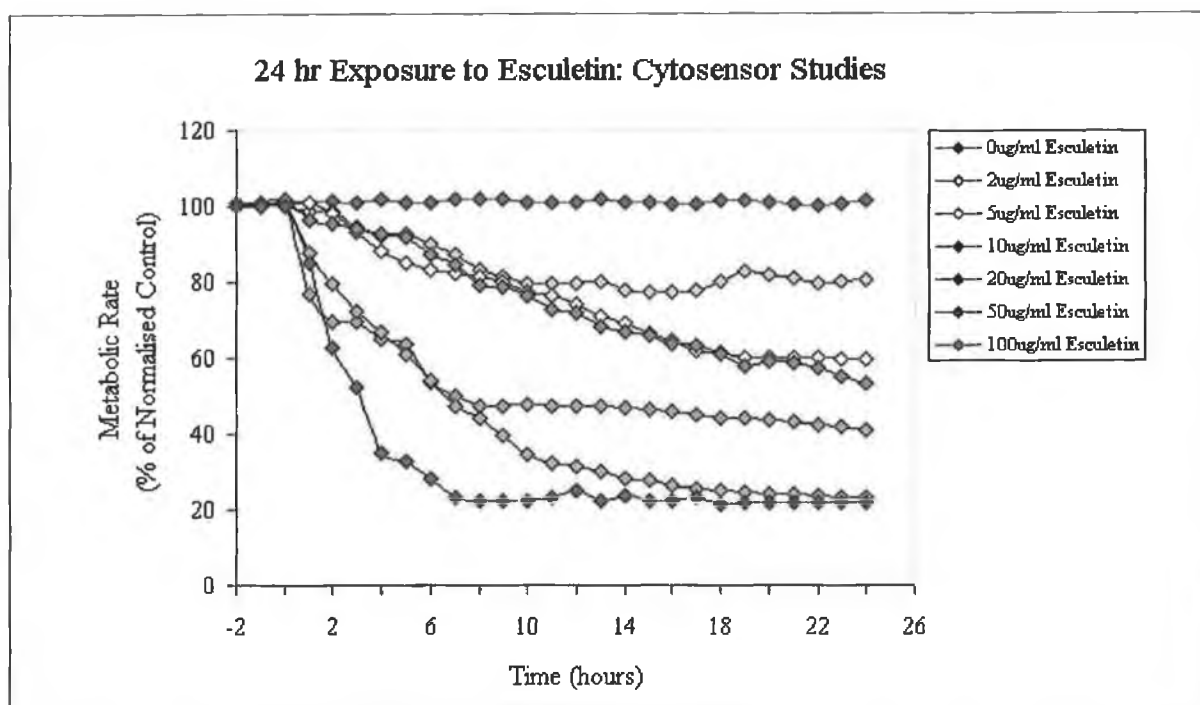
Figure 5.30: *Exposure of MCF-7 cells to various concentrations of esculetin for 24hrs. The above plot shows mean of three experiments conducted on the Cytosensor Microphysiometer, to determine the effects of the drug on cellular metabolism (Section 2.5.5). The cellular acidification rate for each sensor chamber was determined prior to drug exposure, using a 4 min pump cycle, with the acidification rate measured in the final 30secs. of this cycle. This rate was normalised at 100% and all subsequent acidification rates during drug-exposure expressed as a percentage of this normalised value. These values of metabolic rate (mean of three experiments) were plotted vs time in the above graph.*
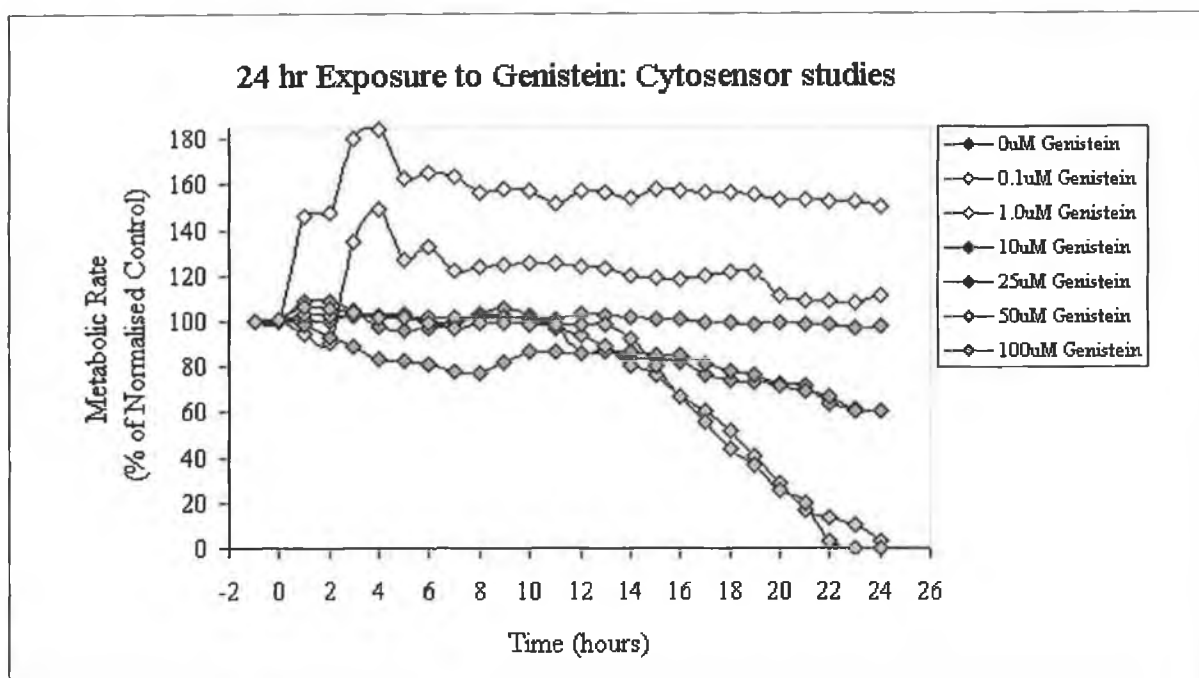
Figure 5.31: *Exposure of MCF-7 cells to various concentrations of genistein for 24hrs. The above plot shows mean of three experiments conducted on the Cytosensor Microphysiometer, to determine the effects of the drug on cellular metabolism (Section 2.5.5). The cellular acidification rate for each sensor chamber was determined prior to drug exposure, using a 4 min pump cycle, with the acidification rate measured in the final 30secs. of this cycle. This rate was normalised at 100% and all subsequent acidification rates during drug-exposure expressed as a percentage of this normalised value. These values of metabolic rate (mean of three experiments) were plotted vs time in the above graph.*
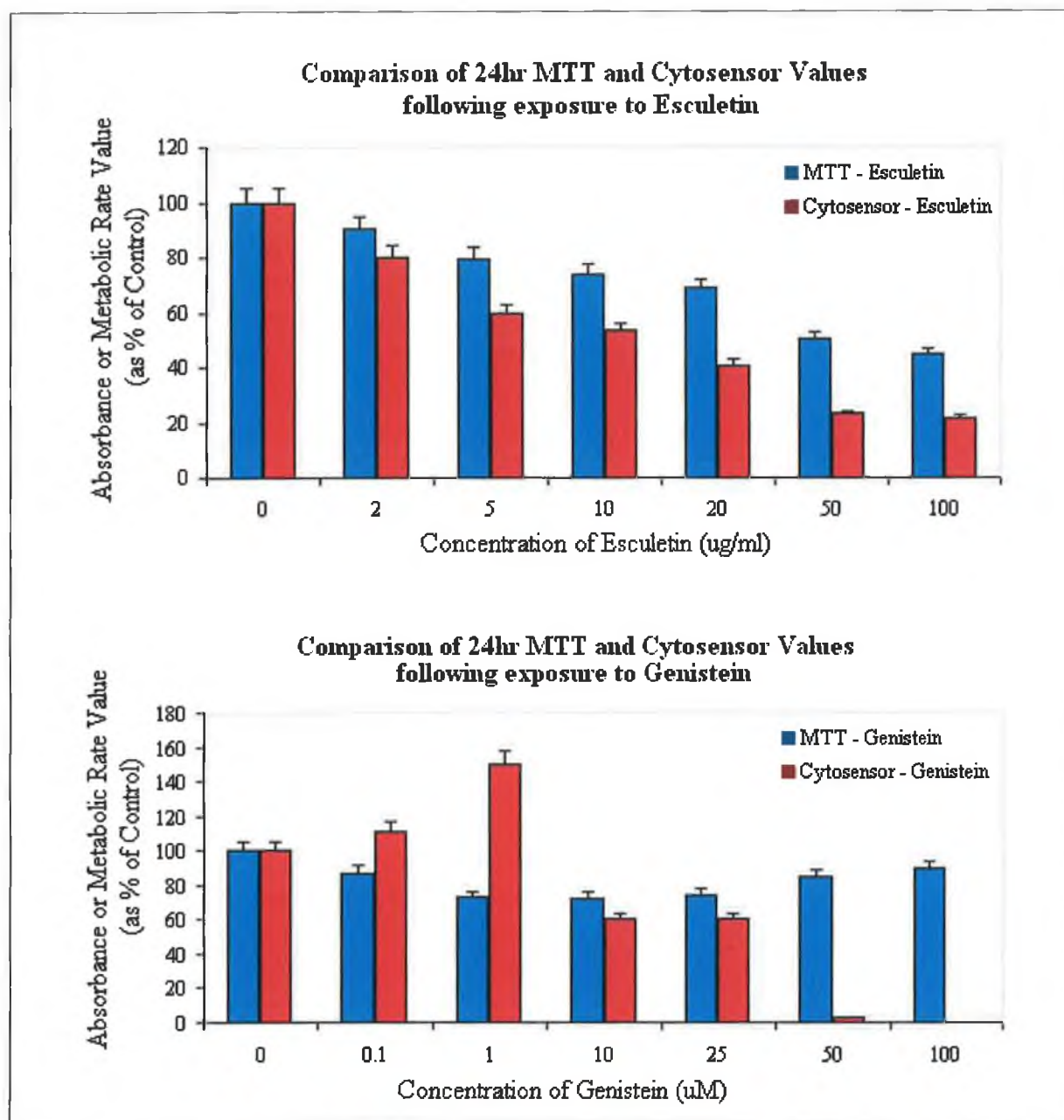
Figure 5.32: *Comparison of values obtained from MTT Assays and Cytosensor Studies on metabolism suppression in MCF-7 cells by esculetin (top), and genistein (bottom) following 24hr exposures. This is clearly evident in the genistein exposure graph where a metabolic rate increase in the range of 0.1-1.0μM genistein is depicted (cytosensor results-red bars). This estrogenic effect that enhances metabolism of MCF-7 cells due to the presence of the estrogen receptor is not evident from the MTT assay results (blue bars) where cells were exposed to the same concentration range (0.1-1.0μM genistein).*

Comparison of 24hr MTT and Cytosensor Values following exposure to Warfarin
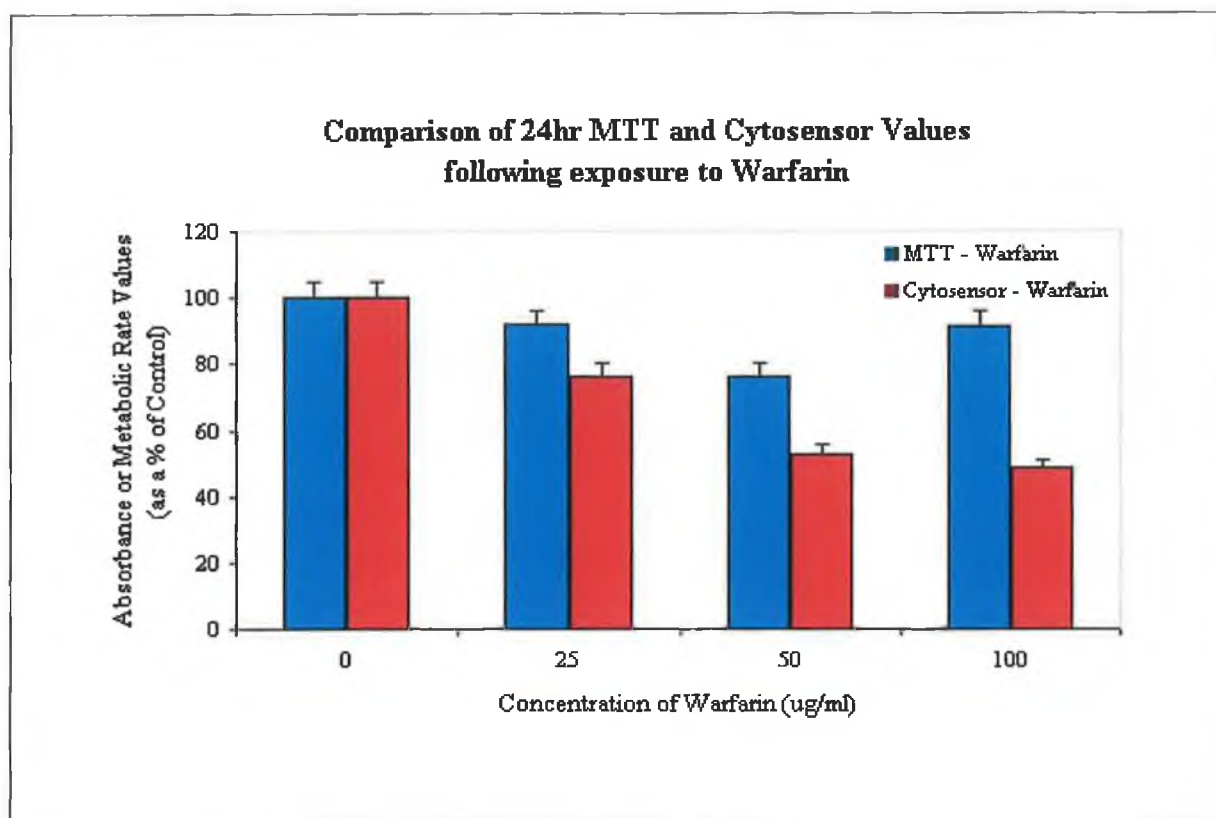
Figure 5.33: Comparison of values obtained from MTT Assays and Cytosensor Studies on metabolism suppression in MCF-7 cells by warfarin, following 24hr exposures. The Cytosensor studies are more sensitive in the prediction of metabolism perturbations (Table 5.9). Section 4.12 explains the cell proliferation overestimation evident at the highest warfarin concentration (MTT results).

Table 5.9: *Significance of difference in sensitivity between the cytosensor microphysiometer and MTT assay. A probability of 0.05 (P<0.05) or less was deemed statistically significant.*

Compound	MCF-7 Significance P Value
Warfarin (μg/ml)	
25	<0.05
50	<0.01
100	<0.01
Esculetin (μg/ml)	
2	<0.01
5	<0.01
10	0.01
20	<0.01
50	<0.01
100	<0.01
Genistein (μM)	
0.1	0.01
1	<0.01
10	<0.05
25	<0.05
50	<0.0001
100	<0.01

5.11.3. Reversibility Studies with the Cytosensor Microphysiometer

Previous reversibility studies of the effects of the benzopyrones on cultured cells have utilised proliferative-based assessments to determine whether cells could recover from exposure to these compounds (Egan *et al.*, 1997; Finn *et al.*, 2002). In most instances, this type of experiment entailed a period of drug exposure, followed by a drug-free recovery growth period for a subpopulation of the original exposed cells. This introduces an element of selection into the reversibility study, i.e.- outgrowth of a subpopulation of drug-resistant cells could account for the appearance of a "reversible effect".

It is, therefore more desirable to assess the recovery of cells exposed to benzopyrones using an alternative method, preferably internally controlled, to avoid the above problems of subpopulation selection. The cytosensor is an ideal instrument for such an experiment- each sensor chamber, with its

encased cells, acts as its own internal control. During exposure of cells to a compound, the metabolic rate of the cells is compared to the metabolic rate of the same sample of cells prior to exposure; during a recovery period the same complete sample of exposed cells, not a subpopulation, are allowed to recover, and again their metabolic rate during recovery is compared to the original metabolic rate. This allows for the complete and valid assessment of the reversibility of the effects of a compound on the cells metabolism.

Reversibility studies were completed for esculetin, warfarin and genistein. Various exposure / recovery periods were assessed, the results of which are shown in Figures 5.34-5.39. The recovery of MCF-7 cells from exposure to warfarin was assessed following both 4hr and 24hr (Figure 5.34. & 5.37.) periods. The effects of warfarin on cellular metabolism have been described in Section 5.11.2.2. and were not as significantly inhibitory in comparison to esculetin and genistein even at the high concentrations used. MCF-7 cells were exposed to warfarin at various concentrations (0-100μg/ml) for 4hrs, after this time the cells were allowed to recover by exposure to normal running media with out warfarin for a further 4hrs. At the highest concentration (100μg/ml) there was a slight drop in metabolic rate (approximately 5%), however once the drug-containing media was removed there was no sign of recovery over the following 4hrs. When cells were exposed to 50μg/ml warfarin for 4hrs there was a slight decrease in metabolic rate to approximately 4% (the same was evident for 20μg/ml exposure over 4hrs). After drug–containing media was removed the cells recovered to their pre-exposure levels, for both 50μg/ml and 20μg/ml pre-exposed MCF-7 cells. Cells were then exposed to warfarin for 24hrs and this was followed by a 24hr recovery period where cells were exposed to drug-free media. The metabolic rate of the cells declined steadily after 24hrs exposure to 100μg/ml warfarin, and attained a metabolic rate approximately 40% below the basal rate. Exposure to 50μg/ml warfarin has similar inhibitory effect on the metabolic rate after 24hrs (Figure 5.37.). However, during the following 24hr recovery period there is significant recovery of metabolic rate (to basal metabolic levels) for cells pre-exposed to 50μg/ml warfarin but not to 100μg/ml warfarin where the metabolic rate continues to drop to approximately 60% below the basal metabolic rate. Recovery of metabolic rate is also apparent in cells pre-exposed to 20μg/ml warfarin with metabolic rate reaching levels that are slightly higher (a maximum of 10%) than the basal metabolic rate. It is therefore, evident that recovery of MCF-7 cells from warfarin exposure is both dose-and time-dependent.

Reversibility studies were also completed for MCF-7 cells exposed to esculetin at various concentrations (0-100μg/ml) over 4hrs and 24hrs (Figure 5.35. & 5.38. respectively). 4hr exposure to esculetin concentrations in the range 20-100μg/ml caused a suppression of cellular metabolism that was both dose-dependent and reversible as illustrated in Figure 5.35. However, following 24hrs of

esculetin exposure, the ability to recover from such severe metabolic suppression (e.g. approx. 80% decrease in metabolic rate in comparison to basal levels) was lost by the cells at all concentrations tested (2-100µg/ml). Data obtained from reversibility studies accomplished with genistein and MCF-7 cells are shown in Figures 5.36. & 5.39. 4 hr exposure of cells to genistein in the range (50-100µM) caused approximately 10% decrease in metabolic rate in comparison to the basal metabolic rate. However, it is evident from Figure 5.36. that no significant recovery took place once the cells were exposed to drug-free media. As expected at the lowest concentration of 1.0µM genistein there was an increase in metabolic rate as genistein exerted its estrogen like effect on the estrogen responsive MCF-7 cell line. Exposure of these cells to drug-free media caused a slight decrease in metabolic rate as the estrogen receptor is no longer stimulated by genistein. Following 24hrs of genistein exposure (50-100µM) the results are similar to esculetin in that the cells lost their ability to fully recover from severe metabolic suppression. Again when cells are exposed to 1.0µM genistein there is an increase in metabolic rate by ~ 60% and like 4hr exposure when cells are introduced to drug-free media there is a decrease in metabolic rate close to basal metabolic levels due to lack of ER stimulation.

The results obtained in these cytosensor studies indicate that the suppression of cellular metabolism in MCF-7 cells exposed to benzopyrones such as esculetin and genistein is not fully reversible following prolonged (24hr) exposure. In previous studies by Cooke, (1999) esculetin was found to irreversibly suppress metabolism in A431 cells over 24hrs. These findings correlate well with the results presented in this study with MCF-7 cells. Since warfarin does not significantly suppress the metabolism of exposed cells over 4hrs there is no significant difference in metabolic rate during warfarin exposure or recovery. Over 24hrs warfarin has an effect on the metabolism of exposed cells (Figure 5.37.), however, only the highest concentration (100µg/ml) irreversibly suppresses the metabolism of the MCF-7 cells tested.
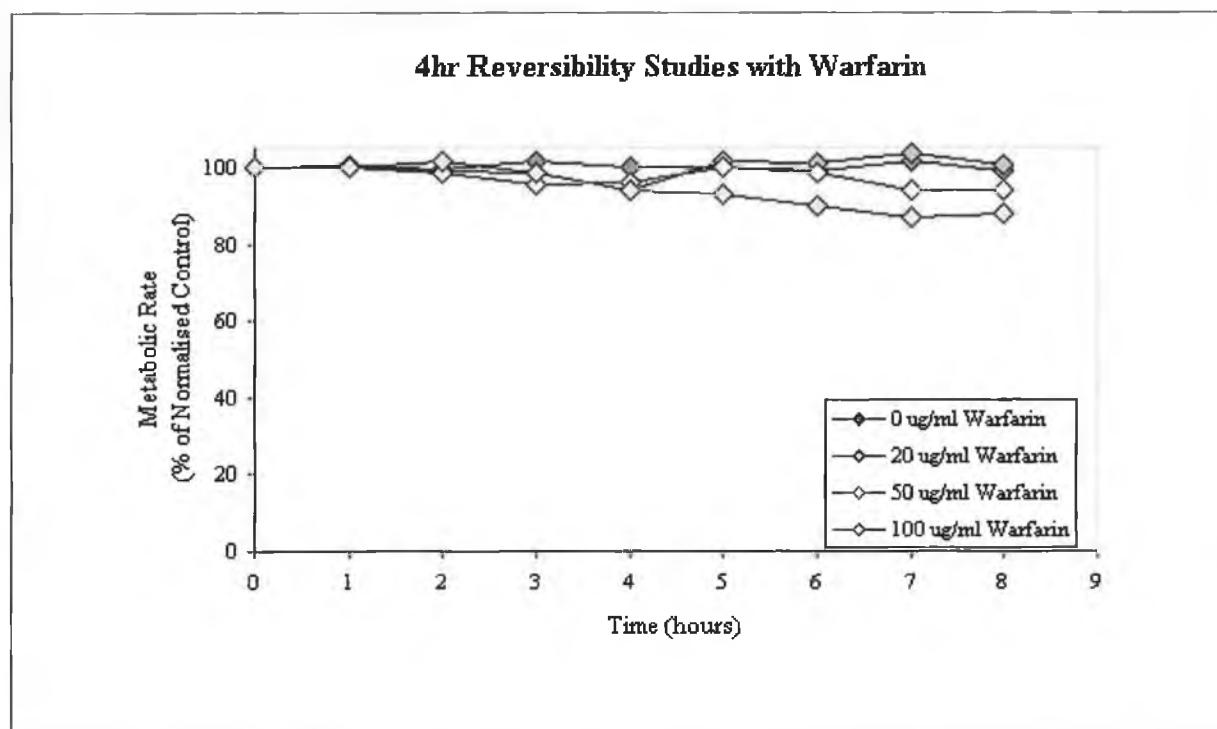
Figure 5.34: *Exposure of MCF-7 cells to various concentrations of warfarin for 4hrs, followed by a further 4hrs period of recovery in drug-free medium. The above plot shows the mean of three experiments conducted on the Cytosensor Microphysiometer, to determine the reversibility of the effects of the drug on cellular metabolism. In individual experiments, the cellular acidification rate for each sensor chamber was determined prior to drug exposure, using a 4 min pump cycle, with the acidification rate measured in the final 30secs. of this cycle. This rate was normalised at 100% and all subsequent acidification rates during exposure and recovery periods were expressed as a percentage of this normalised value. These values of metabolic rate (mean of three experiments) were plotted vs time in the above graph (same conditions for all experiments Figure 5.33-5.38). At the highest concentration (100µg/ml) there was a minor decline in metabolic rate (~5%). However, once the drug media was removed there was no sign of recovery over the following 4hrs. When cells were exposed to 20- 50µg/ml warfarin for 4hrs there was a slight decrease in metabolic rate to ~4%. After drug media was removed the cells recovered to their pre-exposure levels, for both 50µg/ml and 20µg/ml pre-exposed MCF-7 cells.*
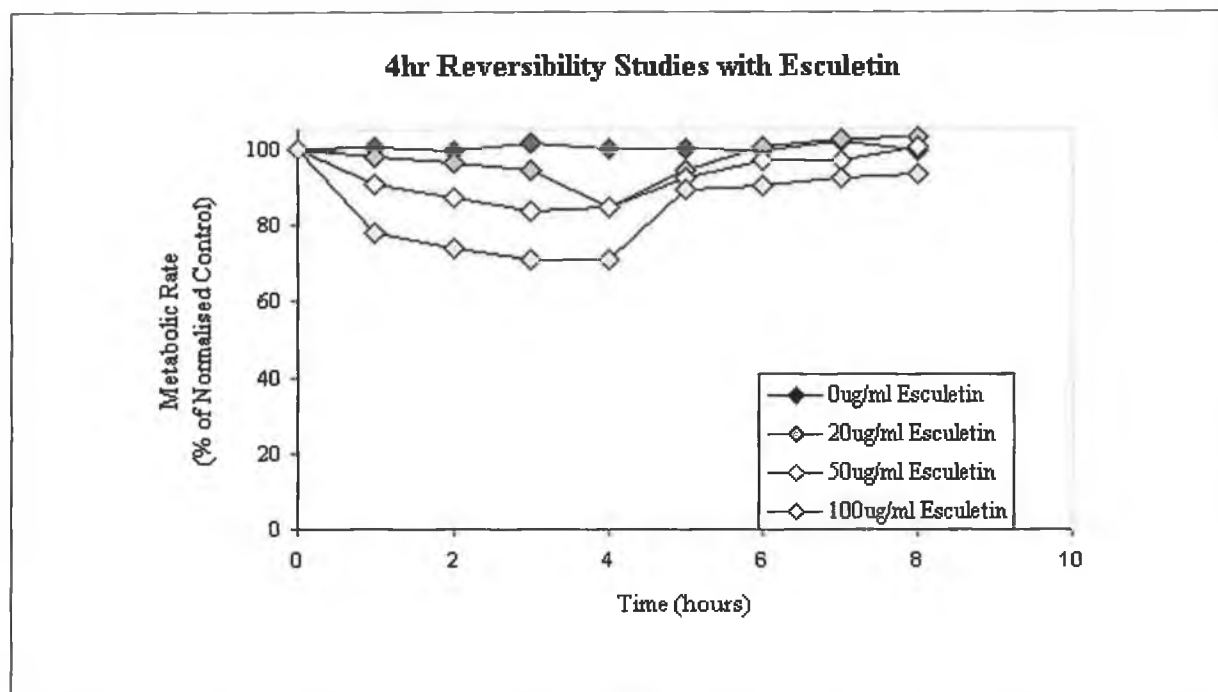
Figure 5.35: *Exposure of MCF-7 cells to various concentrations of esculetin for 4hrs, followed by a further 4hrs period of recovery in drug-free medium. The above plot shows the mean of three experiments conducted on the Cytosensor Microphysiometer, to determine the reversibility of the effects of the drug on cellular metabolism. 4hr exposure to esculetin concentrations in the range 20-100µg/ml caused a suppression of cellular metabolism that was both dose-dependent and reversible as illustrated in the above graph.*

4hr Reversibility Studies with Genistein
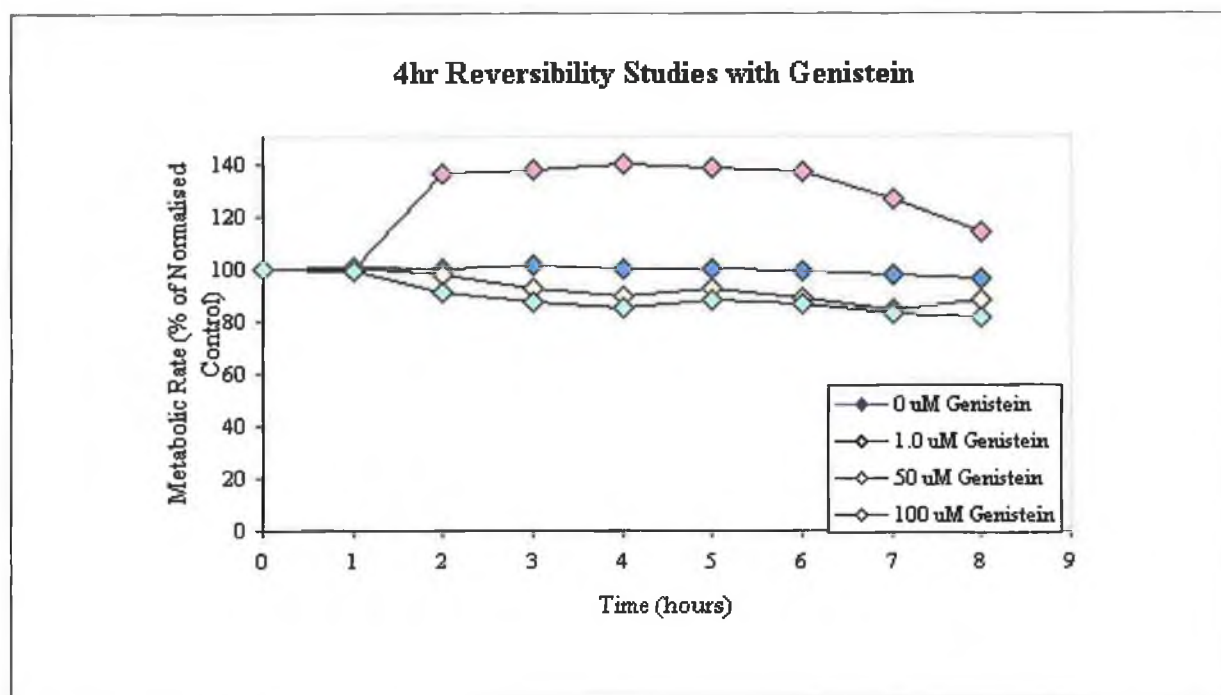
Figure 5.36: Exposure of MCF-7 cells to various concentrations of genistein for 4hrs, followed by a further 4hrs period of recovery in drug-free medium. The above plot shows the mean of three experiments conducted on the Cytosensor Microphysiometer, to determine the reversibility of the effects of the drug on cellular metabolism. 4 hr exposure of cells to genistein in the range (50-100μM) caused ~10% decrease in metabolic rate in comparison to the basal metabolic rate. However, it is evident from the above graph that no significant recovery took place once the cells were exposed to drug-free media. As expected at the lowest concentration of 1.0μM genistein there was an increase in metabolic rate as genistein exerted its estrogenic effect on the estrogen-responsive MCF-7 cell line. Exposure of these cells to drug-free media caused a slight decrease in metabolic rate as the estrogen receptor is no longer stimulated by genistein.
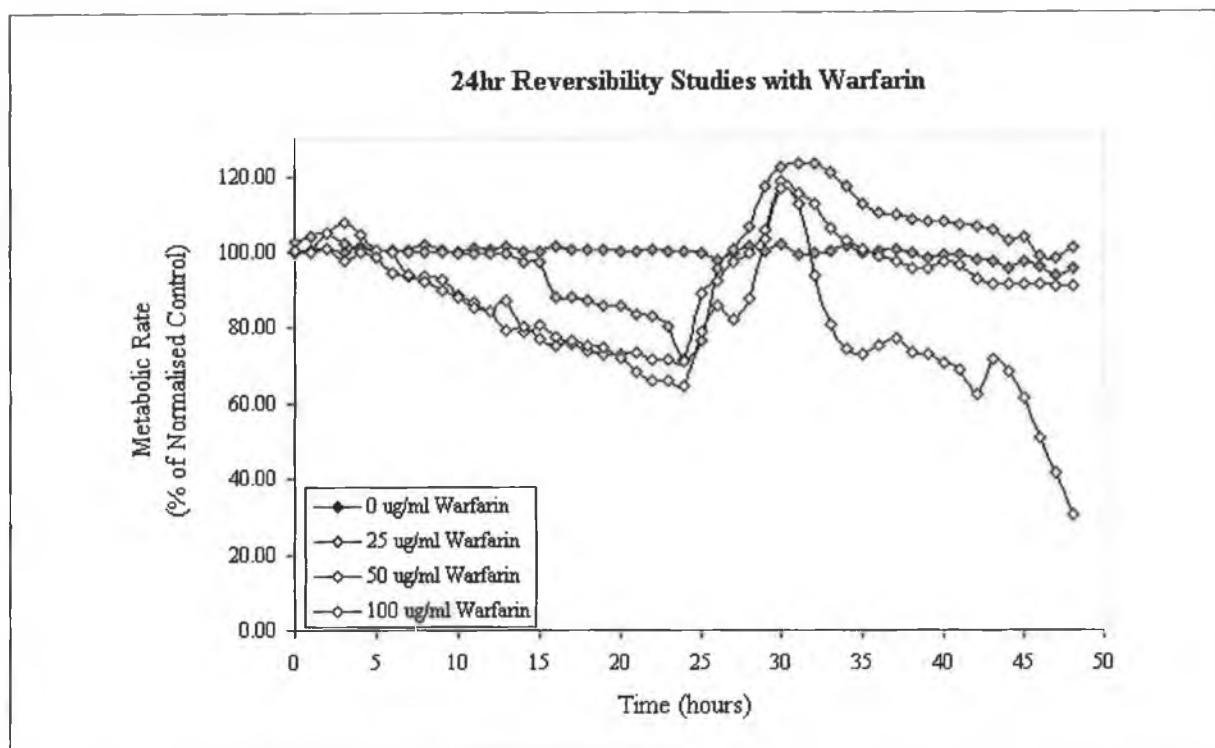
Figure 5.37: *Exposure of MCF-7 cells to various concentrations of warfarin for 24hrs, followed by a further 24hrs period of recovery in drug-free medium. The above plot shows the mean of three experiments conducted on the Cytosensor Microphysiometer, to determine the reversibility of the effects of the drug on cellular metabolism. The metabolic rate of the cells declined steadily after 24hrs exposure to 100μg/ml warfarin, and attained a metabolic rate ~ 40% below the basal rate. Exposure to 50μg/ml warfarin had a similar inhibitory effect on the metabolic rate after 24hrs. However, during the following 24hr recovery period there is significant recovery of metabolic rate (to basal metabolic levels) for cells pre-exposed to 50μg/ml warfarin but not to 100μg/ml warfarin where the metabolic rate continues to drop to ~60% below the basal metabolic rate. Recovery of metabolic rate is also apparent in cells pre-exposed to 20μg/ml warfarin with metabolic rate reaching levels that are slightly higher (a maximum ~10%) than the basal metabolic rate. It is evident that recovery of MCF-7 cells from warfarin exposure is both dose-and time-dependent. During the subsequent 10 hours after the initial 24 hour exposure to warfarin there is a sharp increase followed by a steady decrease in metabolic rate. This increase may represent activation of an ATP-coupled transporter protein e.g. the P-glycoprotein, which results in the efflux of drug from the intracellular environment. Prolonged exposure to high drug concentrations overcomes this efflux mechanism*

24hr Reversibility Studies with Esculetin

Legend:
- 0 ug/ml Esculetin
- 2 ug/ml Esculetin
- 5 ug/ml Esculetin
- 10 ug/ml Esculetin
- 20 ug/ml Esculetin
- 50 ug/ml Esculetin
- 100 ug/ml Esculetin

Y-axis: Metabolic Rate (% of Normalised Control)

X-axis: Time (hours)
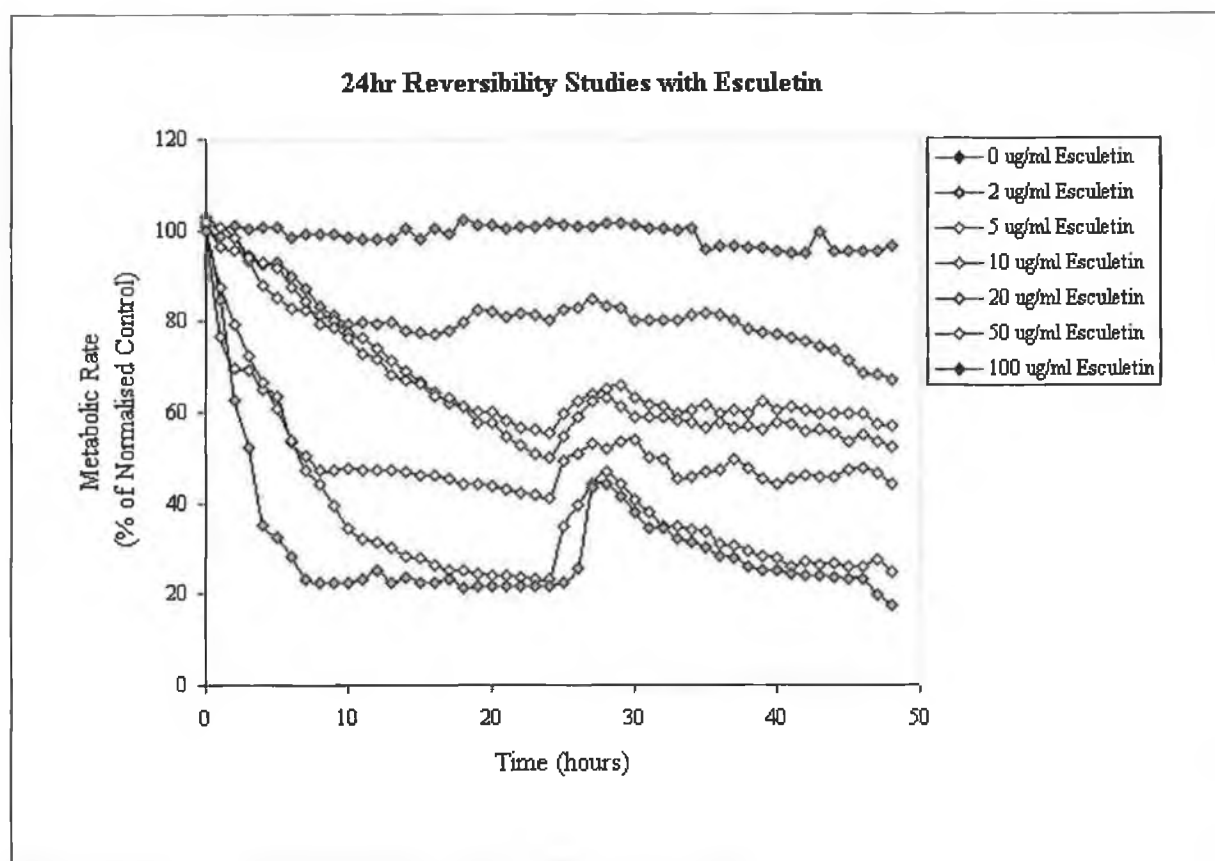
Figure 5.38: Exposure of MCF-7 cells to various concentrations of esculetin for 24hrs, followed by a further 24hrs period of recovery in drug-free medium. The above plot shows the mean of three experiments conducted on the Cytosensor Microphysiometer, to determine the reversibility of the effects of the drug on cellular metabolism. Following 24hrs of esculetin exposure, the ability to recover from such severe metabolic suppression (e.g. ~80% decrease in metabolic rate in comparison to basal levels) was lost by the cells at all concentrations tested (2-100µg/ml).
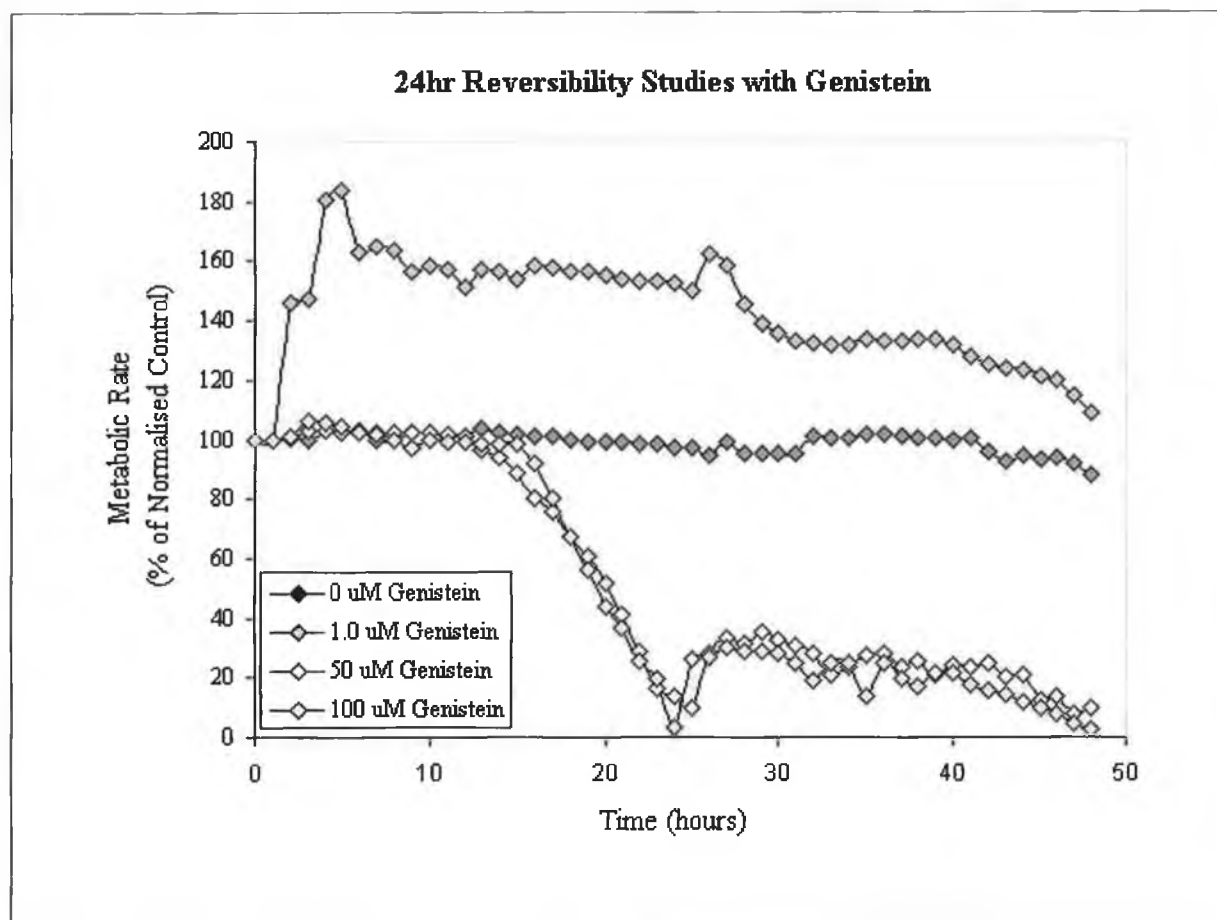
Figure 5.39: *Exposure of MCF-7 cells to various concentrations of genistein for 24hrs, followed by a further 24hrs period of recovery in drug-free medium. The above plot shows the mean of three experiments conducted on the Cytosensor Microphysiometer, to determine the reversibility of the effects of the drug on cellular metabolism. Following 24hrs of genistein exposure (50-100µM) the results are comparable to esculetin as the cells lost their ability to fully recover from severe metabolic suppression. When cells are exposed to 1.0µM genistein there is an increase in metabolic rate by approximately 60%. Similar to the results illustrated in Figure 5.35 there is a decrease in metabolic rate (due to lack of ER stimulation.) close to basal metabolic levels as cells are introduced to drug-free media.*

5.11.4. ELISA-Detection of Tyrosine Phosphorylation in MCF-7 Cells

As outlined in Section 5.9. it was decided to examine the effect of esculetin and warfarin, on total tyrosine phosphorylation in intact MCF-7 cells. An ELISA-based system was used to achieve this. The ELISA used was adapted from the method of Cooke (1999), where it had been used to determine the effect of 7-hydroxycoumarin and esculetin on tyrosine phosphorylation in A431 cells. This cell line is known to over express the EGF-R. When serum-starved A431 cells are exposed to EGF, their signalling pathways become activated, and the overall levels of phosphorylated tyrosine (P-Tyr) within the cells increase. Although the MCF-7 cell line does not over express the EGF-R it is present at lower levels than the ER. Therefore, an increase in P-Tyr levels was expected to be evident for MCF-7 cells stimulated with EGF, like the A431 cells. The phosphorylated tyrosines can be detected in an ELISA-system using anti-phosphotyrosine antibodies. If the cells are exposed to tyrosine kinase inhibitors, and then stimulated with EGF, the increase in P-Tyr should be diminished in inhibitor-treated cells compared to control cells.

Initial experiments were necessary as a number of parameters needed to be optimised (e.g. Cell seeding density, EGF concentration). The optimised ELISA parameters are shown in Table 5.10. The effect of esculetin and warfarin on growth factor stimulated tyrosine phosphorylation was then determined, following pre-exposure periods of 1 and 6 hours. Genistein a well-known tyrosine kinase inhibitor was used as a positive control in this experiment. In all experiments, increases in P-Tyr levels in drug-treated cells were compared to P-tyr increases in control cells, with diminished increases illustrating tyrosine kinase inhibition. The results of these experiments are shown in Tables 5.11.-5.16. and Figures 5.40.-5.45. Tables 5.15-5.16 and Figures 5.44-5.45. illustrates the results for genistein the positive control. After 1 hour pre-exposure, genistein caused a slight inhibition of tyrosine phosphorylation EGF stimulated MCF-7 cells, with 18% inhibition at the highest concentration tested (100µg/ml). Increasing the genistein pre-exposure time to 6 hours caused a major augmentation of this effect, with approximately 40% inhibition of P-Tyr levels at the highest concentration (100µg/ml).

Tables 5.13.-5.14 and Figure 5.42.-5.43 illustrates the results following stimulation of P-Tyr in MCF-7 cells pre-exposed to warfarin. 1 hour pre-exposure to warfarin lead to little or no difference in P-Tyr levels as a 2% decrease at the highest concentration (100µg/ml) is not significant in comparison to control cells. 6 hour pre-exposure of cells to warfarin lead to a slight decrease (approx. 6% at 100µg/ml) of P-Tyr levels. Tables 5.11.-5.12 and Figure 5.40.-5.41 illustrate the results for esculetin. 1 hour pre-exposure of MCF-7 cells to esculetin followed by stimulation with EGF did not affect cellular tyrosine phosphorylation levels as even at the highest concentration there was only a

slight decrease of ~ 8% at 100μg/ml. However, increasing esculetin pre-exposure time to 6 hours, caused a decrease in P-Tyr levels up to 20% inhibition at the highest concentration tested (100μg/ml).

These results indicate that only esculetin inhibits growth factor-stimulated tyrosine phosphorylation by up to 20%. Warfarin is a less potent inhibitor of cell proliferation and metabolic activity than esculetin (Section 5.11.1, Section 5.11.2.2. & 5.11.2.4.) and this may be partly due to the fact that it shows no significant tyrosine phosphorylation inhibition in comparison to both esculetin and genistein. Neither esculetin nor warfarin prevented phosphorylation with the efficiency of genistein the positive control (maximal effect 40% inhibition at 100μg/ml, following 6 hour pre-exposure). The ELISA-based system yielded no information on the effects of the compounds on tyrosine kinase activity. Therefore, the cytosensor microphysiometer was employed for this research. Experimental details are described in Section 2.5.6.2. and involve pre-exposure of MCF-7 cells to either warfarin or esculetin (0-20μg/ml) for either 1 or 6 hours prior to EGF (200ng/ml) stimulation. If either warfarin or esculetin inhibit the signal transduction of metabolically active MCF-7 cells a decrease in EGF stimulated metabolic rate should be evident (Figure 5.44-5.45).

Table 5.10: *Optimised parameters for the ELISA-based assessment of tyrosine phosphorylation in EGF-stimulated MCF-7 cells.*

Variable Examined	Optimal Conditions
Cell Seeding Density	5×10^4 cells/well
EGF Concentration	200ng/ml. 15 mins.
ELISA Blocking Conditions	1.5 hrs @ 37°C, 10% FCS, 0.2% Tween-20 in Tris-Buffered Saline.
Primary Ab (Anti-Phosphotyrosine Exposure	1/750 Dilution 1hr @ 37°C
Secondary Ab (AP-labelled Anti-Mouse IgG) Exposure	1/1500 Dilution 1hr @ 37°C

The significance of any inhibition (by esculetin, warfarin or genistein) of growth factor-stimulated tyrosine phosphorylation was determined using a paired Student's t-test with confidence limits set at 95%. A probability of 0.05 ($P<0.05$) or less was deemed statistically significant.

315

Table 5.11: *ELISA results: Esculetin inhibition of tyrosine phosphorylation in MCF-7 cells*

Concentration of Esculetin (µg/ml)	1hr Drug Pre-exposure	Significance P Value
0	100.00 ± 1.35	-
2	98.18 ± 1.90	>0.05
10	92.04 ± 0.75	<0.01
20	93.57 ± 0.92	0.01
50	94.29 ± 0.87	0.01
100	91.14 ± 1.84	<0.01
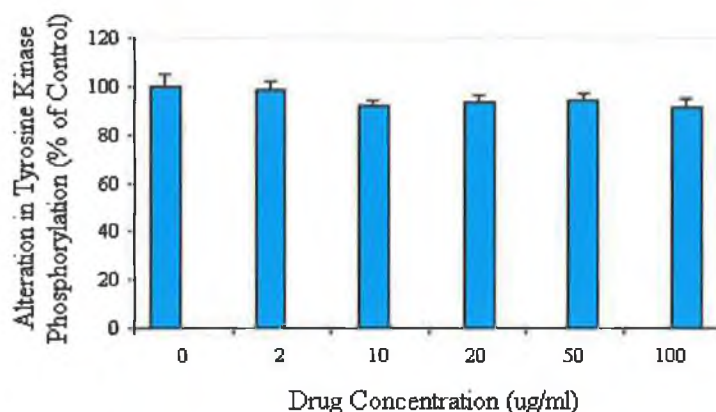
Figure 5.40: *Bar Chart illustrating the inhibition of tyrosine phosphorylation in EGF-stimulated MCF-7 cells by esculetin (1hr pre-exposure) All experiments involved drug samples replicated four times (n=4), and were carried out on three separate occasions (Section 2.2.6.3). The drug-treated cells absorbance values were normalised vs absorbances of untreated control cells. Control absorbance (0 µg/ml Drug/no drug pre-exposure) = 0.896 $\pm$ 0.035.*

Table 5.12: *ELISA results: Esculetin inhibition of tyrosine phosphorylation in MCF-7 cells*

Concentration of Esculetin (µg/ml)	6hr Drug Pre-exposure	Significance P Value
0	100.00 ± 1.48	-
2	91.07 ± 1.21	<0.01
10	84.38 ± 0.98	<0.0001
20	88.39 ± 1.76	<0.0001
50	84.38 ± 1.39	<0.0001
100	83.48 ± 1.05	<0.0001
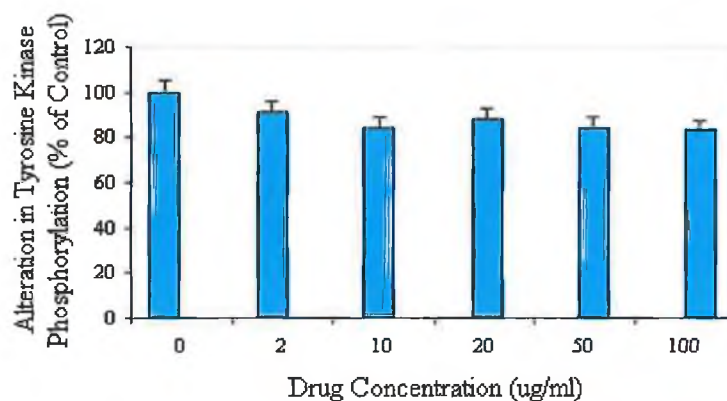
Figure 5.41: *Bar Chart illustrating the inhibition of tyrosine phosphorylation in EGF-stimulated MCF-7 cells by esculetin (6hr pre-exposure) All experiments involved drug samples replicated four times (n=4), and were carried out on three separate occasions (Section 2.2.6.3). The drug-treated cells absorbance values were normalised vs absorbances of untreated control cells. Control absorbance = 0.848 ± 0.041.*

Table 5.13: ELISA results: Warfarin inhibition of tyrosine phosphorylation in MCF-7 cells

Concentration of Warfarin (µg/ml)	1hr Drug Pre-exposure	Significance P Value
0	100.00 ± 1.08	-
2	100.30 ± 2.57	>0.05
10	94.50 ± 1.61	<0.05
20	101.67 ± 2.77	>0.05
50	99.93 ± 1.68	>0.05
100	98.32 ± 1.26	>0.05
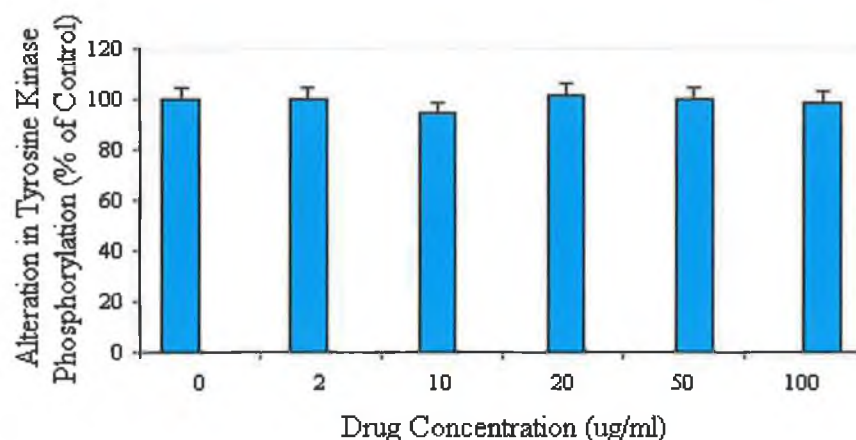
Figure 5.42: Bar Chart illustrating the inhibition of tyrosine phosphorylation in EGF-stimulated MCF-7 cells by warfarin (1hr pre-exposure) All experiments involved drug samples replicated four times (n=4), and were carried out on three separate occasions (Section 2.2.6.3). The drug-treated cells absorbance values were normalised vs absorbances of untreated control cells. Control absorbance = 1.225 ± 0.027.

Table 5.14: ELISA results: Warfarin inhibition of tyrosine phosphorylation in MCF-7 cells

Concentration of Warfarin (μg/ml)	6hr Drug Pre-exposure	Significance P Value
0	100.00 ± 2.51	-
2	100.25 ± 2.49	>0.05
10	102.30 ± 2.93	>0.05
20	99.50 ± 2.74	>0.05
50	96.80 ± 1.87	<0.05
100	94.65 ± 1.03	<0.05
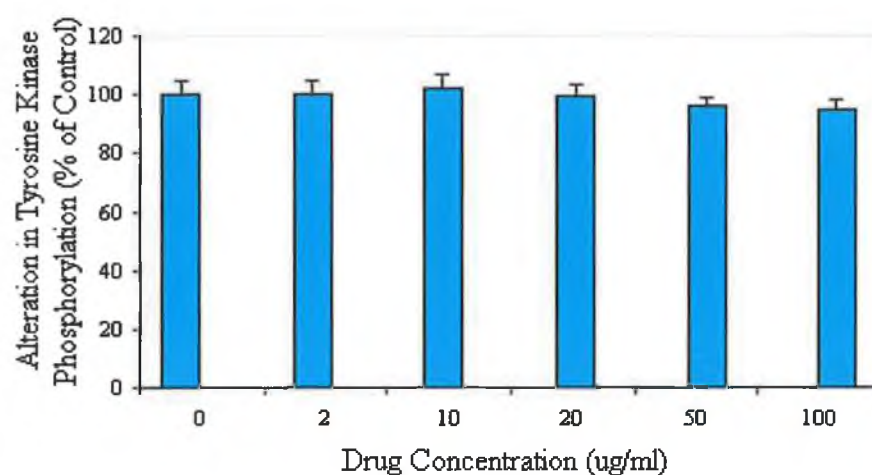
Figure 5.43: Bar Chart illustrating the inhibition of tyrosine phosphorylation in EGF-stimulated MCF-7 cells by warfarin (6hr pre-exposure) All experiments involved drug samples replicated four times (n=4), and were carried out on three separate occasions (Section 2.2.6.3). The drug-treated cells absorbance values were normalised vs absorbances of untreated control cells. Control absorbance = 0.985 ± 0.03.

Table 5.15: *ELISA results: Genistein inhibition of tyrosine phosphorylation in MCF-7 cells*

Concentration of Genistein (μg/ml)	1hr Drug Pre-exposure	Significance P Value
0	100.00 ± 2.31	-
2	82.09 ± 3.15	<0.0001
10	76.60 ± 2.54	<0.0001
20	87.14 ± 1.05	<0.0001
50	85.83 ± 1.89	<0.0001
100	82.41 ± 1.83	<0.0001
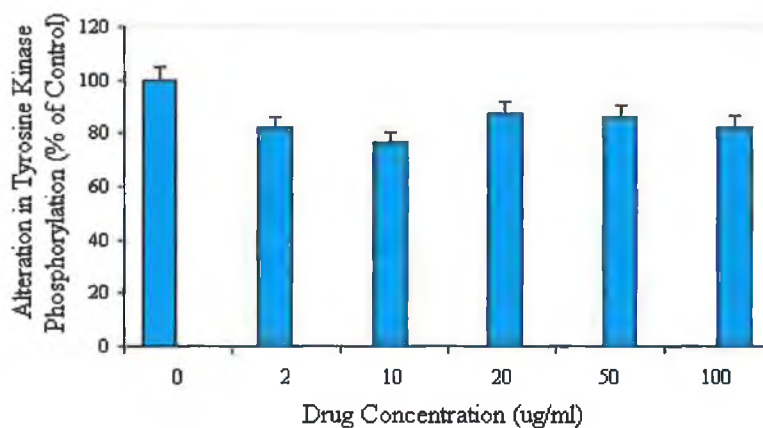
Figure 5.44: *Bar Chart illustrating the inhibition of tyrosine phosphorylation in EGF-stimulated MCF-7 cells by genistein (1hr pre-exposure) All experiments involved drug samples replicated four times (n=4), and were carried out on three separate occasions (Section 2.2.6.3). The drug-treated cells absorbance values were normalised vs absorbances of untreated control cells. Control absorbance = 0.741 ± 0.034.*

Table 5.16: *ELISA results: Genistein inhibition of tyrosine phosphorylation in MCF-7 cells*

Concentration of Genistein (μg/ml)	6hr Drug Pre-exposure	Significance P Value
0	100.00 ± 02.48	-
2	54.21 ± 0.38	<0.0001
10	51.64 ± 0.65	<0.0001
20	65.36 ± 0.96	<0.0001
50	67.86 ± 0.68	<0.0001
100	60.79 ± 0.59	<0.0001
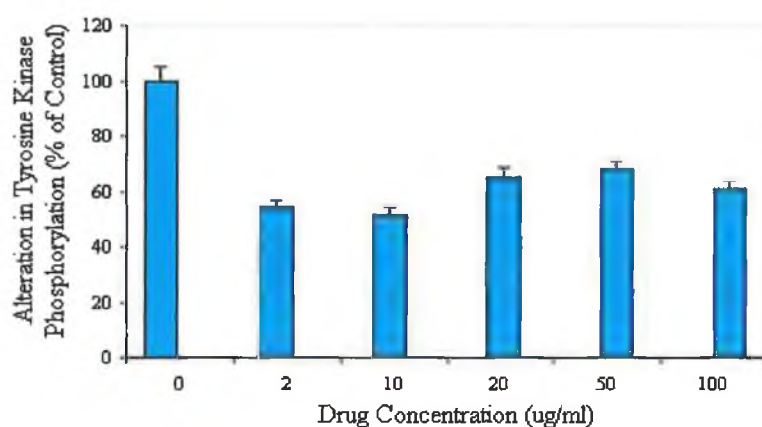
Figure 5.45: *Bar Chart illustrating the inhibition of tyrosine phosphorylation in EGF-stimulated MCF-7 cells by genistein (6hr pre-exposure) All experiments involved drug samples replicated four times (n=4), and were carried out on three separate occasions (Section 2.2.6.3). The drug-treated cells absorbance values were normalised vs absorbances of untreated control cells. Control absorbance = 0.919 $\pm$ 0.037.*

5.11.5. Cytosensor Microphysiometer Studies into Tyrosine Kinase Inhibition

The Cytosensor Microphysiometer system has proven to be a powerful tool for receptor discovery and characterisation and can rapidly and reliably measure cell surface receptor activation. The flexibility of this system is due to its measurement of the extracellular acidification rate (ECAR). Fluctuation in cellular acid excretion is a physiological consequence of receptor activation for all classes of cell surface receptors examined so far. A major advantage of this system is the ability to examine receptor interactions using intact, viable cells, which is an essential condition for evaluating drugs directed at intracellular targets. The cytosensor microphysiometer has been used in the past to dissect various cellular signalling pathways e.g. research stimulation of proton efflux from chondrocytic cells by EGF. The cytosensor has also been used to examine signal transduction of neurohormones. Therefore, we chose to use this instrument to examine the effect of esculetin and warfarin on EGF-stimulated pathways in MCF-7 cells. The cytosensor is an attractive method for examining inhibition of EGF-RTK in MCF-7 cells for two reasons:

1. The study was carried out in intact cells, thereby eliminating worries about receptor stability.
2. Downstream signalling events could be observed concurrently, thereby yielding more information per experiment.

The EGF-stimulation of EGF-RTK in serum-starved MCF-7 cells had to be optimised, as a higher concentration of EGF was required to stimulate these cells than A431 cells. This is due to the fact that the EGF-R although present in MCF-7 cells it is found in low amounts as there are higher levels of ER present (Section 5.5.5.). Maximal stimulation of the cells was with 200ng/ml EGF and this concentration was used in all subsequent experiments. As illustrated in Figure 5.46. exposure of MCF-7 cells to 200ng/ml of EGF caused an increase in the acidification rate of the cells, to a peak of 25% above baseline values. This peak in acidification rate was transient and acidification rate dropped to approximately 5% below baseline values. The initial rise in acidification rate is principally due to the activation of the EGF-Receptor-associated tyrosine kinase activity, as it can be blocked by pre-exposure of cells to the tyrosine kinase inhibitor genistein, for 1 hour or 6 hours, respectively.

Figure 5.46. portrays the activation of EGF-RTK in cells pre-exposed to esculetin for 1 or 6 hours. Pre-exposure of MCF-7 cells to 20µg/ml esculetin prior to EGF stimulation, caused a slight decrease (approx. 10%) in the peak activation of EGF-RTK. However the metabolic rate continued to drop to approximately 15 % below baseline levels and this may indicate a block in the signalling

pathway downstream of the EGF-RTK. 6 hours pre-exposure of the cells to 20µg/ml esculetin prior to EGF stimulation, caused a decrease (approx. 15%) in the peak activation of EGF-RTK. Again, the esculetin-treated cells metabolic rate continued to drop to 20 % below baseline levels suggesting a downstream block of EGF-stimulated signalling pathway.

As shown in Figure 5.47, 1hr pre-exposure of cells to 20µg/ml warfarin did not block activation of the EGF-RTK. However, warfarin results were similar to esculetin 1hr pre-exposure, as there was a continued drop in metabolic rate to approximately 15% below baseline values. After 6 hour pre-exposure to warfarin there was approximately 5% decrease in peak activation of EGF-RTK. The observed results correlate well with the ELISA-TK results of Section 5.11.4. Both sets of results show that esculetin has the ability to inhibit both tyrosine phosphorylation and its kinase activity, whereas warfarin shows no ability to block tyrosine phosphorylation or inhibit its kinase activity. Although the results show some similarity to the work carried out by Cooke (1999) there are some significant differences. This is most likely due to the different cell lines used. The A431 cell line over-expressed the EGF-R and due to this the peak acidification rates (although transient like in MCF-7 cells) were much higher, stimulation of cells with 100ng/ml EGF gave a peak rate of approximately 80% above the baseline values. The cells maintained a higher metabolic rate of approximately 30% above the baseline in A431 cells whereas MCF-7 cells metabolic rate dropped below the base line. In MCF-7 cells the main mitogenic receptor of importance is the ER, which is at much higher levels than EGF-R. In this experiment MCF-7 cells were not exposed to E_2 a well-known mitogenic activator of the ER. Therefore MCF-7 cells stimulated by EGF could indirectly activate the nuclear ER by phosphorylation of Ser 118 through MAP-K and PI3-K pathways. However from the results it seems that by blocking EGF-R phosphorylation the cross-talk between the EGF-R and ER is also blocked. This could explain why there is a drop in metabolic rate after the peak has been reached because the cross-talk is necessary to maintain the basal metabolic rate. Signal transduction through ERK may indirectly influence cell biologic functions via the transactivation of target genes. This was thought to be the exclusive function of the nuclear ER (Glass *et al.,* 1997; Halachmi *et al.,* 1994), but examples are emerging that signalling from the membrane has a similar role. One established mechanism is that growth factor receptors for EGF or IGF can stimulate ERK, leading to the phosphorylation of Ser 118 of the nuclear ER (Bunone *et al.,* 1996). This provides a means by which growth factor signalling transactivates genes, via ER in the absence of E_2 and defines the importance of cross-talk between EGF-R and ER. As stated above, the decrease may be due to downstream block in signalling pathway, which is most likely ERK and nuclear ER phosphorylation in MCF-7 cells. A431 cells do not have the ER present and, therefore, there is no cross talk and metabolic rates remain higher than those of MCF-

7 cells. The rates may also be higher due to the higher levels of EGF-R in A431 cells than MCF-7 cells.
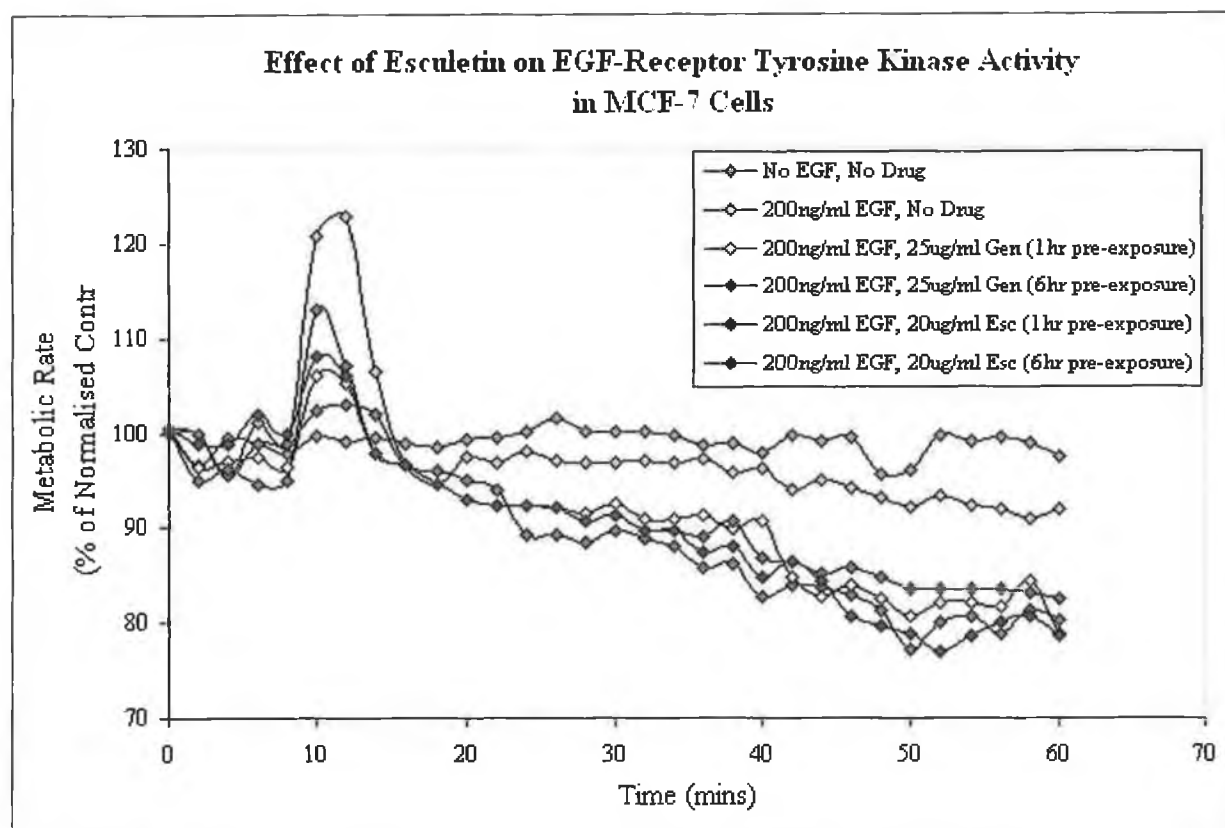
Figure 5.46: *Exposure of MCF-7 cells to esculetin for different time periods, prior to stimulation with 200ng/ml EGF. The above plot shows the experiment conducted on the Cytosensor Microphysiometer to determine the effect of esculetin exposure on the activation of the EGF-RTK in MCF-7 cells. Genistein was included as a positive tyrosine kinase inhibitor control. In individual experiments, the cellular acidification rate for each sensor chamber was determined prior to EGF exposure, using a 2 min cycle, with the acidification rate measured in the final 30 secs. of this cycle. This rate was normalised at 100% and all subsequent acidification rates during and following EGF exposure were expressed as a percentage of this normalised value. These values of metabolic rate (mean of three experiments) were plotted vs time in the above graph.*

Effect of Warfarin on EGF-Receptor Tyrosine Kinase Activity in MCF-7 Cells

Legend:
- No EGF, No Drug
- 200ng/ml EGF, No Drug
- 200ng/ml EGF, 25ug/ml Gen (1hr pre-exposure)
- 200ng/ml EGF, 25ug/ml Gen (6hr pre-exposure)
- 200ng/ml EGF, 20ug/ml War (1hr pre-exposure)
- 200ng/ml EGF, 20ug/ml War (6hr pre-exposure)

Y-axis: Metabolic Rate (% of Normalised Control)
X-axis: Time (mins)
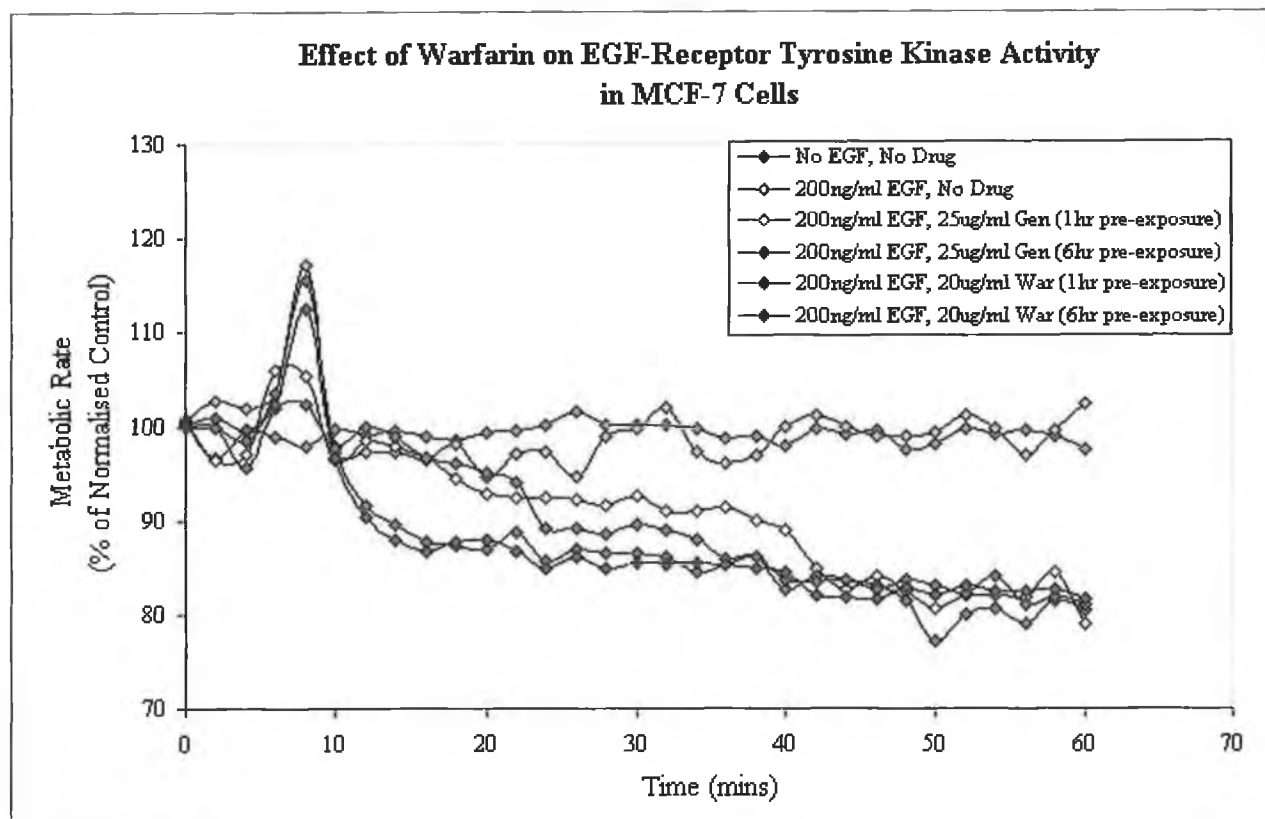
Figure 5.47: Exposure of MCF-7 cells to warfarin for different time periods, prior to stimulation with 200ng/ml EGF. The above plot shows the experiment conducted on the Cytosensor Microphysiometer to determine the effect of warfarin exposure on the activation of the EGF-RTK in MCF-7 cells. Genistein was included as a positive tyrosine kinase inhibitor control. In individual experiments, the cellular acidification rate for each sensor chamber was determined prior to EGF exposure, using a 2 min cycle, with the acidification rate measured in the final 30 secs. of this cycle. This rate was normalised at 100% and all subsequent acidification rates during and following EGF exposure were expressed as a percentage of this normalised value. These values of metabolic rate (mean of three experiments) were plotted vs time in the above graph.

5.11.6. DNA Synthesis Studies

Incorporation of radioactive thymidine is a widely used method to quantify initiation of DNA synthesis by exogenous growth factors, hormones, drugs or other agents in cell culture. Measurement of DNA synthesis with the [3H]-thymidine assay is considered as the 'gold standard' for the assessment of cell growth. Unfortunately this assay has several disadvantages, which have prompted the development of viable non-radioactive alternatives to measure DNA synthesis or cell proliferation in cultured cells. An important development has been the replacement of the [3H]-thymidine assay by

325

the BrdU ELISA. This assay technique is based on the incorporation of the pyrimidine analogue BrdU instead of thymidine into the DNA of proliferating cells. In other words BrdU has the ability to label cell in the S-phase of the cell cycle. After its incorporation into DNA, BrdU is detected by ELISA. Finn *et al.*, (2002) have shown that DNA synthesis is decreased in human renal carcinoma cells exposed to 6-nitro-7-hydroxycoumarin and 7,8-dihydroxycoumarin. BrdU incorporation assays showed that both agents had a concentration-dependent inhibitory effect on DNA synthesis.

It can be seen from Figure 5.48. that all compounds tested seem to affect DNA synthesis of MCF-7 cells. These cells were exposed to warfarin, esculetin or genistein over 96 hours. The microtitre assays for determining the effect of the benzopyrones on proliferation and metabolism indicated that warfarin has the least inhibitory effect on both cell lines examined. Therefore, as expected, warfarin had the least inhibitory effect on DNA synthesis. At the highest concentration of 100µg/ml there was approximately 20% decrease in DNA synthesis levels compared to control cells. Both esculetin and genistein showed time and dose-dependent inhibitory effects on DNA synthesis. At the highest concentration of esculetin there was approximately 80% inhibition of DNA synthesis in MCF-7 cells. There was a sharp decrease in DNA synthesis between 1-10µg/ml esculetin. Genistein (as anticipated) at the lower concentration range (upwards to ~1µg/ml) yielded a slight increase in DNA synthesis. This is due to the fact that genistein is a phytoestrogen (Section 5.12.) and can stimulate the ER in MCF-7 cells at low concentrations. At the higher concentration range between 1-13.5µg/ml there is a sharp decline in DNA synthesis with an inhibition of approximately 75-80% at the highest concentration tested (13.5µg/ml).
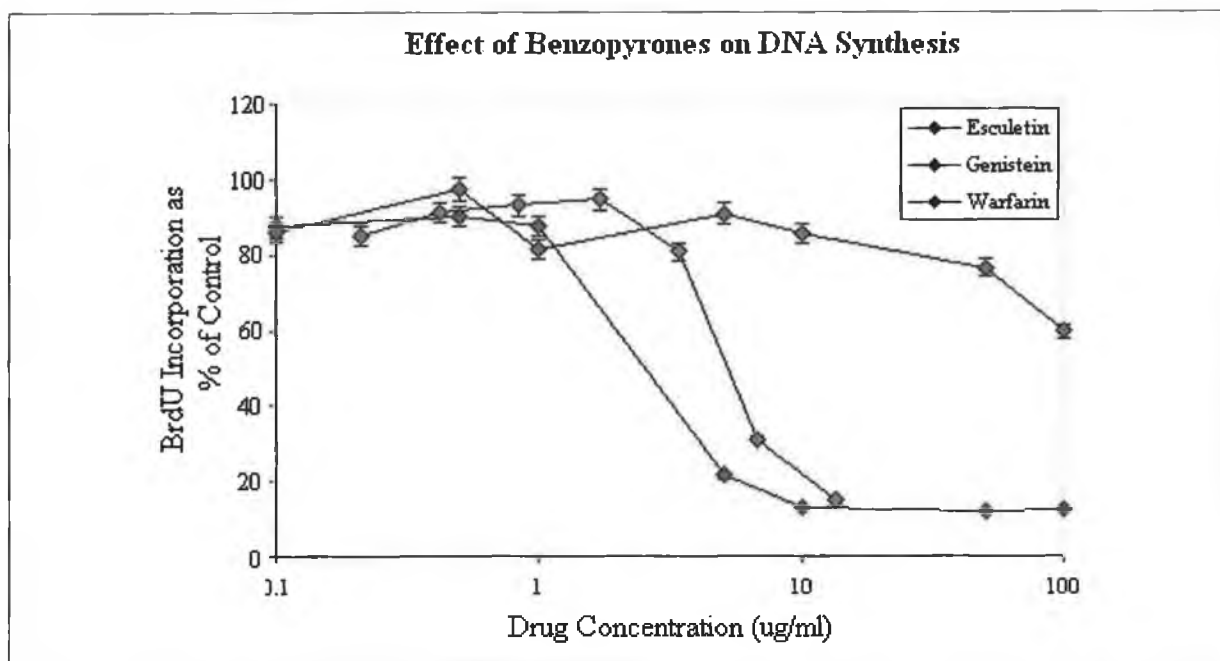
Figure 5.48: *Exposure of MCF-7 cells to various concentrations of genistein, warfarin and esculetin for 96 hrs. This time period was chosen for the reasons outlined in Section 5.12. Optimal assay duration for human cell lines should be a minimum of 4 days to allow for cell death and loss of intracellular activities. The MTT assay was the only microtitre assay performed with drug exposure over 24hrs in order for direct comparison to the 24hr cytosensor assays (Section 5.11.2.4; Figure 5.32-5.33).*

5.12. Conclusions

In this chapter the effect of benzopyrones (warfarin, 7-hydroxycoumarin, esculetin, and genistein) on the growth and metabolism of human tumour cells (MCF-7 & A549) was examined. Signal transduction studies were also performed in order to obtain information regarding the mechanism of action of warfarin, esculetin and genistein on MCF-7 cells. Signalling studies focused on this cell line due to its possession of the ER, which can be stimulated by mitogens such as EGF and estradiol (E_2).

Proliferation assays yielded some interesting information on growth inhibition by benzopyrones:

1. The potency of growth inhibition by genistein was greater than esculetin, which, in turn was greater than warfarin.
2. MCF-7 cells tested were quite sensitive to the effects of all three compounds.
3. A549 cells did not seem to be as sensitive to the effects of all three compounds in comparison to MCF-7 cells. However both genistein and esculetin displayed significant inhibitory effects on A549 cells.

Assessment of leakage of a wide variety of enzymes has been used for cytotoxicity testing endpoints. Lactate dehydrogenase (LDH) is a convenient marker because of the stability of the enzyme activity in the culture system (Martin, 1992). In this study none of the four compounds tested (warfarin, 4-hydroxywarfarin, esculetin and 7-hydroxycoumarin) caused significant membrane damage in both cell lines (MCF-7 and A549) assessed by LDH assay. There are some drawbacks that should be noted when using the LDH assay. If serum contaminates the system with endogenous enzymes they can mask low levels of leached enzymes, which leads to underestimation of LDH present. The main drawback of this assay however, is its reliance on the premise that membrane integrity and cellular viability are closely linked. This is not always the case, at least in the early stages of cell death; so these assays may not always be true / sensitive indicators of viability. Therefore, other assays (MTT, AP) must be performed in order to obtain a complete picture of the effects of benzopyrones on cells under investigation.

The effects of four compounds (warfarin, 7-hydroxycoumarin, esculetin, and genistein) on cellular metabolism was examined using the MTT assay and the cytosensor (where only warfarin and esculetin have been tested on MCF-7 cells). However, the cytosensor method proved to be more useful than the MTT assay.

An important result evident from the data collected, was the fact that the Cytosensor Microphysiometer was more sensitive to the effects of the benzopyrones on cellular metabolism than the MTT assay. For example, the MTT assay detected a decrease in cellular metabolism of ~ 30% when MCF-7 cells were exposed to 20μg/ml esculetin for 24hrs (Figure 5.32.). According to the cytosensor results, the cellular metabolism in cells exposed to 20μg/ml esculetin decreased by approximately 60% over this time period. In fact it would appear from comparing the MTT and Cytosensor results for warfarin, esculetin and genistein (Figure 5.32 & 5.33), that the Cytosensor

328

Microphysiometer is a much more sensitive predictor of metabolic inhibition. These results support previous indications that the cytosensor possesses superior sensitivity in comparison to the MTT assay (Cooke & O'Kennedy, 1999).

The reason for this is unclear but may be coupled to the fact that the MTT assay relies on the activity of just one group of mitochondrial enzymes to predict adverse effects on metabolism, and in doing so may underestimate metabolic effects. The MTT assay has been shown to underestimate the growth inhibitory effects of interferons (IFNs) in the past (Jabbar *et al.*, 1989). Formazan production can also be induced by drugs that cause perturbations of the cell cycle (Supino, 1985). Cells have also been observed to metabolise the tetrazolium dye when lethally damaged and have lost the ability to exclude vital dyes (Maehara *et al.*, 1987). It should be noted that previous studies have shown optimal assay duration for human cell lines is a minimum of four days to allow for cell death and loss of dehydrogenase activity, with a maximum of seven days to obviate the necessity for refeeding cultures (Martin. 1992). The MTT assay was performed over 24 hrs (necessary for direct comparison to the 24hr cytosensor assay) and can only give an indication of the effects of drug exposure to cells (the results on their own cannot be conclusive). However, the data produced from this assay format can be assessed in conjunction with the other 96-well microtitre plate assays to determine the overall effect of the benzopyrones on cell proliferation and metabolism.

Apart from the increased sensitivity of prediction, the Cytosensor has several other advantages over the MTT assay for the detection of metabolic suppression. As mentioned before, the 'real-time' aspect of detection with the cytosensor yields large amounts of information on the nature of the metabolic suppression (*e.g.* time of detrimental effects, *etc.*), per experiment. To attain this information with an end-point system such as the MTT Assay would require multiple, kinetic end-point assays. In addition, the exposure set-up of the Cytosensor (flow-through, perfusive) mimics the *in vivo* drug delivery/exposure more than the static exposure set-up of the MTT Assay. Finally, the Cytosensor Microphysiometer allows for reversibility studies to be performed on drug-treated cells to assess their recovery, an experiment difficult, if not impossible to achieve with cells following the MTT Assay. The tested benzopyrones (warfarin, esculetin and genistein on cytosensor) all displayed a dose- and time-dependent effect on cellular metabolism, with genistein followed by esculetin displaying the most potent effects. For warfarin, only the highest concentration (100µg/ml) irreversibly suppressed the metabolism of the MCF-7 cells tested.

The acid phosphatase (AP) assay is based on hydrolysis of pNPP by intracellular AP in viable cells to produce *p*-nitrophenol. In comparison to [^{3}H] thymidine incorporation, AP assay has similar

329

sensitivity but a wider linear response range. The method also shows higher sensitivity and reproducibility in comparison to cell proliferation assays based on reduction of tetrazolium salts (e.g. MTT assay). Due to its ease of use, sensitivity and low cost the AP assay method is especially suited to applications where a large number of samples are assayed (Yang, et al., 1996; Si, et al., 1999). Results obtained for AP assays carried out on both cell lines showed that all compounds tested (same as MTT assay) had a detrimental effect on cell proliferation with esculetin and genistein being the most potent. Genistein had a proliferative effect at low concentrations only in MCF-7 cells, which was expected and correlates well with previous studies (Hsieh, 1998). Overall the AP assay was found to offer the best combination of sensitivity, linearity, flexibility, ease of performance, reproducibility and precision, of all the 96-well culture plate assays.

The investigation of how esculetin and warfarin affect the signal transduction cascade and cell cycle progression in MCF-7 cells was performed using three different assay formats. An ELISA for detection of tyrosine phosphorylation in whole cells was used in order to determine whether the agents tested inhibit tyrosine phosphorylation of growth factor stimulated EGF-R in MCF-7 cells. The cytosensor microphysiometer was utilised to determine whether esculetin or warfarin inhibit tyrosine kinase activity in EGF stimulated MCF-7 cells. The final assay again utilised the ELISA format, however this time it determined to what extent the agents inhibited DNA synthesis in MCF-7 cells. Previous studies have investigated the effects of E_2 on ER stimulation and signal transduction (Kelly & Wagner, 1999; Migliaccio et al., 1996; Aronica et al., 1994). However, breast cancer cells can be stimulated to proliferate with growth factors in the absence of added estrogen or progesterone. MAP kinase activation increases in response to stimuli such as EGF and IGF-1. Urokinase type plasminogen activator, FGF-2 and insulin activate MAP kinase in MCF-7 cells (Nguyen et al., 2000; Vercoutter-Edouart et al., 2000; Albas et al., 1998). Therefore, it was possible in this study to successfully stimulate the EGF-R in serum-starved MCF-7 cells with EGF and in turn activate the MAP kinase pathway in the absence of E_2.

The regulation of activated MAP kinase in MCF-7 cells involves inhibitory (TNF-α) as well as stimulatory (EGF) pathways. Research has shown that EGF stimulates activated MAP kinase within 1-2 minutes in MCF-7 cells. Maximal stimulation occurs at 6-8 minutes with a decrease in MAP kinase stimulation after this time period (Flury et al., 1997). The cytosensor results reflect this stimulation pattern as after the transient maximal stimulation of EGF-R (which will also transiently stimulate downstream MAP kinase activation), there is a decline in stimulation after a short time period of ~10 minutes. It was important to determine for this study that the EGF-R is tyrosine phosphorylated in MCF-7 cells. This has been demonstrated and tyrosine kinase activity was also

330

detected in Western blots of whole-cell protein extracts from the MCF-7 cell line probed with a phosphotyrosine antibody (Mueller *et al.*, 1994). Therefore, when MCF-7 cells were pre-exposed to either esculetin or warfarin it was possible to determine whether these agents inhibited tyrosine phosphorylation or not.

Esculetin is known to be a cytostatic drug and the inhibition of the cell-cycle at transition G_1/S is consistent with the cytostatic effect of both 7-hydroxycoumarin and esculetin. It is also evident from previous studies that esculetin primarily effects/inhibits events in the G_1 phase of the cell cycle (Jimenez-Orozco *et al.*, 2001; Wang *et al.*, 2002). If cells are arrested in G_1 phase before S phase progression there would be a significant decrease in DNA synthesis expected in these arrested cells. Therefore, the results illustrated in Figure 5.45. indicates there is a significant decrease in DNA synthesis in MCF-7 cells treated with either esculetin or genistein but not warfarin. It is possible that the decrease in DNA synthesis in esculetin-treated MCF-7 cells is due to the agent's ability to induce G_1 arrest with no progression to S phase where DNA synthesis occurs. Genistein seems to affect cell cycle progression differently to esculetin. Figure 5.44. shows that the decline in DNA synthesis occurs at a higher concentration than esculetin and this may be due to the fact that genistein does not arrest cells at G_1 phase. Genistein has been shown to inhibit progression later at G_2/M phase transition (Constantinou *et al.*, 1998; Fioravanti *et al.*, 1998; Papazisis *et al.*, 2000). This is after S phase and therefore, some DNA synthesis may occur. However, this stop in G_2/M phase usually is followed by apoptosis and not progression into mitosis as would happen in normal cycling cells. This leads to a decrease in DNA synthesis as cells die off due to apoptosis.

Taken together the signal transduction and cell cycle regulation results indicate what the possible target of esculetin in MCF-7 cells is and how it affects components of the activated MAP kinase pathway. This is illustrated in Figure 5.49. It is shown in this diagram that (backed up by results in Section 5.11.4.) esculetin can inhibit tyrosine phosphorylation of the stimulated EGF-R. This inhibition affects downstream molecules (e.g. Ras, ERK, Myc and Nuclear ER) with important roles in MAP kinase cascade (Pan *et al.*, 2003). Therefore, esculetin can inhibit the receptor tyrosine kinase activity of growth factor receptors such as EGF-R and ER. This in turn will prevent growth signals reaching other signalling intermediates such as Ras, or activation of transcription factors such as Myc. Another signal transduction pathway involves phosphatidylinositol-3-kinase (PI3-K) heterodimer, which is an important mediator of survival factors, protecting many cell types from multiple apoptosis-inducing stimuli. If PI3-K is inhibited (by esculetin inhibiting phosphorylation) the signalling pathway is interrupted and the cell is unable to progress into the S phase of the cell cycle.

Figure 5.49: *Proposed mechanism of action of esculetin in MCF-7 cells. Esculetin may function by inhibiting the RTK activity of growth factor receptors. This will prevent growth signals reaching other signalling intermediates such as Ras, or activation of transcription factors such as Myc. Alternatively, PI3-K may be a target, if inhibited (by inhibiting phosphorylation) it cannot inhibit GSK-3 which is free to degrade cyclin D1 which inhibits cell cycle progression.*

Given the importance of signalling anomalies in cancer cells, it was of interest to determine if the cellular target of esculetin or warfarin was a signalling pathway component. Since tyrosine phosphorylation is essential to the emanation of growth signals, and esculetin was previously reported to inhibit cellular tyrosine kinases, it was decided to concentrate on this aspect of signalling. The work presented in this chapter outlines the fact that the activity of the EGF-Receptor, tyrosine kinase, is affected adversely by exposure to esculetin but not by warfarin. The downregulation of RTK-induced tyrosine phosphorylation is important for the downstream growth factor signalling, and if inhibited, causes gross perturbation and downregulation of its signalling targets (particularly at the mRNA level). This might explain previous reports of downregulation of *ras* and *c-myc*, in 7-hydroxycoumarin and esculetin-treated cells (Seliger & Pettersson, 1994b; Lu *et al.*, 1996; Pan *et al.,* 2002). Regardless of whether they directly or indirectly inhibit the EGF-RTK, the decrease in tyrosine phosphorylation effected by coumarin compounds such as esculetin may offer an explanation for the precise mode of their anti-tumour action. Anomalies in tyrosine phosphorylation are extremely prevalent in tumour cells, and are responsible for persistent growth signalling in these cells. Interruption/disruption of this persistent signalling suppresses this abnormal proliferation, and therefore any compound, which decreases tyrosine phosphorylation, has anti-proliferative properties and potential clinical applications.

Chapter 6
Overall Conclusions

6.1 Overall Conclusions

The aim of the research performed was to study toxicological and immunological aspects of the benzopyrones. The immunological studies involved the characterisation of an anti-warfarin monoclonal antibody from clone 4-2-25 which was then used for the development of antibody-based assay systems for the detection of warfarin in biological fluids. The purpose of the toxicological studies was to examine the anti-cancer properties of benzopyrone compounds at a cellular level, in order to comprehend the observed clinical properties of these compounds.

Chapter 3 describes the characterisation of the anti-warfarin monoclonal antibody. The antibody was purified using a protein-G column and then utilised for the development of a competitive ELISA for the detection of warfarin in PBS and urine. Intra- and interday variability studies were performed to determine the precision and reproducibility of the assay. The assay proved to be accurate and reproducible with intra- and interday CVs of typically less than 10%. Cross reactivity studies demonstrated that the anti-warfarin mAb shared a common epitope with 4-hydroxycoumarin ring structure and the carbonyl substituent. Acenocoumarin showed the highest degree of cross-reactivity (18%) due to its structural similarities to warfarin. Both 6-hydroxywarfarin and 7-hydroxywarfarin show degrees of cross-reactivity of 8 & 1%, respectively. The method of Friguet *et al.*, (1985) was utilised to measure the affinity of the anti-warfarin mAb, which exhibited excellent specificity towards the parent molecule (warfarin) over structurally-related analogues (acenocoumarin, 6- and 7-hydroxywarfarin). This is evident from the resulting K_D values where the anti-warfarin mAb showed a higher affinity for warfarin ($K_D = 2.0 \times 10^{-8}$) than for any of the hydroxy metabolites assayed ($K_D = 2.0 \times 10^{-6} - 4.0 \times 10^{-7}$).

Chapter 4 involves the use of the anti-warfarin mAb (described in chapter 3) for the development of a BIAcore-based inhibition immunoassay for the detection of warfarin in biological fluids. Two sensor chip surfaces, the warfarin-BSA conjugated immobilised surface and the directly immobilised 4'-aminowarfarin chip surface were utilised. Decreasing concentrations of free warfarin was incubated with anti-warfarin mAb and allowed to equilibrate for 5-10 minutes. The samples were then passed in random order, over the derivatised chip surface. The biosensor-based assay system developed for the detection of warfarin in urine utilised a chip surface to which 4'-aminowarfarin was covalently coupled. Such surfaces demonstrated exceptional stability and reproducibility (% C.V. less than 12%) and were capable of being used for greater than 1,000 assays. In the clinical setting, economics is becoming increasingly more important and the use of such regenerable assay formats

offers a very attractive alternative to current high consumable-based alternatives (i.e. ELISA (immunoplates) and HPLC (solvent waste)).

The initial work in chapter 5, examined the toxicological effects of selected benzopyrones on the growth and metabolism of the two human tumour cell lines (MCF-7 & A549). From the assays performed (MTT, AP, LDH and cytosensor studies) it was evident that both genistein and esculetin exhibit the most potent anti-proliferative effects. Warfarin possessed weaker anti-proliferative effects in comparison to genistein and esculetin. Cell signalling studies are of interest with regard to the search for novel cancer chemotherapeutic agents. Knowledge of the effects of anti-cancer agents on signal transduction and cell cycle of cancer cells may prove useful in controlling the spread of cancer. Given the importance of signalling irregularities in cancer cells, it was of interest to determine if the cellular target of esculetin or warfarin was a signalling pathway component. Tyrosine phosphorylation is essential for the emanation of growth signals, and, since esculetin was previously reported to inhibit cellular tyrosine kinases, it was decided to concentrate on this aspect of signalling. The results presented in chapter 5 indicate that the tyrosine kinase activity of the EGF-Receptor in MCF-7 cells is affected adversely by pre-exposure to esculetin but not by warfarin. Therefore, it was possible to elucidate esculetin's mechanism of action on MCF-7 cells (Figure 5.49), from the results obtained in sections 5.11.4 - 5.11.5.

It is evident that the benzopyrones are a therapeutically interesting group of compounds with many clinically beneficial properties ranging from anti-coagulation (e.g. warfarin) to anti-proliferative effects (e.g. esculetin, genistein). It is apparent from this research that monoclonal antibodies can be produced to successfully detect these compounds (e.g. warfarin) in biological matrices. This thesis illustrates the current and potential clinical benefits of the benzopyrones. Clearly, the benzopyrones deserve further immunological and toxicological studies to facilitate better understanding of their mode of action and how they can be therapeutically applied in the future.

Chapter 7

References

Ad-El, D., Meirvitz, A., Weinberg, A., Kogan, L., Arieli, D., Neuman, A., Linton, D. (2000) Warfarin skin necrosis: local and systemic factors, *Br. J. Plastic Surg.,* **53:** 624-625.

Agarwal, R. (2000) Cell signalling and regulators of cell cycle as molecular targets for prostate cancer prevention by dietary agents, *Biochem. Pharmacol.,* **60:** 1051-1059.

Ahmad, A., Ramakrishnan, A., McLean, M., Breau, A. (2003) Use of surface plasmon resonance biosensor technology as a possible alternative to detect differences in binding of enantiomeric drug compounds to immobilised albumins, *Biosen. Bioelect.,* **18:** 399-404.

Aisner, J., Goutsou, M., Maurer, L.H., Cooper, R., Chahinian, P., Carey, R., Skarin, A., Slawson, R., Perry, M.C., Green, MR. (1992) Intensive combination chemotherapy, concurrent chest irradiation, and warfarin for the treatment of limited-disease small-cell lung cancer: a cancer and leukaemia group b pilot study, *J. Clin. Oncol.,* **10:** 1230-1236.

Akeb, F., Ferrua, B., Creminon, C., Roptin, C., Grassi, J., Nevers, M., Guedj, R., Garraffo, R., Duval, D. (2002) Quantification of plasma and intracellular levels of the HIV protease inhibitor, ritonavir, by competitive ELISA, *J. Immunol. Methods.,* **263:** 1-9.

Akimoto, T., Nonaka, T., Ishikawa, H., Sakurai, H., Saitoh, J.I., Takahashi, T., Mitsuhashi, N. (2001) Genistein, a tyrosine kinase inhibitor, enhanced radiosensitivity in human esophageal cancer cell lines *in vitro*: possible involvement of inhibition of survival signal transduction pathways, *Int. J. Radiation. Oncol. Biol. Phys.,* **50:** 195-201.

Alblas, J., Slager-Davidov, R., Steenbergh, P.H., Sussenbach, J.S., van Der, B. (1998) The role of map kinase in TPA-mediated cell cycle arrest of human breast cancer cells, *Oncogene,* **16:** 131-139.

Anastase-Ravion, S., Ding, Z., Pelle, A., Hoffmann, A., Letoumeur, D. (2001) New antibody purification procedure using a thermally responsive poly(n-isopropylacrylamide)-dextran derivative conjugate, *J. Chromatog. B,* **761:** 247-254.

Anderes, K., Luthin, D., Castillo, R., Kraynov, E., Castro, M., Nared-Hood, K., Gregory, M., Pathak, V., Christie, L., Paderes, G., Vazir, H., Ye, Q., Anderson, M., May, J. (2003) Biological characterisation of a novel, orally active small molecule gonadotropin-releasing hormone (GnRH) antagonist using castrated and intact rats, *J. Pharmacol Exp. Ther.,* **305:** 688-695.

338

Andersson, M., Ronnmark, J., Arestrom, I., Nygren, P.A., Ahlborg, N. (2003) Inclusion of a non-immunoglobulin binding protein in two-site ELISA for quantification of human serum proteins without interference by heterophilic serum antibodies, *J. Immunol. Methods,* **283:** 225-234.

Anfossi, L., Giraudi, G., Tozzi, C., Giovannoli, C., Baggiani, C., Vanni, A. (2004) Development of a non-competitive immunoassay for monitoring DDT, its metabolites and analogues in water samples, *Anal. Chim. Acta,* **506:** 87-95.

Ansel, H., Allen, L., Popovich, N. (1999) *Pharmaceutical Dosage Forms and Drug Delivery Systems,* Seventh Edition, Lippincott, Williams & Wilkens, New York.

Arndt, M. & Krauss J. (2003) Bispecific diabodies for cancer therapy, *Methods Mol. Biol.,* **207:** 305-321.

Aronica, S., Kraus, W., Katzenellenbogen, B. (1994) Estrogen action via the cAMP signalling pathway: stimulation of adenylate cyclase and cAMP-regulated gene transcription, *Proc. Natl. Acad. Sci. USA.,* **91:** 8517-8521.

Arteaga, C. (2003) Targeting HER1/EGFR: a molecular approach to cancer therapy, *Semin. Oncol.,* **30:** 3-14.

Aubrey, N., Devaux, C., Sizaret, P., Rochat, H., Goyffon, M., Billiald, P. (2003) Design and evaluation of a diabody to improve protection against a potent scorpion neurotoxin, *Cell. Mol. Life Sci.,* **60:** 617-628.

Babu, E. & McIntyre, J. (2001) Warfarin-induced changes characteristic of inflammatory carcinoma of the breast, *The Breast,* **10:** 348-359.

Bai, M. (2004) Dimerization of G-protein-coupled receptors: roles in signal transduction, *Cell. Signal.,* **16:** 175-186.

Bain, C., Evall, J., Whitesides, G. (1989) Formation of monolayers by the coadsorption of thiols on gold: variation in the head group, tail group, and solvent, *J. Am. Chem. Soc.,* **111:** 321-335.

Banfield, C. & Rowland, M. (1984) Stereospecific fluorescence high-performance liquid chromatographic analysis of warfarin and its meabolites in plasma and urine, *J. Pharm. Sci.*, **73:** 1392-1396.

Barboule, N., Lafon, C., Chadebech, P., Vidal, S., Valette, A. (1999) Involvement of p21 in the PKC-induced regulation of the G2/M cell cycle transition, *FEBS Letts.*, **444:** 32-37.

Barnard, D., Sun, H., Baker, L., Marshall, M.S. (1998) *In vitro* inhibition of Ras-Raf association by short peptides, *Biochem. Biophys. Res. Commun.*, **247:** 176-180.

Barragan, M., Bellosillo, B., Campas, C., Colomer, D., Pons, G., Gil, J. (2002) Involvement of Protein kinase C and phosphatidylinositol 3-kinase pathways in the survival of B-cell chronic lymphocytic leukaemia cells, *Blood,* **99:** 2969-2976.

Barrett, J. (1996) Phytoestrogens: friends or foes?, *Environ. Health Perspect.*, **104:** 478-482.

Bengten, E., Wilson, M., Miller, N., Clem, L.W., Pilstrom, L., Warr, G.W. (2000) Immunoglobulin isotypes: structure, function, and genetics, *Curr. Top. Microbiol. Immunol.*, **248:**189-219.

Bentley, D., Backhouse, G., Hutchings, A., Haddon, R., Spragg, B., Routledge, P. (1986) Investigation of patients with abnormal response to warfarin, *Br. J. Clin. Pharmacol.*, **22:** 37-41.

Berkner, K. (2000) The vitamin K-dependent carboxylase, *J. Nutr.*, **130:** 1877-1880.

Bertola, J., Mazoyer, E., Bergmann, J., Drouet, L., Simoneau Mahe, I. (2003) Early prediction of the sensitivity of warfarin in elderly patients by the fall in factor VIIc and protein C at the induction of treatment, *Thromb. Res.,* **109:** 287-291.

Bertucci, C. & Cimitan, S. (2003) Rapid screening of small ligand affinity to human serum albumin by an optical biosensor, *J. Pharm. Biomed. Anal.*, **32:** 707-714.

Bertucci, C., Canepa, A., Ascoli, G.A., Guimaraes, L., Felix, G. (1999) Site I on human albumin: differences in the binding of (R)- and (S)-warfarin, *Chirality,* **11:** 675-679.

Bethea, D., Fullmer, B., Syed, S., Seltzer, G., Tiano, J., Rischko, C., Gillespie, L., Brown, D., Gasparro, F. (1999) Psoralen photobiology and photochemotherapy: 50 years of science and medicine, *J. Dermatol. Sci.,* **19:** 78-88.

Bobek, V., Boubelik, M., Kovarik, J., Taltynov, O. (2003) Inhibition of adhesion breast cancer cells by anticoagulant drugs and cimetidine, *Neop.,* **50:** 148-151.

Bobrovnik, S.A. (2003) Determination of antibody affinity by ELISA. Theory, *J. Biochem. Biophys. Methods,* **57:** 213-236.

Boder, E., Midelfort, K., Wittrup, K. (2000) Directed evolution of antibody fragments with monovalent femtomolar antigen-binding site, *Proc. Natl. Acad. Sci., USA.,* **97:** 10701-10705.

Bogan, D., Deasy, B., O'Kennedy, R., Smyth, M. (1995) Determination of free and total 7-hydroxycoumarin in urine and serum by capillary electrophoresis, *J. Chromatogr. B.,* **663:** 371-378.

Bogan, D., Deasy, B., O'Kennedy, R., Smyth, M. (1996) The use of capillary electrophoresis for studying interspecies differences in coumarin metabolism in liver microsomes, *Xenobiotica,* **26:** 437-448.

Bokken, G., Corbee, R., Van Knapen, F., Bergwerff, A. (2003) Immunochemical detection of *salmonella* group B, D and E using an optical surface plasmon resonance biosensor, *FEMS Microbiol. Letts.,* **222:** 75-82.

Boppana, V., Schaefer, W., Cyronak, M. (2002) High-performance liquid-chromatographic determination of warfarin enantiomers in plasma with automated on-line sample enrichment, *J. Biochem. Biophys. Methods,* **54:** 315-326.

Bosland, M.C. (1991) Prostate Cancer, In: *Encyclopaedia of Human Biology,* First Edition, Academic Press, San Diego, **6:** 177-190.

Boulianne, G., Hozumi, N., Shulman, M. (1984) Production of functional chimaeric human/mouse antibody, *Nature (London),* **312:** 643-646.

Bourinbaiar, A. & Jirathitikal, V. (2003) Low-cost anti-HIV compounds: potential application for AIDS therapy in developing countries, *Curr. Pharm. Design,* **9:** 1419-1431.

Bourinbaiar, A., Tan, X., Nagorny, R. (1993) Effect of the oral anticoagulant, warfarin, on HIV-1 replication and spread, *AIDS,* **7:** 129-130.

Brady, H., Desai, S., Gayo-Fung, L.M., Khammungkhune, S., McKie, J.A., O'Leary, E., Pascasio, L., Sutherland, M.K., Anderson, D.W., Bhagwat, S.S., Stein, B. (2002) Effects of SP500263, a novel, potent antiestrogen, on breast cancer cells and in xenograft models, *Cancer Res.,* **62:** 1439-1442.

Breckenbridge, A. & Orme, W. (1973) Kinetics of warfarin absorption in man, *Clin. Pharmacol. Therapeutics,* **14:** 955-961.

Brennan, J., Dillon, P., O'Kennedy, R. (2003) Production, purification and characterisation of genetically-derived scFv and bifunctional antibody fragments capable of detecting illicit drug residues, *J. Chromatogr. B,* **786:** 327-342.

Brooks, C., Rutherford, J., Gould, J., Ramsay, M., James, D. (2002) Warfarin dosage in postpartum women: a case-control study, *Br. J. Obstet. Gynaecol.,* **109:** 187-190.

Bruce, M., Boyd, V., Duch, C., White, J. (2002) Dialysis-based bioreactor systems for the production of monoclonal antibodies - alternatives to ascites production in mice, *J. Immunol. Methods,* **264:** 59-68.

Bruggermann, M., Caskey, I., Teale, C., Walermann, I., Williams, G., Surani, M., Neuberger, M. (1989) A repertoire of monoclonal antibodies with human heavy chains from transgenic mice, *Prac. Natl. Acad. Sci.,USA,* **86:** 6709-6713.

Brunet, A., Roux, D., Lenormand, P., Dowd, S., Keyse, S., Pouysségur, J. (1999) Nuclear translocation of p42/p44 mitogen-activated protein kinase is required for growth factor-induced gene expression and cell cycle entry, *E.M.B.O. J.,* **18:** 664-674.

Bruneton, J. (1999) *Pharmacognosy, Phytochemistry, Medicinal Plants,* Second Edition, Intercept Ltd, Hampshire UK., pp 263-277.

Bruno, J. (1998) Validation BIACORE assay, *BIAjournal*, **2:** 9-11.

Budzisz, E., Brzezinska, E., Krajewska, U., Rozalski, M. (2003) Cytotoxic effects, alkylating properties and molecular modelling of coumarin derivatives and their phosphonic analogues, *Eur. J. Med. Chem.,* **38:** 597-603.

Bunone, G., Briand, P., Miksicek, R., Picard, D. (1996) Activation of the unliganded estrogen receptor by EGF involves the MAP kinase pathway and direct phosphorylation, *E.M.B.O. J.,* **15:** 2174-2183.

Burvall, K., Palmberg, L., Larsson, K. (2002) Metabolic activation of A549 human airway epithelial cells by organic dust: a study based on microphysiometry, *Life Sci.,* **71:** 299-309.

Bush, E., Low, L., Trager, W. (1983) A sensitive and specific stable isotope assay for warfarin and its metabolites, *Biomed. Mass Spec.,* **10:** 395-398.

Buyck, H., Buckley, N., Leslie, M., Plowman, P. (2003) Capecitabine-induced potentiation of warfarin, *Clin. Oncol.,* **15:** 1.

Byrden, T. (1996) The elucidation of the mode of action of coumarin and some specified derivatives, **MSc Thesis,** Dublin City University, Dublin, Ireland.

Cahill, D., Roben, P., Quinlan, N., O'Kennedy, R. (1995) Immunoassays, In: *Encyclopaedia of Analytical Science,* First Edition, (Ed) Townshend A, Academic Press, New York, **7:** 4343-4348.

Cai, B., Zhang, H., Zhang, D., Cui, C., Li, W. (2002) Apoptosis-inducing activity of extract from chinese herb, *Albizzia Lucidior I. Neilsen, Ai Zheng,* **21:** 373-378.

Campbell, H., Smith, W., Roberts, W., Link, K. (1948) Studies on the haemorrhagic sweet clover disease. II. The bioassay of haemorrhagic concentrates by following the prothrombin level in the plasma of rabbit blood, *J. Biol. Chem.,* **138:** 1-20.

Cao, C., Eldefrawi, M., Eldefrawi, A., Burnett, J., Mioduszewski, R., Menking, D., Valdes, J. (1998) Toxicity of sea nettle toxin to human hepatocytes and the protective effects of phosphorylating and alkylating agents, *Toxicon.,* **36:** 269-281.

Cao, C., Mioduszewski, R., Menking, D., Valdes, J., Katz, E., Eldefrawi, M., Eldefrawi, A. (1999) Cytotoxicity of Organophosphate Anticholinesterases, *In Vitro Cell & Dev. Biol.,* **35:** 493-500.

Capitán-Vallvey, L., Deheldel, M., Avidad, R. (1999) Determination of warfarin in waters and human plasma by solid-temperature transmitted phosphorescence, *Arch. Environ. Cont. Toxicol.,* **37:** 1-6.

Caponigro, F. (2002) Farnesyl transferase inhibitors: a major breakthrough in anticancer therapy?, *Anticancer Drugs,* **13:** 891-897.

Cardenas, M., Sanfridson, A., Cutler, N., Heitman, J. (1998) Signal-transduction cascades as targets for therapeutic intervention by natural products, *TIBTECH,* **16:** 427-433.

Carter, S.K., Bakowski, M.T., Hellman, K. (1989) *Chemotherapy of Cancer,* Third Edition, Wiley & Sons, New York.

Casley-Smith, J.R. & Casley-Smith, J.R. (1997) Coumarin in the treatment of lymphoedema and other high-protein oedemas, In: *Coumarins: Biology, Applications and Mode of Action,* (Eds: R O'Kennedy & R.D. Thornes), John Wiley & Sons, Chichester, pp 143-184.

Casley-Smith, J.R. & Casley-Smith, J.R. (1986) *High Protein Oedema and the Benzopyrones,* J.B. Lippincott, Sydney.

Chan, K. & Woo, K. (1988) Determination of warfarin in human plasma by high performance liquid chromatography, *Meth. Findings Exptl. Clin. Pharmacol.,* **10:** 699-703.

Chen, H. & Walsh, C.T. (2001) Coumarin formation in novobiocin biosynthesis: beta-hydroxylation of the aminoacyl enzyme Tyrosyl-S-Novh by a Cytochrome P450 NovI, *Chem Biol.,* **8:** 301-312.

Chiarugi, P. & Cirri, P. (2003) Redox regulation of protein tyrosine phosphatases during receptor tyrosine kinase signal transduction, *TRENDS Biochem. Sci.,* **28:** 509-514.

Chinowsky, T., Quinn, J., Bartholomew, D.U., Kaiser, R., Elkind, J. (2003) Performance of the Spreeta 2000 integrated surface plasmon resonance affinity sensor, *Sens. Actuat. B,* **91:** 266-274.

Cho, H., Choi, D., Ko, B., Nam, C., Park, K., Lee, Y., Lee, S., Lee, J., Lee, K., Lee, E., Ju, S., Kim, B. (2000) Cold preservation of rat cultured hepatocytes: the scoparone effect, *Transplant. Proc.,* **32:** 2325-2327.

Chu, K., Wu, S., Stanley, T., Stafford, D., High, K. (1996) A mutation in the propeptide of factor IX leads to warfarin sensitivity by a novel mechanism, *J. Clin. Invest.,* **98:** 1619-1625.

Chua, M.S., Kashiyama, E., Bradshaw, T., Stinson, S., Brantley, E., Sausville, E., Stevens, M. (2000) Role of CYP1A1 in modulation of antitumour properties of the novel agent 2-(4-Amino-3-methylphenyl)benzothiazole (DF 203, NSC 674495) in human breast cancer cells, *Cancer Res.,* **60:** 5196-5203.

Clark, J. & Bremner, B. (2002) Fatal warfarin-induced skin necrosis after total hip arthroplasty, *J. Arthroplasty,* **17:** 1070-1073.

Clark, M. (2000) Antibody humanisation: a case of the 'emperor's new clothes'?, *Immunol. Today,* **21:** 397-402.

Clarke, R., Hilakivi-Clarke, L., Trock, B. (2001) Breast cancer: dietary and environmental oestrogens, *Biologist,* **48:** 21-26.

Clothier, R. (1985) The FRAME cytotoxicity test (Kenacid blue), In: *Methods in Molecular Biology, vol.43: In vitro Toxicity Testing Protocols,* (Eds: S. O'Hare & C.K. Atterwill), Humana Press Inc.,Totowa, USA, pp 109-118.

Clynes, M., O'Connor, R., O'Driscoll, L., Daly, C., Meleady, P. (2003) Challenges in molecular analysis for individualised cancer therapy, *Drug Disc. Today,* **8:** 531.

Coffey, M., Strong, J., Forsyth, P., Lee, P. (1998) Reovirus therapy of tumours with activated ras pathway, *Science,* **282:** 1332-1334.

Coleman, M., Goldenberg, D., Siegel, A., Ketas, J., Ashe, M., Fiore, J., Leonard, J. (2003) Epratuzumab: targeting b-cell malignancies through CD22, *Clin. Cancer Res.,* **9:** 3991S-4S.

345

Connolly, D., Knight, M., Harakas, N., Wittwer, A., Feder, J. (1986) Determination of the number of endothelial cells in culture using an acid phosphatase assay, *Anal. Biochem.,* **152:** 136-140.

Constantinou, A.I., Kamath, N., Hurley, J.S. (1998) Genistein inactivates Bcl-2, delays the G2/M phase of the cell cycle, and induces apoptosis of human breast adenocarcinoma MCF-7 cells, *Eur. J. Cancer,* **34:** 1927-1934.

Cook, C., Ballentine, D., Seltzman, T., Tallent, C. (1979) Warfarin enantiomer disposition: determination by stereoselective radioimmunoassay, *J. Pharmacol. Exp. Pharm.,* **210:** 391-398.

Cooke, D. & O'Kennedy, R. (1999) Comparison of the tetrazolium salt assay for succinate dehydrogenase with the cytosensor microphysiometer in the assessment of compound toxicities, *Anal. Biochem.,* **274:** 188-194.

Cooke, D., Fitzpatrick, B., O'Kennedy, R., McCormack, T., Egan, D. (1997) Coumarins – multifaceted molecules with many analytical and other applications, In: *Coumarins: Biology, Applications and Mode of Action,* (Eds: R O'Kennedy & R.D. Thornes), John Wiley & Sons, Chichester, pp 303-332.

Cooke, D. (1999) Studies on the mode of action of coumarins (coumarin, 6-hydroxycoumarin, 7-hydroxycoumarin and esculetin) at a cellular level, **PhD Thesis**, Dublin City University, Dublin, Ireland.

Cooper, M.A. (2003) Biosensor profiling of molecular interactions in pharmacology, *Curr. Opin. Pharmacol.,* **3:** 557-562.

Coqueret, O. (2003) New roles for p21 and p27 cell-cycle inhibitors: a function for each cell compartment?, *TRENDS Cell Biol.,* **13:** 65-70.

Corsini, E., Lucchi, L., Binaglia, M., Viviani, B., Bevilacqua, C., Monastra, G., Marinovich, M., Galli, C. (2001) Cloricromene, a semi-synthetic coumarin derivative, inhibits tumour necrosis factor-α production at a pre-transcriptional level, *Eur. J. Pharmacol.,* **418:** 231-237.

Corvera, S. (2001) Phosphatidylinositol 3-Kinase and the control of endosome dynamics: new players defined by structural motifs, *Traffic,* **2:** 859-866.

Cosgriff, T. & Stuart, W. (1953) Chronic anticoagulant therapy in recurrent embolism of cardiac origin, *Ann. Intern. Med.,* **38:** 278-287.

Cotrufo, M., De Feo, M., De Santo, L., Romano, G., Della Corte, A., Renzulli, A., Gallo, C. (2002) Risk of warfarin during pregnancy with mechanical valve prostheses, *Obstet. Gynecol.,* **99:** 35-40.

Crooks, S., McCarney, B., Traynor, I., Thompson, C., Floyd, S., Elliott, C. (2003) Detection of levamisole residues in bovine liver and milk by immunobiosensor, *Anal. Chim. Acta,* **483:** 181-186.

Crowther, J. (1995) *ELISA Theory and Practice*, First Edition, Humana Press, New Jersey.

D'Orazio, P. (2003) Biosensors in clinical chemistry, *Clin. Chim. Acta.,* **334:** 41-69.

Danelian, E., Karlén, A., Karlsson, R., Winiwarter, S., Hansson, A., Löfås, S., Lennernäs, H., Hämäläinen, M. (2000) SPR biosensor studies of the direct interaction between 27 drugs and a liposome surface: correlation with fraction absorbed in humans, *J. Med. Chem.,* **43:** 2084-2087.

Dangi, S., Hyukjin, C., Shapiro, P. (2003) Requirement for phosphatidylinositol-3 kinase activity during progression through S-phase and entry into mitosis, *Cell. Signal.,* **15:** 667-675.

Daniell, H., Streatfield, S., Wycoff, K. (2001) Medical molecular farming: production of antibodies, biopharmaceuticals and edible vaccines in plants, *TRENDS Plant Sci.,* **6:** 219-226.

Danilova, N. (1994) ELISA screening of monoclonal antibodies to haptens: influence of the chemical structure of hapten-protein conjugates, *J. Immunol. Methods,* **117:** 111-117.

Davies, C. (1994a) Antibody structure and function, In: *The Immunoassay Handbook* (Ed. Wlid D), Stockton Press, New York, pp 3-8.

Davies C. (1994b) Immunoassay design, In: *The Immunoassay Handbook* (Ed. Wlid D), Stockton Press, New York, pp 15-44.

De Orsi, D., Gagliardi, L., Turchetto, L., Tonelli, D. (1998) HPLC determination of warfarin and acenocoumarol in raw materials and pharmaceuticals, *J. Pharm. Biomed. Anal.,* **17:** 891-895.

De Rosa, S., Mitova, M., Handjieva, N., Calis, I. (2002) Coumarin glucosides from *Cruciata taurica, Phytochem.,* **59:** 447-450.

De Vries, J., & Schmitz-Kummer, E. (1993) Direct column liquid chromatographic enantiomer separation of the coumarin anticoagulants phenprocoumon, warfarin, acenocoumarol and metabolites on an α-acid glycoprotein chiral stationary phase, *J. Chromatogr.,* **614:** 315-320.

De Vries, J., Harenberg, J., Walter, E., Zimmerman, R., Simon, M. (1982) Determination of the anticoagulant phenprocoumon in human plasma and urine by high-performance liquid chromatography, *J. Chromatogr. Biomed. Appl.,* **231:** 83-92.

De Vries, H., Ronken, E., Reinders, J., Buchner, B., Van Berkel, T., Kuiper, J. (1998) Acute effects of oxidised low density lipoprotein on metabolic responses in macrophages, *FASEB J.,* **12:** 111-118.

De Wildt, R., Mundy, C., Gorick, B., Tomlinson, I. (2000) Antibody arrays for high-throughput screening of antibody-antigen interactions, *Nature Biotechnol.,* **18:** 989-994.

Deasy, B. (1996) Development of novel analytical methods to study the metabolism of coumarin, **PhD Thesis,** Dublin City University, Dublin, Ireland.

Delves, P. (1995) *Antibody Applications-Essential Techniques,* First Edition, John Wiley & Sons, New York.

Dempke, W.C. (2003) Farnesyltransferase inhibitors-a novel approach in the treatment of advanced pancreatic carcinomas, *Anticancer Res.,* **23:** 813-818.

Dempsey, E., O'Sullivan, C., Smyth, M.R., Egan, D., O'Kennedy, R., Wang, J. (1993) Development of an electrochemical biosensor for 7-hydroxycoumarin, *Analyst,* **118:** 411-414.

Deprez, P., Mandine, E., Gofflo, D., Meunier, S., Lesuisse, D. (2002) Small ligands interacting with the phosphotyrosine binding pocket of the Src SH$_2$ protein, *Bioorg. Med. Chem. Letts.,* **12:** 1295-1298.

Desta, Z., Soukhova, N., Mahal, S., Flockhart, D. (2000) Interaction of cisapride with human Cytochrome P450 system: metabolism and inhibition studies, *Drug Metab. Disposition,* **28:** 789-800.

Dexeus, F.H., Logothetis, C.J., Sella, A., Fitz, K., Amato, R., Reuben, J.M., Dozier, N. (1990) Phase II study of coumarin and cimetidine in patients with metastatic renal-cell carcinoma, *J. Clin. Oncol.*, **8:** 325-329.

Dharmaratne, H., Sajeevani, M., Marasinghe, G., Ekanayake, E. (1998) Distribution of pyranocoumarins in calophyllum cordato-oblongum, *Phytochemistry,* **49:** 995-998.

Diawara, M.M., Allison, T., Kulkosky, P., Williams, D.E. (1997) Psoralen-induced growth inhibition in wistar rats, *Cancer Letts.,* **114:** 159-160.

Dillon, P., Daly, S., Manning, B., O'Kennedy, R. (2003) Immunoassay for the determination of morphine-3-glucuronide using a surface plasmon resonance-based biosensor, *Biosen. Bioelect.,* **18:** 217-227.

Dockal, M., Carter, D., Ruker, F. (1999) The three recombinant domains of human serum albumin, *J. Biol. Chem.*, **274:** 29303-29310.

Dueñas, M., Malmborg, A., Casavilla, R., Ohlin, M., Borrebaeck, C. (1996) Selection of phage displayed antibodies based on kinetic constants, *Mol. Immunol.,* **33:** 279-285.

Ebbinghaus, S.W., Mohler, J.L., Marshall, M.E. (1997) Renal cell carcinoma: the background, rationale and current development of coumarin (1,2-benzopyrone) as a potential therapeutic agent, In: *Coumarins: Biology, Applications and Mode of Action,* (Eds: R O'Kennedy & R.D. Thornes), John Wiley & Sons, Chichester, pp 209-239.

Egan, D. & O'Kennedy, R. (1992) Rapid and sensitive determination of coumarin and 7-hydroxycoumarin and its glucuronide conjugate in urine and plasma by high performance liquid chromatography, *J. Chromatogr. B*, **582:** 137-143.

Egan, D. & O'Kennedy, R. (1993a) Spectrofluorimetric method for the quantification of 7-hydroxycoumarin in urine and plasma using both extracted and unextracted samples, *Analyst*, **118:** 201-203.

Egan, D. & O'Kennedy, R. (1993b) The production and characterisation of anti-7-hydroxycoumarin antibodies and their use in the development of an enzyme-linked immunosorbent assay, *J. Ir. Coll. Phys. Surg.*, **22:** 72.

Egan, D., James, P., Cooke, D., O'Kennedy, R. (1997) Studies on the cytostatic and cytotoxic effects and mode of action of 8-nitro-7-hydroxycoumarin *Cancer Letts.*, **118:** 201-211.

Egan, D., O'Kennedy, R., Moran, E., Cox, D., Prosser, E., Thornes, R.D. (1990) The pharmacology, metabolism, analysis and applications of coumarin and coumarin-related compounds, *Drug Metab. Rev.*, **22:** 503-529.

Ekelund, S., Larsson, R., Nygren, P. (2002) Metabolic effects of the cytotoxic guanidino-containing drug CHS 828 in human U-937 lymphoma cells, *Anticancer Res.*, **22:** 2269-2274.

Ekelund, S., Liminga, G., Bjorkling, F., Ottosen, E., Schou, C., Binderup, L., Larsson, R. (2000) Early stimulation of acidification rate by novel cytotoxic pyridyl cyanoguanidines in human tumour cells: comparison with *m*-Iodobenzylguanidine, *Biochem. Pharmacol.*, **60:** 839-849.

Ekelund, S., Sjöholm, Å., Nygren, P., Binderup, L., Larsson, R. (2001) Cellular pharmacodynamics of the cytotoxic guanidine-containing drug CHS 828. Comparison with methylglyoxal-bis(guanylhydrazone), *Eur. J. Pharmacol.*, **418:** 39-45.

Ekins, R. (1992) Immunoassay design and optimisation, In: *Principles and Practice of Immunoassay* (Eds: Price E & Newman D) Stockton Press, New York, pp 96-149.

Ekins, R. (1998) Ligand assay: from electrophoresis to miniaturized microarrays, *Clin. Chem.*, **44:** 2015-2030.

Elian, A. (2003) ELISA detection of clonazepam and 7-aminoclonazepam in whole blood and urine, *Forensic Sci. Int.*, **134:** 54-56.

Elkind, J., Stimpson, D., Strong, A., Bartholomew, D., Melendez, J. (1999) Integrated analytical sensors: the use of the TISPR-1 as a biosensor, *Sens. Actuators, B* **54:** 182–190.

Evans, I., Sayers, M., Gibbons, A., Price, G., Snooks, H., Sugar, A. (2002) Can warfarin be continued during dental extraction? results of a randomised controlled trial, *Br. J. Oral Maxillofacial Surg.,* **40:** 248-252.

Fach, P., Perelle, S., Grout, J., Dilasser, F. (2003) Comparisonm of different PCR tests for detecting shiga toxin-producing *Escherichia coli* O157 and development of an ELISA-PCR assay for specific identification of the bacteria, *J. Microbiol. Methods,* **55:** 383-392.

Fan, J., Banerjee, D., Stambrook, P., Bertino, J. (1997) Modulation of cytotoxicity of chemotherapeutic drugs by activated H-ras, *Biochem. Pharmacol.,* **53:** 1203-1209.

Fan, Y., Wu, D.Z., Gong, Y.Q., Xu, R., Hu, Z.B. (2002) Metabolic responses induced by thrombin in human umbilical vein endothelial cells, *Biochem. Biophys. Res. Commun.,* **293:** 979-985.

Fang, Y., Li, Z., Watanabe, Y. (2003) Pharmacokinetics of a novel anti-asthmatic, scoparone, in the rabbit serum, assessed by a simple HPLC method, *J. Ethnopharmacol.,* **86:** 127-130.

Fasciglione, G., Marini, S., Bannister, J., Giardina, B. (1996) Hapten-carrier interactions and their role in the production of monoclonal antibodies against hydrophobic haptens, *Hybridoma,* **15:** 1-9.

Fasco, M., Piper, L., Kaminsky, L. (1977) Biochemical applications of a quantitative high-pressure liquid chromatographic assay of warfarin and it's metabolites, *J. Chrom.,* **131:** 365-373.

Favata, M., Horiuchi, K., Manos, E., Daulerio, A., Stradley, D., Feeser, W., Van Dyk, D., Pitts, W., Earl, R., Hobbs, F., Copeland, R., Magolda, R., Scherle, P., Trzaskos, J. (1998) Identification of a novel inhibitor of mitogen-activated protein kinase kinase, *J. Biol. Chem.,* **273:** 18623-18632.

Fentem, J. & Fry, J. (1992) Metabolism of coumarin by rat, gerbil and human liver microsomes *Xenobiotica,* **22:** 357-367.

Ferrer, J., Leiton, M., Zaton, A. (1998) The binding of benzopyranes to human serum albumin. A structure-affinity study, *J. Protein Chem.,* **2:** 115-119.

Findlay, J., Smith, W., Lee, J., Nordblom, G., Das, I., DeSilva, B., Khan, M., Bowsher, R. (2000) Validation of immunoassays for bioanalysis: A pharmaceutical industry perspective, *J. Pharm. Biomed. Anal.,* **21:** 1249-1273.

Finn, G., Kenealy, E., Creaven, B., Egan, D. (2002) *In vitro* cytotoxic potential and mechanism of action of selected coumarins, using human renal cell lines, *Cancer Letts.,* **183:** 61-68.

Fioravanti, L., Cappelletti, V., Miodini, P., Ronchu, E., Brivio, M., Di Fronzo, G. (1998) Genistein in the control of breast cancer cell growth: insights into the mechanism of action *in vitro, Cancer Letts.,* **130:** 143-152.

Fischer, H., Seelig, A., Beier, N., Raddatz, P., Seelig, J. (1999) New drugs for the Na+/H+ exchanger. Influence of Na+ concentration and determination of inhibition constants with a microphysiometer, *J. Membr. Biol.,* **168:** 39-45.

Fischer, R,. & Emans, N. (2000) Molecular farming of pharmaceutical proteins, *Transgenic Res.,* **9:** 279-299.

Fitzpatrick, B. (2001) The production, characterisation and applications of polyclonal and monoclonal antibodies to warfarin, **PhD Thesis,** Dublin City University, Dublin, Ireland.

Flood, E., Redish, M., Bociek, S., Shapiro, S. (1943) Thrombophlebitis migrans disseminate: report of a case in which gangrene of the breast occurred: observations on the therapeutic use of dicumarol (3,3¢methylenebis(4-hydroxycoumarin)) *NY. State J. Med.,* **43:** 1121-1124.

Flury, N., Eppenberger, U., Mueller, H. (1997) Tumour-necrosis factor-alpha modulates mitogen-activated protein kinase activity of epidermal-growth-factor-stimulated MCF-7 breast cancer cells, *Eur. J. Biochem.,* **249:** 421-426.

Forero, A., Meredith, R., Khazaeli, M., Carpenter, D., Shen, S., Thornton, J., Schlom, J., LoBuglio, A. (2003) A novel monoclonal antibody design for radioimmunotherapy, *Cancer Biother. Radiopharm.,* **18:** 751-759.

Foster, J., Henley, D., Ahamed, S., Wimalasena, J. (2001) Estrogens and cell-cycle regulation in breast cancer, *TRENDS Endocrinol. Metab.,* **12:** 320-327.

Foster, J., Henley, D., Bukovsky, A., Seth, P., Wimalasena, J. (2001a) Multifaceted regulation of cell cycle progression by estrogen: regulation of Cdk inhibitors and Cdc25A independent of cyclin D1-Cdk4 function, *Mol. Cell. Biol.,* **21:** 794-810.

Frankfurt, O. & Krishan, A. (2001) Enzyme-Linked Immunosorbent Assay (ELISA) for the specific detection of apoptotic cells and its application to rapid drug screening, *J. Immunol. Methods.,* **253:** 133-144.

Friguet, B., Chaffotte, A., Djavadi-Ohaniance, L., Goldberg, M. (1985) Measurements of the true affinity constant in solution of antigen-antibody complexes by enzyme-linked immunosorbent assay, *J. Immunol. Methods,* **77:** 305-319.

Frostell-Karlsson, A., Remaeus, A., Roos, H., Andersson, K., Borg, P., Hamalainen, M. (2000) Biosensor analysis of the interaction between immobilized human serum albumin and drug compounds for prediction of human serum albumin binding levels, *J. Med. Chem.,* **43:** 1968-1992.

Fukazawa, H., Noguchi, K., Murakami, Y., Uehara, Y. (2002) Mitogen-activated protein/extracellular signal-regulated kinase kinase (MEK) inhibitors restore anoikis sensitivity in human breast cancer cell lines with a constitutively activated extracellular-regulated kinase (ERK) pathway, *Mol. Cancer Ther.,* **1:** 303-309.

Gage, B., Fihn, S., White, R. (2000) Management and dosing of warfarin therapy, *Am. J. Med.,* **109:** 481-488.

Galka, M., Lvarrav, V., Lakabevitis, A., Davis, C. (2000) The human immunoglobulin loci introduced into mice: V(D) and J gene segment usage similar to that of adult humans, *Eur. J. Immunol.,* **30:** 534-540.

Gana-Weisz, M., Halaschek-Wiener, J., Jansen, B., Elad, G., Haklai, R., Kloog, Y. (2002) The Ras inhibitor S-trans, trans-farnesylthiosalicylic acid chemosensitizes human tumour cells without causing resistance, *Clin. Cancer Res.,* **8:** 555-565.

Gangolli, S., Shilling, W., Grasso P., Gaunt I. (1974) Studies on the metabolism and hepatotoxicity of coumarin in the baboon, *Biochem. Soc. Trans.,* **2:** 310–312.

Gareil, P., Grammond, J., Guyon, F. (1993) Separation and determination of warfarin enantiomers in human plasma samples by capillary zone electrophoresis using a methylated -cyclodextrin containing electrolyte, *J. Chromatogr.,* **615:** 317-325.

Gaudin, V., Fontaine, J., Maris, P. (2001) Screening of penicillin residues in milk by surface plasmon resonance-based biosensor assay: comparison of chemical and enzymatic sample pre-treatment, *Anal. Chim. Acta,* **436:** 191-198.

Gefter, M., Margulies, D., Scharff, M. (1977) A simple method for polyethylene glycol-promoted hybridization of mouse myeloma cells, *Somatic Cell. Genet.,* **3:** 231-236.

Ghate, M., Monohar, D., Kulkarni, V., Shobha, R., Kattimani, S.Y. (2003) Synthesis of vanillin ethers from 4-(bromomethyl) coumarins as anti-inflammatory agents, *Eur. J. Med. Chem.,* **38:** 297-302.

Gillis, E., Gosling, J., Sreenan, J., Kane, M. (2002) Development and validation of a biosensor-based immunoassay for progesterone in bovine milk, *J. Immunol. Methods,* **267:** 131-138.

Glass, C., Rose, D., Rosenfeld, M. (1997) Nuclear receptor co-activators, *Curr. Opin. Cell Biol.,* **9:** 222-232.

Glennie, M. & Johnson, P. (2000) Clinical trials of antibody therapy, *Immunol. Today,* **21:** 403-410.

Goepel, W. & Heiduschka, P. (1995) Interface analysis in biosensor design, *Biosens. Bioelectron.,* **10:** 853-883.

Goepel, W. (1991) Chemical sensing, molecular electronics and nanotechnology: interface technologies down to the molecular scale, *Sens. Actuat. B,* **4:** 7-21.

Gratzner, H.G. (1982) Monoclonal antibody to 5-bromo and 5-iododeoxyuridine: A new reagent for detection of DNA replication, *Science,* **218:** 474.

Green, L. (1999) Antibody engineering via genetic engineering of the mouse: xenomouse strains are a vehicle for the facile generation of therapeutic human monoclonal antibodies, *J. Immunol. Methods,* **231:** 11-23.

Griffiths, D. & Hall, G. (1993) Biosensors – What real progress is being made?, *TIBTECH*, **11**: 122-30.

Grotz, K.A., Wustenberg, P., Kohnen, R., Al-Nawas, B., Henneicke-von Zepelin, H.H., Bockisch, A., Kutzner, J., Naser-Hijazi, B., Belz, G.G., Wagner, W. (2001) Prophylaxis of radiogenic sialadenitis and mucositis by coumarin/troxerutine in patients with head and neck cancer-a prospective, randomized, placebo-controlled, double-blind study, *Br. J. Oral. Maxillofac. Surg.,* **39**: 34-39.

Grunicke, H., Maly, K., Uberall, F., Schubert, C., Kindler, E., Stekar, J., Brachwitz, H. (1996) Cellular signalling as a target in cancer chemotherapy. Phospholipid analogues as inhibitors of mitogenic signal transduction, *Advan. Enzyme Regul.,* **36**: 385-407.

Grunicke, H. (1995) *Signal Transduction Mechanisms in Cancer*, First Edition, R.G. Landes, Austin.

Grunwald, V. & Hidalgo, M. (2003) Development of the epidermal growth factor receptor inhibitor OSI-774, *Semin. Oncol.,* **30**: 23-31.

Guh, J.H., Yu, S.M., Ko, F.N., Wu, T.S., Teng, C.M. (1996) Antiproliferative effect in rat vascular smooth muscle cells by osthole, isolated from *Angelica pubescens*, *Eur. J. Pharmacol.,* **298**: 191-197.

Guilet, D., Seraphin, D., Rondeau, D., Richomme, P., Bruneton, J. (2001) Cytotoxic coumarins from *Calophyllum dispar, Phytochemistry,* **58**: 571-575.

Gunneriusson, E., Nord, K., Uhlen, M., Nygren, P. (1999) Affinity maturation of a Taq DNA polymerase-specific affibody by helix shuffling, *Protein Eng.,* **12**: 873-878.

Gustavsson, E., Bjurling, P., Sternesjo, A. (2002) Biosensor analysis of penicillin g in milk based on the inhibition of carboxypeptidase activity, *Anal. Chim. Acta,* **468**: 153-159.

Haab, B.B. (2001) Advances in protein microarray technology for protein expression and interaction profiling, *Curr. Opin. Drug Discov. Develop.,* **4**: 116-123.

Haasnoot, W., Beinenmann-Ploum, M., Kohen, F. (2003b) Biosensor immunoassay for the detection of eight sulfonamides in chicken serum, *Anal. Chim. Acta,* **483**: 171-180.

Haasnoot, W., Cazemier, G., Koets, M., Van Amerongen, A. (2003a) Single biosensor immunoassay for the detection of five aminoglycosides in reconstituted skimmed milk, *Anal. Chim. Acta,* **488:** 53-60.

Hafner, F. (2000) Cytosensor microphysiometer: technology and recent applications, *Biosens. Bioelectron.,* **15:** 149-158.

Hahnenberger, K., Krystal, M., Esposito, K., Tang, W., Kurtz, S. (1996) Use of microphysiometry for analysis of heterologous ion channels expressed in yeast, *Nature Biotechnol.,* **14:** 880-883.

Halachmi, S., Marden, E., Martin, G., MacKay, H., Abbondanza, C., Brown, M. (1994) Estrogen receptor-associated proteins: possible mediators of hormone-induced transcription, *Science,* **264:** 1455–1458.

Hallak, H., Wedlund, P., Modi, M., Patel, I., Lewis, G., Woodruff, B., Trowbridge, A. (1993) High clearance of (S)-warfarin in a warfarin-resistant subject, *Br. J. Clin. Pharmacol.,* **35:** 327-30.

Hamburger, A. & Salmon, S. (1977) Primary bioassay of human tumour stem cells, *Science,* **197:** 461-463.

Hansen, M., Nielsen, S., Berg, K. (1989) Re-examination and further development of a precise and rapid dye method for measuring cell growth/cell kill, *J. Immunol. Methods,* **119:** 203-210.

Hansson, M., Ringdahl, J., Robert, A., Power, U., Goetsch, L., Nguyen, T., Uhlén, M., Ståhl, S., Nygren, P. (1999) An *in vitro* selected binding protein (affibody) shows conformation-dependent recognition of the respiratory syncytial virus (RSV) G protein, *Immunotechnol.,* **4:** 237-252.

Harayama, S. (1998) Artificial evolution by DNA shuffling, *TIBTECH,* **16:** 76-82.

Hardie, D. (1991) *Biochemical Messengers. Hormones, Neurotransmitters and Growth Factors,* First Edition, Chapman & Hall, London.

Hartmann, A., Agwrell, E., Beevers, C., Brrendlar-Schwaab, S., Burlinson, B., Clay, P., Collins, A., Smith, A., Speit, G., Thybawd, V., Tice, R. (2003) Recommendations for conducting the *in vivo* alkaline comet assay, *Mutagenesis,* **18:** 45-51.

Hawker, J. (2003) Chemiluminescence-based BrdU ELISA to measure DNA synthesis, *J. Immunol. Methods,* **274:** 77-82.

Hay, F. & Westwood, O. (2002) Practical immunology, Fourth Edition, Blackwell Scientific Publications, Oxford.

Hayhurst, A., Happe, S., Mabry, R., Koch, Z., Iverson, B., Georgiou, G. (2003) Isolation and expression of recombinant antibody fragments to the biological warfare pathogen *Brucella melitensis, J. Immunol. Methods,* **276:** 185-196.

He, M. & Taussig, M. (2001) Single step generation of protein arrays from DNA by cell-free expression and *in situ* immobilisation (PISA method), *Nucleic Acids Res.,* **29:** E73-3.

Heidenreich, A. & Schrader, A. (2003) The treatment of hormone refractory prostate cancer, *EAU Update Series,* **1:** 40-50.

Hejna, M., Raderer, M., Zielinkski, C. (1999) Inhibition of metastasis by anticoagulants, *J. Nat. Cancer Institute,* **91:** 22-36.

Helleday, T. (1998) Session 1: signal transduction, *Toxicol. In Vitro,* **12:** 519-522.

Hemminki, A., Niemi, S., Hautoniemi, L., Soderlund, H., Takkiken, K. (1998) Fine tuning of an anti-testosterone antibody binding site by stepwise optimisation of the CDRs, *Immunotechnology,* **4:** 59-69.

Hensley, P. & Myszka, D. (2000) Analytical Biotechnology -sorting needles and haystacks, *Curr. Opin. Biotechnol.,* **11:** 9-12.

Herbst, R.S. (2003) Erlotinib (Tarceva): An update on the clinical trial program, *Semin. Oncol.,* **30:** 34-46.

Hermans, J. & Thijjsen H. (1989) The *in vitro* ketone reduction of warfarin and analogues. substrate stereoselectivity, product stereoselectivity, and species differences, *Biochem. Pharmacol.,* **38:** 3365-3370.

Hermanson, G. (1996) *Bioconjugate Techniques,* First Edition, Academic Press, London, England.

Herrmann, C., Block, C., Geisen, C., Haas, K., Weber, C., Winde, G., Moroy, T., Muller, O. (1998) Sulindac sulfide inhibits Ras signalling, *Oncogene,* **17:** 1769-1776.

Herzenberg, L. (1978). Mouse immunoglobulin allotypes: description and specific methodology, In: *Handbook of Experimental Immunology,* First Edition, Blackwell Scientific Publications, Oxford, England, pp 1-23.

Hiatt, A., Cafferkey, R., Bowdish, K. (1989) Production of antibodies in transgenic plants, *Nature (London),* **342:** 76-78.

Hirsh, J., Fuster, V., Ansell, J., Halperin, J. (2003) American heart association/american college of cardiology foundation guide to warfarin therapy, *J. Am. Coll. Cardiol.,* **41:** 1633-1652.

Hirsh, J. (1982) Rebound hypercoagulability, *Stroke,* **13:** 527-537.

Hirsh, J. (1995) Optimal intensity and monitoring warfarin, *Am. J. Cardiol.,* **75:** 39B-42B.

Hoelscher, G., Gruber, H., Coldham, G., Grigsby, J., Hanley, E.N. Jr. (2000) Effects of a very high antibiotic concentrations on human intervertebral disc cell proliferation, viability, and metabolism *in vitro, Spine,* **25:** 1871-1877.

Holliger, P., Prospero, T., Winter, G. (1993) Diabodies: small bivalent and bispecific antibody fragments, *Proc. Natl. Acad. Sci., USA,* **90:** 6444-6448.

Homola, J., Yee, S., Gauglitz, G. (1999) Surface plasmon resonance sensors: review, *Sens. Actuators B: Chem.,* **54:** 3-15.

Hoogenboom, H. & Chames, P. (2000) Natural and designer binding sites made by phage display technology, *Immunol. Today,* **21:** 371-377.

Hoogenboom, H., De Bruine, A., Hufton, S., Hoet, R., Arends, J., Roovers, R. (1998) Antibody phage display technology and its applications, *Immunotechnology,* **4:** 1-20.

Høyer-Hansen, G., Hamers, M., Pedersen, A., Jørgen Nielsen, H., Brünner, N., Danø, K., Stephens, R. (2000) Loss of ELISA specificity due to biotinylation of monoclonal antibodies, *J. Immunol. Methods,* **235:** 91-99.

Hsieh, C., Santell, R., Haslem, S., Helferich, W. (1998) Estrogenic effects of genistein on the growth of estrogen receptor-positive human breast cancer (MCF-7) cells *in vitro* and *in vivo, Cancer Res.,* **58:** 3833-3838.

Hua, P., Tsai, W.J., Kuo, S.M. (2003) Estrogen response element-independent regulation of gene expression by genistein in intestinal cells, *Biochim. Biophys. Acta,* **1627:** 63-70.

Huang, H.C., Lee, C.R., Weng, Y.I., Lee, M.C., Lee, Y.T. (1992) Vasodilator effect of scoparone (6,7-dimethoxycoumarin) from chinese herb, *Eur. J. Pharmacol.,* **218:** 123-128.

Huang, Z.Q., Buchsbaum, D., Raisch, K., Bonner, J., Bland, K., Vickers, S. (2003) Differential responses by pancreatic carcinoma cell lines to prolonged exposure to erbitux (IMC-C225) anti-EGFR antibody, *J. Surg. Res.,* **111:** 274-283.

Hudson, L. & Hay, F. (1980) *Practical Immunology,* Second Edition, Blackwell Scientific Publications, Oxford, England.

Hudson, P. & Kortt, A, (1999) High avidity scFv multimers; diabodies and triabodies, *J. Immunol. Methods,* **231:** 177-189.

Hudson, P. & Souriau, C. (2001) Recombinant antibodies for cancer diagnosis and therapy, *Expert. Opin. Biol. Ther.,* **1:** 845-55.

Huong, P., Kolk, A., Eggelte, T., Verstijnen, C., Gilis, H., Hendriks, H. (1991) Measurement of antigen-specific lymphocyte proliferation using 5-Bromo-deoxyuridine incorporation. An easy and low cost alternative to radioactive thymidine incorporation, *J. Immunol. Methods,* **140:** 243-248.

Hutt, A., Hadley, M., Tan, S. (1994) Enantiospecific analysis: applications in bioanalysis and metabolism, *Europ. J. Drug Metab. Pharmacokinet.,* **3:** 241-251.

Iliades, P., Kortt, A., Hudson, P. (1997) Triabodies: single chain Fv fragments without a linker form trivalent trimers, *FEBS Letts,* **409:** 437-441.

Ishibashi, K., Fujishima, A., Watanabe, T., Hashimoto, K. (2000) Detection of active oxidative species in TiO_2 photocatalysis using the fluorescence technique, *Electrochem. Communications,* **2:** 207-210.

Itoh, K., Suzuki, K., Ishiwata, S., Tezuka, T., Mizugaki, M., Suzuki, T. (1999) Application of a recombinant Fab fragment from phage display library for sensitive detection of a target antigen by an inhibition ELISA system, *J. Immunol Methods,* **223:** 107-114.

Ivasenko, I., Shlyakhto, E. (2001) Effect of distributed plasma oxidant homeostasis on haemopoietic differentiation of polypotent bone marrow stem cells in mice treated with dipyridamole, *Bull. Exp. Biol. Med.,* **132:** 766-768.

Jabbar, S.A.B., Twentyman, P.R., Watson, J.V. (1989) The MTT assay underestimates the growth inhibitory effects of interferons, *Br. J. Cancer,* **60:** 523-528.

Jaffers, G., Fuller, T., Cosimi, A., Russell, P., Winn, H., Colvin, R. (1986) Monoclonal antibody therapy. Anti-idiotypic and non-anti-idiotypic antibodies to OKT3 arising despite intense immunosuppression, *Transplantation,* **41:** 572-578.

Jang, M.S., Lee, S.J., Xue, X., Kwon, H.M., Ra, C.S., Lee, Y.T., Chung, T. (2002) Production and characterisation of monoclonal antibodies to a generic hapten for class-specific determination of organophosphorus pesticides, *Bull. Korean Chem. Soc.* **23:** 1116-1120.

Jefferis, R. & Deverill, I. (1992) The antigen antibody reaction, In: *Principles and Practice of Immunoassay* (Eds: Price E & Newman D), First Edition, Stockton Press, New York, pp 1-17.

Jimenez-Orozco, F., Lopez-Gonzalez, J.S., Nieto-Rodriguez, A., Velasco-Velazquez, M.A., Molina-Guarneros, J.A., Mendoza-Patino, N., Garcia-Mondragon, M.J., Elizalde-Galvan, P., Leon-Cedeno, F., Mandoki, J.J. (2001) Decrease of cyclin D1 in the human lung adenocarcinoma cell line A-427 by 7-hydroxycoumarin, *Lung Cancer,* **34:** 185-194.

Jirholt, P., Ohlin, M., Borrebaeck, C., Soderlind, E. (1998) Exploiting Sequence Space: Shuffling *In vivo* formed complentarity determining regions into a master framework, *Gene*, **215**: 471-476.

Jisa, E. & Jungbauer, A. (2003) Kinetic analysis of estrogen receptor homo- and heterodimerisation *in vitro*, *J. Steroid Biochem. Mol. Biol.*, **84**: 141-148.

Jones, G. & Jimenez, J. (1999) Intramolecular photoinduced electron transfer for cations derived from azole-substituted coumarin dyes, *Tetrahedron,* **40**: 8551-8555.

Jones, G. & Jimenez, J. (2001) Azole-linked coumarin dyes as fluorescence probes of domain-forming polymers, *J. Photochem. Photobiol. B: Biol.*, **65**: 5-12.

Jongerius-Gortemaker, B., Goverde, R., Van Knapen, F., Bergwerff, A. (2002) Surface plasmon resonance (BIACORE) detection of serum antibodies against *Salmonella Enteritidis* and *Salmonella Typhimurium*, *J. Immunol. Methods,* **266**: 33-44.

Jönsson, U., Fagerstam, L., Ivarsson, B., Lundh, K., Löfas, S., Persson, B., Roos, H., Rönnberg, L., Sjölander, S., Stenberg, E., Stahlberg, R., Urbaniczky, C., Östlin, H., Malmqvist, M. (1991) Real-time biospecific interaction analysis using surface plasmon resonance and a sensorchip technology, *BioTechniques,* **11**: 620-626.

Kaclikova, E., Kuchta, T., Kay, H., Gray, D. (2001) Separation of *Listeria* from cheese and enrichment media using antibody-coated microbeads and centrifugation, *J. Immunol. Methods,* **46**: 63-67.

Kahn, J. (2003) The end of cancer as we know it, *Wired,* **11**: 108-113

Kai, E., Ikebukuro, K., Hoshina, S., Watanabe, H., Karube, I. (2000) Detection of PCR products of *Escherichia coli* O157:H7 in human stool samples using surface plasmon resonance (SPR), *FEMS Immunol. Med. Microbiol.*, **29**: 283-288.

Kaminsky, L. & Zhang, Z. (1997) Human P450 metabolism of warfarin, *Pharm. Therapeut.*, **73**: 67-74.

Kampranis, S., Gormley, N., Tranter, R., Orphanides, G., Maxwell, A. (1999) Probing the binding of coumarins and cyclothialidines to DNA gyrase, *Biochemistry*, **38:** 1967-1976.

Kangas, L., Gronroos, M., Nieminen, A. (1984) Bioluminescence of cellular ATP: a new method for evaluating cytotoxic agents *in vitro*, *Med. Biol.*, **62:** 338-343.

Katzenellenbogen, B. (1996) Estrogen receptors: bioactivities and interactions with cell signalling pathways, *Biol. Reprod.*, **54:** 287-293.

Kawada, M., Usami, I., Ohba, S.I., Someno, T., Kim, J., Hayakawa, Y., Nose, K., Ishizuka, M. (2002) Hygrolidin induces p21 expression and abrogates cell cycle progression at G1 and S Phases, *Biochem. Biophys. Res. Comm.*, **298:** 178-183.

Kawamura, M., Inoue, Y., Oyama, T., Kobayashi, K. (2002) Chemosensitivity test for unresectable non-small cell lung carcinoma, *Nip. Geka. Gak. Zass.*, **103:** 229-232.

Kawase, M., Sakagami, H., Hashimoto, K., Tani, S., Hauer, H., Chatterjee, S.S. (2003) Structure-cytotoxic activity relationships of simple hydroxylated coumarins, *Anticancer Res.*, **23:** 3243-3246.

Keating, G. & O'Kennedy, R. (1997) The chemistry and occurrence of coumarins, In: *Coumarins: Biology, Applications and Mode of Action*, (Eds: R O'Kennedy & R.D. Thornes), John Wiley & Sons, Chichester, pp 23-66.

Keating, G. (1998) Biosensor-based studies on coumarins, **PhD Thesis**, Dublin City University, Dublin, Ireland.

Kellermann, S.A. & Green, L. (2002) Antibody discovery: the use of transgenic mice to generate human monoclonal antibodies for therapeutics, *Curr. Opin. Biotech.*, **13:** 593-597.

Kelly, M.J. & Wagner, E.J. (1999) Estrogen modulation of G-protein-coupled receptors, *Trends Endocrinol Metab.*, **10:** 369-374.

Khleif, S.N., Abrams, S.I., Hamilton, J.M,, Bergmann-Leitner, E., Chen, A., Bastian, A., Bernstein, S., Chung, Y., Allegra, C.J., Schlom, J. (1999) A phase I vaccine trial with peptides reflecting Ras oncogene mutations of solid tumours, *J. Immunother.*, **22:** 155-165.

Killard, A. (1998) The production of antibodies to coumarin and its major human metabolites, **Ph.D. Thesis**, Dublin City University, Dublin, Ireland.

Kim, S., Kang, J., Hu, W., Evers, B., Chung, D. (2003) Geldanamycin decreases Raf-1 and Akt levels and induces apoptosis in neuroblastomas, *Int. J. Cancer,* **103:** 352-359.

King, S.H., Joslin, M., Raudibaugh, K., Pieniaszek, H., Jr, Benedek, I. (1995) Dose-dependent pharmacokinetics of warfarin healthy volunteers, *Pharm. Res.,* **12:** 1874-1877.

Kipriyanov, S., Moldenhauer, G., Braunagel, M., Reusch, U., Cochlovius, B., Le Gall, F., Kouprianova, O., Von der Lieth, C.W., Little, M. (2003) Effect of domain order on the activity of bacterially-produced bispecific single-chain Fv antibodies, *J. Mol. Biol.,* **330:** 99-111.

Kipriyanov, S.M. (2002) Generation of bispecific and tandem diabodies, *Methods Mol. Biol.,* **178:** 317-331.

Kipriyanov, S.M. (2003) Generation and characterization of bispecific tandem diabodies for tumour therapy, *Methods Mol. Biol.,* **207:** 323-333.

Ko, F.N., Wu, T.S., Liou, M.J., Huang, T.F., Teng, C.M. (1992) Vasorelaxation of rat thoracic aorta caused by osthole isolated from angelica pubescens, *Eur. J. Pharmacol.,* **219:** 29-34.

Kodadek, T. (2001) Protein microarrays: prospects and problems, *Chem. Biol.* **8:** 105-115.

Kohler, G. & Milstein, C. (1975) Continuous culture of fused cells secreting antibody of predefined specificity, *Nature (London),* **256:** 495-497.

Kokron, O., Maca, S., Gasser, G., Schmidt, P.R. (1991) Cimetidine and coumarin therapy of renal cell carcinoma, *Oncology,* **48:** 102-106.

Kolodziej, H., Kayser, O., Woerdenbag, H., van Uden, W., Pras, N. (1997) Structure-cytotoxicity relationships of a series of natural and semi-synthetic simple coumarins as assessed in two human tumour cell lines, *Z. Naturforsch.,* **52:** 240-244.

Kong, A.N., Yu, R., Hebbar, V., Chen, C., Owuor, E., Hu, R., Ee, R., Mandlekar, S. (2001) Signal transduction events elicited by cancer prevention compounds, *Mutation Res./Fund. Mol. Mech. Mutagenesis,* **480:** 231-241.

Kontermann, R., Martineau, P., Cummings, C., Karpas, A., Allen, D., Derbyshire, E., Winter, G. (1997) Enzyme immunoassays using bispecific diabodies, *Immunotechnology,* **3:** 137-144.

Kovich, O. & Otley, C. (2003) Thrombotic complications related to discontinuation of warfarin and aspirin therapy perioperatively for cutaneous operation, *J. Am. Acad. Dermatol.,* **48:** 233-237.

Kowalska-Pylka, H., Majer-Dziedzic, B., Niewiadomy, A., Matysiak, J. (2001) Evaluation of the toxicity of substituted benzthioanilides by using *in vitro* tests, *ATLA,* **29:** 547-556.

Kramer, K. & Hock, B. (2003) Recombinant antibodies for environmental analysis, *Anal. Bioanal. Chem.,* **377:** 417-426.

Kratochwil, N., Huber, W., Muller, F., Kansy, M., Gerber, P. (2002) Predicting plasma protein binding of drugs: a new approach, *Biochem. Pharmacol.,* **64:** 1355-1374.

Krebs, L., Wang, X., Nagy, A., Schally, A., Prasad, P., Liebow, C. (2002) A conjugate of doxorubicin and an analog of luteinizing hormone-releasing hormone shows increased efficacy against oral and laryngeal cancers, *Oral Oncol.,* **38:** 657-663.

Kukanskis, K., Elkind, J., Melendez, J., Murphy, T., Miller, G., Garner, H. (1999) Detection of DNA hybridization using the TISPR-1 surface plasmon resonance, *Anal. Biochem.,* **274:** 7-17.

Kumi-Diaka, J. (2002) Chemosensitivity of human prostate cancer cells PC3 and LNCaP to genistein isoflavone and β-Lapachone, *Biol. Cell,* **94:** 37-44.

Kunze, K., Wienkers, W., Thummel, K., Trager, W. (1996) Inhibition of the human cytochrome P450-dependent metabolism of warfarin by fluconazole: *in vitro* studies, *Drug Metab. Disposition,* **24:** 414-421.

Kuo, R., Mac Ewan, D., Baxter, G. (1994) Cell cycle dependency of the TNF-α effects on TF-1 cells: a role for the TNFRII in mediating apoptosis, *Mol. Biol. Cell.,* **5:** 26a.

Kurbacher, C., Grecu, O., Stier, U., Gilster, T., Janat, M., Untch, M., Konecny, G., Bruckner, H., Cree, I. (2003) ATP chemosensitivity testing in ovarian and breast cancer: early clinical trials, *Recent Results Cancer Res.*, **161**: 221-230.

Kurtoglu, M., Taviloglu, K., Guloglu, R., Barbaros, U., Necefli, A., Yanar, H. (2001) Warfarin-induced skin necrosis: presentation of two cases, *Eur. J. Vasc. Endovasc. Surg. Extra.*, **2**: 91-93.

Lake, B. (1999) Coumarin metabolism, toxicity and carcinogenicity: relevance for human risk assessment, *Food Chem. Tox.*, **37**: 423-453.

Lancet, J.E. & Karp, J.E. (2003) Farnesyl transferase inhibitors in myeloid malignancies, *Blood Rev.*, **17**: 123-129.

Landwojtowicz, E., Nervi, P., Seelig, A. (2002) Real-time monitoring of p-glycoprotein activation in living cells, *Biochemistry*, **41**: 8050-8057.

Lang, R., Berger, A., Hermann, A., Kofler, B. (2001) Biphasic response to human galanin of extracellular acidification in human bowes melanoma cells, *Eur. J. Pharmacol.*, **423**: 135-141.

Lapík, O., Tursa, J., Kleinová, T., Vítková, M., Dvoáková, H., Klejdus, B., Moravcová, J. (2003) Synthesis of hapten and conjugates of coumestrol and development of immunoassay, *Steroids*, **68**: 1147-1155.

Larrick, J. & Thomas, D. (2001) Producing proteins in transgenic plants and animals, *Curr. Opin. Biotechnol.*, **12**: 411-418.

Larrick, J., Yu, L., Chen, J., Jaiswal, S., Wycoff, K. (1998) Production of antibodies in transgenic plants, *Res. Immunol.*, **149**: 603-608.

Lee, K.H,, Chai, H.B,, Tamez, P., Pezzuto, J., Cordell, G., Win, K.K., Tin-Wa, M. (2004) Biologically active alkylated coumarins from *Kayea assamica*, *Phytochemistry*, **64**: 535-541.

Lee, M. & Schwartz, R. (1981) Warfarin resistance and vitamin K, *Ann. Intern.. Med.*, **94**: 140.

Lefrere, J.J., Horellou, M.H., Conard, J., Samama, M. (1987) Proposed classification of resistances to oral anticoagulant therapy, *J. Clin. Pathol.*, **40:** 242.

Leim, L., Choong, L., Woo, K. (2001) Action of dipyridamole and warfarin on the growth of human endothelial cells cultured in serum-free media, *Clin. Biochem.*, **34:** 141-147.

Lennox, A., Smout, J., Shlebak, A., Wolfe, J. (2001) Warfarin-induced skin necrosis: association with heparin-induced thrombocytopenia and protein S deficiency, *Eur. J. Vasc. Endovasc. Surg. Extra.*, **1:** 25-26.

Leonard, P., Hearty, S., Brennan, J., Dunne, L., Quinn, J., Chakraborty, T., O'Kennedy, R. (2003) Advances in biosensors for detection of pathogens in food and water, *Enz. Microbial Tech.*, **32:** 3-13.

Levin, E.R. (2002) Cellular functions of plasma membrane estrogen receptors, *Steroids,* **67:** 471-475.

Levitzki, A. (1996) Targeting signal transduction for disease therapy, *Curr. Opin. Cell Biol.,* **8:** 239-244.

Lewis, R.J. and Trager, W.F. (1970) Warfarin metabolism in man: identification of metabolites in urine, *J. Clin. Invest.*, **49:** 907-913.

Libby, J. (1998) Post-antibiotic effect in *Escherichia coli* determined with real-time metabolic monitoring, *Antimicrob. Agents Chemother.*, **42:** 78-82.

Lickiss, J., Cane, K., & Baikie, G. (1974) *In vitro* drug selection in anti-neoplastic chemotherapy, *Eur. J. Cancer,* **10:** 809-814.

Liedberg, B. & Lundstrom, I. (1993) Principles of biosensing with an extended coupling matrix and surface plasmon resonance, *Sens. Actuat. B,* **11:** 63-72.

Liminga, G., Jonsson, B., Nygren, P., Larsson, R. (1999) On the mechanism underlying calcein-induced cytotoxicity, *Eur. J. Pharmacol.*, **383:** 321-329.

Linder, M. (2001) Genetic Mechanisms for hypersensitivity and resistance to the anticoagulant warfarin, *Clin. Chim. Acta,* **308:** 9-15.

Link, K. (1945) The anticoagulant dicoumarol, *Proc. Inst. Med. Chicago*, **15:** 370-389.

Link, K. (1959) The discovery of dicoumarol and its sequels, *Circulation*, **9:** 97-107.

Link, K. (1948) Dicoumarol - and the estimation of prothrombin, In: *Transactions of the First Conference on Blood Clotting and Allied Problems*, New York, pp 126-136.

Little, M, Kiripanyov, S., Le Gall, F., Moldenhauer, G. (2000) Of mice and men: hybridoma and recombinant antibodies, *Immunol. Today*, **21:** 364-370.

Liu, H.R., Li, Z., Wang, X.H., Han, X.S., Teng, Z., Sun, Z. (2002) Effect of scoparone on $[Ca^{2+}]_i$ of the isolated tracheal smooth muscle cells of guinea-pig, *J.China Med. Uni.*, **31:** 249–251.

Lodwick, A. (1999) Warfarin therapy: a review of the literature since the 'fifth american college of chest physicians' consensus conference on antithrombotic therapy, *Clin. Appl. Thrombosis /Haemostasis*, **5:** 208-215.

Loebstein, R., Yonath, H., Peleg, D., Almog, S., Rotenberg, M., Lubetsky, A., Roitelman, J., Harats, D., Halkin, H., Ezra, D. (2001) Inter-individual variability in sensitivity to warfarin-nature or nurture?, *Clin. Pharmacol. Therapeutics,* **70:** 159-164.

Löfas, S. & Johnsson, B. (1990) A novel hydrogel matrix on gold surfaces in surface plasmon resonance sensors for fast and efficient covalent immobilization of ligands, *J. Chem. Soc. Chem Commun.,* **21:** 1526-1528.

Löfas, S., Malmqvist, M., Ronnberg, I., Stenberg, E., Liedberg, B., Lundstrom, I. (1991) Bioanalysis with surface plasmon resonance, *Sens. Actuators B*, **5:** 79-84.

Loprinzi, C.L., Kugler, J.W., Sloan, J.A., Rooke, T.W., Quella, S.K., Novotny, P., Mowat, R.B., Michalak, J.C., Stella, P.J., Levitt, R., Tschetter, L.K., Windschitl, H. (1999) Lack of effect of coumarin in women with lymphoedema after treatment for breast cancer, *N. Engl. J. Med.*, **340:** 346-350.

Lu, D., Jimenez, X., Zhang, H., Atkins, A., Brennan, L., Balderes, P., Bohlen, P., Witte, L., Zhu, Z. (2003) Di-diabody: a novel tetravalent bispecific antibody molecule by design, *J. Immunol. Methods,* **279:** 219-232.

Luczkiewicz, M. & Glod, D. (2003) Callus cultures of Genista Plants – *In Vitro* material producing high amounts of isoflavones of phytoestrogenic activity, *Plant Sci.,* **165:** 1101-1105.

Lui, K., Panchal, A., Santhanagopal, A., Dixon, S., Bernier, S. (2002) Epidermal growth factor stimulates proton efflux from chondrocytic cells, *J. Cell Physiol.,* **192:** 102-112.

Luo, X., Naiyun, X., Lübai, C., & Huang, D. (2001) Synthesis of coumarin dyes containing N-alkylsulfonamide groups, *Dyes and Pigments,* **51:** 153-159.

Luong, J., Bouvrette, P., Male, K. (1997) Developments and applications of biosensors in food analysis, *TIBTECH,* **15:** 369-377.

Lutomski, D., Palascak, J., Bower, R. (1987) Warfarin resistance associated with intravenous lipid administration, *J. Parenteral Enteral Nutr.,* **11:** 316-318.

Maat, B. (1980) Selective macrophage inhibition abolishes warfarin-induced reduction of metastases, *Br. J. Cancer,* **41:** 313-316.

MacLaren, R., Wachsman, B., Swift, D., Kuhl, D. (1997) Warfarin resistance associated with intravenous lipid administration: discussion of the literature and review of the literature, *Pharmacotherapy,* **17:** 1331-1337.

Madan M & Tcheng J. (2000) Update on Abciximab Readministration During Percutaneous Coronary Interventions, *Curr. Intervent. Cardiol. Reports,* **2:** 244-249.

Madhavan, G., Balraju, V., Mallesham, B., Chakrabarti, R., Lohray, V. (2003) Novel coumarin derivatives of heterocyclic compounds as lipid-lowering agents, *Bioorg. Med. Chem. Letts.,* **13:** 2547-2551.

Maehara, Y., Anai, H., Tamada, R., Sugimachi, K. (1987) The ATP assay is more sensitive than the succinate dehydrogenase inhibition test for predicting cell viability, *Eur. J. Cancer & Clin. Oncol.*, **23:** 273-276.

Makino, T., Wakushima, H., Okamoto, T., Okukubo, Y., Deguchi, Y., Kano, Y. (2002) Pharmacokinetic interactions between warfarin and kangen-karyu, a chinese traditional herbal medicine and their synergistic action, *J. Ethnopharmacol.*, **82:** 35-40.

Malhotra, O., Nesheim, M., Mann, K. (1985) The kinetics of activation of normal and gamma carboxy glutamic acid-deficient prothrombins, *J. Biol. Chem.*, **260:** 279-287.

Malhotra, O. (1981) Degradation of normal and dicoumarol-induced prothrombins with thrombin, *Ann. N.Y. Acad. Sci.*, **370:** 438-52.

Maltese, A. & Bucolo, C. (2002) Simultaneous determination of cloricromene and its active metabolite in rabbit aqueous humor by high-performance liquid chromatography, *J. Chromatogr.*, **767:** 153-158.

Markgren, P., Hämäläinen, M., Danielson, H. (1998) Screening of compounds interacting with HIV-1 proteinase using optical biosensor technology, *Anal. Biochem.*, **265:** 340-50.

Markgren, P., Hämäläinen, M., Danielson, H. (2000) Kinetic analysis of the interaction between HIV-1 protease and inhibitors using optical biosensor technology, *Anal. Biochem.*, **279:** 71-8.

Markowska, J. (2003) Monoclonal antibodies in the treatment of ovarian cancer, *Eur. J. Gynaecol. Oncol.*, **24:** 7-11.

Marshall, M., Kervin, K., Benefield, C., Umerani, A., Albainy-Jenei, S., Zhao, Q., Khazaeli, M. (1994) Growth-inhibitory effects of coumarin (1,2-benzopyrone) and 7-hydroxycoumarin on human malignant cell lines *in vitro*, *J. Cancer Res. Clin. Oncol.*, **120 (Suppl):** S3-S10.

Marshall, M.E., Butler, K., Fried, A. (1991) Phase I evaluation of coumarin (1,2-Benzopyrone) and cimetidine in patients with advanced malignancies, *Mol. Biother.*, **3:** 170-178.

Marshall, M.E., Butler, K., Hermansen, D. (1990) Treatment of hormone-refractory stage-D carcinoma of prostate with coumarin (1,2-benzopyrone) and cimetidine: a pilot study, *Prostate*, **17:** 95-99.

Martin, A. (1992) Cytotoxicity testing *in vitro*: investigation of 5 miniaturised, colorimetric assays, **PhD Thesis,** Dublin City University, Dublin, Ireland.

Matsui, Y., Goto, M., Iwakawa, M., Asano, T., Kenmochi, T., Imai, T., Ochiai, T. (2003) Modified radiosensitivity of pancreatic cancer xenografts by farnesyl protein transferase inhibitor and MEK inhibitor, *Oncol. Rep.* **10:** 1525-1528.

Maurer, H. & Arlt, J. (1998) Detection of 4-hydroxyxcoumarin anticoagulants and their metabolites in urine as part of a systematic toxicological analysis procedure for acidic drugs and poisons by gas chromatography-mass spectrometry after extractive methylation, *J. Chromatogr.,* **714:** 181-195.

Maurer, L.H., Herndon, J.E., Hollis, D.R., Aisner, J., Carey, R.W., Skarin, A.T., Perry, M.C., Eaton, W.L., Zacharski, L.L., Hammond, S., Green, M.R. (1997) Randomized trial of chemotherapy and radiation therapy with or without warfarin for limited-stage small-cell lung cancer: a cancer and leukaemia group B study, *J. Clin. Oncol.,* **15:** 3378-3387.

Mazzocca, A., Giusti, S., Hamilton, A., Sebti, S., Pantaleo, P., Carloni, V. (2003) Growth inhibition by the farnesyltransferase inhibitor FTI-277 involves Bcl-2 expression and defective association with Raf-1 in liver cancer cell lines, *Mol. Pharmacol.,* **63:** 159-166.

McCall, R., Huff, R., Chio, C., TenBrink, R., Bergh, C., Ennis, M., Ghazal, N., Hoffman, R., Meisheri, K., Higdon, N., Hall, E. (2002) Preclinical studies characterising the anti-migraine and cardiovascular effects of the selective 5-HT1D receptor agonist PNU-142633, *Cephalagia,* **22:** 799-806.

McCarney, B., Traynor, I., Fodey, T., Crooks, S., Elliott, C. (2003) Surface plasmon resonance biosensor screening of poultry liver and eggs for nicarbazin residues, *Anal. Chim. Acta,* **483:** 165-169.

Meitner, P. (1991) The fluorescent cytoprint asay: a new approach to *in vitro* chemosensitivity testing, *Oncology,* **5:** 75-81.

Mello, L., & Kubota, L. (2002) Review of the use of biosensors as analytical tools in the food and drink industries, *Food Chem.,* **77:** 237-256.

Mendez, M., Green, L., Corvalan, J.R., Jia, X.C., Maynard-Currie, C., Yang, X., Gallo, M., Louie, D., Lee, D., Erickson, K., Luna, J., Roy, C., Abderrahim, H., Kirschenbaum, F., Noguchi, M., Smith, D., Fukushima, A., Hales, J., Klapholz, S., Finer, M., Davis, C., Zsebo, K., Jakobovits, A. (1997) Functional transplant of megabase human immunoglobulin loci recapitulates human antibody response in mice, *Nature Genet.,* **15:** 146-156.

Mestres-Ventura, P. (2003) Chemosensitivity testing of human tumours using Si-sensor chips, *Recent Results Cancer Res.,* **161:** 26-38.

Meyer, R., Hagemyer, R., Knoth, R., Volk, B. (2001) Oxidative Hydrolysis of scoparone by Cytochrome P450 CYP2C29 reveals a novel metabolite, *Biochem. Biophys. Res. Commun.,* **285:** 32-39.

Migliaccio, A., Castoria, M., Di Domenico, M., de Falco, A., Bilancio, A., Lombardi, M., Bottero, D., Varricchio, L., Nanayakkara, M., Rotondi, A., Auricchio, F. (2003) Sex steroid hormones act as growth factors, *J. Steroid Biochem. Mol. Biol.,* **83:** 31-35.

Migliaccio, A., Di Domenico, M., Castoria, G., de Falco, A., Bontempo, P., Nola, E., Auricchio, F. (1996) Tyrosine kinase/p21ras/MAP-Kinase pathway activation by estradiol-receptor complex in MCF-7 cells, *EMBO J.,* **15:** 1292-1300.

Mohler, J.L., Gomella, L.G., Crawford, E.D., Glode, L.M., Zippe, C.D., Fair, W.R., Marshall, M.E. (1992) Phase II evaluation of coumarin (1,2-benzopyrone) in metastatic prostatic carcinoma, *Prostate,* **20:** 123-131.

Molina, A., Valladares, M., Magadan, S., Sancho, D., Viedma, F., Sanjuan, I., Gambon, F., Sanchez-Madrid, F., Gonzalez-Fernandez, A. (2003) The use of transgenic mice for the production of a human monoclonal antibody specific for human CD69 antigen, *J. Immunol. Methods.,* **282:** 147-158.

Moran, E., O'Keeffe, M., O'Connor, R., Larkin, A., Murphy, P., Clynes, M. (2002) Methods for generation of monoclonal antibodies to the very small drug hapten, 5-benzimidazolecarboxylic acid, *J. Immunol. Methods,* **271:** 65-75.

Moran, E., O'Kennedy, R., Thornes, RD. (1987) Analysis of coumarin and its urinary metabolites by high-performance liquid chromatography, *J. Chromatogr.,* **416:** 165-169.

Moran, E., Prosser, E., O'Kennedy, R., Thornes, R. (1993) The effect of coumarin and 7-hydroxycoumarin on the growth of human tumour cell lines, *J. Ir. Coll. Phys. Surg.,* **22:** 41-43.

Mousa, S. (2002) Anticoagulants in thrombosis and cancer: the missing link, *Expert Rev. Anticancer Ther.,* **2:** 227-233.

Mueller, H., Loop, P., Liu, R., Wosikowski, K., Kueng, W., Eppenberger, U. (1994) Differential signal transduction of epidermal-growth-factor receptors in hormone-dependent and hormone-independent human breast cancer cells, *Eur. J. Biochem.,* **221:** 631-637.

Murakami, A., Yamayoshi, A., Iwase, R., Nishida, J., Yamaoka, T., Wake, N. (2001) Photodynamic antisense regulation of human cervical carcinoma cell growth using psoralen-conjugated oligo(nucleoside phosphorothioate), *Eur. J. Pharm. Sci.,* **13:** 25-34.

Murakami A, Yamayoshi A, Iwase R, Nishida JI, Yamaoka T, Wake N. (2001) Photodynamic Antisense Regulation of Human Cervical Carcinoma Cell Growth Using Psoralen-Conjugated Oligo(nucleoside Phosphorothioate), *Eur. J. Pharm. Sci.,* **13:** 25-34.

Murray RDH, Mendez J, Brown SA. (1982) *The Natural Coumarins – Occurrence, Chemistry and Biochemistry.* John Wiley, Chichester.

Myers, R.B., Parker, M., Grizzle, W.E. (1994) The effects of coumarin and suramin on the growth of malignant renal and prostatic cell lines, *J. Cancer Res. Clin. Oncol.,* **120:** S11-S13.

Myszka, D. & Rich, R. (2000) Implementing surface plasmon resonance biosensors in drug discovery, *Pharmacy Sci.Technol.Today,* **9:** 310-316.

Naidong, W., Ring, P., Midtlein, C., Jiang, X. (2001) Development and validation of a sensitive and robust LC–tandem MS method for the analysis of warfarin enantiomers in human plasma, *J. Pharm. Biomed. Anal.,* **25:** 219-226.

Nakamori, M., Iwahashi, M., Nakamura, M., Yamaue, H. (2003) Clinical benefit of chemosensitivity test for patients with regional lymph node-positive oesophageal squamous cell carcinoma, *J. Surg. Oncol.,* **84:** 10-6.

Nakamura, K., Toyohira, H., Kariyazono, H., Ishibashi, M., Saigenji, H., Shimokawa, S., Taira, A. (1994) Anticoagulant effects of warfarin and kinetics of K vitamin in faeces and blood, *Artery,* **21:** 148-60.

Natsume, T., Nakayama, H., Isobe, T. (2001) BIA-MS-MS: biomolecular interaction analysis for functional proteomics, *TIBTECH,* **19:** S28-S32.

Nelson, R., Krone, J., Jansson, O. (1997b) Surface plasmon resonance biomolecular interaction analysis mass spectrometry. 2. Fiberoptic-based analysis, *Anal. Chem.,* **69:** 4369-4374.

Nelson, R., Krone,, J., Jansson, O. (1997a) Surface plasmon resonance biomolecular interaction analysis mass spectrometry. 1. Chip-based analysis, *Anal. Chem.,* **69:** 4363-4368.

Newton, D., Pollock, D., DiTullio, P., Echelard, Y., Harvey, M., Wilburn, B., Williams, J., Hoogenboom, H., Raus, J., Meade, H., Rybak, S. (1999) Anti-transferrin receptor antibody-Rnase fusion protein expressed in the mammary gland of transgenic mice, *J. Immunol. Methods,* **231:** 147-157.

Nguyen, D.H., Webb, D.J., Catling, A.D., Song, Q., Dhakephalkar, A., Weber, M.J., Ravichandran, K.S., Gonias, S.L. (2000) Urokinase-type plasminogen activator stimulates the Ras/extracellular signal-regulated kinase (ERK) signalling pathway and MCF-7 cell migration by a mechanism that requires focal adhesion kinase, Src, and Shc. Rapid dissociation of GRB2/Sps-Shc complex is associated with the transient phosphorylation of ERK in urokinase-treated cells, *J. Biol. Chem.,* **275:** 19382-19388.

Nieba, L., Krebber, A., Plückthun, A. (1996) Competition BIAcore for measuring true affinities: large differences from values determined from binding kinetics, *Anal. Biochem.,* **234:** 155-165.

Niu, Q., Zhao, C., Jing, Z. (2001) An Evaluation of the colorimetric assays based on enzymatic reactions used in the measurement of human natural cytotoxicity, *J. Immunol. Methods,* **251:** 11-19.

Nolke, G., Fischer, R., Schillberg, S. (2003) Production of therapeutic antibodies in plants, *Expert Opin. Biol. Ther.,* **3:** 1153-62.

Nord, K., Gunneriusson, E., Ringdahl, J., Stahl, S., Uhlen, M., Nygren, P. (1997) Binding proteins selected from combinatorial libraries of an alpha-helical bacterial receptor domain, *Nature Biotechnol.,* **15l:** 772-777.

Nuzzo, R. & Allara, D. (1983) Adsorption of bifunctional organic disulphids on gold surfaces, *J. Am. Chem. Soc.,* **105:** 4481.

O'Reilly, R. (1976) Vitamin K and the oral anticoagulant drugs, *Ann. Rev. Med.,* **27:** 245-61.

O'Shannessy, D., Brigham-Burke, M., Peck, K. (1992) Immobilisation chemistries suitable for use in the biacore surface plasmon resonance detector, *Anal. Biochem.,* **205:** 132-136.

Ojala, T. (2001) Biological screening of plant coumarins, **PhD Thesis,** University of Helsinki, Helsinki, Finland.

Okamoto, T., Kawasaki, T., Hino, O. (2003) Osthole prevents anti-FAS antibody-induced hepatitis in mice by affecting the caspase-3-mediated apoptotic pathway, *Biochem. Pharmacol.,* **65:** 677-681.

Oketch-Rabah, H., Mwangia, J., Lisgartenb, J., Mberuc, E. (2000) A new antiplasmodial coumarin from *Toddalia asiatica* roots, *Fitoterapia,* **71:** 636-640.

Otsuji, E., Matsumura, H., Okamoto, K., Toma, A., Kuriu, Y., Ichikawa, D., Hagiwara, A., Yamagishi, H., (2003) Application of ^{99m}Tc labelled chimaeric fab fragments of monoclonal antibody A7 for immunoscintigraphy of pancreatic carcinoma, *J. Surg. Oncol.,* **84:** 160-164.

Owicki, J. & Parce, J. (1992) Biosensors based on the energy metabolism of living cells: the physical chemistry and cell biology of extracellular acidification, *Biosens. Bioelect.,* **7:** 255-272.

Palaretti, G. & Legnani, C. (1996) Warfarin withdrawal, *Clin. Pharmacokinet.,* **1996:** 300-13.

Pan, S,L., Huang, Y.W., Guh, J.H., Chang, Y.L., Peng, C.Y., Teng, C.M. (2003) Esculetin inhibits ras-mediated cell proliferation and alleviates vascular restenosis following angioplasty in rats, *Biochem Pharmacol.,* **65:** 1897-1905.

Papazisis, K., Zambouli, D., Kimoundri, OT., Papadakis, E.S., Vala, V., Geromichalos, G.D., Voyatzi, S., Markala, D., Destouni, E., Boutis, L., Kortsaris, A.H. (2000) Protein tyrosine kinase inhibitor, genistein, enhances apoptosis and cell cycle arrest in K562 cells treated with γ-irradiation, *Cancer Letts.,* **160:** 107-113.

Pelkonen, O., Maenpaa, J., Taavitsainen, P., Rautio, A., Raunio, H. (1998) Inhibition and induction of human Cytochrome P450 (CYP) enzymes, *Xenobiotica,* **28:** 1203-1253.

Pelkonen, O., Raunio, H., Rautio, A., Pasanen, M., Lang, M.A. (1997) The metabolism of coumarin, In: *Coumarins: Biology, Applications and Mode of Action,* (Eds: R O'Kennedy & R.D. Thornes), John Wiley & Sons, Chichester, pp 67-92.

Pelkonen, O., Rautio, A., Raunio, H., Pasanen, M. (2000) CYP2A6: a human coumarin 7-hydroxylase, *Toxicol.,* **144:** 139-147.

Petersen, C., Ha, C.E., Curry, S., Bhagavan, N.V. (2002) Probing the structure of the warfarin-binding site on human serum albumin using site-directed mutagenesis, *Proteins,* **47:** 116-125.

Petersen, C., Ha, C.E., Harohalli, K., Park, D., Bhagavan, N. (2000) Familial dysalbuminemic hyperthyroxinemia may result in altered warfarin pharmacokinetics, *Chemico-Biol. Inter.,* **124:** 161-172.

Petitpas, I., Bhattacharya Twine, S., East, M., Curry, S. (2001) Crystal structure analysis of warfarin binding to human serum albumin, *J. Biol. Chem.,* **276:** 22804-22809.

Piehler, J., Brecht, A., Giersch, T., Hock, B., Gauglitz, G. (1997) Assessment of affinity constants by rapid solid phase detection of equilibrium binding in a flow system, *J. Immunol. Methods,* **201:** 189-206.

Pluckthun, A. & Pack, P. (1997) New protein engineering approaches to multivalent and bispecific antibody fragments, *Immunotechnology,* **3:** 83-105

Pochet, L., Dieu, M., Frederick, R., Murray, A.M., Kempen, I., Pirotte, B., Masereel, B. (2003) Investigation of the inhibition mechanism of coumarins on chymotrypsin by mass spectrometry, *Tetrahedon,* **59:** 4557-4561.

Pollock, D., Kutzko, J., Birck-Wilson, E., Williams, J., Echelard, Y., Meade, H. (1999) Transgenic milk as a method for the production of recombinant antibodies, *J. Immunol. Methods,* **231:** 147-157.

Prall, O., Rogan, E., Musgrove, E., Watts, C., Sutherland, R. (1998) c-Myc or Cyclin D1 mimics estrogen effects on cyclin E-Cdk2 activation and cell cycle re-entry, *Mol. Cell. Biol.,* **18:** 4499-4508.

Prendergast, G., & Gibbs, J. (1997) Ras regulatory interactions: novel targets for anti-cancer intervention?, *Bioessays,* **16:** 187-191.

Putnam, K., Bombick, D., Doolittle, D. (2002) Evaluation of eight *in vitro* assays for assessing the cytotoxicity of cigarette smoke condensate, *Toxicol. In Vitro,* **16:** 599-607.

Qian, Y., Castranova, V., Shi, X. (2003) New perspectives in arsenic-induced cell signal transduction, *J. Inorg. Biochem.,* **96:** 271-278.

Quinn, J. & O'Kennedy, R. (2001) Biosensor-based estimation of kinetic and equilibrium constants, *Anal. Biochem.,* **290:** 36-46.

Quinn, J., Patel, P., Fitzpatrick, B., Manning, B., Dillon, P., Daly, S., O'Kennedy, R., Alcocer, M., Lee, H., Morgan, M., Lang, K. (1999) The use of regenerable, affinity ligand-based surfaces for immunosensor applications, *Biosen. Bioelectron.,* **14:** 587-595.

Rader, C., Turner, J., Heine, A., Shabat, D., Sinha, S., Wilson, I., Lerner, A., Barbas, C. (2003) A humanised aldolase antibody for selective chemotherapy and adaptor immunotherapy, *J. Mol. Biol.,* **332:** 889.

Ragueneau-Majlessi, I., Levy, R., Meyerhoff, C. (2001) Lack of effect of repeated administration of levetiracetam on the pharmacodynamic and pharmacokinetic profiles of warfarin, *Epilepsy Res.,* **47:** 55-63.

Rajaian, H., Symonds, H., Bowmer, C. (1997) Drug binding sites on chicken albumin: a comparison to human albumin, *J. Vet. Pharmacol. Ther.,* **20:** 421-426.

Ramdas, L., Bunnin, B., Plunkett, M., Sun, G., Ellman, J., Gallick, G., Budde, R. (1999) Benzodiazepine compounds as inhibitors of the src protein tyrosine kinase: screening of a combinatorial library of 1,4-benzodiazepines, *Arch. Biochem. Biophys.,* **368:** 394-400.

Rang, H.P., & Dale, M.M. (1987) *Pharmacology,* First Edition, Churchill Livingstone, Edinburgh.

Ratna, W. (2002) Inhibition of estrogenic stimulation of gene expression by genistein, *Life Sciences,* **71:** 865-877.

Rautio, A., Kraul, H., Kojo, A., Salmela, E., Pelkonen, O. (1992) Interindividual variability in coumarin 7-hydroxylation in healthy individuals, *Pharmacogenetics,* **2:** 227-233.

Ring, P., & Bostick, J. (2000) Validation of a method for the determination of (R)-warfarin and (S)-warfarin in human plasma using LC with UV detection, *J. Pharm. Biomed. Anal.,* **22:** 573-581.

Ritschel, WA., Brady, M.E., Tan, H.S.I., Hoffman, K.A., Yiu, I.M. & Grummich, K.W. (1977) Pharmacokinetics of coumarin and its 7-hydroxy-metabolites upon intravenous and peroral administration of coumarin in man, *Eur. J. Clin. Pharmacol.,* **12:** 457-461.

Ritschel, W.A., Grummich, K.W., Kaul, S., Hardt, T.J. (1981) Biopharmaceutical parameters of coumarin and 7-hydroxycoumarin, *Die Pharma. Ind.,* **43:** 271-276.

Robinson, G. (1995) The commercial development of planar optical biosensors, *Sens. Actuators B: Chem.,* **29:** 31-36.

Roche-Nagle, G., Robb, W., Ireland, A., Bouchier-Hayes, D. (2003) Extensive skin necrosis associated with warfarin sodium therapy, *Eur. J. Vasc. Endovasc Surg.,* **25:** 481-482.

Roderick, L. (1931) A problem in the coagulation of the blood, 'sweet clover disease of cattle', *Am. J. Physiol.,* **96:** 413-25.

Roma, G., Di Braccio, M., Carrieri, A., Grossi, G., Leoncini, G., Signorello, M., Carotti, A. (2003) Coumarin, chromone, and 4(3h)-pyrimidinone novel bicyclic and tricyclic derivatives as antiplatelet agents: synthesis, biological evaluation, and comparitive molecular field analysis, *Bioorg. Med. Chem.,* **11:** 123-138.

Romano, M., Maddox, J., Serhan, C. (1996) Activation of human monocytes and the acute monocytic leukaemia cell line (THP-1) by lipoxins involves unique signalling pathways for lipoxin A4 Versus Lipoxin B4: evidence for differential Ca^{2+} mobilisation, *J. Immunol.,* **157:** 2149-2154.

Ronnmark, J., Hansson, M., Nguyen, T., Uhlen, M., Robert, A., Stahl, S., Nygren, P.A. (2002) Construction and characterisation of affibody-Fc chimeras produced in *Escherichia coli, J. Immunol. Methods,* **261:** 199-211.

Rossi, E., Sharkey, R., McBride, W., Karacay, H., Zeng, L., Hansen, H., Goldenberg, D., Chang, C.H. (2003) Development of new multivalent-bispecific agents for pretargeting tumour localization and therapy, *Clin. Cancer Res.,* **9:** 3886S-3896S.

Rotenstreich, Y., Rubowitz, A., Segev, F., Jaeger-Roshu, S., Assia, E. (2001) Effect of warfarin therapy on bleeding during cataract surgery, *J. Cataract Refract. Surg.,* **27:** 1344-1345.

Rudin, C., Holmlund, J., Fleming, G., Mani, S., Stadler, W., Schumm, P., Monia, B., Johnston, J., Geary, R., Yu, R.Z., Kwoh, T.J., Dorr, F., Ratain, M. (2001) Phase I trial of ISIS 5132, an antisense oligonucleotide inhibitor of c-Raf-1, administered by 24-hour weekly infusion to patients with advanced cancer, *Clin. Cancer Res.,* **7:** 1214-1220.

Santen, R., Song, R., McPherson, R., Kumar, R., Adam, L., Jeng, M.H., Yue, W. (2002) The role of mitogen-activated protein (MAP) kinase in breast cancer, *Steroid Biochem. Mol. Biol.,* **80:** 239-256.

Sardari, S., Mori, Y., Horita, K., Micetich, R., Nishibe, S., Daneshtalab, M. (1999) Synthesis and antifungal activity of coumarins and angular furanocoumarins, *Bioorg. Med. Chem.,* **7:** 1933-1940.

Sarimehmetoglu, B., Kuplulu, O., Celik, H. (2004) Detection of aflatoxin M_1 in cheese samples by ELISA, *Food Control,* **15:** 45-49.

Sblattero, D. & Bradbury, A. (2000) Exploiting recombination in single bacteria to make large phage antibody libraries, *Nature Biotechnol.*, **18:** 75-80.

Schindler, J., Godbey, A., Hood, W., Bolten, S., Broadus, R., Kasten, T., Cassely, A., Hirsch, J., Merwood, M., Nagy, M., Fok, K., Saabye, M., Morgan, H., Compton, R., Mourey, R., Wittwer, A., Monahan, J. (2002) Examination of the kinetic mechanism of mitogen-activated protein kinase activated protein kinase-2, *Biochim. Biophys. Acta,* **1598:** 88-97.

Scholfield, K., Thomson, J., Poller, L. (1987) Protein C response to induction and withdrawal of oral anticoagulant treatment, *Clin. Lab. Haematol.*, **9:** 225-262.

Scordo, M., Pengo, V., Spina, E., Dahl, M., Gusella, M., Padrini, R. (2002) Influence of CYP2C9 and CYP2C19 genetic polymorphisms on warfarin maintence dose and metabolic clearance, *Clin. Pharmacol. Therapeutics,* **72:** 702-710.

Scouten, W., Luong, J., Brown, S. (1995) Enzyme or protein immobilisation techniques for applications in biosensor design, *TIBTECH,* **13:** 178-185.

Seligman, S. (1994) Influence of solid-phase antigen competition enzyme-linked immunosorbent assays (ELISAs) on calculated antigen-antibody dissociation constants, *J. Immunol. Methods,* **168:** 101-110.

Seo, H.S., Journe, F., Larsimont, D., Sotiriou, C., Leclercq, G. (2003) Decrease of estrogen receptor expression and associated ERE-Dependent transcription in MCF-7 breast cancer cells after oligomycin treatment, *Steroids,* **68:** 257-269.

Seyhi, R. (1994) Transducer aspects of biosensors, *Biosens. Bioelectron.,* **9:** 243-264.

Seymour, L. (2003) Epidermal growth factor receptor inhibitors: an update on their development as cancer therapeutics, *Curr. Opin. Investig. Drugs,* **4:** 658-666.

Sharma, S., Neale, M., Di Nicolantonio, F., Knight, L., Whitehouse, P., Mercer, S., Higgins, B., Lamont, A., Osborne, R., Hindley, A., Kurbacher, C., Cree, I. (2003) Outcome of ATP-based tumour chemosensitivity assay directed chemotherapy in heavily pre-treated recurrent ovarian carcinoma, *BMC Cancer,* **3:** 19.

Shepherd, F.A. (2003) Second-line chemotherapy for non-small cell lung cancer, *Expert. Rev. Anticancer Ther.*, **3**: 435-442.

Shilling, W.H., Crampton, R.F., Longland, R.C. (1969) Metabolism of coumarin in man, *Nature (London)*, **221**: 664-665.

Si, F., Shin, S.H., Biedermann, A., Ross, G.M. (1999) Estimation of PC12 cell numbers with acid phosphatase assay and mitochondrial dehydrogenase assay: dopamine interferes with assay based on tetrazolium, *Exp. Brain Res.*, **124**: 145-150.

Sikora, K. & Smedley, H. (1984) Monoclonal antibodies, First Edition, Blackwell Scientific Publications, Oxford.

Simon, R., Beaudin, S., Johnston, M., Walton, K., Shaughnessy, S. (2002) Long-term treatment with sodium warfarin results in decreased femoral bone strength and cancellous bone volume in rats, *Thromb. Res.*, **105**: 353-358.

Sireci, G., Espinosa, E., Di Sano, C., Dieli, F., Fournie, J., Salerno, A. (2001) Differential activation of human gammadelta cells by nonpeptide phosphoantigens, *Eur. J. Immunol.*, **31**: 1628-1635.

Sjolander, S. & Urbanicky, S. (1991) Integrated fluid handling system for biomolecular interaction analysis, *Anal. Biochem.*, **63**: 2338-2345.

Sledge, G. & Miller, K. (2003) Exploiting the hallmarks of cancer: the future conquest of breast cancer, *Eur. J. Can.*, **39**: 1668-1675.

Smith, G., Patel, S., Windass, J., Thornton, J., Winter, G., Griffiths, A. (1998) Small binding proteins selected from a combinatorial repertoire of knottins displayed on phage, *J. Mol. Biol.*, **277**: 317-332.

Sonksen, C., Nordhoff, E., Jansson, O., Malmqvist, M., Roepstorff, P. (1998) Combining MALDI mass spectrometry and biomolecular interaction analysis using a biomolecular interaction analysis instrument, *Anal. Chem.*, **70**: 2731-2736.

Sridhar, S., Seymour, L., Shepherd, F.A. (2003) Inhibitors of epidermal-growth factor receptors: a review of clinical research with a focus on non-small-cell lung cancer, *Lancet Oncol.*, **4**: 397-406.

380

Stahmann, M., Graf, L.H., Heubner, C.F., Roseman, S., Link, K.P. (1944) Studies on the 4-hydroxycoumarins. IV. Esters of the 4-hydroxycoumarins, *J. Am. Chem. Soc.,* **66:** 900-2.

Steen, H., Kuster, B., Fernandez, M., Pandey, A., Mann, M. (2002) Tyrosine phosphorylation mapping of the epidermal growth factor receptor signalling pathway, *J. Biol. Chem.* **277:** 1031-1039.

Stevens, F. (1987) Modificiation of an ELISA-based procedure for affinity determination: correction necessary for use with bivalent antibody, *Mol. Immunol.,* **24:** 1055-1060.

Steward, M. (1984) Antibodies: their structure and function, First Edition, Chapman and Hall, London.

Stewart, Z., Westfall, M., Pietenpol, J. (2003) Cell-Cycle dysregulation and anticancer therapy, *TRENDS Pharmacol. Sci.,* **24:** 139-145.

Steyn, J., Van Der Merwe, H., De Kock, M. (1986) Reversed-phase high-performance liquid chromatographic method for the determination of warfarin from biological fluids in the low nanogram range, *J. Chromatogr.,* **378:** 254-260.

Stocklein, W., Behrsing, O., Scharte, G., Micheel, B., Benkert, A., Schobler, W., Warsinke, A., Scheller, F. (2000) Enzyme kinetic assays with surface plasmon resonance (BIAcore) based on competition between enzyme and creatinine antibody, *Biosen. Bioelect.,* **15:** 377-382.

Stoger, E., Sak, M., Fischer, R., Christou, P. (2002) Plantibodies: applications, advantages and bottlenecks, *Curr. Opin. Biotech.,* **13:** 161-166.

Strasser, A., Dietrich, R., Usleber, E., Martlbauer, E. (2003) Immunochemical rapid test for multiresidue analysis of antimicrobial drugs in milk using monoclonal antibodies and hapten-glucose oxidase conjugates, *Anal. Chim. Acta,* **495:** 11-19.

Strobl, J., Wonderlin, W., Flynn, D.C. (1995) Mitogenic signal transduction in human breast cancer cells, *Gen. Pharmacol.,* **26:** 1643-1649.

Stryer, L. (1995) *Biochemistry,* Fourth Edition, W.H. Freeman, New York.

Su, Y.C., Lim, K.P., Nathan, S. (2003) Bacterial expression of the scFv fragment of a recombinant antibody specific for *Burkholderia pseudomallei* exotoxin, *J. Biochem. Mol. Biol.,* **36:** 493-498.

Sullivan, T., Welsh, E., Kerdel, F., Burdick, A., Kirsner, R. (2003) Infliximab for *Hidradenitis suppurativa, Br. J. Dermatol.,* **149:** 1046-1049.

Summy, J.M. & Gallick, G.E. (2003) Src family kinases in tumour progression and metastasis, *Cancer Metastasis Rev.,* **22:** 337-358.

Sun, L., Ghosh, I., Xu, M.Q. (2003) Generation of an affinity column for antibody purification by intein-mediated protein ligation, *J. Immunol. Methods.,* **282:** 45-52.

Supino, R. (1985) MTT assays, In: *Methods in Molecular Biology, vol.43: In vitro toxicity testing protocols,* (Eds: S. O'Hare & C.K. Atterwill), Humana Press Inc.,Totowa, USA, pp 137-149.

Suttie, J. (1993) Synthesis of vitamin K-dependent proteins, *FASEB J.,* **7:** 445-452.

Svojanosky, S., Egodage, K., Wu, J., Slavik, M., Wilson, G. (1999) High sensitivity ELISA determination of taxol in various human biological fluids, *J. Pharm. Biomed. Anal.,* **20:** 549-555.

Taavitsainen, P. (2001) *Cytochrome P450 Isoform-Specific In Vitro Methods to Predict Drug Metabolism and Interactions,* Oulu University Press, Finland.

Tabrizi, A., Zehnbauer, B., Borecki, I., McGrath, S., Buchman, T., Freeman, B. (2002) The frequency and effects of Cytochrome P450 (CYP) 2C9 polymorphisms in patients receiving warfarin, *J. Am. Coll Surg.,* **194:** 267-273.

Takahashi, H., Kashima, T., Kimura, S., Muramoto, N., Nakahata, H., Kubo, S., Shimoyama, Y., Kajiwara, M., Echizen, H. (1997) Determination of unbound warfarin enantiomers in human plasma and 7-hydroxywarfarin in human urine by chiral stationary-phase liquid chromatography with ultraviolet or fluorescent and on-line circular dichroism detection, *J. Chromatog.,* **701:** 71-80.

Takahashi, H., Wilkinson, G., Caraco, Y., Muszkat, M., Kim, R., Kashima, T., Kimura, S., Echizen, H. (2003) Population differences in S-warfarin metabolism between CYP2C9 genotype-matched caucasian and japanese patients, *Clin. Pharmacol. Therapeutics,* **73:** 253-263.

Takamiya, O. & Yoahioka, A. (1996) Factor VII binding to tissue factor in plasma from warfarin-treated individuals, *Thromb. Res.,* **81:** 657-663.

Takamura, Y., Kobayashi, H., Taguchi, T., Motomura, K., Inaji, H., Noguchi, S. (2002) Prediction of chemotherapeutic response by collagen gel droplet embedded culture-drug sensitivity test in human breast cancers, *Int. J. Cancer,* **98:** 450-455.

Talstad, I. & Gamst, O. (1994) Warfarin resistance due to malabsorption, *J. Internal Med.,* **236:** 465-7.

Tanos, V., Brzezinski, A., Drize, O., Strauss, N., Peretz, T. (2002) Synergistic inhibitory effects of genistein and tamoxifen on human dyplastic and malignant epithelial breast cells *in vitro, Eur. J. Obstet. Gynecol. Reprod. Biol.,* **102:** 188-194.

Thornes, R.D., Daly, L., Lynch, G., Breslin, B., Browne, H., Browne, H.Y., Corrigan, T., Daly, P., Edwards, G., Gaffney, E. (1994) Treatment with coumarin to prevent or delay recurrence of malignant melanoma, *Cancer Res. Clin. Oncol.,* **120:** S32-34.

Thornes, R.D., Edlow, D.W., Wood, S. Jr. (1968) Inhibition of locomotion in cancer cells *in vivo* by anticoagulant therapy. 1. Effect of sodium warfarin on V2 cancer cells, granulocytes, lymphocytes and macrophages in rabbits, *Johns Hopkins Med. J.,* **123:** 305-316.

Thornes, R.D., Lynch, G., Sheehan, M.W. (1982) Cimetidine and coumarin therapy of melanoma, *Lancet,* **320:** 328.

Thornes, R.D. (1983) Acquired immune suppression in chronic brucellosis, *Ir. Med. J.,* **76:** 225.

Thornes, R.D. (1997) Clinical and biological observations associated with coumarins, In: *Coumarins: Biology, Applications and Mode of Action,* (Eds: R O'Kennedy & R.D. Thornes), John Wiley & Sons, Chichester, pp 255-265.

Tishkoff, G. & Hunt, L. (2000) Unexpected molecular mimicry among peptides MHC Class II, blood-clotting factor X, and HIV-1 envelope glycoprotein GP120, *Thromb. Res.,* **98:** 343-346.

Tistravik, D., Huesan, D., Deshpance, U., Kung, A. (1999) differential effects of administration of a human anti-CD4 monoclonal antibody HM6G, in nonhuman primates, *Clin. Immunol.,* **92:** 138-152.

Tomlinson, I. & Holt, L. (2001) Protein profiling comes of age, *Genome Biol.,* **2:** REVIEWS1004.1-REVIEWS1004.3

Tsai, T.H., Tsai, T.R., Chen, C.C., Chen, C.F. (1996) Pharmacokinetics of osthole in rat plasma using high-performance liquid chromatography, *J. Pharm. Biomed. Anal.,* **14:** 749-753.

Tummino, P., Ferguson, D., Hupe, D. (1994) Competitive inhibition of HIV-1 protease by warfarin derivatives, *Biochem. Biophys. Res. Commun.,* **201:** 290-294.

Tveit, K. (1983) Use of xenografts for drug sensitivity testing *in vitro,* In: *Human Tumour Drug Sensitivity Testing In Vitro,* (Eds: P.P. Dendy & B.T. Hill), First Edition, Academic Press, London, pp 201-210.

Uckun, F., Narla, R., Jun, X., Zeren, T., Venkatachalam, T., Waddick, K., Rostostev, A., Myers, D. (1998) Cytotoxic activity of epidermal growth factor-genistein against breast cancer cells, *Clin. Cancer Res.,* **4:** 901-912.

Ullah, N., Ahmed, S., Muhammad, P., Ahmed, Z., Nawaz, H., Malik, A. (1999) Coumarinolognoid glycoside from *Daphne oleoides, Phytochem.,* **51:** 103-105.

Usami, M., Mitsunaga, K., Ohno, Y. (2002) Estrogen receptor binding assay of chemicals with a surface plasmon resonance biosensor, *J. Steroid Biochem. Mol. Biol.,* **81:** 47-55.

Van de Sande, T., De Schrijver, E., Heyns, W., Verhoeven, G., Swinnen, J. (2002) Role of the phosphatidylinositol 3'-Kinase/PTEN/Akt kinase pathway in the overexpression of fatty acid synthase in LNCaP prostate cancer cells, *Cancer Res.,* **62:** 642-646.

van Spriel, A., van Ojik, H., van de Winkel, J. (2000) Immunotherapeutic perspective for bispecific antibodies, *Immunol. Today,* **21:** 391-7.

Vanscheidt, W., Rabe, E., Naser-Hijazi, B., Ramelet, A.A., Partsch, H., Diehm, C., Schultz-Ehrenburg, U., Spengel, F., Wirsching, M., Gotz, V., Schnitker, J., Henneicke-von Zepelin, H.H. (2002) The Efficacy and safety of a coumarin-/troxerutin-combination (SB-LOT) in patients with chronic venous insufficiency: a double blind placebo-controlled randomised study, *Vasa.*, **31:** 185-190.

Vaughan, T., Osbourne, J., Tempest, P. (1998) Human antibodies by design, *Nature Biotechnol.*, **16:** 535.

Velasco-Velazquez, M.A., Agramonte-Hevia, J., Barrera, D., Jimenez-Orozco, A., Garcia-Mondragon, M.J., Mendoza-Patino, N., Landa, A., Mandoki, J. (2003) 4-hydroxycoumarin disorganizes the actin cytoskeleton in B16-F10 melanoma cells but not in B82 fibroblasts, decreasing their adhesion to extracellular matrix proteins and motility, *Cancer Letts.*, **198:** 179-186.

Vercoutter-Edouart, A.S., Lemoine, J., Smart, C.E., Nurcombe, V., Boilly, B., Peyrat, J.P., Hondermarck, H. (2000) The mitogenic signalling pathway for fibroblast growth factor-2 involves the tyrosine phosphorylation of cyclin D2 in MCF-7 human breast cancer cells, *FEBS Letts.*, **478:** 209-215.

Verhagen, H. (1954) Local haemorrhage and necrosis of the skin and underlying tissues, during anti-coagulant therapy with dicumarol or dicumacyl, *Acta Med. Scand.*, **148:** 453-467.

Vitale, N., De Feo, M., Cotrufo, M. (2002) Anticoagulation for prosthetic heart valves during pregnancy: the importance of warfarin daily dose, *Eur. J. Cardio-thoracic Surg.*, **22:** 656-657.

Vitale, N., De Feo, M., De Santo, L., Pollice, A., Tedesco, N., Cotrufo, M. (1999) Dose-dependent fetal complications of warfarin in pregnant women with mechanical heart valves, *J. Am. Coll. Cardiol.*, **33:** 1637-1641.

Vuky, J., Motzer, R.J. (2000) Cytokine therapy in renal cell cancer, *Urol Oncol.*, **5:** 249-257.

Wada, H., Fok, K., Pitchford, S. (1994) Stimulation of peripheral blood t-cells with anti-CD3 and anti-CD28 results in a sustained increase in extracellular acidification rate, *FASEB J.*, **8:** A852

Wada, H., Indelicato, S.R., Meyer, L., Kitamura, T., Miyajima, A., Kirk, G., Muir, V., Parce, J. (1993) GM-CSF triggers a rapid, glucose-dependent extracellular acidification by TF-1 Cells: evidence for sodium/proton antiporter and PKC-mediated activation of acid production, *J. Cell. Physiol.*, **154:** 129-138.

Wada, H., Owicki, J., Bruner, L., Miller, K., Raley-Susman, K., Panfili, P., Humphries, G., Parce, J.W. (1992) Measurement of cellular responses to toxic agents using a silicon microphysiometer, *AATEX*, **1:** 154-164.

Waldmann, H. (1989) Manipulation of T-cell responses with monoclonal antibodies, *Ann. Rev. Immunol.,* **7:** 407-444.

Wang, C.C., Lai, J.E., Chen, L.G., Yen, K.Y., Yang, L.L. (2000) Inducible nitric oxide synthase inhibitors of chinese herbs. Part 2: naturally occurring furanocoumarins, *Bioorg. Med. Chem.,* **8:** 2701-2707.

Wang, C.J., Hsieh, Y.J., Chu, C.Y., Lin, Y.L., Tseng, T.H. (2002) Inhibition of cell cycle progression in human leukaemic HL-60 cells by esculetin, *Cancer Letts.,* **160:** 107-113.

Warrier, I., Brennan, C.A., Lusher, J. (1986) Familial resistance in a black child, *Am. J. Pediatr. Haematol. Oncol.,* **4:** 346-347.

Watanabe, E., Tsuda, Y., Watanabe, S., Ito, S., Hayashi, M., Watanabe, T., Yuasa, Y., Nakazawa, H. (2000) Development of an enzyme immunoassay for the detection of plant growth regulator inabenfide in rice, *Anal. Chim. Acta,* **424:** 149-160.

Wcislo, G. & Szczylik, C. (2003) Interferon: therapy in patients with cutaneous malignant melanoma in adjuvant setting,. *Pol Merkuriusz Lek.,* **15:** 5-8.

Webb, S. & Hall, J. (2001) Polyclonal-based ELISA for the identification of cyclohexanedione analogs that inhibit maize acetyl coenzyme-A carboxylase, *J AOAC Int.,* **84:** 143-149.

Weber, U.S., Steffen, B., Siegers, C.P. (1998) Antitumour-activities of coumarin, 7-hydroxycoumarin and its glucuronide in several human tumour cell lines, *Res. Commun. Mol. Pathol. Pharmacol.,* **99:** 193-206.

Weihua, Z., Andersson, S., Cheng, G., Simpson, E., Warner, M., Gustafsson, A. (2003) The 16th datta lecture update on estrogen signalling, *FEBS Letts.,* **546:** 17-24.

Weinmann, I. (1997) History of the development and applications of coumarin and coumarin-related compounds, In: *Coumarins: Biology, Applications and Mode of Action,* (Eds: R O'Kennedy & R.D. Thornes), John Wiley & Sons, Chichester, pp 1-22.

Weinstein-Oppenheimer, C., Blalock, W., Steelman, L., Chang, F., McCubrey, J. (2000) The Raf Signal Transduction Cascade as a Target for Chemotherapeutic Intervention in Growth Factor-Responsive Tumours, *Pharmacol. Ther.,* **88:** 229-279.

Weisenthal, L. & Kern, D. (1991) Prediction of drug resistance in cancer chemotherapy: the Kern and DiSc assays, *Oncology,* **5:** 93-103.

Weiss, A. & Schlessinger, J. (1998) Switching signals on and off by receptor dimerisation, *Cell,* **94:** 277-280.

Welder, A. & Acosta, D. (1994) Enzyme leakage as an indicator of cytotoxicity in cultured cells, In: *Methods in Toxicology,* (Eds: C.A. Tyson & J.M. Frazier), **vol 1B:** Academic Press, New York, pp 46-49.

West, K., Linnoila, I., Brognard, J., Belinsky, S., Harris, C., Dennis, P. (2003) P-326 tobacco carcinogen-induced cellular transformation increases Akt activation *in vitro* and *in vivo, Lung Cancer,* **41:** S174.

Williams, C. & Addona, T. (2000) The Integration of SPR Biosensors With Mass Spectrometry: Possible Applications for Proteome Analysis, *TIBTECH,* **18:** 45-50.

Wong, R., Mytych, D., Jacobs, S., Bordens, R. (1997) Validation parameters for a novel biosensor assay which simultaneously measures serum concentrations of a humanised monoclonal antibody and detects induced antibodies, *J. Immunol. Methods,* **209:** 1-15.

Wright, I. (1960) Treatment of thromboembolic disease, *JAMA,* **174:** 1921-1924.

Wu, J., Fong, W.F., Zhang, J.X., Leung, C.H., Kwong, H.L., Yang, M.S., Li, D., Cheung, H.Y. (2003) Reversal of multidrug resistance in cancer cells by pyranocoumarins isolated from *Radix peucedani, Eur. J. Pharmacol.,* **473:** 9-17.

Wu, S.N., Lo, Y.K., Chen, C.C., Li, H.F., Chiang, H.T. (2002) Inhibitory effect of the plant-extract osthole on L-Type calcium current in NG108-15 neuronal cells, *Biochem. Pharmacol.,* **63:** 199-206.

Yamazaki, H. & Shimada, T. (1997) Human liver Cytochrome P450 enzymes involved in the 7-hydroxylation of R-and S-warfarin enantiomers, *Biochem. Pharmacol.,* **54:** 1195-1203.

Yang, E.B., Zhao, Y.N., Zhang, K., Mack, P. (1999) Daphnetin, one of the coumarin derivatives is a protein kinase inhibitor, *Biochem. Biophys.Res. Commun.,* **260:** 682-685.

Yang, T.T., Sinai, P., Kain, S.R. (1996) An acid phosphatase assay for quantifying the growth of adherent and nonadherent cells, *Amer. J. Physiol.,* **241:** 103-108.

Yang, X.D., Corvalan, I., Wang, P., Ray, C., Davis, C. (1999a) Fully human anti-Interlueukin-8 monoclonal antibodys: potential therapeutics for the treatment of inflammatory disease states, *J. Leukoc. Biol.,* **66:** 401-410.

Yang, X.D., Lia, X.C., Corvalan, I., Wang, P., Davis, C., Lakabrevits, A. (1999b) Eradication of established tumours by a fully human monoclonal antibody to the epidermal growth factor receptor without concomitant chemotherapy, *Cancer Res.,* **59:** 1236-1243.

Yau, K., Lee, H., Hall, C. (2003) Emerging trends in the synthesis and improvement of hapten-specific recombinant antibodies, *Biotech. Advan.,* **21:** 599-637.

Yeilada, E., Taninaka, H., Takaishi, Y., Honda, G., Sezik, E., Momota, H., Ohmoto, Y., Taki, T. (2001) *In vitro* inhibitory effects of *Daphne oleoides* SPP. *Oleoides* on inflammatory cytokines and activity-guided isolation of active constituents, *Cytokine,* **13:** 359-364.

Zacharski, L., Henderson, W., Rickles, F., Forman, W., Cornell, C. Jr., Jackson Forcier, R., Edwards, R., Headley, E., Kim, S.H., O'Donnell, J., O'Dell, R., Tornyos, K., Kwaan, H. (1984) Effect of warfarin anticoagulation on survival in carcinoma of the lung, colon, head and neck, and prostate. Final report of VA cooperative study no.75, *Cancer,* **53:** 2046-2052.

Zacharski, L. (2002) Anticoagulants in cancer treatment: malignancy as a solid phase coagulopathy, *Cancer Letts.,* **28:** 5-18.

Zacharski, L.R., Howell, A.L., Memoli, V.A. (1992) The coagulation biology of cancer, *Fibrinolysis,* **1:** 39-42.

Zambrano, E., Nathanielsz, P., McDonald, T. (2002) Neonatal ovine adrenal cortical and medullary cell H^+ responses to ACTH and prostaglandin E_2, *Biol. Neonate,* **82:** 243-249.

Zatta, A. & Bevilacqua, C. (1999) Differential inhibition of polymorphonuclear leucocyte functions by cloricromene, *Pharmacol. Res.,* **40:** 525-533.

Zembutsu, H., Ohnishi, Y., Tsunoda, T., Furukawa, Y., Katagiri, T., Ueyama, Y., Tamaoki, N., Nomura, T., Kitahara, O., Yanagawa, R., Hirata, K., Nakamura, Y. (2002) Genome-wide cDNA microarray screening to correlate gene expression profiles with sensitivity of 85 human cancer xenografts to anti-cancer drugs, *Cancer Res.,* **62:** 518-527.

Zhang, Z., Fasco, MJ, Huang, Z., Geungerich, P., Kaminsky, L.S. (1995) Human Cytochromes P4501A1 and P4501A2: R-warfarin metabolism as a probe, *Drug Metab. Dispos.,* **23:** 1339-1345.

Zhou, Q. & Chan, E. (2002) Effect of 5-flurouracil on the anticoagulant activity and the pharmacokinetics of warfarin enantiomers in rats, *Eur. J. Pharm. Sci.,* **17:** 73-80.

Zhu, G., Yang, B., Jennings, R. (2000) Quantitation of basic fibroblast growth factor by immunoassay using BIAcore 2000, *J. Pharm. Biomed. Anal.,* **24:** 281-290.

Zhu, Z. (2003) Aberrant tumour vasculature and angiogenesis: new opportunities for cancer therapy, *Drug Discovery Today,* **8:** 827-828.

Zimbelman, J., Lefkowitz, Schaeffer, C., Hays, T., Manco-Johnson, M., Manhalter, C., Nuss, R. (2000) Unusual complications of warfarin therapy: skin necrosis and priapism, *J. Pediatrics,* **137:** 266-268.

Zingarelli, B., Carnuccio, R., Di Rosa, M. (1993) Cloricromene inhibits the induction of nitric oxide synthase, *Eur. J. Pharmacol.,* **243:** 107-111.

Appendix

Appendix 1A

1A.1. Glossary of Terms and Definitions Commonly Employed in Bioanalytical Validation Procedures:

The terms listed below are commonly referred to in bioanalytical validation procedures and the criteria which they can be defined under have been extensively reviewed (Findlay *et al.*, 2000).

Mean

Describes the average of replicate (x) measurements. (i.e. $n_1+n_2+\ldots\ldots n_x/x$)

Accuracy

Is defined as the closeness of agreement between a measured test result and its expected true reference value.

Precision

Is defined as the closeness of agreement, or variance between independent test results of multiple measurements of the same sample obtained under a set of specified analytical test conditions. It is normally expressed in terms of the relative standard deviation (% R.S.D.), or the coefficient of variation (% C.V.) of the determined concentration of a replicate number of assays. The degree of precision assessed between replicates (i.e. % C.V.) performed during a single assay batch, is commonly referred to as the intra-assay variation (also referred to as repeatability). The term inter-assay variation (also referred to as reproducibility) is used to describe the precision between assays when related to multiple batches.

Limit of Detection (L.O.D.)

Defines the lowest concentration of analyte that the analytical technique can differentiate from background.

Lower Limit of Quantitation (L.O.Q.):

The lowest concentration of analyte that can be measured from the calibration curve with acceptable levels of precision and accuracy.

Robustness:

Is a term used to describe the ability of an analytical technique to withstand fluctuations in the described analytical test conditions. For immunoassay procedures the term could be used to describe changes in the ionic strength of the matrix, as well as pH and temperature changes.

Standard Curve:

This describes the relationship between the measured analyte response (i.e. absorbance, response units) and the analyte concentration.

Coefficient of Variation (% C.V.)

A quantitative measure of the precision of an analytical measurement expressed as a percent function of the mean value, also referred to as the Relative Standard Deviation (% R.S.D.).

$$\% \text{ C.V.} = [\text{S.D./Mean value}] \times 100$$

Batch/Run:

Refers to a single set of samples (standards) analysed together as a single sample set using the same analytical technique.

Residual:

Describes the difference between the value described by the equation model and the true value.

Precision profile:

A quantitative measure of the variation between measurements, usually the coefficient of variation versus the nominal concentration of analyte in the sample.

Normalised Response Values:

The response recorded in response units (R) at each particular antigen concentration divided by the response recorded in the presence of zero antigen (R/Ro).

i.e.

Normalised Response　＝　　　Response measured at particular antigen concentration
　　　　　　　　　　　　　　　　Response measured at zero antigen concentration

Normalised Absorbance Values:

The absorbance recorded (A) at each particular antigen concentration divided by the absorbance recorded in the presence of zero antigen (A/Ao).

i.e.

Normalised Absorbance = $\dfrac{\text{Absorbance measured at particular antigen concentration}}{\text{Absorbance measured at zero antigen concentration}}$

Appendix 1B

1B.1. 'Student's' t Test (For Paired Samples)

"Student" (real name: W. S. Gossett [1876-1937]) developed statistical methods to solve problems stemming from his employment in Guinness's brewery. Student's *t*-test deals with the problems associated with inference based on "small" samples: the calculated mean (X_{avg}) and standard deviation (σ) may by chance deviate from the "real" mean and standard deviation (i.e., what one would measure if many more data items were available: a "large" sample).

Definition: It is the statistical test used to evaluate if two groups are significatively different according to their means.

Example using EXCEL

t-Test: Paired Two Sample for Means		
	Variable 1	Variable 2
Mean	0.6393	0.5537
Variance	0.000492	0.001044
Observations	10	10
Pearson Correlation	0.216921	
Hypothesized Mean Difference	0	
df	9	
t Stat	7.734238	
P(T<=t) one-tail	1.45E-05	
t Critical one-tail	1.833114	
P(T<=t) two-tail	2.90E-05	
t Critical two-tail	2.262159	